METHODS IN MOLECULAR MEDICINE™

Autoimmunity

Methods and Protocols

Edited by

Andras Perl, MD, PhD

HUMANA PRESS

Autoimmunity

METHODS IN MOLECULAR MEDICINE™

John M. Walker, SERIES EDITOR

112 **Molecular Cardiology:** *Methods and Protocols,* edited by *Zhongjie Sun, 2005*

111 **Chemosensitivity:** *Volume 2, In Vivo Models, Imaging, and Molecular Regulators,* edited by *Rosalyn D. Blumethal, 2005*

110 **Chemosensitivity:** *Volume 1, In Vitro Assays,* edited by *Rosalyn D. Blumethal, 2005*

109 **Adoptive Immunotherapy,** *Methods and Protocols,* edited by *Burkhard Ludewig and Matthias W. Hoffman, 2005*

108 **Hypertension,** *Methods and Protocols,* edited by *Jérôme P. Fennell and Andrew H. Baker, 2005*

107 **Human Cell Culture Protocols,** *Second Edition,* edited by *Joanna Picot, 2005*

106 **Antisense Therapeutics,** *Second Edition,* edited by *M. Ian Phillips, 2005*

105 **Developmental Hematopoiesis:** *Methods and Protocols,* edited by *Margaret H. Baron, 2005*

104 **Stroke Genomics:** *Methods and Reviews,* edited by *Simon J. Read and David Virley, 2004*

103 **Pancreatic Cancer:** *Methods and Protocols,* edited by *Gloria H. Su, 2004*

102 **Autoimmunity:** *Methods and Protocols,* edited by *Andras Perl, 2004*

101 **Cartilage and Osteoarthritis:** *Volume 2, Structure and In Vivo Analysis,* edited by *Frédéric De Ceuninck, Massimo Sabatini, and Philippe Pastoureau, 2004*

100 **Cartilage and Osteoarthritis:** *Volume 1, Cellular and Molecular Tools,* edited by *Massimo Sabatini, Philippe Pastoureau, and Frédéric De Ceuninck, 2004*

99 **Pain Research:** *Methods and Protocols,* edited by *David Z. Luo, 2004*

98 **Tumor Necrosis Factor:** *Methods and Protocols,* edited by *Angelo Corti and Pietro Ghezzi, 2004*

97 **Molecular Diagnosis of Cancer:** *Methods and Protocols, Second Edition,* edited by *Joseph E. Roulston and John M. S. Bartlett, 2004*

96 **Hepatitis B and D Protocols:** *Volume 2, Immunology, Model Systems, and Clinical Studies,* edited by *Robert K. Hamatake and Johnson Y. N. Lau, 2004*

95 **Hepatitis B and D Protocols:** *Volume 1, Detection, Genotypes, and Characterization,* edited by *Robert K. Hamatake and Johnson Y. N. Lau, 2004*

94 **Molecular Diagnosis of Infectious Diseases,** *Second Edition,* edited by *Jochen Decker and Udo Reischl, 2004*

93 **Anticoagulants, Antiplatelets, and Thrombolytics,** edited by *Shaker A. Mousa, 2004*

92 **Molecular Diagnosis of Genetic Diseases,** *Second Edition,* edited by *Rob Elles and Roger Mountford, 2004*

91 **Pediatric Hematology:** *Methods and Protocols,* edited by *Nicholas J. Goulden and Colin G. Steward, 2003*

90 **Suicide Gene Therapy:** *Methods and Reviews,* edited by *Caroline J. Springer, 2004*

89 **The Blood–Brain Barrier:** *Biology and Research Protocols,* edited by *Sukriti Nag, 2003*

88 **Cancer Cell Culture:** *Methods and Protocols,* edited by *Simon P. Langdon, 2003*

87 **Vaccine Protocols,** *Second Edition,* edited by *Andrew Robinson, Michael J. Hudson, and Martin P. Cranage, 2003*

86 **Renal Disease:** *Techniques and Protocols,* edited by *Michael S. Goligorsky, 2003*

85 **Novel Anticancer Drug Protocols,** edited by *John K. Buolamwini and Alex A. Adjei, 2003*

84 **Opioid Research:** *Methods and Protocols,* edited by *Zhizhong Z. Pan, 2003*

83 **Diabetes Mellitus:** *Methods and Protocols,* edited by *Sabire Özcan, 2003*

82 **Hemoglobin Disorders:** *Molecular Methods and Protocols,* edited by *Ronald L. Nagel, 2003*

81 **Prostate Cancer Methods and Protocols,** edited by *Pamela J. Russell, Paul Jackson, and Elizabeth A. Kingsley, 2003*

80 **Bone Research Protocols,** edited by *Miep H. Helfrich and Stuart H. Ralston, 2003*

79 **Drugs of Abuse:** *Neurological Reviews and Protocols,* edited by *John Q. Wang, 2003*

78 **Wound Healing:** *Methods and Protocols,* edited by *Luisa A. DiPietro and Aime L. Burns, 2003*

METHODS IN MOLECULAR MEDICINE™

Autoimmunity

Methods and Protocols

Edited by

Andras Perl, MD, PhD

Departments of Medicine, Microbiology, and Immunology, State University of New York, Upstate Medical University, College of Medicine, Syracuse, NY

HUMANA PRESS TOTOWA, NEW JERSEY

999 Riverview Drive, Suite 208
Totowa, New Jersey 07512

www.humanapress.com

This publication is printed on acid-free paper. ∞

ANSI Z39.48-1984 (American Standards Institute) Permanence of Paper for Printed Library Materials.

Production Editor: Angela Burkey

Cover design by Patricia F. Cleary.

Cover illustration: Histopathology of EAU in the B10.RIII mouse (Chapter 21, Fig. 3.; *see* page 411 for complete legend and discussion on page 410).

For additional copies, pricing for bulk purchases, and/or information about other Humana titles, contact Humana at the above address or at any of the following numbers: Tel.: 973-256-1699; Fax: 973-256-8341; E-mail: humana@humanapr.com; or visit our Website: www.humanapress.com

Printed in the United States of America. 10 9 8 7 6 5 4 3 2 1

eISBN: 1-59259-805-6

ISSN: 1543-1894

Library of Congress Cataloging-in-Publication Data

Autoimmunity : methods and protocols / edited by Andras Perl.
p. ; cm. -- (Methods in molecular medicine ; 102)
Includes bibliographical references and index.
ISBN 1-58829-231-2 (alk. paper)
1. Autoimmune diseases--Laboratory manuals. 2. Autoimmunity--Laboratory manuals.
[DNLM: 1. Autoimmunity--physiology--Laboratory Manuals. 2. Autoimmune Diseases--physiopathology--Laboratory Manuals. 3. Models, Immunological--Laboratory Manuals. 4. T-Lymphocytes--immunology--Laboratory Manuals. QW 25 A938 2004] I. Perl, Andras. II. Series.
RC600.A852 2004
616.97'8--dc22

2004000177

To my parents,

Ibolya and Miklos,

and family,

Katalin, Annmarie, Marcel, and Daniel,

for their inspiration, support, and love

in my pursuit of medicine and science

Preface

> "Research is to see what everybody else has seen, and to think what nobody else has thought." — *Albert Szentgyörgyi*

Autoimmunity: Methods and Protocols is intended to serve as a ready-to-use guide to establish and interrogate human and animal models of autoimmune diseases. The first chapter, "Pathogenesis and Spectrum of Autoimmunity," discusses major hypotheses driving this most tantalizing area of research since Paul Ehrlich proposed the concept of autoimmunity in 1900. Considering the great diversity and ever-changing spectrum of autoimmunity, it has not been possible to include models and experimental protocols for each known disorder. Rather, several chapters have been devoted to the most prevalent and complex diseases, such as rheumatoid arthritis, systemic lupus erythematosus, insulin-dependent diabetes mellitus, and multiple sclerosis. The chapters are contributed by laboratories actively using the models presented. Each chapter contains an introductory section that discusses the relevance of the model for a particular disease and for autoimmunity in general.

Part I contains methods and protocols to assess immunological and biochemical pathways relevant for disease pathogenesis. Chapters in this section focus on methods to identify susceptibility genes, intercellular signaling via cytokines, intracellular signaling through the T-cell receptor and signal processing via protein kinases, identification and enumeration of autoantigen-specific T cells and autoantibodies, and the dysregulation of apoptosis and its role in modification of self-antigens. Part II contains protocols to establish and assess inflammatory arthritis, systemic lupus erythematosus, myocarditis, thyroiditis, experimental autoimmune encephalomyelitis, insulin-dependent diabetes mellitus, scleroderma, uveitis, and vitiligo. The methods center on the assessment of genetic, immunological, and biochemical parameters underlying spontaneous or exogenous antigen-induced diseases. Although the individual protocols focus on a specific disease, they can be adapted to investigate additional signaling pathways or pathogenic autoantigens.

Autoimmunity: Methods and Protocols should supplement those laboratory manuals that contain recipes for standard cell and molecular biology and immunology techniques, such as cell culture, gene cloning, sequencing, and amplification by polymerase chain reaction, vector design for the generation of transgenic and knockout animals, flow cytometry, fluorescence microscopy, electrophoresis, and gene and protein microarray methods.

Although these general methods are not described in detail here, they are appropriately referenced in each section.

I am grateful to Professor John Walker for his invitation and help with organizing and formatting this book and to Dr. Paul Phillips for his continued encouragement and support. With both my colleagues in the field and newcomers in mind, step-by-step protocols and detailed troubleshooting guides supplement all chapters. I am grateful to the distinguished authors for the time, expertise, and devotion that made this book possible.

If the reader feels that a particularly relevant disease or model is missing, I should be held responsible. Refining and extracting new meaning from old models and developing new ones is a constantly ongoing process. Therefore, our readers are invited to approach the authors with questions and comments or offer new models and protocols for a future edition.

Andras Perl, *MD, PhD*

Contents

Part II. Animal Models of Autoimmunity

Contributors

Marina Afanasyeva • *Department of Medicine, University of Calgary, Calgary, Alberta, Canada*

Rajeev K. Agarwal • *Laboratory of Immunology, National Eye Institute, National Institutes of Health, Bethesda, MD*

Katalin Banki • *Department of Pathology, State University of New York, Upstate Medical University College of Medicine, Syracuse, NY*

David D. Brand • *Department of Medicine, University of Tennessee Health Sciences Center; Veterans Affairs Medical Center, Memphis, TN*

Livia A. Casciola-Rosen • *Departments of Medicine and Dermatology, The Johns Hopkins University School of Medicine, Baltimore, MD*

Rachel R. Caspi • *Laboratory of Immunology, National Eye Institute, National Institutes of Health, Bethesda, MD*

Arpita Choudhury • *Division of Rheumatology, Department of Medicine, University of Pennsylvania, Philadelphia, PA*

Daniela Čiháková • *Division of Immunology, Department of Pathology, Johns Hopkins Medical Institutions, Baltimore, MD*

Mary K. Crow • *Mary Kirkland Center for Lupus Research, Hospital for Special Surgery, New York, NY*

J. Ludovic Croxford • *Department of Microbiology–Immunology and Interdepartmental Immunobiology Center, Northwestern University Feinberg School of Medicine, Chicago, IL*

George S. Eisenbarth • *Barbara Davis Center for Childhood Diabetes, University of Colorado Health Sciences Center, Denver, CO*

Robert Eisenberg • *Division of Rheumatology, Department of Medicine, University of Pennsylvania, Philadelphia, PA*

DeLisa Fairweather • *Division of Immunology, Department of Pathology, Johns Hopkins Medical Institutions, Baltimore, MD*

Kevin G. Fuller • *Department of Microbiology–Immunology and Interdepartmental Immunobiology Center, Northwestern University Feinberg School of Medicine, Chicago, IL*

Peter Gergely • *Division of Rheumatology, Department of Medicine, State University of New York, Upstate Medical University College of Medicine, Syracuse, NY*

Tibor T. Glant • *Section of Biochemistry and Molecular Biology, Department of Orthopedic Surgery and Department of Biochemistry, Rush University School of Medicine, Chicago, IL*

John B. Harley • *Arthritis and Immunology Program, Oklahoma Medical Research Foundation; Departments of Medicine and Pathology, University of Oklahoma Health Sciences Center, and the Department of Veterans Affairs Medical Center, Oklahoma City, OK*

Laurence M. Howard • *Department of Microbiology–Immunology and Interdepartmental Immunobiology Center, Northwestern University Feinberg School of Medicine, Chicago, IL*

Arthur A. Hurwitz • *Department of Microbiology and Immunology, State University of New York Upstate Medical University, Syracuse, NY; Laboratory of Molecular Immunoregulation, National Cancer Institute, Frederick, MD*

Qingyong Ji • *Department of Microbiology and Immunology, State University of New York Upstate Medical University, Syracuse, NY*

Gary M. Kammer • *Section on Rheumatology and Clinical Immunology, Department of Internal Medicine; Department of Microbiology and Immunology, Wake Forest University Health Sciences, Winston-Salem, NC*

Andrew H. Kang • *Department of Medicine, University of Tennessee Health Sciences Center; Veterans Affairs Medical Center, Memphis, TN*

Jennifer A. Kelly • *Arthritis and Immunology Program, Oklahoma Medical Research Foundation, Oklahoma City, OK*

Islam U. Khan • *Section on Rheumatology and Clinical Immunology, Department of Internal Medicine, Wake Forest University Health Sciences, Winston-Salem, NC*

Kyriakos A. Kirou • *Mary Kirkland Center for Lupus Research, Hospital for Special Surgery, New York, NY*

Sandeep Krishnan • *Department of Cellular Injury, Walter Reed Army Institute of Research, Silver Spring; Department of Medicine, Uniformed Services University of the Health Sciences, Bethesda, MD*

Gabriella Lakos • *Section of Rheumatology, University of Illinois at Chicago College of Medicine, Chicago, IL*

Christina Lee • *Mary Kirkland Center for Lupus Research, Hospital for Special Surgery, New York, NY*

Edwin Liu • *Barbara Davis Center for Childhood Diabetes, University of Colorado Health Sciences Center, Denver, CO*

Clayton Mathews • *Diabetes Institute Division of Immunogenetics, Rangos Research Center, Department of Pediatrics, Children's Hospital of Pittsburgh, University of Pittsburgh, Pittsburgh, PA*

Katalin Mikecz • *Section of Biochemistry and Molecular Biology, Department of Orthopedic Surgery, Department of Biochemistry, Rush University Medical Center, Chicago, IL*

STEPHEN D. MILLER • *Department of Microbiology–Immunology and Interdepartmental Immunobiology Center, Northwestern University Feinberg School of Medicine, Chicago, IL*

MARTHA J. MILTON • *Diabetes Institute Division of Immunogenetics, Rangos Research Center, Department of Pediatrics, Children's Hospital of Pittsburgh, University of Pittsburgh, Pittsburgh, PA*

HIROAKI MORIYAMA • *Barbara Davis Center for Childhood Diabetes, University of Colorado Health Sciences Center, Denver, CO*

GYORGY NAGY • *Division of Rheumatology, Department of Medicine, College of Medicine, Upstate Medical University, State University of New York, Syracuse, NY*

MADHUSOODANA P. NAMBIAR • *Department of Cellular Injury, Walter Reed Army Institute of Research, Silver Spring; Department of Medicine, Uniformed Services University of the Health Sciences, Bethesda, MD*

SWAPAN K. NATH • *Arthritis and Immunology Program, Oklahoma Medical Research Foundation, Oklahoma City, OK*

BRIAN NILAND • *Departments of Medicine, Microbiology, and Immunology, College of Medicine, Upstate Medical University, State University of New York, Syracuse, NY*

JULIE K. OLSON • *Department of Microbiology–Immunology and Interdepartmental Immunobiology Center, Northwestern University Feinberg School of Medicine, Chicago, IL*

STANFORD L. PENG • *Department of Internal Medicine/Rheumatology, Department of Pathology and Immunology, Washington University School of Medicine, St. Louis, MO*

ANDRAS PERL • *Division of Rheumatology, Departments of Medicine and of Microbiology and Immunology, College of Medicine, Upstate Medical University, State University of New York, Syracuse, NY*

JON D. PIGANELLI • *Diabetes Institute Division of Immunogenetics, Rangos Research Center, Department of Pediatrics, Children's Hospital of Pittsburgh, University of Pittsburgh, Pittsburgh, PA*

MICHELLE POULIN • *Diabetes Institute Division of Immunogenetics, Rangos Research Center, Department of Pediatrics, Children's Hospital of Pittsburgh, University of Pittsburgh, Pittsburgh, PA*

FERENC PUSKAS • *Division of Rheumatology, Department of Medicine, College of Medicine, Upstate Medical University, State University of New York, Syracuse, NY*

YUEMING QIAN • *Division of Rheumatology, Department of Medicine, College of Medicine, Upstate Medical University, State University of New York, Syracuse, NY*

PRAVEEN RAO • *Department of Neurology, University of Rochester School of Medicine and Dentistry, Rochester, NY*
DONNA RAY • *Department of Internal Medicine, University of Michigan, Ann Arbor, MI*
BRUCE RICHARDSON • *Department of Internal Medicine, University of Michigan and the Ann Arbor Veteran's Affairs Hospital, Ann Arbor, MI*
KATHRYN M. ROBERTS • *Department of Medicine, The Johns Hopkins University School of Medicine, Baltimore, MD*
NOEL R. ROSE • *Division of Immunology, Department of Pathology, and Feinstone Department of Molecular Microbiology and Immunology, Johns Hopkins Medical Institutions, Baltimore, MD*
ANTONY ROSEN • *Department of Medicine, Cell Biology, and Pathology, The Johns Hopkins University School of Medicine, Baltimore, MD*
EDWARD F. ROSLONIEC • *Veterans Affairs Medical Center and the Departments of Medicine and Pathology, University of Tennessee Health Sciences Center, Memphis, TN*
R. HAL SCOFIELD • *Arthritis and Immunology Program, Oklahoma Medical Research Foundation, Departments of Medicine and Pathology, University of Oklahoma Health Sciences Center; Department of Veterans Affairs Medical Center, Oklahoma City, OK*
BENJAMIN M. SEGAL • *Department of Neurology, University of Rochester School of Medicine and Dentistry, Rochester, NY*
RAJNI B. SHARMA • *Division of Immunology, Department of Pathology, Johns Hopkins Medical Institutions, Baltimore, MD*
SHINSUKE TAKAGAWA • *Section of Rheumatology, University of Illinois at Chicago College of Medicine, Chicago, IL*
GEORGE C. TSOKOS • *Department of Cellular Injury, Walter Reed Army Institute of Research, Silver Spring; Department of Medicine, Uniformed Services University of the Health Sciences, Bethesda, MD*
JOHN VARGA • *Section of Rheumatology, University of Illinois at Chicago College of Medicine, Chicago, IL*
VISHAL G. WARKE • *Department of Cellular Injury, Walter Reed Army Institute of Research, Silver Spring; Department of Medicine, Uniformed Services University of the Health Sciences, Bethesda, MD*
LIPING YU • *Barbara Davis Center for Childhood Diabetes, University of Colorado Health Sciences Center, Denver, CO*
RAYMOND YUNG • *Department of Internal Medicine, University of Michigan and the Ann Arbor Veteran's Affairs Hospital, Ann Arbor, MI*

1

Pathogenesis and Spectrum of Autoimmunity

Andras Perl

Summary

The immune system specifically recognizes and eliminates foreign antigens and thus protects the integrity of the host. During maturation of the immune system, tolerance mechanisms develop that prevent or inhibit potentially harmful reactivities to self-antigens. Autoreactive B and T cells that are generated during immune responses are eliminated by apoptosis in the thymus, lymph nodes, or peripheral circulation or are actively suppressed by regulatory T cells. However, autoreactive cells may survive because of failure of apoptosis or molecular mimicry, that is, presentation and recognition of cryptic epitopes of self-antigens or aberrant lymphokine production. Development of immune responses and tolerance is determined by an interplay of genetic and environmental factors. Autoimmunity is a result of the breakdown of one or more of the mechanisms of immune tolerance.

Key Words: Apoptosis; autoantibodies; autoimmunity; cytokines; molecular mimicry; T-cell signaling.

One of the basic functions of the immune system is to recognize and eliminate foreign antigens specifically and thus protect the integrity of the host. Through rearrangements and somatic mutations of gene segments encoding T- and B-cell receptors and antibody molecules, the immune system acquires tremendous diversity. During maturation of the immune system, recognition of self-antigens plays an important role in shaping the repertoires of immune receptors. Tolerance mechanisms develop that prevent or inhibit potentially harmful reactivities to self-antigens. These self-defense mechanisms are mediated on the levels of central and peripheral tolerance; that is, autoreactive T cells are either eliminated by apoptosis in the thymus, lymph nodes, or peripheral circulation or actively suppressed by regulatory T cells. Likewise, autoreactive B cells are eliminated in the bone marrow or peripheral lymphoid organs. However, immune responses triggered by foreign antigens may be sustained by

From: *Methods in Molecular Medicine, Vol. 102: Autoimmunity: Methods and Protocols*
Edited by: A. Perl © Humana Press Inc., Totowa, NJ

Table 1
Exogenous and Endogenous Factors Involved in Autoimmunity

	Example	Disease	Mechanism	Reference
Exogenous agents				
Virus	Coxsackie	Diabetes	Mimicry	***23***
Bacterium	Klebsiella	Reactive arthritis	Mimicry	***24***
Drug, chemical, ultraviolet light	5-Azacytidine	Lupus	Demethylation	***25,26***
Endogenous agents				
Gene	MHC locus	Thyroiditis	Antigen presentation	***5,27***
	Complement	Lupus	Immune complex formation	***4***
Hormone	Estrogen	Lupus	Gene expression	***28***
Cytokine	Interleukin 10	Lupus	T-cell dysfunction	***18,29***
Transcription factor	NF-κB	Lupus	T-cell dysfunction	***30***
Dysregulated apoptosis	Fas mutation	ALPS	Defective apoptosis	***13,14***
Dysregulated apoptosis	Caspase 10 mutation	ALPS	Defective apoptosis	***15***

NF-κB, nuclear facotr κβ; ALPS, autoimmune lymphoproliferative syndrome.

molecular mimicry (i.e., presentation and recognition of cryptic epitopes of self-antigens). Further downstream, execution of immune responses depends on cooperation of many cell types, cytokines, and intracellular signaling networks. Therefore, autoimmunity represents the end result of the breakdown of one or more of the basic mechanisms of immune tolerance (**Table 1**).

Autoimmunity may occur in normal individuals, with a higher frequency in older people. Infectious diseases often elicit autoreactivities based on similarity between exogenous and self-antigens. Infection-induced autoimmunity usually is self-limited by elimination of the antigen-producing cell or organism. However, self-reactivity may be sustained through molecular mimicry ***(1)*** (i.e., homology between exogenous and endogenous epitopes) and the inability of the immune system to destroy self-reactive B or T cells via apoptosis, anergy, or other regulatory mechanisms. Nevertheless, autoimmunity does not necessarily lead to tissue injury. Autoantibodies, such as rheumatoid factor or antinuclear antibodies occur in more than 5% of normal subjects without ever resulting in rheumatoid arthritis (RA) or systemic lupus erythematosus (SLE), which are characterized by the very presence of such antibody reactivities.

Table 2
Systemic Autoimmune Diseases

Disease	Organ system involvement and immunopathology
SLE	All, primarily joints, skin, blood vessels, serous membranes, kidney, lung, heart; antinuclear antibodies
RA	Joints, blood vessels, serous membranes, lung; anti-immunoglobulin G immunoglobulin M rheumatoid factor
Ankylosing spondylitis	Axial > peripheral joints, uveitis, aortitis
Scleroderma	Skin, blood vessels, gut, lung, heart, kidney
Psoriasis	Skin, joints
Sjögren's syndrome	Salivary and lacrimal glands, pancreas, lung, kidney; antibodies SSA and SSB, lymphocytic infiltration of involved tissues
Dermatomyositis	Skin, muscle, blood vessels
Inflammatory bowel disease	Small and/or large intestine, joint, uvea; perinuclear antineutrophil cytoplasmic antibodies directed to myeloperoxidase
Wegener's granulomatosis	Blood vessel inflammation in kidney, lung, skin; cytoplasmic antineutrophil cytoplasmic antibodies directed to proteinase 3
Goodpasture syndrome	Kidney, lung, antibody to basement membrane
Periarteritis nodosa	Blood vessel inflammation in all tissues (typically kidney, skin, intestines) except lung

SSA, Sjögren syndrome A; SSB, Sjörgen syndrome B.

Autoimmunity can damage nearly every tissue or cell type of the body. The spectrum, severity, and duration of disease vary widely. Depending on the organ systems involved, systemic and organ-specific autoimmune diseases have been delineated. Systemic autoimmune diseases include SLE, RA, scleroderma, Wegener's granulomatosis, Goodpasture syndrome, Sjögren's syndrome, dermatomyositis, psoriasis, ankylosing spondylitis, and inflammatory bowel diseases (**Table 2**).

Although SLE can involve almost any tissue of the body, inflammatory bowel diseases extend to fewer tissues, the gut, the joints, and the eye. Organ-specific diseases include insulin-dependent diabetes mellitus (IDDM), multiple sclerosis (MS), uveitis, thyroiditis, pernicious anemia, autoimmune hemolytic anemia, thrombocytopenia, hepatitis, primary biliary cirrhosis, pemphigus, pemphigoid, and vitiligo (**Table 3**). Individual patients may have more than one autoimmune disorder concurrently and subsequently.

Table 3
Organ-Specific Autoimmune Diseases

Disease	Typical involvement and immunopathology
Insulin-dependent diabetes mellitus	Pancreas; antiinsulin and anti-glutamic acid decarboxylase antibodies
Multiple sclerosis	Central nervous system; antimyelin T-cell and antibody reactivities
Myasthenia gravis	Peripheral nervous system; antibody to acetylcholine receptor
Thyroiditis	Thyroid gland; antithyroid antibodies
Uveitis	Uvea; antibody and T-cell mediated
Pernicious anemia	Stomach; antibody to intrinsic factor required for absorption of vitamin B_{12}
Pemphigus	Skin; antibody to intercellular adhesion molecule desmoglein-3
Pemphigoid	Skin
Vitiligo	Skin
Myocarditis	Heart
Autoimmune hemolytic anemia	Erythrocytes; antibody mediated
Autoimmune thrombocytopenia	Platelets; antibody mediated
Acquired thrombotic thrombopenic purpura	Antibody to von Willebrand factor-cleaving metalloprotease
Primary biliary cirrhosis	Liver; antibody-mediated targeting pyruvate dehydrogenase
Autoimmune hepatitis	Liver; antibody-mediated targeting cytochrome P450

Although the causes of autoimmune diseases have not been defined, independent lines of evidence have implicated environmental factors and genetic determinants of the host ***(2)***. As shown in **Table 1**, polymorphisms of HLA molecules that regulate antigen presentation ***(3)*** and complement deficiency states ***(4)*** have been identified as inherited factors influencing disease susceptibility. Concordance rates for autoimmune diseases such as SLE, IDDM, RA, and MS are approx 25% in monozygotic twins. Alternatively, the discordance rate may be as high as 70% among monozygotic twins ***(5)***, suggesting a significant role for exogenous agents ***(6)***.

The concept of autoimmunity, designated as *horror autotoxicus*, was first proposed by Ehrlich in 1900 ***(7)***. The clonal selection theory and specific elimination of self-reactive "forbidden" clones as a means of preventing autoimmu-

nity was hypothesized by Burnet ***(7)***. The first organ-specific autoimmune disease, experimental thyroiditis, was described by Rose and Witebsky in 1956 ***(8)***.

Rose and Vladutiu were the first to recognize the influence of the major histocompatibility (MHC) gene locus on development of autoimmunity ***(27)***. Similar to the consequences of microbial infections, autoimmune diseases are characterized by polyclonal T-cell expansions and antibody production, suggesting an antigen-driven process ***(1,2)***.

During the past century, tremendous efforts were made to identify self-antigens and infectious agents capable of inducing autoimmunity in humans and animal models. Such studies led to the discovery of disease-specific autoantigens that have become instrumental in clinical diagnosis ***(9)***. As examples, antinuclear antibodies, rheumatoid factor, proteinase 3-specific cytoplasmic antineutrophil cytoplasmic antibodies, antiglomerular basement membrane antibodies, and thyroglobulin antibodies are routinely used to establish a diagnosis of SLE, RA, Wegener's granulomatosis, Goodpasture syndrome, and Hashimoto's thyroiditis, respectively.

Various antigens from tissues targeted by organ-specific autoreactivities have been used to generate useful animal models. Joint cartilage-derived antigens, such as collagen (*see* Chapter 16) and proteoglycan (*see* Chapter 17), can induce inflammatory arthritis in mice. Myelin-derived antigens, myelin basic protein, myelin oligodendrocyte glycoprotein, and proteolipid protein (*see* Chapters 18 and 19), as well as mimicking viral antigens, can trigger encephalomyelitis resembling MS (*see* Chapter 18). Certain animal strains spontaneously develop IDDM, characterized by autoreactivities to pancreas-derived antigens such as insulin or glutamic acid decarboxylase (*see* Chapters 11 and 12). These animal models provide new information on the pathogenesis of autoimmunity: They identify and confirm relevant autoantigens and delineate critical checkpoints of signaling networks that can be targeted for therapeutic interventions.

As an example, tumor necrosis factor (TNF)-α antagonists reduced the severity of collagen-induced arthritis in animal models and became a major breakthrough in the treatment of RA and other types of inflammatory arthritis. Interestingly, TNF-α antagonists enhanced production of antinuclear antibodies and induced flare of lupus and demyelination in patients with MS. Along the same line, TNF-α has been shown to protect against lupus ***(10)*** and experimental allergic encephalomyelitis in animal models ***(11,12)***. Such clinical and experimental observations indicate significant differences in pathogenesis between autoimmune diseases. TNF-α triggers programmed cell death; therefore, its blockade is thought to hinder elimination of autoreactive cells via this mechanism.

Defects in apoptosis underlie the pathology of human autoimmune lymphoproliferative syndromes ***(13–15)*** and animal models of SLE ***(16)*** (**Table 1**). Methods to assess apoptosis are described in Chapters 6 and 7. Development of autoimmunity is also influenced by the cytokine milieu (*see* Chapter 8). Although patients with MS overproduce Th1-type cytokines ***(17)***, lupus is characterized by predominance of Th2 cytokines, such as interleukin 10 ***(18)***. Signaling through the T-cell receptor, adaptor molecules, and kinases is markedly altered in SLE (*see* Chapters 3–6 and 8).

The expression profiles of genes regulating T-cell activation show dramatic changes with respect to healthy donors and other autoimmune patients ***(19)***. Genomewide surveys with microsatellite markers confirmed the importance of the MHC locus and identified additional genome segments that may influence susceptibility to SLE ***(20)***, MS ***(21)***, and IDDM ***(22)***. Microarray analyses have revealed an upregulation of interferon-α-inducible genes, suggestive of infectious etiology and cytokine imbalance in patients with SLE (*see* Chapter 8). Coordinated efforts toward delineating the role of triggering antigens, alterations in signaling networks, and underlying genetic mutations are required to understand pathogenesis and thus design specific interventions to treat each autoimmune disease.

Acknowledgments

This work was supported in part by grants DK 49221 and AI 48079 from the National Institutes of Health, RG-2466 from the National Multiple Sclerosis Society, and the Central New York Community Foundation.

References

1 Oldstone, M. B. A. (1987) Molecular mimicry and autoimmune disease. *Cell* **50,** 819–820.
2 Steinberg, A. D., Gourley, M. F., Klinman, D. M., Tsokos, G. C., Scott, D. E., and Krieg, A. M. (1991) Systemic lupus erythematosus. *Ann. Intern. Med*. **115,** 548–559.
3 Silverstein, A. M. and Rose, N. R. (1997) On the mystique of the immunological self. *Immunol. Rev*. **159,** 197–206.
4. Agnello, V. (1986) Lupus diseases associated with hereditary and acquired deficiencies of complement. *Springer Semin. Immunopathol*. **9,** 183–219.
5 Arnett, F. C. and Reveille, J. D. (1992) Genetics of systemic lupus erythematosus. *Rheum. Dis. Clin. North Am*. **18,** 865–892.
6 Perl, A. (1999) Mechanisms of viral pathogenesis in rheumatic diseases (invited review). *Ann. Rheum. Dis.* **58,** 454–461.
7. Ehrlich, P. (1900) On immunity with special reference to cell life. *Proc. R. Soc. Lond. B Biol. Sci.* **66,** 428–448.
8 Rose, N. R. and Witebsky, E. (1956) Studies on organ specificity. V. Changes in the thyroid glands of rabbits following active immunization with rabbit thyroid extracts. *J. Immunol.* **76,** 417–427.

9. Samter, M., Talmage, D. W., Frank, M. M., Austen, K. F., and Claman, H. N. (1988) *Immunological Diseases*, Little Brown, Boston.
10 Mageed, R. A. and Isenberg, D. A. (2002) Tumour necrosis factor (in systemic lupus erythematosus and anti-DNA autoantibody production. *Lupus* **11,** 850–855.
11 Wang, J., Asensio, V. C., and Campbell, I. L. (2002) Cytokines and chemokines as mediators of protection and injury in the central nervous system assessed in transgenic mice. *Curr. Top. Microbiol. Immunol*. **265,** 23–48.
12 Ghezzi, P. and Mennini, T. (2001) Tumor necrosis factor and motorneuronal degeneration: an open problem. *Neuroimmunomodulation* **9,** 178–182.
13 Fisher, G. H., Rosenberg, F. J., Straus, S. E., Dale, J. K., Middleton, L. A., Lin, A. Y., et al. (1995) Dominant interfering Fas gene mutations impair apoptosis in a human autoimmune lymphoproliferative syndrome. *Cell* **81,** 935–946.
14 Drappa, J., Vaishnaw, A. K., Sullivan, K. E., Chu, J.-L., and Elkon, K. B. (1996) *Fas* gene mutations in the Canale-Smith syndrome, an inherited lymphoproliferative disorder associated with autoimmunity. *N. Engl. J. Med.* **335,** 1643–1649.
15 Wang, J., Zheng, L., Lobito, A., Chan, F. K., Dale, J., Sneller, M., et al. (1999) Inherited human caspase 10 mutations underlie defective lymphocyte and dendritic cell apoptosis in autoimmune lymphoproliferative syndrome type II. *Cell* **98,** 47–58.
16 Cohen, P. L. and Eisenberg, R. A. (1991) *Lpr* and *gld*: single gene models of systemic autoimmunity and lymphoproliferative disease. *Annu. Rev. Immunol.* **9,** 243–269.
17 Clerici, M., Fusi, M. L., Caputo, D., Guerini, F. R., Trabattoni, D., Salvaggio, A., et al. (1999) Immune responses to antigens of human endogenous retroviruses in patients with acute or stable multiple sclerosis. *J. Neuroimmunol.* **99,** 173–182.
18 Georgescu, L., Vakkalanka, R. K., Elkon, K. B., and Crow, M. K. (1997) Interleukin-10 promotes activation-induced cell death of SLE lymphocytes mediated by Fas ligand. *J. Clin. Invest*. **100,** 2622–2633.
19 Kammer, G. M., Perl, A., Richardson, B. C., and Tsokos, G. C. (2002) Abnormal T cell signal transduction in systemic lupus erythematosus. *Arthritis Rheum*. **46,** 1139–1154.
20 Harley, J. B., Moser, K. L., Gaffney, P. M., and Behrens, T. W. (1998) The genetics of human systemic lupus erythematosus. *Curr. Opin. Immunol*. **10,** 690–696.
21 Haines, J. L., Ter-Minassian, M., Bazyk, A., Gusella, J. F., Kim, D. J., Terwedow, H., et al. (1996) A complete genomic screen for multiple sclerosis underscores a role for the major histocompatibility complex. *Nature Genet*. **13,** 469–471.
22 Cox, N. J., Wapelhorst, B., Morrison, V. A., Johnson, L., Pinchuk, L., Spielman, R. S., et al. (2001) Seven regions of the genome show evidence of linkage to type 1 diabetes in a consensus analysis of 767 multiplex families. *Am. J. Hum. Genet*. **69,** 820–830.
23 Tian, J., Lehmann, P. V., and Kaufman, D. L. (1994) T cell cross-reactivity between Coxsackie virus and glutamate decarboxylase is associated with a murine diabetes susceptibility allele. *J. Exp. Med*. **180,** 1979–1984.

24 Baum, H., Davies, H., and Peakman, M. (1996) Molecular mimicry in the MHC: hidden clues to autoimmunity? *Immunol. Today* **17,** 64–70.
25 Richardson, B. C., Strahler, J. R., Pivirotto, T. S., Quddus, J., Bayliss, G. E., Gross, L. A., et al. (1992) Phenotypic and functional similarities between 5-azacytidine-treated T cells and a T-cell subset in patients with active systemic lupus erythematosus. *Arthritis Rheum*. **35,** 647–662.
26 Reap, E. A., Roof, K., Maynor, K., Borrero, M., Booker, J., and Cohen, P. L. (1997) Radiation and stress-induced apoptosis: a role for Fas/Fas ligand interactions. *Proc. Natl. Acad. Sci. U S A* **94,** 5750–5755.
27 Vladutiu, A. O. and Rose, N. R. (1971) Autoimmune murine thyroiditis relation to histocompatibility (H-2) type. *Science* **174,** 1137–1139.
28 Lockshin, M. D. (2002) Sex ratio and rheumatic disease: excerpts from an Institute of Medicine report. *Lupus* **11,** 662–666.
29 Llorente, L., Zou, W., Levy, Y., Richaud-Patin, Y., Wijdenes, J., Alcocer-Varela, J., et al. (1995) Role of interleukin 10 in the B lymphocyte hyperactivity and autoantibody production of human systemic lupus erythematosus. *J. Exp. Med.* **181,** 839–844.
30. Wong, H. K., Kammer, G. M., Dennis, G., and Tsokos, G. C. (1999) Abnormal NF-(B activity in T lymphocytes from patients with systemic lupus erythematosus is associated with decreased p65-RelA protein expression. *J. Immunol*. **163,** 1682–1689.

I

Models of Pathogenesis in Human Autoimmune Disorders

2

Mapping the Systemic Lupus Erythematosus Susceptibility Genes

Swapan K. Nath, Jennifer A. Kelly, John B. Harley, and R. Hal Scofield

Summary

Systemic lupus erythematosus (SLE) is a prototype systemic, autoimmune inflammatory disease that can involve virtually any organ or tissue type. The disease has a strong familial tendency but, like most human illness, has a complex pattern of inheritance that is consistent with multiple susceptibility genes as well as environmental risk factors. Association studies have been performed, especially for the major histocompatibility complex on chromosome 6 and for various complement components. Several large familial studies have begun to report results for genetic linkage. Linkage has been established for many genetic intervals. SLE is a complex clinical illness, and investigation of the genetics of the illness based on clinical manifestations revealed linkages not found without consideration of the phenotype of the disease.

Key Words: Autoantibodies; autoantigens; complement; genetic association; genetic linkage; HLA; systemic lupus erythematosus;

1. Introduction

Systemic lupus erythematosus (SLE) is a complex disease in which immune responses are directed against a multitude of self-antigens. SLE in humans manifests with a diverse array of clinical symptoms that potentially involve multiple organ systems. At least a portion of the pathophysiology is attributed to deposition of immune complexes, which are continuously formed by autoantigens and autoantibodies, in various tissues. Thus, pathogenesis is related to dysregulation of self-reactive B cells. In addition, immune dysfunction of the T lymphocytes involved in the adaptive immune system and elements of the innate immune system, such as complement protein deficiencies, are also involved in disease expression.

From: *Methods in Molecular Medicine, Vol. 102: Autoimmunity: Methods and Protocols*
Edited by: A. Perl © Humana Press Inc., Totowa, NJ

Although SLE is a clinically heterogeneous disease, current guidelines require a set of 4 of 11 American College of Rheumatology criteria for classification of a patient as having SLE ***(1)***; the hallmark feature is the production of autoantibodies against nuclear components. As a result, antinuclear antibody (ANA) testing is very sensitive for the disease, although not highly specific because ANAs are sporadically detected in as much as 2% of the female population over the age of 40 yr as well as in the sera of persons with other diseases.

On the other hand, antibodies to double-stranded DNA (dsDNA) and the Sm protein are very specific for SLE. The overall estimated prevalence in the United States is approx 12–64 cases per 100,000 individuals ***(2,3)***. Significant gender differences are observed in prevalence (female:male = 9:1), age at onset, premorbid conditions, clinical expression, course of illness, response to treatment, and morbid risk. In addition, there are important racial differences in disease manifestations. For example, at least a two- to fourfold higher incidence in non-Caucasian as compared with Caucasian population has been observed ***(4)***.

The familial nature of SLE suggests an underlying genetic susceptibility, but environmental, stochastic, or epigenetic factors must be important because even monozygotic twins are not always concordant for disease. Substantial evidence has shown that the disease clusters in families, with 7–12% increased risk among the first- or second-degree relatives of a proband ***(5)***. An increased concordance rate in identical twins (15–69%) as opposed to dizygotic twins (2–5%) ***(6)*** shows support for genetic basis. The relative risk ratio for the siblings of an affected proband λ_s varies from 20 to 40 ***(7)***. Moreover, the complex pattern of inheritance of SLE suggests multigenic inheritance, requiring interaction of various combinations of contributing genes at multiple loci in individual patients; these combinations are likely to contribute to clinically diverse phenotypes. Finally, various environmental factors, perhaps interacting with specific genes, also may play a significant role in development of SLE.

Often, lupus shows familial cosegregation with other autoimmune diseases, like rheumatoid arthritis, Sjögren's syndrome, or antiphospholipid antibody syndrome. In fact, studies show that 10–20% of lupus probands have at least one first or second-degree relative afflicted with other autoimmune diseases. In a classic study, Bias et al. ***(8)*** defined an "autoimmune phenotype" in lupus pedigrees based on the presence of an autoimmune disease or high titers of autoantibodies (e.g., rheumatoid factors, anti-smooth muscle antibodies, anti-acetylcholin-esterase antibodies, thyroid insufficiency). Bias and coworkers found that the most parsimonious model for the mode of inheritance of this new phenotype was autosomal dominant with variable penetrance (92 and 49% for women and men, respectively). This led to the hypothesis that a single gene confers susceptibility to autoimmunity, and other genes (such as HLA, T-cell

receptors, immunoglobulin allotypes) bestow specificity to the autoimmune phenotype developed.

Becker et al. ***(9)*** compared linkage results from 23 autoimmune or inflammatory disease studies and showed clustering of mapped candidate autoimmune loci to 18 genomic regions, supporting the hypothesis of a possible shared genetic basis. Genes that predispose to SLE are undoubtedly related to key events in pathogenesis and may be involved in the expression of various other autoimmune diseases.

For disorders with a poorly known biochemical basis like SLE, identification of the genes is a prerequisite or key to an increased understanding of the biological basis. Therefore, identification of the genes contributing to susceptibility for SLE will contribute to understanding of the development and pathogenesis of the disease and may lead to novel therapeutic interventions. Such information may be valuable in predicting the course of SLE in individual patients, and this could prove to be an important guide to therapy and monitoring. In addition, genetic screening could be used to identify individuals who are at risk so that they can take advantage of early diagnosis and treatment.

2. Methods for Identifying Genes

The situation of gene discovery in humans changed markedly two decades ago when it was recognized that variations in human DNA could be assayed directly and used as genetic markers in linkage studies ***(10)***. The identification of restriction fragment length polymorphism (RFLP) markers and, subsequently, abundant highly polymorphic short tandem repeat (STR) microsatellite markers ***(11,12)*** led to the mapping and identification of many single-gene, Mendelian diseases.

Such mapping is based on the meiotic mapping process of recombination. Naturally occurring mutations are identified on the basis of their chromosomal location through meiotic events as manifested in families segregating for the disease. Typically, the markers closer to the disease gene show the strongest genotype–phenotype correlations. Markers showing the strongest correlation with disease in families are assumed to be closest to the disease locus. Such a strategy ultimately leads to positional cloning of the culprit gene.

The remarkable success of linkage analysis and positional cloning has generated a strong sense of optimism in identifying genes for a range of common, familial, and non-Mendelian diseases such as SLE. Currently, for complex diseases, two kinds of fundamentally different strategies have been used to identify genetic susceptibility factors: the whole genome search by linkage analysis and the study of candidate genes. In principle, both approaches are very simple.

When screening the whole genome, the objective is to find a genome area in which a disease risk factor is present. This is done by studying the entire

genome with a dense collection of genetic markers, typically 300–400. Then, linkage statistics are calculated either by parametric (penetrance-dependent) or nonparametric allele-sharing (penetrance-independent) model-free methods at each position of the genome. In this way, genomic intervals are identified in which the statistics show a significant deviation from what would be expected under independent assortment.

In contrast to relying on genomewide, evenly spaced linkage study, candidate gene studies focus on genes selected because of an *a priori* hypothesis about the candidate gene's etiological role in the pathogenesis. Although a linkage study analyzes the cosegregation of two parameters (disease and marker) in families, the association study investigates the coexistence (nonindependence) of alleles in individuals. Thus, collection of families is not necessarily needed in this last method.

Although these methods have been relatively successful in identifying some suspected genomic regions, they have not yet been highly successful in identifying genes involved in the pathogenesis of SLE. In the single instance in which a specific disease-causing gene and allele have been identified, information from a knockout mouse phenotype greatly aided the gene discovery process. Lindqvist and colleagues ***(13)*** mapped, confirmed, and localized an SLE susceptibility gene on a chromosome. Genetic knockout of the programmed cell death 1 gene, which lies within the mapped interval, results in an SLE phenotype. Thus, this gene became a high-priority candidate, and a regulatory polymorphism upstream of the coding region of this gene appears to be the sequence predisposing to SLE ***(14)***.

The inability to identify susceptibility genes may be the result of a combination of the following causes. First, SLE varies in severity of symptoms, race, gender, and age at onset, which results in difficulty selecting the best populations to study. Second, SLE can vary in its etiological mechanisms, which might involve various biological pathways. Third, SLE, like other complex diseases, is more likely caused by several genes with small overall contributions and relative risks. Because of these factors, researchers now apply another approach, which is an association study based on a candidate gene approach.

2.1. Sources of Complexity and Clinical Heterogeneity in SLE

Clearly, SLE is a clinically complex disease such that two patients may share no common feature and yet still be diagnosed as having the illness. This fact is exemplified in the classification criteria, for which presence of any 4 of 11 criteria allows classification as SLE ***(1)***. SLE may involve almost any organ system with the mucocutaneus, musculoskeletal, neurological, hematological, immunological, cardiovascular, pulmonary, and renal systems all included in the criteria. Thus, the pattern of manifestations varies greatly between indi-

viduals, making the disease as clinically diverse as any single entity in modern medicine. So, it can easily be imagined that the complex clinical picture will have an impact on and produce an equally complex genetic etiology.

In general, SLE may range from not much more than a nuisance to an immediately life-threatening illness. Mortality in SLE is associated with several disease features, including thrombocytopenia most prominently ***(15,16)***. Nonetheless, prediction of severity of disease or mortality in an individual remains virtually impossible. Thus, the disease has marked heterogeneity regarding its severity as assessed by mortality.

Another area in which there is great heterogeneity in SLE is the immunological manifestations. Although almost every patient has ANAs, the specificity of these autoantibodies varies widely. There are four prominent protein autoantigen specificities. Anti-Ro (or SSA) is found in the sera of about 40% of patients with SLE, some of whom also have anti-La (or SSB), which is never found without the simultaneous presence of anti-Ro. An analogous situation exists for anti-RNP and anti-Sm. Anti-RNP is found in the sera of about 40–50% of patients with SLE, and anti-Sm is found in 5–20% of sera but is always found in conjunction with anti-RNP. There are many clinical, immunological, and immunogenetic associations for each of these autoantibodies. For example, anti-Ro is strongly associated with genetic deficiency of early complement components, such as C2 and C4 (reviewed in **ref. *17***), and is associated with neutropenia ***(18)***. Of course, the other prominent autoantibody system in SLE is that binding native (double-stranded) DNA. The presence of anti-dsDNA is associated with kidney disease.

Overall, the large variety of clinical/immunological changes noted and the variability seen across subjects imply that SLE is an etiologically heterogeneous disease phenotype. In addition, the number of major anomalies observed in different body organs or systems demonstrates a very likely complex etiology for SLE. Because SLE is an extremely complex disease, genetic susceptibility to SLE is likely to be polygenic, involving several genes of low penetrance with allelic (different variants within the same gene) as well as locus (genetic variants in separate genes) heterogeneity and complicated epitasis, gene–environmental interactions.

2.2. Replication and Its Importance

A handful of susceptibility genes for common and complex diseases such as *BRCA1* and *BRCA2* in breast cancer ***(19,20)***, *Calpain10* in NIDDM ***(21)***, *NOD2* in Crohn's disease ***(22,23)***, *Neuregulin 1* in schizophrenia ***(24)***, and *ADAM33* in asthma ***(25)*** have been identified. Despite these successes, linkage studies of complex diseases have been difficult to replicate. A review of the linkage findings of 31 complex human diseases based on whole genome scan concluded

that genetic localization of most susceptibility loci is still imprecise and difficult to replicate ***(26)***.

This difficulty is, in part, because of the inability to measure the precise underlying phenotype, small sample sizes, genetic heterogeneity, inaccurate genetic model, and statistical methods employed in analysis. In another similar review, Hirschhorn et al. ***(27)*** reviewed genetic association studies and concluded that only a few were reproducible. Success has been elusive because almost all complex diseases are the combination of multiple genes and environmental factors. Unlike the so-called monogenic diseases, there is no "smoking gun," that is, associated disease mutations obviously deleterious to protein function. Instead, there are likely to be alleles with subtle functional changes that are neither necessary nor sufficient to cause disease.

Replication of initial linkage signals from independent samples is considered an important and crucial step toward distinguishing between true positives and false positives ***(28)***. The basis of all scientific research is hypothesis testing and validation of results by independent researchers or data. Independent replication is typically viewed as the *sine qua non* for accepting a hypothesis, but this is an extremely difficult issue in genetic studies for a complex disease, especially when genetic effects are weak and possibly context dependent (e.g., incidence may vary by sex, ethnicity, or precision of diagnosis), even with a reasonably large sample ***(29,30)***.

2.3. Application of Association to SLE

Association studies are used to localize genetic effects and identify differences in the distribution of allele frequencies according to the phenotypic status within a population. To date, there have been numerous candidate genes studied with SLE. Efforts have focused on genes identified based on some theoretical or actual knowledge of disease mechanisms associated with biologic pathways implicated in SLE. Because the loss of immune tolerance to self-components is the basis of disease etiology, many genes encoding proteins with significant functions in the immune system have been considered as candidates. Several reviews ***(31–34)*** provide a comprehensive catalog of potential candidate genes. An updated list of candidate genes showing significant association with SLE is given in **Table 1**.

Evidence supporting associations has been observed for numerous genes and genomic regions, including within the major histocompatibility complex in both class II and class III as well as for several cell surface immunoglobulin receptors, among others. However, there has been no, or very few, consistent replication of positive findings for any of these disease genes. There is a potentially good explanation for this phenomenon. Inconsistencies in these genetic association studies may stem from reliance on the population genetic property

Table 1
Association Studies in SLE

Chromosome	Gene	Reference
1p36	C1q	***44***
1q22-23	FcGR2A	***45***
1q22-23	FcGR3A	***46***
1q22-23	TcR-ζ	***47–49***
1q31-32	IL10	***50–52***
2q33	CTLA-4	***53***
6p21	HLA-DR3, HLA-DR2	***54,55***
6p21	TNF-α	***56–58***
6p21, 19p13, 6p21	C2, C3, C4	***59***
10q11.2-q21	MBP	***60–62***
10q24, 1q23	FAS/FASL	***63***
18q21	Bcl-2	***50***

of linkage disequilibrium to detect an association between what is actually a "marker" polymorphism in a candidate gene and the unobserved true SLE-predisposing variant. Moreover, the complexity of SLE demands studies that have very strong statistical power. The sample sizes of most of the candidate gene studies to date have been inadequate to make conclusive statements about the role of the specific alleles in a complex clinical phenotype.

Although population-based association methodology is statistically powerful, similar to other disease association studies, false-positive results may occur if cases and controls are not drawn from the same population with a matched genetic history. In addition, modest genetic effects and allelic heterogeneity contribute to difficulty in replication and confirmation of the candidate genes implicated in SLE in the last several years.

2.4. Application of Linkage to SLE

There are several different study designs with variable ascertainment approaches that have been used for genomewide scan to identify novel susceptibility loci for SLE. Some of the study designs involve (a) sibling pairs who may or may not have parents available or (b) small and large pedigrees with several generations. Numerous genome scans have been made by the four major scientific groups (located in California, Oklahoma, and Minnesota in the United States and in Sweden), revealing many loci spread across the genome (reviewed in **refs.** ***33*** and ***34***). There are seven major cytogenetic locations, which show significant evidence of linkage to SLE based on the recommended criteria

Table 2
Different Studies for Whole-Genome Scan for Finding SLE Susceptibility Loci

Study center	Study design	Number of families	Major ethnicity (%)	Major linkage findings	Reference
OMRF 1	Extended pedigrees	94	Caucasian (58), African American (33)	1q23, 1q25, 13q32, 20q13	***64***
OMRF 2	Extended pedigrees	126	Caucasian (63), African American (27)	4p16-16, 1q22-24	***65***
UMN 1	Sibpairs	105	Caucasian (80), Hispanic (8), African American (5)	6p11-21, 16q13, 14q21, 20p12	***66***
UMN 2	Sibpairs	82	Caucasian (78), African American (15), Hispanic (6)	7p22, 7q21, 10p13, 7q36	***67***
UMN 1 + 2	Sibpairs	187	Caucasian (79), African American (10), Hispanic (7)	6p11-12, 16q13, 2p15	***67***
USC	Extended pedigrees	80	Caucasian (46), Hispanic (54)	1q43	***68***
Uppsala	Extended pedigrees	17	Caucasian (100)	2q37, 4p15-13, 19p13, 19q13	***13***

OMRF, Oklahoma Medical Research Foundation; USC, University of Southern California; UMN, University of Minnesota; Uppsaella, Uppsala University, Sweden.

for genome scan. These key regions, along with several suggested regions identified by at least two independent groups, are summarized in **Table 2** and **Fig. 1**.

However, for the reasons discussed, linkages to many loci have not been replicated across different population groups and studies, although replication in SLE may be better than that in many other genetically complex human diseases (*see* **ref. *34*** for complete details of these data). Thus far, genomewide scanning has led to the identification of only one susceptibility gene for SLE, the programmed cell death 1 gene (PDCD1, also called PD-1) ***(14)***.

2.4.1. Pedigree Stratification Strategy

As discussed, SLE is a complex autoimmune disease with a definite genetic predisposition. However, the exploration of SLE genetics is in its infancy. SLE is an extremely complicated clinical illness with a wide range of manifestations. Clinical manifestations of SLE can be very diverse, with glomerulonephritis, dermatitis, thrombosis, vasculitis, seizures, arthritis, hemolytic anemia, and thrombocytopenia counted among the disease's manifestations. Consequently, the variation between patients is incredible. Indeed, it is possible to have two patients afflicted with SLE who satisfy the classification criteria three different ways with no features in common. This degree of clinical heterogeneity may be because of the involvement of multiple major and modifier genes. Thus far, the genome scans have been performed using a general SLE phenotype.

As an alternative, a set of "etiologic classes" could be considered, reflecting different genes or interactive combinations resulting in SLE for particular subsets of individuals or families (the "pedigree stratification approach"). Detection of a main effect will depend on the relative proportion of individuals carrying a particular genetic variant (or interactive combination that includes that gene) among the individuals studied. As this proportion is likely to fluctuate between data sets, it is unlikely that a particular linkage finding could be replicated in many other data sets, even if the same underlying model were at play. This is because the combination of families from different "classes" in the same linkage or association study will reduce the ability to detect the effects of any particular gene. The well-known example is the BCR1 gene, found only when early-onset breast cancer was considered among families that also had ovarian cancer.

The strategy of using pedigree stratification as a way to discover linkage effects has only been pursued by our Oklahoma group. We have taken the advantage of a pedigree stratification strategy from our huge collection of pedigrees with relevant clinical and medical information available for each individual, especially for the patients with SLE. Therefore, the extraordinary clinical heterogeneity in lupus is consistent with this phenotype as a treasure trove of genetic linkages based on stratifying pedigrees by clinical or demographic features. The rationale behind the subgrouping of the SLE families with a common clinical feature is to make the SLE families more genetically homogeneous. It was anticipated that, regardless of the actual number of genes involved in SLE, decreasing sample heterogeneity by subgrouping families based on race and common associated traits would increase the likelihood of identifying genes for SLE. Although this approach has many advantages, the major disadvantage is the reduced sample size after phenotype stratification, which urgently requires independent verification of the findings.

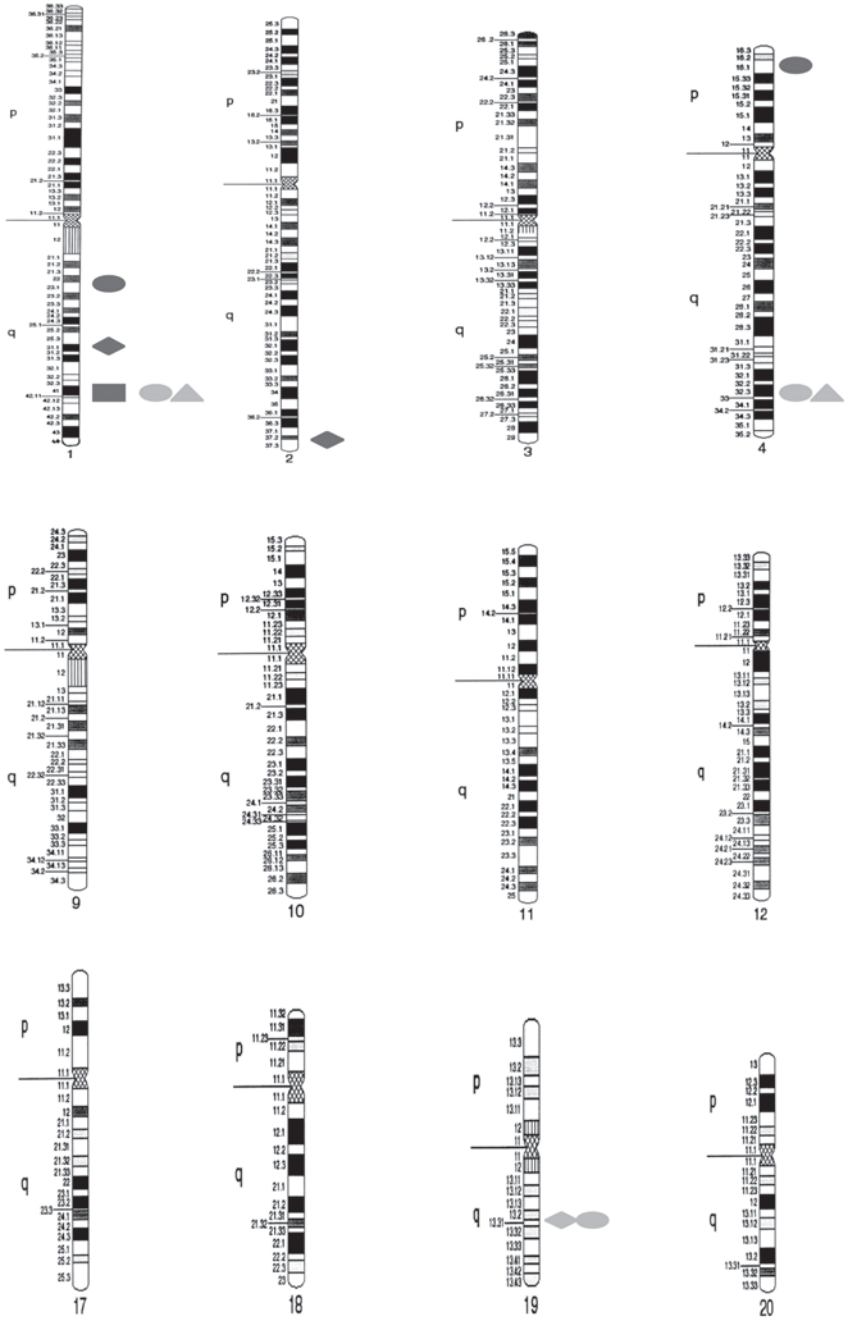
p
q
1
2
3
4
9
10
11
12
17
18
19
20

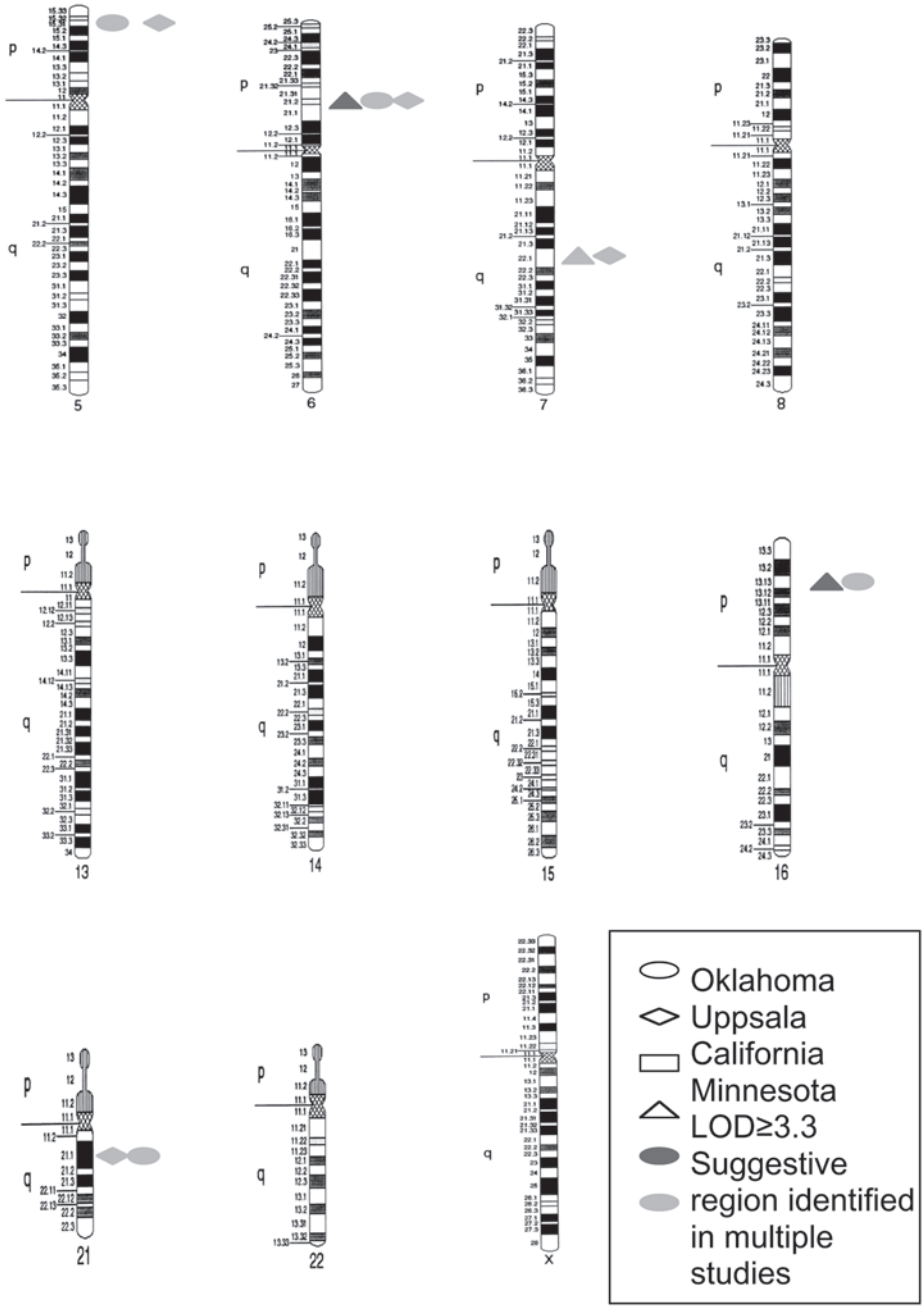

Fig. 1. Several groups have performed independent genomewide linkage studies. Results established and confirmed, or with suggestive conformation, are shown by chromosomal location. Oklahoma, Oklahoma Medical Research Foundation; Uppsala, Uppsala University, Sweden; California, University of Southern California; Minnesota, University of Minnesota.

2.4.2. Effect of Stratification

Because we are using a pedigree stratification strategy and dealing with a very low number of families, there is always a chance for false-positive results. Here, we have used an *ad hoc* criterion to adjust the critical value for declaring the significance of a linkage. For example, we performed the linkage analyses on a subset from our total pedigree collection, in which pedigrees were ascertained by the presence or absence of a certain phenotype (e.g., rheumatoid arthritis positive or negative, although study phenotype for linkage was maintained as SLE), and six different parametric models (based on different penetrances because the true model is unknown) along with a nonparametric model were tested in initial genome screen so that several genome scans were performed. This is a case of a multiple testing problem in which 14 [2 × (6 + 1)] tests were performed.

To assess the significance of any linkage findings, we may use two types of experimental solutions. First, we took a simulation-based approach. We randomly selected *n* (number of pedigrees used for subset analysis) pedigrees from the total available pedigrees 10,000 times (sampling with replacement) and calculated the logarithmic odds (LOD) score at the peak marker for each resampled set of *n* to determine an empirical distribution of LOD scores. Therefore, this gives an empirical *p* value for our original *n* selected pedigrees from the observed LOD score distribution.

Second, we have used an *ad hoc* correction designed to maintain the overall genomewide significance level (5% level) to detect the significant linkage by raising the LOD score limit to 4.4. This is calculated as $LOD_{(new)} = LOD_{(conv)} + \log_{10}(\#test)$ ***(35,36)***, where $LOD_{(conv)}$ is the conventional LOD score to be significant at 3.3. To date, we have identified many genomic regions with high statistical significance that may harbor genes predisposing to SLE. Some of the most convincing linkage results (**Table 3**) have been found by subgrouping the SLE families based on a specific autoimmune feature, for example, thrombocytopenia, hemolytic anemia, or diagnosis of rheumatoid arthritis.

3. Discussion and Future Directions

We anticipate that family-based classical linkage analysis followed by the association-based positional cloning approach will continue to advance the understanding of the biology of SLE disease phenotypes by identifying the underlying susceptibility genes. The availability of the human genome sequence, as well as that of model organisms, should expedite this effort. The full-scale analysis of genetic variation of genes in regions linked to disease will require the development of cost-effective, high-throughput single-nucleotide polymorphism genotyping. Considering the present advancement in the field, these advanced technologies and appropriate and powerful study designs will bring success to SLE genetics.

Table 3
Convincing Linkage Results Published (Exceeding Lander-Kruglyak Significance and/or Our Ad Hoc Criteria) With Lupus From Oklahoma Pedigree Collection Based on Pedigree Stratification Strategy

Region	Marker	Race	No. of pedigrees	Phenotype	LOD/ *p* value	Reference
2q34-35	D2s1384-D2s434	AA	40	Renal	1×10^{-6}	***68***
4p16-15	D4s3007	EA	23	Neuropsychiatric	5.19	***69***
5p15.3	D5s2505	EA	14	Rheumatoid arthritis	6.9	***70***
10q22.3	D10s2470	EA	31	Renal	8×10^{-7}	***68***
11p13	D11s1392	AA	13	Thrombocytopenia	5.72	***16***
11q14	D11S2002	AA	16	Hemolytic anemia	4.70	***71***
11q14	D11S2002	AA	12	Nucleolar ANA	5.62	***72***
17p13	D17s974-D17s1298	EA	16	Vitiligo	3×10^{-5}	***73***
19p13.3	D19s714	EA	37	dsDNA	4.93	***74***

AA, African-American; EA, European-American.

As discussed here, individuals affected with SLE are extraordinarily different from one another by clinical and laboratory measures. This variation may have a genetic basis; if so, it is advantageous to incorporate measures of between-family clinical variability as covariates in a genetic linkage analysis of affected relative pairs to allow for locus heterogeneity. This approach was applied to genome scan marker data from the Oklahoma Medical Research Foundation and identified some new genetic linkage for SLE ***(37)***. So, allowing for locus heterogeneity through the incorporation of covariates in linkage analysis is a useful way to dissect the genetic contributions to SLE and uncover new genetic effects. A few other variants of this method have been developed that take into account the locus heterogeneity measured by covariates, thereby allowing the discovery of evidence for linkage that might otherwise be obscured ***(38–40)***.

It is estimated that the human genome contains approx 30,000 genes. It seems likely that one day there will be the capacity to assess each individual gene and its significance to SLE in a very inexpensive way. Finding the predisposing genes may then be less difficult than it is today. But, the major challenge will be in understanding the biology and characterization of the genetic mechanisms responsible for SLE susceptibility. Consequently, a significant amount of time will be required to understand the biology of many of the real genetic effects now being discovered. For example, HLA-B27 and its significant association with ankylosing spondylitis have been known for 30 yr ***(41)***, yet the biology, disease mechanism, and why the association exists are not understood.

The DNA-based approach is also not without its shortcomings. This is particularly apparent when complex diseases like SLE are considered, for which the disease phenotype is more likely influenced by many different genes together with a modifying effect of the environment. These gene–gene and gene–environment interactions that combine to cause the disease complicate the interpretation of the data generated from family-based linkage and association studies.

As an alternative to this, an RNA-based approach could also be used to identify the important genes that are responsible for the development of the complex phenotype for SLE. By comparing gene expression in normal and disease states, differentially expressed genes are identified and may represent candidate genes for further investigation. For example, this technology has identified the *Nba2*, a murine SLE susceptibility locus ***(42)***. The use of gene expression arrays in human SLE has identified a pattern of interferon-inducible gene expression signature ***(43)***. So, this new approach will likely complement the DNA-based approach and further advance the knowledge about SLE biology.

Acknowledgments

This work was supported in part by grants from the National Institutes of Health to J. B. Harley, R. H. Scofield, and S. K. Nath as well a contract to J. B. Harley.

References

1 Tan, E. M., Cohen, A. S., Fries, J. F., Masi, A. T., McShane, D. J., Rothfield, N. F., et al. (1982) The 1982 revised criteria for the classification of systemic lupus erythematosus. *Arthritis Rheum.* **25,** 1271–1277.

2. Hochberg, M. C. (1997) The epidemiology of systemic lupus erythematosus, in *Dubois' Lupus Erythematosus* (Wallace, D. J., Hahn, B. H., eds.), Williams and Wilkins, Baltimore, MD, pp. 49–65.

3 Lawrence, R. C., Helmick, C. G., Arnett, F. C., Deyo, R. A., Felson, D. T., Giannini, E. H., et al. (1998) Estimates of the prevalence of arthritis and selected musculoskeletal disorders in the United States. *Arthritis Rheum*. **41,** 778–799.

4 Petri, M. (1998) The effect of race on incidence and clinical course in systemic lupus erythematosus: the Hopkins Lupus Cohort. *J. Am. Med. Womens Assoc.* **53,** 9–16.

5 Vyse, T. J. and Todd, J. A. (1996) Genetic analysis of autoimmune disease. *Cell* **85,** 311–318.

6 Deapen, D., Escalante, A., Weinrib, L., Horwitz, D., Bachman, B., Roy-Burman, P., et al. (1992) A revised estimate of twin concordance in systemic lupus erythematosus. *Arthritis Rheum.* **35,** 311–318.

7 Wandstrat, A. and Wakeland, E. (2001) The genetics of complex autoimmune diseases: non-MHC susceptibility genes. *Nat. Immunol*. **2,** 802–809.

8 Bias, W. B., Reveille, J. D., Beaty, T. H., Meyers, D. H., and Arnett, F. C. (1986) Evidence that autoimmunity in man is a Mendelian dominant trait. *Am. J. Hum. Genet*. **39,** 584–602.

9 Becker, K. G., Simon, R. M., Bailey-Wilson, J. E., Freidlin, B., Biddison, W. E., McFarland, H. F., et al. (1998) Clustering of non-major histocompatibility complex susceptibility candidate loci in human autoimmune diseases. *Proc. Natl. Acad. Sci. U S A* **95,** 9979–9984.

10 Botstein, D., White, R. L., Skolnick, M., and Davis, R. W. (1980) Construction of a genetic linkage map in man using restriction fragment length polymorphisms. *Am. J. Hum. Genet.* **32,** 314–331.

11 Weber, J. L. and May, P. E. (1989) Abundant class of human DNA polymorphisms which can be typed using the polymerase chain reaction. *Am. J. Hum. Genet.* **44,** 388–396.

12 Litt, M. and Luty, J. A. (1989) A hypervariable microsatellite revealed by in vitro amplification of a dinucleotide repeat within the cardiac muscle actin gene. *Am. J. Hum. Genet.* **44,** 397–401.

13 Lindqvist, A. K., Steinsson, K., Johanneson, B., Kristjansdottir, H., Arnasson, A., Grondal, G., et al. (2000) A susceptibility locus for human systematic lupus erythematosus (hSLE1) on chromosome 2q. *J. Autoimmun.* **14,** 169–178.

14 Prokunina, L., Castillejo-Lopez, C., Oberg, F., Gunnarsson, I., Berg, L., Magnusson, V., et al. (2202) A regulatory polymorphism in PDCD1 is associated with susceptibility to systemic lupus erythematosus in humans. *Nature Genet.* **32,** 666–669.

15 Reveille, J. D., Bartolucci, A., and Alarcon, G. S. (1990) Prognosis in systemic lupus erythematosus. Negative impact of increasing age at onset, black race, and thrombocytopenia, as well as causes of death. *Arthritis Rheum.* **33,** 37–48.

16 Scofield, R. H., Bruner, G. R., Kelly, J. A., Kilpatrick, J., Bacino, D., Nath, S. K., et al. (2003) Thrombocytopenia identifies a severe familial phenotype of systemic lupus erythematosus and reveals genetic linkages at 1q22 and 11p13. *Blood* **101,** 992–997.

17 Walport, M. J. (2002) Complement and systemic lupus erythematosus. *Arthritis Res.* **4(Suppl. 3),** S279–S293.

18 Kurien, B. T., Newland, J., Paczkowski, C., Moore, K. L., and Scofield, R. H. (2000) Association of neutropenia in systemic lupus erythematosus with anti-Ro and binding of an immunologically crossreactive neutrophil membrane antigen. *Clin Exp Immunol.* **120,** 209–217.

19 Miki, Y., Swensen, J., Shattuck-Eidens, D., Futreal, P. A., Harshman, K., Tavtigian, S., et al. (1994) A strong candidate for the breast and ovarian cancer susceptibility gene *BRCA1*. *Science* **266,** 66–71.

20 Wooster, R., Bignell, G., Lancaster, J., Swift, S., Seal, S., Mangion, J., et al. (1995) Identification of the breast cancer susceptibility gene *BRCA2*. *Nature* **378,** 789–792.

21 Horikawa, Y., Oda, N., Cox, N. J., Li, X., Orho-Melander, M., Hara, M., Hinokio, Y., et al. (2000) Genetic variation in the gene encoding calpain-10 is associated with type 2 diabetes mellitus. *Nat Genet.* **26,** 163–175.
22 Hugot, J. P., Chamaillard, M., Zouali, H., Lesage, S., Cezard, J. P., Belaiche, J., et al. (2001) Association of NOD2 leucine-rich repeat variants with susceptibility to Crohn's disease. *Nature* **411,** 599–603.
23 Ogura, Y., Bonen, D. K., Inohara, N., Nicolae, D. L., Chen, F. F., Ramos, R., et al. (2001) A frameshift mutation in NOD2 associated with susceptibility to Crohn's disease. *Nature* **411,** 603–606.
24 Stefansson, H., Sigurdsson, E., Steinthorsdottir, V., Bjornsdottir, S., Sigmundsson, T., Ghosh, S., et al. (2002) Neuregulin 1 and susceptibility to schizophrenia. *Am J Hum Genet.* **71,** 877–892.
25 Van Eerdewegh, P., Little, R. D., Dupuis, J., Del Mastro, R. G., Falls, K., et al. (2002) Association of the ADAM33 gene with asthma and bronchial hyperresponsiveness. *Nature* **418,** 426–430.
26 Altmuller, J., Palmer, L. J., Fischer, G., Scherb, H., and Wjst, M. (2001) Genomewide scans of complex human diseases: true linkage is hard to find. *Am J Hum Genet.* **69,** 936–950.
27 Hirschhorn, J. N., Lohmueller, K., Byrne, E., and Hirschhorn, K. (2002) A comprehensive review of genetic association studies. *Genet Med.* **4,** 45–61.
28 Lander, E. S. and Kriglyak, L. (1995) Genetic dissection of complex traits: guidelines for interpreting and reporting linkage results. *Nat Genet.* **11,** 241–247.
29 Risch, N. and Merikangas, K. (1996) The future of genetic studies of complex human diseases. *Science* **273,** 1,516,151–1,516,157.
30. Risch, N. (2000) Searching for genes in complex diseases: lessons from systemic lupus erythematosus. *J. Clin. Invest.* **105,** 1503–1506.
31 Schur, P. H. (1995) Genetics of systemic lupus erythematosus. *Lupus* **4,** 425–437.
32 Mohan, C. (2001) Murine lupus genetics: lessons learned. *Curr. Opin. Rheumatol.* **13,** 352–360.
33. Johanneson, B. and Alarcon-Riquelme, M. E. (2001) An update on the genetics of systemic lupus erythematosus. *Israel Med Assoc J.* **3,** 88–93.
34 Kelly, J. A., Moser, K. L., and Harley, J. B. (2002) The genetics of systemic lupus erythematosus: putting the pieces together. *Genes Immun.* **3 (Suppl. 1),** S71–S85.
35. Kidd, K. K. and Ott, J. (1984) Power and sample size in linkage studies. *Cytogenet. Cell Genet.* **37,** 510–511.
36. Ott, J. (1999) *Analysis of Human Genetic Linkage*, 3rd ed., Johns Hopkins University Press, Baltimore, MD.
37 Olson, J. M., Song, Y., Dudek, D. M., Moser, K. L., Kelly, J. A., Bruner, G. R., et al. (2002) A genome screen of systemic lupus erythematosus using affected-relative-pair linkage analysis with covariates demonstrates genetic heterogeneity. *Genes Immun.* **3(Suppl. 1),** S5–S12.
38 Rice, J. P., Rochberg, N., Neuman, R. J., Saccone, N. L., Liu, K. Y., Zhang, X., et al. (1999) Covariates in linkage analysis. *Genet Epidemiol.* **17(Suppl. 1),** S691–S695.

39 Alcais, A. and Abel, L. (2001) Incorporation of covariates in multipoint model-free linkage analysis of binary traits: how important are unaffecteds? *Eur. J. Hum. Genet.* **9,** 613–620.
40 Glidden, D. V., Liang, K. Y., Chiu, Y. F., and Pulver, A. E. (2003) Multipoint affected sibpair linkage methods for localizing susceptibility genes of complex diseases. *Genet Epidemiol.* **24,** 107–117.
41 Brewerton, D. A., Hart, F. D., Nicholls, A., Caffrey, M., James, D. C., and Sturrock, R. D. (1973) Ankylosing spondylitis and HL-A 27. *Lancet* **1(7809),** 904–907.
42 Wither, J. E., Paterson, A. D., and Vukusic, B. (2000) Genetic dissection of B cell traits in New Zealand black mice. The expanded population of B cells expressing up-regulated costimulatory molecules shows linkage to Nba2. *Eur. J. Immunol.* **30,** 356–365.
43 Baechler, E. C., Batliwalla, F. M., Karypis, G., et al. (2003) Interferon-inducible gene expression signature in peripheral blood cells of patients with severe lupus. *Proc. Natl. Acad. Sci. U. S. A.* **100,** 2610–2615.
44 Slingsby, J. H., Norsworthy, P., Pearce, G., Vaishnaw, A. K., Issler, H., Morley, B. J., and Walport, M. J. (1996) Homozygous hereditary C1q deficiency and systemic lupus erythematosus. A new family and the molecular basis of C1q deficiency in three families. *Arthritis Rheum.* **39,** 663–670.
45 Salmon, J. E., Millard, S., Schachter, L. A., Arnett, F. C., Ginzler, E. M., and Gourley, M. F., et al. (1996) Fc gamma RIIA alleles are heritable risk factors for lupus nephritis in African Americans. *J. Clin. Invest.* **97,** 1348–1354.
46. Wu, J., Edberg, J. C., Redecha, P. B., Bansal, V., Guyre, P. M., Coleman, K., et al. (1997) A novel polymorphism of FcgammaRIIIa (CD16) alters receptor function and predisposes to autoimmune disease. *J. Clin. Invest.* **100,** 1059–1070.
47. Liossis, S. N., Ding, X. Z., Dennis, G. J., and Tsokos, G. C. (1998) Altered pattern of TCR/CD3-mediated protein-tyrosyl phosphorylation in T cells from patients with systemic lupus erythematosus. Deficient expression of the T cell receptor zeta chain. *J. Clin. Invest.* **101,** 1448–1457.
48. Vassilopoulos, D., Kovacs, B., and Tsokos, G. C. (1995) TCR/CD3 complex-mediated signal transduction pathway in T cells and T cell lines from patients with systemic lupus erythematosus. *J. Immunol.* **155,** 2269–2281.
49. Tebib, J. G., Alcocer-Varela, J., Alarcon-Segovia, D., and Schur, P. H. (1990) Association between a T cell receptor restriction fragment length polymorphism and systemic lupus erythematosus. *J. Clin. Invest.* **86,** 1961–1967.
50. Llorente, L., Richaud-Patin, Y., Couderc, J., Alarcon-Segovia, D., Ruiz-Soto, R., Alcocer-Castillejos, N., Alcocer-Varela, J., et al. (1997) Dysregulation of interleukin-10 production in relatives of patients with systemic lupus erythematosus. *Arthritis Rheum.* **40,** 1429–1435.
51. Llorente, L., Zou, W., Levy, Y., Richaud-Patin, Y., Wijdenes, J., Alcocer-Varela, J., et al. (1995) Role of interleukin 10 in the B lymphocyte hyperactivity and autoantibody production of human systemic lupus erythematosus. *J. Exp. Med.* **181,** 839–844.
52. Mehrian, R., Quismorio, F. P., Jr., Strassmann, G., Stimmler, M. M., Horwitz, D. A., Kitridou, R. C., et al. (1998) Synergistic effect between IL-10 and bcl-2 geno-

types in determining susceptibility to systemic lupus erythematosus. *Arthritis Rheum.* **41,** 596–602.
53. Ahmed, S., Ihara, K., Kanemitsu, S., Nakashima, H., Otsuka, T., Tsuzaka, K., et al. (2001) Association of CTLA-4 but not CD28 gene polymorphisms with systemic lupus erythematosus in the Japanese population. *Rheumatology* **40,** 662–667.
54. Reinersten, J. L., Klippel, J. H., Johnson, A. H., Steinberg, A. D., Decker, J. L., and Mann, D. L. (1982) Family studies of B lymphocyte alloantigens in systemic lupus erythematosus. *J. Rheumatol.* **9,** 253–262.
55. Arnett, F. C. (1985) HLA and genetic predisposition to lupus erythematosus and other dermatologic disorders. *J. Am. Acad. Dermatol.* **13,** 472–481.
56. Fugger, L., Morling, N., Ryder, L. P., Georgsen, J., Jakobsen, B. K., Svejgaard, A., et al. (1989) NcoI restriction fragment length polymorphism (RFLP) of the tumor necrosis factor (TNF a) region in four autoimmune diseases. *Tissue Antigens* **34,** 17–22.
57. Sullivan, K. E., Wooten, C., Schmeckpeper, B. J., Goldman, D., and Petri, M. A. (1997) A promoter polymorphism of tumor necrosis factor alpha associated with systemic lupus erythematosus in African-Americans. *Arthritis Rheum.* **40,** 2207–2211.
58. Wilson, A. G., Gordon, C., di Giovine, F. S., de Vries, N., van de Putte, L. B., Emery, P., et al. (1994) A genetic association between systemic lupus erythematosus and tumor necrosis factor alpha. *Eur. J. Immunol.* **24,** 191–195.
59. Arnett, F. C. (1997) In *Dubois' Lupus Erythematosus* (Wallace, D. J., Hahn, B. H., eds.), Williams and Wilkins, Baltimore, MD.
60. Davies, E. J., Snowden, N., Hillarby, M. C., Carthy, D., Grennan, D. M., Thomson, W., et al. (1995) Mannose-binding protein gene polymorphism in systemic lupus erythematosus. *Arthritis Rheum.* **38,** 110–114.
61. Ip, W. K., Chan, S. Y., Lau, C. S., and Lau, Y. L. (1998) Association of systemic lupus erythematosus with promoter polymorphisms of the mannose-binding lectin gene. *Arthritis Rheum.* **41,** 1663–1668.
62. Sullivan, K. E., Wooten, C., Goldman, D., and Petri, M. (1996) Mannose-binding protein genetic polymorphisms in black patients with systemic lupus erythematosus. *Arthritis Rheum.* **39,** 2046–2051.
63. Wu, J., Metz, C., Xu, X., Abe, R., Gibson, A. W., Edberg, J. C., et al. (2003) A novel polymorphic CAAT/enhancer-binding protein beta element in the FasL gene promoter alters Fas ligand expression: a candidate background gene in African American systemic lupus erythematosus patients. *J Immunol.* **170,** 132–138.
64. Moser, K. L., Neas, B. R., Salmon, J. E., Yu, H., Gray-McGuire, C., Asundi, N., et al. (1998) Genome scan of human systemic lupus erythematosus: evidence for linkage on chromosome 1q in African-American pedigrees. *Proc. Natl. Acad. Sci. USA* **95,** 14,869–14,874.
65. Gray-McGuire, C., Moser, K. L., Gaffney, P. M., Kelly, J., Yu, H., Olson, J. M., et al. (2000) Genome scan of human systemic lupus erythematosus by regression modeling: evidence of linkage and epistasis at 4p16-15.2. *Am. J. Hum. Genet.* **67,** 1460–1469.

66. Gaffney, P. M., Kearns, G. M., Shark, K. B., Ortmann, W. A., Selby, S. A., Malmgren, M. L., et al. (1998) A genome-wide search for susceptibility genes in human systemic lupus erythematosus sib-pair families. *Proc. Natl. Acad. Sci. U S A* **95,** 14,875–14,879.
67. Gaffney, P. M., Ortmann, W. A., Selby, S. A., Shark, K. B., Ockenden, T. C., Rohlf, K. E., et al. (2000) Genome screening in human systemic lupus erythematosus: results from a second Minnesota cohort and combined analyses of 187 sib-pair families. *Am. J. Hum. Genet.* **66,** 547–556.
68. Shai, R., Quismorio, F. P., Jr., Li, L., Kwon, O. J., Morrison, J., Wallace, D. J., et al. (1999) Genome-wide screen for systemic lupus erythematosus susceptibility genes in multiplex families. *Hum. Mol. Genet.* **8,** 639–644.
69. Quintero-Del-Rio, A. I., Kelly, J. A., Kilpatrick, J., James, J. A., and Harley, J. B. (2002) The genetics of systemic lupus erythematosus stratified by renal disease: linkage at 10q22.3 (SLEN1), 2q34-35 (SLEN2), and 11p15.6 (SLEN3). *Gene Immun.* **3,** S57–S62.
70. Nath, S. K., Kelly, J. A., Reid, J., Lam, T., Gray-McGuire, C., Namjou, B., et al. (2002) SLEB3 in systemic lupus erythematosus (SLE) is strongly related to SLE families ascertained through neuropsychiatric manifestations. *Hum Genet.* **111,** 54–58.
71. Namjou, B., Nath, S. K., Kilpatrick, J., Kelly, J. A., Reid, J., James, J. A., et al. (2002) Stratification of pedigrees multiplex for systemic lupus erythematosus and for self-reported rheumatoid arthritis detects a systemic lupus erythematosus susceptibility gene (SLER1) at 5p15.3. *Arthritis Rheum.* **46,** 2937–2945.
72. Kelly, J. A., Thompson, K., Kilpatrick, J., Lam, T., Nath, S. K., Gray-McGuire, C., et al. (2002) Evidence for a susceptibility gene (SLEH1) on chromosome 11q14 for systemic lupus erythematosus families characterized by hemolytic anemia. *Proc. Natl. Acad. Sci. U S A* **99,** 11,766–11,771.
73. Sawalha, A. H., Namjou, B., Nath, S. K., Kilpatrick, J., Germundson, A., Kelly, J. A., et al. (2002) Genetic linkage of systemic lupus erythematosus with chromosome 11q14 (SLEH1) in African-American families stratified by a nucleolar antinuclear antibody pattern. *Gene Immun.* **3,** S31–S44.
74. Nath, S. K., Kelly, J. A., Namjou, B., Lam, T., Bruner, G. R., Scofield, R. H., et al. (2001) Evidence for a susceptibility gene, SLEV1, on chromosome 17p13 in families with vitiligo-related systemic lupus erythematosus. *Am. J. Hum. Genet.* **69,** 1401–1406.
75. Namjou, B., Nath, S. K., Kilpatrick, J., Kelly, J. A., Reid, J., Reichlin, M., et al. (2002) Genome scan stratified by the presence of anti-double-stranded DNA (dsDNA) autoantibody in pedigrees multiplex for systemic lupus erythematosus (SLE) establishes linkages at 19p13.2 (SLED1) and 18q21.1 (SLED2). *Gene Immun.* **3,** S35–S41.

3

T-Cell Signaling Abnormalities in Human Systemic Lupus Erythematosus

Madhusoodana P. Nambiar, Sandeep Krishnan, and George C. Tsokos

Summary

Abnormal expression of key signaling molecules and defective functions of T lymphocytes play a significant role in the pathogenesis of systemic lupus erythematosus (SLE). T-cell receptor (TCR)/CD3-mediated stimulation of SLE T cells shows increased protein tyrosine phosphorylation of cellular proteins, with faster kinetics, heightened calcium response, and decreased interleukin (IL)-2 production. The molecular mechanism of T-cell signaling abnormalities in SLE T cells is complex and cannot be explained fully by the current theories of T-cell signaling. Current research on lymphocyte signaling abnormalities in SLE has been directed toward investigating various factors that contribute to abnormal tyrosine phosphorylation, intracellular calcium response, and cytokine production. Latest developments suggest multiple components, including altered receptor structure, supramolecular assembly, modulation of membrane clustering, aberrant cellular distribution, and precompartmentalization with lipid rafts invariably contributing to abnormal T-cell signaling in SLE T cells. The methods and protocols described here pertaining to T-cell signaling abnormalities in SLE T cells are very much optimized in many ways, and they were derived by the combined tasks and continuous efforts of many researchers in the laboratory over a long period. These simplified protocols can be readily applied to study T-cell signaling abnormalities in SLE to identify the genetic, molecular, and biochemical factors contributing to aberrant immune cell function and unravel the pathophysiology of SLE.

Key Words: Autoimmune disease; calcium response; cell proliferation; cell signaling; cytokines; immunoblotting; T-cell isolation; tyrosine phosphorylation.

1. Introduction

1.1. T-Cell Receptor Signaling

One of the earliest steps in the signal transduction after T-cell receptor (TCR)/CD3 engagement is the phosphorylation of the tyrosine residues within the three immunoreceptor tyrosine-based activation motifs (ITAMs) of the ζ-chain

From: *Methods in Molecular Medicine, Vol. 102: Autoimmunity: Methods and Protocols*
Edited by: A. Perl © Humana Press Inc., Totowa, NJ

by Lck and Fyn leading to the association and activation of ζ-chain-associated protein-70 (ZAP-70) ***(1–4)***. Once activated, Fyn, Lck, Syk, and ZAP-70 cooperate in the tyrosine phosphorylation, activation, and juxtaposition of downstream signal transducers that contribute to the initiation of mitogen-activated protein (MAP) kinase cascades, phosphatidyl inositol 3 (PI3)-kinase activation, and Ca^{2+} flux. Increase in the intracellular Ca^{2+} after T-cell activation gives rise to sequential activation of sets of genes that in turn initiate proliferation, differentiation, and effector functions.

Basically, in addition to the complete investigation of the expression of various signaling molecules, T-lymphocyte signaling is analyzed at four stages to compare the signaling (1) early (1, 2, and 3 min) tyrosine phosphorylation of the cellular proteins, (2) intracellular calcium response, (3) expression of cytokines, and (4) cell proliferation. In normal T cells, the intensity of the T-cell signaling directly correlates with the level of expression of the critical T-cell signaling molecule, such as TCR ζ-chain. TCR ζ-chain is the limiting factor in T-cell receptor assembly, transport, and surface expression and receptor function ***(5,6)***. However, in autoimmune disorders, the cell signaling remains abnormal and appears to correlate inversely with the level of TCR ζ-chain. The exact nature of the mechanism that triggers the inverse correlation has become a topic of intense interest to many researchers.

1.2. Applications

Signaling studies have several applications in SLE and other autoimmune disorders. The precise pathological mechanisms behind abnormal T-cell functions in SLE remain incompletely understood. Identification of underlying genetic, molecular, and biochemical mechanisms responsible for aberrant T-cell signaling will contribute to the understanding of the etiopathogenesis of SLE as well as provide novel targets for future pharmacological intervention.

1.3. Study Design

Normal T cells or autoimmune disease controls such as rheumatoid arthritis, Sjögren's syndrome, Still's disease, limited systemic sclerosis, mixed connective tissue disorder, antiphospholipid syndrome, and dermatositis can be used as controls for SLE studies. Samples taken on different dates can be compared by normalizing the data against a proper internal control. It is important to distinguish between TCR/CD3-mediated signaling from nonreceptor-mediated signaling abnormalities in SLE T cells by TCR/CD3 activation using antibodies or by nonreceptor-mediated stimulation using phorbol-12-myristate 13-acetate/ionomycin, respectively.

Studies of T-cell signaling abnormalities should be correlated with the SLE disease activity index, current medication, demographics (race, gender, age) to

distinguish abnormalities that are intrinsic to the disease from abnormalities associated with disease activity. Medication should include both current medications and previous medications because the effects of some cytotoxic drugs are presumed to last longer.

Studies can also be performed on primary SLE T cells, which can be cultured and maintained up to 30–40 d. To confirm the results further, the study should be designed to follow up the patients over a period of 3–4 yr, during which the SLE disease activity will improve considerably. If possible, it is also a good idea to request the patients not to take any medication at least 24 h before drawing the blood sample to reduce the effects of medication.

2. Materials

2.1. General Materials and Supplies

1. RPMI-1640 (without L-glutamine) stored at 4°C (Quality Biological Inc., Gaithersburg, MD).
2. Fetal bovine serum (FBS), heat inactivated, endotoxin tested (Quality Biological Inc.).
3. Ficoll-Hypaque, Lymphoprep™ (Axis-Shield PoC AS, Oslo, Norway).
4. Phosphate-buffered saline (PBS) 10X, pH 7.4 (Quality Biological Inc.).
5. Bovine serum albumin (BSA), Fraction V (Sigma Aldrich, St. Louis, MO).
6. Trypan blue 0.4% (Sigma Aldrich).
7. 200 m*M* L-Glutamine (Quality Biological Inc.).
8. 0.5 *M* ethylenediaminetetraacetic acid (EDTA) (Biofluids Inc., Rockville, MD).
9. 1 *M* HEPES buffer (Sigma Aldrich).
10. 15- and 50-mL disposable polypropylene conical tubes (Fisher Scientific, Suwanee, GA).
11. 6-Well flat bottom tissue culture polystyrene plates with lids (BD Pharmingen, San Diego, CA).
12. 24- and 96-well flat-bottom tissue culture polystyrene plates with lids (Corning Inc., Corning, NY).
13. Disposable syringe filter assembly, 0.45 or 0.22 μm (USA/Scientific Plastics, Ocala, FL).
14. Polyallomer centrifuge tubes 14 × 89 mm (Beckman, Palo Alto, CA).
15. Antibiotics used were penicillin-streptomycin (10,000 U/mL penicillin and 10,000 U/mL streptomycin) (Quality Biological Inc.).

2.2. Antibodies and Kits

1. Anti-CD3ε immunoglobulin G (IgG), clone-OKT3 (Orthobiotech, Raritan, NJ). It is available as 5-mL ampules of 0.5 mg/mL. After opening the ampule, the antibody should be aliquoted into 100 μL under a sterile hood and stored at 4°C.
2. Anti-CD3ε IgG, clone-UCHT1 (BD Pharmingen).
3. Anti-CD3ε IgM, clone-2Ad2a2, was a generous gift from Dr. Ellis Reinherz, Dana Farber Cancer Institute, Boston, MA.
4. Anti-CD28 IgG (NA/LE™), clone-CD 28.2 (BD Pharmingen).

5. The crosslinking antibody was goat antimouse IgG (Santa Cruz Biotechnology, Santa Cruz, CA).
6. The isotype controls were mouse IgG (Santa Cruz Biotechnology).
7. Antiphosphotyrosine antibody horseradish peroxidase (Ab-HRP) conjugated or unconjugated, clone 4G10 (Upstate Biotechnology, New York).
8. Phosphotyrosine antibody mouse monoclonal IgG2b, clone PY99 (Santa Cruz Biotechnology).
9. Goat antimouse IgG-HRP (Santa Cruz Biotechnology).
10. Panhuman T-cell isolation kit (Miltenyi Biotech).
11. RosetteSep™ human T-cell enrichment cocktail (StemCell Technologies Inc., Vancouver, BC, Canada).
12. Quantikine human IL-2 immunoassay kit (R&D Systems Inc., Minneapolis, MN).
13. Protein assay kit (Bio-Rad, Hercules, CA).

2.3. Electrophoretic, Western Transfer, Immunoblotting, and Immunoprecipitation Reagents

1. Novex precast gels 4–12% Bis-Tris NuPAGE™ gels (Invitrogen, Carlsbad, CA).
2. Whatman filter papers (Fisher Scientific).
3. Polyvinylidene fluoride (PVDF) membrane, Immobilon-P, pore size 0.45 μm (Sigma Aldrich).
4. NuPAGE antioxidant (Invitrogen)
5. NuPAGE -20X morpholino ethane sulfonic acid (MES) running buffers.
6. NuPAGE 20X 3-(*N*-morpholino) propane sulfonic acid (MOPS) running buffer.
7. NuPAGE transfer buffer 20X.
8. NuPAGE LDS (laureal dodecyl sulfate) sample buffer (4X) (Invitrogen).
9. SeeBlue® Plus 2 protein ladder (Invitrogen).
10. Protein A/G plus-agarose, 2 mL 50% slurry (Santa Cruz Biotechnology).
11. Phenyl phosphate disodium salt (Sigma Aldrich).
12. Kodak X-ray film (Sigma Aldrich).
13. Tween-20 (Sigma Aldrich).
14. Triton X-100 (Fisher Scientific).

2.4. Flow Cytometry Reagents

Fluorescence-activated cell sorter (FACS) tubes, 12 × 75 mm polypropylene test tubes without cap (Fisher Scientific) were used for the flow cytometry reagents.

2.5. Instruments

1. Tabletop centrifuge, Sorvall-RT 6000D, rotor H-1000 B (Kendro Laboratory Products, Newtown, CT).
2. Refrigerated tabletop microtube centrifuge, Biofuge-Fresco (Kendro Laboratory Products).

3. Nonrefrigerated Micromax centrifuge (International Equipment Co., Needham Heights, MA).
4. Hemocytometer and coverslips (Fisher Scientific).
5. Water bath (Precision Scientific Group, Thomas Scientific, Swedesboro, NJ).
6. Flow cytometer, model FACSCalibur (Becton Dickinson, San Jose, CA).
7. Epics Altra flow cytometer (Coulter Beckmann, Hialeah, FL).
8. Spectrophotometer (UVSpec) and software (Amersham Pharmacia, Piscataway, NJ).
9. Thermomax plate reader (Molecular Devices, Sunnyvale, CA; Software-SoftPro10).
10. Gel docking station and software (Software, Quantity One, Bio-Rad).
11. NuPAGE gel casts and transfer casts (Invitrogen).
12. Power supplies, Bio-Rad Power Pac 300 (Bio-Rad).
13. Light microscope, Olympus (OPELCO, Dulles, VA).
14. CO_2 incubator (Forma Scientific Inc., Marietta, OH).
15. Sterile hood (Nuaire, Biological Safety Cabinets, Plymouth, MN).

3. Methods

3.1. Isolation and Cell Culture of T Lymphocytes

3.1.1. Separation of Peripheral Blood Mononuclear Cells

The blood should be collected in heparin green-top blood collection tubes and kept at room temperature. Peripheral blood mononuclear cells (PBMCs) are isolated by density gradient centrifugation over Ficoll-Hypaque, and the whole process is done at room temperature.

1. The blood is aliquoted into 10 mL in each 50-mL conical disposable centrifuge tube.
2. Add 30 mL RPMI-1640 medium with Pen-Strep, cap it, and mix by inverting.
3. Carefully underlay the sample with 10 mL Lymphoprep.
4. Centrifuge in a Sorvall tabletop centrifuge at 800*g* for 45 min. Do not apply brake during centrifugation to prevent mixing of the density gradient layers during the deceleration process.
5. Remove the interface of the white ring or buffy coat containing PBMCs and transfer to new 50-mL conical tubes.
6. Dilute the PBMCs with three volumes of RPMI-1640 with Pen-Strep, mix, and centrifuge at 400*g* for 5 min.
7. Discard the supernatant and resuspend the cells in appropriate volume of RPMI-1640.
8. Count the cells using a hemocytometer by diluting 10-mL samples with 200 mL trypan blue. The cells should be counted from all four corner cubes, and the total number obtained should be more than 200 for accurate results. Total number of cells = cell count/4 × 20 × 10^4 cells/mL.

Note that trypan blue exclusion will be used to determine the viability of PBMCs. If the PBMCs are contaminated with red blood cells (RBCs) and the sample appears red, it can be hemolyzed using ACK lysis buffer (0.15*M* NH_4Cl, 1 m*M* $KHCO_3$, and 0.1 m*M* EDTA). If used immediately, the isolated PBMCs should be kept in RPMI-1640 containing Pen-Strep at 37°C in a CO_2 incubator. If the cells need to be kept for a longer time, maintain in RPMI containing Pen-Strep and 10% FBS at 37°C in a CO_2 incubator.

3.1.2. Isolation of T Lymphocytes From PBMCs

Any of the following three different protocols can be used to isolate T lymphocytes from PBMCs. Magnetic separation and RosetteSep methods routinely yield greater than 97% CD3-positive T lymphocytes and have distinct advantages. Rosetting using sheep red blood cells (SRBCs) routinely yields around 93% CD3-positive cells; however, it is inexpensive.

3.1.2.1. Magnetic Separation Using Microbeads

T cells can be isolated by negative depletion by magnetic separation using a kit from Miltenyi Biotech. This procedure is simple and involves incubation of the PBMCs with a cocktail of hapten-conjugated antibodies that bind to non-T lymphocytes, followed by removal of the antibody-bound non-T lymphocyte by a magnetic bead coated with secondary antihapten antibody. The non-T lymphocytes bound to the magnetic beads are retained in a column under the influence of a powerful magnet. The flowthrough containing purified T cells is used for the studies.

Although the manufacturer's protocol suggests that PBMCs may be stored in the refrigerator overnight in PBS containing 2 m*M* EDTA supplemented with 10% autologous serum after the last washing step before separation using an magnetic cell sorting (MACS) column, we found that storing SLE PBMCs under these conditions sometimes results in large clumps that fail to resuspend and later clog the separation column and decrease the flow and yield. Overnight incubation of SLE PBMCs also leads to decreased viability of the cells and cell lysis. Occasionally, in some SLE patients, increased attachment of the cells to the surface walls of the 50-mL conical tube was encountered.

1. Count the PBMCs and wash them in 10 mL MACS buffer (1X PBS, 1% FBS or 0.5% BSA, 2 m*M* EDTA).
2. Remove the supernatant very carefully and resuspend the cells in 80 μL (per 10^7 cells) ice-cold MACS buffer.
3. Add 20 μL hapten-antibody cocktail per 10^7 cells, mix well, and incubate at 6°C for 10 min.
4. Wash two times with MACS buffer (20 times the labeling volume).

5. Resuspend the cells in 80 μL MACS buffer and add 20 μL MACS antihapten microbeads per 10^7 cells, mix well, and incubate at 6°C for 15 min.
6. Wash the cells one time as in **step 4** and resuspend in 500 μL MACS buffer.
7. Set up the MACS column between the magnet and wash the column with 3 mL of MACS buffer.
8. Load the cells to the column, collect the flowthrough, and wash with 10 mL of MACS buffer.
9. Centrifuge the T lymphocytes at 300*g* for 5 min in the Sorvall tabletop centrifuge and discard the supernatant.
10. Resuspend the cells in an appropriate volume of RPMI-1640 containing 10% FBS and Pen-Strep.

3.1.2.2. RosetteSep

T lymphocytes can be directly isolated from the SLE blood samples using this protocol. The method of T-cell isolation by RosetteSep is essentially based on crosslinking the non-T lymphocytes with antibodies coated to latex beads that separate with RBCs in Ficoll-Hypaque density gradient centrifugation. This negative selection protocol takes less time than MACS separation. However, the yield of purified T lymphocytes is slightly lower than with MACS isolation.

1. Take 10 mL of SLE blood in each 50-mL conical tube.
2. Add 250 μL of the StemCell T-cell isolation antibody. Mix well using a 25-mL pipet and incubate at room temperature for 20 min.
3. Add 30 mL of prewarmed RPMI-1640 containing Pen-Strep and mix it.
4. Underlay the sample with 10 mL of Lymphoprep and centrifuge at 800*g* for 40 min at room temperature.
5. Collect the interphase layer of cells in fresh tubes, dilute with RPMI-1640, and spin at 500*g* for 10 min.
6. Resuspend the purified T cells in an appropriate volume of RPMI-1640 containing 10% FBS plus Pen-Strep.

3.1.2.3. Rosetting With SRBCs

This old protocol of T-cell isolation is less expensive. It is based on rosetting the T cells with SRBCs, followed by separation of the rosettes and hypotonic lysis of the SRBCs ***(7)***.

3.1.2.3.1. Preparation of SRBCs

1. Transfer 7.5 mL SRBCs to a 50-mL conical tube.
2. Fill the tube with cold RPMI-1640 and centrifuge at 200*g* for 5 min at 4°C.
3. Repeat the washing two more times and restore the volume to 7.5 mL with RPMI-1640.
4. Prepared SRBCs can be stored at 4°C for a few days.

3.1.2.3.2. Rosetting With SRBCs

1. Adjust the cells to a final concentration of 10×10^6 cells/mL.
2. Add an equal volume of solution that contains 10% washed SRBCs, 20% FBS, and 70% RPMI-1640.
3. Mix well using a pipet and incubate at room temperature for 20 min.
4. Centrifuge the suspension at 50*g* for 10 min at room temperature and incubate for 2 h or overnight at 4°C.
5. Gently resuspend the rosetted cells by laying the tube on the bench and rolling it slowly around its long axis.
6. The suspension is underlayed with 10 mL ice-cold Ficoll-Hypaque and centrifuged at 800*g* for 35 min at 10°C.
7. Collect the interphase containing B lymphocytes and discard the supernatant without disturbing the cell pellet at the bottom.
8. Wash the rosetted T-cell pellet with 20 mL RPMI-1640 twice by centrifuging at 300*g* for 10 min.
9. Subject the cell pellet to hypotonic lysis of SRBCs using 10 mL ACK lysis buffer (0.15 *M* NH_4Cl, 1 m*M* $KHCO_3$, and 0.1 m*M* EDTA) for 3 min.
10. Fill the tube with RPMI-1640 and centrifuge at 300*g* for 10 min. Wash the T-cell pellet two times with RPMI-1640, resuspend in 2 mL RPMI-1640, and count the cells.

3.1.3. Cell Culture of T Lymphocytes

1. Prepare the culture medium by mixing 70% RPMI-1640, 5% FBS, and 20% HL1 medium.
2. Add 1 μg/mL phytohemagglutinin.
3. Resuspend the T cells at a concentration of 1×10^6 cells/mL in the above medium and start cell culture.
4. After 2 d, centrifuge the cells at 300*g* for 5 min and resuspend in fresh culture medium containing 1 μg/mL phytohemagglutinin and 25 U/mL IL-2.
5. Change the medium when the color becomes yellow (2 d at the beginning and later 5 d). Always resuspend the cells at 1×10^6 cells/mL).

Note that SLE T cells grow under these conditions and can be maintained up to 40 d. It should be always kept in mind that it is not clear how many of the sick SLE T cells die under these conditions and how many unaffected cells grow.

3.2. Analysis of TCR/CD3-Mediated Signaling in Lymphocytes

3.2.1. Measurement of TCR/CD3-Mediated Intracellular Calcium Response in SLE T Cells

Intracellular calcium response is measured by flow cytometry after labeling the cells with INDO-1 (Molecular Probes, Eugene, OR) ***(8)***. INDO-1-loaded cells are analyzed using an Epics Altra (Coulter Beckmann) flow cytometer

equipped with a high-power, dual-wavelength (365 nm and 488 nm) argon laser and ultraviolet source. In each run, first the cells are run unstimulated to record the baseline fluorescence ratio, which represents the resting $[Ca^{2+}]_i$ levels. After 40 s, antibody OKT3, other activating antibodies, or the isotype control $mIgG_{2a}$ is added to the tube, followed by crosslinking with the goat antimouse IgG at 130 s; the calcium response is recorded for 10 min. The mean fluorescence ratio calculated by the software MultiTime (version 3, Phoenix Flow Systems, San Diego, CA) is directly proportional to the free cytosolic Ca^{2+}.

It is very important to perform the calcium analysis as soon as possible after blood collection to be very close to the signaling in vivo. Isolated T lymphocytes (5×10^6/mL) should be recovered in RPMI-1640 containing 10% FBS and Pen-Strep at 37°C in 5% CO_2 for 4–6 h for an optimal response and should not be maintained more than 16 h. Longer periods of incubation of the lymphocytes in culture medium may decrease the effective calcium response qualitatively and quantitatively. Also, longer periods of incubation could affect the results of T-cell signaling abnormalities because gene expression can change in cells incubated with the culture medium. When comparing the intracellular calcium response of SLE T cells to that of normal T cells, the experiment should be done simultaneously on the same day to avoid instrumental variations.

1. Prepare 100 mL of RPMI-1640 medium containing 1% FBS, 10 m*M* pH 7.4 HEPES, and Pen-Strep. Filter the medium through a 0.45-μ*M* filter and prewarm to 37°C.
2. Take 1 mL of SLE T cells maintained in RPMI-1640 (1×10^6 cells/mL) in a flow cytometry tube. Add 1 μL INDO-1 (add 50 μL DMSO to 1 vial of 50 μg INDO-1, keep it covered with aluminum foil) and incubate at 37°C for 1 h.
3. Dilute 200 μL INDO-1 loaded T lymphocytes to 2 mL in 37°C prewarmed culture medium and loaded to Epics Altra flow cytometer.
4. The sample should be run at a data rate of approx 150 to increase the efficiency. Therefore, the flow rate has to be adjusted if there is variation in cell number among samples. Too many cells in the sample may decrease the flow rate and ultimately clog the tubes. If the data rate is decreased while running, increase the flow rate to adjust the data rate.
5. After recording the baseline for 40 s, add 2.5 μg/mL OKT3, mix the samples, and allow to run for another 50 s.
6. Add 20 μg/mL goat antimouse antibody, mix, and allow to run for 10 min with intermittent shaking.
7. Data can be analyzed using MultiTime software and plotted as the mean ratio or percentage responding cells.

Note that the mean fluorescence ratio calculated by the MultiTime software is directly proportional to the free cytosolic Ca^{2+} (**Fig. 1**). The intracellular

calcium response can also be represented as a percentage of responding cells. A positive responding cell is one with $[Ca^{2+}]_i$ that is increased by two standard deviations above the mean background levels. Intracellular calcium response data can be interpreted by calculating the total area under the response curve or by taking the peak mean ratio at a selected time. After the peak response, lack of a gradual decrease in the intracellular calcium response to the baseline suggests a sustained response and is interpreted as abnormal termination of T-cell signaling. More than 1 μL INDO-1 per 1 mL of cells should not be added because the high DMSO may reduce the calcium response. When running at a high flow rate, a 10-min recording may require more than 2 mL of cells.

As an alternative to OKT3, an anti-CD3 IgM antibody can be used. The calcium response is much higher following activation with pentameric IgM antibody because of better crosslinking. Addition of secondary crosslinking antibody is not necessary when stimulating with IgM antibody. To study or compare with non-TCR-mediated calcium response, the cells can be activated by phorbol-12-myristate 13-acetate/ionomycin.

3.2.2. Tyrosine Phosphorylation of Cellular Protein Substrates

3.2.2.1. Cell Activation and Lysis

1. Transfer 5 million SLE T cells in 500 μL serum-free RPMI-1640 medium to a 1.5-mL microfuge tube.
2. Incubate the cells at 37°C for 10 min in a water bath.
3. Stimulate the cells with the addition of 1 μg/mL OKT3 for 0, 1, or 2 min at 37°C. (Antibody 2Ad2a2:IgM 1:200 dilution or UCHT1 10 μg/mL antibody can be substituted for OKT3. When using OKT3 Ab, it can be crosslinked by adding 10 μg/mL goat antimouse antibody immediately to increase the level of tyrosine phosphorylation.)
4. Stop the reaction by the addition of 0.5 mL ice-cold 2X stop buffer (50 m*M* Tris-HCl, 100 m*M* NaCl, 100 m*M* NaF, 2 m*M* Na_3VO_4, 10 m*M* EDTA, 10 m*M* sodium pyrophosphate, 2 m*M* phenylmethane sulfonyl fluoride (PMSF), 20 μg/mL leupeptin, and 20 μg/mL aprotinin).
5. Cells were pelleted and lysed in lysis buffer (working solution for 1 mL, 500 μL 2X stop buffer , 483 μL water; 5 μL 0.5*M* EDTA, 1 μL aprotinin, 1 μL 5 mg/mL leupeptin; 5 μL 0.2*M* PMSF; 5 μL 200 m*M* sodium vanadate) containing 1% Nonidet P-40 (Sigma Aldrich).
6. Incubate the cells at 4°C for 1 h in a shaker in the cold room.
7. Centrifuge the cells at 18,000*g* for 10 min at 4°C and collect the supernatant. The pellet, which can be used to evaluate tyrosine phosphorylation of proteins in detergent-insoluble membrane fractions, should be washed twice with 100 μL lysis buffer.
8. Freeze both the pellet and the cytoplasmic protein extract at –80°C.

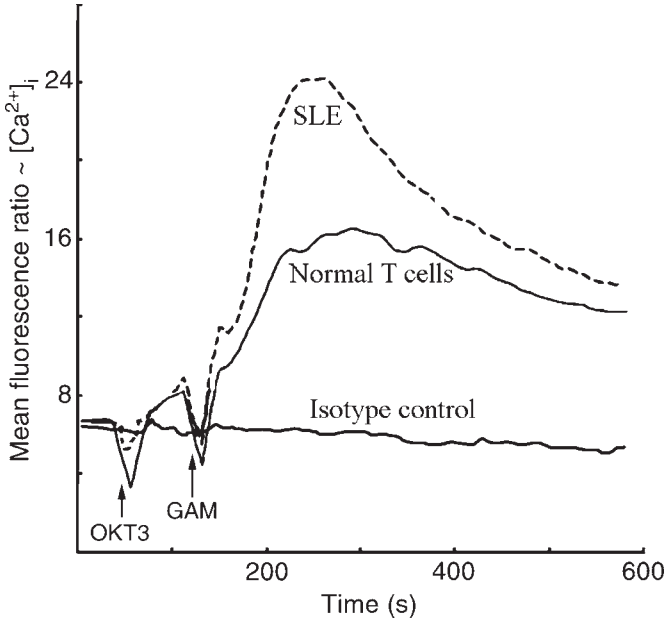

Fig. 1. TCR/CD3-induced intracellular calcium response in SLE T cells. For this, 1×10^6 SLE T cells were resuspended in 1 mL prewarmed culture medium and loaded with 1 μL (1 μg/mL in DMSO) INDO-1 (Molecular Probes) for 60 min at 37°C. INDO-1-loaded cells were diluted 10 times (0.2 –2 mL) with prewarmed, filtered RPMI-1640 containing 1% FBS. After establishing the baseline fluorescence ratio that represents the resting $[Ca^{2+}]_i$ levels for 40 s, the cells were stimulated with either OKT3 (2.5 μg/mL) or the isotype control mIgG2a, followed by 10 μg/mL of goat antimouse antibody at 130 s. The intracellular calcium response was continuously monitored for 10 min with intermittent shaking.

3.2.2.2. Bio-Rad Protein Assay

1. Take a flat-bottom, 96-well culture plate.
2. Pipet a row of 0, 2, 4, 6, 8, and 10 μL protein standard (1 mg/mL BSA in distilled water) and add 10, 8, 6, 4, 2, and 0 μL, respectively, of distilled water to make up the final volume to 10 μL.
3. For cell lysates, pipet 2 μL of the samples to the wells and add 8 μL of distilled water.
4. Add 90 μL of the Bio-Rad protein assay reagent concentrate to each well (if the concentration of the samples is very low, then increase the volume of the cell lysate and adjust the volume to 10 μL with distilled water). The blue color reaction is noted, and the plate is read at 595 nm in a microplate reader using SOFTmaxPro software (Molecular Devices, Sunnyvale, CA) to obtain the con-

centration of the protein in each sample. Each protein value is multiplied by 5 (dilution) to obtain the concentration of proteins in micrograms per microliter. The Bio-Rad protein assay can also be done in 1-mL plastic disposable cuvets using 200 µL Bio-Rad protein assay reagent and 800 µL protein solution plus water.

Note that normal T lymphocytes yield approx 5 µg/µL protein if 5 million cells are lysed in 100 µL lysis buffer. Jurkat T lymphoma cell lines yield approx 20 µg/µL protein if 5 million cells are lysed in 150 µL lysis buffer. Pipetting errors can interfere with the result. Avoid any bubbles in the wells or results may be affected. Generally, electrophoresis of 15–20 µg of the protein sample is required for decent detection by immunoblotting.

3.2.2.3. Protein Separation by Polyacrylamide Gel Electrophoresis

3.2.2.3.1. Sodium Dodecyl Sulfate-Polyacrylamide Gel Electrophoresis Using NuPAGE. Depending on the molecular weight of the protein under investigation, different gel types can be used for sodium dodecyl sulfate-polyacrylamide gel electrophoresis (SDS-PAGE). Higher molecular weights (above 100 kDa) can be better resolved with a 6% gel, molecular weights of 50–100 kDa can be better resolved with a 10% gel, and to visualize lower molecular weight proteins, a 12% gel can be used. Sometimes, a gradient gel, such as a 4–12% Bis-Tris gel may be necessary to see the whole spectrum of proteins. The Invitrogen-Novex precast gel is set up after removing the stripe and comb in the electrophoresis apparatus according to manufacturer's instructions, and the outer chamber is filled with running buffer (50 mL 20X MOPS or MES, depending on the resolution required, plus 950 mL distilled water). The inner chamber is filled with 200 mL of running buffer containing 0.5 mL of antioxidant (supplied by the manufacturer) to cover the loading wells. The samples are denatured in SDS and reduced using dithiothreitol or 2-mercaptoethanol ***(9)***. Protein sample preparation for loading is as follows:

1. Pipet 10–15 µg protein lysate from different samples in a 1.5-mL microfuge tube.
2. Add an equal volume of 4X loading buffer (Invitrogen-Novex, Carlsbad, CA) containing bromophenol blue, SDS, and 2 mercaptoethanol. The total volume of the sample should not exceed 32 µL. Therefore, it is necessary to use 5X loading buffer for dilute samples.
3. Boil for 5 min in a water bath and cool at room temperature.

The following is the procedure for loading samples to gels:

1. Clean the wells by flushing with the running buffer using a pipet.
2. Gels are carefully loaded with samples using thin pipet tips.
3. On one end of the well, the SeeBlue-2 or rainbow protein ladder is added.

4. The gel is run for 1 h at a constant 150–170 V until the bromophenol blue reaches the bottom of the gel. Remove the running buffer, take the gel out, and continue with staining or Western blotting.

Note that care should be taken to avoid spillage of samples into adjacent wells. The voltage should be reduced if "smiling" of the gel occurs or if the proteins run weirdly. If gels heat up during the run, it should be run at 4°C in the cold room. Optionally, to make sure loading is equal, the gels can be stained with Coomassie brilliant blue to visualize the proteins.

3.2.2.3.2. Sodium Dodecyl Sulfate-Polyacrylamide Gel Electrophoresis

1. Remove the stripe from precast 10% SDS-PAGE gels and fit into the chamber.
2. Remove the comb, fasten the device, and fill running buffer (dilute 10X Tris-glycine/SDS buffer; Invitrogen).
3. Add an equal volume of 2X SDS-PAGE loading buffer containing 2-mercaptoethanol to 10–15 μg protein samples, boil for 5 min, and load to the gel along with prestained SeeBlue protein marker.
4. Run the gel at 125 V for 2 h until bromophenol blue reaches the bottom of the gel. Remove the running buffer, take the gel out, and proceed with Western blotting.

3.2.2.3.3. Coomassie Blue Staining

1. Incubate the gel for 2 h in fixing solution (50% methanol, 10% acetic acid, 40% water).
2. Wash the gel with water and stain for 4 h in Coomassie brilliant blue staining solution (50% methanol, 0.05% Coomassie brilliant blue R-250, 10% acetic acid, 40% water).
3. Destain the gel with 50 mL destaining solution (5% methanol, 7% acetic acid, 88% water).
4. Change the destaining solution a few times until blue bands and clear backgrounds are obtained. Store the gel in 7% acetic acid or water.

3.2.2.4. Western Blotting

1. Wear gloves and cut the PVDF membrane 1–2 mm larger than the gel.
2. Soak pads, filters, and membranes for 15 min in transfer buffer (for 1 L, use 50 mL 20X transfer buffer available, 849 mL distilled water, 1 mL antioxidant, and 100 mL methanol; if methanol is not available, the same volume of 200 proof ethanol can be substituted).
3. Disassemble gel sandwich and equilibrate gel for 5 min in transfer buffer at room temperature.
4. For one membrane, assemble transfer sandwich in the following order: negative electrode, pad, pad, filter, gel, membrane, filter, pad, pad, positive electrode. For two membranes, assemble transfer sandwich in the following order: negative electrode, pad, pad, filter, gel, membrane, filter, pad, filter, gel, membrane, filter, pad, pad, positive electrode.

5. Remove any bubbles between the filter paper, gel, and PVDF membrane by rolling a pipet from one side to the other. This is important to avoid improper transfer of the proteins.
6. Fill the chamber with transfer buffer until the pads are just covered.
7. Run at a constant 30 V for 1 h (at 4°C)
8. Disassemble the sandwich and mark the front side of the membrane with a pen.

Note that the membrane can be stained with Ponceau S (0.3% Ponceau S in 5% trichloroacetic acid) to confirm the transfer. Place the membrane in Ponceau S solution for 5 min at room temperature, destain with water, photograph it, and completely destain with water by soaking for 10 min. Alternatively, the unusable transferred gel can be stained with Coomassie brilliant blue to evaluate the amount transferred. Overtransfer and loss of proteins may occur if transfer is prolonged beyond 1 h. For overnight transfers, a constant 14 V is applied.

3.2.2.5. Immunoblotting

1. Rinse the membrane in 1X PBS or 1X Tris-buffered saline (TBS) and transfer it to a plastic box.
2. Block the membrane with 3–5% BSA for 1 h in PBS or TBS.
3. Transfer the membrane to a plastic bag with 7 mL of blocking solution, add antiphosphotyrosine-HRP antibody (1:1500 dilution), remove the bubbles, and seal the bag. The membrane is incubated for 2–3 h or overnight at 4°C with agitation using a nutator.
4. Remove the membrane and wash three times for 10 min each in 15 mL of PBST (1X PBS, 0.1% Tween-20) or TBST (1X TBS, 0.1% Tween-20).
5. Wash the membrane in PBS or TBS once.

3.2.2.6. Detection

1. Warm and mix enhanced chemiluminescent (ECL) reagents 1 and 2 (Amersham Pharmacia) and mix mL of each to make 8 mL reagent per blot.
2. Incubate the membrane in the ECL reagent for 1 min. Make sure that the reagent spreads over the entire membrane.
3. Drain the ECL reagent from the membrane, dry the membrane gently, and then put it between a plastic envelope or saran wrap and place it on a detection cassette.
4. Cut Kodak X-ray film (Sigma Aldrich) to the appropriate size, bend the upper right-hand corner to identify the position, put the film on the membrane, expose for 10 s, and expose a second film for 1 min.
5. Develop the film in a Kodak automatic processor. If necessary, increase or decrease the exposure time to obtain a good autoradiogram.

Note that if the antibody used is not conjugated with HRP, then a second step of incubation for 1 h with antimouse HRP is required after the primary anti-

body, followed by three washes of PBST and one wash with PBS as described in **Subheading 3.2.2.5., step 4** before development. The antiphosphotyrosine antibody (clone 4G10) from Upstate Biotechnology can be frozen and reused at least three times. Immunoblotting for phosphotyrosine should be done at first if the blot is going to be probed for other molecules of interest (**Fig. 2**). HRP-conjugated antiphosphotyrosine antibody 4G10 works better and saves time compared to non-HRP-conjugated antiphosphotyrosine primary antibody and an antimouse goat IgG coupled to HRP. Do not let the blot dry out during any step of immunoblotting as this will increase background staining.

3.2.3. Kinetics of Tyrosine Phosphorylation of Cellular Proteins

The kinetics of early tyrosine phosphorylation of cellular proteins can be studied by activation of SLE T cells for 0, 1, 2, and 3 min and analysis of tyrosine-phosphorylated proteins as mentioned in **Subheading 3.2.2.** The kinetics of phosphorylation of cellular protein substrates is faster in SLE T cells compared with normal T cells (**Fig. 2**).

3.2.4. Cell Proliferation Assay

1. Antigen proliferation assays are set up in 96-well culture plates containing 1×10^5 SLE T cells/well (triplicates) in RPMI-1640 containing 10% FBS.
2. The cells are treated with immobilized OKT3 (10 μg/mL) and immobilized anti-CD28 antibody (2.5 μg/mL).
3. Cells are incubated at 37°C for 3 d.
4. Add 1 μCi of [^{3}H] thymidine/well (6.7 Ci/mmol) and incubate for 18 h.
5. Harvest the cells using a Tomtec 96-well plate harvester (Wallac, Gaithersburg, MD).
6. Incorporated radioactivity is quantitated using a Microbeta Tri-luxe plate scintillation counter (Wallac).

3.2.5. Cytokine Expression

1. 5 million T cells are plated in 1 mL medium in a 24-well culture plate.
2. Cells are activated via TCR/CD3 complex with 10 μg/mL anti-CD3 monoclonal antibody plus 2.5 μg/mL anti-CD28 monoclonal antibody for 24 or 48 h.
3. The samples are transferred to a microfuge tube and centrifuged at 18,000*g* for 2 min at 4°C.
4. The supernatants are collected, and IL-2 is measured using 100 μL of the culture supernatant in triplicates by Quantikine enzyme-linked immunosorbent assay (ELISA) kit (R&D Systems, Minneapolis, MN).
5. The levels of interferon-γ and IL-4 or other cytokines in culture supernatants are measured by ELISA using minikits (Endogen, Cambridge, MA).
6. The absorbance of the color reactions is read at 450 nm in an ELISA microplate reader (Bio-Rad).

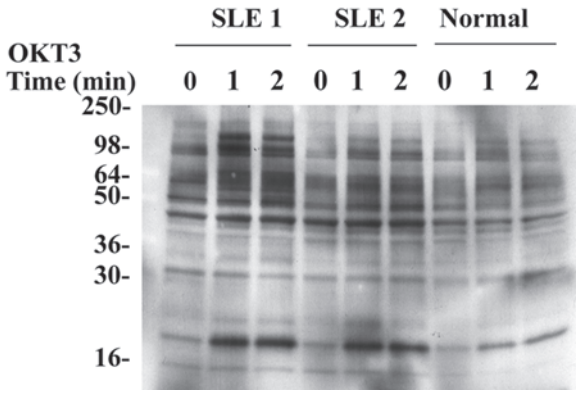

Fig. 2. Increased phosphorylation of TCR/CD3-mediated phosphorylation of TCR ζ-chain with faster kinetics in SLE T cells. Magnetically purified SLE T cells were stimulated through TCR/CD3 with 10 μg/mL of OKT3 and 20 μg/mL goat antimouse antibody for 0, 1, and 2 min and lysed. Proteins (15 μg) were analyzed on NuPAGE under reducing conditions and immunoblotted with horseradish peroxidase-conjugated antiphosphotyrosine antibody 4G10. SLE T cells showed supranormal phosphorylation of cellular protein substrates with faster kinetics compared with normal T cells.

4. Notes

1. Keeping the SLE blood at 4°C is not advisable because of the cryoglobulins present in SLE. Storing the blood for a longer duration reduces the yield of PBMCs because of the possible aggregation between lymphocytes or with other blood cells, forming clumps as well as lysis. Also, long-time incubation of blood results in increased adhesion of RBCs to PBMCs, making it slightly reddish. If this happens, RBCs need to be lysed before proceeding; otherwise, the protein and the proteolytic activity from RBCs may bias the results.
   The same-day use of the SLE blood sample is advised for maximum yield of viable PBMCs and best reproducible results. If the cells are used for transfection or nucleoporation procedures as described in Chapter 4, purification of lymphocytes on the same day significantly improves the transfection efficiency. Do not incubate the cells more than 1 min with ACK lysis buffer because it may damage the lymphocytes.
2. The negatively selected lymphocytes obtained by MACS separation are "untouched"; thus, this technique is superior to positive selection methods. To improve the yield of lymphocytes by MACS separation, elute the column with three times the column volume of buffer. Also, failure to degas the buffer each time impedes the speed of elution and decreases the yield of elution. The purity of the isolated T lymphocytes can be determined by CD3e staining and flow cytometry.
   Although rosetting with SRBCs is an inexpensive method to isolate T cells from

blood, it takes longer compared to the MACS separation or RosetteSep. Rosetted cells need to be rested 4–6 h before the signaling experiments. If hypotonic lysis of SRBCs is prolonged, it can affect the functions of T cells.

3. Because SLE T cells produce low amounts of IL-2, it is good to increase the cell number if possible. The cell pellet obtained after separation of the culture supernatant can be lysed in RLT cell lysis buffer supplied with RNeasy mini kit (Qiagen Inc., Valencia, CA) to determine the level of IL-2 messenger RNA expression.

References

1 Irving, B. A., Chan, A. C., and Weiss, A. (1993) Functional characterization of a signal transducing motif present in the T cell antigen receptor zeta chain. *J. Exp. Med.* **177 ,** 1093–1103.

2 Zenner, G., Vorherr, T., Mustelin, T., and Burn, P. (1996) Differential and multiple binding of signal transducing molecules to the ITAMs of the TCR-zeta chain. *J. Cell Biochem.* **63,** 94–103.

3 Kersh, E. N., Shaw, A. S., and Allen, P. M. (1998) Fidelity of T cell activation through multistep T cell receptor zeta phosphorylation. *Science* **281,** 572–575.

4 Kersh, E. N., Kersh, G. J., and Allen, P. M. (1999) Partially phosphorylated T cell receptor zeta molecules can inhibit T cell activation. *J. Exp. Med.* **190,** 1627–1636.

5 Weiss, A. and Littman, D. R. (1994) Signal transduction by lymphocyte antigen receptors. *Cell* **76,** 263–274.

6 Wange, R. L. and Samelson, L. E. (1996) Complex complexes: signaling at the TCR. *Immunity* **5,** 197–205.

7 Falkoff, R. M., Peters, M., and Fauci, A. S. (1982) T cell enrichment and depletion of human peripheral blood mononuclear cell preparations. Unexpected findings in the study of the functional activities of the separated populations. *J. Immunol. Meth.* **50,** 39–49.

8 Liossis, S. N., Ding, D. Z., Dennis, G. J., and Tsokos, G. C. (1998) Altered pattern of TCR/CD3-mediated protein-tyrosyl phosphorylation in T cells from patients with systemic lupus erythematosus. Deficient expression of the T-cell receptor zeta chain. *J. Clin. Invest.* **101 ,** 1448–1457.

9. Laemmli, U. K. (1970) Cleavage of structural proteins during the assembly of the head of bacteriophage T4. *Nature* **227,** 680–685.

4

TCR ζ-Chain Abnormalities in Human Systemic Lupus Erythematosus

Madhusoodana P. Nambiar, Sandeep Krishnan, Vishal G. Warke, and George C. Tsokos

Summary

A growing number of studies have revealed that the expression of many genes is abnormal in T lymphocytes of patients with systemic lupus erythematosus (SLE). Although aberrant expression of signaling molecules may arise intrinsically or in response to the environment, these abnormalities play a significant role in the pathogenesis of this autoimmune disease. Modern research on lymphocyte signaling abnormalities in SLE has been directed toward identifying defective expression of various signaling molecules, understanding the molecular basis of the deficiency, and dissecting the T-cell signaling abnormalities that result from abnormal gene expression. The developments suggest that interplay of abnormal transcriptional factor, aberrant messenger RNA processing/editing, ubiquitination, proteolysis, oxidative stress, and changes in chromatin structure invariably contribute to the abnormal expression of numerous signaling molecules in SLE T cells. The contribution of each of these mechanisms in the abnormal expression of signaling molecules in SLE T cells is not known. In addition to abnormalities in gene expression, multiple factors, including altered cellular distribution of the protein, rewiring of the receptor, modulation of membrane clustering, and lipid raft distribution of signaling molecules and defective signal-silencing mechanisms play a key role in delivering the anomalous T-cell receptor/CD3-mediated intracellular calcium response in SLE T cells. The optimized methods and protocols described here pertaining to TCR ζ-chain expression and related T-cell signaling abnormalities can be very well applied to other molecules aberrantly expressed in SLE T cells.

Key Words: Chromatin immunoprecipitation; cloning and sequencing; electroporation; flow cytometry; gene expression; immunoprecipitation; lipid rafts; nuclear extract; RT-PCR; signaling molecules; T-cell signaling.

From: *Methods in Molecular Medicine, Vol. 102: Autoimmunity: Methods and Protocols*
Edited by: A. Perl © Humana Press Inc., Totowa, NJ

1. Introduction

1.1. TCR ζ-Chain

The T-cell receptor (TCR) ζ-chain is a vital T-cell signaling molecule that is considered the limiting factor among the eight subunits of the TCR in receptor assembly, transport, and surface expression and is crucial to receptor signaling function ***(1,2)***. The ζ-chain transcript is generated as the spliced product of eight exons separated by distances of 0.7 to more than 8 kb ***(3)***.

The ζ-chain exists in multiple forms and membrane fractions with distinct functions in antigen (Ag)-mediated signaling process. In addition to the soluble 16-kDa unphosphorylated form, the detergent-soluble fraction of TCR ζ-chain includes the phosphorylated p21- and p23-kDa forms and mono- and polyubiquitinated forms. The detergent-insoluble membrane fraction includes the actin cytoskeleton-bound form and lipid raft-associated forms of the TCR ζ-chain. Systemic lupus erythematosus (SLE) T cells display low levels of p16, p21, and 23-kDa and detergent-insoluble membrane-bound forms of the TCR ζ-chain. In contrast, ubiquitinated forms of the ζ-chain are high in SLE T cells.

We reported that the levels of residual TCR ζ-chain associated with lipid rafts and the membrane clustering of the TCR ζ-chain are significantly increased in SLE T cells. A majority of patients with SLE also display decreased expression of TCR ζ-chain messenger RNA (mRNA) ***(4,5)***.

1.2. Applications

Discovery of abnormal expression of genes in SLE is important for identification of the molecules that may predispose to aberrant immune responses to autoantigens and cause pathologic autoantibody production. Studies of abnormal gene expression will unfold the pathologic mechanisms behind abnormal T-cell functions in SLE. Identification of underlying genetic, molecular, and biochemical mechanisms will provide novel targets for future pharmacological intervention and complement existing therapeutic modalities. In the coming years, gene expression studies are expected to define a molecular signature with respect to genes and signaling for immune cells in patients with SLE, which may dictate treatment.

1.3. Study Design

When applying these methods to study other signaling molecules, it is important to design the study to analyze various forms and fractions of the molecules by using antibodies that can bind to multiple forms rather than one structural epitope. Normal T cells or autoimmune disease controls such as rheumatoid arthritis, Sjögren's syndrome, Still's disease, limited systemic sclerosis, mixed connective tissue disorder, antiphospholipid syndrome, and dermatositis can

be used as controls for SLE. Similarly, when the size of the molecule of interest and endogenous controls are significantly different, it is reasonable to combine the antibodies when probing the immunoblots to reduce experimental time and too much stripping of blots. Samples taken on different dates can be compared by normalizing the data against a proper internal control.

Studies showed that, in addition to abnormal expression of key signaling molecules, the downstream signaling molecules that associate and participate in signaling function are altered in SLE T cells. Accordingly, it is important to include studies of downstream signaling molecules and their function in SLE T cells by TCR activation using antibodies or by non-receptor-mediated stimulation using phorbol-12-myristate 13-acetate/ionomycin. Abnormalities in signaling molecules should be correlated with the SLE disease activity index, current medication, and demographics (race, gender, age) to distinguish abnormalities intrinsic to the disease from those associated with disease activity. If possible, it is also a good idea to request that patients not take any medication at least 24 h before drawing the blood sample to reduce the effects of medication. To confirm the results further, the study should be designed to follow up the patients over a period of 3–4 yr, during which the SLE disease activity will improve considerably.

2. Materials

In addition to the materials described in Chapter 3, the materials described here are required.

2.1. Electrophoretic, Western Transfer, Immunoblotting, and Immunoprecipitation Reagent

Blotto nonfat dry milk (Santa Cruz Biotechnology, Santa Cruz, CA) is used as a reagent.

2.2. Antibodies

2.2.1. Staining Antibodies

1. Anti-CD3ε, clone M-20 (Santa Cruz Biotechnology).
2. Anti-CD3ζ, carboxy terminal binding antibody, clone C-20 (Santa Cruz Biotechnology).
3. Anti-FcRγ (Upstate Biotechnology, Waltham, MA).
4. Anti-linker for activated T cells (LAT), clone-FL-233 (Santa Cruz Biotechnology).
5. Antiactin, clone-I-19 (Santa Cruz Biotechnology).

2.2.2. Isotype Controls

1. Goat immunoglobulin G (IgG) (Santa Cruz Biotechnology).
2. Rabbit IgG (Santa Cruz Biotechnology).
3. Mouse IgG (Santa Cruz Biotechnology).

2.2.3. Blocking Antibodies

Human IgG (Sigma Aldrich, St Louis, MO) was used for blocking antibodies.

2.2.4. Secondary Fluorescent-Labeled Antibodies

All the immunoglobulins have minimum crossreactivity with bovine, chicken, goat, guinea pig, Syrian hamster, horse, human, mouse (except three), rat, and sheep IgG.

1. Tetramethylrhodamine isothiocyanate (TRITC)-labeled donkey antirabbit IgG (H + L) (Jackson ImmunoResearch Lab, West Grove, PA).
2. TRITC-labeled donkey antigoat IgG (H + L) (Jackson ImmunoResearch Lab).
3. Fluorescein isothiocyanate (FITC)-labeled antimouse IgG (H + L) (Jackson ImmunoResearch Lab).
4. FITC-labeled donkey antirabbit IgG (H + L) (Jackson ImmunoResearch Lab).

2.2.5. Secondary HRP-Labeled Antibodies

1. Goat antirabbit IgG-HRP (Santa Cruz Biotechnology).
2. Antigoat IgG-HRP (Santa Cruz Biotechnology).
3. Antimouse IgG-HRP (Santa Cruz Biotechnology).

2.3. Kits

1. RNeasy mRNA isolation kit (Qiagen Inc., Valencia, CA).
2. Reverse transcriptase polymerase chain reaction (RT-PCR) kit (Promega Corp., Madison, WI).
3. Plasmid miniprep isolation kit (Qiagen Inc.).
4. Nucleoporation kit (Amaxa Corp., Köln, Germany).

2.4. RT-PCR, Gene Expression Analysis

1. Ethidium bromide (Sigma Aldrich).
2. Seakem gametic technology grade (GTG) agarose (FMC BioProducts, Rockland, ME).
3. Taq polymerase (Promega Corp.).
4. PCR beads (Amersham Pharmacia, Piscataway, NJ).
5. X-gal (Sigma-Aldrich).

2.5. Density Gradient Centrifugation and Protein Concentration

1. Sucrose (Bio-Rad, Hercules, CA).
2. Trichloroacetic acid (TCA) (Sigma Aldrich).
3. Sodium chloride (Sigma Aldrich).
4. Morpholino ethane sulfonic acid (MES) (Sigma Aldrich).
5. Brij58 (Sigma Aldrich).
6. Triton X-100 (Fisher Scientific, Suwanee, GA).
7. Acetone (Fisher Scientific).

2.6. Flow Cytometry and Fluorescence Microscopy Reagents

1. FACS tubes, 12 × 75 mm polypropylene test tubes without cap (Fisher Scientific).
2. Polylysine-coated Poly Prep slides (Sigma Aldrich).
3. Pap pen with normal large tip (Electron Microscopy Sciences, Washington, PA).
4. Cover glasses that are 22 × 22 mm by 0.13–0.17 mm thick (VWR Scientific, Buffalo Grove, IL).
5. Gel/Mount™ (Biomedia Corp., Hayward, CA).
6. Colorless nail polish from any local store.
7. Saponin (Sigma Aldrich).
8. Digitonin (Sigma Aldrich).
9. Glycine (Bio-Rad).

2.7. Instruments

1. Dounce homogenizer (Fisher Scientific).
2. Beckman ultracentrifuge and SW41 rotor (Palo Alto, CA).
3. Flow cytometer, model FACSCalibur (Becton Dickinson, San Jose, CA).
4. PCR machine, T3 thermocycler (Biometra, Heidelberg, Germany).
5. Confocal microscope, Bio-Rad Radiance 2100, ×10–×100 (Bio-Rad; Laser Sharp 2000 software)
6. Olympus model IX70 fluorescence microscope (OPELCO, Dulles, VA).
7. Nucleoporator (Amaxa Corp.).
8. Sonicator (Fisher Scientific).

3. Methods

3.1. Biochemical Analysis of Abnormalities in T-Cell Signaling Molecules

3.1.1. Preparation of Cytoplasmic Extract and Detergent-Insoluble Cell Membrane Extract of SLE T Cells

1. Take 5 million cells in a 1.5-mL microfuge tube and add 100 μL of freshly prepared NP-40 cell lysis buffer (working solution for 1 mL, 500 μL stop buffer 2X, 483 μL water, 5 μL 0.5 *M* ethylenediaminetetraacetic acid [EDTA], 1 μL aprotinin, 1 μL 5 mg/mL leupeptin; 5 μL 0.2 *M* PMSF; 5 μL 200 m*M* sodium vanadate containing 1% Nonidet P-40 (Sigma Aldrich).
2. Vortex the cell lysate in the cold room for 1 h.
3. Centrifuge the sample at 18,000*g* for 10 min at 4°C in a microfuge.
4. Separate the cytoplasmic extract from the detergent-insoluble membrane pellet and store it at –80°C.
5. Wash the detergent-insoluble membrane pellet two times with 100 μL lysis buffer and freeze at –80°C until use.

3.1.2. Preparation of Nuclear Extracts

1. Take 5 million T cells in a 15-mL conical tube and centrifuge at 400*g* for 5 min.
2. Wash cells with 10 mL phosphate-buffered saline (PBS) or TBS and transfer it into a microfuge tube; centrifuge at 18,000*g* for 15 s.
3. Remove the TBS and resuspend the cell pellet in 400 mL cold buffer A (10 m*M* HEPES at pH 7.9, 10 m*M* KCl, 0.1 m*M* EDTA, and 0.1 m*M* EGTA) by gentle pipetting using microtips. Freshly add 1 μL 1 *M* dithiothreitol [DTT], 10 μL 50 m*M* PMSF, and 0.5 μL aprotinin for 1 mL of buffer A. Prepare 1 *M* stock solution of DTT by adding 1.09 g DTT in 20 mL of 0.01 *M* sodium acetate at pH 5.2, filter, and store as 1-mL aliquots at –20°C.
4. Allow the cells to swell on ice for 15 min.
5. Add 25 mL of 10% Nonidet-P40 and vigorously vortex the tube for 10 s.
6. Centrifuge the homogenate for 30 s at 18,000*g* in a microfuge tube at 4°C.
7. Resuspend the nuclear pellet in 40 μL of ice-cold buffer C (20 m*M* HEPES at pH 7.9, 0.4 m*M* NaCl, 1 m*M* EDTA, and 1 m*M* EGTA). Freshly add 1 μL 1 *M* DTT, 20 μL 50 m*M* PMSF, and 0.5 μL aprotinin for 1 mL of buffer C.
8. Vigorously rock the tube at 4°C for 45 min on a shaking platform.
9. Centrifuge the nuclear extract for 5 min in a microfuge tube at 4°C.
10. Freeze the supernatants in aliquots at –80°C.
11. Estimate the protein using Bio-Rad protein assay reagent as described in Chapter 3, **Subheading 3.2.2.2.**

3.1.3. Separation of Proteins by Polyacrylamide Gel Electrophoresis and Western Blotting

Proteins (10–15 μg) were separated by sodium dodecyl sulfate-polyacrylamide gel electrophoresis (SDS-PAGE) or NuPAGE (Invitrogen, Carlsbad, CA) gel electrophoresis under reducing conditions and Western blotted to PVDF membranes as described in Chapter 3, **Subheading 3.2.2.3.**

3.1.3.1. Gel Electrophoresis of Detergent-Insoluble Membrane Fraction

The detergent-insoluble membrane pellet from 5 million cells was solubilized by mechanical agitation and sonication in the presence of 4% SDS in the loading buffer. The mixture was boiled for 20 min in sample buffer containing 4% SDS and centrifuged; the supernatant was loaded to gels ***(6,7)***.

3.1.3.2. Immunoblotting

1. Unlike phosphotyrosine blotting, the blocking solution for immunoblotting with signaling proteins is 5% milk in PBS or TBS.
2. After 1 h blocking, discard the blocking solution, transfer the membrane to a plastic bag, and seal the four sides.
3. Cut a corner of the plastic bag and add N-terminal or C-terminal TCR ζ-chain antibody (1:1000) diluted in 5 mL fresh blocking solution, reseal, and incubate at room temperature for 2–3 h in a nutator.

4. Remove the membrane from the plastic bag and wash as described earlier.
5. Incubate the membrane in a plastic bag with 5 mL blocking solution for 1 h with antimouse HRP secondary antibody followed by three washes of PBST and one wash with PBS as described in Chapter 3, **Subheading 3.2.2.6.** before development. The blots were developed using ECL reagents as described above.

3.1.4. Western Blot Stripping and Reprobing

1. Membranes were stripped with immunopure stripping buffer (Pierce Chemical Co., Rockford, IL) for 90 min at room temperature.
2. The membranes were washed with PBS or TBS, blocked, and immunoblotted with control antibody or other antibodies of interest as described in **Subheading 3.1.3.2.**

3.1.5. Immunoprecipitation

1. Lyse 20 million cells in 250 μL lysis buffer and prepare the cytoplasmic extract as described in **Subheading 3.1.2.**
2. Preclear the cell lysate by adding protein A/G agarose/Sepharose by adding 25 μL of 50% slurry and incubate at 4°C for 10 min on a rocker or orbital shaker.
3. Remove the protein A/G agarose beads by centrifugation at 14,000*g* at 4°C for 10 min and transfer the supernatant to a fresh tube.
4. Add 10 μg of CD3ε antibody and mix for 2 h or possibly overnight at 4°C on a rocker or orbital shaker.
5. Capture the immunocomplex by adding 25 μL protein A or protein G agarose/Sepharose bead slurry (50% slurry) by gently rocking in a rocker or orbital shaker for 2 h or overnight at 4°C.
6. Collect the agarose/Sepharose beads by centrifugation for 15 s at 18,000*g*.
7. Discard the supernatant and wash the beads three times with 25 μL lysis buffer.
8. Resuspend the agarose in 2X sample buffer, mix, and boil for 5 min before loading to SDS-PAGE or NuPAGE.
9. Western blot the samples to PVDF membranes and immunoblot with TCR ζ-chain antibody or antibodies to downstream signaling molecule as described in **Subheading 3.1.3.2.**

3.1.6. Estimation of Lipid Raft-Associated TCR ζ-Chain

The functionally important lipid raft-associated form of the TCR ζ-chain is quantitated by treating the SLE T cells with cholesterol-solubilizing agent methyl-β-cyclodextrin, which disrupts lipid rafts. The increase in the amount of TCR ζ-chain in the detergent-soluble fraction after treatment corresponds to the lipid raft-associated form of TCR ζ-chain. We have successfully applied this method to SLE T cells and discovered that the residual TCR ζ-chain is more associated with the lipid rafts in T cells of patients with SLE ***(4,8)*** (**Fig. 1A**).

1. Pipet 5 million cells into two microfuge tubes and resuspend in 1 mL of culture medium without serum.
2. T cells are treated with or without 30 m*M* methyl-β-cyclodextrin (Sigma Aldrich) for 30 min at 25°C.

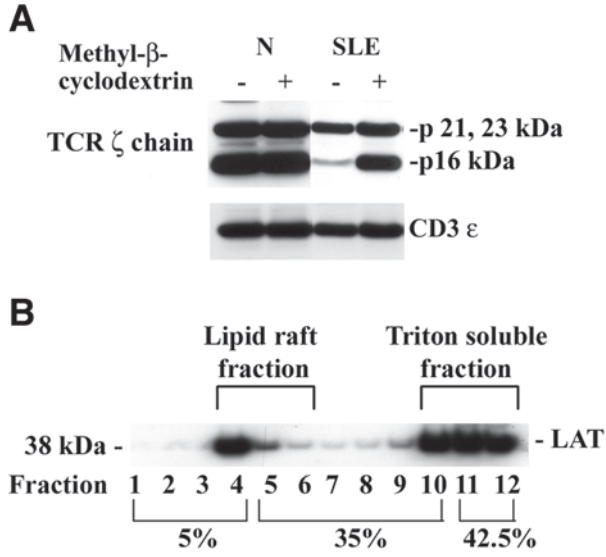

Fig. 1. **(A)** Analysis of the membrane lipid raft-associated and actin cytoskeleton-associated forms of the TCR ζ-chain in SLE T cells. **(A)** SLE T cells were treated with the lipid raft-disrupting agent methyl-β-cyclodextrin for 30 min. The cells were lysed, and the detergent-soluble and detergent-insoluble fractions were collected by centrifugation, separated by SDS-PAGE, transferred, and blotted with the TCR ζ-chain C-terminal monoclonal antibody (MAb). On treatment with methyl-β-cyclodextrin, the increased level of the p16 and p21 23-kDa forms of the TCR ζ-chain in the detergent-soluble fraction represent lipid raft-associated TCR ζ-chain. Densitometric analysis showed that, in SLE T cells, the lipid raft-associated TCR ζ-chain is increased compared to normal donors. **(B)** Sucrose density gradient analysis showing distribution of LAT in raft and nonraft fractions; 100×10^6 cells were lysed with a lysis buffer containing 1% Brij58 and fractionated by discontinuous sucrose gradient. Immunoblot analysis of LAT was performed with an equal volume of cell lysate from each fraction. Raft and nonraft fractions were as indicated.

3. Lyse cells in 1% NP-40 lysis buffer as described above and centrifuge at 18,000*g* for 10 min at 4°C.
4. The detergent-soluble and insoluble fractions were electrophoretically separated in a 12% gel and transferred to PVDF membranes (Millipore, Bedford, MA). The membranes were immunoblotted with TCR ζ-chain C-terminal antibody and other relevant antibodies and developed as described in **Subheading 3.1.3.2.**

3.1.7. Lipid Raft Isolation

Lipid raft and associated proteins can be isolated from T cells using density gradient centrifugation in an ultracentrifuge ***(9,10)***.

1. T cells (25 million) are pelleted and lysed in 1 mL of 1% Brij58 or 0.2% Triton X-100 lysis buffer (0.2% Triton X-100 or 1% Brij58 in MES-buffered saline [MBS] buffer [25 m*M* MES, 150 m*M* NaCl, pH 6.5], supplemented with 1 m*M* sodium orthovanadate, 2 m*M* EDTA, 1 m*M* PMSF, and 1 μg/mL aprotinin). The lysis buffer is prepared as follows for 200 mL stock solution: 2 g 1% Brij58 or 400 μL 0.2% Triton X-100 400, 1.0665 g 25 m*M* MES, 1.743 g 150 m*M* NaCl. Freshly add 800 μL 2 m*M* EDTA of 0.5 *M*, 1 m*M* Na_3VO_4, 1 m*M* PMSF, and 1 μg/mL aprotinin.
2. Homogenize the cell lysate with 15 strokes of loose-fitting Dounce homogenizer and incubate on ice for 30 min.
3. Mix the lysate with an equal volume of 85% sucrose and placed at the bottom of a 12-mL ultracentrifuge tube. Sucrose gradient solutions are 85% w/v sucrose in MBS (42.5 g in 50 mL MBS), 35% w/v sucrose in MBS (17.5 g in 50 mL MBS), and 5% w/v sucrose in MBS (2.5 g in 50 mL MBS).
4. Place a step gradient of 6 mL of 35% sucrose and 4 mL of 5% sucrose solution containing 1 m*M* Na_3VO_4 and 2 m*M* EDTA on top of the lysate.
5. Centrifuge samples for 18–22 h at 200,000*g* (39,000 rpm) at 4°C using a SW-41 rotor in a Beckmann ultracentrifuge.
6. Collect 1-mL fractions starting from the top with a 1-mL pipet (12 fractions). The 1-mL samples can also be collected from the bottom by carefully piercing the bottom of tube using a syringe needle.
7. When 1-mL samples are collected from the top, fractions 4 and 5 contain the cloudy band and are indicative of rafts, and fractions 11 and 12 are soluble fractions (**Fig. 1B**).

3.1.8. Concentration of Proteins in Lipid Raft Fractions by TCA Precipitation

This step is optional and may be required to concentrate proteins from the fractions, especially if using fewer cells.

1. Add 250 μL of 100% TCA (add 350 mL water to 500 g TCA; store at room temperature).
2. Mix and incubate on ice for 10 min.
3. Centrifuge in a microfuge at 18,000*g* for 5 min.
4. Remove the supernatant carefully, leaving behind the white pellet.
5. Wash the pellet twice with 200 μL cold acetone by resuspending and spinning in the microfuge at 18,000*g* for 5 min.
6. Air-dry the pellet for 5–10 min to dry residual acetone.
7. Add 2X SDS-PAGE sample buffer with reducing agent (5% 2-mercaptoethanol or 0.1 *M* DTT), boil for 10 min, and load on SDS-PAGE.

3.2. Molecular Biology Studies of Signaling Molecule in SLE T Cells

3.2.1. Reverse Transcriptase Polymerase Chain Reaction

3.2.1.1. Isolation of mRNA

1. Lyse 5×10^6 cells in 600 μL RLT buffer supplied with Qiagen RNeasy minikit (Qiagen Inc.). If not used immediately, the sample can be frozen at –80°C for several months.
2. Homogenize the samples by centrifugation at 18,000*g* for 2 min in a Qiashredder.
3. Add 600 μL of 70% ethanol to the homogenized lysate and mix well by pipetting.
4. Apply 700 μL of the sample to RNeasy minicolumn placed in a 2-mL collection tube and spin at 8000*g* for 15 s. Discard the filtrate, reload the remaining sample, and spin again.
5. Add 700 μL of buffer RW1 to the RNeasy column and spin at 8000*g* for 15 s. Discard the flowthrough and collection tube.
6. Transfer RNeasy column to a new 2-mL collection tube and pipet 500 μL buffer RPE; centrifuge the tube at 18,000*g* for 15 s. Discard the flowthrough.
7. Add 500 μL RPE buffer to the RNeasy column and centrifuge at 18,000*g* for 1 min.
8. Transfer the RNeasy column to a new 1.5-mL collection tube. Pipet 50 μL RNase-free water directly onto the RNeasy silica gel membrane. Centrifuge at 8000*g* for 1 min. Keep the 30–40 μL RNA recovered from the column and immediately place on ice.

3.2.1.2. Estimation of the Amount of Total RNA

1. Dilute 2 μL RNA into 100 μL of RNase-free water.
2. Transfer 100 μL of the diluted RNA to a quartz cuvet and read the absorbance ratio at 260–280 nm in a Amersham Pharmacia UVSpec spectrophotometer.
3. Optical density (OD) value × 40 (factor for RNA) × 50 (dilution) = μg/mL of RNA.

3.2.1.3. Reverse Transcription

1. Take 500 ng total RNA in 10 μL water and add 1 μL of oligo$(dT)_{15}$ primer. Heat the sample for 5 min at 65°C and cool at room temperature.
2. Prepare 9.1 μL reactions by adding 4 μL of 25 m*M* $MgCl_2$, 2 μL of 10X reverse transcription buffer, 2 μL 10 m*M* deoxyribonucleotide triphosphates, 0.5 μL recombinant RNasin ribonuclease inhibitor, and 0.6 μL AMV reverse transcriptase (15 units). Add the mix to the RNA samples. For multiple samples, a master mix should be prepared excluding the RNA, which has to be added at the end.
3. Incubate the samples at 45°C for 15–60 min.
4. Heat the samples at 95°C for 5 min and immediately cool on ice. The single-stranded cyclic DNA can be stored at –80°C if necessary.

3.2.1.4. Polymerase Chain Reaction

1. On ice, prepare 47-μL reaction in a thin-wall, 0.5-mL PCR tube by adding 5 μL 10X PCR buffer, 3 μL 25 m*M* $MgCl_2$ (final concentration 1.5 m*M*), 2 μL 10X dNTPs, 1 μL 10 pmol TCR ζ-chain forward primer and 1 μL 10 pmol TCR ζ-chain reverse primer 34 μL water, and 1 μL Taq DNA polymerase (2.5 units); add 2 μL of the reverse transcription product.
2. Place a drop of paraffin oil on the top.
3. Set up PCR conditions in a Biometra thermocycler as follows: 94°C denaturation for 5 min, followed by 36 cycles at 94°C for 1 min, 67°C annealing for 1 min, 72°C extension for 2 min, and a final extension at 72°C for 7 min.

3.2.1.5. Agarose Gel Electrophoresis

1. Run 12 μL of samples mixed with 3 μL of 5X loading buffer in 1.2% Seakem agarose gel using 1X Tris-borate-EDTA buffer.
2. Stain the sample with 5 μL of ethidium bromide (10 mg/mL) and visualize under ultraviolet illuminator or Bio-Rad gel imaging station. Ethidium bromide can also be included in the gel just before casting. Alternatively, the gels can be stained with 5 μL SYBRGreen in 50 mL TE buffer (Molecular Probes, Eugene, OR), which is 100-fold more sensitive and less mutagenic than ethidium bromide.

3.2.1.6. TA Cloning

To identify mutations on the TCR ζ-chain gene, the PCR products can be cloned in a TOPO TA cloning vector (Invitrogen). Recombinant clones (5–10) should be sequenced to identify mutations.

1. Take 1 μL PCR product and clone to TOPO TA cloning kit (Invitrogen) according to manufacturer's instructions.
2. Transform 2 μL of the PCR product to competent cell supplied in the kit as suggested and plate 50- and 100-μL samples in two LB agar plates containing 100 μg/mL ampicillin and X-gal.
3. Grow 12 white recombinant colonies in 5 mL LB medium containing 100 μg/mL ampicillin.
4. Prepare miniprep plasmids from 12 white recombinant colonies using Qiagen plasmid miniprep kit.
5. Digest 1 μg of the purified plasmid with EcoRI and analyze by agarose gel electrophoresis and ethidium bromide staining to verify the presence of inserts.

3.2.1.7. DNA Sequencing

1. Take 5 μL (500 ng) of the plasmid in a thin-wall PCR tube.
2. Mix with 1.6 pmol M13 reverse or T7 primer.
3. Cycle sequence on an ABI 377 sequencer using an ABI dye terminator cycle sequencing kit (ABI PRISM, Applied Biosystems Inc., Foster City, CA) system as described by the manufacturer.
4. Analyze sequences using the Lasergene (DNASTAR, Madison, WI) software program.

3.2.2. Real-Time PCR

1. The reaction is set up in 25 μL volume using PCR beads from Amersham Pharmacia.
2. Add 0.2 μL of 2X diluted single-stranded cyclic DNA obtained by reverse transcription to the PCR beads.
3. Add 1 μL of 100X diluted SYBRGreen and adjust the volume to 25 μL using nuclease-free water.
4. Transfer the sample to 25-μL real-time PCR cuvets (VWR Scientific) and briefly spin in a microfuge to remove any air bubbles.
5. Tightly cap the tube and place it on a SmartCycler (SmartCycler™, Cepheid, Sunnyvale, CA).
6. Run the PCR under the following conditions: 94°C denaturation for 1 min, followed by 45 cycles of 94°C for 15 s, 67°C annealing for 15 s, 72°C extension for 30 s.
7. Analyze samples based on the fluorescence cycle threshold (Ct) differences between various times compared to their controls. Also analyze samples based on the difference between the numbers of cycles at 50% fluorescence. A temperature denaturation curve should be simultaneously analyzed to verify for specific products.
8. The sample can also be run on agarose gel electrophoresis to verify for specific products.

3.2.3. mRNA Stability Assay

SLE T cells can be treated with 10 μg/mL actinomycin D to arrest RNA synthesis and can be incubated for different times. At the end of each period, the total RNA is isolated, and RT-PCR or real-time PCR is carried out as described above. The decrease in the level of TCR ζ-chain mRNA at different times compared to 0 time gives an indication of mRNA stability.

3.2.4. Electroporation

After several modifications of the electroporation method, we established this method to transfect primary T cells routinely with 25–30% efficiency ***(11,12)***. The technique is mainly based on making the T cells more electrocompetent by incubating the peripheral blood mononuclear cells (PBMCs) overnight at 37°C in culture medium in the presence of 1 μg/mL phytohemagglutinin. T cells are isolated from the PBMCs on the next day as described in **Subheading 2.** and transfected.

1. Incubate the PBMCs overnight at a density of 3×10^6/mL in RPMI-1640 containing penicillin/streptomycin and 10% fetal bovine serum (FBS) or autologous serum and 1 μg/mL phytohemagglutinin for 18–20 h.
2. Isolate T cells by negative selection of non-T cells using MACS separation as described in Chapter 3, **Subheading 3.1.2.**

3. Resuspend 5 × 10^6 to 20 × 10^6 of the purified T cells in 500 μL Opti-MEM medium and transfer to a Gene Pulser cuvet (Bio-Rad).
4. Add plasmid DNA (10–15 μg) and mix gently.
5. Electroporate the cells at 300 V/1000 μF in a Bio-Rad electroporator at room temperature.
6. Transfer the cells to a 15-mL conical tube; wash with prewarmed culture medium and resuspend in AIM-V (Invitrogen, Carlsbad, CA) medium. Electroporated cells are incubated in the presence of 10 U interleukin 2/mL at 37°C for 48–72 h for optimum gene expression.

3.2.5. Nucleofection

Nucleofection is a technique that introduces the DNA directly to the nucleus. It has a great advantage in that it is not necessary to activate or manipulate the cells before nucleofection. Nucleofection works well with 1–5 μg DNA.

1. Add 0.5 mL supplement to 2.25 mL Nucleofector solution and mix gently (stable for 3 mo at 4°C). Prewarm the nucleofector solution to room temperature.
2. Prepare 6-well plates by pipetting 3.5 mL of culture medium and preincubate the plates at 37°C.
3. Transfer 5 × 10^6 cells to an Eppendorf tube, centrifuge, and discard the supernatant so that no residual medium covers the cell pellet.
4. Resuspend the pellet in 100 μL Nucleofector solution at room temperature.
5. Immediately add 5 μg DNA. The cell number can be increased up to 20 × 10^6 cells, but the DNA should be kept at 5 μg. An increased concentration of DNA can lead to decreased transfection efficiency
6. Transfer the sample into an Amaxa certified cuvet, avoid air bubbles, and close the cuvet with a blue cap.
7. Insert the cuvet into the cuvet holder and rotate the turning wheel clockwise to the final position.
8. Select program U-14 and press the X key to start the program; the display should show OK.
9. Remove the samples from the cuvet immediately after the program has finished using the plastic pipets provided. To transfer the cells, add 0.5 mL prewarmed culture medium to the cuvet and then pipet the cells to the prepared 6-well plate.
10. Incubate the cells in a humidified 37°C/5% CO_2 incubator.

3.2.6. Chromatin Immunoprecipitation Assay

The chromatin immunoprecipitation assay (ChIP) is a powerful technique to analyze the amount of TCR ζ-chain transcription factor, Elf-1, or acetylated histones bound to the promoter DNA in live SLE T cells.

3.2.6.1. Preparation of Salmon Sperm DNA-Blocked Sepharose Protein A/G

1. Incubate 10 μg/μL sonicated salmon sperm DNA at 45°C for 10 min.
2. Wash 50 μL (50% slurry) of Sepharose protein A/G two times with blocking buffer (10 m*M* Tris-HCl, 150 m*M* NaCl, 1m*M* EDTA, 0.05% NaN_3 at pH 7.5).

3. Resuspend the beads in 100 μL blocking buffer and add 1.2 μL of 10 μg/μL salmon sperm DNA and 3 μL of 10 mg/mL bovine serum albumin.
4. Incubate in the cold room overnight in an orbital or rotating shaker.

3.2.6.2. Crosslinking of the Cells and Preparation of Cell Extract

1. Take 1×10^6 T cells. Activate the cells as you wish.
2. Add 1/37 volume of 37% formaldehyde to the cells and mix immediately. Close the cap and incubate the cells 20 min at 37°C.
3. Add 1–2 vol of ice-cold PBS to cells to stop the reaction. Spin down the cells at 2000 rpm for 5 min.
4. Wash cells twice with ice-cold PBS.
5. Lyse the cells in an Eppendorf tube at room temperature in lysis buffer (50 m*M* Tris-HCl, 10 m*M* EDTA, 1% SDS at pH 8.1; just before use, add 1 m*M* PMSF, 1 μg/mL aprotinin, and 1 μg/mL leupeptin) at 1×10^6 cells/200 μL. Incubate on ice for 10 min.
6. Sonicate samples on ice five times, with the duration of each burst 10 s at continuous output and with a 30-s pause between each burst.
7. Spin cells at 1500 rpm for 15 min at 4°C. Transfer the supernatant to another tube and discard the pellet.
8. Freeze the sample at –70°C or proceed with immunoprecipitation.

3.2.6.3. Chromatin Immunoprecipitation

1. Thaw the frozen sample and add 1.8 mL of ChIP dilution buffer (0.01% SDS, 1.1% Triton X-100, 1.2 m*M* EDTA, 16.7 m*M* Tris-HCl at pH 8.1, 167 m*M* NaCl; just before use, add the protease inhibitors).
2. To reduce nonspecific background, preclear the 2 mL diluted sample with 80 μL of salmon sperm DNA-blocked protein A/G Sepharose bead (50% slurry). Incubate the samples 1 h at 4°C, shaking in a nutator.
3. Pellet the protein A/G agarose by centrifugation at 18,000*g* for 30 s and transfer the supernatant to a new tube.
4. Add TCR ζ-chain transcription factor, Elf-1 antibody (6–12 μg/2 mL) and incubate overnight with shaking at 4°C. For a negative control, use a no antibody or isotype control antibody immunoprecipitation by incubating the supernatant fraction with 60 μL PBS or with isotype control antibody.
5. Add 60 μL of salmon sperm-blocked protein A/G Sepharose bead (50% slurry) to each sample and incubate at 4°C for 2 h or overnight.
6. Centrifuge the samples at 18,000*g* for 30 s and discard the supernatant.
7. Wash the protein A/G Sepharose/antibody/Elf-1 complex for 5 min on a rotating platform twice with 1 mL of low-salt immune complex wash buffer.
8. Wash the protein A/G Sepharose/antibody/Elf-1 complex for 5 min on a rotating platform once with 1 mL of lithium chloride wash buffer.
9. Wash the protein A/G Sepharose/antibody/Elf-1 complex for 5 min on a rotating platform twice with 1 mL of 1X Tris-EDTA buffer.

10. Resuspend in 100 μL Tris-EDTA buffer containing 0.5% SDS.
11. Digest the sample with 0.5 μL of proteinase K (20 mg/mL) for 2 h at 45°C.
12. Reverse crosslink the protein from DNA by incubating at 65°C for 4–6 h.
13. Extract the DNA using a Qiagen DNA purification kit.
14. Amplify the DNA by PCR using the TCR ζ-chain promoter forward primer 5' CCA TCG AGA ACT TGT ATT TG 3', –307 to –288 sense bps, and reverse primer 5' GCC CTA CCT GTA ATC GG 3', +129 to +113 antisense bps, according to the numbering of Rellahan et al. ***(13)***, or using two primers located approx 300 bp apart.

3.2.7. ChIP to Detect the Binding of Phosphorylated Transcription Factors

The ChIP protocol can also be exploited to analyze the level of phosphorylated transcription factor bound to promoter DNA by first immunoprecipitation with antiphosphotyrosine antibody and then with the antibody of interest.

1. Immunoprecipitate the cell lysates with antiphophotyrosine antibody 4G10 (12 μL per 2 mL) or antiphosphoserine and antiphosphothreonine for 1 h and capture with 80 μL (50% slurry) of protein A/G Sepharose.
2. Elute the antiphosphotyrosine immunoprecipitates from the protein A/G Sepharose beads by incubating with 10 m*M* phenyl phosphate in lysis buffer containing 1% NP-40 at 4°C for 15 min.
3. Reprecipitate phosphotyrosine-immunoprecipitated samples with the antibody of interest, and the ChIP assay is continued as described above.

3.3. Cell Biology Studies of Signaling Molecules in SLE T Cells

Expression of signaling molecules can be determined using fluorescence labeling and flow cytometry technologies. Similarly, distribution of a particular signaling molecule in the cell can be analyzed by direct or indirect fluorescence microscopy. These techniques can be applied to nonpermeable and permeabilized cells to distinguish surface expression and intracellular expression, respectively.

3.3.1. Flow Cytometry

3.3.1.1. Flow Cytometry Using Nonpermeabilized Cells

The technique can be applied to molecules that have extracellular domains, and antibodies directed to the extracellular domain are readily available. For each assay, a sample with an isotype control of the primary antibody is required to determine the background binding. Before adding the antibodies, the nonspecific Fc receptor binding should be blocked using excess human IgG. It is important to precool the centrifuge and to perform the experiment at 4°C. When

discarding the solution after centrifugation, be careful not to disturb the small pellet, which may not be seen very clearly.

1. Transfer 1–2 million cells to flow cytometry tubes.
2. Centrifuge the cells at 400*g* at 4°C in a Sorvall tabletop centrifuge for 5 min.
3. Discard the media, resuspend the cells in 200 μL PBS, and centrifuge as in **step 2**. If any activation is required, it has to be done before adding paraformaldehyde using 10 μg/mL of OKT3 (Orthobiotech, Raritan, NJ) plus goat antimouse IgG (Santa Cruz Biotechnology).
4. Mildly fix the cell by adding 200 μL 0.1% paraformaldehyde in PBS and incubate in ice for 10 min.
5. Centrifuge the sample again as in **step 2** and discard the supernatant.
6. Resuspend the cells in 200 μL staining buffer, add 50-fold excess human IgG, and incubate on ice for 30 min.
7. Incubate the sample with 2 μg of the murine antihuman CD3ε or isotype control antibody for 30 min on ice.
8. Wash twice with 2 mL ice-cold staining buffer as in **step 2**.
9. Resuspend the sample in 200 μL staining buffer, add 50-fold excess human IgG to block the Fc receptor binding, and incubate with 2 μL of goat antimouse FITC-conjugated antibodies for 30 min on ice in the dark.
10. Wash three times with 2 mL staining buffer and resuspend in 200 μL PBS containing 1% paraformaldehyde and loaded onto the flow cytometer.

Levels of expression can be quantitated by either percentage of cells expressing the signaling molecule or by mean fluorescence intensity. If the cells are analyzed by flow cytometry using the same settings, the level of expression on different samples on different days can be normalized by adjusting against the readings of an untreated control ***(14)***.

3.3.1.2. Flow Cytometry Using Permeabilized Cells

Flow cytometry using permeabilized cells can be applied to the TCR ζ-chain or other signaling molecules that do not have substantial extracellular domains or antibodies directed to the extracellular domain. Flow cytometry using permeabilized cells will provide an estimate of the total level of expression of the TCR ζ-chain. For each assay, a sample with an isotype control of the primary antibody is required to determine the background binding. Before adding the antibodies, the nonspecific Fc receptor binding should be blocked using excess human IgG. It is important to precool the centrifuge and to perform the experiment at 4°C, except for permeabilization with detergents, which is done at room temperature. When discarding the solution after centrifugation, be careful not to disturb the pellet, which is tiny and may not be seen very clearly.

1. Transfer 1–2 million cells to flow cytometry tubes.
2. Centrifuge the cells at 400*g* at 4°C in a Sorvall tabletop centrifuge for 5 min.

3. Discard the media, resuspend the cells in 200 μL PBS, centrifuge as in **step 2**. Activate the cells if necessary at this stage using 10 μg/mL of OKT3 (Orthobiotech) plus goat antimouse IgG (Santa Cruz Biotechnology).
4. Mildly fix the cell by adding 200 μL 0.1% paraformaldehyde in PBS and incubate in ice for 10 min.
5. Centrifuge the sample again as in **step 2** and discard the supernatant.
6. Resuspend the cells in 200 μL digitonin or saponin permeabilization buffer and incubate at room temperature for 10 min.
7. Centrifuge as in **step 2**.
8. Suck off the supernatant, resuspend the cells in permeabilization buffer, and add 50-fold excess human IgG and incubate for 30 min on ice.
9. Incubate the sample with 2 μg of the murine antihuman TCR ζ- (6B1.02) or isotype control antibody for 30 min on ice.
10. Wash twice with 2 mL ice-cold staining buffer as in **step 2**.
11. Resuspend the sample in 200 μL permeabilization buffer, add 50-fold excess human IgG to block the Fc receptor binding, and incubate with 2 μL of goat antimouse FITC-conjugated antibodies for 30 min on ice in the dark.
12. Wash three times with 2 mL staining buffer and resuspend in 200 μL PBS containing 1% paraformaldehyde and loaded onto the flow cytometer.

Levels of expression can be quantitated by either percentage of cells expressing the signaling molecule or by mean fluorescence intensity. If the cells are analyzed by flow cytometry using the same settings, the level of expression on different samples on different days can be normalized by adjusting against the readings of an untreated control ***(14)***.

3.3.2. Fluorescence Microscopy

The distribution of the TCR ζ-chain in lymphocytes is visualized by fluorescence microscopy. Although not very quantitative, fluorescence microscopic images will also give a broad idea of the gross level of expression of the TCR ζ-chain (**Fig. 2A**). The cells can be permeabilized and stained in the tube or can be adhered to slides and stained. The staining procedure in the tubes results in increased recovery of the cells because T cells of patients with SLE do not attach well to the polylysine-coated slides. Appropriate markers like LAT or Cholera toxin B subunit can be used for localizing the TCR ζ-chain to lipid rafts. When double labeling, the TCR ζ-chain can be stained with PE-labeled secondary antibody, and markers can be labeled with FITC-labeled antibody. Isotype control is necessary to ensure specific staining.

1. Transfer 1–2 million cells to flow cytometry tubes.
2. Centrifuge the cells at 400*g* at 4°C in a Sorvall tabletop centrifuge for 5 min.
3. Discard the media, resuspend the cells in 100 μL PBS, and centrifuge as in **step 2**.
4. Mildly fix the cell by adding 100 μL 0.25% paraformaldehyde in PBS and incubate on ice for 10 min.

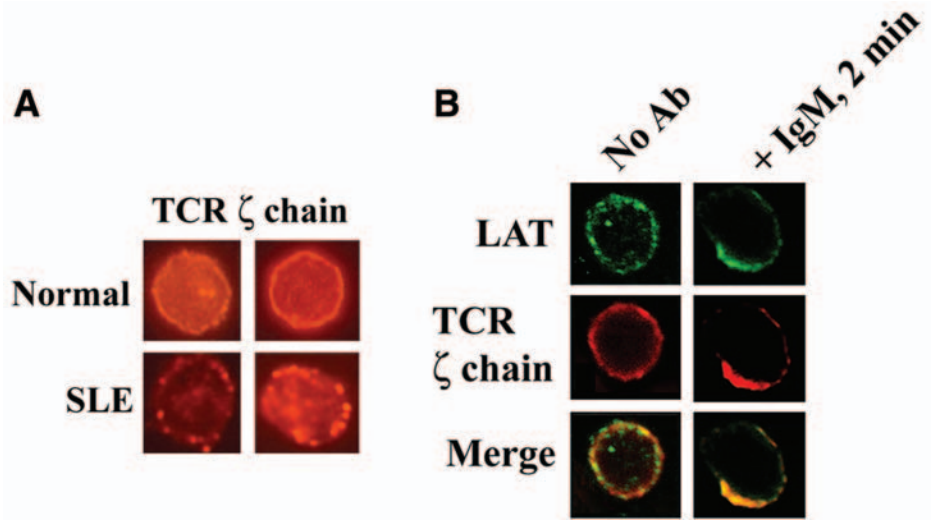

Fig. 2. Fluorescence microscopy of the TCR ζ-chain in SLE T cells showed increased clustering. **(A)** Two million T cells of patients with SLE or normal donors were fixed with 0.25% paraformaldehyde and permeabilized with digitonin. Cells were incubated with antimouse TCR ζ-chain C-terminal monoclonal antibody for 1 h and then washed in staining buffer. Rhodamine-labeled antimouse goat IgG secondary antibody was added, and the sample was incubated for 1 h. The cells were washed and mounted on slides, and the samples were visualized in an Olympus fluorescence microscope at ×100. Staining of the TCR ζ-chain was enhanced in SLE T cells to reveal the distribution. **(B)** Confocal microscopy of the TCR ζ-chain in SLE T cells. SLE T cells adhered on polylysine-coated slides by incubating for 1 h at room temperature. The cells were activated with anti-CD3-IgM (clone 2Ad2A2) at 37°C for 2 min. The reaction was stopped with 3% paraformaldehyde for 15 min, and cells were permeabilized with a buffer containing 0.05% saponin and the blocking antibody human IgG 1 μg. Cells were stained with anti-CD3ζ (clone C-20) and anti-LAT (clone FL-233) for 1 h at room temperature and counterstained with antigoat TRITC and antirabbit FITC, respectively for 30 min. Cells were washed; air-dried, and mounted using Gel/Mount. Coverslips were applied, and the edges were sealed with clear nail polish. Samples were analyzed with a laser scanning confocal fluorescence microscope with a 1 × 70 scope, Bio-Rad Lasersharp 2000 software. Unlike the normal T cells, preformed membrane clustering of the TCR ζ-chain in SLE T cells led to TCR capping within 2 min of activation.

5. Centrifuge the sample again as in **step 2** and discard the supernatant.
6. Resuspend the cells in 100 μL digitonin or saponin permeabilization buffer and incubate at room temperature for 10 min; centrifuge as in **step 2**.
7. Resuspend the cells in permeabilization buffer, add 50-fold excess human IgG, and incubate for 30 min.

8. Incubate the sample with 2 μg of the murine antihuman TCR ζ- (6B1.02) or isotype control antibody for 30 min on ice.
9. Wash twice with 2 mL ice-cold staining buffer as in **step 2**.
10. Resuspend the sample in 100 μL permeabilization buffer, add 50-fold excess human IgG to block the Fc receptor binding, and incubate with 2 μL of goat antimouse FITC-conjugated antibodies for 30 min on ice in the dark.
11. Wash three times with 2 mL staining buffer, resuspend in 20 μL Gel/Mount, and apply a drop on a glass slide; carefully place the coverslip, avoiding air bubbles, and seal the sides with nail polish. The slide is ready to view under a fluorescence microscope. Keeping the stained cells for a long time may lead to leakage of the stain.

3.3.3. Confocal Microscopy

Confocal microscopy can be used to determine the distribution of the expressed TCR ζ-chain at three dimensions in SLE T cells before and after activation (**Fig. 2B**). The microscope will take sectioned images of the stained cells, and the overall distribution of the TCR ζ-chain can be analyzed. Also, there is better resolution of the specimen by confocal microscopy because the laser is focused on a single plane, as opposed to the diffuse direction of the laser beam in fluorescence microscopy. An isotype control is required for both nonactivated and activated samples.

1. Make two circles on a polylysine-coated slide using the pap pen and add 1 million cells in 100 μL RPMI-1640 containing 1% FBS.
2. Place the slides in a box and keep the box at room temperature for 1 h to adhere the cells.
3. Activate the cells by OKT3 or anti-CD3 IgM antibody at 37°C for the time required. Clustering requires a short time activation of 2–3 min, whereas capping requires activation for 10 min.
4. Remove the medium by suction and fix the cells in 3.7% paraformaldehyde (dissolve 3.7% paraformaldehyde in approx 50 mL PBS, increase the pH using NaOH to dissolve, and readjust the final pH to 7.0 using 6*N* HCl and make up the volume to 100 mL) for 30 min. Alternatively, the cells can also be activated in a microfuge tube and then adhered to the polylysine-coated glass slides.
5. Wash with 200 μL PBS.
6. Permeabilize using 100 μL permeabilization buffer, add 50 μg of human IgG to block Fc receptor binding, and incubate at room temperature for 15 min.
7. Remove the permeabilization buffer and stain with anti-TCR ζ-chain antibody in 100 μL permeabilization buffer for 1 h along with excess human IgG at room temperature.
8. Wash three times, 5 min each, with 200 μL permeabilization buffer.
9. Stain with secondary FITC- or PE-labeled goat antimouse IgG in 100 μL permeabilization buffer containing excess human IgG for 30 min at room temperature.

10. Wash four times, 5 min each, with PBS at room temperature. This step is critical to remove any residual FBS, which can otherwise give high background. Dry the samples for 15 s.
11. Add a drop of Gel/Mount and place the coverslips carefully to avoid air bubble trapping. Seal the sides of the coverslips with nail polish and view the slide with an Olympus confocal microscope (1 × 70 scope, software, Bio-Rad LaserSharp 2000). Slides may be stored at 2–8°C for up to 5 d if necessary, and initial signals will be strong enough.

4. Notes

1. The N-terminal TCR ζ-chain antibody recognizes 16-kDa and ubiquitinated forms of the TCR ζ-chain. We demonstrated that the C-terminal antibody recognizes the phosphorylated p21- and p23-kDa form of the ζ-chain in addition to 16-kDa and ubiquitinated forms. Both the antibodies were able to detect a novel 14-kDa form of the TCR ζ-chain ***(4)***. It is important to run the detergent-soluble cytosolic fraction along with the detergent-insoluble membrane fraction to confirm ζ-chain deficiency rather than a translocation between compartments. Membrane translocation is one of the causes for decreased expression of the TCR ζ-chain in heat-shocked T cells ***(15)***. The membranes should be stripped and reprobed with control actin antibody to confirm equal loading and the integrity of the samples. If there is a variation of actin between samples, the expression of the TCR ζ-chain can be quantitated by densitometry and taking the ratio against the level of actin between samples.
   After a few experiments, immunoblotting can be done with two antibodies together if the molecular weight of the proteins is significantly different. Combining multiple antibodies will reduce the time of the experiment and the life of the membrane. The membranes can be stripped and reprobed approx 5–6 times with very highly reproducible results. Careful consideration should be given to some antibodies that do not strip well and may give background bands when probing with new antibodies. Stripping and reprobing the blot is also important to confirm ubiquitination, phosphorylation, or other modification of the molecule of interest. If the membranes are going to be reprobed for phosphotyrosine, this should be done last.
2. The increase in the amount of TCR ζ-chain in the detergent-soluble fraction after incubating with methyl-β-cyclodextrin was considered a lipid raft-associated fraction (**Fig. 1**). CD3ε or actin can be used as a control in this experiment. Similar to lipid raft-bound TCR ζ-chain, the actin-bound TCR ζ-chain can be estimated by treating the cells with or without 10 μ*M* cytochalasin D, which disrupts actin polymerization, leading to accumulation of the TCR ζ-chain in the detergent-soluble cytoplasmic fraction. An increase in the level of the TCR ζ-chain in the detergent-soluble fraction after 3 h treatment with cytochalasin D will provide an estimate of the actin-bound form of the TCR ζ-chain ***(6,16,17)***.
   If activation of cells is necessary for the experiments, it should be done before lysis of cells. A minimum of 25×10^6 cells is required for proper isolation of lipid

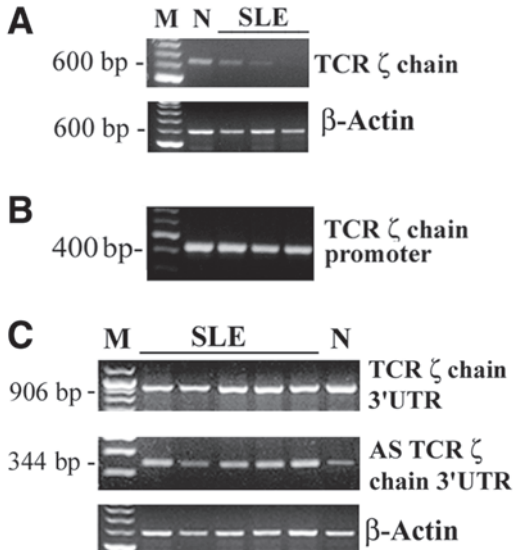

Fig. 3. RT-PCR analysis of the expression of TCR ζ-chain mRNA in normal donor and SLE T lymphocytes. **(A)** Total RNA was isolated from 5×10^6 T lymphocytes and reverse transcribed; the TCR ζ-chain was amplified by specific primers. The PCR products (15 μL) were electrophoresed in 1.2% agarose gel and visualized by ethidium bromide staining. M is the 100-bp DNA ladder molecular weight marker; N is the normal donor. **(B)** PCR amplification of TCR ζ-chain promoter from T cells of SLE and normal healthy control subjects. Genomic DNA was isolated from T lymphocytes or granulocytes, and the promoter region was PCR amplified using specific primers. The PCR products (10 μL) were electrophoresed in 1.2% agarose gel and visualized by ethidium bromide staining. **(C)** RT-PCR analysis of the expression of TCR ζ-chain mRNA 3(untranslated region SLE T lymphocytes. Total RNA was reverse transcribed, and the normal or alternatively spliced TCR ζ-chain mRNA 3(untranslated region or β-actin was amplified by specific primers. The PCR products (15 μL) were electrophoresed in 1.2% agarose gel and visualized by ethidium bromide staining. M is the 100-bp DNA ladder molecular weight marker; N indicates normal donor.

rafts. Very fine balancing of the tubes before centrifugation is required for good results. The buckets of rotors should be properly tightened; otherwise, the tube will flatten, and the vacuum will suck off the samples during centrifugation, resulting in loss of sample. Collection of the 1-mL fraction should be accurate; otherwise, it may lead to crosscontamination.

3. Five million SLE T cells yield approx 3 μg total RNA. If the OD 260 is very low, then decrease the dilution of the total RNA. A 260/280 OD ratio of 1.8 to 2.0 represents pure RNA.
   A control PCR using β-actin is necessary to evaluate the integrity and equal loading of the RNA (**Fig. 3**). If there is any variation of control β-actin, the level of

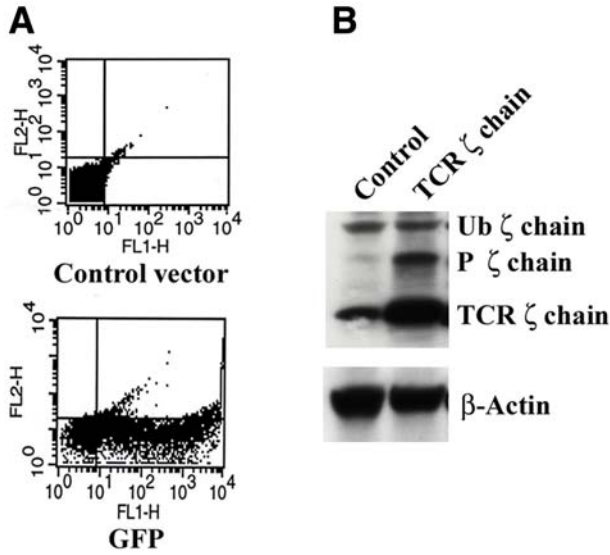

Fig. 4. Transfection and expression of TCR ζ-chain by nucleoporation in SLE T cells. **(A)** Analysis of transfection efficiency by nuceloporation in SLE T cells. SLE T cells were transfected by nucleoporation with a GFP expression plasmid or control β-galactosidase plasmid. After 18 h, the cells were directly analyzed for GFP expression by flow cytometry. A representative of five experiments using cells from different patients is shown. The transfection efficiency was 70–75%. **(B)** Analysis of TCR ζ-chain expression by Western blotting in nucleoporated SLE T cells. After 18 h, transfected cells (5×10^6) were lysed, and the detergent-soluble and detergent-insoluble fractions were collected. Protein from the detergent-soluble fraction (10 μg) was analyzed on 4–12% NuPAGE gel under reducing conditions, transferred to PVDF membrane, and immunoblotted with TCR ζ-chain C-terminal MAb. The membrane was stripped and reprobed with CD3ε MAb and β-actin antibody. The membrane was stripped and reprobed with β-actin antibody.

TCR ζ-chain mRNA should be normalized against the level of actin for comparison between samples. The primers (Genosys, The Woodlands, TX) for PCR amplification of TCR ζ-chain coding region are forward 5'AGC CTC TGC CTC CCA GCC TCT TTC TGA G 3' (35–62 sense bps) and reverse 5' TCA GTG GCT GAG AAG AGT GAA CCG GGT TG 3' (669–641 antisense bps according to numbering of ***18***) (**Fig. 3A**). Primers for amplifying the TCR z-chain promoter are as follows: forward primer, 5'CCA TCG AGA ACT TGT ATT TG 3',–307 to –288 sense basepairs; and reverse primer, 5'GCC CTA CCT GTA ATC GG 3', +129 to +113 antisense bps according to the numbering of Rellahan et al. ***(13)*** specific for TCR ζ-chain promoter (**Fig. 3B**). The primers for amplifying the TCR ζ-chain 3' untranslated region are as follows: forward primer, 5'CAG CCA

GGG GAT TTC CAC CAC TCA AAG 3' (567–592 sense basepairs); and reverse primer, 5'CCC TAG TAC ATT GAC GGG TTT TTC CTG 3' (1472–1443 antisense bps) (**Fig. 3C**). b-Actin is used as a control, and the primers are as follows: forward primer, 5'CAT GGG TCA GAA GGA TTC CT 3'; and reverse primer, 5'AGC TGG TAG CTC TTC TCC A 3'. Addition of excess SYBRGreen gives false-positive results in real-time RT-PCR.

Each clone should be sequenced from both the orientations to verify mutations. The presence of the same mutations in more than one clone distinguishes artifacts from mutations. A patient sample obtained a second time in a follow-up study can also be used to confirm mutations.

4. Enhanced green florescence protein cloned in pIRES2 vector (pIRES2-EGFP, Clontech, Palo Alto, CA) can be used as controls to determine the transfection efficiency (**Fig. 4A**). The nucleofection protocol routinely gives 70–75% transfection efficiency with enhanced green fluorescent protein. Following nucleofection, the TCR z-chain is expressed after 3 h, and an approx 10-fold increase in expression was observed after 12 h (**Fig. 4B**). More than 8 h incubation of purified T cells before transfection reduces the efficiency of transfection. If the cell number is decreased, then the culture volume can be reduced accordingly. Reduction in the volume of Nucleofector solution significantly reduces the transfection efficiency. To reuse the electroporation cuvettes, wash with bleach and rinse six times with water. Rinse with 95% ethanol twice, replace the cap, and dry upside down in the hood.

References

1 Weiss, A. and Littman, D. R. (1994) Signal transduction by lymphocyte antigen receptors. *Cell* **76 ,** 263–274.

2 Wange, R. L. and Samelson, L. E. (1996) Complex complexes: signaling at the TCR. *Immunity* **5,** 197–205.

3 Jensen, J. P., Hou, D., Ramsburg, M., Taylor, A., Dean, M., and Weissman, A. M. (1992) Organization of the human T cell receptor zeta/eta gene and its genetic linkage to the Fc gamma RII-Fc gamma RIII gene cluster. *J. Immunol.* **148,** 2563–2571.

4 Nambiar, M. P., Enyedy, E. J., Fisher, C. U., Krishnan, S., Warke, V. G., Gilliland, W. R., et al. (2002) Abnormal expression of various molecular forms and distribution of T cell receptor zeta chain in patients with systemic lupus erythematosus. *Arthritis Rheum.* **46,** 163–174.

5 Takeuchi, T., Tsuzaka, K., Pang, M., Amano, K., Koide, J., and Abe, T. (1998) TCR zeta chain lacking exon 7 in two patients with systemic lupus erythematosus. *Int. Immunol.* **10,** 911–921.

6 Caplan, S. and Baniyash, M. (1996) Normal T cells express two T cell antigen receptor populations, one of which is linked to the cytoskeleton via zeta chain and displays a unique activation-dependent phosphorylation pattern. *J. Biol. Chem.* **271,** 20,705–20,712.

7. Caplan, S. and Baniyash, M. (2000) Searching for significance in TCR–cytoskeleton interactions. *Immunol. Today* **21,** 223–228.

8 Abe, T., Toguchi, T., Takeuchi, T., Kiyotaki, M., and Homma, M. (1981) Mitogenic responses to lipopolysaccharide by B lymphocytes from patients with systemic lupus erythematosus. *Scand. J. Immunol.* **15,** 475–482.
9 Darlington, P. J., Baroja, M. L., Chau, T. A., Siu, E., Ling, V., Carreno, B. M., et al. (2002) Surface cytotoxic T lymphocyte-associated antigen 4 partitions within lipid rafts and relocates to the immunological synapse under conditions of inhibition of T cell activation. *J. Exp. Med.* **195,** 1337–1347.
10 Xavier, R., Brennan, T., Li, Q., McCormack, C., and Seed, B. (1998) Membrane compartmentation is required for efficient T cell activation. *Immunity* **8,** 723–732.
11 Herndon, T. M., Juang, Y. T., Solomou, E. E., Rothwell, S. W., Gourley, M. F., and Tsokos, G. C. (2002) Direct transfer of p65 into T lymphocytes from systemic lupus erythematosus patients leads to increased levels of interleukin-2 promoter activity. *Clin. Immunol.* **103,** 145–153.
12 Nambiar, M. P., Fisher, C. U., Kumar, A., Tsokos, C. G., Warke, V. G., and Tsokos, G. C. (2003) Forced expression of the Fc receptor gamma-chain renders human T cells hyperresponsive to TCR/CD3 stimulation. *J. Immunol.* **170,** 2871–2876.
13 Rellahan, B. L., Jensen, J. P., Howcroft, T. K., Singer, D. S., Bonvini, E., and Weissman, A. M. (1998) Elf-1 regulates basal expression from the T cell antigen receptor zeta-chain gene promoter. *J. Immunol.* **160,** 2794–2801.
14 Valensin, S., Paccani, S. R., Ulivieri, C., Mercati, D., Pacini, S., Patrussi, L., et al. (2002) F-actin dynamics control segregation of the TCR signaling cascade to clustered lipid rafts. *Eur. J. Immunol.* **32,** 435–446.
15 Nambiar, M. P., Fisher, C. U., Enyedy, E. J., Warke, V. G., Krishnan, S., and Tsokos, G. C. (2000) Heat stress downregulates TCR zeta chain expression in human T lymphocytes. *J. Cell Biochem.* **79,** 416–426.
16 Rozdzial, M. M., Malissen, B., and Finkel, T. H. (1995) Tyrosine-phosphorylated T cell receptor zeta chain associates with the actin cytoskeleton upon activation of mature T lymphocytes. *Immunity* **3,** 623–633.
17. Rozdzial, M. M., Pleiman, C. M., Cambier, J. C., and Finkel, T. H. (1998) pp56Lck mediates TCR zeta-chain binding to the microfilament cytoskeleton. *J. Immunol.* **161,** 5491–5499.
18. Weissman, A. M., Baniyash, M., Hou, D., Samelson, L. E., Burgess, W. H., and Klausner, R. D. Molecular cloning of the zeta chain of the T cell antigen receptor. *Science* **239,** 1018–1021.

5

Protein Kinase A and Signal Transduction in T Lymphocytes

Biochemical and Molecular Methods

Islam U. Khan and Gary M. Kammer

Summary

Abnormal T-cell effector functions in systemic lupus erythematosus (SLE) are present and may be associated with disease immunopathogenesis. Our work has led to the characterization of a signaling defect, involving protein kinase A (PKA), leading to abnormal T-cell effector functions in SLE. PKA is a component of the adenylyl cyclase/cyclic adenosine monophosphate/PKA (AC/cAMP/PKA) pathway, a principal signal transduction system in T cells. The aim of this chapter is to provide a comprehensive, technical, step-by-step approach to studying PKA function in T cells. The methods detailed here are (a) chromatographic fractionation of PKA-I and PKA-II isozymes and PKA phosphotransferase activity in purified T cell populations, (b) Western immunoblotting to identify the presence of regulatory (R)-subunit proteins of PKA, and (c) isolation of RNA, and quantification of PKA R subunit-specific transcripts by competitive polymerase chain reaction. Although our emphasis in the chapter is T cells, these methods may be useful for investigation of signaling via PKA in other cell types as well.

Key Words: Cloning; competitive PCR; FPLC; protein kinase A; sequencing; signal transduction; SLE; T cells; Western blotting.

1. Introduction

Current evidence supports the concept that altered signal transduction in T lymphocytes of subjects with the autoimmune disease systemic lupus erythematosus (SLE) is present and may be associated with disease immunopathogenesis ***(1)***. Rather than a single signaling defect, however, SLE T cells appear to express multiple abnormalities that span the proximal, middle, and distal

From: *Methods in Molecular Medicine, Vol. 102: Autoimmunity: Methods and Protocols*
Edited by: A. Perl © Humana Press Inc., Totowa, NJ

segments of the signaling pathway. Because signaling research in SLE is still in early development, insufficient information is currently available to determine whether certain signaling defects will be identified in subpopulations of lupus subjects and whether particular defects might be associated with specific clinical manifestations of the disease or organ involvement. However, in the near term, it seems likely that future research will focus on the identification of new signaling defects and further characterization of current signaling defects with relation to gene expression and, ultimately, abnormal T-cell effector functions in SLE.

The initial signaling abnormality in SLE T cells was identified in the cyclic adenosine monophosphate (cAMP)/protein kinase A (PKA) pathway ***(2)***. This report led to the identification of impaired cAMP-dependent protein phosphorylation ***(3)*** because of deficient PKA isozyme activities ***(4,5)***.

The aim of this chapter is to provide a comprehensive, technical, step-by-step approach to studying PKA function in T lymphocytes. Although our emphasis is the T lymphocyte, these methods may be useful for investigation of signaling via PKA in other cell types as well.

2. Materials

2.1. Fractionation of PKA Into PKA Isozymes and PKA Phosphotransferase Assay

1. Buffer A: 10 m*M* K_2HPO_4 and 1 m*M* ethylenediaminetetraacetic acid (EDTA). Bring pH to 7.2 with H_3PO_4, filter through 500-mL vacuum filter, and degas for 20 min with stir bar, tapping container to release bubbles.
2. Buffer B: Buffer A + 1 *M* NaCl. Bring pH to 7.2 with H_3PO_4, filter through 500-mL vacuum filter, and degas for 20 min with stir bar, tapping container to release bubbles.
3. HiTrap Q columns, 1 mL (Amersham Pharmacia, Piscataway, NJ).
4. cAMP stock (10^{-2} *M*) (Sigma, St. Louis, MO) is diluted to a final concentration of 10^{-4} *M*, which is the working solution of cAMP.
5. Reaction mix (5 mL total): 0.5 mL of 400 m*M* Tris-HCl + 10 m*M* ethyleneglycoltetraacetic acid (EGTA) at pH 7.2.; 0.5 mL 200 m*M* $MgCl_2$; 1.0 mL 1 m*M* Kemptide (Sigma); 1.0 mL 2.5 mg/mL bovine serum albumin (BSA; Sigma); 2.0 mL dH_2O.
6. [^{32}P] adenosine triphosphate (ATP) mix: 44 µL 10% 2 m*M* ATP (Sigma); 6.6 µL 1.5% [^{32}P]ATP; bring to 440 µL with distilled (d)H_2O.
7. PKA type I isoenzyme (PKA-I) standard (Sigma).

2.2. Western Immunoblotting

1. Tris-HCl-buffered saline-Tween (TBS-T): 100 m*M* Tris-HCl at pH 7.6, 500 m*M* NaCl, 0.1% Tween-20.
2. Blocking buffer: TBS-T + 1% BSA.

Primary antibodies: anti-PKA-RI, -RIIα and -RIIβ monoclonal antibodies (MAbs) (Transduction Laboratories, Lexington, KY).
Secondary antibody: horseradish peroxidase (HRP)-labeled antimouse antibody (Amersham Life Science, Piscataway, NJ).

2.3. Genetic

1. Random primer (Amersham Pharmacia).
2. M-MLV H^- reverse transcriptase (Gibco BRL, Gaithersburg, MD).
3. Neutral DNA fragments (BamHI/EcoRI fragment of V-erb B; Clone Tech, Palo Alto, CA).
4. PKA RIα and RIβ subunit-specific MIMICs (synthesized as described in **Subheading 3.4.1.**).
5. Taq polymerase and other PCR reagents (PerkinElmer-Cetus, Emeryville, CA).
6. DNA thermal cycler (PerkinElmer-Cetus).
7. HAEIII-digested øx174 DNA (Gibco BRL).
8. DNA sequencer (ABI Prism 377; Applied Biosystems; Foster City, CA).
9. pCR2.1-TOPO vectors and TOP10 chemically competent cells (Invitrogen, Carlsbad, CA).
10. Wizard Plus DNA purification system (Promega, Madison, WI).

3. Methods

The following methods describe (a) fast protein liquid chromatography (FPLC) by the GradiFrac method to separate the type I and type II PKA isozymes (PKA-I and PKA-II); (b) the PKA phosphotransferase assay for quantification of PKA-I and PKA-II isozyme activities; (c) Western immunoblotting to quantify the regulatory (R)-subunit (i.e., RIα, RIβ, RIIα, and RIIβ) protein content of PKA-I and PKA-II isozymes; (d) construction of PKA RIα- and RIβ-subunit MIMICs for competitive polymerase chain reaction (C-PCR); (e) quantification of RIα and RIβ transcripts; and (f) cloning and sequencing of PKA RIα complementary DNA (cDNA) and genomic DNA from human T lymphocytes.

The PKA isozymes are partially purified by FPLC (GradiFrac; Amersham Pharmacia Biotech, Piscataway, NJ) using HiTrap Q columns, anion monobead exchange columns.

3.1. GradiFrac Control Settings

1. Control unit UV-1: Knob set to 0.5, switch set to “range AU.”
2. Pump P-50: Flow rate adjustments will be made using the control panel on the fraction collector.
3. Chart recorder: Chart speed set to 5 mm/min, blue pen range set to 10 mV, and red pen range set to 1 V.

For operation, the valve settings of the GradiFrac are shown in **Fig. 1**.

Fig. 1. Valve settings of the GradiFrac.

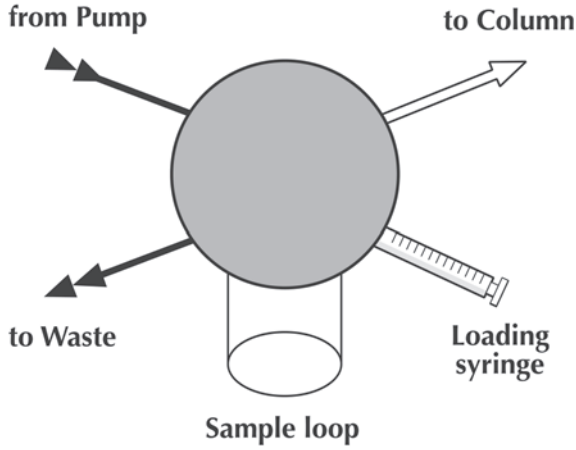

Fig. 2. Schematic representation of the tubing connection on the main port of the GradiFrac.

The wash valve setting is used during washing of the tubing and column. The flow is from the pump directly to waste (**Fig. 2**). It is useful for flushing the tubing prior to use of the column. The flow rate can be set to high for fast flushing because the flow is not going through the column.

The load is the setting for normal operation (**Fig. 1**). The flow is from the pump to the column, bypassing the sample loop (**Fig. 2**). This is also the position used when loading the sample from the syringe into the sample loop ("LOAD" means to load the sample into the loop).

The injection (INJ) is the setting that moves the sample out of the sample loop and onto the column (**Fig. 1**). The flow is from the pump, through the sample loop, and to the column (**Fig. 2**). Although it seems counterintuitive, INJ is *not* the setting that the sample is injected from the syringe into the sample loop. LOAD is used to load the sample into the sample loop, and INJ is used for the pump to inject the sample onto the column.

Starting the system and cleaning and equilibrating the column are performed as follows:

1. Turn on the power to the pump. The RUN light should come on. On the control panel at the front of the fraction collector, press the down arrow until it reads MANUAL RUN. Press ENTER. The display should now read CONC %B. Leave it at 0 and press ENTER. The display should now read FLOW in milliliters/minute. Enter 0.5 and press ENTER. The pump will now start. The display should now read FRACTN ml (FRACTN = fraction). After 10–20 min, press the up arrow until the display reads CONC %B. Enter 1 and press ENTER; 1% B means 10 mM NaCl. Move the valve to INJ (injection) to allow the buffer flow to flush the sample loop.
2. Insert the blue and red pens into their respective holders on the chart recorder and press the buttons to move the pens to the down position. Turn on the power to the recorder.
3. After 10–20 min or when the blue pen is steady, first move the valve back to LOAD to close the sample loop. Then, press the up arrow until the display reads CONC %B. Enter 100 and press ENTER; 100% B means 1 M NaCl. Let it run at 1 M NaCl to clean any previous sample that is still retained in the column. Although HiTrap Q columns can be reused, we recommend that these disposable columns be changed after each usage.
4. When the blue pen has returned to baseline, press the up arrow until the display reads CONC %B. Enter 1 and press ENTER. Let it flow through the column until several column volumes have passed through and the blue pen has settled to baseline. The column should now be equilibrated at 10 mM NaCl. Adjust the chart recorder pens so that the red pen is at the 1% line and the blue pen is at the 10% line.
5. Add six or seven small glass tubes to the collection rack. Rotate the tray, and position the arm on the fraction collector over the first tube. Press the down arrow until the display reads FRACTN ml. Enter 5 and press ENTER. Allow a few milliliters (it does not need to be the full 5 mL) to flow into the collection tube. This is to flush the tubing leading from the fraction control switch to the tubes. Press the up arrow until the display reads FRACTN ml. Enter 0 and press ENTER. Rotate the tray until the arm is over a clean tube. Discard the first tube.
6. To load the sample, press PAUSE. Move the valve to INJ and remove the syringe. Fill the syringe with buffer A (from a separate container), then eject it into waste to flush the syringe. Add the blunt-end needle to the syringe. Draw the sample into the syringe. Optimally, 1 mg of T-cell lysate is used for the chromatographic separation. If the sample volume is small, more buffer may be drawn into the syringe. Do not exceed 2 mL volume in the syringe as the sample loop capacity is 2 mL. Remove the needle and then flick out any air bubbles from the syringe. Screw the syringe back onto the valve. Move the valve back to LOAD. Push the plunger in to load the sample into the sample loop. Press CONTINUE to start the buffer flow again. Move the valve to INJ to begin the flow through the

sample loop. After 10–15 min, when the entire sample has moved onto the column, move the valve back to LOAD for normal operation. Label six 2.0-mL tubes for aliquots (three for each fraction). Keep the tubes on ice.

7. To elute fractions, wait until the blue pen has settled to baseline. Fraction I, which contains the PKA-I holoenzyme, can then be eluted. Press the up arrow until the display reads CONC %B. Enter 20 and press ENTER; 20% B means 200 mM NaCl. The red pen should move up to the 20% line. Press the down arrow until the display reads FRACTN ml. Enter 5, but do not press ENTER yet. Fraction collection will not begin until the ENTER button is pressed. At a rate of 0.5 mL/min, the first fraction will elute in around 8–9 min.
8. Typically, right before the first peak begins to come off, the blue pen will dip slightly below the baseline. When the blue pen begins to move up, press ENTER to begin collecting the fraction. The blue pen will make a tick mark at the beginning of the fraction. While it is collecting, you may press the up arrow to return to the FRACTN ml display and enter 0. The fraction will continue collecting until ENTER is pressed. Typically, fraction 1 will require more than 5 mL to collect the entire peak. The blue pen will make a tick mark at the 5-mL point but will continue collecting until 0 mL is entered. If more than 5 mL is required and the collection tube is full, simply rotate the tray to the next tube and continue collecting the fraction.
9. To stop collecting the first fraction, press ENTER to enter 0 mL. Rotate the tray to the next tube. Remove the tube(s) containing fraction 1 and put on ice. If it is in more than one tube, then pool them together into a 15-mL tube on ice. Pipet the fraction up and down several times to ensure that it is thoroughly mixed. Aliquot the fraction into the labeled tubes and immediately store at –70°C. When the blue pen has returned to baseline, press the up arrow to return to FRACTN ml. Enter 5 and press ENTER. Allow a few milliliters to flush the tubing leading to the fraction collector. Press the up arrow and enter 0 mL to stop the collection. Rotate the tray to the next tube and discard the first one.
10. When the second fraction (fraction 2, predominantly PKA-II holoenzyme) is ready for collection, press the up arrow until the display reads CONC %B. Enter 40 and press ENTER; 40% B means 400 mM NaCl. The red pen should move up to the 40% line. Press the down arrow until the display reads FRACTN ml and enter 5, but do not press ENTER until ready to begin collecting the second fraction. Typically, the blue pen will also dip slightly right before the second peak begins to come off. When the blue pen begins to move up, press ENTER to start collecting the fraction. The blue pen will make a tick mark. Press the up arrow and enter 0, but do not press ENTER until ready to stop collecting the fraction.
11. Usually, 5 mL is sufficient to collect all of fraction 2. The blue pen will make a tick mark after 5 mL have been collected. Press ENTER to stop the collection. Rotate the tray and remove the tube containing fraction 2. Place the tube on ice. Pipet the fraction up and down several times to ensure that it is thoroughly mixed. Aliquot the fraction into the labeled tubes and immediately store at –70°C.

12. Press the up arrow and enter 100% B. Let it flow at 1 M NaCl to clean any remaining protein on the column. When the blue pen has come back down, enter 0% B. Let it flow at 0% NaCl so that no salt will remain in the pump (buffers containing salt may damage the pump after long periods of time). At the end of fractionation, press the red END button to stop the pump. Turn off the power button on the pump. Move the pens to the up position and remove them. Replace the pen caps so they will not dry out. Press the recorder ON/OFF button to stop the recorder. Press the down arrow button on the chart recorder to feed the paper quickly.

A typical chromatogram of PKA-I and PKA-II separation from T-cell lysate by FPLC using an anion exchange column is shown in **Fig. 3**.

3.2. PKA Assay

PKA phosphotransferase activity is quantified by measuring the transfer of phosphate-32 from [γ-^{32}P]ATP to the synthetic heptapeptide (Kemptide), leu-arg-arg-ala-**ser**-leu-gly (**Table 1**).

In a separate tube, add 20 µL "hot" [^{32}P]ATP mix to 180 µL dH_2O. Add 20 µL of this to two scintillation vials (for duplicates) to count the isotopic standard. Keep the tubes in a rack on ice while mixing. Add the components to the tubes, saving [^{32}P]ATP mix for last. Vortex to mix. Then, incubate in a 30°C oscillating water bath for 5 min.

Return the tubes to the ice. Add 100 µL stop solution (2.5% BSA + 0.02% sodium deoxycholate) to each tube. Vortex to mix. Add 3 mL wash solution (0.86% H_3PO_4) to each tube. Vortex to mix. Set up the vacuum apparatus with presoaked Whatman P81 filter paper circles (Fisher, Pittsburgh, PA). Add the tube contents to the filters and be careful to disperse the contents over the entire filter. Incubate on filters for 5 min. Add 5 mL wash solution to the empty tubes. After the 5-min incubation, open the valves to drain for 1 min. Close the valves, then add the wash solution from the tubes. Incubate for 5 min to wash the filters. Again, drain for 1 min. Repeat this wash three more times, then drain and allow the filters to dry under the vacuum flow for 15 min. Transfer the filter papers to scintillation vials. Add 5 mL EcoLite scintillation fluid (ICN, Irvine, CA). Measure in a scintillation counter.

3.3. Western Immunoblotting of PKA R-Subunit Proteins

The purity of PKA holoenzyme after FPLC is regularly monitored by Western immunoblotting. The presence of RI and RII subunits of PKA in the chromatographic eluate is determined by a method detailed in **ref. *7***. Briefly, the fraction 1 (eluate from 200 m*M* extraction, predominantly PKA-I holoenzyme) and fraction 2 (eluate from 400 m*M* extraction, predominantly PKA-II holoen-

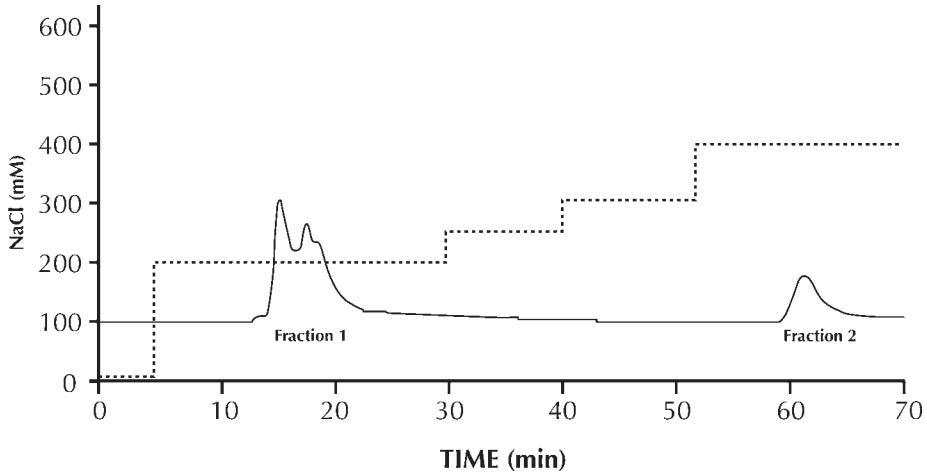

Fig. 3. FPLC elution profile of PKA isozymes at 280 nm; 1 mg of T-cell lysate is loaded onto a Mono Q column and eluted with a discontinuous NaCl gradient. The dotted line represents the molarity of NaCl at the peaks representing fraction 1 and fraction 2.

zyme) are desalted and concentrated through a Centricon-30 filter (Amicon, Beverly, MA), lyophilized, and reconstituted in water to a concentration of 1 μg/μL. Twenty μg of protein is used for sodium dodecyl sulfate-polyacrylamide gel electrophoresis (SDS-PAGE) analysis for the presence of PKA R-subunit proteins. The samples are boiled in Laemmli's sample buffer, followed by loading onto a 10% one-dimensional SDS-PAGE gel.

To determine the molecular weight of R-subunit proteins, molecular weight standards (Amersham) are also loaded on the gel. The gel is run for approx 5 h at a constant current of 35 mA. The proteins are transferred to the polyvinylidene fluoride (PVDF) membrane (Millipore, Bedford, MA) for 1 h at 1 A using a Bio-Rad transblot apparatus (Hercules, CA).

The whole procedure of immunoblotting is performed in an Autoblot microhybridization oven (Bellco Glass Inc., Vineland, NJ) at room temperature. After protein transfer, the membrane is incubated with rotation for 1 h in blocking buffer and then followed by two washings with TBS-T for 15 min each and by one 5-min washing with TBS-T. The membrane is incubated with any of the primary antibody (1:1000 dilution in blocking buffer) for 1 h, followed by three washings as before. After washing, the membrane is incubated with secondary antibody (1:3000 dilution in blocking buffer) for 1 h. Thereafter, the membrane is washed three times with TBS-T as before.

Table 1
Quantification of PKA Phosphotransferase Activity

PKA isozyme	cAMP	Tube no.	Distilled H_2O (μL)	Sample (μL)	Reaction mix (μL)	cAMP (μL)	[^{32}P] ATP mix (μL)
Type I	–	1	20	60	100	—	20
	–	2	20	60	100	—	20
	–	3	20	60	100	—	20
	+	4	—	60	100	20	20
	+	5	—	60	100	20	20
	+	6	—	60	100	20	20
Type II	–	7	20	60	100	—	20
	–	8	20	60	100	—	20
	–	9	20	60	100	—	20
	+	10	—	60	100	20	20
	+	11	—	60	100	20	20
	+	12	—	60	100	20	20
	–	13	60	20	100	—	20
PKA-I	–	14	60	20	100	—	20
standard	–	15	60	20	100	—	20
(Sigma)	+	16	40	20	100	20	20
(1 μg/μL)	+	17	40	20	100	20	20
	+	18	40	20	100	20	20

Immunoblots are developed using Western Lightning enhanced chemiluminescence (ECL) reagents (PerkinElmer Life Sciences, Boston, MA). The blot is usually probed by PKA-RI MAb first; this MAb detects both RIα and RIβ subunits. To detect the presence of RIIα and RIIβ, the blot is first stripped with 20 m*M* glycine (pH 2.0) solution at 50°C in a microhybridization oven for 30 min, followed by three washings with TBS-T. The remainder of the procedure is as described in **Subheading 3.3.** A representative blot is shown in **Fig. 4**, demonstrating the presence of RIα- and RIβ-subunit proteins in fraction 1 and RIIα- and RIIβ-subunit proteins in fraction 2.

3.4. Isolation of Genomic DNA, RNA, and cDNA Synthesis

Genomic DNA and total cellular RNA are extracted from 10×10^6 T lymphocytes using standard protocols *(7)*. Single-stranded cDNA (sscDNA) is synthesized from 1–2 μg of total RNA using random primers (Amersham Pharmacia) and Maloney-Murine leukemia virus ribonuclease (M-MLV) H^- reverse transcriptase, according to the manufacturer's instructions (Gibco BRL).

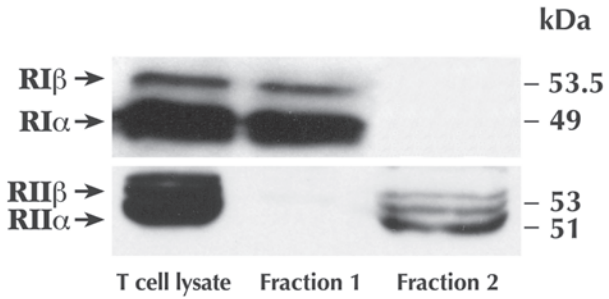

Fig. 4. Immunoblot of T-lymphocyte PKA R-subunit proteins. Nuclei-free T-cell lysate is partially purified by FPLC. Fractions 1 and 2 (each 20 μg), along with the T-cell lysate (150 μg), are loaded on the same gel. RI-subunit proteins are identified by anti-RI MAb. The same blot is stripped, and RII-subunit proteins are identified by anti-RIIα and anti-RIIβ MAbs. The blot confirms that there is almost no contamination of RII-subunit proteins in fraction 1 and no contamination of RI-subunit proteins in fraction 2.

3.4.1. Construction of PKA RIα- and RIβ-Subunit MIMICs for C-PCR

Neutral 580-bp DNA fragments (BamHI/EcoRI fragment of V-erb B; Clone Tech) are used to construct RIα- and RIβ-subunit MIMICS. Composite primers containing RIα- and RIβ-subunit gene-specific primer sequences and 20 nucleotides that hybridize to the neutral DNA fragments are designed using the Oligomer version 5.0 program (Molecular Biology Insights, Cascade, CO) *(7)*. RIα and RIβ subunit-specific MIMICs are generated by selecting neutral DNA fragment regions containing an identical GC content of the amplified RIα- or RIβ-subunit segments and by using RIα and RIβ subunit-specific composite and gene-specific primers in PCR amplification of neutral DNA fragments.

The size of RIα and RIβ MIMICs is adjusted to 353 and 535 bp long, respectively, by choosing appropriate sequences along the neutral DNA fragment as the primer template to distinguish RIα and RIβ PCR products of 227 and 342 bp long, respectively. This yields neutral DNA fragments with RIα or RIβ gene-specific sequences incorporated at the ends and designated as RIα and RIβ MIMICs. Molar quantities of these MIMICs are calculated, diluted with MIMIC dilution solution (50 μg/mL of ultrapure glycogen) to a concentration of 100 attomol/μL, and used as stock solution for internal standards (MIMICs) to quantify RIα and RIβ transcripts using C-PCR.

The use of MIMICs containing the same primer sequences and identical proportions of GC content in the amplified RIα- or RIβ-subunit segments make it possible to quantify transcripts of each subunit in cDNA samples more accu-

rately because MIMICs and RIα or RIβ are amplified with equal efficiencies. In a series of experiments, we used the following concentrations of RIα- and RIβ-subunit MIMICs as internal standards along with equal quantities of cDNA samples because the RIα- and RIβ-subunit transcripts were within this range.

3.4.2. Quantification of RIα and RIβ Transcripts

The twofold dilutions of MIMICS mentioned in **Subheading 3.4.1.** are spiked into PCR reaction tubes containing equal amounts of cDNA samples (10% of sscDNA synthesized from 1 μg of total cellular RNA) and 25 pmol of each primer, 1X PCR buffer (10 m*M* Tris-HCl at pH 8.3, 50 m*M* KCl), 200 m*M* of each deoxynucleotide 5'-triphosphate, 25 m*M* $MgCl_2$, 1.25 U of Taq polymerase, and double-distilled water to a final volume of 50 μL. The reaction mixtures are overlaid with mineral oil (Sigma) or PCR gems (PerkinElmer-Cetus) and subjected to 30 cycles of denaturation at 94°C for 1 min, primer annealing (temperature dependent on primer pair) for 2 min, and extension at 72°C for 3 min plus 2 s added for each cycle utilizing a DNA thermal cycler (PerkinElmer-Cetus).

Amplified RIα and its MIMIC and RIβ and its MIMIC are distinguished by electrophoresing in a 2% agarose gel and staining with ethidium bromide because the MIMICs and the RIα- and RIβ-specific PCR products have different basepair lengths. Gels are photographed using an ultraviolet transilluminator and 667 Polaroid film. The amount of RIα and/or RIβ is estimated by comparing with different concentrations of known standard (MIMIC) and identifying which concentration of standard matches that of the gene product ***(7)***.

3.5. Oligonucleotide Primers for PCR Amplification

Oligonucleotide primers for the PKA RIα coding region corresponding to nucleotides 285–679 have been designed based on published sequences ***(8)*** using the Oligomer version 5.0 program and synthesized by Sigma Genosys (Woodlands, TX).

3.5.1. Amplification of PKA RIα cDNA

cDNAs are amplified as follows: Each reaction mixture consists of 10% of a single sscDNA reaction, 25 pmol of each primer, 1X PCR buffer (10 m*M* Tris-HCl at pH 8.3, 50 m*M* KCl), 2.5 m*M* $MgCl_2$, 200 μM of each deoxynucleotide 5'-triphosphate, 1.25 U of Taq polymerase (PerkinElmer-Cetus), and double-distilled water to a final volume of 50 μL. The reaction mixture is subjected to 30 cycles of denaturation (94°C, 1 min), primer annealing (51°C, 1 min) for 2 min, and extension for 3 min at 72°C plus 2 s added for each cycle utilizing a DNA thermal cycler. Then, 5 μL of reaction mixture is analyzed on a 2% agarose gel in Tris-HCl/acetate/EDTA buffer. One μg of HAEIII-digested

øx174 DNA (Gibco BRL) is used as molecular weight markers: 1353, 1078, 872, 603, 310, and 234 bps. PCR products are purified using the Wizard Plus purification system (Promega, Madison, WI). Specific gene amplification is confirmed by sequencing of PCR products by an automatic DNA sequencer (ABI Prism 377).

3.5.2. Cloning and Sequencing of PKA RIα cDNA and Genomic DNA

The amplified products of the PKA RIα coding region corresponding to positions 285–679 are cloned and sequenced as follows: PCR products are t-tailed with Taq polymerase, cloned into the pCR2.1-TOPO vector according to the manufacturer's instructions (Invitrogen), and sequenced using T7, M13 primers and an ABI-377 sequencer. Genomic DNA samples are amplified using exon-specific primer sets as described in **ref. *6***. Amplified products of exons 3, 4, and 6 are sequenced directly from purified PCR products. Because exon 5 is only 58 bp long, we have subcloned the PCR products of this exon into pCR2.1-TOPO cloning vectors and sequenced using an automated DNA sequencer.

4. Notes

1. We always use a fresh HiTrap column for each separation. During the chromatographic separation of type I and type II PKA isozymes, we always wash the HiTrap column after the elution of fraction 1 with a gradual increase of NaCl (from 250 to 300 m*M*) before eluting fraction 2. This additional washing avoids any contamination of type I isozyme in the fraction collected for type II isozyme.
2. We have used neutral DNA fragments (BamHI/EcoRI fragment of V-erb B) 580 bp long to construct RIα- and RIβ-subunit MIMICS. Other neutral DNA fragments, such as of Lambda ZAP II Vector (Stratagene, La Jolla, CA), can be used to construct gene-specific MIMICs, depending on GC content of the target gene. Selecting a neutral DNA fragment region containing an identical GC content amount of the amplified gene segment for MIMIC construction is important in quantifying transcripts in cDNA samples more accurately because MIMICs containing an identical GC content of the amplified segment will amplify with equal efficiencies.
3. In our experiments, transcripts of PKA RIα were cloned into the pCR2.1-TOPO vectors and TOP10 chemically competent cells. Because of the rapid advancement of molecular biology techniques, several vectors and competent cells were developed. Using these improved reagents and techniques, the efficiency of cloning and sequencing of genes of interest can be enhanced considerably.

Acknowledgments

This work was supported by U.S. Public Health Service grants RO1 AR39501 and RO1 AI46526.

References

1 Kammer, G. M., Perl, A., Richardson, B. C., and Tsokos, G. C. (2002) Abnormal T cell signal transduction in systemic lupus erythematosus. *Arthritis Rheum.* **46,** 1139–1154.

2 Mandler, R., Birch, R. E., Polmar, S., Kammer, G. M., and Rudolph, S. A. (1982) Abnormal adenosine-induced immunosuppression and cAMP metabolism in T lymphocytes of patients with systemic lupus erythematosus. *Proc. Natl. Acad. Sci. USA* **79,** 7542–7546.

3 Hasler, P., Schultz, L. A., and Kammer, G. M. (1990) Defective cAMP-dependent phosphorylation of intact T lymphocytes in active systemic lupus erythematosus. *Proc. Natl. Acad. Sci. USA* **87,** 1978–1982.

4 Kammer, G. M., Khan, I. U., and Malemud, C. J. (1994) Deficient type I protein kinase A isozyme activity in systemic lupus erythematosus T lymphocytes. *J. Clin. Invest.* **94,** 422–430.

5 Mishra, N., Khan, I. U., Tsokos, G. C., and Kammer, G. M. (2000) Association of deficient type II protein kinase A activity with aberrant nuclear translocation of the RIIβ_subunit in systemic lupus erythematosus T lymphocytes. *J. Immunol.* **165,** 2830–2840.

6 Laxminarayana, D., Khan, I. U., and Kammer, G. M. (2002) Transcript mutations of the α regulatory subunit of protein kinase A and up-regulation of the RNA-editing gene transcript in lupus T lymphocytes. *Lancet* **360,** 842–849.

7 Laxminarayana, D., Khan, I. U., Mishra, N., Olorenshaw, I., Taskén, K., and Kammer, G. M. (1999) Diminished levels of protein kinase A RIα and RIβ transcripts and proteins in systemic lupus erythematosus T lymphocytes. *J. Immunol.* **162,** 5639–5648.

8. Solberg, R., Sandberg, M., Natarajan, V., Torjesen, P. A., Hansson, V., Jahnsen, T., et al. (1997) The human gene for the regulatory subunit RIα of cyclic adenosine 3',5'-monophosphate-dependent protein kinase: two distinct promoters provide differential regulation of alternately spliced messenger ribonucleic acids. *Endocrinology* **138,** 169–181.

6

Apoptosis and Mitochondrial Dysfunction in Lymphocytes of Patients With Systemic Lupus Erythematosus

Andras Perl, Gyorgy Nagy, Peter Gergely, Ferenc Puskas, Yueming Qian, and Katalin Banki

Summary

Systemic lupus erythematosus (SLE) is characterized by abnormal activation and cell death signaling within the immune system. Activation, proliferation, or death of cells of the immune system are dependent on controlled reactive oxygen intermediate (ROI) production and ATP synthesis in mitochondria. The mitochondrial transmembrane potential ($\Delta\Psi_m$) reflects the energy stored in the electrochemical gradient across the inner mitochondrial membrane, which in turn is used by F_0F_1-ATPase to convert adenosine 5'-diphosphate to ATP during oxidative phosphorylation. Mitochondrial hyperpolarization and transient ATP depletion represent early and reversible steps in T-cell activation and apoptosis. By contrast, T lymphocytes of patients with SLE exhibit elevated $\Delta\Psi_m$, that is, persistent mitochondrial hyperpolarization, cytoplasmic alkalinization, increased ROI production, as well as diminished levels of intracellular glutathione and ATP. Oxidative stress affects signaling through the T-cell receptor as well as the activity of redox-sensitive caspases. ATP depletion may be responsible for diminished activation-induced apoptosis and sensitize lupus T cells to necrosis. Mitochondrial dysfunction is identified as a key mechanism in the pathogenesis of SLE.

Key Words: Apoptosis; ATP depletion; caspases; cytoplasmic alkalinization; glutathione depletion; mitochondrial hyperpolarization; necrosis; reactive oxygen intermediates; systemic lupus erythematosus.

1. Introduction

Systemic lupus erythematosus (SLE) is a chronic inflammatory disease characterized by T- and B-cell dysfunction and production of antinuclear antibodies. Abnormal T-cell activation and cell death underlie the pathology of SLE ***(1,2)***. Potentially autoreactive T and B lymphocytes during development ***(3)***

From: *Methods in Molecular Medicine, Vol. 102: Autoimmunity: Methods and Protocols*
Edited by: A. Perl © Humana Press Inc., Totowa, NJ

and after completion of an immune response are removed by apoptosis *(4)*. Paradoxically, lupus T cells exhibit both enhanced spontaneous apoptosis and defective activation-induced cell death (AICD). Increased spontaneous apoptosis of peripheral blood lymphocytes (PBLs) has been linked to chronic lymphopenia *(5)* and compartmentalized release of nuclear autoantigens in patients with SLE *(6)*. By contrast, defective CD3-mediated cell death may be responsible for persistence of autoreactive cells *(7)*.

1.1. Mitochondrial Checkpoints of T-Cell Activation and Apoptosis

Both cell proliferation and apoptosis are energy-dependent processes. Energy in the form of adenosine triphosphate (ATP) is provided through glycolysis and oxidative phosphorylation. The mitochondrion (**Fig. 1**), the site of oxidative phosphorylation, has long been identified as a source of energy and cell survival *(8)*. The synthesis of ATP is driven by an electrochemical gradient across the inner mitochondrial membrane maintained by an electron transport chain and the membrane potential (negative inside and positive outside). A small

---

Fig. 1. Overview of mitochondrial redox and metabolic checkpoints of T-cell activation and apoptosis signals. Antigen binding-initiated signaling through the T-cell receptor complex/CD3 and the CD28 costimulatory molecule activate phosphatidylinositol 3-kinase (PI3K) and protein tyrosine kinases (PTK). Increased cytosolic Ca^{2+} concentration activates the serine/threonine phosphatase calcineurin, which dephosphorylates the nuclear factor for activated T cells (NFAT). Dephosphorylated NFAT can translocate to the nucleus, where it promotes transcription of IL-2 in concert with AP-1, NF-κB, and Oct-1. $Ca2^{+}$ flux into mitochondria increases production of ROS and NF-κB activation *(88–90)*. Mitochondrial membrane integrity is maintained by a balance of membrane-stabilizing bcl-2 and bcl-X_L and pore-inducing bax and bad *(34)* as well as the metabolic capacity to synthesize reducing equivalents, NADPH, GSH, and TRX. Controlled increase of ROS levels activates NF-κB and promotes cell growth. Excess ROS production and disruption of $\Delta\Psi_m$ lead to AICD executed by caspase-3 (digesting vitally important proteins PARP, 70K U1RNP, lamin, and actin) and caspase-3-dependent DNase (CAD; causing nuclear DNA fragmentation). Cleavage by caspase-3 is thought to expose cryptic epitomes and cause autoantigenicity of self-antigens *(91)*. Activity of redox-sensitive transcription factors NF-κB, p53, AP-1, and Sp1 is regulated through release from inhibitor complexes and conformational changes in their active sites. Intracellular antioxidants reduced glutathione (GSH) and thioredoxin (TRX) are regenerated at the expense of NADPH supplied primarily through metabolism of glucose via the PPP *(92)*. Among PPP products, ribose 5-phosphate is required for nucleotide and DNA synthesis and supports cell growth, C3–C7 sugars influence mitochondrial function and reactive oxygen species

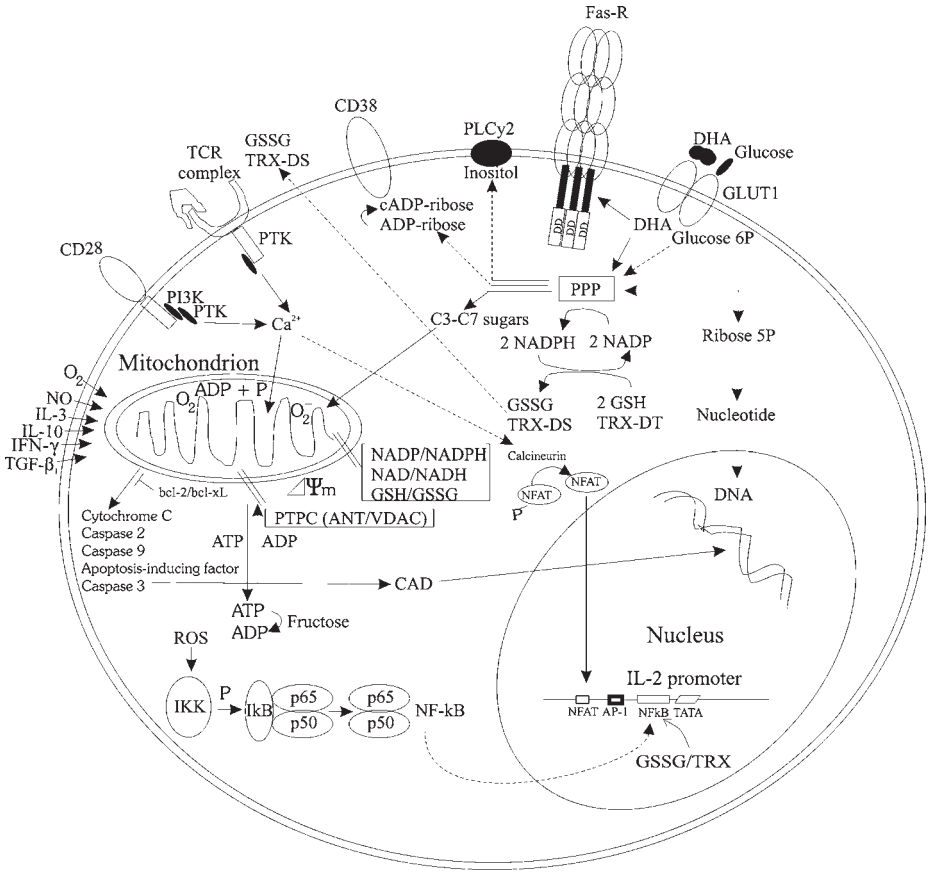

Fig. 1. (*continued*) (ROS) production, inositol and ADP-ribose serve as precursors for second messengers inositol phosphates and cADP-ribose, respectively. Dehydroascorbate (DHA) is imported through glucose transporter 1 (GLUT1). DHA is metabolized through the PPP, thereby enhancing GSH levels. DHA also increases surface expression of Fas-R ***(93)***. Glutathione reductase and TRX reductase synthesize GSH and reduced TRX (TRX-DT) at the expense of NADPH. Formulation of the PPP and its efficiency to provide NADPH is dependent on the expression of G6PD and TAL ***(14,15)***. $\Delta\Psi_m$ is controlled by intracellular GSH/NADH/NADPH levels; integrity of the permeability transition pore complex (PTPC), largely comprised of adenine nucleotide translocator (ANT; inner membrane); voltage-dependent anion channel (VDAC; outer membrane); and translocation and dimerization of pro- and antiapoptotic bcl-2 family members in the intermembrane space ***(34)***. Phosphorylation of BAD by mitochondria-anchored PKA results in antiapoptotic sequestration of BAD into the cytosol ***(94)***. Signaling through cell death receptors, such as Fas(15), CD3/CD28 costimulation ***(36, 7)***, ROS ***(24)***, NO ***(29)***, as well as lymphokines, IL-3, IL-10, IFN-γ, and TGF-β_1 influence $\Delta\Psi_m$, ATP synthesis, and susceptibility to apoptosis ***(37)***.

fraction of electrons react directly with oxygen and form reactive oxygen intermediates (ROIs).

Disruption of the mitochondrial membrane potential has been proposed as the point of no return in apoptotic signaling ***(9–11)***. Mitochondrial membrane permeability is subject to regulation by an oxidation–reduction equilibrium of ROIs, pyridine nucleotides (NADH/NAD + nicotinamide adenine dinucleotide phosphate [NADPH]/NADP), and glutathione (GSH) levels ***(12)***. Regeneration of GSH by glutathione reductase from its oxidized form, GSSG, depends on NADPH produced by the pentose phosphate pathway (PPP) ***(13)***. ROI levels and $\Delta\Psi_m$ are regulated by the supply of reducing equivalents from PPP ***(14,15)***. Although ROIs have been considered toxic byproducts of aerobic existence, evidence is now accumulating that controlled levels of ROIs modulate various aspects of cellular function and are necessary for signal transduction pathways, including those mediating T-cell activation and apoptosis ***(16)***.

Increased production of ROIs was demonstrated in cell death mediated by tumor necrosis factor (TNF) ***(17–19)*** and Fas ***(9,14,20–23)***. Disruption of the mitochondrial membrane potential $\Delta\Psi_m$ has been proposed as the point of no return in apoptotic signaling ***(9–11)***. Interestingly, elevation of $\Delta\Psi_m$, mitochondrial hyperpolarization, and ROI production precede phosphatidylserine (PS) externalization and a disruption of $\Delta\Psi_m$ in Fas- ***(15)*** and H_2O_2-induced apoptosis of Jurkat human leukemia T cells and normal human PBLs ***(24)***. These observations were extended to apoptosis induced by p53 ***(25)***, TNF-α ***(26)***, staurosporin ***(27)***, camptothecin ***(28)***, and nitric oxide ***(29)***.

Elevation of $\Delta\Psi_m$ is independent from activation of caspases and represents an early event in apoptosis ***(15,25)***. Pretreatment with caspase inhibitor peptides, DEVD, Z-VAD, and Boc-Asp, completely abrogated Fas-induced PS externalization, indicating that activation of caspase-3, caspase-8, and related cysteine proteases was absolutely required for cell death ***(30–33)***. ROI levels were partially inhibited in DEVD-treated Jurkat cells, suggesting that caspase-3 activation, perhaps through damage of mitochondrial membrane integrity, contributes to ROI production and serves as a positive-feedback loop at later stages of the apoptotic process. Nevertheless, ROI levels remained significantly elevated after pretreatment with caspase inhibitors. This suggested that activation of caspase-3 or -8 was not required for increased ROI production and ($\Delta\Psi_m$) ($\Delta\Psi_m$) hyperpolarization.

By contrast, DEVD, Z-VAD, and Boc-Asp blocked PS externalization and decline of $\Delta\Psi_m$ in annexin V-positive Jurkat cells, suggesting that disruption of $\Delta\Psi_m$ (a) was a relatively late event with respect to ROI production and $\Delta\Psi_m$ hyperpolarization, and (b) depended on activation of caspase-3 and related proteases. The precise mechanism by which Fas and TNF signaling leads to changes in $\Delta\Psi_m$ and ROI levels remains to be defined. Cleavage of

cytosolic bid by caspase-8 generates a p15 carboxyterminal fragment that translocates to mitochondria. This may represent the initial insult to mitochondria in the Fas/TNF pathway ***(34)***.

Mitochondrial hyperpolarization appears to be the earliest change associated with Fas ***(15)***, H_2O_2 ***(24)***, human immunodeficiency virus 1 ***(35)***, p53 ***(25)***, TNF-α ***(26)***, staurosporin ***(27)***, camptothecin ***(28)***, and nitric oxide (NO)-induced apoptosis ***(29)***. Elevation of $\Delta\Psi_m$ is also triggered by activation of the CD3/CD28 complex ***(36)*** or stimulation with concanavalin A (Con A) ***(15)***, interleukin (IL)-10, IL-3, interferon (IFN)-γ, or transforming growth factor (TGF)-β ***(37)***. Therefore, elevation of $\Delta\Psi_m$ or mitochondrial hyperpolarization represents an early, but reversible, switch not exclusively associated with apoptosis. With $\Delta\Psi_m$ hyperpolarization and extrusion of H^+ ions from the mitochondrial matrix, the cytochromes within the electron transport chain become further reduced, which favors generation of ROIs ***(38)***. Thus, mitochondrial hyperpolarization is a likely cause of increased ROI production and may be ultimately responsible for increased susceptibility to apoptosis following T-cell activation.

1.2. Death Pathway Selection in Mitochondria

The mitochondrion is the site of ATP synthesis via oxidative phosphorylation. The synthesis of ATP is driven by an electrochemical gradient across the inner mitochondrial membrane maintained by an electron transport chain and the membrane potential. Activity of caspases require ATP to the extent that depletion of ATP by inhibition of F_0F_1-ATPase with oligomycin ***(39)*** or exhaustion of intracellular ATP stores by prior apoptosis signals, Fas stimulation ***(39)***, or H_2O_2 pretreatment leads to necrosis ***(40)***. Thus, intracellular ATP concentration is a key switch in the cell's decision to die via apoptosis or necrosis ***(39)***.

Extracellular ATP and adenosine have long been known to be cytotoxic. Adenosine may act through P1 purinoreceptors, raising intracellular Ca^{2+} and causing oxidative stress. ATP could also activate ectoenzymes as a phosphate donor or, through stimulation of $P2X_7$ purinoreceptors, deplete intracellular K^+, resulting in activation of caspases ***(41)***. Sustained increase of intracellular Ca^{2+} concentration mediates coupling of ATP production to metabolic need during T-cell activation ***(42)***. In fact, increased cytosolic Ca^{2+} concentration could be responsible for elevation of $\Delta\Psi_m$, which is a primary driving force of ATP synthesis ***(43)***. As noted, further reduction of the cytochromes within the electron transport chain by $\Delta\Psi_m$ hyperpolarization favors increased ROI generation ***(38)***. Subsequent damage to mitochondrial membranes leads to release of mitochondrial Ca^{2+} stores and a secondary increase of cytosolic Ca^{2+} concentration ***(8)***. Ca^{2+} serves as a cofactor for activation of caspases and endonucleases during the execution phase of apoptosis ***(44)***.

Table 1
Signaling Abnormalities of T-Cell Death in Patients With SLE

Signal	Effect	Reference
($\Delta\Psi_m$) ↑	ROI ↑, ATP ↓	***36***
ROI ↑	Spontaneous apoptosis ↑, IL-10 production↑	***36,37***
GSH ↓	ROI ↑, spontaneous apoptosis ↑	***14,36***
Spontaneous apoptosis ↑	Compartmentalized autoantigen release, disease activity ↑	***5,6,36,60***
H_2O_2	Apoptosis ↓, necrosis ↑	***36***
CD3/CD2↑	AICD ↓, necrosis ↑	***37***
ATP ↓	Predisposes for necrosis	***36,39***
Necrosis ↑	Inflammation ↑	***36,86***
AICD ↓	Persistence of autoreactive cells	***7,37***
FasR ↑	Spontaneous apoptosis ↑	***60***
FasL ↑	Spontaneous apoptosis ↑	***61***
IL-10↑	Selective induction of apoptosis in SLE	***37,61,87***
NO ↑	Disease activity↑	***62***
IL-10 blockade	Spontaneous apoptosis ↓, ROI ↓	***37,61***
IL-12	Spontaneous apoptosis ↓, ROI ↓	***37***

↑, increase; ↓, decrease.

1.3. Mitochondrial Dysfunction in Lupus T Cells

SLE T cells exhibit both defective AICD and enhanced spontaneous apoptosis (**Table 1**). Coordinate mitochondrial hyperpolarization and ATP depletion play key roles in abnormal T-cell death of patients with SLE ***(36)***, $\Delta\Psi_m$ and ROI levels as well as cytoplasmic pH are elevated in patients with SLE in comparison to healthy or controls with rheumatoid arthritis ***(36,37)***. Baseline mitochondrial hyperpolarization and ROI levels correlated with diminished GSH levels, suggesting increased utilization of reducing equivalents in patients with SLE.

It is presently unclear whether synthesis of GSH or its regeneration from its oxidized form is deficient in lupus patients. GSH is also required for interleukin-2-dependent T-cell proliferation ***(45)*** as well as CD2- and CD3-mediated T-cell activation ***(46)***. Thus, a low GSH content may also inhibit CD3-induced H_2O_2 production. Nevertheless, GSH deficiency predisposes cells for ROI-induced cell death ***(14,24,47)***. Diminished H_2O_2-induced apoptosis of cells with low baseline GSH levels indicates a severe dysfunction of redox signaling in patients with SLE.

Increased ROI production may lead to skewed expression of redox-sensitive surface receptors and lymphokines. As examples, ROIs regulate gene transcription and release of TNF-α and IL-10 ***(48)***, both of which are elevated in sera ***(49,50)*** and freshly isolated PBLs of patients with SLE ***(51,52)***. Expression of TCR ζ-chain is sensitive to oxidative stress ***(53)***, and thus increased ROI levels may explain, at least in part, low TCR ζ-chain expression in lupus T cells ***(54)***. Cell surface expression of the Fas receptor ***(55–57)*** and Fas ligand is also redox sensitive ***(58)***. Increased ROI levels may be related to increased IL-10 production, release of FasL, and overexpression of the FasR in SLE ***(59–61)***. Elevated NO production may also contribute to increased spontaneous apoptosis ***(62,63)***. Mitochondrial ROI production and $\Delta\Psi_m$ are early checkpoints in Fas- ***(15)*** and H_2O_2-induced apoptosis ***(24)***. Increased ROI levels confer sensitivity to H_2O_2-, NO-, TNF-α-, or Fas-induced cell death ***(14)***. Therefore, elevated baseline ROI and $\Delta\Psi_m$ levels may have key roles in enhanced spontaneous death of PBLs in patients with SLE.

1.4. Mitochondrial Hyperpolarization and ATP Depletion Predispose Lupus T Cells to Necrosis

In response to treatment with exogenous H_2O_2, a precursor, or ROI, lupus T cells failed to undergo apoptosis, and cell death preferentially occurred via necrosis. As noted in **ref. *24***, H_2O_2 triggered a rapid increase of $\Delta\Psi_m$ and ROI production, which was followed by apoptosis of PBLs in healthy subjects. By contrast, H_2O_2 failed to elevate $\Delta\Psi_m$, ROI production, and apoptosis, but rather elicited necrosis in patients with lupus. Both CD3/CD28-induced H_2O_2 production and H_2O_2-induced apoptosis require mitochondrial ROI production. Therefore, diminished CD3/CD28-induced H_2O_2 production and H_2O_2-induced apoptosis together with deficient elevation of $\Delta\Psi_m$ and ROI levels reveal deviations of key biochemical checkpoints in mitochondria of patients with SLE.

1.5. Pharmacological Targeting of Mitochondrial Dysfunction in SLE

Mitochondrial hyperpolarization predisposes for increased ROI production ***(38)***. Oxidative stress affects the activity of transcription factors activation protein (AP-1) and NF-κB ***(64,65)*** and, further downstream, may lead to the skewed expression of IL-2, TNF, and IL-10 ***(48)***. Increased spontaneous apoptosis of lymphocytes has been linked to increased IL-10 production, release of Fas ligand, and overexpression of Fas receptor in SLE ***(61)***. Because increased ROI levels confer sensitivity to H_2O_2-, NO-, TNF-, and Fas-induced cell death ***(14,15)***, elevated baseline $\Delta\Psi_m$, ROI production, and intracellular pH may have key roles in altered activation and death of lupus T cells. Although mitochondrial hyperpolarization was not affected, IL-10 antibody or IL-12 normalized ROI

production and intracellular alkalinization in lupus PBLs ***(37)***. Therefore, IL-10 antagonists may partially correct signaling dysfunction in lupus. A proapoptotic 1,4-benzodiazepine (Bz-423) has been found to promote ROI-mediated apoptosis of germinal center B cells and ameliorate glomerulonephritis in lupus-prone NZB/W mice ***(66)***. The mechanism of mitochondrial hyperpolarization and ATP depletion require further studies, which in turn could identify novel targets for pharmacological intervention in patients with SLE.

2. Materials

1. Ficoll-Paque Plus (Amersham Pharmacia, Uppsala, Sweden).
2. RPMI-1640 medium, fetal calf serum (FCS), penicillin, streptomycin, amphotericin B (Life Technologies, Grand Island, NY).
3. OKT3 monoclonal antibody (MAb; CRL 8001, ATCC, Rockville, MD).
4. CD28.2 MAb (Pharmingen, San Diego, CA).
5. Cytokines IL-2, IL-3, IL-4, IL-6, IL-7, IL-10, IL-12, IL-15, TNF-α, TGF-β_1, and IFN-γ (PeproTech, Rocky Hill, NJ).
6. Polyclonal goat antihuman IL-10 neutralizing antibody (R&D Systems, Minneapolis, MN).
7. Annexin binding buffer: 10 m*M* HEPES at pH 7.4, 140 m*M* NaCl, and 2.5 m*M* $CaCl_2$.
8. Phosphate-buffered saline (PBS): 8 g NaCl, 0.2 g of KCl, 1.44 g Na_2HPO_4, 0.24 g KH_2PO_4 dissolved in 1 L of H_2O with pH adjusted to 7.4.
9. Fluorescein isothiocyanate-conjugated annexin V (annexin V-FITC) and phycoerythrin-conjugated annexin V (annexin V-PE; R&D Systems).
10. Propidium iodide (PI; R&D Systems).
11. Triton X-100 (Sigma, St. Louis, MO).
12. Hydroethidine (HE; Molecular Probes, Eugene, OR).
13. Quantum Red/Cy5-conjugated MAbs directed to CD3, CD4, CD8, CD14 (Sigma) and CD45RA and CD45RO (Pharmingen).
14. Fluorescence microscope: Nikon Eclipse E800 camera (Nikon Corp., Tokyo, Japan) equipped with SPOT digital camera (Diagnostic Instruments, Sterling Heights, MI).
15. Becton Dickinson (Franklin Lake, NJ) FACStar Plus flow cytometer equipped with an argon ion laser delivering 200 mW power at 488 nm.
16. Oxidation-sensitive fluorescent probes 5,6-carboxy-2',7'-dichlorofluorescein-diacetate (DCFH-DA), dihydrorhodamine 123 (DHR), and HE (Molecular Probes).
17. Cationic lipophilic dyes with high binding affinity to mitochondria: 3,3'-dihexyloxacarbocyanine iodide ($DiOC_6$); 5,5',6,6'-tetrachloro-1,1',3,3'-tetraethylbenzimidazolocarbocyanine iodide (JC-1); tetramethylrhodamine, methyl ester, perchlorate (TMRM) (all from Molecular Probes).
18. Carbonyl cyanide *m*-chlorophenylhydrazone (mClCCP; Sigma).
19. Luminometer: AutoLumat LB953 (Berthold GmbH, Wildbad, Germany).

20. ATP determination kit (Molecular Probes).
21. ApoGlow kit (Lumitech, Nottingham, UK).
22. Carboxy SNARF-1-acetoxymethyl ester acetate (SNARF-1; Molecular Probes).
23. Dimethyl sulfoxide (DMSO; Sigma).
24. High K^+ buffers of varying pH values (120 m*M* KCl, 30 m*M* NaCl, 0.5 m*M* $MgSO_4$, 1 m*M* $CaCl_2$, 1 m*M* $NaHPO_4$, 5 m*M* glucose, and 10 m*M* HEPES).
25. Nigericin (Sigma; diluted from a stock solution of 500 μg/mL in ethanol).
26. Deproteinizing buffer for GSH assay: 70% perchloric acid and 15 m*M* bathophenanthrolinedisulfonic acid (BPDS; Sigma).
27. γ-Glutamyl glutamate (γ-Glu-Glu; Sigma) as internal standard for GSH assay.
28. After repeated freezing and thawing, samples were centrifuged at 15,000g for 3 min and 50 mL of 100 m*M* mono-iodo-acetic acid in 0.2 m*M* m-cresol purple was added to 500 mL supernatant. Samples were neutralized by addition of 480 mL of 2 *M* KOH and 2.4 *M* $KHCO_3$ and incubated in the dark at room temperature for 10 min. Then, 1 mL of 1% fluoro-dinitro-benzene was added, and the samples were incubated in the dark at 4°C overnight. After centrifugation and filtering, 100 mL of supernatant were injected into the high-performance liquid chromatography (HPLC) model 2690 (Waters Alliance System, Milford, MA) equipped with a model 996 photodiode array detector and Spherisorb NH_2 column (4.6 × 250 mm; 10 mm; Waters).
29. 7-Amino-4-trifluoromethyl-coumarin (AFC; Sigma).
30. Caspase substrate peptides: DEVD-AFC, Z-IETD-AFC, where Z represents a benzyloxycarbonyl group; caspase inhibitor peptides Z-Val-Ala-Asp(Ome).fmk (Z-VAD), Boc-Asp.fmk (Boc-Asp), as well as noncaspase cysteine protease inhibitor Z-Phe-Ala.fmk (Z-FA) (Enzyme Systems Products, Livermore, CA).
31. Caspase assay buffer: 250 m*M* sucrose, 20 m*M* HEPES-KOH at pH 7.5, 50 m*M* KCl, 2.5 m*M* $MgCl_2$, 1 m*M* dithiothreitol (DTT).
32. Versene (Life Technologies).
33. Con A (Sigma).
34. Goat antimouse immunoglobulin G (IgG; ICN, Aurora, OH).
35. Tritiated thymidine (^{3}HTdR; ICN).
36. CH-11 IgM MAb to Fas/Apo-1/CD95 (Upstate Biotechnology, Saranac Lake, NY).
37. Complete RPMI medium: RPMI-1640 supplemented with 10% FCS, 2 m*M* L-glutamine, 100 IU/mL penicillin, 100 μg/mL gentamicin, and 10 μg/mL amphotericin B.
38. Plastic tissue culture dishes (Becton Dickinson).
39. Phenol, chloroform, isoamyl alcohol, proteinase K, agarose (all RNase and DNase free, molecular biology grade; Sigma).
40. Spectrophotometer.
41. Luminometer.
42. Carbonyl cyanide *m*-chlorophenylhydrazone (mClCCP, Sigma).
43. Folin and Ciocalteu's Phenol Reagent Solution (Sigma).
44. A 4-mm diameter, 0.45-μm polypropylene filter (Whatman, Mainstead, UK).

45. MAb to poly(ADP-ribose) polymerase (PARP) C-2-10 ***(67)***.
46. MAb 5F7 directed to C-terminal amino acids 176–460 of human FLICE/Mch5/caspase-8 (Panvera, Madison, WI).
47. MAb 31A1067 directed to caspase-3 (Gene Therapy Systems, San Diego, CA).
48. MAb C4 directed to human β-actin (Boehringer, Indianapolis, IN).
49. Biotinylated secondary antibodies and horseradish peroxidase-conjugated avidin (Jackson Laboratories, West Grove, PA).
50. 4-Chloronaphthol (Sigma).
51. Enhanced chemiluminescence detection kit (Western Lightning Chemiluminescence Reagent Plus, PerkinElmer Life Sciences, Boston, MA).
52. Kodak Image Station 440CF equipped with Kodak 1D Image Analysis Software (Eastman Kodak Company, Rochester, NY).

3. Methods

The methods described here outline (a) in vitro lymphocyte culture, activation, and apoptosis assays; (b) flow cytometric analysis of ($\Delta\Psi_m$); (c) ROI production; (d) intracellular pH; (e) measurement of intracellular ATP and ADP; (f) HPLC analysis of reduced (GSH) and oxidized (GSSG) forms of glutathione; and (g) caspase enzyme assays.

3.1. Lymphocyte Culture, Activation, and Viability Assays

3.1.1. Separation of Peripheral Blood Mononuclear Cells

1. Collect peripheral blood in sterile tubes containing 50 U heparin (Sigma) per milliliter of blood.
2. Layer blood diluted 1:1 with PBS on Ficoll-Paque. Typically, layer 10 mL diluted blood over 5 mL of Ficoll-Paque.
3. Centrifuge cells at 500*g* for 30 min with centrifuge brake off.
4. Remove peripheral blood mononuclear cells (PBMCs) from interface between Ficoll-Paque and plasma with pipettor.
5. Wash PBMCs three times in PBS by centrifugation at 300*g* for 10 min.
6. PBMCs are resuspended at 10^6 cells/mL in complete RPMI medium, and incubated for experiments at 37°C in a humidified atmosphere with 5% CO_2.

3.1.2. Separation of Monocytes and PBLs

1. Precoat Petri dishes with autologous serum for 30 min at 37°C.
2. Add 5 mL of PBMCs (maximum 5×10^6/mL) to serum-pretreated dishes and incubate for 1 h at 37°C.
3. Remove nonadherent cells by washing three times with 5 mL of warm (37°C) complete RPMI medium.
4. To obtain a monocyte-enriched cell fraction, wash dishes vigorously with warm medium.

5. Add 4 mL of ice-cold 0.05% Versene and 1 mL autologous serum to each dish for 15 min at room temperature.
6. Scrape off loosely adherent monocytes with a rubber policeman under inverse microscopic control.
7. The monocyte-depleted fraction of PBLs should contain less than 2% monocytes, and the monocyte-enriched fraction should contain 90 to 95% monocytes by staining with CD14 MAb.

3.1.3. Cell Culture, Activation, and Viability Assays

Human PBLs undergo apoptosis in response to repetitive activation through the T-cell receptor (i.e., CD3/CD28 costimulation), resulting in AICD ***(36,37)***, crosslinking of cell surface death receptors such as Fas/Apo-1/CD95 ***(15)***, or elevation of intracellular ROI levels after treatment with H_2O_2 ***(24,36)***. Monocytes/macrophages remove apoptotic bodies via phagocytosis; therefore, processing of cell death signals by lymphocytes is best evaluated using PBLs.

3.1.3.1. CD3/CD28 Costimulation of PBLs

1. Precoat 10-cm diameter plastic Petri dishes with 100 μg/mL goat antimouse IgG (diluted in PBS) for 2 h at 37°C.
2. Wash plates with PBS, add OKT3 MAb (1 μg/mL), and incubate for 1 h at 37°C.
3. Add PBLs (10^6 cells/mL in complete RPMI medium).
4. For CD28 costimulation, add 500 ng/mL MAb CD28.2 and incubate cells at 37°C for the desired period of time.

3.1.3.2. Triggering Fas-Mediated Cell Death of PBLs

1. Sensitize peripheral blood T cells for Fas-mediated apoptosis by CD3/CD28 costimulation or treatment with 5 μg/mL Con A for 5–7 d.
2. Monitor blast transformation by measurement of increased side scatter (SSC) using flow cytometry ***(16)*** or ^{3}HTdR incorporation via pulse labeling with 0.4 μCi of ^{3}HTdR of 10^5 cells in 100 μL per well of a 96-well plate ***(68)***.
3. Determine cell viability by staining with 0.25% trypan blue in 0.9% NaCl. Viable cells should not stain with trypan blue.
4. Pellet and resuspend cells at 2×10^6 cells/mL in complete RPMI medium.
5. Add an equal volume of complete RPMI medium without (control) or with 2 μg/mL of CH11 IgM MAb.
6. Incubate cells at 37°C for the desired period of time.

3.1.3.3. Treatment With H_2O_2

1. Prepare fresh 10 m*M* H_2O_2 in PBS from 30% stock solution.
2. Seed PBLs at 2×10^6 cells/mL in complete RPMI medium.
3. Add an equal volume of complete RPMI medium without (control) or with 100 μ*M* H_2O_2.
4. Incubate cells at 37°C for the desired period of time.

3.1.3.4. Monitoring of Cell Death

Apoptosis is monitored by observing cell shrinkage while counting trypan blue-stained cells and DNA fragmentation using agarose gel electrophoresis and quantified by flow cytometry after concurrent staining with annexin V-FITC (fluoresence channel [FL-1]) and PI (FL-2) as described elsewhere ***(14,15,69,70)***. Staining with annexin V-PE was used to monitor PS externalization (FL-2) in parallel with measurement of ROI levels and $\Delta\Psi_m$ (*see* below). Apoptosis rates are expressed as percentage of annexin V-positive/PI-negative cells. Necrosis is assessed by observing cellular and nuclear swelling. Swollen nuclei of necrotic cells can be observed by staining with PI (50 μg/mL). Necrotic cells are enumerated by direct PI staining using flow cytometry and fluorescence microscopy. Necrosis rates are expressed as percentage of PI-positive population within annexin-positive cells ***(36)***.

3.1.3.4.1. DNA Fragmentation Assay

1. Wash cells three times in PBS using screw-capped 15-mL polypropylene tubes.
2. Resuspend up to 5×10^7 cells in 100 m*M* NaCl, 10 m*M* Tris-HCl at pH 8.0, and 1 m*M* ethylenediaminetetraacetic acid (EDTA).
3. Add 250 μL of 10% sodium dodecyl sulfate (SDS).
4. Add 200 μg/mL proteinase K (keep 5-mg/mL aliquots at –20°C).
5. Incubate overnight at 37°C.
6. Extract twice with an equal volume of phenol. Remove aqueous phase only. Do not remove interface.
7. Extract twice with equal volume of chloroform:isoamylalcohol (24:1).
8. Precipitate DNA from aqueous phase with two volumes of absolute ethanol for 10 min at room temperature.
9. Transfer DNA with Pasteur pipet to 500 μL of TE (10 m*M* Tris, 1 m*M* EDTA) in Eppendorf tube and let it dissolve for 30 min.
10. Add 1/10 volume of 3 *M* sodium acetate.
11. Add two volumes of absolute ethanol.
12. Precipitate DNA for 10 min at room temperature.
13. Repeat **steps 9–12**.
14. Dissolve DNA in 500 μL of 10 m*M* Tris-HCl at pH 8.0 and 1 m*M* EDTA.
15. Quantify DNA by reading optical density (OD) at 260 nm (OD260). Read OD at 280 nm as well. OD260/280 should be 1.8–2.0. An OD of 1 corresponds to a DNA concentration of 50 μg/mL.
16. Store DNA at 4°C until analysis in a 2% agarose gel ***(14)***.

3.1.3.4.2. Assessment of Apoptosis and Necrosis by Flow Cytometry

1. Resuspend 2×10^5 cells to be analyzed in 200 μL of annexin binding buffer.
2. Add 5 μL of annexin V-FITC (10 μg/mL) and 5 μL of PI (50 μg/mL).
3. Incubate cells at room temperature in the dark.

4. Analyze by flow cytometry by electronic gating on live cells based on forward scatter (FSC) and SSC and measuring annexin-FITC binding on the FL-1 channel (emission at 530 nm) and PI staining on the FL-2 channel (emission at 625 nm).

3.2. Flow Cytometric Analysis of the Mitochondrial Transmembrane Potential $\Delta\Psi_m$

Mitochondrial transmembrane potential $\Delta\Psi_m$ can be estimated by cationic lipophilic dyes with high binding affinity to the negatively charged inner mitochondrial membrane ***(9,71,72)***. Because binding characteristics do not completely overlap, parallel staining with several dyes is recommended.

1. Resuspend 2×10^5 cells in 200 µL of annexin binding buffer if concurrently stained with annexin V-FITC or annexin V-PE matching a potentiometric dye emitting FL-2 or FL-1 fluorescence, respectively. Alternatively, 2×10^5 cells can be resuspended in 200 µL 5 m*M* HEPES-buffered saline (HBS; containing 0.9% NaCl at pH 7.4). This buffer, lacking Ca^{2+}, does not allow concurrent staining with annexin V.
2. Aliquots of cell suspensions are stained with several potentiometric dyes in parallel.
   a. Add 200 µL of dye solution containing 20 n*M* $DiOC_6$ (excitation 488 nm, emission 525 nm recorded in FL-1). This dye can be added in combination with annexin V-PE emitting FL-2 fluorescence.
   b. Add 200 µL of dye solution containing 1 µ*M* TMRM (excitation 549 nm, emission 573 nm recorded in FL-2). This dye can be added in combination with annexin V-FITC emitting FL-1 fluorescence.
   c. Add 200 µL of dye solution containing 0.5 µM JC-1. JC-1 selectively incorporates into mitochondria, where it forms monomers (fluorescence in green, 527 nm) or aggregates at high transmembrane potentials (fluorescence in red, 590 nm) ***(73,74)***.
3. Parallel cell suspensions should be treated with 5 µM mClCCP. Cotreatment with this protonophore for 15 min at 37°C results in decreased $DiOC_6$, TMRM, and JC-1 fluorescence and serves as a positive control for disruption of mitochondrial transmembrane potential ***(15)***.
4. Incubate cells in the dark for 15 min at 37°C before flow cytometry.
5. For each sample, measurements are carried out on 10,000 cells.

3.3. Measurement of ROI Production

Production of ROI can be assessed fluorometrically using oxidation-sensitive fluorescent probes DCFH-DA, DHR, and HE as described elsewhere ***(14)***. Cells are stained in annexin-binding buffer or HBS with 0.1 µM DHR for 2 min, 1 µM DCFH-DA for 15 min, or 1 µM HE for 15 min, and samples are analyzed using a Becton Dickinson FACStar Plus flow cytometer equipped with an argon ion laser delivering 200 mW of power at 488 nm.

Fluorescence emission from 5,6-carboxy-2',7'-dichlorofluorescein (DCF; green) or DHR (green) is detected at a wavelength of 530 ± 30 nm. Fluorescence emission from oxidized HE, ethidium (red), was detected at a wavelength of 605 nm. Dead cells and debris are excluded from the analysis by electronic gating on FSC and SSC measurements. Although R123, the fluorescent product of DHR oxidation, binds selectively to the inner mitochondrial membrane, ethidium and DCF remain in the cytosol of living cells ***(75)***, thus allowing measurement of ROI levels in different subcellular compartments.

1. Following apoptosis assay, wash cells two times in 5 m*M* HBS (containing 0.9% NaCl) at pH 7.4.
2. Resuspend 2×10^5 cells in 200 µL of annexin-binding buffer if concurrently stained with annexin V-FITC or annexin V-PE matching oxidation-sensitive dyes emitting FL-2 (HE) or FL-1 (DCF, R123) fluorescence, respectively. Alternatively, 2×10^5 cells can be resuspended in 200 µL of 5 m*M* HBS. This buffer, lacking Ca^{2+}, does not allow concurrent staining with annexin V.
3. Subsequently, aliquots of cell suspensions are stained with several potentiometric dyes in parallel.
   a. Add 200 µL of dye solution containing 0.1 µ*M* DHR (excitation 488 nm, emission 530 nm recorded in FL-1). This dye can be added in combination with annexin V-PE emitting FL-2 fluorescence. Staining is done in the dark at room temperature for 2 min, timed with a stopwatch, followed by running on the flow cytometer.
   b. Add 200 µL of dye solution containing 1 µ*M* DCFH-DA (excitation 488 nm, emission 525 nm recorded in FL-1). This dye can be added in combination with annexin V-PE emitting FL-2 fluorescence. Staining is done in the dark at room temperature for 15 min, timed with a stopwatch, followed by running on the flow cytometer.
   c. Add 200 µL of dye solution containing 1 µM HE (excitation 488 nm, emission 605 nm recorded in FL-2). This dye can be added in combination with annexin V-FITC emitting FL-1 fluorescence. Staining is done in the dark at room temperature for 15 min, timed with a stopwatch, followed by running on the flow cytometer.
4. For each sample, measurements are carried out on 10,000 cells.

3.4. Intracellular pH Measurement

Intracellular pH measurements are carried out with flow cytometry using the pH-sensitive dye SNARF-1 as described by Wieder et al. ***(76)***. SNARF-1 enters cells passively as a nonpolar ester. It is then hydrolyzed by intracellular esterases into a polar compound unable to leave membrane-intact cells. The emission spectrum of SNARF-1 undergoes a pH-dependent wavelength shift.

The ratio of fluorescence intensities emitted at two different wavelengths (FL-2 at 580 nm and FL-3 at 650 nm) is used for determination of pH.

1. Make fresh 0.5 mg/mL stock solutions of SNARF-1 daily in DMSO.
2. Resuspend 5×10^5 cells in 500 µL of PBS.
3. Add 5 µg/mL SNARF-1 to the cells and incubate samples 30 min at 37°C.
4. Wash cells once in 1 mL of PBS and resuspend in 500 µL of PBS.
5. Analyze on a Becton Dickinson FACStar Plus flow cytometer. The SNARF-1 dye is excited with 200 mW of the 488-nm argon laser, and fluorescence is collected in two wavelengths (FL-2 at 580 nm and FL-3 at 650 nm) in the pulse processing mode.
6. Generate a standard calibration curve for each experiment by staining the cells in high K^+ buffers of varying pH values (120 m*M* KCl, 30 m*M* NaCl, 0.5 m*M* $MgSO_4$, 1 m*M* $CaCl_2$, 1 m*M* Na_2HPO_4, 5 m*M* glucose, and 10 m*M* HEPES) in the presence of 5 µg/mL nigericin to equilibrate the intracellular/extracellular pH.
7. Calculate intracellular pH based on the FL-3/FL-2 ratio.

3.5. Measurement of Intracellular ATP and ADP Levels

T-cell activation and apoptosis require the energy provided by ATP ***(77)***. Intracellular ATP concentration is a key switch in the cell's decision to die via apoptosis or necrosis ***(39)***; therefore, depletion of ATP may be responsible for defective apoptosis and a predisposition to necrosis in patients with SLE ***(36)***. Intracellular ATP levels can be determined with great sensitivity and specificity using the luciferin–luciferase method ***(78)***. Addition of luciferin and firefly luciferase to an ATP-containing biological sample results in light emission. The luminometric ATP assay is based on the firefly luciferase reaction:

$$\text{ATP} + \text{D-Luciferin} + O_2 \rightarrow \text{AMP} + \text{Pyrophosphate} + \text{Oxyluciferin} + CO_2 + \text{Light}$$

The quantum efficiency is very high, resulting in almost 1 photon per ATP molecule consumed in the reaction. The light is measured in luminometer. Under assay conditions of constant luciferase activity, the intensity of the emitted light is proportional to the ATP concentration. The assay is calibrated by the addition of a known amount of ATP.

3.5.1. Collection of Cells for ATP Assay

1. Collect 5×10^6 PBLs by centrifugation at 300*g* for 10 min and wash once in PBS.
2. Resuspend the cell pellet in 50 µL of PBS and mix with equal volumes of 2.5% trichloroacetic acid. Such extracts can be stored at –20°C.
3. Measure the total protein content of each sample using the Lowry assay ***(79)***.

3.5.2. Lowry Assay

The stock solutions for the Lowry assay are

Lowry A: 2% Na_2CO_3 in 0.1 *M* NaOH.
Lowry B: 1% $CuSO_4$ in diH_2O.
Lowry C: 2% Sodium potassium tartrate ($NaKC_4H_4O_6 \cdot 4H_2O$).

The reagents are

Lowry stock reagent: 49 mL Lowry A, 0.5 mL Lowry B, 0.5 mL Lowry C.
Folin's reagent: 2N Phenol reagent (Folin-Ciocalteau reagent). Dilute 1:1 in diH_2O before use.

Bovine serum albumin standard solution is prepared as described in **Table 2**. The standard calibration solution is dissolved at a concentration of 1 mg/mL in a buffer similar to the biological sample of unknown protein content, such as PBS. For the assay procedure:

1. Add 100 μL of sample (sample + buffer = 100 μL) per tube.
2. Add 1.0 mL of Lowry stock reagent to each tube.
3. Incubate 30 min at room temperature.
4. Add 100 mL of Folin's reagent to each tube.
5. Incubate 30 min at room temperature.
6. Read in a spectrophotometer at 595 nm.

3.5.3. ATP Assay

The ATP contents of PBLs from patients with SLE and control donors were assayed in parallel. The bioluminescence assay was performed in an AutoLumat LB953 automated luminometer using an ATP determination kit according to the manufacturer's instructions. ATP standard curves are established in each experiment and should be linear in the 5- to 5000-n*M* range. To eliminate the impact of nonspecific inhibitors in the cellular extracts, standard amounts of ATP were added to the reaction mixtures as controls, and ATP levels were remeasured ***(80)***. In our laboratory, the sample volume added to the reaction mixtures was less than 2% of the total assay volume.

3.5.3.1. Precautions

- Because of the high sensitivity of the luciferin–luciferase reaction, avoid contamination with ATP from exogenous biological sources, such as bacteria or fingerprints. Therefore, latex or vinyl gloves are to be worn at all times.
- Protect the D-luciferin and firefly luciferase reagents from light.
- Mix solutions containing firefly luciferase gently, for example, by inversion; vortex mixing may denature the enzyme.
- Arsenate compounds may inhibit the reaction.
- The temperature optimum for the reaction is 28°C. At higher temperatures, the reaction is slower.

Table 2
Preparation of Protein Standard Solution for Lowry Assay

Standard solution protein amount (μg)	Standard solution volume (μL)	Buffer volume (μL)
0	0	100
10	10	90
20	20	80
30	30	70
50	50	50
75	75	25
100	100	0

The standard calibration solution is dissolved at a concentration of 1 mg/mL in a buffer similar to the biological sample of unknown protein content, such as PBS.

3.5.3.2. Reagents

1. D-Luciferin (MW 302): 3 mg of lyophilized powder per vial.
2. Firefly recombinant luciferase: 40 μL of a 5-mg/mL solution in 25 m*M* Tris-acetate at pH 7.8, 0.2 *M* ammonium sulfate, 15% (v/v) glycerol, and 30% (v/v) ethylene glycol.
3. 25 mg DTT (MW 154).
4. ATP: 400 μL of a 5 m*M* solution in TE buffer.
5. 20X reaction buffer: 10 mL of 500 m*M* Tricine buffer at pH 7.8, 100 m*M* $MgSO_4$, 2 m*M* EDTA, and 2 m*M* sodium azide.
6. Standard reaction solution containing 0.5 m*M* D-luciferin, 1.25 μg/mL firefly luciferase, 25 m*M* Tricine buffer at pH 7.8, 5 m*M* $MgSO_4$, 100 μ*M* EDTA, and 1 m*M* DTT.

Store reagent frozen at –80°C. Avoid repeated freezing and thawing.

3.5.3.3. ATP Assay Protocol

1 Make 1.0 mL of 1X reaction buffer by adding 50 μL of 20X. reaction buffer to 950 μL of deionized autoclaved H_2O. This volume will be sufficient to make 1 mL of 10 m*M* D-luciferin stock solution.
2. Make 1 mL of a 10 m*M* D-luciferin stock solution by adding 1 mL of 1X reaction buffer (prepared in **step 1**) to one vial of D-luciferin (3 mg of lyophilized powder). Protect from light until use. The D-luciferin stock solution is reasonably stable for several weeks if stored at –20°C and protected from light.
3. Prepare a 100 m*M* DTT stock solution by adding 1.62 mL of H_2O to 25 mg of DTT. Aliquot into ten 160-μL volumes and store frozen at –20°C. Stock solutions of DTT stored properly are stable for 6 mo to 1 yr. Thawed aliquots should be kept on ice until ready for use.

4. Prepare low-concentration ATP standard solutions from 5 n*M* to 5 μ*M* by diluting the 5 m*M* ATP stock solution in H_2O. These dilute solutions are stable for several weeks when stored at –20°C.
5. Make 10 mL of a standard reaction solution by combining the following:
   8.9 mL distilled H_2O.
   0.5 mL 20X reaction buffer.
   0.1 mL 0.1 *M* DTT.
   0.5 mL 10 m*M* D-luciferin.
   2.5 μL of firefly luciferase 5 mg/mL stock solution.
6. Gently mix the tube by inverting three times. The firefly luciferase enzyme is easily denatured by vortexing. Keep the reaction solution protected from light until use.
7. Create standard curve:
   a. Measure luminescence of standard reaction solution (prepared in **step 5**), which is considered as background.
   b. Start the reaction by adding the desired amount of dilute ATP standard solution (prepared in **step 4**) and read the luminescence. The volume of the dilute ATP standard solution added to the standard assay solution should be no more than 10%, preferably less than 2%, of the total assay volume.
   c. Subtract the background luminescence.
   d. Generate a standard curve for a series of ATP concentrations. Be sure always to add a constant sample volume of the ATP-containing solution as an internal standard.
8. For sample analysis, add an experimental sample to the standard reaction solution. The total volume of the experimental sample assays should be equal to that of the ATP standard assays, with the amount of experimental sample added no more than 10% of the total assay volume.
9. Calculate the amount of ATP in the experimental samples from the standard curve.

3.5.3.4. Assessment of ATP/ADP Ratio and ADP Levels

ADP can be measured by its conversion to ATP using the ApoGlow kit. The ATP produced is then detected by the luciferin–luciferase method.

1. Dispense 100 μL of standard reaction solution with the experimental sample as described in **Subheading 3.5.3.3., step 8** into 96-well plates.
2. Load plate into 96-well plate reader and record luminescence (reading A).
3. After 10-min lag period, add 20 μL of ADP-converting reagent to each well using multichannel pipettor or autodispenser built into luminometer if available.
4. Take a 1-s integrated reading (reading B). If autoinjector is unavailable, reading B should be taken before addition of ADP-converting reagent.
5. After 5-min incubation allowing conversion of ADP to ATP, take a final 1-s integrated reading (reading C).
6. The ADP:ATP ratio is calculated as follows: (C – B)/A.

3.6. HPLC Assay of Glutathione Levels

Reduced (GSH) and oxidized (GSSG) glutathione as well as other intermediates of GSH metabolism can be concurrently measured by reverse-phase ion-exchange HPLC using ultraviolet detection at 365 nm ***(81)***.

1. Wash 2×10^7 PBLs once in 5 mL of PBS and store cell pellet at –80°C until assay.
2. Resuspend cell pellet in 250 μL of H_2O. Use 10 μL of cell suspension to measure protein content as described in **Subheading 3.5.2.**
3. Add 50 μL of 70% perchloric acid and 25 μL of 15 m*M* BPDS to deproteinize sample as well as 25 μL of γ-Glu-Glu as internal standard.
4. Vortex, freeze, and thaw the sample in two cycles.
5. Pellet sample in microcentrifuge at 15,000*g* for 5 min and save supernatant.
6. Add 25 μL of 100 m*M* mono-iodo-acetic acid in 0.2 m*M* m-cresol purple to 250 μL of supernatant.
7. Adjust pH of acidic solution (pink in color) to pH 8.0–9.0 (purple in color) by addition of 240 μL of 2 *M* KOH and 2.4 *M* $KHCO_3$.
8. Incubate sample in the dark at room temperature for 10 min.
9. Add 1 mL of 1% fluoro-dinitro-benzene, vortex, and incubate the samples in the dark at 4°C overnight.
10. Centrifuge sample at 15,000*g* for 10 min at 4°C.
11. Filter supernatant through 4-mm diameter 0.45-μm polypropylene filter.
12. Inject 50 μL of each sample into HPLC equipped with a model 996 photodiode array detector and a Waters Spherisorb 3-NH_2-propyl column (4.6 × 250 mm; 10 μm). An ultraviolet detector set to a wavelength of 365 nm can also be used.
13. After sample injection, a mobile phase of HPLC comprised of 80% mobile phase solution A (80% methanol) and 20% mobile phase solution B (0.5 *M* sodium acetate dissolved in 64% methanol) is maintained for 5 min, followed by a 10-min linear gradient to 1% mobile phase solution A/99% mobile phase solution B at a flow rate of 1.5 mL/min. Then, the mobile phase is held at 99% mobile phase solution B until the final compound, usually GSSG, has eluted (5–10 min).

3.7. Caspase Enzyme Assays

Activation of the caspase enzyme cascade is a hallmark of apoptosis. Caspase-3 is a key effector of all apoptosis pathways, amplifying the signal from initiator caspases (such as caspase-8) and indicating a final commitment to cellular disassembly. In addition to cleaving other caspases in the enzyme cascade, caspase-3 has been shown to cleave PARP, DNA-dependent protein kinase, protein kinase Cδ, the 70-kD component of U1 small nuclear ribonucleoprotein (snRNP), and actin.

1. Induce apoptosis in cells by the desired method. Remember to incubate a concurrent control culture without induction. Include cells treated with caspase inhibitor DEVD-CHO as a negative control ***(15)***.

2. After washing cells once in PBS, pellet 10^6 cells per experimental sample at 400*g* for 5 min. The cell pellet can be stored at –80°C until measurement.
3. Resuspend the cell pellet in 25 μL of chilled cell lysis buffer comprised of 10 m*M* HEPES/KOH (pH 7.4), 2 m*M* EDTA, 0.1% CHAPS, 5 m*M* DTT, 1 m*M* phenylmethylsulphonylfluoride, 10 μg/mL pepstatin A, 20 μg/mL leupeptin, 10 μg/mL aprotinin. Alternatively, cell lysis buffer from Clontech can be used.
4. Incubate cell lysate on ice for 15 min.
5. Pellet cell lysates in a microcentrifuge at 15,000*g* for 10 at 4°C.

Transfer the supernatants to new microcentrifuge tubes. Samples may be assayed immediately or frozen at –80°C until measurement.

6. Add 25 μL of 2X reaction buffer containing 80 μ*M* zDEVD-AFC substrate (derived from 1 m*M* stock in DMSO), 250 m*M* sucrose, 20 m*M* HEPES-KOH (pH 7.5), 50 m*M* KCl, 2.5 m*M* MgCl, 1 m*M* freshly added DTT. Set up parallel samples lacking zDEVD-AFC substrate and containing caspase-3 inhibitor peptide zDEVD-AFC.
7. Incubate at 37°C for 15–60 min (depending on caspase activity) and add ice-cold H_2O to 1 mL. Reaction can be stored frozen at –80°C for later measurement.
8. Prepare 12-point calibration curve with 0.002–4 μ*M* AFC.
9. Read fluorescence of experimental samples with 400-nm excitation filter and 505-nm emission filter.
10. After reading the fluorescence, take 0.4-mL aliquot from experimental samples and add 0.4 mL Lowry reagent and 0.2 mL Folin reagent (according to Lowry protocol described in **Subheading 3.5.2.**) to measure protein content. Add lysis and reaction buffers to set up standard blank tubes.
11. Express caspase activity as picomoles AFC per minute per milligram protein. Activities vary between 1000 and 5000 U/mg protein.

3.8. Western Blot Analysis of Caspase Activity

Caspases are activated through proteolysis that can be monitored by Western blot analysis.

1. For visualization of PARP caspase-3 and caspase-8, lyse 2×10^6 cells in 100 μL of 62.5 m*M* Tris-HCl at pH 6.8, 6 *M* urea, 10% glycerol, 2% SDS, 0.00125% bromophenol blue, and 5% β-mercaptoethanol.
2. Sonicate lysate for 15 s, boil for 5 min, and store at –80°C. ***(67)***.
3. Assess protein concentration by Lowry method (*see* **Subheading 3.5.2.**).
4. Separate 40 μg of total cell lysate in 10 μL per well by SDS polyacrylamide gel electrophoresis and electroblot to nitrocellulose ***(82)***.
5. Incubate nitrocellulose strips in 100 m*M* Tris-HCl at pH 7.5, 0.9% NaCl, 0.1% Tween-20, and 5% skim milk with the primary antibodies anti-PARP MAb C-2-10 ***(67)***, anti-caspase-3 (GTS), anti-caspase-8 (Panvera), or actin MAb C4 at a 1000-fold dilution at room temperature overnight.

6. After washing, incubate blots with biotinylated secondary antibodies and subsequently with horseradish peroxidase-conjugated avidin. Between incubations, the strips are vigorously washed in 0.1% Tween-20, 100 m*M* Tris-HCl at pH 7.5, and 0.9% NaCl.
7. The blots can be developed with a substrate comprised of 1 mg/mL 4-chloronaphthol and 0.003% hydrogen peroxide or using enhanced chemiluminescence detection.
8. Activation of the caspase cascade is monitored by cleavage of caspase-3 (32-kD precursor into 17-kD active form), caspase-8 (55-kD precursor into 42-kD active doublet), and PARP (116-kD precursor into 85-kD fragment).

4. Notes

1. When assessing T-cell activation and apoptosis in PBLs of patients with SLE, parallel processing of PBLs from control donors who are healthy and who have inflammatory disease, such as rheumatoid arthritis, is essential. We typically establish values for normal donors and process cells from two controls in parallel with cells from two patients. Whenever possible, we use freshly isolated cells. Alternatively, PBLs frozen in complete RMPI-1640 medium with 7.5% DMSO/30% FCS can be used when viability of defrosted cells exceeds 98% by trypan blue staining.
2. Testing of apoptosis by PBMCs vs PBLs may reflect influence of phagocytic activity by monocytes/macrophages. Such comparative analysis should be supplemented by direct analysis of macrophage phagocytosis. However, phagocytosis depends on many factors, such as Fc receptor polymorphisms or release of macrophage-activating factors by T and B cells. Therefore, we routinely analyze PBLs as effectors.
3. Fluorochromes are kept as highly concentrated (>10 m*M*) stock solutions in DMSO at –80°C, unless indicated otherwise. SNARF-1 is kept aliquoted in powder form and reconstituted in DMSO on the day of assay.
4. PI directly stains necrotic cells. As described elsewhere ***(14,83)***, live or apoptotic cells do not stain with PI and require permeabilization with 0.1% Triton X-100. When using HE (FL-2) for ROI measurement, cells are costained with annexin V-FITC (FL-1). Thus, annexin V-PE or annexin V-FITC are matched with emission spectra of potentiometric and oxidation-sensitive fluorescent probes. Staining with annexin V alone or in combination with DHR or $DiOC_6$ was carried out in 10 m*M* HEPES at pH 7.4, 140 m*M* NaCl, and 2.5 m*M* $CaCl_2$. Using three-color fluorescence, mitochondrial ROI levels, $\Delta\Psi_m$, and PS externalization within T-cell subsets can be concurrently analyzed by parallel staining with DHR or $DiOC_6$ (FL1), annexin V-PE (FL2), and Quantum Red/Cy5-conjugated MAbs directed to CD3, CD4, CD8 (Sigma; FL-3), CD45RA and CD45RO (Pharmingen). Quantum Red contains two covalently linked fluorochromes, PE and Cy5. PE absorbs light energy at 488 nm and emits at 670 nm, in the excitation range of Cy5, which acts as an acceptor dye. For fluoresence microscopy, cells were photographed

using a Nikon Eclipse E800 camera. Green and red fluorescent images were digitally superimposed using SPOT software (Diagnostic Instruments).

5. Mitochondrial transmembrane potential ($\Delta\Psi_m$) can be estimated by cationic lipophilic dyes with high binding affinity to the negatively charged inner mitochondrial membrane ***(9,71,72)***. Because binding characteristics do not completely overlap, parallel staining with several dyes is recommended.
6. The AFC calibration curve is very stable when measured on the same instrument and setting. The caspase assay is time and protein dependent when done with the suggested cell number and substrate concentration. Specificity of the enzymatic reaction was tested by using caspase-3 inhibitor DEVD-CHO and caspase-1/interleukin-converting enzyme (ICE) inhibitor tyrosinyl-valyl-alanyl-aspartate-chloromethyl-ketone (YVAD)-CMK at a concentration range of 50–300 μM ***(84)***. Caspase-8 activity can be tested using Z-IETD-AFC as a substrate. Caspase inhibitors Z-VAD and Boc-Asp as well as noncaspase cysteine protease inhibitor Z-FA were tested at concentrations of 20 μM, 50 μM, and 300 μM ***(85)***.

Acknowledgments

This work was supported in part by grants DK 49221 and AI 48079 from the National Institutes of Health, RG-2466 from the National Multiple Sclerosis Society, and the Central New York Community Foundation.

References

1 Elkon, K. B. (1994) Apoptosis in SLE—too little or too much? *Clin. Exp. Rheumatol.* **12,** 553–559.
2. Perl, A. and Banki, K. (1999) Molecular mimicry, altered apoptosis, and immunomodulation as mechanisms of viral pathogenesis in systemic lupus erythematosus, in *Lupus: Molecular and Cellular Pathogenesis* (Kammer, G. M. and Tsokos, G. C., eds.), Humana Press, Totowa, NJ, pp. 43–64.
3 Cohen, J. J., Duke, R. C., Fadok, V. A., and Sellins, K. S. (1992) Apoptosis and programmed cell death in immunity. *Annu. Rev. Immunol.* **10**, 267–293.
4 Thompson, C. B. (1995) Apoptosis in the pathogenesis and treatment of disease. *Science* **267,** 1456–1462.
5 Emlen, W., Niebur, J. A., and Kadera, R. (1994) Accelerated in vitro apoptosis of lymphocytes from patients with systemic lupus erythematosus. *J. Immunol.* **152,** 3685–3692.
6 Casciola-Rosen, L. A., Anhalt, G., and Rosen, A. (1994) Autoantigens targeted in systemic lupus erythematosus are clustered in two populations of surface structures on apoptotic keratinocytes. *J. Exp. Med*. **179,** 1317–1330.
7 Kovacs, B., Vassilopoulos, D., Vogelgesang, S. A., and Tsokos, G. C. (1996) Defective CD3-mediated cell death in activated T cells from patients with systemic lupus erythematosus: role of decreased intracellular TNF-alpha. *Clin. Immunol. Immunopathol*. **81,** 293–302.
8 Skulachev, V. P. (1999) Mitochondrial physiology and pathology; concepts of programmed death of organelles, cells and organisms. *Mol. Aspects Med.* **20,** 139–140.

9. Xiang, J., Chao, D. T., and Korsmeyer, S. J. (1996) BAX-induced cell death may not require interleukin 1b-converting enzyme-like proteases. *Proc. Natl. Acad. Sci. USA* **93,** 14,559–14,563.
10 Susin, S. A., Zamzami, N., Castedo, M., Daugas, E., Wang, H.-G., Geley, S., et al. (1997) The central executioner of apoptosis: multiple connections between protease activation and mitochondria in Fas/Apo-1/CD95- and ceramide-induced apoptosis. *J. Exp. Med.* **186,** 25–37.
11 Vander Heiden, M., Chandel, N. S., Williamson, E. K., Schumaker, P. T., and Thompson, C. B. (1997) Bcl-X_L regulates the membrane potential and volume homeostasis of mitochondria. *Cell* **91,** 627–637.
12 Constantini, P., Chernyak, B. V., Petronilli, V., and Bernardi, P. (1996) Modulation of the mitochondrial permeability transition pore by pyridine nucleotides and dithiol oxidation at two separate sites. *J. Biol. Chem.* **271,** 6746–6751.
13. Mayes, P. A. (1993) The pentose phosphate pathway and other pathways of hexose metabolism, in *Harper's Biochemistry* (Murray, R. K., Granner, D. K., Mayes, P. A., and Rodwell, V. W., eds.), Appleton and Lange, Norwalk, CT, pp. 201–211.
14 Banki, K., Hutter, E., Colombo, E., Gonchoroff, N. J., and Perl, A. (1996) Glutathione levels and sensitivity to apoptosis are regulated by changes in transaldolase expression. *J. Biol. Chem.* **271,** 32,994–33,001.
15. Banki, K., Hutter, E., Gonchoroff, N., and Perl, A. (1999) Elevation of mitochondrial transmembrane potential and reactive oxygen intermediate levels are early events and occur independently from activation of caspases in Fas signaling. *J. Immunol.* **162,** 1466–1479.
16 Perl, A., Gergely, P., Jr., Puskas, F., and Banki, K. (2002) Metabolic switches of T-cell activation and apoptosis. *Antioxid. Redox Signal*. **4,** 427–443.
17 Meier, B., Radeke, H. H., Selle, S., Younes, M., Sies, H., Resch, K., et al. (1989) Human fibroblasts release reactive oxygen species in response to interleukin-1 or tumor necrosis factor-α. *Biochem. J.* **263,** 539–545.
18 Hennet, T., Richter, C., and Peterhans, E. (1993) Tumor necrosis factor-α induces superoxide anion generation in mitochondria of L929 cells. *Biochem. J.* **289,** 587–592.
19 Schulze-Osthoff, K., Krammer, P. H., and Droge, W. (1994) Divergent signaling via APO-1/Fas and the TNF receptor, two homologous molecules involved in physiological cell death. *EMBO J.* **13,** 4587–4596.
20 Gergely, P., Nekam, K., Lang, I., Kalmar, L., Gonzalez-Cabello, R., and Perl, A. (1984) Ketoconazole in vitro inhibits mitogen-induced blastogenesis, antibody-dependent cellular cytotoxicity, natural killer activity and random migration of human leukocytes. *Immunopharmacology* **7,** 167–170.
21 Williams, M. S. and Henkart, P. A. (1996) Role of reactive oxygen intermediates in TCR-induced death of T cell blasts and hybridomas. *J. Immunol.* **157,** 2395–2402.
22 Gulbins, E., Brenner, B., Schlottmann, K., Welsch, J., Heinle, H., Koppenhoefer, U. L., et al. (1996) Fas-induced programmed cell death is mediated by a Ras-regulated O2- synthesis. *Immunology* **89,** 205–212.

23 Um, H. D., Orenstein, J. M., and Wahl, S. M. (1996) Fas mediates apoptosis in human monocytes by a reactive oxygen intermediate dependent pathway. *J. Immunol.* **156,** 3469–3477.
24 Puskas, F., Gergely, P., Banki, K., and Perl, A. (2000) Stimulation of the pentose phosphate pathway and glutathione levels by dehydroascorbate, the oxidized form of vitamin C. *FASEB J.* **14,** 1352–1361.
25 Li, P.-F., Dietz, R., and von Harsdorf, R. (1999) p53 regulates mitochondrial membrane potential through reactive oxygen species and induces cytochrome *c*-independent apoptosis blocked by bcl-2. *EMBO J.* **18,** 6027–6036.
26 Gottlieb, E., Vander Heiden, M. G., and Thompson, C. B. (2000) Bcl-X_L prevents the initial decrease in mitochondrial membrane potential and subsequent reactive oxygen species production during tumor necrosis factor alpha-induced apoptosis. *Mol. Cell. Biol.* **20,** 5680–5689.
27 Scarlett, J. L., Sheard, P. W., Hughes, G., Ledgerwood, E. C., Ku, H.-H., and Murphy, M. P. (2000) Changes in mitochondrial membrane potential during staurosporin-induced apoptosis in Jurkat cells. *FEBS Lett.* **475,** 267–272.
28 Sanchez-Alcazar, J. A., Ault, J. G., Khodjakov, A., and Schneider, E. (2000) Increased mitochondrial cytochrome *c* levels and mitochondrial hyperpolarization precede camptothecin-induced apoptosis in Jurkat cells. *Cell Death Differ.* **7,** 1090–1100.
29 Almeida, A., Almeida, J., Bolanos, J. P., and Moncada, S. (2001) Different responses of astrocytes and neurons to nitric oxide: the role of glycolytically generated ATP in astrocyte protection. *Proc. Natl. Acad. Sci. USA* **98,** 15,294–15,299.
30 Tewari, M. and Dixit, V. M. (1995) Fas- and tumor necrosis factor-induced apoptosis is inhibited by the Poxvirus *crmA* gene product. *J. Biol. Chem.* **270,** 3255–3260.
31 Los, M., Van de Craen, M., Penning, L. S., Schenk, H., Westendorp, M., Baeuerle, P. A., et al. (1995) Requirement of an ICE/CED-3 protease for Fas/Apo-1-mediated apoptosis. *Nature* **375,** 81–83.
32 Enari, M., Hug, H., and Nagata, S. (1995) Involvement of an ICE-like protease in Fas-mediated apoptosis. *Nature* **375,** 78–81.
33 Salvesen, G. S. and Dixit, V. M. (1997) Caspases: intracellular signaling by proteolysis. *Cell* **91,** 443–446.
34 Gross, A., McDonnell, J. M., and Korsmeyer, S. J. (1999) BCL-2 family members and the mitochondria in apoptosis. *Genes Dev.* **13,** 1899–1911.
35 Banki, K., Hutter, E., Gonchoroff, N. J., and Perl, A. (1998) Molecular ordering in HIV-induced apoptosis: oxidative stress, activation of caspases, and cell survival are regulated by transaldolase. *J. Biol. Chem.* **273,** 11,944–11,953.
36 Gergely, P. J., Grossman, C., Niland, B., Puskas, F., Neupane, H., Allam, F., et al. (2002) Mitochondrial hyperpolarization and ATP depletion in patients with systemic lupus erythematosus. *Arthritis Rheum.* **46,** 175–190.
37 Gergely, P. J., Niland, B., Gonchoroff, N., Pullmann, R., Jr., Phillips, P. E., and Perl, A. (2002) Persistent mitochondrial hyperpolarization, increased reactive oxygen intermediate production, and cytoplasmic alkalinization characterize altered IL-

10 signaling in patients with systemic lupus erythematosus. *J. Immunol.* **169,** 1092–1101.
38. Stryer, L. (1988) *Biochemistry*, Freeman, New York, pp. 397–426.
39 Leist, M., Single, B., Castoldi, A. F., Kuhnle, S., and Nicotera, P. (1997) Intracellular adenosine triphosphate (ATP) concentration: a switch in the decision between apoptosis and necrosis. *J. Exp. Med.* **185,** 1481–1486.
40. Lee, Y. and Shacter, E. (1999) Oxidative stress inhibits apoptosis in human lymphoma cells. *J. Biol. Chem.* **274,** 19,792–19,798.
41 Chow, S. C., Kass, G. E. N., and Orrenius, S. (1997) Purine and their role in apoptosis. *Neuropharmacology* **36,** 1149–1156.
42 Lewis, R. S. (2001) Calcium signaling mechanisms in T lymphocytes. *Annu. Rev. Immunol.* **19,** 497–521.
43 LaNoue, K. F. and Duszynski, J. (1992) Kinetic studies of ATP synthase: the case for the positional change mechanism. *J. Bioenerg. Biomembr.* **24,** 499–506.
44 McConkey, D. J. and Orrenius, S. (1996) The role of calcium in the regulation of apoptosis. *J. Leukoc. Biol.* **59,** 775–783.
45 Hamilos, D. L. and Wedner, H. J. (1985) The role of glutathione in lymphocyte activation. I. Comparison of inhibitory effects of buthionine sulfoximine and 2-cyclohexene-1-one by nuclear size transformation. *J. Immunol.* **135,** 2740–2747.
46 Suthanthiran, M., Anderson, M. E., Sharma, V. K., and Meister, A. (1990) Glutathione regulates activation-dependent DNA synthesis in highly purified normal human T lymphocytes stimulated via the CD2 and CD3 antigens. *Proc. Natl. Acad. Sci. USA* **87,** 3343–3347.
47 Salvemini, F., Franze, A., Iervolino, A., Filosa, S., Salzano, S., and Ursini, M. V. (1999) Enhanced glutathione levels and oxidoresistance mediated by increased glucose-6-phosphate dehydrogenase expression. *J. Biol. Chem.* **274,** 2750–2757.
48 Le Moine, O., Louis, H., Stordeur, P., Collet, J. M., Goldman, M., and Deviere, J. (1997) Role of reactive oxygen intermediates in interleukin 10 release after cold liver ischemia and reperfusion in mice. *Gastroenterology* **113,** 1701–1706.
49 al Janadi, M., al Balla, S., al Dalaan, A., and Raziuddin, S. (1993) Cytokine profile in systemic lupus erythematosus, rheumatoid arthritis, and other rheumatic diseases. *J. Clin. Immunol.* **13,** 58–67.
50 Studnicka-Benke, A., Steiner, G., Petera, P., and Smolen, J. S. (1996) Tumour necrosis factor alpha and its soluble receptors parallel clinical disease and autoimmune activity in systemic lupus erythematosus. *Br. J. Rheumatol.* **35,** 1067–1074.
51 Swaak, A. J., van den Brink, H. G., and Aarden, L. A. (1996) Cytokine production (IL-6 and TNF alpha) in whole blood cell cultures of patients with systemic lupus erythematosus. *Scand. J. Rheumatol.* **25,** 233–238.
52. Handwerger, B. S., Luzina, I., Da Silva, L., Storrer, C. E., and Via, C. S. (1999) Cytokines in the immunopathogenesis of lupus, in *Lupus: Molecular and Cellular Pathogenesis* (Kammer, G. S. and Tsokos, G. C., eds.) Humana, Totowa, NJ, pp. 321–340.
53 Otsuji, M., Kimura, Y., Aoe, T., Okamoto, Y., and Saito, T. (1996) Oxidative stress by tumor-derived macrophages suppresses the expression of CD3 zeta chain

of T-cell receptor complex and antigen-specific T-cell responses. *Proc. Natl. Acad. Sci. USA* **93,** 13,119–13,124.

54 Liossis, S. N., Ding, X. Z., Dennis, G. J., and Tsokos, G. C. (1998) Altered pattern of TCR/CD3-mediated protein-tyrosyl phosphorylation in T cells from patients with systemic lupus erythematosus. Deficient expression of the T cell receptor zeta chain. *J. Clin. Invest.* **101,** 1448–1457.

55 Li, D., Yang, B., and Mehta, J. L. (1998) Ox-LDL induces apoptosis in human coronary artery endothelial cells: role of PKC, PTK, bcl-2, and Fas. *Am. J. Physiol.* **275,** H568–H576.

56. Orlinick, J. R., Vaishnaw, A., Elkon, K. B., and Chao, M. V. (1997) Requirement of cysteine-rich repeats of the Fas receptor for binding of the Fas ligand. *J. Biol. Chem.* **272,** 28,889–28,894.

57 Bennett, M., Macdonald, K., Chan, S.-W., Luzio, J. P., Simari, R., and Weissberg, P. (1998) Cell surface trafficking of Fas: a rapid mechanism of p53-induced apoptosis. *Science* **282,** 290–293.

58 Kasibhatla, S., Genestier, L., and Green, D. R. (1999) Regulation of Fas ligand expression during activation-induced cell death in T lymphocytes. *J. Biol. Chem.* **274,** 987–992.

59 He, J., Choe, S., Walker, R., Di Marzio, P., Morgan , D. O., and Landau, N. R. (1995) Human immunodeficiency virus type 1 viral protein R (vpr) arrests cells in the G2 phase of the cell cycle by inhibiting p34cdc2 activity. *J. Virol.* **69,** 6705–6711.

60 Lorenz, H. M., Grunke, M., Hieronymus, T., Herrmann, M., Kuhnel, A., and Manger, B. (1997) In vitro apoptosis and expression of apoptosis-related molecules in lymphocytes from patients with systemic lupus erythematosus and other autoimmune diseases. *Arthritis Rheum.* **40,** 306–317.

61 Georgescu, L., Vakkalanka, R. K., Elkon, K. B., and Crow, M. K. (1997) Interleukin-10 promotes activation-induced cell death of SLE lymphocytes mediated by Fas ligand. *J. Clin. Invest.* **100,** 2622–2633.

62 Oates, J. C., Christensen, E. F., Reilly, C. M., Self, S. E., and Gilkeson, G. S. (1999) Prospective measure of serum 3-nitrotyrosine levels in systemic lupus erythematosus: correlation with disease activity. *Proc. Assoc. Am. Phys.* **111,** 611–621.

63 Cooper, G. S., Dooley, M. A., Treadwell, E. L., St. Clair, E. W., Parks, C. G., and Gilkeson, G. S. (1998) Hormonal, environmental, and infectious risk factors for developing systemic lupus erythematosus. *Arthritis Rheum.* **41,** 1714–1724.

64 Sen, C. K. and Packer, L. (1996) Antioxidant and redox regulation of gene transcription. *FASEB J.* **10,** 709–720.

65 Li, N. and Karin, N. (1999) Is NF-kB the sensor of oxidative stress? *FASEB J.* **13,** 1137–1143.

66 Blatt, N. B., Bednarski, J. J., Warner, R. E., Leonetti, F., Johnson, K. M., Boitano, A., et al. (2002) Benzodiazepine-induced superoxide signals B cell apoptosis: mechanistic insight and potential therapeutic utility. *J. Clin. Invest.* **110,** 1123–1132.

67 Lamarre, D., Talbot, B., De Murcia, G., LaPlante, C., LeDuc, Y., Mazen, A., et al. (1988) Structural and functional analysis of poly(ADP-ribose) polymerase: an immunological study. *Biochim. Biophys. Acta* **950,** 147–160.

68 Colombo, E., Banki, K., Tatum, A. H., Daucher, J., Ferrante, P., Murray, R. S., et al. (1997) Comparative analysis of antibody and cell-mediated autoimmunity to transaldolase and myelin basic protein in patients with multiple sclerosis. *J. Clin. Invest.* **99,** 1238–1250.

69 Vermes, I., Haanen, C., Steffens-Nakken, H., and Reutelingsperger, C. (1995) A novel assay for apoptosis. Flow cytometric detection of phosphatidylserine expression on early apoptotic cells using fluorescein labelled annexin V. *J. Immunol. Meth.* **184,** 39–51.

70 Martin, S. J., Reutelingsperger, C. P. M., McGahon, A. J., Rader, J. A., van Schie, C. A. A., LaFace, D. M., et al. (1995) Early redistribution of plasma membrane phosphatidylserine is a general feature of apoptosis regardless of the initiating stimulus: inhibition by overexpression of bcl-2 and Abl. *J. Exp. Med.* **182,** 1545–1556.

71 Petit, P. X., O'Connor, J. E., Grunwald, D., and Brown, S. C. (1990) Analysis of the membrane potential of rat- and mouse-liver mitochondria by flow cytometry and possible applications. *Eur. J. Biochem.* **194,** 389–397.

72 Tanner, M. K., Wellhausen, S. R., and Klein, J. B. (1993) Flow cytometric analysis of altered mononuclear cell transmembrane potential induced by cyclosporin. *Cytometry* **14,** 59–69.

73 Smiley, S. T., Reers, M., Mottola-Hartshorn, C., Lin, M., Chen, A., Smith, T. W., et al. (1991) Intracellular heterogeneity in mitochondrial membrane potentials revealed by a J-aggregate-forming cation JC-1. *Proc. Natl. Acad. Sci. USA* **88,** 3671–3675.

74 Cossarizza, A., Franceschi, C., Monti, D., Salvioli, S., Bellesia, E., Rivabene, R., et al. (1995) Protective effect of N-acetylcysteine in tumor necrosis factor-a-induced apoptosis in U937 cells: the role of mitochondria. *Exp. Eye Res.* **220,** 232–240.

75. Royall, J. A. and Ischiropoulos, H. (1993) Evaluation of 2(,7(-dichlorofluorescein and dihydrorhodamine 123 as fluorescent probes for intracellular H_2O_2 in cultured endothelial cells. *Arch. Biochem. Biophys.* **302,** 348–355.

76 Wieder, E. D., Hang, H., and Fox, M. H. (1993) Measurement of intracellular pH using flow cytometry with carboxy-SNARF-1. *Cytometry* **14,** 916–921.

77 Fiers, W., Beyaert, R., Declercq, W., and Vandenabeele, P. (1999) More than one way to die: apoptosis, necrosis and reactive oxygen damage. *Oncogene* **18,** 7719–7730.

78 Lundin, A. (2000) Use of firefly luciferase in ATP-related assays of biomass, enzymes, and metabolites. *Meth. Enzymol.* **305,** 346–370.

79 Lowry, O. H., Rosebrough, N. J., Farr, A. L., and Randall, R. J. (1951) Protein measurement with the Folin phenol reagent. *J. Biol. Chem.* **193,** 265–275.

80. Lundin, A. (1994) ATP extractants neutralized by cyclodextrins, in *Bioluminescence and Chemiluminescence* (Campbell, A. K., Kricka, L. J., and Stanley, P. E., eds.) Wiley, Chichester, UK, pp. 399–402.

81 Fariss, M. W. and Reed, D. J. (1987) High-performance liquid chromatography of thiols and disulfides: dinitrophenol derivatives. *Meth. Enzymol.* **143,** 101–109.

82 Towbin, H. H., Staehelin, T., and Gordon, J. (1979) Electrophoretic transfer of proteins from polyacrylamide gels to nitrocellulose sheets: procedure and some applications. *Proc. Natl. Acad. Sci. USA* **76,** 4350–4354.
83 Nicoletti, I., Migliorati, G., Pagliacci, M. C., Grignani, F., and Riccardi, C. (1991) A rapid and simple method for measuring thymocyte apoptosis by propidium iodide staining and flow cytometry. *J. Immunol. Meth.* **139,** 271–279.
84 Nicholson, D. W., Ali, A., Thornberry, N. A., Vaillancourt, J. P., Ding, C. K., Gallant, M., et al. (1995) Identification and inhibition of ICE/CED-3 protease necessary for mammalian apoptosis. *Nature* **376,** 37–43.
85 Armstrong, R. C., Aja, T., Xiang, J., Gaur, S., Krebs, J. F., Hoang, K., et al. (1996) Fas-induced activation of the cell death-related protease CPP32 is inhibited by bcl-2 and by ICE family protease inhibitors. *J. Biol. Chem.* **271,** 16,850–16,855.
86 Eisner, M. D., Amory, J., Mullaney, B., Tierney, L., Jr., and Browner, W. S. (1996) Necrotizing lymphadenitis associated with systemic lupus erythematosus. *Semin. Arthritis Rheum.* **26,** 477–482.
87 Llorente, L., Zou, W., Levy, Y., Richaud-Patin, Y., Wijdenes, J., Alcocer-Varela, J., et al. (1995) Role of interleukin 10 in the B lymphocyte hyperactivity and autoantibody production of human systemic lupus erythematosus. *J. Exp. Med.* **181,** 839–844.
88 Green, J. M. and Thompson, C. B. (1994) Modulation of T cell proliferative response by accessory cell interactions. *Immunol. Res.* **13,** 234–243.
89 Los, M., Schenk, H., Hexel, K., Baeuerle, P. A., Droge, W., and Schulze-Osthoff, K. (1995) IL-2 gene expression and NF-kappa B activation through CD28 requires reactive oxygen production by 5-lipoxygenase. *EMBO J.* **14,** 3731–3740.
90 Tatla, S., Woodhead, V., Foreman, J. C., and Chain, B. M. (1999) The role of reactive oxygen species in triggering proliferation and IL-2 secretion in T cells. *Free Radic. Biol. Med.* **26,** 14–24.
91. Casciola-Rosen, L. A., Miller, D. K., Anhalt, G. J., and Rosen, A. (1994) Specific cleavage of the 70 kDa protein component of the U1 small nuclear ribonucleoprotein is a characteristic biochemical feature of apoptotic cell death. *J. Biol. Chem.* **269,** 30,757–30,760.
92 Perl, A. and Banki, K. (2000) Genetic and metabolic control of the mitochondrial transmembrane potential and reactive oxygen intermediate production in HIV disease. *Antioxid. Redox Signal* **2,** 551–573.
93 Puskas, F., Gergely, P. J., Niland, B., Banki, K., and Perl, A. (2002) Differential regulation of hydrogen peroxide and Fas-dependent apoptosis pathways by dehydroascorbate, the oxidized form of vitamin C. *Antioxid. Redox Signal* **4,** 358–369.
94. Harada, H., Becknell, B., Wilm, M., Mann, M., Huang, L. J., Taylor, S. S., et al. (1999) Phosphorylation and inactivation of BAD by mitochondria-anchored protein kinase *A. Mol. Cell* **3,** 413–422.

7

Methods for Inducing Apoptosis

Kathryn M. Roberts, Antony Rosen, and Livia A. Casciola-Rosen

Summary

Apoptotic cells are sources of tolerogenic material during tissue homeostasis; abnormalities in apoptosis or in the clearance of apoptotic material generate a novel source of antigens against which an autoimmune response may be initiated. In our laboratory, we study the biochemistry and cell biology of systemic autoimmune disease autoantigens during different forms of cell death. Several different methods for inducing apoptosis, and for assaying the induction of this cellular process, are routinely performed. This chapter describes methods for inducing apoptosis via ultraviolet B irradiation, small molecule drug treatments, death receptor ligation, and exposure to granule components of cytotoxic lymphocytes. Assays to confirm the induction of apoptosis by quantifying changes in mitochondrial membrane potential, phosphatidylserine membrane localization, DNA content, and autoantigen cleavage are also detailed.

Key Words: Apoptosis; autoantigens; autoimmunity; caspase; cytotoxic lymphocytes; Fas ligation; granzyme B; UVB irradiation.

1. Introduction

Systemic autoimmune diseases encompass a broad spectrum of multisystem illnesses characterized by immune-mediated tissue damage and the presence of high-titer autoantibodies to a diverse array of autoantigens. There is an emerging consensus that the apoptotic cell is a potent source of tolerogenic material during homeostatic tissue turnover, and that abnormalities in the signaling, execution, and clearance of apoptotic material may be an important source of antigens in systemic autoimmune diseases.

Studies performed in our laboratory addressed the cell biologic and biochemical fate of systemic disease autoantigens during different forms of cell death. We have shown that (a) autoantigens are clustered and concentrated in the surface blebs of apoptotic cells ***(1,2)***, and (b) many of these proteins are cleaved during cell death by several families of apoptotic proteases, including

From: *Methods in Molecular Medicine, Vol. 102: Autoimmunity: Methods and Protocols*
Edited by: A. Perl © Humana Press Inc., Totowa, NJ

caspases and granzyme B (GrB, a protease released from cytotoxic lymphocyte granules during target cell killing) ***(3–7)***. These studies require the quantitative analysis of cell death pathways and their biochemical signatures, the methods for which are reviewed in detail in this chapter.

Apoptosis is a highly conserved cell death process mediated in part by a family of cysteine proteases (caspases) that achieve the final apoptotic phenotype through cleavage of a specific group of downstream substrates. Although numerous upstream mediators engage a restricted group of upstream molecular pathways to initiate apoptosis, they mostly converge on a common set of downstream pathways through activation of effector caspases. Initiating signals can be delivered and transduced at several different subcellular sites, including plasma membrane, mitochondria, endoplasmic reticulum, and the Golgi apparatus ***(8)***. In each case, initiation rests on the assembly of a multimolecular complex, which functions to activate effector caspases that cleave downstream substrates.

All the assays described in this chapter focus on the downstream biochemical features of apoptosis, which include evidence of cleavage of signature caspase substrates ***(9,10)***, exposure of phosphatidylserine (PS) at the outer surface of the plasma membrane bilayer ***(11)***, alterations of mitochondrial membrane potential ***(12)***, or internucleosomal DNA fragmentation ***(13,14)***. Many apoptosis initiators involve incubating cells with small molecules that engage relevant proapoptotic signaling pathways (e.g., staurosporine, brefeldin A), and these are dealt with in **Subheading 3.2.**. Other pathways of apoptosis induction involve the ligation of a cell surface receptor (e.g., FasR) by a proapoptotic ligand (**Subheading 3.3.**), exposure to ultraviolet irradiation (**Subheading 3.1.**), and exposure to cytotoxic lymphocyte granule components (**Subheadings 3.4.** and **3.5.**).

2. Materials

2.1. Ultraviolet B Irradiation of Cultured Cells

1. Cultured cells.
2. Dulbecco's phosphate-buffered saline (PBS).
3. Ultraviolet B (UVB) source (Spectra Mini II, DaarLin Company, Bryan, OH). The UVB output must be measured; this can be done using a UVX digital radiometer with a UVX-31 sensor (calibration wavelength 310 nm).

2.2. Drug Treatment of Cultured Cells

1. Staurosporine. Make a 1 m*M* stock solution in dimethyl sulfoxide (DMSO) and store at –20°C protected from light.
2. C2-Ceramide (*N*-acetyl-D-sphingosine) or C6-ceramide (*N*-hexanoyl-D-sphingosine). Make 10 m*M* stock solutions in DMSO and store at –20°C.
3. 2-Deoxyglucose. Make a 1 *M* stock solution in H_2O and store at –20°C.

4. DMEM (Dulbecco's modified Eagle's medium) without glucose and without sodium pyruvate (Gibco 11966-025, Gibco/Invitrogen, Carlsbad, CA).
5. Brefeldin A. Make a 10 mg/mL stock in DMSO and store at –20°C.
6. Thapsigargin. Make a 1 m*M* stock in DMSO and store at –20°C protected from light.

2.3. Fas Ligation of Cultured Cells

1. Anti-Fas monoclonal antibody (clone CH-11).
2. Fas-positive target cells (e.g., Jurkat cells).

2.4. Incubation of Cultured Cells With Cytotoxic Lymphocyte Granule Contents

1. Granule contents purified from YT cells (*see* **Subheading 3.4.**); store at –80°C.
2. Relaxation buffer (10 m*M* Pipes at pH 6.8, 100 m*M* KCl, 3.5 m*M* $MgCl_2$, 1.25 m*M* ethyleneglycol-bis (2-aminoethyelether) *N*,*N*,*N'*,*N'*-tetraacetic acid (EGTA), 1 m*M* adenosine triphosphate [ATP]).
3. Cultured cells (may be adherent or suspension cultures).
4. Cell lifters for lifting adherent cells off culture dishes (cat. no. 3008, Corning Costar, Corning, NY).
5. Hanks balanced salt solution (HBSS) without calcium and magnesium, stored at 4°C.
6. HBSS without calcium and magnesium supplemented with 10 m*M* HEPES at pH 7.4 and 10 m*M* $MgSO_4$ (HBSS/HEPES/Mg), stored at 4°C.
7. 150 m*M* $CaCl_2$ stock solution (0.22-μm filtered).

2.5. Lymphokine-Activated Killer Cell Assay

1. Sterile PBS.
2. Blood collection equipment, including collection tubes with heparin or citrate anticoagulant.
3. Ficoll-Paque™ Plus (Amersham Biosciences, Piscataway, NJ, cat. no. 17-1440-02).
4. Sterile HBSS at room temperature.
5. Lymphokine-activated killer (LAK) medium (RPMI, 2% autologous human plasma, L-glutamine, penicillin, streptomycin, 10 m*M* HEPES at pH 7.4, sterile filtered through 0.22-μm filter).
6. Recombinant human interleukin 2 (cat. no. 356043, BD Biosciences, San Diego, CA; to minimize loss of activity, aliquot into small volumes, store at –80°C, and avoid multiple freezing and thawing).
7. K562 target cells (CCL-243, ATCC, Manassas, VA) cultured in RPMI-1640, 10% fetal calf serum (not heat inactivated), L-glutamine.
8. Round-bottom, 96-well plates and centrifuge with a 96-well plate holder.

2.6. Assays to Confirm Induction of Apoptosis

The necessary reagents vary widely, depending on which assay for apoptosis is used. Because detailing all assays is beyond the scope of this chapter, we describe four commonly used methods to confirm apoptosis. *See* **Subheading 4.6.** for references to other assays.

2.6.1. Cleavage of Autoantigens by Apoptotic Proteases as Assayed by Immunoblotting

1. Lysis buffer: 1% Nonidet P-40, 20 m*M* Tris-HCl at pH 7.4, 150 m*M* NaCl, 1 m*M* ethylenediaminetetraacetic acid (EDTA). Store at 4°C. Add protease inhibitors (antipain, [1 μg/mL], leupeptin [1 μg/mL], chymostatin [1 μg/mL], pepstatin [1 μg/mL], phenylmethyl sulfonyl fluoride [1 m*M*]) immediately before use.
2. 5X gel application buffer: 10% sodium dodecyl sulfate (SDS), 20% glycerol, 200 m*M* Tris-HCl, pH 6.8, 3 mg bromophenol blue. Store at room temperature. Add 5% 2-mercaptoethanol to this buffer immediately before use on lysates.
3. Apparatus and reagents to run SDS-polyacrylamide gels and transfer proteins to membranes (e.g., nitrocellulose or immobilon). All are detailed in **ref. *15***. Reagents, buffers, and antibodies to perform Western blots are as described in **ref. *15***.

2.6.2. Assay of Mitochondrial Membrane Potential ($\Delta\Psi_m$)

1. JC-1 (5,5',6,6'-tetrachloro-1,1',3,3'-tetraethylbenzimidazolyl carbocyanine iodide) can be purchased from several vendors. Make a 1- to 5-mg/mL stock solution in DMSO and store protected from light at –20°C in single-use aliquots.
2. PBS.

2.6.3. Annexin V Staining

1. Fluorescently conjugated annexin V (also available as an annexin V staining kit).
2. 10X binding buffer: 0.1 *M* HEPES at pH 7.4, 1.4 *M* NaCl, 25 m*M* $CaCl_2$, diluted to 1X before use (or use the binding buffer recommended by the annexin V supplier).
3. PBS.

2.6.4. Propidium Iodide Staining

1. PBS.
2. Propidium iodide (PI) staining solution: 10 μg/mL PI, 50 μg/mL ribonuclease A, in PBS. Make this solution fresh before use and protect from light. PI is commercially available as a solution or solid. If using the solid, make a 1-mg/mL stock solution in water and store at 4°C, protected from light.
3. 75% ethanol at 4°C.

3. Methods

Five different methods frequently used to induce apoptosis in intact cells are described in this section. They range from treatment of cultured cells with chemical reagents (*see* **Subheading 3.2.**) to the physiological cytotoxic lymphocyte-induced cytotoxicity of intact target cells (LAK cell assay; *see* **Subheading 3.5.**). In addition, methods to verify and quantitate the induction of apoptosis are detailed or referenced (*see* **Subheading 3.6.**).

3.1. UVB Irradiation of Cultured Cells

1. Both adherent and nonadherent cell types can be used. Wash cells twice with PBS and leave cells in PBS for UVB irradiation. Resuspend nonadherent cells at 1×10^5 to 1×10^6 cells/mL for irradiation. Irradiate adherent cell cultures in tissue culture dishes (use 10 mL PBS for a 10-cm culture dish).
2. Irradiate cells for the required amount of time to deliver the desired dose of UVB (*see* **Note 1**).
3. Remove PBS and replace with the appropriate culture medium. Place cells in a 37°C humidified incubator (*see* **Note 2**).
4. Harvest the cells after they have been incubated for the optimal amount of time to induce apoptosis (*see* **Note 3**).

3.2. Drug Treatment of Cultured Cells

1. Plate cells (suspension or adherent cultures) at a moderate density in dishes; include additional dishes for untreated and vehicle-treated controls.
2. Dilute drug to be used in normal growth medium, unless otherwise specified, at the following final concentrations (these are given as general guidelines, but should be optimized by performing a dose–response assessment): 1 μ*M* staurosporine, 20 μ*M* ceramide, 1 μg/mL brefeldin A, 0.2 μ*M* thapsigargin, and 10 m*M* 2-deoxyglucose. For 2-deoxyglucose treatment, wash the cells several times in medium without glucose and pyruvate before incubating with glucose- and pyruvate-free medium to which 10 m*M* 2-deoxyglucose has been added.
3. Add drugs to cells and incubate in a humidified atmosphere at 37°C. During the incubation, cultures can be visually inspected with phase contrast microscopy to monitor morphological drug-induced changes (*see* **Note 4**). Perform a time course to optimize the length of the incubation as this will vary depending on cell type and drug dose used. The following times are given as general guidelines for different treatments: staurosporine, 4–6 h; ceramide, brefeldin A, and 2-deoxyglucose, 16–24 h; thapsigargin, 24 h.
4. Harvest cells for study and/or assay for induction of apoptosis after incubation for the optimal time (*see* **Subheading 3.6.**).

3.3. Fas Ligation

1. This procedure can only be used on Fas-positive target cells. The method described here has been optimized for Jurkat cells. Of note, cycloheximide frequently is added to other cell types in combination with anti-Fas antibody to augment induction of apoptosis ***(16–18)*** (*see* **Note 5**). Similar principles apply to other receptor-induced death pathways (e.g., that induced by tumor necrosis factor).
2. Plate Jurkat cells, suspended $0.5–1 \times 10^6$ cells/mL in culture medium, in a six-well dish.
3. Add anti-Fas monoclonal antibody CH-11 at a final concentration of 1 μg/mL.
4. Incubate cells in a 37°C, 5% CO_2 humidified incubator and harvest cells at appropriate times. Using cleavage of the autoantigen poly(ADP-ribose) poly-

merase (PARP) as a readout of apoptosis (*see* **Subheading 3.6.**), we found that approx 50% of PARP is cleaved after 90 min, and PARP cleavage is more than 95% complete at 3 h, confirming that Jurkat cells are rapidly induced to become apoptotic ***(19)***. Weis et al. ***(20)*** used various other assays to confirm apoptosis induced by anti-Fas antibody incubation with Jurkat cells.

3.4. Incubation of Cultured Cells With Cytotoxic Lymphocyte Granule Contents

1. Prepare granule contents from cultured YT cells (a human natural killer leukemia cell line) using a method based on that described by Peitsch and Tschopp ***(21)***. Briefly, culture the cells in medium consisting of RPMI-1640, 10% heat-inactivated fetal bovine serum (HIFBS). Wash 10^8–10^9 cells in relaxation buffer and resuspend them at 5×10^7 cells/mL in ice-cold relaxation buffer. Break the cells open by nitrogen cavitation (30 bar pressure on ice for 20 min) and centrifuge the resulting homogenate (300*g*, 5 min, 4°C). Load the supernatant onto linear 0–90% Percoll gradients (dilute with relaxation buffer to make the gradients) and centrifuge in a swinging bucket rotor (30,000*g*, 4°C, 45 min). Collect 0.8-mL fractions and assay these for the presence of GrB, which is used as a readout for the presence of granules (*see* **Note 6**). Pool the granule-containing fractions, centrifuge them (100,000*g*, 4°C) and discard most of the clear supernatant. Use the residual volume (approx 1 mL) to aspirate the pelleted granules from the centrifuge tube. To break open the intact granules, add 1.5 volumes of 3 *M* NaCl and keep the solution on ice for 30 min before centrifuging (100,000*g*, 4°C). Dialyze the resulting supernatant (containing GC) against PBS at 4°C. Aliquot the preparation into small volumes and store at –80°C.
2. Wash cultured cells twice in HBSS. If using suspension cultures, resuspend these after washing, at 8×10^6 cells/mL, in HBSS/HEPES/Mg buffer. Adherent cultures may be removed from the culture dishes by gently scraping the cells off in sheets with a cell scraper (*see* **Note 7**), aspirating a few times to dissociate the cells, centrifuging, and resuspending the cells at 8×10^6 cells/mL in HBSS/HEPES/Mg buffer. These cells can be incubated approx 10 min in a humidified incubator to allow cell membranes to reseal.
3. Set up cell-killing reactions on ice. Use 25 µL of suspended cells (aliquoted into a 1.5-mL microfuge tube) for a single reaction as this represents an amount of protein that can readily be immunoblotted in a single SDS PAGE gel lane (*see* **Subheading 3.6.**); if larger reactions are needed, scale up all the individual components proportionally. Add GC (*see* **Notes 8** and **9**), gently mix cells by manual pipetting a few times, and incubate on ice for 5 min. Control reactions are set up by adding an equivalent volume of PBS instead of GC.
4. Add $CaCl_2$ to a final concentration of 1.5 m*M* and incubate reactions at 37°C for the optimal time to induce apoptosis (*see* **Note 8**). Mix the reaction tubes gently every 15 min to prevent the cells from settling in the bottom of the tubes.
5. Terminate reactions at the appropriate time and assay as described to confirm apoptosis (*see* **Subheading 3.6.**). Note that reactions may be microfuged before

terminating so that intact apoptotic and normal cells (pellet) and the apoptotic material that has leaked out of the cells (supernatant) can be analyzed separately.

3.5. LAK Cell Assay

The following procedure is based on methods described by Topalian et al. ***(22)*** and Andrade et al. ***(23)***.

1. Collect 40 mL of blood with heparin or citrate anticoagulant. Dilute 1:1 (v/v) with sterile, room temperature PBS.
2. Add 12 mL Ficoll-PaquePlus into each of two 50-mL tubes. Carefully layer 35–40 mL of blood/PBS on top.
3. Centrifuge at 900*g* for 30 min at 20°C, with no brake.
4. Remove the supernatants and save them (the supernatants are the autologous serum needed to make up LAK medium).
5. Carefully transfer the whitish interface layers containing the peripheral blood mononuclear cells to a new tube. Wash three times with at least three volumes of room temperature HBSS. Pellet the cells by centrifuging (10 min, 400*g*, 20°C). Resuspend cells in LAK medium at 1×10^6 cells/ml.
6. Add 1000 Cetus U/mL recombinant interleukin (IL)-2 and culture cells for 6–7 d.
7. Wash cultured K562 cells twice with LAK medium, count, and resuspend at 1×10^6 cells/mL.
8. Resuspend LAK cells in fresh LAK medium at 3×10^6 cells/mL for a 3:1 effector:target ratio (*see* **Note 10**).
9. Pipet 100 µL each of K562 cells and LAK cells into a round-bottom, 96-well plate. Reactions should include LAK cells alone, K562 cells alone, and LAK cells plus K562 cells.
10. Briefly centrifuge the cells together in a centrifuge with a 96-well plateholder (3 min, 200*g*, room temperature), then incubate in a 37°C incubator for the desired time (*see* **Note 10**).
11. At completion of the incubation, assay as described in **Subheading 3.6.**. For biochemical analysis, 5X gel application buffer should be added directly to the incubation mixture, and washing should be avoided.

3.6. Assays to Confirm the Induction of Apoptosis

3.6.1. Immunoblotting to Assess Autoantigen Cleavage

1. Lyse cells in lysis buffer and generate samples for electrophoresis by adding the appropriate volume of 5X gel application buffer. Gels lanes can be loaded either based on equal cell numbers (when dealing with suspension cultures or the methods described in **Subheadings 3.4.** and **3.5.**) or based on equal protein loads. For the latter, a protein assay must be performed on an aliquot of lysate.
2. Run the gel samples on SDS polyacrylamide gels and subsequently transfer the proteins to nitrocellulose ***(15)***. Immunoblot as described ***(15)*** using a protein known to be cleaved during apoptosis (*see* **Note 12**). Apoptosis is quantified by measuring the amount of protein cleaved (*see* **Fig. 1**).

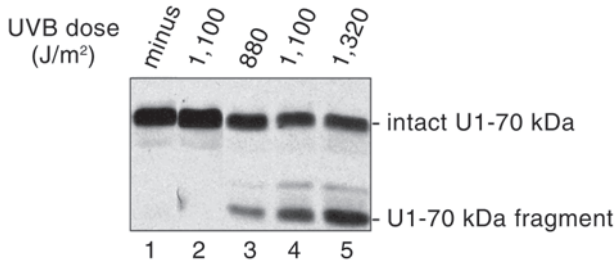

Fig. 1. Dose–response of UVB irradiation to determine optimal amount to induce apoptosis in cultured human keratinocytes. Cultured human keratinocytes (third passage) were irradiated with the indicated doses of UVB (lanes 2–5) or were not irradiated (lane 1). After irradiation, the cells either were harvested immediately (lane 2) or were incubated in fresh growth medium at 37°C for 16 h before harvesting. Cell lysates (50 μg/lane) were electrophoresed on 10% SDS polyacrylamide gels and immunoblotted with a patient serum monospecific for U1-70 kDa as described in **Subheading 3.6.** Intact U1-70 kDa and the 40-kDa fragment generated by caspase-3 cleavage during apoptosis are marked on the figure.

3.6.2. Assay of Mitochondrial Membrane Potential ($\Delta\Psi_m$)

Mitochondrial membrane potential changes can be detected using JC-1 (*see* **Note 13**) and analyzed by fluorescence-activated cell sorting (FACS) ***(12,24,25)***.

1. Dissociate cells with trypsin/EDTA if necessary and wash with serum-containing medium.
2. Resuspend cells at 1×10^6 cells/mL in medium.
3. Add JC-1 to a final concentration of 10 μg/mL. Incubate at 37°C, protected from light, for 10 min.
4. Wash cells twice with PBS and assay by FACS using a 488-nm argon-ion laser source. Collect emissions simultaneously on FL-1 and FL-2 channels.

3.6.3. Annexin V Staining

Annexin V staining specifically detects PS in the outer leaflet of the plasma membrane, an early feature of apoptotic cells ***(26)*** (*see* **Note 14**).

1. Collect cells. For adherent cells, trypsinize and wash in serum-containing medium, followed by PBS washes.
2. Rinse 1×10^5 to 1×10^6 cells in binding buffer and resuspend cells in binding buffer as indicated by annexin V supplier.
3. Add annexin V as indicated by supplier and incubate 10 min in the dark (from this point on and for any other manipulations, samples must be protected from light).

4. Analyze by FACS immediately or continue with PI staining before FACS analysis.

3.6.4. PI Staining to Determine Sub-G_0/G_1 Cell Population

The procedure described next is based on the method described by Telford et al. ***(27)***.

1. Collect cells and wash in PBS. For adherent cells, collect floaters and dissociate cells as described in **Subheading 3.6.3.**
2. Pellet cells by centrifugation.
3. Add 500 μL of cold 75% ethanol per 1×10^6 cells. Flick tube to resuspend the cells.
4. Leave at 4°C (30 min to overnight).
5. Wash in PBS.
6. Add 500 μL of PI solution (made fresh and protected from light). Incubate 10 min at room temperature before analyzing by FACS.

4. Notes

1. Of note, different cell types vary in their susceptibility to UVB irradiation. For example, approx 35% of a HeLa cell culture irradiated with 1650 J/m^2 UVB become apoptotic 7–8 h after irradiation. In contrast, cultured human muscle cells are unresponsive to this dose of UVB, and 293T cells are also fairly resistant to UVB irradiation. Jurkat cells, however, are more sensitive than HeLa cells to induction of apoptosis by UVB irradiation. The amount of UVB used must be optimized for each cell type by doing a dose–response analysis. The data presented in **Fig. 1** show that, with increasing doses of UVB irradiation, increased amounts of apoptosis are generated. Immunoblotting of the 40-kDa fragment, generated during apoptosis by caspase-3 cleavage of the U1-70-kDa protein, is used as a readout of apoptosis in this assay (*see* **Subheading 3.6.**).
2. The length of time taken to induce apoptosis after exposure to UVB differs for various cell types and should be optimized for each cell type by performing a time course of 37°C incubation after UVB irradiation (a 0- to 24-h range should be tested).
3. In the case of adherent cell cultures irradiated with UVB, the appearance of apoptotic cells can be readily observed using a standard tissue culture microscope. As the cells become apoptotic, they round up and become "blebbed." This can be used as an easy and helpful readout of how the cells are responding to UVB irradiation prior to harvesting them. In the earlier stages of apoptosis, the cells remain adherent, but will finally float into the medium. If the cells are harvested when many have detached, care should be taken to analyze both the remaining adherent cells as well as the floaters.
4. Treatment of adherent cell lines with the drugs described in **Subheading 3.2.** alters cell morphology as visualized by light microscopy; such changes are frequently not indicative of cell death. For example, staurosporine-treated HeLa cells begin to look flattened rapidly after treatment (within 1.5 h), although this

precedes detection of apoptosis by several hours. Ceramide treatment causes HeLa cells to become rounded and to detach, with little evidence of blebbing. HeLa cells treated with the other drugs described in **Subheading 3.2.** also become rounded, with the extent of blebbing varying and often seen only in the detached population of cells.

5. Although lymphocyte-derived cell lines (e.g., Jurkat cells) often are used in experiments involving induction of apoptosis via Fas ligation, the use of many other cell types has been reported in the literature. As the scope of this chapter precludes a full discussion, we include only a brief discussion of the issues here. There are many reports that pretreatment of cells with interferon-γ before Fas ligation can enhance susceptibility to Fas ligation ***(28–30)***. The commonly used HeLa cell line can be made susceptible to apoptosis induced by fas ligation when treated with PD98059 (a mitogen-activated protein kinase inhibitor), the protein synthesis inhibitor cycloheximide, or under serum starvation conditions ***(31)***. When using cell lines other than Jurkat cells, we suggest that the literature first be consulted to see if that cell type has been used previously. If not, we recommend starting with Fas ligation alone and in combination with other treatments, such as with preincubation with interferon-γ or cycloheximide.
6. To confirm which fractions contain granules, immunoblot a small amount (approx 1–2 μL) of each fraction with an antibody to GrB (an abundant protease in granules). Antibodies against GrB are commercially available from several different sources (e.g., cat no. 804-121-C100 Alexis Corp., San Diego, CA). Alternately, in vitro assays measuring cleavage of immunoblotted antigens to assess which fractions have GrB protease activity can be performed ***(5,23)***.
7. Methods other than mechanical lifting, which may cause some damage to cell membranes if performed too vigorously, may be used to remove adherent cells from culture dishes. EDTA (0.5–1 m*M*) can be used for this purpose, but it should be noted that not all cell types detach using this reagent. Alternately, treatment with trypsin/EDTA can be used, but caution should be exercised as trypsin can cleave cell surface proteins and decrease cell viability. After treatment with trypsin and/or EDTA, the cells must be thoroughly washed to remove these reagents before adding the GC.
8. The amount of GC to be added to each cytotoxicity assay and the length of incubation at 37°C must be optimized for each batch of GC and for each cell type used. Using cleavage of autoantigens as a readout of apoptosis (see **Subheading 3.6.**), we typically find that the first cleaved fragments appear within 15–30 min, with incubations generally carried out for 60–120 min. The amount of GC to be used in a 25 mL reaction depends on the concentration of the preparation and the activity of the GrB; in our experience, 2–2.5 μL of GC induce apoptosis effectively.
9. The specificity of GrB varies depending on the species (L. A. Casciola-Rosen, M. Garcia-Calvo, N. Thornberry, and A. Rosen, unpublished observations, 2004). Therefore, it is important, for example, to use GC prepared from human YT cells on cultured human cells. It is also important to define which granzymes are present because some cells (e.g., YT cells) express GrB, but lack granzyme A.

10. For each LAK preparation, it is important to optimize the ratio of effector cells to target cells (E:T), as well as the length of incubation for this assay, because the activity of different preparations varies. We recommend that the E:T ratios be titrated over a range of 1:1 to 10:1. We frequently find that the optimal ratio (for K562 targets) is 3:1 or 5:1 when the incubations are performed for 3–4 h.
11. Many methods can be used to detect apoptosis. The *Wiley Current Protocols* volumes have well-detailed methods as well as background information and commentary on most of the methods listed here, as well as for additional assays of apoptosis. The *Wiley Current Protocols* series is available on-line at http://www.mrw2.interscience.wiley.com/cponline/.
12. PARP cleavage during apoptosis, from the 116-kDa intact protein to an 89-kDa fragment generated by caspase-3, has been well characterized ***(32–34)***. For this reason, and because antibodies that immunoblot robustly are commercially available (e.g., cat. no. 9542 Cell Signalling Technology, Beverly, MA; cat. no. 06-557, Upstate Char-lottesville, VA), this is a protein of choice for immunoblotting in this assay.
13. JC-1 is a fluorescent dye that exists as a monomer at low membrane potential and as an aggregate at higher membrane potential. The monomeric form of JC-1 exhibits green fluorescence, whereas the aggregate exhibits red fluorescence. This dye is useful for detecting changes in membrane potential because healthy cells have red mitochondrial staining (indicating normal high mitochondrial membrane potential), whereas apoptotic cells fluoresce green (reflecting the decreased apoptotic mitochondrial membrane potential) ***(12,24,25)***.
14. PS is normally localized to the inner leaflet of the plasma membrane. Early in apoptosis, PS flips from the inner leaflet to the outer leaflet ***(11)***. Annexin V displays specific and high-affinity binding to PS, and its binding can be used as a marker for apoptosis ***(11,26)***. For annexin V to specifically stain extracellular PS, it must be used on unfixed cells because membrane damage that occurs during fixation can allow annexin V to enter the cell and also bind PS in the inner leaflet of the plasma membrane. When additional staining procedures are being performed on the same cell sample, annexin V staining must be done first. The cells can then be washed to remove unbound annexin V prior to fixation and other staining procedures.

Acknowledgments

This work was supported by National Institutes of Health grants AR 44684 (L. Casciola-Rosen) and R37 DE 12354 (A. Rosen), the Edmund C. Lynch Fellowship in Arthritis Research, and an Arthritis Foundation Maryland Chapter MARRC grant. A. Rosen is supported by a Burroughs Wellcome Fund Translational Research Award.

References

1 Rosen, A., Casciola-Rosen, L., and Ahearn, J. (1995) Novel packages of viral and self-antigens are generated during apoptosis. *J. Exp. Med.* **181,** 1557–1561.

2 Casciola-Rosen, L. A., Anhalt, G., and Rosen, A. (1994) Autoantigens targeted in systemic lupus erythematosus are clustered in two populations of surface structures on apoptotic keratinocytes. *J. Exp. Med.* **179,** 1317–1330.
3 Casciola-Rosen, L. A., Anhalt, G. J., and Rosen, A. (1995) DNA-dependent protein kinase is one of a subset of autoantigens specifically cleaved early during apoptosis. *J. Exp. Med.* **182,** 1625–1634.
4 Rosen, A. and Casciola-Rosen, L. (1999) Autoantigens as substrates for apoptotic proteases: implications for the pathogenesis of systemic autoimmune disease. *Cell Death Differ.* 6, **6–12.**
5 Casciola-Rosen, L., Andrade, F., Ulanet, D., Wong, W. B., and Rosen, A. (1999) Cleavage by granzyme B is strongly predictive of autoantigen status: implications for initiation of autoimmunity. *J. Exp. Med.* **190,** 815–826.
6 Casciola-Rosen, L. A., Pluta, A. F., Plotz, P. H., Cox, A. E., Morris, S., Wigley, F. M., et al. (2001) The DNA mismatch repair enzyme PMS1 is a myositis-specific autoantigen. *Arthritis Rheum.* **44,** 389–396.
7 Nagaraju, K., Cox, A., Casciola-Rosen, L., and Rosen, A. (2001) Novel fragments of the Sjögren's syndrome autoantigens alpha-fodrin and type 3 muscarinic acetylcholine receptor generated during cytotoxic lymphocyte granule-induced cell death. *Arthritis Rheum.* **44,** 2376–2386.
8 Ferri, K. F. and Kroemer, G. (2001) Organelle-specific initiation of cell death pathways. *Nat. Cell Biol.* **3,** E255–E263.
9 Casciola-Rosen, L. A., Miller, D. K., Anhalt, G. J., and Rosen, A. (1994) Specific cleavage of the 70-kDa protein component of the U1 small nuclear ribonucleoprotein is a characteristic biochemical feature of apoptotic cell death. *J. Biol. Chem.* **269,** 30,757–30,760.
10. Casciola-Rosen, L., Nicholson, D. W., Chong, T., Rowan, K. R., Thornberry, N. A., Miller, D. K., et al. (1996) Apopain/CPP32 cleaves proteins that are essential for cellular repair: a fundamental principle of apoptotic death. *J. Exp. Med.* **183,** 1957–1964.
11 Fadok, V. A., Voelker, D. R., Campbell, P. A., Cohen, J. J., Bratton, D. L., and Henson, P. M. (1992) Exposure of phosphatidylserine on the surface of apoptotic lymphocytes triggers specific recognition and removal by macrophages. *J. Immunol.* **148,** 2207–2216.
12 Zamzami, N., Marchetti, P., Castedo, M., Zanin, C., Vayssiere, J. L., Petit, P. X., et al. (1995) Reduction in mitochondrial potential constitutes an early irreversible step of programmed lymphocyte death in vivo. *J. Exp. Med.* **181,** 1661–1672.
13 Wyllie, A. H. (1980) Glucocorticoid-induced thymocyte apoptosis is associated with endogenous endonuclease activation. *Nature* **284,** 555–556.
14 Gavrieli, Y., Sherman, Y., and Ben Sasson, S. A. (1992) Identification of programmed cell death in situ via specific labeling of nuclear DNA fragmentation. *J. Cell Biol.* **119,** 493–501.
15 Casciola-Rosen, L. and Nagaraju, K. (2002) Immunoblotting of single cell types isolated from frozen sections by laser microdissection. *Methods Enzymol.* **356,** 70–79.

16 Nophar, Y., Holtmann, H., Ber, R., and Wallach, D. (1988) Dominance of resistance to the cytocidal effect of tumor necrosis factor in heterokaryons formed by fusion of resistant and sensitive cells. *J. Immunol.* **140,** 3456–3460.
17 Wallach, D. (1997) Cell death induction by TNF: a matter of self control. *Trends Biochem. Sci.* **22,** 107–109.
18 Hahn, T., Toker, L., Budilovsky, S., Aderka, D., Eshhar, Z., and Wallach, D. (1985) Use of monoclonal antibodies to a human cytotoxin for its isolation and for examining the self-induction of resistance to this protein. *Proc. Natl. Acad. Sci. USA* **82,** 3814–3818.
19 Greidinger, E. L., Miller, D. K., Yamin, T. T., Casciola-Rosen, L., and Rosen, A. (1996) Sequential activation of three distinct ICE-like activities in Fas-ligated Jurkat cells. *FEBS Lett.* **390,** 299–303.
20 Weis, M., Schlegel, J., Kass, G. E., Holmstrom, T. H., Peters, I., Eriksson, J., et al. (1995) Cellular events in Fas/APO-1-mediated apoptosis in Jurkat T lymphocytes. *Exp. Cell Res.* **219,** 699–708.
21 Peitsch, M. C. and Tschopp, J. (1994) Granzyme B. *Methods Enzymol.* **244,** 80–87.
22 Topalian, S. L., Solomon, D., and Rosenberg, S. A. (1989) Tumor-specific cytolysis by lymphocytes infiltrating human melanomas. *J. Immunol.* **142,** 3714–3725.
23 Andrade, F., Roy, S., Nicholson, D., Thornberry, N., Rosen, A., and Casciola-Rosen, L. (1998) Granzyme B directly and efficiently cleaves several downstream caspase substrates: implications for CTL-induced apoptosis. *Immunity* **8,** 451–460.
24 Reers, M., Smith, T. W., and Chen, L. B. (1991) J-Aggregate formation of a carbocyanine as a quantitative fluorescent indicator of membrane potential. *Biochemistry* **30,** 4480–4486.
25 Smiley, S. T., Reers, M., Mottola-Hartshorn, C., Lin, M., Chen, A., Smith, T. W., et al. (1991) Intracellular heterogeneity in mitochondrial membrane potentials revealed by a J-aggregate-forming lipophilic cation JC-1. *Proc. Natl. Acad. Sci. USA* **88,** 3671–3675.
26 Koopman, G., Reutelingsperger, C. P., Kuijten, G. A., Keehnen, R. M., Pals, S. T., and van Oers, M. H. (1994) Annexin V for flow cytometric detection of phosphatidylserine expression on B cells undergoing apoptosis. *Blood* **84,** 1415–1420.
27 Telford, W. G., King, L. E., and Fraker, P. J. (1994) Rapid quantitation of apoptosis in pure and heterogeneous cell populations using flow cytometry. *J. Immunol. Methods* **172,** 1–16.
28 Gannot, G., Bermudez, D., Lillibridge, D., and Fox, P. C. (1998) Fas and Fas-mediated effects on a human salivary cell line in vitro: a model for immune-mediated exocrine damage in Sjögren's syndrome. *Cell Death Differ.* **5,** 743–750.
29 Li, J. H., Kluger, M. S., Madge, L. A., Zheng, L., Bothwell, A. L., and Pober, J. S. (2002) Interferon-gamma augments CD95(APO-1/Fas) and pro-caspase-8 expression and sensitizes human vascular endothelial cells to CD95-mediated apoptosis. *Am. J Pathol.* **161,** 1485–1495.
30 Wen, L. P., Madani, K., Fahrni, J. A., Duncan, S. R., and Rosen, G. D. (1997) Dexamethasone inhibits lung epithelial cell apoptosis induced by IFN-gamma and Fas. *Am. J. Physiol.* **273,** L921–L929.

31 Holmstrom, T. H., Tran, S. E., Johnson, V. L., Ahn, N. G., Chow, S. C., and Eriksson, J. E. (1999) Inhibition of mitogen-activated kinase signaling sensitizes HeLa cells to Fas receptor-mediated apoptosis. *Mol. Cell Biol.* **19,** 5991–6002.
32 Tewari, M., Quan, L. T., O'Rourke, K., Desnoyers, S., Zeng, Z., Beidler, D. R., et al. (1995) Yama/CPP32 beta, a mammalian homolog of CED-3, is a CrmA-inhibitable protease that cleaves the death substrate poly(ADP-ribose) polymerase. *Cell* **81,** 801–809.
33 Nicholson, D. W., Ali, A., Thornberry, N. A., Vaillancourt, J. P., Ding, C. K., Gallant, M., et al. (1995) Identification and inhibition of the ICE/CED-3 protease necessary for mammalian apoptosis. *Nature* **376,** 37–43.
34. Lazebnik, Y. A., Kaufmann, S. H., Desnoyers, S., Poirier, G. G., and Earnshaw, W. C. (1994) Cleavage of poly(ADP-ribose) polymerase by a proteinase with properties like ICE. *Nature* **371,** 346–347.

8

Measurement of Cytokines in Autoimmune Disease

Kyriakos A. Kirou, Christina Lee, and Mary K. Crow

Summary

Systemic autoimmune diseases are characterized by extensive alterations in immune system function, with cytokines and autoantibodies contributing to impaired immunoregulation and tissue damage. Characterization of the expression and function of cytokines is important for elucidation of pathogenic mechanisms and for identification of therapeutic targets and strategies. We reviewed the utility of assays that reflect individual variability in cytokine gene sequence, expression of messenger ribonucleic acid (mRNA) or protein, as well as measurement of expression of target genes regulated by cytokines. Real-time reverse transcriptase polymerase chain reaction and intracellular staining for cytokine expression are two sensitive and quantitative approaches for analysis of cytokine mRNA and protein, respectively. Detailed methods are provided for these assays.

Key Words: Assay; autoimmunity; cytokine; interferon; interleukin.

1. Introduction

The immune system alterations that characterize systemic autoimmune diseases, with systemic lupus erythematosus (SLE) the prototype, extend to virtually all components of the innate and adaptive immune responses. A current paradigm suggests that a host microenvironment that favors maturation of antigen-presenting cells can promote activation of autoantigen-specific lymphocytes and result in chronic immune system activation and tissue damage ***(1–3)***. This scenario involves dendritic cells, T cells, and B cells, as well as the products of inflammatory cells of the innate immune system, including monocytes and neutrophils. The effector functions implemented by these immune system cells are induced and mediated by cytokines, along with autoantibodies and products of the complement system.

From: *Methods in Molecular Medicine, Vol. 102: Autoimmunity: Methods and Protocols*
Edited by: A. Perl © Humana Press Inc., Totowa, NJ

1.1. Cytokines in SLE

The cytokines produced by antigen-presenting cells and lymphocytes, including the interferons (IFNs) and interleukins (ILs), work together to control the form of the normal and pathological immune response. The global cytokine profile of a disease such as SLE is highly complex ***(4)***. The complement of cytokines observed is likely a product of whatever endogenous and exogenous triggers are inducing autoimmunity as well as the efforts of the immune system to gain control over the activated immune system. Elucidation of the balance of cytokines produced and the response of cells to those cytokines should permit new insight into the pathogenic mechanisms that drive autoimmunity as well as identification of potential therapeutic targets.

Several patterns of cytokine expression have been clearly documented in SLE. IL-10 and IL-6 levels in peripheral blood, as measured by enzyme-linked immunosorbent assay (ELISA), are high in patients with active SLE ***(5–13)***. The source of these cytokines likely includes monocytes as well as T lymphocytes ***(14)***. Although IL-10 is considered an immunosuppressive cytokine, when it binds to activated monocytes, as may occur in autoimmune disease, the IL-10 may not effectively generate intracellular signals ***(14)***. The predicted functional effects of IL-10 in SLE are also complex because of its positive actions on B cells. IL-10 augments B-cell proliferation as well as immunoglobulin (IG) class switching ***(15)***. So, although IL-10 might be considered a cytokine that could potentially dampen immune system activation, its overall effects may be mixed in view of its less-efficacious inhibition of activated, compared with unstimulated, monocytes and its positive actions on B cells ***(15,16)***. Similarly, IL-6 has positive effects on B cells, promoting terminal B-cell differentiation, and may support production of autoantibodies ***(17)***.

Of great interest are compelling data indicating overexpression of type I IFN, as well as IFN target genes, in SLE. The type I IFNs include the products of 13 IFN-α genes, as well as IFN-β, IFN-κ, IFN-τ, and IFN-ω ***(18)***. IFN-α is elevated in serum of patients with active SLE, as measured many years ago based on its capacity to inhibit viral infection of cells and more recently based on ELISA and polymerase chain reaction (PCR) analysis ***(19–22)***.

The presence of active IFN in many patients with SLE has been detected based on microarray studies of peripheral blood mononuclear cells (PBMCs) ***(23–26)***. In those studies, genes regulated by IFN were overexpressed in SLE blood compared to blood cells of disease control subjects, and we have confirmed the IFN-induced gene expression with real-time PCR analysis (K. A. Kirou, C. Lee, and M. K. Crow, unpublished observations, 2003). The major cellular source of IFN-α is the plasmacytoid dendritic cell, which can be induced by virus, unmethylated cytosine phosphate guanosine (CpG DNA), or lipopolysaccharide ***(27–31)***.

The pathogenic role of type I IFN in SLE, and possibly other autoimmune diseases, is supported by numerous reports of induction of disease after therapeutic administration of type I IFN in cases of hepatitis virus infection or malignancy ***(32)***. The number of cases of autoimmune disease triggered by type I IFN is a small proportion of those patients receiving this therapy, but these cases strongly indicate that, in the setting of genetic factors that predispose to SLE, type I IFN can allow disease expression.

SLE is characterized by production of autoantibodies, and abundant data indicate that those autoantibodies are both antigen driven and depend on T-cell help. The T-cell-derived signals that drive B-cell expansion and IG class switching to produce the potentially pathogenic isotypes IgG and IgA comprise those delivered by cell contact, such as those mediated by the CD154 (CD40 ligand)/CD40 pathway, as well as signals delivered by T-cell-derived cytokines ***(33)***. Although the classical Th1/Th2 paradigm might suggest that Th2 cytokines would predominate in SLE because Th2 cytokines are thought to drive B-cell differentiation, in fact the cytokine picture in SLE is complex ***(4)***. In murine lupus models, the IgG subclass that makes up a substantial proportion of the autoantibodies found in serum is IgG_{2a}, a subclass supported by the Th1 cytokine IFN-γ ***(34)***. Moreover, lupus mice deficient in IFN-γ are protected from nephritis, suggesting an important role for that cytokine in lupus disease ***(35–37)***. On the other hand, IL-10, a product of Th2 cells, is elevated in SLE as discussed. Careful measurement of cytokines derived from T cells, monocytes, and dendritic cells, as well as definition of the cells that produce those cytokines, will be important for more complete characterization of the pathogenic mechanisms that contribute to disease in SLE and other autoimmune syndromes.

1.2. Genetic Polymorphisms That Contribute to Altered Cytokine Production

The production of cytokines is a function of the activating and inhibiting signals delivered to the cell surface of immune and inflammatory cells by their ligands. However, the degree of expression of individual cytokines is also regulated based on individual genetic differences that translate into variable efficiency in cytokine production. The extent of genetic polymorphisms that contribute to SLE has not been fully characterized. However, variable sequences in the promoter region of tumor necrosis factor (TNF) may contribute to other autoimmune diseases, including juvenile dermatomyositis, and IL-6 polymorphisms have been associated with SLE ***(38–40)***. Genetic variability can be localized to regulatory regions of genes, potentially modifying the level of expression, or can be in coding sequences, sometimes resulting in an altered amino acid sequence and modified conformational structure. More complete

study of the genetic variants associated with disease activity and clinical disease subsets is likely to provide new understanding of the basis of the immune system alterations that contribute to autoimmune disease and inflammation.

1.3. Approaches to Analysis of Cytokines in Autoimmune Disease

The expression of cytokines and the capacity to produce cytokines in an individual can be assessed using numerous distinct and complementary approaches (*see* **Subheading 4.1.**). The identification of genetic polymorphisms that modify expression or function of cytokine gene products, along with understanding the role of those cytokines in immunopathogenesis, may permit assignment of disease susceptibility to an individual. Measurement of messenger RNA (mRNA) encoding a cytokine can be used to provide a reasonable indication of the amount of cytokine protein produced. However, the variable stability of one or another mRNA must be considered, and the presence of mRNA may not necessarily indicate that the mRNA is translated and the corresponding protein generated.

Direct measurement of protein, as by ELISA, is a fairly reliable indicator of the presence of that protein, but issues of protein degradation and variable detection, based on the antibodies used and the availability of their corresponding epitopes, suggest that confirmation of protein concentration using alternative approaches can be valuable ***(4)***. Although ELISA determines quantity of protein per volume of fluid, usually serum or plasma, intracellular staining for cytokine protein and the enzyme-linked immunospot (ELISPOT) assay determine the percentage of cytokine-producing cells in a cell preparation and permit identification of those cells ***(41–45)***. The latter approach provides important information because some of the pathogenic cytokines are products of multiple cell types. Knowing the major cell source can assist in development of therapeutic strategies to inhibit (or augment) production of the cytokine.

Because some cytokines may be short-lived, in some cases measurement of the activation of signaling molecules induced by a cytokine or expression of the target genes regulated by a cytokine may be a more sensitive measure than assay of the cytokine itself. For example, phosphorylation of components of the Janus kinase signal transducer and activator of transcription (Jak-STAT) pathway of signaling molecules can indicate recent binding of the relevant cytokine to its receptor ***(16)***. A more "downstream" target, gene transcription, can also be measured as a readout of recent cytokine activity. For example, use of microarray technology has indicated that a set of genes regulated by IFN is activated in patients with SLE; this is based on increased relative expression of mRNA corresponding to those target genes ***(23–26)***. As any given gene target can usually be induced by multiple triggers, inhibition of gene expression with an antibody (Ab) that neutralizes activity of a specific cytokine can be used to demonstrate the relevance of that cytokine to the induction of the target mRNA (or protein) measured.

1.4. Assays of Cytokine Expression

In our experience, real-time PCR of cells assayed both immediately ex vivo and after in vitro culture with activating stimuli has proved useful for determining relative quantity of cytokine mRNA in cells from patients with SLE and control subjects (*see* **Subheadings 4.2.** and **4.3.**). Parallel studies of intracellular cytokine expression confirm the PCR data and provide an indication of the cellular source of the cytokine. We are also measuring mRNA specific for cytokine target genes in peripheral blood cells studied immediately ex vivo to support an important functional role for the cytokine in immune system function. It is this redundant approach using complementary assays that is most likely to generate accurate and interpretable data leading to new understanding and treatments of the altered immune function of patients with autoimmune disease.

This review provides detailed methodology for two currently used approaches for measurement of cytokine mRNA and protein: real-time PCR and intracellular staining using flow cytometry. A more comprehensive list of methods of analysis of cytokine expression is provided, with selected references.

1.5. List of Cytokine Assays

1.5.1. Genomic Variability

1. Single-nucleotide polymorphisms (SNPs).
2. Haplotype clusters.

Individual variability in genome sequence, whether in regulatory regions, introns, or coding sequences, may confer variable expression or function of gene products. Determination of SNPs by allele-specific PCR often is used to assign a polymorphism to an individual ***(46)***. Statistical approaches can be used to relate the allele to cytokine expression or functional properties. Current multicenter efforts are defining large stretches of genome sequence that are inherited as blocks ***(47)***. Future studies will be able to relate inheritance of haplotype blocks to cytokine expression or clinical phenotype.

1.5.2. Messenger RNA

1. Northern blot.
2. RNase protection.
3. Reverse transcriptase PCR (RT-PCR).
4. Competitive PCR.
5. Real-time RT-PCR.

The presence of mRNA specific for a cytokine provides a reasonable measure of the presence of the corresponding protein. Measurement of mRNA is an appropriate strategy when reagents are not available for determination of protein expression or as a complementary approach to protein determination. It

should be recognized that the presence of mRNA does not ensure translation into protein or that any protein that might be generated from the message is functional. Nevertheless, measurement of cytokine mRNA provides an excellent measure of recent specific gene transcription. Northern blot and RNase protection assays use an mRNA-specific probe, usually radioactively labeled, that directly binds to the message and is visualized after electrophoresis through a gel ***(48)***.

Northern blot determination of a specific mRNA is usually compared to the presence of a stable mRNA detected with a distinct labeled probe. Commonly used control mRNAs include glyceraldehyde-3-phosphate dehydrogenase, hypoxanthine phosphoribosyltransferase 1 (HPRT1), and β-glucuronidase. Advantages of these techniques include the specificity of the data and the ability to detect transcripts of variable size in the case of Northern blot, sometimes reflecting splice variants. Disadvantages of the techniques are the requirement for relatively high cell numbers and the use of radioactive reagents.

RT-PCR uses reverse transcriptase to convert cellular mRNA to complementary DNA (cDNA) and then uses specific oligonucleotide primers to amplify cDNA that corresponds to the gene product, cytokine, of interest ***(49)***. This approach is routinely performed in many laboratories and has the advantage that primers specific for virtually any mRNA can be made as long as its sequence is known. A disadvantage is that RT-PCR is only relatively quantitative. Competitive RT-PCR is more quantitative than RT-PCR but requires the production of a construct that includes a DNA sequence corresponding to the gene product of interest ***(50)***. When amplified with specific primers, this competing construct shows a distinct size compared to the target amplicon and is included in the PCR reaction in a range of concentrations. The concentration at which the target cDNA outcompetes the artificial construct is recorded, allowing comparison of mRNA quantity among various cell samples.

This approach provides an accurate relative comparison of mRNA among samples, but is labor intensive, sometimes requiring multiple assays of a given sample to fine-tune the range of concentrations of competitor that allows the target cDNA to compete effectively with the added construct. Real-time PCR (*see* **Subheading 3.1.**) described in detail below, has the advantages of requiring only small numbers of cells to generate sufficient cDNA for analysis, the assay is simple to perform once the conditions for detecting a specific transcript are established, and the assay is quantitative ***(51,52)***.

1.5.3. Protein

1. ELISA.
2. Western blot.
3. ELISPOT.
4. Intracellular immunofluorescence staining.

Measurement of cytokine protein is obviously the most definitive approach to determining the availability of that cytokine in functional form and is desired when the appropriate detecting reagents (usually specific antibodies) are available. However, it must be considered that protein can be degraded, whether in cells or after secretion into the extracellular compartment, so protein concentration at a point in time does not necessarily reflect the amount of that protein recently produced.

When determination of total cytokine protein is desired, ELISA is a commonly used and easily performed assay. In addition to protein concentration, usually measured in a body fluid (serum or plasma) or in cell culture supernatants, it is often valuable to determine the cellular source of the protein and, in some cases, the frequency of cells that are producing the protein.

Western blot is another valuable approach to demonstrate the presence of cytokine protein in a cell population or in serum or culture supernatants. Polyclonal antibodies are usually used to identify protein bands resolved on a polyacrylamide gel and then transferred to a nitrocellulose membrane. Western blot is only relatively quantitative, and the amount of total cell protein loaded for resolution by electrophoresis must be carefully determined and comparable among samples.

ELISPOT assay, a method that identifies cells producing cytokine based on Ab recognition of the specific cytokine, followed by detection of deposited enzyme-linked anticytokine Ab with an enzyme substrate, is a valuable measure of the number of cells in a preparation that make that specific cytokine product ***(43–45)***. ELISPOT has high sensitivity and can be combined with selection of cells bearing a particular phenotypic marker to determine the number of cytokine-producing cells in a particular cell subset.

Intracellular staining is a versatile technique that is readily performed for most cytokines, with data derived from cytofluorograph analysis. The percentage of cytokine-producing cells in a population can be determined, as well as the phenotype of those cells, by combining intracellular staining for the cytokine with cell surface analysis of lineage-specific or activation markers. In addition, a relative quantification of cytokine protein can be assessed based on fluorescence intensity. Our protocol for intracellular staining is presented in detail.

1.5.4. Cytokine Target Activation

1. Phosphorylation of intracellular signaling molecules.
2. Target gene mRNA or protein expression.

In some cases, cytokine mRNA and protein are only briefly expressed, and the consequences of cytokine receptor ligation and expression of gene products induced by those cytokines are more readily detected. For example, our

data and data from other laboratories have detected increased expression of mRNA specific for genes induced by type I and type II IFN ***(23–26)***. In the setting of this striking IFN-induced gene expression signature, expression of IFN protein has been difficult to detect using ELISA. Real-time RT-PCR can be used to detect the targets of a cytokine's activity. Inhibition of the activity of that cytokine with a neutralizing Ab can be used to support a specific role for the cytokine in the gene expression observed.

2. Materials

2.1. Real-Time PCR

2.1.1. PBMC Isolation

1. Green-top tubes (BD Vacutainer™ sodium heparin, Becton Dickinson and Company, Franklin Lakes, NJ).
2. Ficoll-Paque™ Plus (Amersham Biosciences, Piscataway, NJ).
3. Hanks balanced salt solution (HBSS; Mediatech Inc., Holly Hill, FL).
4. Red blood cell lysis buffer (Roche Diagnostics, Indianapolis, IN).
5. Complete medium: 10% fetal calf serum in RPMI-1640 solution (Mediatech Inc.) supplemented with 2 m*M* of L-glutamine, 100 U/mL penicillin, and 100 μg/mL streptomycin.
6. Trypan blue solution (Mediatech Inc.).
7. Hemocytometer.

2.1.2. Cell Lysis

1. Phosphate-buffered saline (PBS) tablets (Sigma Aldrich, St. Louis, MO).
2. RLT buffer (Qiagen RNeasy® minikit) (Qiagen, Valencia, CA).
3. 2-Mercaptoethanol or β-mercaptoethanol (β-ME; Sigma).
4. 3-mL syringes.
5. 20-ga needles.

2.1.3. RNA Isolation and Measurement

1. 70% ethanol (ETOH) (Sigma).
2. Qiagen RNeasy minikit. In addition to RLT buffer, this also contains buffers RW1 and RPE, RNeasy minispin columns, collection tubes, and RNase-free water.
3. Diethylpyrocarbonate (DEPC)-treated water (Ambion®, Ambion, Inc., Austin, TX).

2.1.4. Primer Design and Preparation

1. Beacon Designer 2.06 (Premier Biosoft International, Palo Alto, CA).
2. DNA mfold (version 3.1) Web server (by Zucker and Turner); available free at www.bioinfo.rpi.edu/applications/mfold/old/dna.

2.1.5. Reverse Transcription

1. SuperScript™ III RNase H^- reverse transcriptase (Invitrogen Corp., San Diego, CA). This contains SuperScript III RT (200 U/mL), 0.1 *M* dithiotreitol, and 5X first-strand buffer.

2. 10 m*M* deoxynucleotide triphosphate (dNTP) Mix, PCR grade (Invitrogen). This contains 10 m*M* each of deoxyadenine triphosphate (dATP), deoxycytosine triphosphate (dCTP), deoxyguanine triphosphate (dGTP), and deoxythymine triphosphate (dTTP).
3. Oligo$(dT)_{12–18}$ Primer (Invitrogen).
4. Ribonuclease H (Invitrogen).
5. RNaseOUT™ recombinant RNase inhibitor (Invitrogen).

2.1.6. Real-Time Quantitative Amplification of Gene Expression and Analysis

1. 2X iQ™ SYBR→ Green Supermix (Bio-Rad Laboratories, Hercules, CA). This contains stabilizers, salts, 0.4 m*M* each of dNTP, 50 μ/mL iTac DNA polymerase, SYBR Green I, and 20 n*M* fluorescein (for well factor correction).
2. 96-well PCR plates (DNase and Rnase free) (Bio-Rad Laboratories).
3. Optical tape (Bio-Rad Laboratories).
4. DEPC-treated water (Ambion).
5. Ethidium bromide.
6. NuSieve® 3:1 agarose (BioWhittaker Molecular Applications, Rockland, ME).

2.2. Intracellular Staining

2.2.1. PBMC Isolation

The PBMC materials are the same as in **Subheading 2.1.1.**

2.2.2. Inhibition of Golgi Function

1. Brefeldin A (Sigma).
2. Dimethyl sulfoxide.
3. 5-mL (15 × 75 mm) polystyrene round-bottom tubes (Falcon brand, Becton Dickinson). These are called flow tubes hereafter.

2.2.3. Cell Surface Staining

1. PBS tablets (Sigma).
2. Bovine serum albumin (BSA).
3. Sodium azide.
4. Normal human serum (to block Fc receptors on cells).
5. Cell surface antibodies. Usually fluorescein isothiocyanate (FITC) labeled (i.e., anti-CD4-FITC) (BD Pharmingen, San Diego, CA).

2.2.4. Intracellular Staining and Flow Cytometry Analysis

1. Saponin (Sigma).
2. Sodium azide (Fisher, Pittsburgh, PA).
3. PBS tablets (Sigma).
4. Formalin (methanol free, 10% ultrapure, EM grade, in water; Polysciences International).
5. Antibodies for intracellular cytokines, usually labeled with R-phycoerythrin (R-PE).
6. FACScan or FACScalibur (BD Biosciences)

3. Methods

3.1. Real-Time PCR

3.1.1. PBMC Isolation

After informed consent, heparinized blood (in 10-mL green-top tubes) is obtained by venipuncture from each individual.

1. Blood is mixed with an equal amount of HBSS and layered carefully over 12 mL of Ficoll-Paque Plus in a 50-mL Falcon tube. Spin at 700*g* for 20 min with brakes off (gradient centrifugation).
2. With a Pasteur pipet, remove carefully the PBMC cell layer from the interface between Ficoll and diluted plasma. Try to avoid obtaining too much Ficoll. Spin at 300*g* for 10 min.
3. Wash cells by resuspending the cell pellet in 30 mL HBSS. Spin at 300*g* and repeat. Because many of our disease samples (from SLE or rheumatoid arthritis) contain a substantial amount of red blood cells (RBCs), we always lyse the RBCs in the pellets by resuspending in 2 mL of RBC lysis buffer for 3–5 min before washing for the second time. This step allows more accurate counting of our PBMCs, which is performed by diluting an aliquot of the cell suspension (usually 1:3) in trypan blue and using a hemocytometer. Although cell viability (assessed by the trypan blue staining) is not an issue in freshly obtained cells, it will be compromised when dealing with cells cultured or stimulated in vitro for more than 1 d.
4. Finally, cells are resuspended in fresh medium at a concentration of 4 million/mL; and 0.5 mL (2 million cells) is aliquoted in each of four 1.5-mL Eppendorf tubes (for lysis and RNA isolation as detailed below) or in flow tubes; these are placed in the incubator until ready to use for flow cytometric analysis.

Each 10-mL tube yields between 10 and 20 million PBMCs, but some lymphopenic SLE patients may have as few as 5 million cells. We always try to isolate the PBMCs as quickly as possible so that the specimen is representative of the in vivo situation. For the same reason, we try to keep the cells on ice for as long as possible during the isolation procedure.

Flow cytometric analysis is done not only for measuring intracellular cytokine levels, but also to determine the cell constitution of PBMCs that will be lysed and used for mRNA quantitation. The major components of these samples (lymphocytes, monocytes, or sometimes even neutrophils) can be differentiated by their forward and side scatter characteristics. When only certain cells are desired to be studied, flow cytometry and staining for cell surface markers will help verify the efficiency of the cell isolation techniques (usually magnetic beads or fluorescence activated cell sorter [FACS]). Although fractionation of PBMCs will allow more specific measurement of mRNA, the longer manipulation process might alter the ex vivo gene expression and compromise the validity of the data.

3.1.2. Cell Lysis

Before cells are lysed, they are washed with sterile PBS, and then the Qiagen RNeasy minikit protocol is followed.

1. Briefly, a fresh lysis buffer is prepared by mixing RLT buffer with β-ME (10 μL/mL RLT). This procedure is performed in the fume hood because β-ME fumes are toxic and foul smelling.
2. Cell pellets are broken by rubbing the tubes on a rough surface; then, the cell pellets are lysed by adding 350 μL RLT (for up to 5 million pelleted cells; 600 μL for 5–10 million cells) solution to the cell pellet.
3. To homogenize the samples, we first vortex vigorously for 10–20 s, and then we pass the samples through a 20-ga needle in a 3-mL syringe 10–20 times. The samples can then be stored at –70°C for more than 6 mo.

3.1.3. RNA Isolation and Measurement

Again, the Qiagen RNeasy minikit protocol is followed. Be sure to perform RNA isolation in a well-ventilated area because fumes from reagents are unpleasant. The protocol is performed at room temperature, so it must be done as quickly as possible.

1. Briefly, RNA is thawed in a 37°C water bath for 2 min to ensure that all salt is dissolved. An equal volume of 70% ETOH (350 μL for 2–5 million cells) is added to each tube, and samples are mixed by pipetting. A precipitate may form, which is normal.
2. Place 700 μL of sample (including precipitate) onto an RNeasy minispin column (in a 2-mL collection tube). Centrifuge for 15 s at maximum speed. If volume is more than 700 μL, do this step in successive aliquots. Discard flowthrough (contains RLT or RW1, not compatible with bleach), but reuse collection tube.
3. Pipet 700 μL buffer RW1 onto column and spin for 15 s at maximum speed to wash. Discard flowthrough and collection tube.
4. Transfer column into a new 2-mL collection tube. Pipet 500 μL buffer RPE (with ETOH) onto column and spin for 15 s at maximum speed to wash. Discard flowthrough and reuse collection tube.
5. Pipet 500 μL RPE onto column. Spin 2 min at maximum to dry the RNeasy membrane. Remove column carefully so that it does not contact the flowthrough. Discard collection tube with filtrate.
6. Transfer column into a new 1.5-mL collection tube and pipet 30–50 μL of RNase-free water directly onto the RNeasy membrane. Spin for 1 min at maximum speed to elute. Repeat (using the same tube) if the expected RNA yield is more than 30 μg.
7. To measure RNA, we usually place 8 μL into 72 μL of DEPC-treated water (dilution factor [DF] = 10) on ice. After washing the RNA/DNA cuvette and selecting the nucleotide mode, we sequentially read the measurements for the blanks (80 μL of DEPC-treated water) and the samples. Calculation of the RNA content is per-

formed by using the formula A_{260} (sample absorbance at 260 nm) × DF × 40. Results are expressed in micrograms per milliliter (or nanograms per microliter), and values above 0.15 are needed to ensure significance. The ratio of the sample absorbances at 260 and 280 nm (A_{260}/A_{280}) estimates its RNA purity and should be greater than 1.5. Our typical yield is 3–8 μg of RNA per 2 million PBMCs.

8. RNA can be used immediately or stored at –20°C to –70°C for months. Excessive freeze–thaw cycles should be avoided.

3.1.4. Primer Design and Preparation

We use the Beacon Designer 2.06 software to design our primers. This program can also be used to design TaqMan® probes and molecular beacons.

1. After program initiation, create a new folder and choose the Open Sequence From Entrez icon. Type in the accession number for the gene(s) of interest so that the program can import the mRNA sequence(s). There are two modes of primer search. We use the Beacon Design option because the TaqMan Design chooses both a primer set and a TaqMan probe at the same time.
2. We then choose Analyze and Primer Search. In the Primer Parameter window, we set the Target TaOpt at 50 ± 2°C and Length Range at 19–23 bp. In the Specify Amplicon Length option, we select 75–200 bp because larger amplicons will not perform well in the real-time PCR reaction.
3. Each selected primer pair is shown with all associated parameters (rating, sequences, position, length, T_m, guanine cytosine (GC)%, hairpin ΔG, self-dimer ΔG, run length, GC clamp, cross dimer ΔG, and the corresponding amplicon's length, T_m, and optimal annealing temperature [TaOpt]).
4. To ensure that no significant secondary structure exists within the amplicon, we cut the corresponding mRNA sequence from the Entrez Browser Nucleotide Search option and insert it into the special box in the DNA mfold (version 3.1) Web server ***(53)***. We specify the folding temperature empirically at 52°C and then set the ionic conditions at 50 m*M* for Na^+ and 3 m*M* for Mg^{++}. An e-mail address must be provided before the program returns the results. All sequences with any secondary structure with ΔG less than (2.0 kcal/mol are rejected, and a new amplicon (for another primer set) is tested until these requirements are met.
5. Finally, BLAST searches are performed on Beacon Designer, and the specificity of the primer set is defined.
6. Primers are ordered salt free at the 10- to 50-n*M* scale; on arrival, they are reconstituted with 100 μL of DEPC-treated water.
7. The concentration of each primer solution is determined spectrophotometrically after a 1-μL aliquot is diluted in 299 μL of water (DF = 1:300).
8. The formula $A_{260} \times 50 \times DF \times 1000$ calculates the concentration of the primer in picograms per microliter, and the result is divided by the molecular weight (MW) of each primer (provided by the manufacturing company) to convert to picomoles per microliter.
9. Finally, 10,000 pmol of the sense (S) and antisense (AS) primers of a given gene are mixed in a total volume of 1 mL DEPC-treated water to obtain final concentrations of 10 m*M* each.

10. Many aliquots (50 μL per 0.5-mL Eppendorf tube) are made to ensure minimal freeze–thaw cycles, which could degrade the primers.

3.1.5. Reverse Transcription

For reverse transcription into cDNA, many systems are available. Because we have primarily used the Superscript III reverse transcriptase system, we describe that procedure below. The total reaction volume is 20 μL, and the full procedure lasts approx 80 min.

1. We thaw on ice and prepare all required reagents.
2. Prepare two master mixes of the reagents (avoid pipetting errors). We always make more of the mix than needed to avoid not having enough: For *N* samples, we use *N* + 2 (or more for more than 10 samples).
   a. Mix 1: In a 0.5-mL Eppendorf tube, add (*N* + 2) μL of Oligo(dT) and (*N* + 2) μL of 10 m*M* dNTP.
   b. Mix 2: In a 0.5-mL Eppendorf tube, add (*N* + 2) × 4 μL of 5X first-strand buffer, (*N* + 2) μL of 0.1 *M* dithiothreitol, (*N* + 2) μL of RNAseOUT (40 U/μL), and (*N* + 2) μL of Superscript III.
3. In each of *N* 0.2-mL PCR tubes, add 2 μL of mix 1 and variable volumes of total RNA, depending on the concentration of the RNA in each sample (not to exceed 11 μL). Add RNAse-free water, if needed, to make the total reaction volume 13 μL. We typically use 1 μg of RNA.
4. Place PCR tubes in a thermal cycler (PerkinElmer) preset to the following program:
   a. START program at 65°C for 5 min, then 4°C for 1 min.
   b. PAUSE program to add 7 μL of mix 2 to each sample. Mix by pipetting and spin down if necessary.
   c. RESUME the program at 25°C for 5 min, then at 50°C for 50 min. This can also be run at 55°C for 30–60 min if using gene-specific primers with templates that have high secondary structure. The program continues at 70°C for 15 min and finishes at 4°C, at which time samples are ready to be removed from the machine.
5. Make a 1:10 dilution of cDNA (18 μL in 162 μL DEPC-treated water) and freeze at –20°C after previously aliquoting into many tubes for one-time use only. This ensures minimum freeze–thaw cycles of samples and minimal degradation of cDNA.

3.1.6. Real-Time Quantitative Amplification of Gene Expression and Analysis

There are several competing thermal cyclers on the market for quantitative PCR analysis on the market. We describe here our experience with the Bio-Rad iCycler IQ Real-Time Detection System. Quantitation is achieved by measuring the increase in fluorescence during the exponential phase of the amplification, which is in real time. An excitation system via an excitation filter wheel directs the light onto all the wells of a 96-well plate. Then, fluores-

cent molecules from each well emit fluorescent light through an emission filter wheel and an image intensifier; this light is eventually detected by the CCD detector. The data are transferred to a computer and analyzed with the Bio-Rad software.

There are currently four techniques used in real-time PCR applications: molecular beacons, hydrolysis probes (TaqMan), hybridization probes, and DNA-binding dyes (SYBR Green I). A detailed review of those, which is beyond the scope of this article, was made by Bustin ***(51)***. Although the method described here cannot be used for multiplexing (multiple gene amplification in the same tube) and lacks specificity with regard to amplicon measured, it is nevertheless reliable, and the specificity problem is corrected by running a melt curve analysis of the PCR products at the end of the reaction ***(54)***. The target and housekeeping genes are amplified in separate wells from the same template. The technique is also cheaper. Because we have used primarily the SYBR Green I method, a brief description of the procedure is given next.

1. Prepare cDNA standards for each gene to be amplified. We used plasmids for this, but most often we just use a known sample with high expression for the tested gene. For example, for IFN-induced protein with tetratricopeptide repeats 1 (IFIT1), an IFN-α-inducible protein, we use a sample obtained from 2 million PBMCs stimulated with 1000 U/mL of IFN-α for 24 h. Again, we prepare many aliquots of these to minimize the need for repeated use, which is complicated by degradation. Prior to PCR, we make all cDNA dilutions for our standard curves: Initially, three 10-fold dilutions in duplicate per plate are used; later, when performance of the reaction is established, only two dilutions are made (*see* **Subheading 4.3.**).
2. Make 1:10 dilutions of all unknown cDNA samples and add 10 μL (for more accurate pipetting) of each in duplicate wells in the 96-well PCR plate.
3. Prepare Supermix for each primer set used: $(N + 2) \times 12.5$ μL of Bio-Rad SybrGreen Mix; $(N + 2)$ μL of the S and AS primer solution; and $(N + 2) \times 1.5$ μL of DEPC-treated water. Add 15 μL of the Supermix to each well. The final volume per reaction is 25 μL, with concentrations of 0.4 μM for each primer, of 25 U/mL of iTac DNA polymerase, of 0.2 m*M* each of dNTPs , and of 3 m*M* of Mg^{++}. The supermix also contains SybrGreen I, a DNA-intercalating dye responsible for the fluorescence emission during the reaction and used to determine the starting quantity of the gene in question. As the cDNA is amplified during the successive reaction cycles, more and more dye binds to DNA, and more fluorescence is emitted.
4. Place sealing optical tape on plate.
5. Spin the contents of the plate in the centrifuge at 300*g* (at 4°C) for 3–5 min.
6. Make sure to cover plate with foil and keep refrigerated (4°C) until placed into machine. Minimize time between preparation and run.

7. Run the PCR reaction by placing the 96-well plate in the PCR machine and opening the iCycler software. Select the Library window and the View Protocol tab and select the most suitable protocol for your reaction. This will most likely be the 2StepAmp+Melt.tmo, which includes five cycles. Cycle 1 consist of 1 repeat and 1 step with dwell time of 3 min at 95°C. Cycle 2 consists of 40 repeats of step 1 (10-s dwell time at 95°C) and step 2 (45 s of dwell time at 55°C). Cycles 3 and 4 each have 1 repeat and 1 step, with 1-min dwell times at 95 and 55°C, respectively. Finally, cycle 5 consists of 80 repeats of step 1 with a 10-s dwell time starting at 55°C and positive increments of 0.5°C for every repeat. Then, click Edit This Protocol. This will transfer you to the Workshop window, where you can change the settings according to your needs. Our settings differ only at the annealing temperature, which is set at 58°C. We amplify at minimum two genes: our target gene and a housekeeping gene, which will serve as the internal control for each sample. We are currently using HPRT1 (NM_000194) and glyceraldehyde-3-phosphate dehydrogenase (NM_002046) housekeeping genes (*see* **Subheading 4.4.**). Specificity of the PCR reactions for the amplified genes is confirmed by examining the melting curve (which is generated during cycle 5 of the reaction) for each gene amplification (*see* **Subheadings 4.5.** and **4.6.**).
8. Analyze the data by opening the file with the Bio-Rad iCycler iQ (version 3.0a) software. For convenience, this can be done later, on the investigator's personal computer, away from the PCR machine. First, select the View Post Run Data tab, then select the experiment file and hit Analyze Data. The amplification curves from all wells are displayed on the Data Analysis window under the PCR Quantification tab (the *x*-axis represents the PCR cycle and the *y*-axis the fluorescence intensity). The melting curves and the standard curves can also be viewed by clicking on the corresponding tabs.
9. To assess the expression of each gene for all unknown samples, select the corresponding wells for that gene (unknowns and standards) by checking the Select Wells box, highlighting the relevant wells, and clicking the Analyze Selected Wells button. The program then automatically sets the best possible threshold line that will horizontally intersect all amplification curves at their exponential phase. This is best visualized when Analysis Mode is set at the PCR Baseline Cycle Subtracted option and with the graph adjusted so that the fluorescence intensity axis is expressed in a Log scale (*see* **Figs. 1** and **2**). The threshold line will determine the threshold cycle of amplification for each sample and will plot it (*y*-axis) against the Log Starting Quantity of the particular gene (*x*-axis). The latter is known for the standards (and typically set as 1, 10, 100 according to their dilutions) and calculated for the unknowns in the standard curve view of the results. The standard curve will also give the correlation coefficient (optimally above 0.98) and the PCR efficiency (optimally between 80 and 120%).
10. Only one melting peak should be present for each amplified gene (*see* **Figs. 1** and **2**). If more than one peak is present, a primer dimer (melt peak lower than amplicon peak) might have been formed, or another gene might have been concurrently amplified. Both situations are undesirable because they will produce

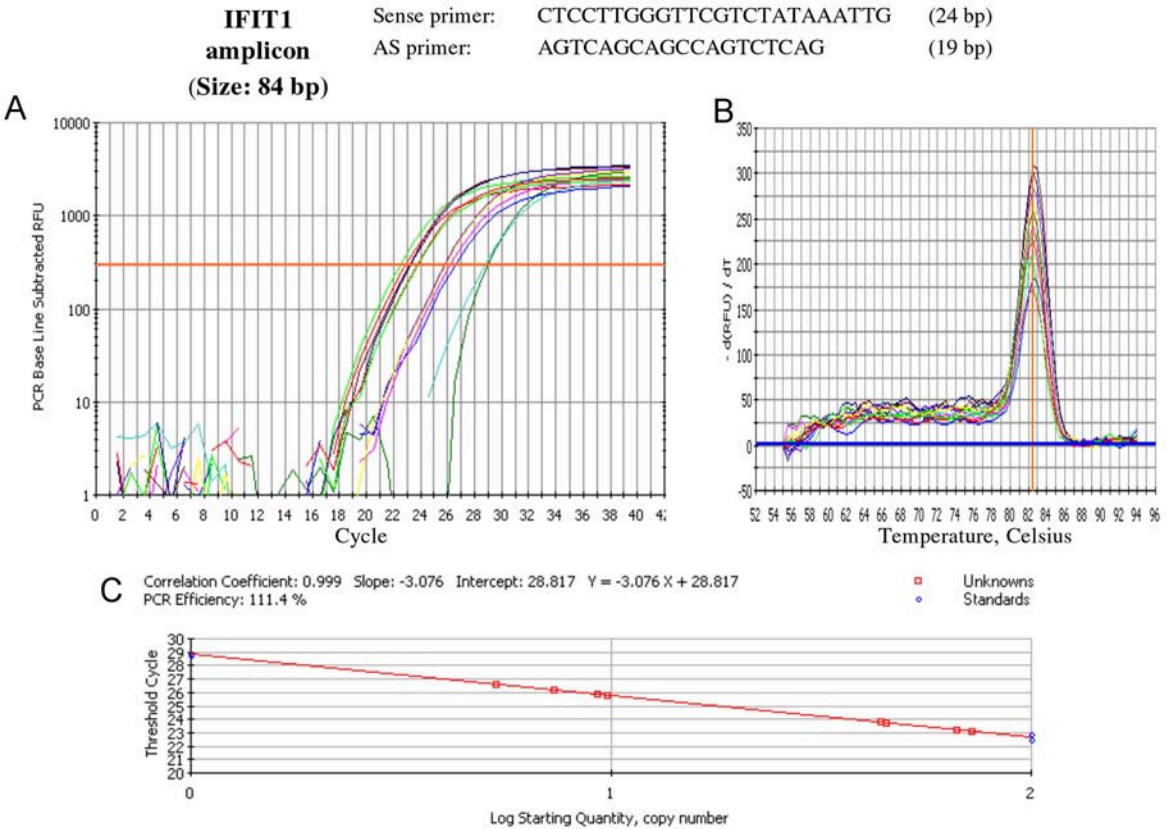

Figs. 1 and 2. Illustrative examples of a target gene amplification (IFIT1; **Fig. 1**) and housekeeping gene amplification (HPRT1; **Fig. 2**) by real-time PCR. Freshly isolated PBMCs (2 million per circumstance) from a healthy donor were either left untreated (sample 1) or were cultured with 200 U/mL IFN-α for 24 h (samples 2–4). Samples 3 and 4 also received anti-IFN-α Ab (200 neutralization units/mL) or an isotype control Ab, respectively. Cell lysis, RNA isolation, reverse transcription, and real-time PCR amplification followed for IFIT1 (NM_001548) in **Fig. 1** and for HPRT1 (NM_000194) in **Fig. 2**. The amplicon sizes and primer

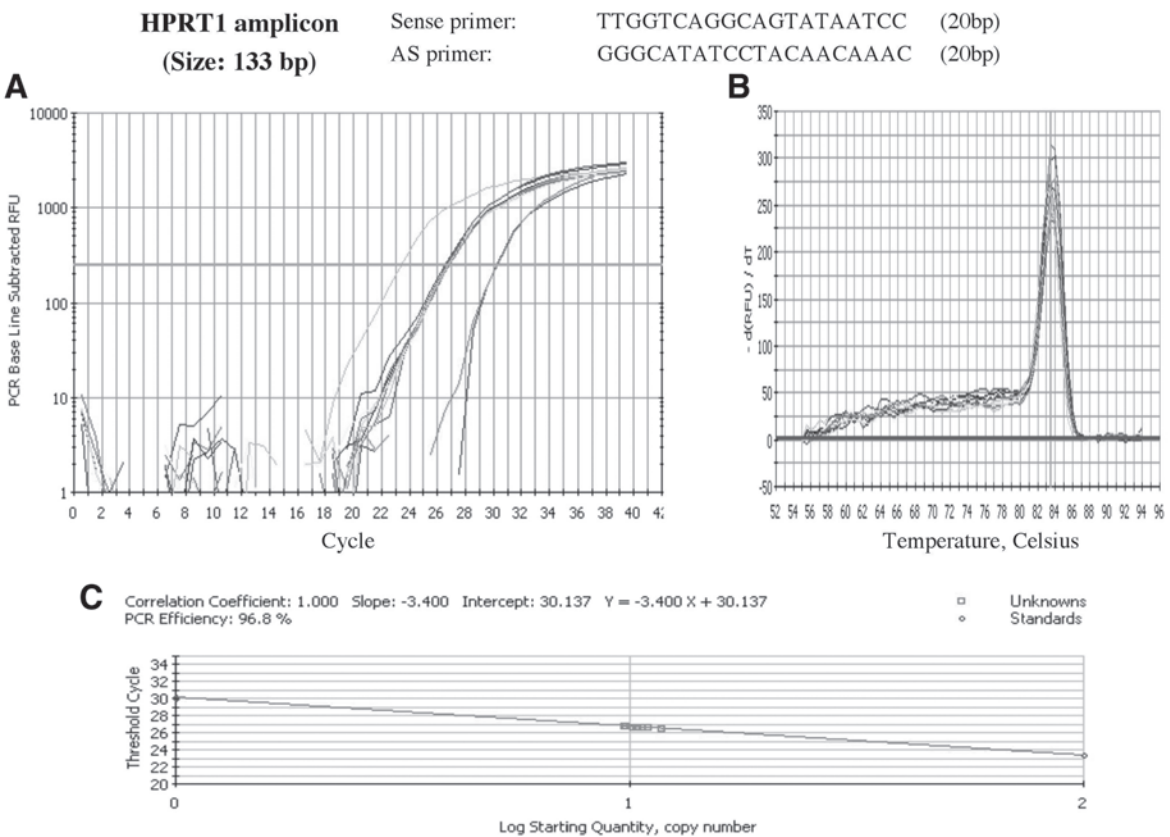

sequences are shown on the top of each figure, and the amplification, melt, and standard curves for each gene are shown in panels **A**, **B**, and **C**, respectively. The efficiency for each reaction is also shown: 111.4% (or $E = 1.114$) for IFIT1 and 96.8% (or $E = 0.968$) for HPRT1. Please note that, because the linearity of the reaction was established in earlier experiments, only two standard dilutions were included in this reaction.

false results. In our experience, unless the primer dimer peak is tiny, these data should be rejected, and the experiment should be repeated.

11. Threshold cycle values for the target and reference genes for each sample are entered into an Excel file and subtracted from the corresponding values of a reference sample (usually the one with no stimulation). These differences are then used as exponents with base the sum of the efficiency of that PCR reaction expressed as a decimal plus 1 (i.e., for efficiency of 98%, this would be 1.98; ***55***). By definition, therefore, the corresponding differences of the reference sample for both the target and housekeeping genes will be 0, which when used as exponents will result in values of 1. Finally, the target gene values are divided by the housekeeping gene values for each sample, and the result is the relative expression value for each unknown sample (*see* **Subheading 4.7.**).
12. An example of the technique is shown in **Figs. 1** and **2** and **Table 1**. In this experiment, PBMCs from a healthy donor either were left untreated (sample 1) or were cultured with 200 U/mL IFN-α (samples 2–4). Samples 3 and 4 also received anti-IFN-α Ab at a concentration of 200 neutralization units/mL or an isotype control Ab, respectively. Cell lysis, RNA isolation, reverse transcription, and real-time PCR amplification followed for IFIT1 and HPRT1 (housekeeping gene). The amplification, melt, and standard curves for each gene are shown in **Figs. 1** and **2**. The efficiency for each reaction is also shown: 111.4% or E = 1.114 for IFIT1 and 96.8% or E = 0.968 for HPRT1. The threshold cycles (Ct) for each sample and for each gene are shown in columns 1 and 2 of **Table 1**. Columns 3 and 4 show the ΔCt's or differences of the Ct of each cycle from the Ct of medium (reference sample) for the two genes. Columns 5 and 6 show the $E + 1$ for each gene (2.114 and 1.968) raised to the corresponding ΔCt power for each sample. Finally, the last column depicts the division of the values in column 5 by the values in column 6 for each sample, which constitutes the relative expression RE of IFIT1 for that sample

3.2. Intracellular Staining of Cytokines

Intracellular expression of cytokines can be measured in either unstimulated or in vitro stimulated cells.

3.2.1. PBMC Isolation

The isolation of PBMCs is the same as in **Subheading 3.1.1.**

3.2.2. Inhibition of Cytokine Secretion by the Golgi System

After PBMC counting and resuspension in 0.5 mL medium (at 4 million/mL), add brefeldin A to a final concentration of 1–2 μg/mL and incubate cells in flow tubes at 37°C and 5% CO_2 for 6–18 h. This inhibits vesicular protein transport from the rough endoplasmic reticulum to the Golgi complex, and therefore will result in accumulation of the cytokines in the rough endoplasmic reticulum for optimal intracellular staining (*see* **Subheading 4.8.**).

Table 1
Calculation of Relative Expression of IFIT1 mRNA in PBMCs by Real-Time PCR

	IFIT1 *Ct*	HPRT1 *Ct*	IFIT1 Δ*Ct*	HPRT1 Δ*Ct*	IFIT1 $(E + 1)^{\Delta Ct}$	HPRT1 $(E+1)^{\Delta Ct}$	IFIT1 *RE*
1. Medium	26.4	26.6	0	0	1	1	1
2. IFN-α	23.2	26.7	3.2	–0.1	11.0	0.9	11.7
3. IFN-α+ anti-IFN-α	25.8	26.7	0.6	–0.2	1.6	0.9	1.7
4. IFN-α+ isotype control	23.6	26.8	2.8	–0.2	8.1	0.9	9.3

Ct, threshold cycle for amplification of each gene for each sample; Δ*Ct*, *Ct* of medium sample minus *Ct* of each sample for each gene; *E*, efficiency of PCR reaction expressed as a decimal.

We performed this procedure primarily to assess the ex vivo (without in vitro stimulation) ability of PBMCs from patients with rheumatic inflammatory diseases to express cytokines such as TNF, IFN-γ-inducible protein 10 (IP10), CD40 ligand (CD40L), TNF-related apoptosis-inducing ligand (TRAIL), and the like. However, this technique can also be applied in cells stimulated in vitro with various stimuli. As an example, phorbol dibutyrate (PDB) and ionomycin stimulation of lymphocytes is used for 4–6 h to help determine whether T cells are of the Th1 or Th2 effector subtypes by checking expression of IFN-α and IL-4, respectively.

Note that brefeldin A is dissolved in dimethyl sulfoxide and is solid at 4°C. Thaw before use.

3.2.3. Cell Surface Staining

Before cell fixation and permeabilization for intracellular staining, we perform cell surface staining as follows:

1. Prepare staining buffer (SB): 1% BSA and 0.1% sodium azide in PBS. Dissolve 5 g BSA and 0.5 g sodium azide in 500 mL PBS. Adjust pH to 7.4–7.6 and filter with a 0.2-μm pore membrane before use. Store at 4°C.
2. Split each cell culture equally in two tubes so that one will be stained with the anticytokine monoclonal antibody (MAb) and the other with the isotype control MAb (each tube contains 1 million cells). Centrifuge cells at 300*g* for 8 min. Discard supernatant by inverting the tube (only once) and drying it on a paper towel. Reinvert to normal position and place on ice.
3. Wash cells once by adding 1–2 mL SB to each flow tube, vortexing gently, and centrifuging at 300*g* for 8 min. Repeat drying procedure as in **step 3**.
4. For *N* samples to stain, prepare $(N + 2) \times 40$ μL SB and add $(N + 2) \times 4$ μL of human serum plus $(N + 2)$ (1 μL of anti-CD4-FITC (and/or another antibody for

another cell marker). Vortex and aliquot 40 µL onto each pellet, resuspend, and incubate for 20 min on ice in the dark. Human serum will block the PBMC Fc receptors, whereas the anti-CD4 MAb will label the $CD4^+$ cells with FITC. Wash once as in **step 3**.

3.2.4. Intracellular Staining

1. Prepare the fixation/permeabilization buffer: 0.1% (w/v) saponin, 4% (v/v) formaldehyde in PBS. A practical preparation example follows: Mix 10 mL of 10X PBS plus 40 mL of 10% formalin in water plus 50 mL H_2O (total volume 100 mL) and dissolve 100 mg of saponin in it.
2. Prepare the intracellular wash buffer (IWB): 0.1% saponin, 0.1% (w/v) sodium azide, in PBS. Practically dissolve 100 mg saponin and 100 mg sodium azide in 100 mL PBS. Adjust pH to 7.4–7.6. Filter with 0.2-µm pore membrane. Store at 4°C.
3. Fix and permeabilize cells: Add 100 µL fixation/permeabilization buffer onto cell pellets and resuspend well. Incubate for 20 min on ice in the dark. Wash cells once with 1 mL IWB and centrifuge/dry as in **Subheading 3.2.3., step 3**.
4. Prepare Abs for intracellular staining. Optimal concentrations should be individually determined for each Ab. A good starting staining Ab concentration might be 2 µg/mL. For example to stain *N* samples with the anti-TNF-PE MAb (0.2 mg/mL from BD Pharmingen), prepare $(N + 2) \times 40$ µL of IWB and add $(N + 2) \times 0.4$ µL anti-TNF. Vortex and add 40 µL to each cell pellet. Incubate on ice for 20 min in the dark and wash once with IWB.
5. Resuspend the cell pellets with 400 µL SB and analyze by FACS. Alternatively, you can store the samples at 4°C for 1–2 d before analysis.
6. To ensure specificity of intracellular staining, always perform a parallel stain with an isotype Ab control. Additional steps to ensure specificity include preincubation of the labeled Ab with an excess amount of the target recombinant cytokine or preincubation of the cells with an excess of the Ab in an unlabeled form. All these controls should be negative for the target cytokine tested.
7. As the procedure described here requires data acquisition in two colors (FITC in FL-1 and R-PE in FL-2), it is necessary to prepare some samples to help with optimization of compensation parameters. We typically use fresh PBMCs that are not stained and others that are stained with either anti-CD3-FITC or anti-CD3-R-PE. All three samples must undergo fixation and permeabilization to have forward and side scatter parameters comparable to the rest of the cells.
8. An example of intracellular staining for TNF is shown in **Fig. 3**.

4. Notes

1. For a complete understanding of the capacity of a cell population to produce a cytokine, it is probably desirable to use a set of complementary approaches, including measurement of mRNA using a quantitative assay and measurement of protein by assay of serum or plasma along with identification of the cells that produce the cytokine using a technique such as intracellular staining or ELISPOT. It may also be desirable to document cytokine production in untreated cells studied imme-

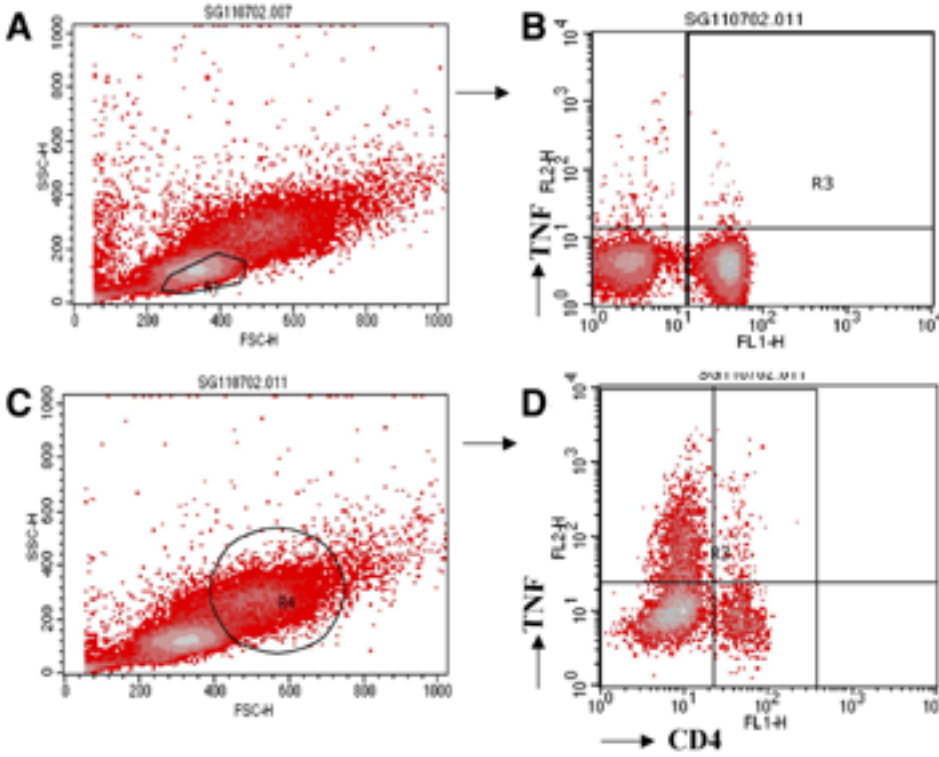

Fig. 3. Unstimulated monocytes from a patient with SLE express high levels of TNF. Freshly isolated PBMCs from a patient with SLE were cultured with brefeldin A for 6 h. After cell surface staining with anti-CD4-FITC, the cells were fixed, permeabilized, and stained intracellularly with either anti-TNF-R-PE or isotype control-R-PE. Finally, the cells were analyzed by two-color flow cytometry. Panels **A** and **C** plot the cells according to their size (forward scatter, FSC) and granularity (side scatter, SSC), and panels **B** and **D** depict the cells gated on R1 (lymphocytes) and R4 (monocytes), respectively, according to their fluorescence on the *x*-axis (FL1, representing the FITC-labeled CD4 cells) and the *y*-axis (FL2, representing R-PE-labeled TNF-expressing cells). Isotype control stained cells were negative for FL2 fluorescence (not shown).

diately ex vivo as well as after several days of culture in both the absence and the presence of cytokine-inducing stimuli. Also desirable and increasingly feasible is to correlate cytokine production with genetic variants in cytokine DNA sequence ***(38–40)***. Although it would seem most likely that alterations in the sequence of the gene promoter would result in increased or decreased gene transcription, altered sequence in the 3' untranslated region of the gene may alter protein production based on variable stability of the mRNA, a feature usually controlled by sequences in that 3' region.

2. Interpretation of the role of a cytokine in the complex pathogenic process that results in autoimmune disease can be fraught with complexity. In addition to the somewhat variable results that can be obtained when assaying for differences in gene sequence, mRNA expression, protein expression, and protein function, the most appropriate assay material for study must be considered. Numerous publications have used mononuclear cells isolated from blood or a disease site that are then activated in vitro with mitogens or triggers that mimic antigen-mediated stimulation ***(56,57)***. It should be recognized that the experience of immune system cells in vivo, often characterized by repeated stimulation through antigen receptors and costimulatory molecules as well as cytokines, may confer on a cell population a relative refractoriness or altered response to further activation ex vivo. The intracellular signaling pathways that are activated in vivo may, with time in culture, return to a more quiescent state, permitting more accurate comparison of cytokine production (or response) in patient cells and control cells.
3. To compare data obtained in different plates (PCR reactions), it is necessary to prepare many aliquots of the same reference cDNA sample and use these in quadruplicate wells in all PCR reactions. Optimally, this should express the target and housekeeping gene at a level close to that of the unknown samples.
4. It should be emphasized here that no housekeeping gene is perfect, and all will vary somewhat with cell stimulation or among various individuals ***(51,58)***.
5. To prevent PCR reaction contamination by amplification products, always discard the PCR plates once the reaction is finished and never place them on the PCR preparation laboratory bench. No-template and no-RT controls should reassure against the presence of contaminating DNA in the reaction.
6. In addition to melt curve analysis, amplification specificity can also be confirmed by gel electrophoresis (on an ethidium bromide-stained 4% NuSieve 3:1 agarose). For PCR fragments smaller than 100 bp, the gel is run at 80–100 V for 45–60 min, and for PCR fragments of 100–250 bp, the gel is run at 100–115 V for 1–1.5 h.
7. In addition to the method of calculating relative expression of a gene described in this chapter, one could directly use the starting quantity values given by the standard curve analysis for each gene and then divide the target gene value by the housekeeping gene value. Finally, all results are corrected so that the reference sample value for the target gene is 1.
8. Monensin can also be used with analogous effects to brefeldin A ***(59)***. Both chemicals are toxic, and contact with skin, eyes, and mucous membranes should be avoided.

References

1 Ronnblom, L. and Alm, G.V. (2001) A pivotal role for the natural interferon αα-producing cells (plasmacytoid dendritic cells) in the pathogenesis of lupus. *J. Exp. Med.* **194,** 59–63.

2 Chernysheva, A. D., Kirou, K. A., and Crow, M. K. (2002) T cell proliferation induced by autologous non-T cells is a response to apoptotic cells processed by dendritic cells. *J. Immunol.* **169,** 1241–1250.

3 Crow, M. K. (2003) Studies of autologous T cell activation in the Kunkel laboratory. *Lupus* **12,** 163–169.
4 Kirou, K. A., and Crow, M. K. (1999) New pieces to the SLE cytokine puzzle. *Clin. Immunol.* **91,** 1–5.
5. Llorente, L., Richaud-Patin, Y., Fior, R., Alcocer-Varela, J., Wijdenes, J., Fourrier, B. M., et al. (1994) In vivo production of interleukin-10 by non-T cells in rheumatoid arthritis, Sjögren's syndrome, and systemic lupus erythematosus. *Arthritis Rheum.* **11,** 1647–1655.
6 Hagiwara, E., Gourley, M. F., Lee, S., and Klinman, D. M. (1996) Disease severity in patients with systemic lupus erythematosus correlates with an increased ratio of interleukin-10:interferon-γ-secreting cells in the peripheral blood. *Arthritis Rheum.* **39,** 379–385.
7 Akira, S., Taga, T., and Kishimoto, T. (1993) IL-6 in biology and medicine. *Adv. Immunol.* **54,** 1–78.
8 Itoh, K. and Hirohata, S. (1995) The role of IL-10 in human B cell activation, proliferation, and differentiation. *J. Immunol.* **154,** 4341–4350.
9 Linker-Israeli, M., Deans, R. J., Wallace, D. J., Prehn, J., Ozeri-Chen, T., and Klinenberg, J. R. (1991) Elevated levels of endogenous IL-6 in systemic lupus erythematosus. A putative role in pathogenesis. *J. Immunol.* **147,** 117–123.
10 Al-Janadi, M., al-Balla, S., al-Dalaan, A., and Raziuddin, S. (1993) Cytokine profile in systemic lupus erythematosus, rheumatoid arthritis, and other rheumatic diseases. *J. Clin. Immunol.* **13,** 58–67.
11 Richaud-Patin, Y., Alcocer-Varela, J., and Llorente, L. (1995) High levels of TH2 cytokine gene expression in systemic lupus erythematosus. *Rev. Invest. Clin.* **47,** 267–272.
12 Swaak, A. J., van den Brink, H. G., and Aarden, L. A. (1996) Cytokine production (IL-6 and TNF alpha) in whole blood cell cultures of patients with systemic lupus erythematosus. *Scand. J. Rheumatol.* **25,** 233–238.
13 Barcellini, W., Rizzardi, G. P., Borghi, M. O., Nicoletti, F., Fain, C., Del Papa, N., et al. (1996) In vitro type-1 and type-2 cytokine production in systemic lupus erythematosus: lack of relationship with clinical disease activity. *Lupus* **5,** 139–145.
14 Linker-Israeli, M., Honda, M., Nand, R., Mandyam, R., Mengesha, E., Wallace, D. J., et al. (1999) Exogenous IL-10 and IL-4 down-regulate IL-6 production by SLE-derived PBMC. *Clin. Immunol.* **91,** 6–16.
15 Cerutti, A., Zan, H., Schaffer, A., Bergsagel, L., Harindranath, N., Max, E. E., et al. (1998) CD40 ligand and appropriate cytokines induce switching to IgG, IgA, and IgE and coordinated germinal center and plasmacytoid phenotypic differentiation in a human monoclonal IgM + IgD + B cell line. *J. Immunol.* **160,** 2145–2157.
16 Ji, J. D., Tassiulas, I., Park-Min, K. H., Aydin, A., Mecklenbrauker, I., Tarakhovsky, A., et al. (2003) Inhibition of interleukin 10 signaling after Fc receptor ligation and during rheumatoid arthritis. *J. Exp. Med.* **197,** 1573–1583.
17 Chen-Kiang, S. (1995) Regulation of terminal differentiation of human B-cells by IL-6. *Curr. Top. Microbiol. Immunol.* **194,** 189–198.
18 Biron, C. A. (2001) Interferons alpha and beta as immune regulators—a new look. *Immunity* **4,** 661–664.

19 Hooks, J. J., Moutsopoulos, H. M., Geis, S. A., Stahl, N. I., Decker, J. L., and Notkins, A. L. (1979) Immune interferon in the circulation of patients with autoimmune disease. *N. Engl. J. Med.* **301,** 5–8.

20 Preble, O. T., Black, R. J., Friedman, R. M., Klippel, J. H., and Vilcek, J. (1982) Systemic lupus erythematosus: presence in human serum of an unusual acid-labile leukocyte interferon. *Science* **216,** 429–431.

21 Yee, A. M., Yip, Y. K., Fischer, H. D., and Buyon, J. P. (1990) Serum activity that confers acid lability to alpha-interferon in systemic lupus erythematosus: its association with disease activity and its independence from circulating alpha-interferon. *Arthritis Rheum.* **33,** 563–568.

22 Blanco, P., Palucha, A. K., Gill, M., Pascual, V., and Banchereau, J. (2001) Induction of dendritic cell differentiation by IFN-alpha in systemic lupus erythematosus. *Science* **294,** 1540–1543.

23 Crow, M. K., George, S., Paget, S. A., Ly, N., Woodward, R., Fry, K., et al. (2002) Expression of an interferon-alpha gene program in SLE. *Arthritis Rheum.* **46,** S281.

24 Baechler, E. C., Batliwalla, F. M., Karypis, G., Gaffney, P. M., Ortmann, W. A., Espe, K. J., et al. (2003) Interferon-inducible gene expression signature in peripheral blood cells of patients with severe lupus. *Proc. Natl. Acad. Sci. USA* **100,** 2610–2615.

25 Bennett, L., Palucka, A. K., Arce, E., Cantrell, V., Borvak, J., Banchereau, J., et al. (2003) Interferon and granulopoiesis signatures in systemic lupus erythematosus blood. *J. Exp. Med.* **197,** 711–723.

26 Han, G.-M., Chen, S.-L., Shen, N., Ye, S., Bao, C.-D., and Gu, Y.-Y. (2003) Analysis of gene expression profiles in human systemic lupus erythematosus using oligonucleotide microarray. *Genes Immun.* **4,** 177–186.

27 Siegel, F. P., Kadowaki, N., Shodell, M., Fitzgerald-Bocarsly, P. A., Shah, K., Ho, S., et al. (1999) The nature of the principal type I interferon-producing cells in human blood. *Science* **284,** 1835–1837.

28 Svensson, H., Johannisson, A., Nikkila, T., Alm, G. V., and Cederblad, B. (1996) The cell surface phenotype of human natural interferon-αα producing cells as determined by flow cytometry. *Scand. J. Immunol.* **44,** 164–172.

29 Vallin, H., Blomberg, S., Alm, G. V., Cederblad, B., and Ronnblom, L. (1999) Patients with systemic lupus erythematosus (SLE) have a circulating inducer of interferon-alpha (IFN-αα) production acting on leukocytes resembling immature dendritic cells. *Clin. Exp. Immunol.* **115,** 196–202.

30 Bave, U., Vallin, H., Alm, G. V., and Ronnblom, L. (2001) Activation of natural interferon-alpha producing cells by apoptotic U937 cells combined with lupus IgG and its regulation by cytokines. *J. Autoimmun.* **17,** 71–80.

31 Magnusson, M., Magnusson, S., Vallin, H., Ronnblom, L., and Alm, G. V. (2001) Importance of CpG dinucleotides in activation of natural IFN-alpha-producing cells by a lupus-related oligodeoxynucleotide. *Scand. J. Immunol.* **54,** 543–550.

32 Ronnblom, L. E., Alm, G. V., and Oberg, K. E. (1990) Possible induction of systemic lupus erythematosus by interferon-αα treatment in a patient with a malignant carcinoid tumor. *J. Intern. Med.* **227,** 207–210.
33 Crow, M. K. and Kirou, K.A. (2001) Regulation of CD40 ligand expression in systemic lupus erythematosus. *Curr. Opin. Rheumatol.* **13,** 361–369.
34 Santiago-Raber, M. L., Baccala, R., Haraldsson, K. M., Choubey, D., Stewart, T. A., Kono, D. H., et al. (2003) Type-I interferon receptor deficiency reduces lupus-like disease in NZB mice. *J. Exp. Med.* **197,** 777–788.
35 Peng, S. L., Moslehi, J., and Craft, J. (1997) Roles of interferon-gamma and interleukin-4 in murine lupus. *J. Clin. Invest.* **99,** 1936–1946.
36 Balomenos, D., Rumold, R., and Theophilopoulos, A. N. (1998) Interferon-gamma is required for lupus-like disease and lymphoaccumulation in MRL-lpr mice. *J. Clin. Invest.* **101,** 364–371.
37 Haas, C., Ryffel, B., and Le Hir, M. (1998) IFN-gamma receptor deletion prevents autoantibody production and glomerulonephritis in lupus-prone (NZB x NZW)F1 mice. *J. Immunol.* **160,** 3713–3718.
38 Pachman, L. M., Liotta-Davis, M. R., Hong, D. K., Kinsella, T. R., Mendez, E. P., Kinder, J. M., et al. (2000) TNFα-308A allele in juvenile dermatomyositis: association with increased production of tumor necrosis factor α, disease duration, and pathologic calcifications. *Arthritis Rheum.* **43,** 2368–2377.
39 Wilson, A. G., DiGiovine, F. S., Blakemore, A. I. F., and Duff, G. W. (1992) Single base polymorphism in the human tumor necrosis factor (TNFα). *Hum. Mol. Genet.* **1,** 353.
40 Linker-Israeli, M., Wallace, D. J., Prehn, J., Michael, D., Honda, M., Taylor, K. D., et al. (1999) Association of IL-6 gene alleles with systemic lupus erythematosus (SLE) and with elevated IL-6 expression. *Genes Immun.* **1,** 45–52.
41 Ansari, A. A. and Mayne, A. E. (2002) Cytokine analysis by intracellular staining. *Methods Mol. Med.* **72,** 423–435.
42 Loza, M. J., Faust, J. S., and Perussia, G. (2003) Multiple color immunofluorescence for cytokine detection at the single-cell level. *Mol. Biotechnol.* **23,** 245–258.
43 Kalyuzhny, A. and Stark, S. (2001) A simple method to reduce the background and improve well-to-well reproducibility of staining in ELISPOT assays. *J. Immunol. Methods* **257,** 93–97.
44 Mashishi, T. and Gray, C. M. (2002) The ELISPOT assay: an easily transferable method for measuring cellular responses and identifying T cell epitopes. *Clin. Chem. Lab. Med.* **40,** 903–910.
45 Van Besouw, N. M., Vaessen, L. M., Zuijderwijk, J. M., van Vliet, M., Ijermans, J. N., van Der Meide, P. H., et al. (2003) The frequency of interferon-γ producing cells reflects alloreactivity against minor histocompatibility antigens. *Transplantation* **75,** 1400–1404.
46 Salmon, J. E., Millard, S., Schachter, L. A., Arnett, F. C., Ginzler, E. M., Gourley, M. F., et al. (1996) Fc gamma RIIA alleles are heritable risk factors for lupus nephritis in African Americans. *J. Clin. Invest.* **97,** 1348–1354.

47 Gabriel, S. B., Schaffner, S. F., Nguyen, H., Moore, J. M., Roy, J., Blumenstiel, B., et al. (2002) The structure of haplotype blocks in the human genome. *Science* **296,** 2225–2229.
48 Von Wolff, M. and Tabibzadeh, S. (1999) Multiprobe Rnase protection assay with internally labeled radioactive probes, generated by RT-PCR and nested PCR. *Front. Biosci.* **4,** C1–C3.
49 Ceol, M., Forino, M., Gambaro, G., Sauer, U., Schleicher, E. D., D'Angelo, A., et al. (2001) Quantitation of TGF-beta1 mRNA in porcine mesangial cells by comparative kinetic RT/PCR: comparison with ribonuclease protection assay and in situ hybridization. *J. Clin. Lab. Anal.* **15,** 215–222.
50 Glue, C., Hansen, J. B., Schjerling, P., Jinquan, T., and Poulsen, L. K. (2002) LPS-induced cytokine production in the monocytic cell line THP-1 determined by multiple quantitative competitive PCR (QC-PCR). *Scand. J. Clin. Lab. Invest.* **62,** 405–412.
51. Bustin, S. A. (2002) Quantification of mRNA using real-time reverse transcription PCR (RT-PCR): trends and problems. *J. Mol. Endocrinol*. **29,** 23–-39.
52 Ramos-Payan, R., Aguilar-Medina, M., Estrada-Parra, S., Gonzalez-Y-Merchand, J. A., Favila-Castillo, L., Monroy-Ostria, A., et al. (2003) Quantification of cytokine gene expression using an economical real-time polymerase chain reaction method based on SYBR Green I. *Scand. J. Immunol.* **57,** 439–445.
53 Zuker, M. (2003) Mfold web server for nucleic acid folding and hybridization prediction. *Nucleic Acids Res.* **31**, 3406–3415.
54 Ririe, K. M., Rasmussen, R. P., and Wittwer, C. T. (1997) Product differentiation by analysis of DNA melting curves during the polymerase chain reaction. *Anal. Biochem.* **245,** 154–160.
55 Pfaffl, M. W. (2001) A new mathematical model for relative quantification in real-time RT-PCR. *Nucleic Acids Res.* **29,** E45–E45.
56 Murakawa, Y., Takada, S., Ueda, Y., Suzuki, N., Hoshino, T., and Sakane, T. (1985) Characterization of T lymphocyte subpopulations responsible for deficient interleukin 2 activity in patients with systemic lupus erythematosus. *J. Immunol.* **134,** 187–195.
57 Solomou, E. E., Juang, Y. T., Gourley, M. F., Kammer, G. M., and Tsokos, G. C. (2001) Molecular basis of deficient IL-2 production in T cells from patients with systemic lupus erythematosus. *J. Immunol.* **166,** 4216–4222.
58 Schmittgen, T. D. and Zakrajsek, B. A. (2000) Effect of experimental treatment on housekeeping gene expression: validation by real-time, quantitative RT-PCR. *J. Biochem. Biophys. Methods* **46,** 69–81.
59. O'Neil-Andersen, N. J. and Lawrence, D. A. (2002) Differential modulation of surface and intracellular protein expression by T cells after stimulation in the presence of monensin or brefeldin A. *Clin. Diagn. Lab. Immunol.* **9,** 243–250.

9

Evaluation of Autoimmunity to Transaldolase in Multiple Sclerosis

Brian Niland and Andras Perl

Summary

Transaldolase is a target of autoimmunity mediated by T cells and antibody (Ab) in patients with multiple sclerosis. Functional T-cell assays, T- and B-cell epitope mapping, and detection of transaldolase-specific antibodies in patients with multiple sclerosis are described. Recombinant transaldolase was produced in a prokaryotic expression vector for use in Western blot analysis of sera of these patients. Overlapping transaldolase peptides 15 amino acids (aa) long were synthesized onto cellulose membranes to map immunodominant B-cell epitopes. Amino acid sequence homologies between viral peptides and immunodominant B-cell epitopes of transaldolase were identified using a computer-based algorithm. Direct assessment of molecular mimicry between transaldolase B-cell epitopes and related viral peptides is also shown. T-cell epitopes are mapped in a T-cell proliferation assay using multiple sclerosis patient and control donor cells. Autoantigen-specific T cells are identified by MHC–peptide tetramer staining using flow cytometry analysis.

Key Words: Autoimmunity; epitope mapping; MHC–tetramer; molecular mimicry; multiple sclerosis; transaldolase.

1. Introduction

Evidence suggests that infections may trigger autoimmune disease in genetically susceptible hosts by the proposed mechanism of *molecular mimicry* ***(1)***. In this scenario, antibodies (Abs) or T cells generated in response to an infectious agent, such as a retrovirus, also crossreact with self-antigens ***(2)***. The crossreactive epitopes of these exogenous agents could play a key role in breaking the tolerance toward self-proteins and the induction of autoimmune disease ***(3)***. Abs crossreactive with a number of viral proteins have been described in patients with multiple sclerosis (MS) ***(4)***.

From: *Methods in Molecular Medicine, Vol. 102: Autoimmunity: Methods and Protocols*
Edited by: A. Perl © Humana Press Inc., Totowa, NJ

Multiple sclerosis is an autoimmune disease involving the central nervous system (CNS). MS lesions contain macrophages and T cells and are characterized by a progressive loss of oligodendrocytes and demyelination of the white matter of the CNS ***(3)***. Although the antigen driving this self-destructive process has not been identified, the importance of myelin-derived antigens was demonstrated by their abilities to elicit an MS-like demyelinating disease, experimental allergic encephalomyelitis, in various animal models ***(5)***. Myelin basic protein (MBP) and proteolipid protein, which make up as much as 30 and 50% of CNS myelin, respectively ***(6)***, are likely targets of an autoimmune response secondary to tissue injury in the CNS.

Another possible autoantigen in MS is the human transaldolase enzyme (TAL-H) ***(4)***. Transaldolase is a rate-limiting enzyme of the pentose phosphate pathway (PPP) that generates the reducing agent nicotinamide adenine dinucleotide phosphate required in lipid biosynthesis, which is necessary for myelination, among other metabolic pathways. This may explain the relatively high level of TAL-H expression in oligodendrocytes of the brain ***(4)***.

The characterization of transaldolase as an autoantigen in MS is used to illustrate methods used in autoepitope mapping and identification of candidate autoantigens.

2. Materials

1. Recombinant TAL-H (rTAL-H) fusion protein with glutathione-*S*-transferase (GST) encoded by pGEX-2T plasmid vector/Gene Fusion System (Amersham Biosciences, Piscataway, NJ) ***(7)***.
2. Isopropylthio-β-galactoside (Gold BioTechnology, St. Louis, MO).
3. Glutathione-coated agarose beads (Sigma Chemical, St. Louis, MO).
4. Thrombin (Sigma Chemical).
5. Affinity-purified GST protein, purified from same *Escherichia coli* strain as the rTAL-H (Amersham Biosciences) ***(7)***.
6. Human sera from patients with MS, systemic lupus erythematosus (SLE), other neurological diseases (ONDs) and healthy blood donors ***(8)***.
7. Anti-TAL-H polyclonal rabbit Ab raised against affinity-purified and enzymatically active full-length recombinant TAL-H ***(7)***.
8. Negative control preimmune rabbit sera ***(7)***.
9. PAGEr Gold precast 12% Tris-glycine polyacyrlamide protein gel (Cambrex, Rockland, ME).
10. 4X sodium dodecyl sulfate (SDS) sample buffer: 1 mL of 0.5 *M* Tris-HCl at pH 6.8, 0.8 mL of glycerol, 1.6 mL of 10% SDS, 0.4 mL of 2-mercaptoethanol, 0.2 mL of 0.05% (w/v) bromophenol blue in H_2O.
11. Trans-Blot 0.45-μm nitrocellulose transfer membrane (Bio-Rad, Hercules, CA).
12. TBS (1X): 100 m*M* Tris-buffered saline at pH 7.4, 150 m*M* NaCl.
13. T-TBS (1X): 100 m*M* Tris-buffered saline at pH 7.4, 150 m*M* NaCl, 0.1% Tween-20.

14. Powdered skim milk (Difco, Sparks, MD).
15. Horseradish peroxidase (HRP)-conjugated goat antirabbit immunoglobulin G (IgG) (Boehringer Mannheim, Indianapolis, IN).
16. Biotinylated goat antihuman serum (Jackson ImmunoResearch, West Grove, PA).
17. HRP-conjugated streptavidin (Jackson ImmunoResearch).
18. 4-Chloro-1-naphthol (Sigma Chemical).
19. Hydrogen peroxide (H_2O_2) 30% (w/w) solution (Sigma-Aldrich).
20. Chloronapthol development solution: 3 mL methanol, 12 mL TBS, 9 mg 4-chloro-1-napthol, and 6 μL H_2O_2.
21. 33 synthetic peptides (32that are 15 aa long, and 1 that is 17 aa long) overlapping TAL-H by 5 aa (Abimed, Langenfeld, Germany).
22. Spot Synthesizer automated solid-phase peptide synthesizer (Abimed).
23. Biotinylated goat $(Fab()_2$ fragments directed against human IgA, IgG, and IgM (Jackson ImmunoResearch).
24. Enhanced Chemiluminescence (ECL™) substrate (Amersham, Little Chalfont, UK).
25. Computerized automated densitometer (Bio-Rad).
26. University of Wisconsin Genetics Computer Group (UWGCG) software ***(9)***.
27. HLA Peptide Binding Prediction (National Institutes of Health [NIH] BioInformatics and Molecular Analysis Section [BIMAS] website: http://bimas.dcrt.nih.gov/molbio/hla_bind/) ***(10)***.
28. Ficoll-Paque™ Plus Ficoll-Hypaque gradient (Amersham Biosciences, Uppsala, Sweden).
29. RPMI-1640 medium supplemented with 10% fetal bovine serum, 2 m*M* L-glutamine, 100 IU/mL penicillin, and 100 μg/mL gentamicin (Mediatech, Herndon, VA).
30. 96-well microtiter plate (Costar, Corning, NY).
31. Recombinant human interleukin-2 (rIL-2) (McKesson BioServices Corp., Rockville, MD).
32. Concanavalin A (Sigma Chemical).
33. [^{3}H]Thymidine (^{3}H-TdR; ICN Biomedicals, Aurora, OH).
34. Skatron semiautomatic cell harvester (Molecular Devices, Sunnyvale, CA).
35. Skatron FilterMAT glass fiber filter (Molecular Devices).
36. 1600 TR liquid scintillation analyzer (Packard Instrument, Downers Grove, IL).
37. Multimeric peptide–major histocompatibility complex (MHC) tetrameric streptavidin-labeled complexes (NIH Tetramer Facility at Emory University, Atlanta, GA).
38. FACStar^{Plus} flow cytometer (BD Biosciences, Palo Alto, CA).

3. Methods

The methods described here outline (a) detection of transaldolase-specific Abs in patients with MS, (b) B-cell epitope mapping of transaldolase, and (c) T-cell epitope mapping of transaldolase and functional T-cell assays.

3.1. Detection of Transaldolase-Specific Antibodies in Patients With MS

By Western blot analysis, Abs to affinity-purified rTAL-H were found in 29/94 sera samples from patients with MS, and Abs to MBP were undetectable in sera of these same patients ***(8)***. Anti-TAL-H Abs were undetectable in sera samples of appropriate negative controls, including 10 patients with SLE, 9 patients with ONDs, and 74 control healthy blood donors ***(8)***. Sera reactivity to rTAL-H of patients with MS was compared to positive control rabbit sera raised against rTAL-H ***(4,8)***. TAL-H-specific seropositivity is based on immunoreactivity to 500 ng rTAL-H per lane at serum dilutions of 100-fold or higher.

3.1.1. Prokaryotic Expression of rTAL-H

Briefly, full-length TAL-H protein, coding for 337 aa, was expressed as a fusion protein with GST encoded by pGEX-2T plasmid vector ***(4,11)***. Optimum stimulation of expression of the recombinant fusion protein was obtained with 1 m*M* isopropylthio-β-galactoside for 4 h at 37°C.

The TAL-H/GST fusion protein was affinity purified through binding of GST to glutathione-coated agarose beads and cleaved from GST by 1 NIH unit of thrombin ***(4,12)***. Functional activity of each batch was analyzed in the transaldolase enzyme assay ***(7)***, showing a specific activity of more than 10 U/mL protein (*see* **Note 1**).

3.1.2. Western Blot Analysis of MS Patient Sera vs rTAL-H

1. Load 500 ng rTAL-H protein in 10 μL SDS sample buffer per well; separate by SDS-PAGE (polyacrylamide gel electrophoresis) and electroblot onto nitrocellulose membrane ***(8,13)***.
2. Incubate nitrocellulose strips in T-TBS and 5% skim milk with either patient or donor sera (at a 100-fold or greater dilution) overnight at room temperature ***(8)***.
3. Incubate separate strips overnight at room temperature with positive control rabbit anti-TAL-H Ab ***(4)*** (*see* **Note 2**)
4. Wash nitrocellulose membrane vigorously six times with T-TBS.
5. For detection using rabbit Ab, incubate with HRP-conjugated goat antirabbit IgG at a 1000-fold dilution in T-TBS and 5% skim milk ***(8)***.
6. For detection using human Abs, incubate with biotinylated goat antihuman serum and subsequently with HRP-conjugated streptavidin, both at 1000-fold dilutions in T-TBS and 5% skim milk ***(8)***.
7. Wash nitrocellulose membrane vigorously six times with T-TBS between incubations.
8. Develop the blots with chloronapthol development solution (*see* **Fig. 1**).
9. The presence of transaldolase-specific autoantibodies in patients with MS was compared with patients with ONDs and healthy control donors using a chi-square test.

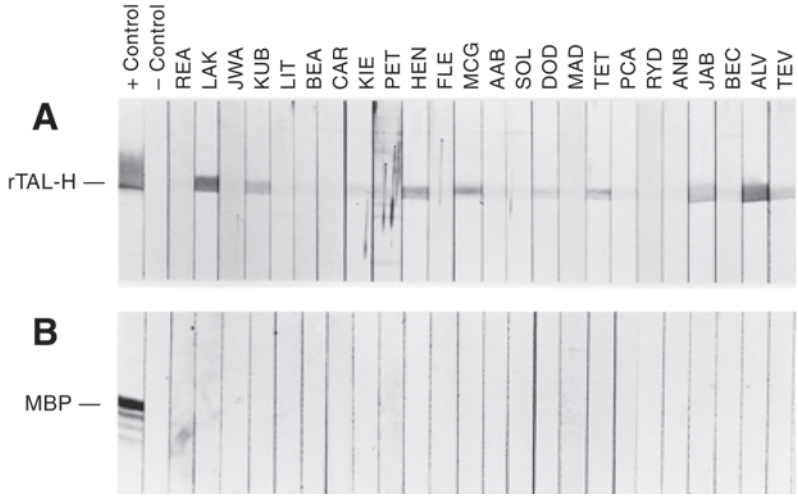

Fig. 1. Western blot reactivity to affinity-purified 38-kD full-length rTAL-H (**A**, 500 ng/lane) and human MBP (**B**, 500 ng/lane) of sera from patients with MS at a dilution of 1:100. + Control indicates rTAL-H-specific rabbit antibody in **A** and MBP-specific rabbit antibody in **B**; – Control indicates normal human serum ***(8)***.

3.2. B-Cell Epitopes

An epitope is the small region of a protein molecule to which the immune system recognizes and responds. Although T-cell epitopes are linear fragments of the original protein molecule, B-cell epitopes can be either linear fragments or folded three-dimensional regions of the intact molecule. Abs induced as a consequence of immunization with a whole protein antigen are often directed toward three-dimensional epitopes, most often composed of sets of residues that are discontinuous and brought together by folding ***(14)***.

These discontinuous linear segments, which represent significant antigenic sites when brought together as a composite site by tertiary structure folding, can be positively identified by testing the antigenicity of overlapping synthetic peptides that ideally cover the complete amino acid sequence of the antigen of interest. ***(15)***. B cell epitopes are usually comprised of 5 aa or fewer in contiguity ***(16)***. Peptides approx 15 aa long can assume ordered conformations that mimic the native protein ***(17)***.

To identify immunodominant epitopes in TAL-H, a total of 33 peptides (32 were 15 aa long, 1 was 17 aa long) overlapping TAL-H (337 aa) by 5 aa was synthesized onto cellulose membranes ***(18,19)***. To map epitopes exposed on native TAL-H, a polyclonal rabbit Ab raised against the full length and enzymatically active TAL-H was used ***(12)***. This polyclonal rabbit Ab binds native

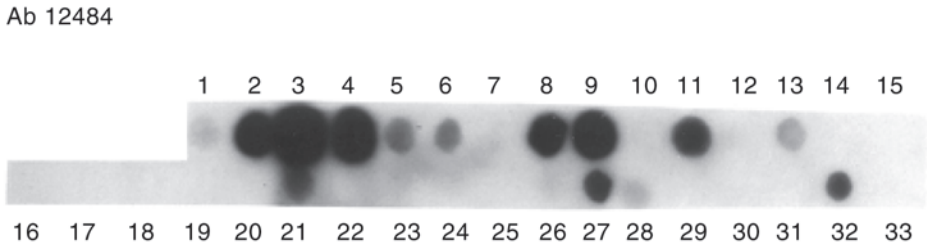

Fig. 2. Recognition by rabbit anti-TAL-H antibody 12484 of 33 cellulose-bound synthetic peptides overlapping TAL-H. The peptides were incubated with Ab 12484 at a 3000-fold dilution. After washing, the strips were incubated with HRP-conjugated goat antirabbit IgG, developed with a chemiluminescent substrate, and exposed to X-ray film. Quantification of antibody reactivities with each peptide was conducted with a computerized automated densitometer ***(18)***.

TAL-H and inhibits its catalytic activity ***(12)***. In Western blot assay, recognition by the rabbit anti-TAL-H sera of individual TAL-H peptides was assessed at a 3000-fold dilution by chemiluminescent detection (*see* **Fig. 2**).

Peptide reactivity with anti-TAL-H Abs was quantified by automated densitometry and expressed as relative binding intensity on a 0–2 scale. Immunodominant epitopes with high binding affinity to anti-TAL-H Abs were defined as having a binding intensity of 1 or higher, that is, 10-fold or more over background.

Subsequently, four immunodominant B-cell epitopes of TAL-H were identified by autoantibodies of patients with MS. Two of these peptides were recognized by both MS sera and rabbit anti-TAL-H sera ***(18)***.

3.2.1. Mapping of Immunodominant B-Cell Epitopes in TAL-H and B-Cell Epitopes in Patients With MS

1. Bind the 33 TAL-H overlapping synthetic peptides (32 are 15 aa long, 1 is 17 aa long) to cellulose strips via $(\beta\text{-Ala})_2$ spacers using the Spot Synthesizer (*see* **Note 3**).
2. Wet membranes in methanol for 10 min.
3. Wet membranes in TBS for 10 min.
4. Incubate peptide-containing strips with sera of control donors and sera of MS patients having Ab reactivities to human rTAL-H at a 1000-fold dilution or with positive control polyclonal rabbit anti-TAL-H Ab at a 3000-fold dilution in T-TBS and 5% skim milk at room temperature overnight. Additional controls included sera from TAL-H Western blot-negative patients with MS and preimmune rabbit serum.
5. Wash the strips vigorously six times with T-TBS.
6. For detection using rabbit Ab, incubate with HRP-conjugated goat antirabbit IgG.

7. For detection using human Abs, incubate with biotinylated goat $(Fab()_2$ fragments directed against human IgA, IgG, and IgM and subsequently with HRP-conjugated avidin.
8. Between the incubations, vigorously wash the strips six times in T-TBS.
9. Incubate the blots with ECL chemiluminescent substrate.
10. Develop by exposure to X-ray film.
11. Quantify Ab reactivities with each peptide using a computerized automated densitometer.
12. Express peptide reactivity with Ab as relative binding intensity on a 0–2 scale (*see* **Note 4**).
13. Compare reactivity levels of polyclonal rabbit sera with human sera peptide recognition (*see* **Note 5**).

3.2.2. Analysis of Amino Acid Sequence Homologies Between Viral Peptides and Immunodominant B-Cell Epitopes of TAL-H Recognized by Patients With MS

Protein comparison with viral peptides can be investigated using computer programs designed to reveal percentage homologies and position of identical residues per sequence alignment. To analyze the identified immunodominant B-cell epitopes, the GAP program of UWGCG Software was applied ***(9)***. All four immunodominant peptides from **Subheading 3.2.1.** showed sequence homology to viral antigens (*see* **Fig. 3**).

3.2.3. Direct Assessment of Molecular Mimicry Between TAL-H B-Cell Epitopes and Related Viral Peptides

To investigate crossreactivity, immunodominant TAL-H epitopes and related viral peptides (*see* **Subheading 3.2.2.**) were synthesized onto cellular membranes and tested in parallel for comparative recognition by rabbit anti-TAL-H sera and MS sera (*see* **Subheading 3.2.1.**). Correlations of crossreactivities between TAL-H and viral peptides were analyzed with Pearson's multivariate χ^2 test ***(18,20)***.

Resultant data provided direct evidence of MS crossreactivity between common viral antigens and the immunodominant epitope of TAL-H in a subset of patients with MS ***(18)***. As a control, sera of patients with MS who lacked TAL-H autoantibodies failed to recognize viral peptides ***(18)***.

3.3. T-Cell Epitopes

3.3.1. T-Cell Proliferation Assay

Antigenic exposure of suspended lymphocytes can result in cellular proliferation with increased DNA synthesis, which can be measured by the incorporation of [^{3}H]thymidine. The stimulation index (SI) is a ratio of the ^{3}H-TdR

```
TAL-H                    101   GRVSTEVDARLSFDK
                               :||     ||||   :
HSV-1 helicase           167   ARVAEHPDARLAWAR 40% (53%)

TAL-H                    231   TIVMGASFRNTGEIK
                                ||:    : : :|||
Measles/SSPE env         281   FIVLSIAYPTLSEIK 33% (60%)

TAL-H                    271   VPVLSAKAAQASDLE
                               ||||    ||     ||
EBV capsid BOLF1         306   VPVLAFDAARLRLLE 53%

TAL-H                    271   VPVLSAKAAQASDLE
                                ||:    ||  |:||
HSV-1 capsid VP5         410   NPVMERFAAHAGDLV 46% (60%)

TAL-H                    311   GIRKFAADAVKLERM
                               ||: : | :: :||
HIV-1 env gp160          572   GIKQLQARVLAVERY 33% (66%)
```

Fig. 3. Amino acid sequence homologies between immunodominant B-cell epitopes of TAL-H recognized by patients with MS and viral peptides. Homologies between TAL-H and viral sequences from herpes simplex type 1 (HSV-1) helicase, measles/subacute sclerosing panencephalitis (SSPE) virus, Epstein–Barr virus (EBV) capsid protein BOLF1, HSV-1 capsid protein VP5, and HIV-1 env gp160 were detected with the UWGCG software ***(9)***. Percentage homologies, percentage similarities (numbers in parentheses), position of identical residues (vertical bars), and position of functionally similar amino acids (colons), as well as amino acid position of the first residue of each peptide, are indicated ***(18)***.

uptake to a specific material compared to a control. To investigate whether TAL-H may be a target of autoreactive cells in patients with MS, its effect on proliferation of lymphocytes was evaluated. Subsequently, TAL-H caused aggregate formation and stimulated proliferation of peripheral blood lymphocytes (PBLs) from patients with MS (*see* **Fig. 4**).

1. Blood donors were recruited among patients with MS, SLE, and ONDs and healthy controls.
2. Peripheral blood mononuclear cells were isolated from heparinized venous blood on Ficoll-Paque gradient. Blood donors were recruited among three groups: those with MS, those with OND, and healthy controls.
3. Cells were resuspended in RPMI -1640 medium supplemented with 10% fetal bovine serum, 2 m*M* L-glutamine, 100 IU/mL penicillin, and 100 μg/mL gentamicin.

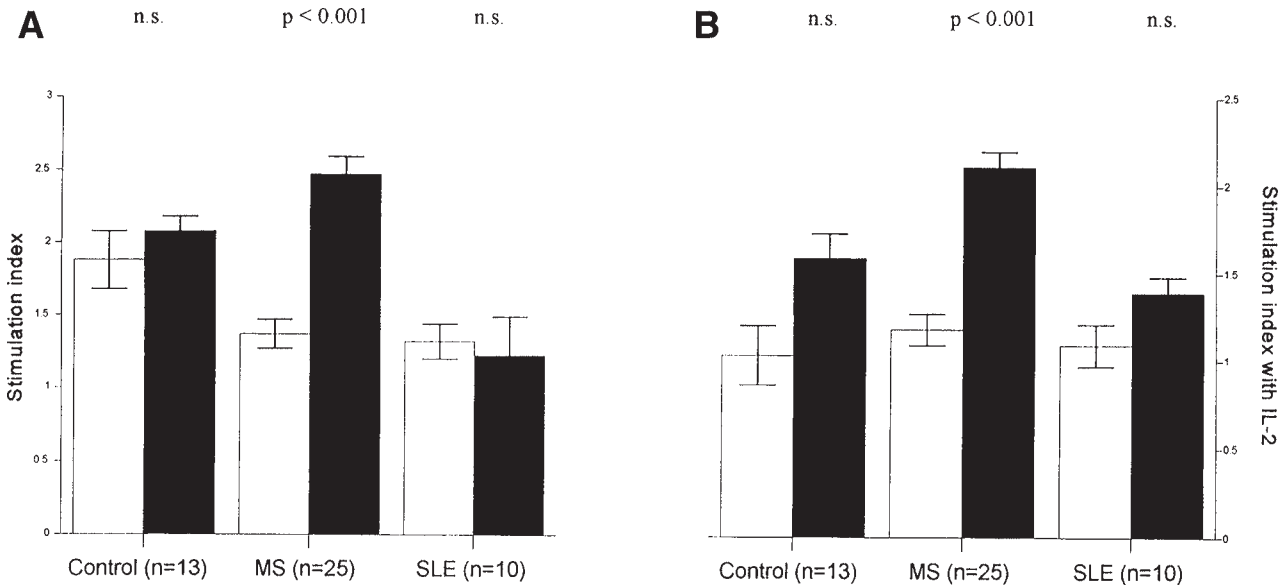

Fig. 4. Proliferative responses to TAL-H and MBP by PBLs from 13 control donors, 25 patients with MS, and 10 patients with SLE. SIs were measured in the absence or presence of 50 U/mL human recombinant IL-2 in response to 5 μg/mL TAL-H (shaded bars) or 30 μg/mL MBP (open bars). Significant differences were observed in patients with MS between responses to TAL-H and MBP in the presence or absence of IL-2 ($p < 0.001$); n.s., not significant ***(8)***.

4. 10^5 cells were incubated in each well of a 96-well microtiter plate, using six parallel samples, in the presence or absence of 50 U/mL human rIL-2 (NIH).
5. rTAL-H and MBP were separately added at empirically determined optimal concentrations of 5 μg/mL and 30 μg/mL, respectively ***(8)*** (*see* **Note 6**).
6. Negative control (5 μg/mL affinity-purified GST protein purified from the same *E. coli* strain as the rTAL-H) and positive control cultures (containing 10 μg/mL concanavalin A) were included in each experiment.
7. Plates were incubated at 37°C in a humidified atmosphere with 5% CO_2 for 72 h.
8. Approximately 8–12 h prior to termination, the cultures were pulsed with 0.4 μCi ^{3}H-TdR.
9. Prior to harvesting the cells, place the 96-well microtiter plate on a bright field microscope to confirm visually antigen-driven blastogenesis and aggregation, seen at a magnification of ×400 ***(4)***.
10. Cells were harvested onto glass fiber filter mats using a semiautomatic cell harvester.
11. ^{3}H-TdR incorporation was measured using a liquid scintillation analyzer ***(8)***.
12. Results are expressed in counts per minute (cpm) as mean plus or minus the standard error (SE) of six parallel cultures.
13. Calculate the SI, given as mean plus or minus the standard deviation (SD) of *n* experiments (*see* **Note 7**).
14. Statistical analysis of mean values was performed with Student's *t*-test. Correlations were analyzed by linear regression. The *p* values less than 0.05 were considered significant ***(8)***.
15. Recombinant TAL-H stimulated proliferation and caused aggregate formation of PBLs from patients with MS ***(4)***.

3.3.2. Mapping of MHC-Restricted TAL-H Epitopes

As demonstrated in **Subheading 3.2.2.**, a candidate protein's potential as an autoantigen can be indicated by comparing its amino acid sequence with that of human viral proteins. Amino acid sequence homologies were analyzed by the GAP program UWGCG software ***(9)***. Detection of conserved residues shared between MHC class I-restricted binding motifs of TAL-H and viral antigens included gag/core proteins of human T lymphotrophic virus I (HTLV-I) and human immunodeficiency virus 1 (HIV-1) ***(4)***.

3.3.3. Predicted Binding Stability of Autoantigen With MHC (Class I)

Incorporation of a typical peptide 8–9 aa long is required for the stabilization of MHC class I heavy chain and β_2 microglobulin (β_2m) complexes and their transport to the cell surface ***(21)***. Binding affinity to MHC class I molecules reliably predicts the capacity of a peptide epitope to elicit a cytotoxic T-cell response ***(22,23)***.

To determine if a protein contains candidate autoantigenic epitopes that may be presented in an MHC-restricted fashion, a computer-based algorithm can be

used. Computer analysis based on the coefficient tables of Dr. Kenneth Parker is made available by the NIH BioInformatics and Molecular Analysis Section (BIMAS) Web site server (http://bimas.dcrt.nih.gov/molbio/hla_bind/) ***(10)***. These computer-based algorithms are designed to predict the binding stability of HLA–antigen/peptide complexes by quantitating positive and negative effects on binding of each amino acid within an octamer, nonamer, and so on from the full-length peptide ***(24)***.

Therefore, the TAL-H amino acid sequence was analyzed for the presence of nonamer peptides with HLA class I binding motifs ***(24)***. Three peptides with predicted HLA-A2 binding stabilities greater than 100 min $t_{1/2}$ at 37°C were identified from the full-length TAL-H amino acid sequence (*see* **Table 1**).

3.3.4. Tetramer Staining for Flow Cytometry Analysis

Antigen-specific T cells can be identified by staining techniques using soluble MHC–peptide tetramer reagents, which bind their specific T-cell receptor ***(25)***. MHC–peptide tetramers are made by folding MHC heavy chain in the presence of high concentrations of the desired antigenic peptide and β_2m if using MHC class I heavy chain. Biotinylation of the carboxy terminus of one chain of the MHC molecule allows the MHC–peptide complex to be bound to streptavidin. Because streptavidin has four biotin-binding sites, four MHC molecules can be linked together in a single complex ***(26)*** (*see* **Fig. 5**).

These multimeric peptide–MHC complexes bind more than one T-cell receptor and thus have a relatively slow dissociation rate ***(26)*** and allow for staining and detection of epitope-specific T cells by flow cytometry when the streptavidin used is fluorophore labeled ***(27)***. The NIH Tetramer Facility (Emory University, Atlanta, GA) provides MHC class I tetramers for human, murine, macaque, and chimpanzee MHC alleles. MHC allele protein production and folding are free to registered investigators, who must provide the antigenic peptide of interest ***(28)***.

The established limiting dilution analysis method has been used to measure the frequency of an antigen-specific T-cell response. However, limiting dilution analysis may underestimate the number of T cells that respond to a particular antigen as it cannot detect cells that can no longer divide that are part of the expanded effector population ***(29)***. Staining of freshly isolated PBLs with the MHC–peptide tetramer can more directly reflect the frequency of MHC-restricted, peptide-specific T cells in vivo.

1. Wash and resuspend 1×10^6 cells of interest (PBLs, T-cell line, etc.) in 100 μL PBS.
2. Incubate cells with tetramer and without tetramer (negative control) for 30 min at 4°C (an irrelevant tetramer can also be used as a negative control) (*see* **Note 8**).
3. Wash cells three times with 1 mL PBS.

Table 1
Identification and Ranking of Potential HLA-A2-Binding TAL-H Peptides

Scoring results			
Rank	Start position	Subsequence residue listing	Score (predicted $t_{1/2}$ in min)
1	168	LLFSFAQAV	1662.432
2	263	LLQDNAKLV	484.777
3	325	MLTERMFNA	461.924
4	252	FLTISPKLL	98.267
5	246	ALAGCDFLT	43.222
6	165	NMTLLFSFA	37.495
7	167	TLLFSFAQA	34.925
8	182	GVTLISPFV	33.472
9	124	RLIELYKEA	30.553
10	142	KLSSTWEGI	30.417
11	54	QMPAYQELV	24.614
12	296	WLHNEDQMA	22.853
13	14	ALDQLKQFT	16.394
14	53	AQMPAYQEL	12.021
15	111	LSFDKDAMV	11.709
16	193	ILDWHVANT	11.655
17	154	KELEEQHGI	10.771
18	245	KALAGCDFL	10.355
19	81	KNAIDKLFV	8.740
20	138	RILIKLSST	8.720

Binding stability was based on calculated half-life (predicted $t_{1/2}$ in minutes at 37°C) of the dissociation of peptide–HLA class I complexes.

4. Resuspend cells in 250 μL PBS.
5. Detect tetramer-stained fluorescent cells using appropriate flow cytometry fluorescent channel (i.e., FL-2 for phycoerythrin) (*see* **Fig. 6**).
6. During tetramer/CD8 double staining of cells, some anti-CD8 Abs may interact with the tetramer to decrease or inhibit antigen-specific tetramer binding.

4. Notes

1. TAL-H enzyme activity was tested in the presence of 3.2 m*M* D-fructose-6-phosphate, 0.2 m*M* erythrose-4-phosphate, 0.1 m*M* nicotinamide adenine dinucleotide hydrogen (NADH), 10 μg α-glycerophosphate dehydrogenase/triosephosphate isomerase at a 1:6 ratio at room temperature by continuous absorbance reading at 340 nm for 20 min ***(4)***.

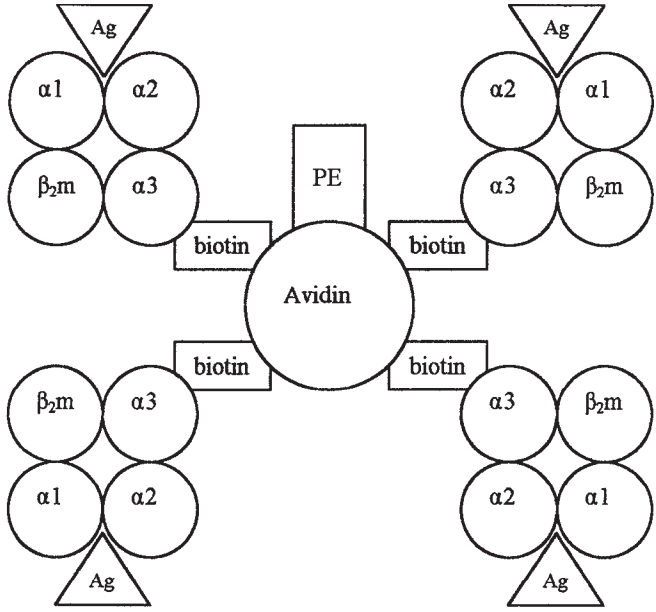

Fig. 5. Schematic diagram of a tetrameric MHC–antigen complex or tetramer. Four antigen-bearing MHC molecules (heavy-chain subunits with β_2-microglobulin) are attached via biotin to a single molecule of phycoerythrin (PE)-labeled streptavidin.

2. Highly specific polyclonal Abs against rTAL-H were raised in New Zealand white rabbits immunized on two separate occasions 3 wk apart with 500 mg of gel-purified rTAL-H protein ***(7)***. Specific reactivity of immune sera was evaluated by Western blot analysis using preimmune rabbit sera as a negative control ***(7)***.
3. The Abimed (Langenfeld, Germany) automated solid-phase peptide synthesizer uses N-terminal Fmoc (9-fluorenylmethoxycarbonyl) amino acid protection chemistry (based on the Merrifield method) for assembling spot-synthesized peptides ***(19)*** directly on the surface of a polyethylene glycol (PEG)-modified and $(\beta\text{-alanine})_2$-functionalized cellulose membrane ***(30)*** (e.g., GRVSTEVDARLSFDK-β alanine-PEG-cellulose). The cellulose membrane's porous and hydrophilic qualities allow measurement of aqueous solutions ***(31)***. PEG and $(\beta\text{-Ala})_2$ act as spacers, improving peptide accessibility and preserving the natural conformation of the C-terminus attached peptide. The $(\beta\text{-Ala})_2$ anchor provides a uniform start for synthesis, following the removal of its Fmoc group, allowing receipt of the incoming protected and activated amino acids to be spotted by the Abimed ASP 422 robotic arm ***(31)***.

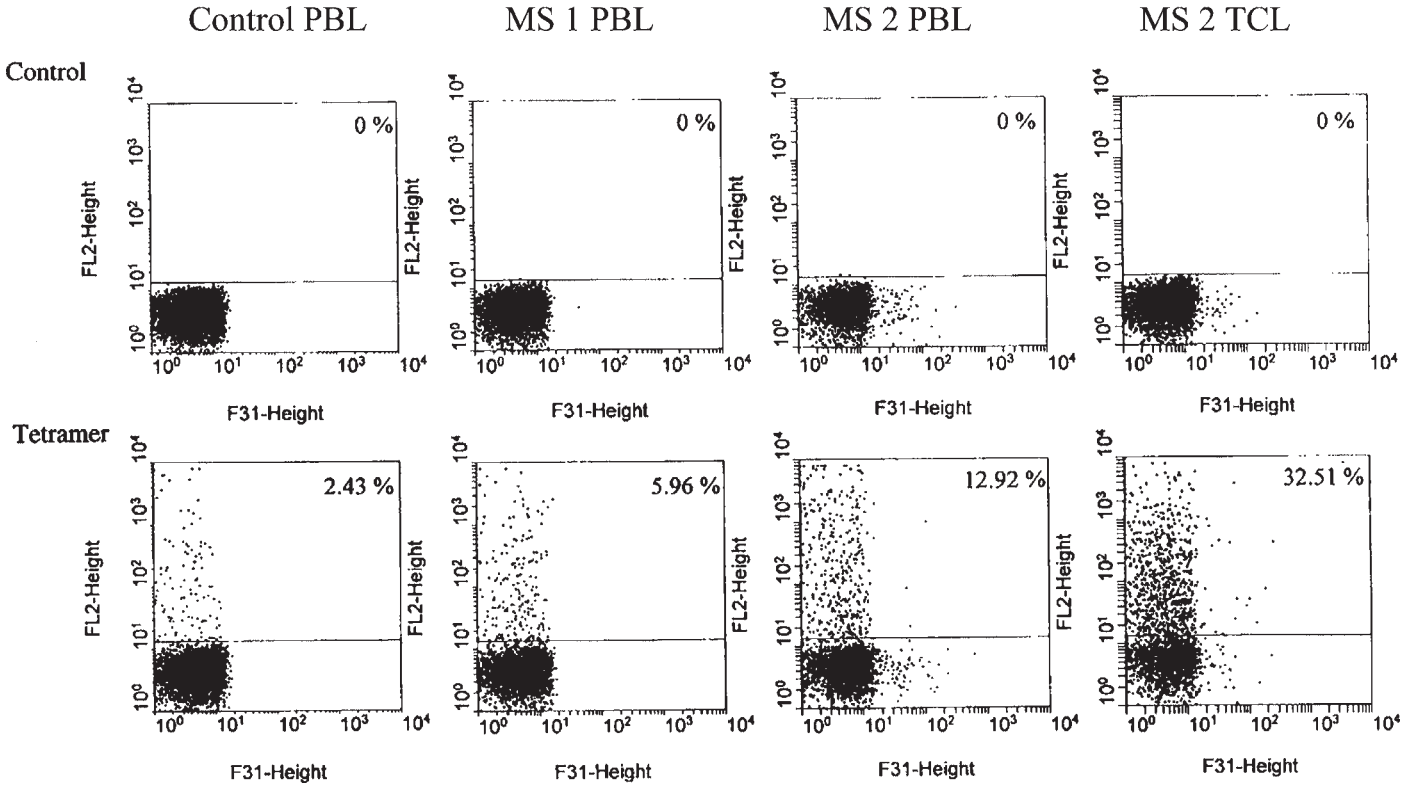

Fig. 6. Flow cytometry analysis of PBLs of control and patients with MS as well as T-cell line (TCL) from patient MS 2. Control cells were unstained, and tetramer-stained cells were stained with TAL-H 168-176/HLA*0201 tetramer for 30 min at 4°C.

4. Cutoff levels are set at 3 SDs over reactivity of negative control sera. Reactivities at or below cutoff levels are set at 0. Maximum reactivity with a single peptide is set at 2.0 for each Ab. Immunodominant epitopes with high binding affinity to Ab were defined as having a binding intensity of half-maximal reactivity (1.0) or above, that is, 10-fold or more over background. Repeat experiments should give variations of less than 10% for peptide-binding values ***(18)***.
5. TAL-H peptides not recognized by the polyclonal rabbit sera (raised against full-length TAL-H) but recognized by MS sera may indicate nonimmunogenic peptides in the rabbit. However, this may indicate a cryptic epitope, perhaps resulting from proteolytic degradation after TAL-H release during demyelination in the human MS brain ***(8,18)***.
6. Previously, concentration ranges of 1–30 μg/mL for TAL-H and 1–100 μg/mL for MBP were tested to find the optimal concentration for inducing cell proliferation ***(8)***. MBP was purified from neurologically normal human brain according to the procedure of Deibler et al. ***(32)***.
7. SI = (Measurement for target material)/(Measurement for control material). An SI value of 3.5 (i.e., an average of 3.5-fold increase of ^{3}H-TdR incorporation in peripheral blood mononuclear cells in response to a single in vitro exposure to antigen) is considered highly significant.
8. Initially, determine optimal tetramer concentration during incubation (e.g., 100-fold dilution, 1000-fold dilution). Also, staining should be tried at 4°C, room temperature, and 37°C. To optimize the signal-to-noise ratio, incubate for 15–60 min, decreasing the time used for staining as the temperature increases ***(28)***.

Acknowledgment

This work was supported by grant RG 2466 from the National Multiple Sclerosis Society.

References

1 Oldstone, M. B. A. (1998) Molecular mimicry and immune-mediated diseases. *FASEB J.* **12,** 1255–1265.
2 Wucherpfennig, K. W. and Strominger, J. L. (1995) Molecular mimicry in T cell-mediated autoimmunity: viral peptides activate human T cell clones specific for myelin basic protein. *Cell* **80,** 695–705.
3 Martin, R., McFarland, H. F., and McFarlin, D. E. (1992) Immunological aspects of demyelinating diseases. *Annu. Rev. Immunol.* **10,** 153–187.
4 Banki, K., Colombo, E., Sia, F., Halladay, D., Mattson, D., Tatum, A., et al. (1994) Oligodendrocyte-specific expression and autoantigenicity of transaldolase in multiple sclerosis. *J. Exp. Med.* **180,** 1649–1663.
5 Roder, J. and Hickey, W. F. (1996) Mouse models, immunology, multiple sclerosis and myelination. *Nat. Genet.* **12,** 6–8.
6. Lees, M. B. and Brostoff, S. W. (1984) Proteins of myelin, in *Myelin* (Morell, P., ed), Plenum Press, New York, pp. 197–224.

7 Banki, K., Halladay, D., and Perl, A. (1994) Cloning and expression of the human gene for transaldolase: a novel highly repetitive element constitutes an integral part of the coding sequence. *J. Biol. Chem.* **269,** 2847–2851.
8 Colombo, E., Banki, K., Tatum, A. H., Daucher, J., Ferrante, P., Murray, R. S., et al. (1997) Comparative analysis of antibody and cell-mediated autoimmunity to transaldolase and myelin basic protein in patients with multiple sclerosis. *J. Clin. Invest.* **99,** 1238–1250.
9 Devereux, J., Haeberli, P., and Smithies, O. (1984) A comprehensive set of sequence analysis programs for the VAX. *Nucleic Acids Res.* **12,** 387–395.
10. Parker, K. HLA peptide binding predictions. NIH BIMAS website: http://bimas.dcrt.nih.gov/molbio/hla_bind/. Accessed April, 2003.
11. Smith, D. B. and Johnson, K. S. (1988) Single-step purification of polypeptides expressed in *Escherichia coli* as fusions with glutathione S-transferase. *Gene* **67,** 31–40.
12. Banki, K. and Perl, A. (1996) Inhibition of the catalytic activity of human transaldolase by antibodies and site-directed mutagenesis. *FEBS Lett.* **378,** 161–165.
13. Towbin, H., Staehelin, T., and Gordon, J. (1979) Electrophoretic transfer of proteins from polyacrylamide gels to nitrocellulose sheets: procedure and some applications. *Proc. Natl. Acad. Sci. USA* **76,** 4350–4354.
14. Geysen, H. M., Meloen, R. H., and Barteling, S. J. (1984) Use of peptide synthesis to probe viral antigens for epitopes to a resolution of a single amino acid. *Proc. Natl. Acad. Sci. USA* **81,** 3998–4002.
15. Geysen, H. M. (1990) Molecular technology: peptide epitope mapping and the pin technology. *Southeast Asian J. Trop. Med. Public Health* **21,** 523–533.
16. Williams, R.C., Jr., Staud, R., Malone, C. C., Payabyab, J., Byres, L., and Underwood, D. (1994) Epitopes on proteinase-3 recognized by antibodies from patients with Wegener's granulomatosis. *J. Immunol.* **152,** 4722–4737.
17. Lang, E., Szendrei, G., Lee, V. M., and Otvos, L., Jr. (1994) Spectroscopic evidence that monoclonal antibodies recognize the dominant conformation of medium-sized synthetic peptides. *J. Immunol. Methods* **170,** 103–115.
18. Esposito, M., Venkatesh, V., Otvos, L., Weng, Z., Vajda, S., Banki, K., et al. (1999) Human transaldolase and cross-reactive viral epitopes identified by autoantibodies of multiple sclerosis patients. *J. Immunol.* **163,** 4027–4032.
19. Frank, R. (1992) Spot-synthesis: an easy technique for the positionally addressable, parallel chemical synthesis on a membrane support. *Tetrahedron* **48,** 9217–9232.
20. Fleiss, J. L. (1981) *Statistical Methods for Rates and Proportions*, Wiley, New York.
21. Germain, R. N. (1994) MHC-dependent antigen processing and peptide presentation: providing ligands for T lymphocyte activation. *Cell* **76,** 287–299.
22. Sette, A., Vitiello, A., Reherman, B., Fowler, P., Nayersina, R., Kast, W. M., et al. (1994) The relationship between class I binding affinity and immunogenicity of potential cytotoxic T cell epitopes. *J. Immunol.* **153,** 5586–5592.

23. Tsuchida, T., Parker, K. C., Turner, R. V., McFarland, H. F., Coligan, J. E., and Biddison, W. E. (1994) Autoreactive CD8+ T-cell responses to human myelin protein-derived peptides. *Proc. Natl. Acad. Sci. U S A* **91,** 10,859–10,863.
24. Parker, K. C., Bednarek, M. A. and Coligan, J. E. (1994) Scheme for ranking potential HLA-A2 binding peptides based on independent binding of individual peptide side-chains. *J. Immunol.* **152,** 163–175.
25. Altman, J. D., Moss, P. A., Goulder, P. J., Barouch, D. H., McHeyzer-Williams, M. G., Bell, J. I., et al. (1996) Phenotypic analysis of antigen-specific T lymphocytes. *Science* **274,** 94–96. Published erratum appears in *Science* (1998) **280,** 1821.
26. Bodinier, M., Peyrat, M. A., Tournay, C., Davodeau, F., Romagne, F., Bonneville, M., et al. (2000) Efficient detection and immunomagnetic sorting of specific T cells using multimers of MHC class I and peptide with reduced CD8 binding. *Nat. Med.* **6,** 707–710.
27. Kuroda, M. J., Schmitz, J. E., Barouch, D. H., Craiu, A., Allen, T. M., Sette, A., et al. (1998) Analysis of Gag-specific cytotoxic T lymphocytes in simian immunodeficiency virus-infected rhesus monkeys by cell staining with a tetrameric major histocompatibility complex class I-peptide complex. *J. Exp. Med.* **187,** 1373–1381.
28. National Institutes of Allergy and Infectious Diseases (NIAID), Tetramer Facility Guide, McKesson Biosciences Corp. http://www.niaid.nih.gov/reposit/tetramer/index.html. April 2003
29. McMichael, A. J. and O'Callaghan, C. A. (1998) A new look at T cells. *J. Exp. Med.* **187,** 1367–1371.
30. Rudiger, S., Germeroth, L., Schneider-Mergener, J., and Bukau, B. (1997) Substrate-specificity of the DnaK chaperone determined by screening cellulose-bound peptide libraries. *EMBO J.* **16,** 1501–1507.
31. Otvos, L., Jr., Pease, A. M., Bokonyi, K., Giles-Davis, W., Rogers, M. E., Hintz, P. A., et al. (2000) *In situ* stimulation of a T helper cell hybridoma with a cellulose-bound peptide antigen. *J. Immunol. Methods* **233,** 95–105.
32. Deibler, G. E., Martenson, R. E., and Kies, M. W. (1972) Large scale preparation of myelin basic protein from central nervous tissue of several mammalian species. *Prep. Biochem.* **2,** 139–165.

II

Animal Models of Autoimmunity

10

Animal Models for Autoimmune Myocarditis and Autoimmune Thyroiditis

Daniela Čiháková, Rajni B. Sharma, DeLisa Fairweather, Marina Afanasyeva, and Noel R. Rose

Summary

This chapter describes four murine models of autoimmune diseases: two related to autoimmune myocarditis and two related to autoimmune thyroiditis. The first model, Coxsackie virus B3 (CB3)-induced myocarditis, results in the development of acute myocarditis in susceptible as well as resistant mouse strains, whereas chronic myocarditis develops only in genetically susceptible mice. CB3-induced myocarditis closely resembles the course of human myocarditis, which is believed to be initiated by viral infection. Mouse cardiac myosin heavy chain has been identified as the major antigen associated with the late chronic phase of viral myocarditis. The second model is cardiac myosin-induced experimental autoimmune myocarditis (EAM) and, in a modification, cardiac α-myosin heavy chain peptide-induced myocarditis. In the EAM model, cardiac myosin or the relevant peptide in Freund's complete adjuvant (FCA)is injected subcutaneously into mice. The immune response, the histological changes, and the genetic susceptibility seen in EAM are similar to those of CB3-induced myocarditis. The third model is experimental autoimmune thyroiditis (EAT). EAT can be induced in genetically susceptible strains of mice by immunization with mouse thyroglobulin in FCA or lipopolysaccharide. Mice susceptible to EAT have the H-2A^{k}, H-2A^{s}, or H-2A^{q} alleles. We describe here a standard technique for the induction of EAT; it was developed in our laboratory and is widely used as a model for studying Hashimoto's thyroiditis. The fourth model presented in this chapter is that of spontaneous autoimmune thyroiditis in NOD.H2^{h4} mice. These mice express the H-2A^{k} allele on an NOD genetic background and develop spontaneous thyroiditis, which is exacerbated with dietary iodine.

Key Words: Autoimmunity; Coxsackie virus B3 (CB3); Freund's complete adjuvant (FCA); myocarditis; myosin; thyroiditis; NOD.H2^{h4}.

From: *Methods in Molecular Medicine, Vol. 102: Autoimmunity: Methods and Protocols*
Edited by: A. Perl © Humana Press Inc., Totowa, NJ

1. Introduction

Experimental mouse models have contributed greatly to the understanding of the immune mechanisms involved in human autoimmune diseases. This chapter describes two models of autoimmune myocarditis and two models of autoimmune thyroiditis.

Myocarditis is an important cause of heart disease, predominantly among young people. It may progress to dilated cardiomyopathy, which is a common cause of heart failure ***(1,2)***. In an effort to study the pathogenic factors responsible for autoimmune myocarditis in humans, we have developed two murine models of myocarditis: Coxsackievirus B3 (CB3)-induced myocarditis and cardiac myosin-induced experimental autoimmune myocarditis (EAM). The latter can also be induced by immunization with peptides derived from the α-cardiac myosin heavy chain.

The CB3-induced myocarditis model involves infection with CB3, which is the most common virus associated with human myocarditis in the United States ***(3)***. Chronic myocarditis is observed in only a few patients after an otherwise common self-limited CB3 infection, suggesting a role for genetic predisposition ***(4)***. CB3-induced myocarditis closely resembles chronic human myocarditis because it also has two phases of infection and only genetically susceptible mice proceed to the second, chronic stage of the disease ***(4,5)***. The initial phase peaks around days 7–14 postinfection, is associated with the presence of infectious CB3 virus, and is characterized by infiltrates of mononuclear and polymorphonuclear inflammatory cells ***(5)***. This early, acute phase of CB3-induced myocarditis develops in all strains of mice studied.

However, only some strains of mice will develop a late, chronic phase of CB3-induced myocarditis (**Fig. 1**). The chronic myocarditis is characterized by a diffuse mononuclear infiltration ***(5)***. In susceptible BALB/c mice, chronic myocarditis develops from day 28 and persists to at least day 56.

Infectious virus can be isolated from the heart by plaque assay in the acute phase, but cannot be detected in the chronic stage of the disease (after day 14 postinfection). However, viral messenger RNA (RNA) can always be detected by *in situ* hybridization or polymerase chain reaction. During viral infection, immunoglobulin M (IgM) and IgG autoantibodies against cardiac myosin are produced in both susceptible and resistant mouse strains. However, susceptible mouse strains produce higher levels of IgG autoantibodies (especially IgG1) to cardiac myosin ***(6)***.

We identified mouse cardiac myosin heavy chain as the major antigen associated with viral myocarditis and were able to induce EAM in mice by immunization with cardiac myosin purified from murine hearts and adjuvant ***(6,7)***. In some mouse strains (A/J, BALB/c), the cardiac α-myosin heavy-chain peptide sequences that are able to induce EAM were identified ***(8–10)***. Therefore,

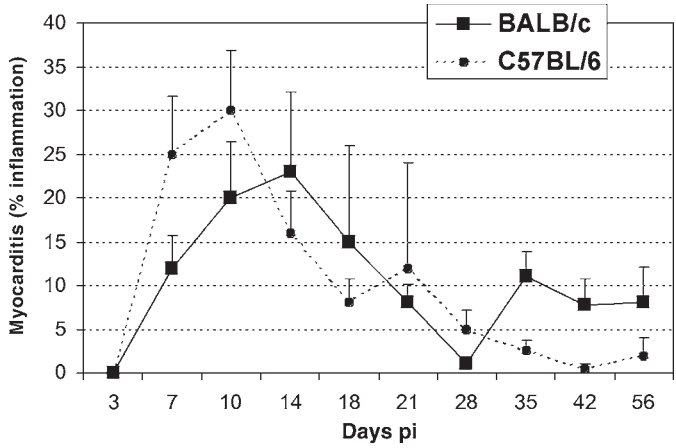

Fig. 1. Comparison of CB3-induced myocarditis in BALB/c and C57BL/6 mice. There were 7–10 mice examined for the histological presence of myocarditis at a number of time-points after CB3 infection. C57BL/6 mice do not develop chronic myocarditis. Results are presented as standard errors of the mean.

it is possible to use the synthetically prepared peptide for induction of EAM. The immune response and the histological changes in this model closely resemble CB3-induced myocarditis.

To produce EAM, Freund's complete adjuvant (FCA) is injected with the antigen (myosin or myosin peptide) twice within 7 d. Inflammation in the heart appears about 14 d after the first injection, peaks around day 21, then declines, but can persist in some mice at least up to day 60. At later time-points, inflammation is reduced, and fibrosis is present in the heart.

Only certain mouse strains are susceptible to cardiac myosin-induced myocarditis. Highly susceptible strains usually have an "A" background, such as A/J, A.CA, and A.SW. Moderate responders are BALB/c mice; C57BL/10 and C57BL/6 are resistant to EAM ***(7)***. The susceptibility is because of non-major histocompatibility complex (MHC) genes, but major histocompatibility locus of class II genes (H-2) modifies the severity of disease.

The third model is murine thyroglobulin (mTg)-induced experimental autoimmune thyroiditis (EAT). Mice are immunized with either homologous or heterologous Tg in combination with FCA or lipopolysaccharide (LPS). Susceptibility to EAT is linked to the I-A subregion of H-2. Murine strains that express H-2A-$^{k,\ q,\ or\ s}$ (CBA/J, DBA/1J, SWR/J, A.SW/J, SJL/J) are predisposed to EAT, whereas the other strains with allelic expression of H-2$^{a,\ b,\ or\ d}$ (B10.A, C57BL/6J, BALB/c, DBA/2J) are poor responders and do not develop severe disease ***(11)***.

The fourth model represents spontaneous experimental autoimmune thyroiditis (SAT) in the NOD.H2^{h4} mouse. The NOD.H2^{h4} mouse was originally developed by Linda Wicker (Merck Pharmaceuticals, Rahway, NJ). It was established from a cross of the nonobese diabetic mouse (NOD) with the B10.A (4R) strain. Repetitive backcrosses to NOD produced progeny expressing the MHC haplotype of B10.A (4R). The backcrossed mice express H-2A^{k}, a susceptible allele for autoimmune thyroiditis in mice with a NOD genetic background. Unlike the parental NOD, the NOD.H2^{h4} mice do not develop diabetes; however, a small percentage develop autoimmune thyroiditis, which is significantly enhanced after feeding iodine ***(12,13)***. NOD.H2^{h4} mice express high antibody levels to mTg and mononuclear cell infiltration in the thyroid gland, which closely resembles Hashimoto's thyroiditis.

2. Myosin- or Peptide-Induced EAM

2.1. Materials

2.1.1. Myosin Preparation

1. 160 mice hearts; at least half of the hearts should be from a susceptible mouse strain.
2. Sterile Teflon-glass homogenizer.
3. Motor-driven homogenizer (Omni International, Warrenton, VA).
4. Beckman 60-Ti/SW50.1 rotor ultracentrifuge.
5. Double-distilled water (ddH_2O) at 4°C.
6. For establishing myosin concentration: BCA (bicinchoninic acid) protein assay reagent kit (Pierce, IL) or spectrophotometer.
7. 1 L buffer 1 (modified Hasselbach-Schneider solution): 22.35 g 0.30 *M* KCl (mol wt 74.5), 26.1 g 0.15 *M* K_2HPO_7 (mol wt 174.0), 2.66 g 0.01 *M* $Na_4P_2O_7$ (mol wt 266.0), 0.095 g 1 m*M* $MgCl_2$ (mol wt 95.0),.
8. Buffer 2 (extraction buffer): 22.35 g 0.30 *M* KCl (mol wt 74.5), 0.681 g 0.01 *M* imidazole (mol wt 68.1), 0.475 g 5 m*M* $MgCl_2$ (mol wt 95.0).
9. Buffer 3 (extraction buffer): 22.35 g 0.30 *M* KCl (mol wt 74.5), 0.681 g 0.01 *M* imidazole (mol wt 68.1).
10. Buffer 4 (extraction buffer): 22.35 g 0.30 *M* KCl (mol wt 74.5), 0.681 g 0.01 *M* imidazole (mol wt 68.1).

All buffers are made using ddH_2O.

2.1.2. Myosin or Peptide Immunization

2.1.2.1. Mice

Use a susceptible mouse strain, either sex, typically age 6–8 wk (we have successfully used BALB/c mice as old as 12 wk).

2.1.2.2. Myosin or Peptide Immunization

1. Cardiac myosin (prepared as in **Subheading 2.2.1.**) or α-cardiac myosin heavy-chain peptide (referred to as peptide here) is used for EAM induction. For A/J mice, the peptide is mc-myhc-position 334–352 with the amino acid sequence, DSAF DVLS FTAE EKAG VYK ***(10)***. For BALB/c mice, it is the peptide position 614–643 with the sequence Ac-SLKLMATLFSTYASADTGDSGKGK GGKKKG ***(9)***. A short version of this peptide (myhc-α 614–629) was used (AcSLKLMATLFSTYASAD-OH) ***(8)***.
2. FCA (Sigma-Aldrich Chemicals, St. Louis, MO).
3. *Mycobacterium tuberculosis* (Difco). When using in A/J mice, FCA is supplemented with 5 mg/mL.
4. *Bordetella pertussis* toxin (List Biological Laboratories); prepare 50 μg/100 mL stock dilution in sterile ddH_2O.
5. 1% sterile phosphate-buffered saline (PBS) (Biofluids).
6. Two 1-mL glass syringes with slots (Hamilton, NV).
7. 25-ga sterile needles.
8. 1-mL plastic syringes.

2.2. Methods

2.2.1. Myosin Purification

We use a modification of the procedure described by Shiverick et al. ***(14)***.

2.2.1.1. Heart Preparation

About 160 mice hearts are needed. The hearts can be freshly collected or frozen (–70 to –80°C). Freshly collected hearts are preferred.

Sacrifice mice and remove their hearts quickly, rinse in ice cold PBS, and place in cold PBS. Remove the atria and coronary groove adipose tissue. Freeze the hearts at –80°C. One day in advance, collect as many fresh hearts as possible; store at 4°C overnight in PBS.

2.2.1.2. Myosin Preparation Day 0

Prepare all buffers. All steps are on ice or at 4°C; buffers should be stored at 4°C.

2.2.1.3. Myosin Preparation Day 1

1. To 250 mL of buffer 1, add 0.08 g dithiothreitol (DTT) (mol wt154.2), 250 μL leupeptin (1.0 mg/mL, aliquoted), and 350 μL PMSF (phenylmethyl-sulfonyl-fluoride; 50 mg/mL) (the final solution should contain 2 m*M* DTT, 1 μg/mL leupeptin, and 1 m*M* PMSF). The final pH should be 6.8 (original pH 8.7; use HCl).

2. Thaw hearts, rinse with cold PBS. Weigh all mice hearts (160 hearts should be approx 22 g wet weight).
3. Mince the hearts on ice with a razor blade. Add 100 mL of buffer 1 (with DDT, leupeptin, and PMSF).
4. Homogenize with motor-driven homogenizer (30 mL of heart/buffer solution in 50 mL tube, speed 3–4 for 20–30 s; total makes 3 aliquots). Add another 100 mL buffer 1. Homogenize the whole volume for 1 min, let it rest for 1 min, and homogenize for another 5 min.
5. Extract the homogenate with gentle stirring for 80–90 min in a cold room (at 4°C).
6. Centrifuge at 12,000*g* for 12 min (taking 2 min to reach the speed); collect supernatant.
7. Centrifuge supernatant at 140,000*g* for 4 h in ultracentrifuge; use Ti60 rotor.
8. Collect the supernatant.
9. Dilute supernatant (around 195 mL) with 20 times the volume of ddH_2O (4°C) (about 3900 mL) by pouring myosin supernatant carefully into water. Let myosin precipitate settle overnight in a cold room (4°C).

2.2.1.4. Myosin Preparation Day 2

1. To 200 mL of buffer 2, add 0.552 g ATP disodium salt (Na_2ATP) (mol wt 551.1; Sigma-Aldrich), 0.062 g DTT (mol wt154.2), 200 μL leupeptin (1.0 mg/mL, aliquoted), and 300 μL PMSF (50 mg/mL). The final solution should contain 5 m*M* Na_2ATP, 2 m*M* DTT, 1 μg/mL leupeptin, and 1 m*M* PMSF. The final pH should be 6.8 (original pH 6.4–6.5; use NaOH).
2. Very carefully pour the supernatant from the precipitated myosin. Do not pour all the supernatant so the myosin is not lost.
3. Centrifuge at 12,000*g* for 14 min. Get rid of supernatant.
4. Dissolve the pellet in 100 mL buffer 2; add additional 100 mL buffer 2 to reach a 200-mL final volume.
5. Homogenize with a Teflon-glass homogenizer.
6. Centrifuge the solution at 43,000*g* for 30 min to remove actin. Use Ti60 rotor and ultracentrifuge.
7. Collect supernatant.
8. Myosin is precipitated from the supernatant (200 mL) by adding eight times the volume of ddH_20 (1600 mL) and allowing it to stand overnight in the cold room (at 4°C). The precipitation is seen very soon after water is added.

2.2.1.5. Myosin Preparation Day 3

1. To 150 mL of buffer 3, add 0.048 g DDT (mol wt154.2), 150 μL leupeptin (1.0 mg/mL, aliquoted), and 225 μL PMSF (50mg/mL). The final solution should contain 2 m*M* DTT, 1 μg/mL leupeptin, and 1 m*M* PMSF at pH 6.8 (original pH 8.0–8.5; use HCl).
2. Stir gently to mix precipitation.
3. Centrifuge at 14,077*g* for 14 min. Collect pellet. Spin supernatant again to increase yield. Collect pellet.

4. Dissolve pellet with 150 mL buffer 3 and homogenize it with a Teflon-glass homogenizer.
5. Centrifuge the solution at 43,000*g* for 30 min to remove actomyosin; use Ti60 rotor.
6. Collect supernatant (a sample of solution can be taken at this point to run on gel).
7. Myosin precipitate is collected by centrifugation at 14,077*g* for 18 min. Collect pellet; the supernatant should be clear.
8. Redissolve pellet with 15 mL buffer 4 (pH 6.8) without DDT and protease inhibitor. Homogenize it with a Teflon-glass homogenizer. Add 3mL buffer 4, aliquot myosin (0.2–0.5 mL), and freeze aliquots immediately. Myosin can be stored up to 1 yr at –80°C, or up to 1 mo in 4°C.
9. Myosin concentration can be established by spectrophotometer or by BCA protein assay.

2.2.3. Myosin or Peptide Immunization

2.2.3.1. Day –1: Peptide Reconstitution

For one mouse, 100 nmol of peptide is needed, but allow 10% more for losses. Dilute the peptide in 1% PBS or ddH_2O at a concentration of 100 nmol of peptide per 50 μL (which is the dose for one mouse). Leave the peptide at room temperature to dissolve for 30 min, then store at 4°C for the next day.

2.2.3.2. Day 0: Preparation of a Myosin/FCA or Peptide/FCA Emulsion: Injection

1. Cardiac myosin is dissolved in buffer 4 at a concentration of 100–250 μg/50 μL (dose for one mouse), depending on the degree of disease desired. Add 10–20% for losses. Final emulsion will be diluted at a ratio of 1:1 with FCA; myosin concentration will be 100–250 μg/100 μL.
2. Emulsify cardiac myosin or peptide solution in FCA. The volume of the glass syringe should be more then twice the volume of the myosin or peptide needed. Take up all the peptide or myosin into the syringe, take the needle out, get rid of all bubbles, and push the solution to the edge of a syringe orifice. Vortex FCA (for A/J mice supplemented FCA in a final concentration of 5 mg/mL), mix it well, and transfer an equal volume immediately into a second glass syringe. Connect a coupler to the FCA syringe; push FCA in the coupler until it is visible in the opposite opening. Place the first syringe with the peptide or myosin on the coupler.
3. Push FCA very slowly into the syringe with myosin/peptide. During the process, rotate both syringes so that the oily FCA mixes with the watery myosin or peptide. Repeat very slowly, mixing the substance and pushing it from one syringe to the other. Mix until the fluid in the syringes is homogeneous.
4. Start to mix faster, ensuring that the coupler is tight and the emulsion is not leaking. The process of mixing can take about 45–60 min or longer. The key is to make a very thick emulsion. When there is resistance while mixing, test the thick-

ness of the emulsion by placing a drop on the surface of water in small beaker. The drop should keep its shape rather than dispersing. A proper emulsion is the key step in the EAM induction.
5. Dilute pertussis toxin from stock (concentration 50 μg/100 μL) 1:100 in sterile 1% PBS (final concentration 500 ng/100 μL). The dose for one mouse is 500 ng in 100 μL. Take the final dilution of toxin to 1-mL plastic syringes.
6. Anesthetize the mouse.
7. Inject the mouse subcutaneously with 0.1 mL of emulsion. Choose one injection side for all mice in the posterior axillary area (all mice should be injected on the same side).
8. Inject 0.1 mL of the pertussis toxin intraperitoneally (the dose should be 500 ng/mouse).

2.2.3.3. Day 7: Boost

Repeat the steps from day 0, but do not use pertussis toxin. Inject an emulsion into the side opposite the one used on day 0.

2.2.3.4. Day 21: Sacrifice Day

Mice are anesthetized; sera are obtained by retroorbital bleeding. Afterward, the mice are euthanized and weighed; their hearts are removed, and blood is gently squeezed from them; the hearts are weighed (low body weight and high heart weight are signs of cardiomyopathy). Immediately after the sacrifice, each heart is scored grossly. Gross score is based on the percentage of the heart's surface that has evidence of inflammation. It is helpful to use the scoring system described in **Table 1**. Fix the heart in 10% formalin for hematoxylin and eosin staining. Make serial sections through the heart, staining every fifth section.

2.2.3.5. Histology Assessment of EAM

Measure the percentage of myocardium infiltrated with mononuclear cells and fibrosis under a microscope, using the scoring system in **Table 1**. For calculating the percentage of inflammation in myocardium, use low magnification so that the whole section can be seen. It is necessary to look at all sections because the inflammation is often spotty rather than diffuse. A grid in the microscope is helpful for the calculation. It is desirable that two independent researchers score all slides separately in a blind manner.

2.3. Notes

2.3.1. Myosin Preparation

1. All material must be 4°C, including the centrifuge rotors and the homogenizer. All work must be done on ice or in a cold room. Carry the centrifuge tubes to and from the centrifuge on ice.

Table 1
EAM Severity Grading (Use for the Gross Score as Well as for Histology)

Score	Inflammation in the heart
1	Less than 10%
2	10–30%
3	30–50%
4	50–90%
5	More than 90%

2. Pay particular attention to final pH of buffers.
3. When homogenizing, try to minimize foaming and heating. Work on ice and make breaks between homogenization, as described. The hearts should be kept on ice all the time.
4. If you want to break the whole process into more days, the possible break points are after **Subheading 2.2.1.3. step 5** (extract the homogenate) and after **Subheading 2.2.1.4. step 5** (homogenize with a Teflon-glass homogenizer).

2.3.2. Myosin or Peptide Immunization

5. FCA contains dead *M. tuberculosis*, which cannot cause infection but is immunogenic. Therefore, caution is necessary when working with FCA. Wear a mask and gloves.
6. A thick, well-mixed emulsion is a critical step for EAM induction.
7. If the emulsion is mixed for a very long time (1 h) and is still liquid, the emulsion is probably too hot. Try to place both syringes with coupler on ice for a time, and the emulsion may become denser.
8. It is critical that each mouse receive the same amount of antigen. To ensure that each mouse is injected with the same amount of the emulsion, all bubbles must be removed from the emulsion. Be careful when removing the needle from the mouse skin so that the emulsion does not leak.

3. CB3-Induced Myocarditis

3.1. Materials

1. Vero cells (American Type Culture Collection [ATCC]; Manassas, VA).
2. Minimum essential medium (MEM), liquid and powder (Mediatech).
3. Sodium bicarbonate ($NaHCO_3$).
4. Heat-activated fetal bovine serum (FBS).
5. Penicillin/streptomycin 5000 U (Pen/Strep) (Mediatech).
6. Trypsin (1X 0.25% trypsin 1 m*M* ethylenediaminetetraacetic acid) (Gibco).
7. PBS (without calcium or magnesium) (Biofluids).
8. CB3, Nancy strain (ATCC).
9. Susceptible mice age 6–8 wk.

10. Bleach (Clorox).
11. Methyl cellulose (4000 centipoises; Fischer).

3.2. Methods

3.2.1. Maintenance of Vero Cells

1. Grow Vero cells in MEM supplemented with Pen/Strep and 10% FBS (10% MEM) until confluent at 37°C and 5% CO_2 (37°C).
2. Remove media and wash cells with PBS to remove FBS prior to the addition of trypsin.
3. Split cells by adding trypsin solution for 5 min at 37°C because Vero cells adhere to the flask.
4. Wash cells from flask and immediately inactivate trypsin by adding 10% MEM.
5. Spin cells at 130*g* for 10 min to pellet cells.
6. Resuspend the pellet and add a small portion of cells to the flask with fresh 10% MEM.

3.2.2. Tissue Culture Virus

1. When Vero cells are confluent, replace the media with MEM supplemented with 2% FBS (2% MEM) and Pen/Strep.
2. CB3 is infectious for people as well as mice; 20% bleach solution or ultraviolet light will kill the virus. Always wear a protective mask and replace gloves immediately after working with the virus to reduce its spread. Wash all surfaces, utensils, and contaminated surfaces with bleach and turn on the ultraviolet light in the hood after working with the virus.
3. Add CB3 from ATCC to a confluent flask of Vero cells in 2% MEM (FBS inhibits viral entry).
4. Incubate virus and cells in an incubator at 37°C as before, until cells round up and detach from the flask (approx 2 d).
5. Carefully collect cells and supernatant (flask full of infectious virus), spin at 795*g* for 20 min, and collect supernatant.
6. Aliquot supernatant and freeze at –80°C.
7. Add bleach to flask and centrifuge tube to kill the virus, and discard.

3.2.3. Heart Passage of the Virus

1. Inoculate 6- to 8-wk-old susceptible mice with 0.1 mL of tissue culture virus intraperitoneally.
2. Two days later, sacrifice the mice and collect the hearts.
3. Sera and organs from these mice contain infectious virus, so use appropriate care.
4. Blot excess blood from hearts and immediately add to cold 2% MEM (10% w/v).
5. Homogenize with the electric homogenizer and spin at 795*g* for 20 min.
6. Collect supernatant and aliquot into useful quantities for later injection of mice.
7. Freeze aliquots at –80°C until used in experiments. Stock should last at least 1 yr at –80°C.

3.2.4. Determination of Viral Titer by Plaque Assay

1. The plaque assay determines the amount of infectious virus in a sample by the degree of killing observed in Vero cells.
2. The level of infectious virus in the heart-passaged virus stock needs to be determined by plaque assay.

3.2.5. Splitting Vero Cells to Trays for Plaque Assay

1. Split cells as described in **Subheading 3.2.1.** to a 24-well culture tray for the plaque assay.
2. Split cells when 80–90% confluent.
3. When cell pellet is obtained after trypsin treatment, resuspend pellet in 1 mL of 2% MEM (FBS hinders virus infection of Vero cells).
4. Count cells by trypan blue exclusion and dilute in 2% MEM to 2×10^5 cells/mL.
5. Add 1 mL to each well of a 24-well culture plate and incubate at 37°C until cells are 80–90% confluent (proper level of confluency is crucial for success of the assay).

3.2.6. Making Methyl Cellulose for the Plaque Assay

1. Add 8.75 g methyl cellulose to 250 mL distilled water (do not mix).
2. Tighten lids only finger tight and autoclave.
3. Just before the mixture comes to room temperature, shake vigorously. The methyl cellulose should be gooey and full of bubbles. If the mixture becomes too cold, lumps will form, and it will be necessary to make a new batch.
4. At least 1 d before the plaque assay, add double-strength MEM (2X MEM) to methyl cellulose and leave in a water bath until "melted" together (this step takes overnight).
5. Make 2X from MEM powder (19.1 g MEM powder to 1 L of water, mix, then add 4.4 g sodium bicarbonate and stir; filter through a 0.2-μm filter to make sterile).
6. Add 250 mL 2X MEM to 250 mL methyl cellulose after both have warmed in 37°C water bath for a few hours.
7. Shake vigorously until mixed.
8. Add FBS to make 2% and mix gently.
9. Methyl cellulose is now ready for the assay.

3.2.7. Plaque Assay

1. Vero cells in 24-well plates must be 80–90% confluent.
2. Prewarm methyl cellulose/MEM and other media in a 37°C water bath.
3. Add 225 μL 2% MEM to each well of a 96-well plate for dilution of virus stock.
4. Remove media with a suction system and glass pipets. Waste container must contain bleach to inactivate virus later in assay.
5. Immediately, so that cells do not dry out, add 1 mL warm 2% MEM to each well and return the plate to the incubator.
6. Add 75 μL heart-passaged virus stock to top row of 96-well plate and serially dilute (fourfold dilutions).

7. Add 200 μL of virus diluent to Vero after removing all of the 2% MEM just prior to addition of virus (do 12 wells at a time so Vero cells do not dry out).
8. Incubate for 1 h at 37°C to allow virus to infect cells. Tip plate to ensure cells are covered well.
9. After 1 h, remove the virus diluent into the bleach waste and immediately add 1 mL of prewarmed methyl cellulose (2% MEM).
10. Incubate for 3 d at 37°C to allow plaque formation.

3.2.8. Staining Plaque Assay

Add 0.5–1.0 mL of 1% methylene blue (in 10% formalin) per well and leave at room temperature overnight. Formalin kills the virus, and plates can be left on the bench. If there are any spills, alcohol will clean the methylene blue.

3.2.9. Destaining Plaque Assay

1. The next day, wash wells vigorously with tap water and dry overnight at room temperature inverted with lids off on absorbent paper or pads.
2. If Vero cells were overconfluent, they will wash off at this step.
3. Make sure that all of the blue dye and methyl cellulose have been removed before drying. Otherwise, plates will be difficult to read.

3.2.10. Counting Plaques

1. Areas where Vero cells have been killed by CB3 will be rounded up in obvious clumps. Some clumps will have clear areas in the centers where cells have died and left an opening. This is a plaque.
2. Count plaques under an inverted microscope and determine the number of plaque forming units (PFUs) per well.

3.2.11. Plaque Calculations

1. Count the number of PFU for each well.
2. Calculate the number of PFU per milliliter by multiplying the PFU/well ratio by the dilution factor and multiplying it by 5 to bring up to 1 mL (200 μL × 5= 1 mL).

3.2.12. Infection of Mice

1. Infect 6- to 8-wk-old mice with 0.1 mL (10^3 PFU of heart-passaged virus [day 0]).
2. Collect hearts for analysis of acute myocarditis from days 7 to 12 postinfection or chronic myocarditis from days 35 to 45 postinfection.

4.Tg-Induced EAT

4.1. Materials

4.1.1. Tg Preparation

1. Susceptible mouse strain, either sex, typically age 6–8 wk.
2. mTg.

3. FCA (Sigma-Aldrich).
4. Bacterial LPS (Sigma-Aldrich).
5. Glass syringes with slots (Hamilton).
6. Three-way plastic stopcock.
7. Beckman 60-Ti/SW50.1 rotor ultracentrifuge.
8. Sephacryl S300HR column (Sigma-Aldrich).
9. BCA protein assay kit (product 23227, Pierce, Rockford, IL).
10. Heparinized capillary tubes (inner diameter 1.1–1.2 mm).
11. PBS.
12. Stainless steel homogenizer.
13. ddH_2O, 4°C.
14. Buffer 1, protease inhibitor buffer (freshly prepared): 0.5 m*M* ethylenediaminetetracetic acid, 0.5 m*M* PMSF, 1 μg/mL pepstatinA, 1 μg/mL aprotinin, and 1 μg/mL leupeptin prepared in PBS.

4.1.2. Assessment of EAT

1. Immunol II 96-well plates (Dynatech, USA).
2. PBS.
3. Tween-20.
4. Sodium carbonate.
5. Sodium bicarbonate.
6. Diethanolamine.
7. Magnesium chloride hexahydrate.
8. Bovine serum albumin (Sigma-Aldrich).
9. Alkaline phosphatase-conjugated IgG mouse antibodies (secondary antibody) (Sigma-Aldrich).
10. Buffers for enzyme-linked immunosorbent assay (ELISA): coating buffer/carbonate-bicarbonate buffer at pH 9.6: 0.795 g sodium carbonate and 1.465 g sodium bicarbonate, make volume to 500 mL with ddH_2O.
11. Diethanolamine buffer (pH 9.8): 9.7 mL diethanolamine (Sigma-Aldrich D-8885) and 10 mg magnesium chloride hexahydrate; bring volume to 100 mL with ddH_2O.
12. Substrate: alkaline phosphatase/*p*-nitrophenyl phosphate, with 10 mg/plate *p*-nitrophenyl phosphate (Sigma Aldrich 104) dissolved in 10 mL/plate diethanolamine buffer.

4.2. Methods

4.2.1. Tg Preparation

Tg is a 660-kDa dimer that can be purified from pooled thyroid glands ***(15)***.

1. Dissect 250–300 thyroid glands from mice and preserve at –80°C still attached to the tracheas.
2. On the day of antigen preparation, both lobes from all thyroids are detached from the trachea and kept wet in ice-cold PBS. The lobes are then gently homogenized

for 5–6 s in the presence of protease inhibitor buffer (*see* **Subheading 4.1.1.**), also known as homogenizing buffer. Approximately 2.5 mL of buffer per 100 thyroids is used. The whole procedure described above is performed at 4°C.
3. Cell debris, membranes, and mTg aggregates are removed by centrifugation at 4300*g* for 30 min. Supernatant is decanted and centrifuged at 110,000*g* for 60 min at 4°C using a Beckman 60-Ti/SW50.1 rotor.
4. The supernatant is then applied to a 1.6 × 88 cm^2 Sephacryl S300HR column equilibrated with 1% PBS at pH 7.2 and 4°C. The column speed is adjusted to 18–20 mL/h. Fractions of 1 mL are collected. For each fraction, the concentration of mTg is measured spectrophotometrically at 280 nm (usually ranges from 2.5 to 5.0 mg/mL). The optical density (OD) thus obtained is plotted against eluted volume. The mTg is typically eluted in three protein peaks. The first peak and the second peak are pooled separately. The second peak is a major source of mTg. The third peak has a low OD and is not used. Total protein content is further assessed by the BCA protein assay.
5. Small 0.5-mL aliquots are then frozen at –20°C until use. Repeated freezing and thawing of Tg is not recommended because it causes the loss of activity because of aggregation. As mTg is a very large and highly hydrophobic molecule that can easily be contaminated with LPS, it is necessary that all the glassware, surgical instruments, and tubing be autoclaved or heated at 200°C for 30 min before use and check each preparation for LPS contamination by the Limulus amebocyte lysate test ***(16)*.**

4.2.2. Tg Immunization

4.2.2.1. Tg Immunization With FCA

1. The standard protocol is a refinement of the original protocol developed by our research group ***(17)***. Mice age 8–10 wk are injected subcutaneously twice at an interval of 7 d with 50 μg of mTg emulsified with FCA. To achieve this concentration, 1 mg mTg/mL is emulsified in FCA containing *M. tuberculosis* H37Ra at a 1:1 ratio.
2. The emulsion of FCA and mTg is prepared similarly as described in the **Subheading 2.2.3.2**. The emulsion should be well prepared, and a drop of emulsion should not disperse when suspended on water.
3. Mice are injected on day 0 and day 7 alternately into thighs. The severity of the disease varies with the dose of mTg and the antigenicity of each preparation. Usually, all mice will develop EAT within 21–28 d of immunization (*see* **Note 2**).

4.2.2.2. Tg Immunization With LPS

1. Another method of EAT induction uses bacterial LPS as an adjuvant. This method has been adopted by several groups ***(18–20)*** because it shows a uniform induction of EAT without requiring emulsion in FCA ***(21)***.
2. The standard protocol involves intravenous injections with 40 μg of mTg on days 0 and 7, followed 3 h later by 20 μg of LPS (trichloroacetic acid precipitated

Salmonella enteritidis or *Escherichia coli*) ***(22)***.

3. The disease develops within 21–28 d of immunization. Severity of the disease is dose dependent. For example, a dose of 20 μg of mTg with 10 μg of LPS given to ASW or SJL strains successfully induces EAT, and higher doses (40 μg) produce a greater lesion score.
4. For adjuvant-free induction of EAT, *see* **Note 4**.
5. For EAT evaluation, *see* **Subheading 5.2.2**.

4.3. Notes

1. As a large protein, Tg is easily hydrolyzed. Therefore, the use of protease inhibitors and special precautions for low temperature are recommended.
2. To achieve an efficient and uniform induction of the disease, all mice in a given experiment should receive the same preparation of antigen.
3. Repeated freezing and thawing reduce the antigenicity of Tg and should be avoided.
4. Adjuvant-free immunization has also been achieved by injecting low concentrations of mTg repeatedly over a period of 4 wk ***(23)***. Effects of other adjuvants, like SGP (a synthetic copolymer of starch, acrylamide, and sodium acrylate) and Quil A ***(13)***, on induction of EAT have also been studied. Granulomatous thyroiditis (G-EAT) induction in CBA/J was achieved by two intravenous injections at 10-d intervals with 150 μg mTg and 15 μg LPS (*E. coli*; Sigma-Aldrich). In another study, autoantigen conjugated to mAbs specific for determinants on APCs were used as an alternative to adjuvant-free induction of EAT ***(24)***.

5. NOD.H2^{h4}: Spontaneous Model of Autoimmune Thyroiditis

5.1. Materials

1. Sodium iodine (Sigma).
2. Food colors (McCormick).

5.2. Animals

Mice (age 3–4 wk) are caged under conventional housing conditions with regular day and night cycles. Regular feed and tap water are used for maintaining the colony. Both sexes develop SAT with low incidence, which is exacerbated by supplementation of dietary sodium iodine (NaI) in their drinking water.

5.3. Methods

5.3.1. NaI Treatment

Dietary iodine is an important environmental factor that plays a key role in the formation of thyroid hormone and regulation of thyroid function. Mice are fed a dose of NaI (0.05–0.15%) mixed in their drinking water. We designate a color code, using food color for each NaI concentration. Food color is added to

water along with NaI. Normally, a dose of 0.05% NaI will induce SAT within 8 wk. Time-course and sex-related differences in iodine-induced autoimmune thyroiditis in NOD.H2^{h4} mice have been studied ***(25)***. Excess iodine intake, leading to the development of autoimmune thyroiditis in humans as well as mice, is evidenced by a large body of literature of epidemiological and research studies.

5.3.2. Evaluation of EAT and SAT

In EAT, the disease pathology usually correlates with the Tg antibody response, but it may not be consistent in all experiments. No direct correlation between disease pathology and serum antibody levels has been observed in our colony of NOD.H2^{h4} mice.

A prebleed (day 0) is performed on all NOD.H2^{h4} mice at the beginning of the treatment to exclude preexisting thyroiditis (*see* **Note 2.**).

5.3.3. Serum Collection and Tg Antibody-Specific Enzyme-Linked Immunosorbent Assay

On days 0, 7, and 28 after injection with mTg or treatment with iodine, mice are anesthetized, and a small volume (200 μL) of blood is collected from the retroorbital venous plexus using heparinized capillary tubes (inner diameter 1.1–1.2 mm). Blood is incubated at room temperature for 60 min, and serum is collected after centrifugation. Serum is stored at –80°C until used.

Purified mTg is coated onto 96-well Immunolon II plates at a concentration of 2 μg/mL in carbonate/bicarbonate buffer (pH 9.6) and incubated overnight at 4°C. The plates are washed four times with PBS-Tween-20 (0.05%) and blocked for 2 h with 1% bovine serum albumin-PBS. Plates are then washed three times and incubated overnight with appropriate mouse sera diluted 1:100 in PBS. After washing, mTg-specific IgG subclasses are detected using appropriate dilutions of secondary antibodies against IgG1 and IgG2b. Color is developed with *p*-nitrophenyl phosphate substrate and OD is read at 405 nm using a microplate reader (Dynatech Laboratories).

5.3.4. Tissue Collection and Histology

Immediately after euthanasia, tracheas with attached thyroids are collected and fixed in 10% phosphate-buffered formalin for 2 d and submitted for histological staining. Thyroids are sectioned at 4–5 μm thicknesses and stained with hematoxylin and eosin. The thyroid histology is assessed as a 5-point score, depending on the percentage of thyroidal inflammation indicated by intrafollicular infiltration of lymphocytes ***(17)***. A 0 score is assigned for no lesions, 1 for less than 20% infiltration, 2 for 20–30%, 3 for 30–50%, and 4 for more than 50 % involvement of the thyroid. The extent of the mononuclear cell

infiltration is assessed on both lobes of thyroid glands on at least 4–6 sections per animal. Statistical differences in the pathological scores are determined by the nonparametric Mann-Whitney U test ***(26)***.

5.3.5. Course of the Disease

Mononuclear cell infiltration into the thyroid reaches a maximum by day 21 postinjection with mTg and does not show regression until day 30 ***(27,28)***. However, several factors play a key role in determining the severity and incidence of disease in a given mouse strain.

5.4. Notes

1. The genetics of the mice is the first concern in inducing EAT. Strains of mice that do not express H-$2^{k\ or\ s}$ genes may develop a low incidence of disease. There is a high degree of variance in severity of thyroiditis even in the same experiment.
2. A prebleed is useful to eliminate animals that may have developed a low degree of spontaneous disease, as indicated by the presence of Tg-specific autoantibodies in their serum.

References

1 Rose, N. R. and Hill, S. L. (1996) Autoimmune myocarditis. *Int. J. Cardiol.* **54,** 171–175.

2 Rose, N. R. and Afanasyeva, M. (2003) From infection to autoimmunity: the adjuvant effect. *ASM News* **69,** 32–137.

3. Rose, N. R., Neumann, D. A., and Herkowitz, A. (1992) Coxsackievirus myocarditis, in *Advances in Internal Medicine* (Stollerman, G. H, LaMont, J. T., Leonard, J. J., and Siperstein, M. D., eds.), Mosby-Year Book, St. Louis, MO, pp. 411–429.

4. Rose, N. R., Wolfgram, L. J., Herkowitz, A., and Beisel, K. W. (1986) Postinfectious autoimmunity: two distinct phases of Coxsackievirus B3-induced myocarditis. *Ann. NY Acad. Sci.* **475,** 146–156.

5 Fairweather, D., Kaya, Z., Shellam, G. R., Lawson, C. M., and Rose, N. R. (2001) From infection to autoimmunity. *J. Autoimmun.* 16, 175–186.

6 Neu, N., Beisel, K. W., Traystman, M. D., Rose, N. R., and Craig, S. W. (1987) Autoantibodies specific for the cardiac myosin isoform are found in mice susceptible to Coxsackievirus B3-induced myocarditis. *J. Immunol.* **138,** 2488–2492.

7 Neu, N., Rose, N. R., Beisel, K. W., Herskowitz, A., Gurri-Glass, G., and Craig, S. W. (1987) Cardiac myosin induces myocarditis in genetically predisposed mice. *J. Immunol.* **139,** 3630–3636.

8 Eriksson, U., Kurrer, M. O., Sonderegger, I., Iezzi, G., Tafuri, A, Hunziker, L., et al. (2003) Activation of dendritic cells through the interleukin 1 receptor 1 is critical for the induction of autoimmune myocarditis. *J. Exp. Med.* **197,** 323–331.

9 Pummerer, C. L., Luze, K., Grassl, G., Bachmaier, K., Offner, F., Burrell, S. K., et

al. (1996) Identification of cardiac myosin peptides capable of inducing autoimmune myocarditis in BALB/c mice. *J. Clin. Invest.* **97,** 2057–2062.
10 Donermeyer, D. L., Beisel, K. W., Allen, P. M., and Smith, S. C. (1995) Myocarditis-inducing epitope of myosin binds constitutively and stably to I-Ak on antigen-presenting cells in the heart. *J. Exp. Med.* **182,** 1291–1300.
11 Vladutiu, A. O. and Rose, N. R. (1975) Cellular basis of the genetic control of immune responsiveness to murine thyroglobulin in mice. *Cell. Immunol.* **17,** 106–113.
12 Rasooly, L., Burek, C. L., and Rose, N. R. (1996) Iodine-induced autoimmune thyroiditis in NOD-H-2h4 mice. *Clin. Immunol. Immunopathol.* **81,** 287–292.
13 Braley-Mullen, H., Sharp, G. C., Medling, B., and Tang, H. (1999) Spontaneous autoimmune thyroiditis in NOD.H-2h4 mice. *J. Autoimmun.* **12,** 157–165.
14 Shiverick, K. T., Thomas, L. L., and Alpert, N. R. (1975) Purification of cardiac myosin. Application to hypertrophied myocardium. *Biochim. Biophys. Acta* **393,** 124–133.
15 Tomazic, V. and Rose, N. R. (1977) Autoimmune murine thyroiditis IX. Relationship of humoral and cellular immunity to thyroiditis in high and low responder mice. *Eur. J. Immunol.* **7,** 40–43.
16. El Rehewy, M., Kong, Y. M., Giraldo, A. A., and Rose, N. R. (1981) Syngeneic thyroglobulin is immunogenic in good responder mice. *Eur. J. Immunol.* **11,** 146–151.
17 Rose, N. R., Twarog, F. J., and Crowle, A. J. (1971) Murine thyroiditis: importance of adjuvant and mouse strain for the induction of thyroid lesions. *J. Immunol.* **106,** 698–704.
18 Zhang, W., Flynn, J. C., and Kong, Y. C. (2001) IL-12 prevents tolerance induction with mouse thyroglobulin by priming pathogenic T cells in experimental autoimmune thyroiditis: role of IFN-gamma and the costimulatory molecules CD40l and CD28. *Cell. Immunol.* **208,** 52–61.
19 Braley-Mullen, H., Johnson, M., Sharp, G. C., and Kyriakos, M. (1985) Induction of experimental autoimmune thyroiditis in mice with in vitro activated splenic T cells. *Cell. Immunol.* **93,** 132–143.
20 Parish, N. M., Roitt, I. M., and Cooke, A. (1988) Phenotypic characteristics of cells involved in induced suppression to murine experimental autoimmune thyroiditis. *Eur. J. Immunol.* **18,** 1463–1467.
21 Esquivel, P. S., Rose, N. R., and Kong, Y. C. (1977) Induction of autoimmunity in good and poor responder mice with mouse thyroglobulin and lipopolysaccharide. *J. Exp. Med.* **145,** 1250–1263.
22 Zaccone, P., Fehervari, Z., and Cooke, A. (2003) Tumour necrosis factor-alpha is a fundamental cytokine in autoimmune thyroid disease induced by thyroglobulin and lipopolysaccharide in interleukin-12 p40 deficient C57BL/6 mice. *Immunology* **108,** 50–54.
23 Rose, N. R., Kong, Y. C., Okayasu, I., Giraldo, A. A., Beisel, K., and Sundick, R. S. (1981) T-cell regulation in autoimmune thyroiditis. *Immunol Rev.* **55,** 299–314.
24 Balasa, B. and Carayanniotis, G. (1993) Immunotargeting of thyroglobulin on

antigen presenting cells abrogates natural tolerance in the absence of adjuvant. *Cell. Immunol.* **150,** 453–458.

25 Rasooly, L., Burek, C. L., and Rose, N. R. (1996) Iodine-induced autoimmune thyroiditis in NOD-H2^{h4} mice. Clin. Immunol. Immunopathol. 81, 287–292.

26 Kong, Y. M., Waldmann, H., Cobbold, S., Giraldo, A. A., Fuller, B. E., and Simon, L. L.(1989) Pathogenic mechanisms in murine autoimmune thyroiditis: short- and long-term effects of in vivo depletion of CD4$^+$ and CD8$^+$ cells. *Clin. Exp. Immunol.* **77,** 428–433.

27 Twarog, F. J. and Rose, N. R. (1969) The adjuvant effect of pertussis vaccine in experimental thyroiditis of the rat. *Proc. Soc. Exp. Biol. Med.* **130,** 434–439.

28. Lillehoj, H. S. and Rose, N. R. (1982) Humoral and cellular immune response to thyroglobulin in different inbred rat strains. *Clin. Exp. Immunol.* **47,** 661–669.

11

Animal Models of Insulin-Dependent Diabetes

Edwin Liu, Liping Yu, Hiroaki Moriyama, and George S. Eisenbarth

Summary

Animal models have contributed enormously to study in the field of type 1 diabetes. Perhaps the most intensively studied model is the nonobese diabetic (NOD) mouse, which develops an autoimmune-mediated spontaneous diabetes associated with the development of insulin autoantibodies and insulitis. Accurate measurement of antiislet autoantibodies by radioassay and detection of antigen-specific T cells using major histocompatibility complex tetramers are possible. Various strategies have been developed in preventing diabetes in animal models; a peptide-induced model of type 1 diabetes has been described. Finally, the development of peptide vaccines is hampered by the risk of anaphylaxis in both mouse and humans. In this chapter, methods and strategies to measure antiinsulin autoantibodies, to detect antigen-specific T cells by tetramer analysis, and to prevent diabetes using peptide vaccines are discussed. Along with these topics, a protocol of peptide-induced diabetes and peptide vaccine-induced anaphylaxis are described, serving as a reminder of the potential dangers that could exist in human trials. In summary, animal models have become necessary in the study of type 1 diabetes and provide researchers important tools to conduct studies that could not otherwise be performed in humans.

Key Words: Anaphylaxis; animal model; autoantibody; autoimmune; insulin; NOD mouse; peptide; radioassay; radioimmunoassay; tetramer; type 1 diabetes; vaccine.

1. Introduction

A series of important animal models for research related to type 1A diabetes (immune mediated) is now available. Studies using animal models have been critical in elucidating the pathogenesis of type 1 diabetes, defining disease-susceptible and resistance genes, identifying putative islet autoantigens, and characterizing various immune cells and immune mediators. Although we cannot overstate the utility of animal models in type 1 diabetes, it is often difficult to interpret data obtained from animals to the actual human condition. Clearly,

From: *Methods in Molecular Medicine, Vol. 102: Autoimmunity: Methods and Protocols*
Edited by: A. Perl © Humana Press Inc., Totowa, NJ

the direct application of animal data to humans needs to be taken cautiously. Nevertheless, animal models provide researchers the opportunity to create experimental conditions that would be unsafe for humans.

There are many rodent models for type 1 diabetes, and they can be generally classified as spontaneous, chemically induced, and transgenic or knockout models (**Table 1**). In particular, the nonobese diabetic (NOD) mouse is the most intensively studied spontaneous model ***(1)***. As in humans, these mice are characterized by lymphocyte infiltration of pancreatic islets (insulitis), complex polygenic disease susceptibility (idd loci) with essential major histocompatibility complex (MHC) genetic influence, and the development of spontaneous antiinsulin autoantibodies ***(2)***.

Transgenic and gene knockout technologies have enabled development of additional animal models for type 1 diabetes ***(3)***. Several T-cell receptor (TCR) transgenic (Tg) mice have been generated from diabetogenic T-cell clones of NOD mice. Many animal models have been modified to express immunologically important molecules by β-cells (using the rat insulin promoter [RIP] to drive transgenes). Specifically, artificially induced β-cell antigens include neoself-antigens such as viral lymphocytic choriomeningitis virus, hemagglutinin, and ovalbumin such that when an immune response is elicited against the neoantigen (i.e., immunization or infection), specific β-cell destruction occurs. Other genes introduced in β-cells include immune mediators such as interleukin (IL)-2 , IL-10, IL-13, interferon (IFN)-γ, and IFN-α.

One particularly interesting mouse is the RIP-B7.1 transgenic mouse, which we utilized to develop a mouse model of type 1 diabetes that is induced by a major diabetes autoantigen, insulin peptide B:9–23 ***(4)***. This experimental autoimmune diabetes model artificially expresses the costimulatory B7.1 molecule on β-cells, enhancing their propensity to be targeted by immune cells. On other hand, several animal models knocking out important molecules have also been developed. Besides knocking out immune mediators, animal models lacking candidate autoantigens such as proinusulin and glutamic acid decarboxylase (GAD) have been created to evaluate the contribution of those molecules to the pathogenesis of type 1 diabetes ***(5,6)***.

Thus, animal models have contributed enormously to the study of type 1 diabetes. Although it is understood that there are limitations to animal models in the study of a human disease, these models will nonetheless contribute to the understanding of this complex disease and to development of novel preventive and therapeutic approaches. In this chapter, we focus on the following relevant protocols in the study of animal models for type 1 diabetes:

Anti-islet autoantibody assays, utilization of tetramers in the study of autoreactive T cells, diabetes prevention in the NOD mouse, peptide induction model of type 1 diabetes, and peptide vaccine-induced anaphylaxis in the NOD mouse.

Table 1
Rodent Models for Type 1 Diabetes

Type of animal model	Pros	Cons
Spontaneous	Similar to human condition Major HLA contribution	Takes too long to develop diabetes
NOD mouse	Polygenic model Very well studied Spontaneous IAA	Relatively easy to prevent diabetes Sex difference (females > males)
BB rat	Oligogenic model Very well studied No sex difference	T-cell lymphopenia (Ian gene)
LETL rat	Oligogenic model No sex difference	Not popular model yet Cblb gene mutant
Chemical-induced models	Rapid onset of diabetes Exact time of injury known	Not sure if immune mediated
Streptozocin	Low dose has immune component	Direct islet toxicity
Alloxan		Direct islet toxicity
Poly-IC	Induction RT1^u rats, B7.1 mice	Protection of NOD mice
Transgenic (Tg) models		
TCR-Tg	Uniform antigen-T cell specificity Highly pathogenic monoclonal T cells	Often specific antigen is unknown
BCD2.5		Unknown antigen, no increase in diabetes mellitus
8.3 TCRab	Antigen islet glucose-related phosphatase, tetramer CD8	
NOD.AI4ab		
RIP-neoantigen Tg	Diabetes-inducing antigen is known Exact time of injury known	Antigen irrelevant to type 1 diabetes
RIP-LCMV	Multiple models	
RIP-HA	Combination with TCR transgene	
RIP-OVA	Combination with TCR transgene	
RIP-B7.1	Enhances islet targeting without neoantigens	Enhanced diabetes development
	Good for combination with other trangenic models	Human DQ8 combined with RIP-B7.1 develops spontaneous diabetes.
	Necessary in autoantigen-induced diabetes	
Knockout (KO) models	Provides information about role of specific genes	Possible passenger gene segments from original strain may influence diabetes
Insulin 1 KO NOD	Prevention of diabetes	
Insulin 2 KO NOD	Acceleration of diabetes	
Anti-sense GAD NOD	One report of prevention	Lack of confirmation with GAD tolerance

1.1. Anti-Islet Autoantibody Assays

Type 1A diabetes mellitus, as defined by an expert panel of the American Diabetes Association, is characterized by the presence of antiislet autoantibodies. The presence of islet autoantibodies in individuals who otherwise seem healthy denotes an increased risk for later development of type 1A diabetes. The early expression of insulin autoantibodies (IAAs) is associated with early development of diabetes in young children and NOD mice. IAAs appear early and then disappear at approximately the time of onset of hyperglycemia in most NOD mice.

There has been tremendous progress in defining islet autoantigens and developing antiislet autoantibody assays. Multiple Immunology of Diabetes Workshops have been held to evaluate assays for IAAs, GAD65 autoantibodies (GAAs), and ICA512 (IA-2) autoantibodies (ICA512AAs); a Diabetes Antibody Standardization Program has been established.

For NOD mice, two International Diabetes Antibody Workshops have been organized by the Immunology and Diabetes Society since 2000. The results from these two NOD antibody workshops demonstrated that IAAs measured by sensitive radio-binding assay (RBA) are a marker of autoimmunity in NOD mice; disappointingly, enzyme-linked immunosorbent assays (ELISA) were discordant with the results obtained by RBA. GAAs and ICA512AAs by both RBA and ELISA were increased in NOD mice compared with control mice at diabetes onset, but GAAs and ICA512AAs frequencies varied significantly with respect to the source colony of NOD mice. Furthermore, sera with increased binding to GADs and ICA512 also had increased binding to the unrelated antigen myelin oligodendrocyte glycoprotein, and binding to GADs could not be inhibited with excess unlabeled GADs, suggesting nonspecific interactions. The above has led to questions regarding the true nature of reported GAAs and ICA512AAs in this animal model.

1.2. Utilization of Tetramers in the Study of Autoreactive T Cells

Autoantibody assays in radioimmunoassay formats have demonstrated disease specificity and sensitivity (e.g., IAAs) for the NOD mouse model. Although it has traditionally been easier to study the humoral component of the immune system, the development of tetramers to study antigen-specific $CD4^+$ and $CD8^+$ T cells has led to improved studies of cellular immunity in type 1 diabetes. MHC–peptide tetramers are soluble complexes of major histocompatibility complex (MHC) molecules bound to streptavidin through its four biotin-binding sites, making an MHC molecule:streptavidin core ratio of 4:1. A peptide (usually 8–10 amino acids long for class I MHC and 13–15 amino acids long for class II MHC) is bound in the MHC groove (for example, human class I HLA-A

or class II HLA-DR and mouse class I H2-K^d or class II I-A^{g7} in NOD mice). The tetramer with bound peptide binds to the T-cell receptor (TCR) of appropriate T cells. Through cooperative multivalent binding, the avidity of a tetramer (compared to a single MHC–peptide complex) is increased, enabling T cells with receptors specific for the MHC–peptide complex to be detected. Binding of fluorescently labeled tetramer to T cells is usually detected by flow cytometry.

Some examples of MHC tetramers used to characterize autoreactive T cells in type 1 diabetes include the use of the mouse class I K^d tetramer to present insulin peptide B:15-23 or islet glucose-related phosphatase peptide (e.g., NRP-V7 [a mimitope designed from the diabetogenic 8.3 T-cell clone]) to islet infiltrates of young NOD mice. Early in the development of insulitis, $CD8^+$ T cells in the islets recognize insulin peptide B:15-23 when presented in the context of class I K^d ***(7)***. Higher numbers of islet-infiltrating and peripheral blood $CD8^+$ T cells that recognize the NRP-V7-K^d tetramer were described. NOD mice with a greater percentage of NRP-V7 reactive T cells more often developed diabetes.

Thus, potential uses for MHC–peptide tetramers are the identification of new T-cell epitopes and the development of new strategies to predict disease. Other potential uses would include the further characterization of T cells in a patient with type 1 diabetes, monitoring disease course or response to therapy, and isolation of antigen-specific T cells for study. In this section, the protocol used to stain mouse peripheral blood for autoreactive T cells is described using the NRP-V7-K^d tetramer as described in **ref. *8*** for the NOD mouse and shared by Tan and colleagues. NOD mice have the highest number of NRP-V7-K^d-reactive T cells in peripheral blood between ages 9 and 15 wk. These mice and this tetramer can be used as positive controls for the study of other tetramers and mouse models of type 1 diabetes.

1.3. Diabetes Prevention in the NOD Mouse

There are literally over 100 "therapies" known to prevent diabetes in the NOD mouse ***(1)***. Some agents used in the mouse model have included immunosuppressive drugs such as azathioprine, corticosteroids, cyclophosphamide, cyclosporin, and methotrexate. These agents generally have nonspecific immune activities that do not target specific autoreactive T lymphocytes. Furthermore, they do not appear to be effective over the long term, with disease recurrence once the drug is withdrawn.

Other strategies have targeted T cells by presumably interfering with T-cell activation, such as the use of cytokines, antibodies that modulate costimulatory or coreceptor molecules or deplete T cells. Some promising therapies proven to be effective in the NOD mouse include the use of anti-CD3 ***(9)*** and nondepleting anti-CD4 therapy ***(10)***. Even though such treatment of mice with

antibody therapy may induce antigen-specific tolerance, the risk of generalized immune suppression remains. Regardless, these two antibodies are examples of experience in animal models that have led to clinical trials in humans, using non-Fc-binding humanized anti-CD3 (hOKT3 Ala-Ala) ***(11)***and nondepleting humanized anti-CD4 (OKT4A) ***(12)***.

Finally, antigen-specific therapy is under study in type 1 diabetes and other autoimmune diseases for which the autoantigens have been identified. Potential autoantigens include insulin B-chain and insulin B:9–23 peptide, GAD, and heat shock protein (p277 peptide of HSP60). Autoantigen peptide vaccination is perhaps the most specific type of immunotherapy in both humans and the mouse, but has properties of a "double-edged" sword; although such therapy may prevent diabetes, there is also potential to accelerate or even induce disease. The precise rules in immunotherapy to modulate the immune system toward disease induction or remission are not well understood, and it is likely that dose, timing, and route of administration will be important factors in the design of peptide vaccines.

Keeping in mind the narrow therapeutic window between the onset of hyperglycemia and critical β-cell mass loss, only two published therapies, antilymphocyte serum and anti-CD3 antibody ***(13)***, have been demonstrated to reverse hyperglycemia in recently diabetic NOD mice, demonstrating the difficulties in treating overtly diabetic mice.

Considering all the available therapies in the NOD mouse, it is likely that diabetes prevention through true antigen-specific T-cell tolerance will require a combination of both autoantigen and potent immunomodulation. Numerous therapies that have been effective in preventing diabetes in the NOD mouse model have failed to influence development of diabetes in humans (injections of subcutaneous insulin, oral insulin, and nicotinamide), and most investigators now believe that therapies that are only effective early in the life of the NOD mouse (e.g., therapy begun at age 4 wk) are unlikely to be effective in humans.

We believe that the later a therapy is effective in the NOD mouse (after insulitis has begun or at onset of diabetes), the more likely such a therapy (e.g., anti-CD3) may be effective in humans. In addition, therapies that completely eliminate insulitis or are effective in more stringent models of diabetes (such as the NOD mouse that lack the insulin 2 gene) may be better preclinical models or end points.

The insulin B-chain B:9–23 peptide is a major diabetes autoantigen of the NOD mouse. A single subcutaneous injection of the peptide with Freund's incomplete adjuvant (FIA) in female NOD mice at age 4 wk prevents diabetes ***(14)***. Not only are mice protected from diabetes, they also produce IAAs. These IAAs are absorbed by whole insulin and not by the peptide itself ***(15)***. In this

section, the standard immunization and follow-up protocol for diabetes protection for B:9–23 compared to a control tetanus toxoid peptide, TT:830–843, is described.

1.4. Peptide Induction Model of Type 1 Diabetes (Experimental Autoimmune Diabetes)

Diabetes or insulitis can be induced in animals. For example, high doses of streptozotocin can rapidly induce diabetes in several strains of mice ***(16)***, and low doses can create a more chronic form of diabetes ***(17)***. Administration of polyinosinic polycytidylic acid (poly-IC), which has been used as a viral RNA mimic to stimulate the innate immune system, can induce insulitis and diabetes in RT1u rat strains ***(18)*** similar to that seen with the Kilham rat virus ***(19)***. We found that immunization with insulin peptide B:9–23 induces IAA expression in normal mice with MHC H-2^d and H-2^{g7} but not H-2^b ***(15)*** and, if combined with poly-IC, induces insulitis. With the introduction of the B7.1 islet transgene to this model, B:9–23 peptide can induce diabetes ***(4)***. In this section, this disease induction model in mice with insulin peptide B:9–23 is described.

1.5. Peptide Vaccine-Induced Anaphylaxis in the NOD Mouse

The identification of autoantigens in autoimmune diseases such as type 1 diabetes or multiple sclerosis has made peptide immunotherapy possible. In fact, peptide vaccine trials are currently underway in type 1 diabetes for an altered peptide ligand of insulin peptide B:9–23 ***(20)***, for GAD peptides, and for heat shock protein 60 (HSP60) (p277) ***(21)***. However, in mouse studies of peptide vaccination, anaphylaxis has been reported in diabetes experiments using the B:9–23 peptide ***(22)*** and GAD peptides ***(23)*** and in multiple sclerosis studies (experimental autoimmune encephalitis) using proteolipid protein (PLP) (139–151) and myelin oligodendrocyte glycoprotein (MOG) (35–55) peptides ***(24)***. Even more concerning is the report of systemic hypersensitivity reactions in humans during phase II trials with an altered peptide ligand for myelin basic protein (MBP) (83–99) ***(25,26)***, which led to the premature discontinuation of therapy in some patients. More research into peptide-induced anaphylaxis, specifically regarding prediction and prevention is needed to gain better understanding of this added risk in peptide immunotherapy.

In this section, we describe an established model of B:9–23-induced anaphylaxis that is consistent and usually fatal for NOD mice 6 wk after the start of injections. Mice receiving repeated injections of B:9–23 peptide develop high titers of immunoglobulin G1 (IgG1) anti-B:9–23 antibodies. We have not been able to detect specific antipeptide IgE antibodies even though, for pathogenesis, both IgG and IgE are important, and anaphylaxis is mediated by both platelet-activating factor and histamine ***(22)***.

2. Materials

2.1. Anti-Islet Autoantibody Assays

1. Buffer 1: 20 m*M* Tris-HCl at pH 7.4, 150 m*M* NaCl, 0.1% bovine serum albumin (BSA), 0.15% Tween-20, 0.1% sodium azide.
2. Buffer 2: 20 m*M* Tris-HCl at pH 7.4, 150 m*M* NaCl, 1.0% BSA, 0.15% Tween-20, 0.1% sodium azide.
3. Protein A-Sepharose (Amersham, Piscataway, NJ, cat. no. 17097402).
4. Protein G-Sepharose (Amersham, cat. no. 17061802).
5. ^{125}I-insulin (Amersham, cat. no. IM166).
6. 96-well polymerase chain reaction (PCR) plate (Fisher, Hampton, NH, cat. no. 05500-48).
7. 96-well filtration plates (Fisher, cat. no. 3504).
8. Bottle-Top 500-mL filters (Fisher, cat. no. 09-740-22J).
9. TopSeal (PerkinElmer, Boston, MA, cat. no. 6005185).
10. Microscint-20 (PerkinElmer, cat. no. 6013621).

The following equipment is used:

TopCount β-counter (PerkinElmer).
Vacuum-operated 96-well plate washer (Millipore, Billerica, MA).
96-well plate shaker (Wallac-Delfia, Torrance, CA).
Fume hood.
Biological and radio safety cabinet.
–20°C freezer.
4°C refrigerator.
Pipette-Aid.

2.2. Utilization of Tetramers in the Study of Autoreactive T Cells

1. Female NOD mouse between ages 9 and 15 wk.
2. Phycoerythren (PE)-labeled NRP-V7-K^d tetramer (NRP-V7 sequence: KYNKA NVFL).
3. PE-labeled TUM-K^d tetramer (control tetramer, sequence KYQAVTTTL).
4. Microhematocrit capillary tubes (Fisher, cat. no. 22-362-566).
5. Bio-Rad Titertube® Micro Tubes (Bio-Rad, Hercules, CA, cat. no. 223-9391), 1-mL volume.
6. Red blood cell (RBC) lysis buffer (*see* **Subheading 1.2.**).
7. Fluorescence-activated cell sorter (FACS) staining buffer (*see* **Subheading 1.2.**).
8. FACS machine and appropriate FACS tubes.
9. Antimouse CD8-FITC (fluorescein isothiocyanate), CD8-PE, and B220-PerCP (Pharmingen, cat. no. 553031, 553033, and 553093) (*see* **Subheading 1.2.**).

2.3. Diabetes Prevention in the NOD Mouse

1. Female NOD mice, age 4 wk (Taconic Farms, Germantown, NY).
2. Insulin peptide B:9–23 (SHLVEALYLVCGERG) and the control peptide TT:830–843 (QYIKANSKFIGITE) are more than 90% pure following high-

performance liquid chromatographic (HPLC) purification (Synpep Corp., Dublin, CA).
3. FIA (cat. no. F-5506, Sigma, St. Louis, MO).
4. Lipopolysaccharide (LPS)-free sterile saline.

2.4. Peptide Induction Model of Type 1 Diabetes (Experimental Autoimmune Diabetes)

1. BALB/c mice or RIP-B7.1-BALB/c mice (backcross one generation), age 4 wk.
2. Insulin peptide B:9–23 (SHLVEALYLVCGERG) and the control peptide TT:830–843 (QYIKANSKFIGITE) are purchased more than 90% pure by HPLC purification (Synpep Corp.).
3. FIA (cat. no. F-5506, Sigma).
4. Poly-IC (cat. no. P-153, Sigma).
5. LPS-free sterile saline and sterile PBS (phosphate-buffered saline).

2.5. Peptide Vaccine-Induced Anaphylaxis in the NOD Mouse

1. Female NOD mice, age 4 wk (Taconic Farms).
2. Insulin peptide B:9–23 (SHLVEALYLVCGERG) is more than 90% pure following HPLC purification (Synpep Corp.).
3. LPS-free sterile saline.
4. Rectal temperature probe (451 Probe and 4600 Precision Thermometer, Yellow Springs Instrument Co., Yellow Springs, OH).

3. Methods

3.1. Anti-Islet Autoantibody Assays

On day 1, in the morning, retrieve and thaw sera to be tested. At midday:

1. Set up incubation of sera in buffer 1.
2. Prepare protein A/G-Sepharose in buffer 1.
3. Coat the 96-well plates with buffer 1.

On the morning of day 2:

4. Add above sera plus buffer 1 to protein A/G-Sepharose in 96-well filtration plates.
5. Wash plates with buffer 2.
6. Dry plates.
7. Add scintillation liquid.

In the afternoon:

8. Count.
9. Analyze data.

The methods described below outline the following:

Incubation of serum with labeled antigen with and without cold insulin overnight.
Precipitation of antibody-bound labeled antigens with protein A/G-Sepharose in a 96-well plate format, with each serum tested in duplicate.

Washing of the 96-well plates to remove unbound labeled antigens.
Counting of each well with a 96-well plate β-counter.
Results expressed as an index.

3.1.1. Incubation of Serum Samples With ^{125}I-Insulin

Each 96-well plate is sufficient for testing 24 samples in duplicate (24 duplicates with cold insulin and 24 duplicates without cold insulin; usually, four plates can easily be run at one time, for a total of 96 samples).

1. Spin sera to remove fibrin clots (otherwise, these may partially block membrane in bottom of wells).
2. Prepare the stock solution of ^{125}I-insulin: Use 1 mL of 5% BSA in PBS to dissolve the powder of 10 μCi of ^{125}I-insulin.
3. Calculate how much ^{125}I-insulin and cold insulin is required.

To process two plates, 6.4 mL of washing buffer is required: 48 × 4.2 × 30 = 6 mL (48 samples, with 30 μL/well; in duplicate for both with and without cold insulin wells, but multiply by 4.2 rather than 4 to allow for extra volume). For each well, 20,000 cpm is used.

3040 μL buffer 1 + 160 μL ^{125}I-insulin = 3.2 mL

2784 μL buffer 1 + 160 μL ^{125}I-insulin + 256 μL humulin (or Novolin) = 3.2 mL

Keep the buffer with labeled antigen mixture on ice.

1. Mix each serum sample with buffer-antigen mixture in a PCR tube (or similar tube): use 6 μL serum and 30 μL buffer; use 2 wells for each sample; and use the same control samples for every assay.
2. Vortex and incubate 2 h at room temperature and overnight at 4°C.

3.1.2. Preparation of 96-Well Filtration Plates and Protein A/G-Sepharose

1. Coat the plate with BSA by adding 150 μL of buffer 1 to each well.
2. Incubate overnight at room temperature after placing the plate on aluminum foil.
3. Remove the washing buffer.
4. The plates are now ready for running the assay, but can be stored at 4°C if necessary.
5. Prepare protein A/G-Sepharose.

3.1.3. Prepare Protein A-Sepharose

1. Use only plastic tubes because protein A sticks to glass.
2. For each plate, take 5 mL protein A-Sepharose in a 50-mL tube. Spin and remove the fluid phase. Wash twice times with buffer 1.
3. Finally, add buffer 1 to give 62.5% concentration of protein A-Sepharose by volume.

3.1.4. Prepare Protein G-Sepharose

1. Use only plastic tubes because protein G sticks to glass.
2. For each plate, take 1 mL protein G-Sepharose in buffer 1 in a 50-mL tube. Spin and remove the fluid phase. Repeat once with buffer 1.
3. Finally, add buffer 1 to give 40% concentration of protein A-Sepharose by volume.

3.1.5. Mix Protein A/G-Sepharose

Mix protein A/G-Sepharose at a 4:1 ratio (final concentration 50% protein A/8% protein G).

3.1.6. Immunoprecipitation With Protein A-Sepharose

1. Add 50 μL of protein A/G-Sepharose mixture to each well. Use Eppendorf multipipettor and resuspend the protein A/G-Sepharose after each row of the plate is done (5 mL of protein A/G-Sepharose are needed per plate).
2. Add 30 μL of overnight incubate to each well (i.e., each serum will be tested in duplicate).
3. Shake the plate on a plate shaker for 45 min at 4°C. Accurate timing is important.
4. Place the plate on a Millipore plate washer device (with vacuum set low).
5. Wash the plate three times with 200 μL of washing buffer per well.
6. Add 130 μL of washing buffer to each well. Shake for at least 5 min at 4°C.
7. Wash the plate four times with 200 μL of washing buffer per well (change the plate direction after two times of washing at this stage).
8. Place the plate under a lamp for approx 10 min to dry. Rotate the plate several times to ensure even drying and check its appearance. Drying is complete when deep fissures in the Sepharose are visible in the bottom of the wells. Do not overdry and be careful not to melt the plastic parts of the plate.
9. Add 50 μL of scintillation cocktail (Microscint-20) to each well.
10. Count on TopCount 96-well plate β-counter.

3.1.7. Data Analysis

1. Delta cpm: Mean cpm of duplicates without cold insulin (Mean cpm of duplicates with cold (unlabeled) insulin.
2. For the cpm index for each sample:

(Sample delta cpm – NC delta cpm)/(PC delta cpm – NC delta cpm)

where NC is the negative control serum, and PC is the positive control serum.

3.2. Utilization of Tetramers in the Study of Autoreactive T Cells

1. Bleed NOD mouse to fill heparinized capillary tube (approx 70 μL blood). Use 70 μL blood per FACS tube to be stained (*see* **Subheading 1.2.**).
2. Insert each Bio-Rad Titertube Micro Tube into an FACS tube. All processing of blood and tetramer will take place in the microtube on ice.

3. RBC lysis: Push blood into microtube and flush with a total of 500 μL RBC lysis buffer (*see* **Subheading 1.2.**). Let RBC lysis occur for 10 min.
   a. Dilute with 500 μL PBS to stop lysis.
   b. To pellet, spin at 450*g* and 4°C for 5 min.
   c. Carefully suction out supernatant (preserve the cell pellet). Do not pour because the pellet does not adhere to the bottom of the tube.
   d. Repeat lysis as needed (*see* **Subheading 1.2.**).
   e. Following the last lysis procedure, dilute with PBS/10% fetal bovine serum.
   f. Spin to pellet and begin washing procedure.
4. Washing procedure:
   a. Wash with 900 μL PBS. Be sure to agitate cells with pipet to ensure thorough washing.
   b. Spin to pellet at 450*g* and 4°C for 5 min.
   c. Repeat washing, but this time use FACS staining buffer.
   d. After pelleting the cells, carefully suction supernatant, leaving approx 70–100 μL of supernatant in the tube. Be sure to leave approximately the same volume in each tube for equal staining.
5. Staining procedure (*see* **Fig. 1**):
   a. Add 1 μL tetramer (NRP-V7 or TUM) to corresponding experimental tubes (*see* **Subheading 1.2.**).
   b. Keep on ice, shielded from light, on a gentle shaker for 2.5 h.
   c. After 2.5 h, add antibodies to corresponding tubes and stain for an additional 30 min: For compensation tubes, to unstained, do not add antibody; for CD8-FITC, add 1 μL of antibody; for CD8-PE, add 1 μL of antibody; for B220-PerCP, add 1 μL of antibody. For experimental tubes with tetramer, add CD8-FITC and B220-PerCP (1 μL each).
   d. Wash three times with FACS staining buffer.
   e. After final wash, pellet cell and suction supernatant, leaving again approx 100 μL per tube for FACS analysis.
   f. For FACS analysis, use the following general strategy:
      Set lymphocyte gate; adjust settings/compensation using the compensation tubes; acquire 20–30,000 gated events per tube; exclude all $B220^+$ cells from gate for $tetramer^+/CD8^+$ T cells. The percentage tetramer staining cells is based on

      $$(Tetramer^+\ CD8^+\ B220^-\ cells)/(all\ CD8^+\ B220^-\ cells)$$

      The percentage NRP-V7 tetramer-positive cells is derived from

      $$\%\ NRP\text{-}V7\ tetramer\ positive - \%\ TUM\ tetramer\ positive$$

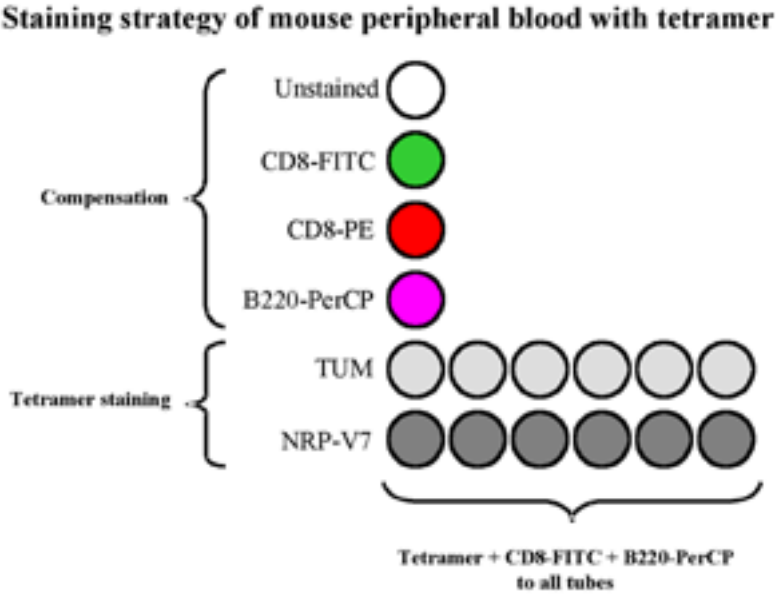

Fig. 1. Staining strategy of mouse peripheral blood with tetramer.

3.3. Diabetes Prevention in the NOD Mouse

1. Prepare the peptide vaccine. (*See* **Subheading 1.3.**)
   a. Resuspend each peptide in sterile LPS-free saline at a concentration of 2 mg/mL.
   b. Adjust the pH to 7.0 with 1 *M* NaOH or 1 *M* HCL.
   c. For each mouse to be immunized, transfer 100 μL of peptide into a 1.5-mL microcentrifuge tube.
   d. Add IFA to tube at a 1:1 volume with peptide (final concentration of peptide is now 1 mg/mL).
   e. Vortex the peptide/IFA vigorously to emulsify (we seal the tube, secure it to the vortexer, and leave on for at least 10 min). Emulsification occurs when vaccine has the consistency of mayonnaise.
   f. Centrifuge briefly to concentrate vaccine to the bottom of the tube for collection.
   g. Transfer the vaccine into 1-mL syringes.
2. Female NOD mice are injected with 100 μL (100 μg peptide) of emulsified vaccine subcutaneously in the back of the neck at age 4 wk.

3. For monitoring, blood is obtained every 4 wk for IAA determination. Blood glucose is measured weekly (usually by tail bleed) starting at age 12 wk and using standard home glucose monitors. A mouse with a blood sugar above 250 mg/dL on two separate days is considered diabetic. Diabetes usually develops between 16 and 30 wk, but follow-up to 1 yr for diabetes is recommended, depending on the experimental regimen.

3.4. Peptide Induction Model of Type 1 Diabetes (Experimental Autoimmune Diabetes)

1. Prepare the peptide vaccine (*see* **Subheading 1.4.**).
2. Prepare the poly-IC in PBS solution (1.5 mg/mL).
3. B:9–23 peptide in IFA is given subcutaneously to BALB/c mice or B7.1-BALB/c mice at age 4 wk (day 1). In addition, poly-IC (7.5 μg/g body weight on days 1–5 and 8–14) is administered intraperitoneally to the mice.
4. For monitoring, blood glucose is measured weekly starting at age 4 wk, and the mice are considered diabetic after two consecutive blood values greater than 250 mg/dL. IAA expression is also measured beginning at age 4 wk until the development of diabetes or until age 32 wk. At the end of the experiments, islet histology is analyzed.

3.5. Peptide Vaccine-Induced Anaphylaxis in the NOD Mouse

1. Prepare the peptide vaccine (*see* **Subheading 1.5.**):
   a. Resuspend each peptide in sterile LPS-free saline at a concentration of 1 mg/mL.
   b. Adjust the pH to 7.0 with 1 *M* NaOH or 1 *M* HCl.
2. Sensitization phase: Female NOD mice at age 4 wk are injected subcutaneously with B:9–23 peptide in the back of the neck on days 1–5 and 8, then weekly thereafter.
3. Induction phase: At age 10 wk (sometimes as early as 9 wk), mice are considered sensitized. Observe for signs of anaphylaxis induction within 30 min after injection, starting at age 9–10 wk.

4. Notes

4.1. Anti-Islet Autoantibody Assays

1. Buffer should be filtered (0.45-μm filter) to prevent any particles blocking the membrane in the bottom of the wells of the 96-well plate (which would decrease washing efficiency and increase the assay background). Store buffers at 4°C in a sterile bottle for up to 3 mo.
2. The standard positive sample should be selected from new-onset diabetic patient(s) with a high positivity of mIAA (cpm range 1000 to 2000) and before insulin injection.
3. All assays are run in duplicates, along with standard positive and negative control serum samples. If the positive control is above or below 30% of its standard cycles per minute, results are regarded as invalid, and the test is rerun until the

positive control result falls within this range. One internal low positive control should be used for monitoring the sensitivity and variability of assay.

4. This assay could be performed without a TopCount β-counter. The MultiScreen filtration plate and a punch-out system (Millipore) could be used for regular scintillation vials and regular β-counter, but this is less convenient.
5. The assay is not able to distinguish between natural IAAs and insulin antibodies induced following insulin injections.

4.2. Utilization of Tetramers in the Study of Autoreactive T Cells

6. RBC lysis buffer: 8.29 g NH_4Cl (0.15 *M*), 1 g $KHCO_3$ (1.0 m*M*), 37.2 mg Na_2EDTA; add 800 µL of H_2O and adjust pH to 7.2–7.4 with 1*N* HCl; add H_2O to 1 L; and filter-sterilize with 0.2-µm filter and store at room temperature.
7. FACS staining buffer: 0.1% sodium azide, 1 m*M* EDTA, 2% fetal bovine serum, and 1X Hanks' balanced salt solution (no phenol red; - Gibco cat. no. 14025-092).
8. CD8-PE is used for PE control during FACS analysis compensation. B220-PerCP is for B-cell staining and exclusion during FACS analysis.
9. Determine number of tubes needed for staining: Four extra tubes will be needed for compensation and the like (unstained, CD8-FITC alone, CD8-PE alone, and B220-PerCP alone). For each experimental point, only two tubes will be needed: one for NRP-V7 tetramer PE plus CD8 FITC plus B220-PerCP and one for TUM tetramer PE plus CD8 FITC plus B220-PerCP.
10. Be sure to agitate the cells gently using pipet to prevent clumping and ensure good RBC lysis.
11. Cell lysis is time consuming, but is more efficient than using Ficoll gradient in preserving cell numbers. We find that adequate RBC lysis requires at least three cycles of lysis and spinning. The red color does not have to be entirely clear because RBCs can be gated out during FACS analysis.

4.3. Peptide Vaccine-Induced Anaphylaxis in the NOD Mouse

12. Signs of anaphylaxis: Within 30 min of injection with B:9–23, mice induced to anaphylax will initially have decreased movement and appear hunched over. The respiratory rate increases. Excessive scratching is noted. As anaphylaxis progresses, mice begin to lay prone; extremities turn blue. Later, body temperature decreases. Death can occur within 30 min. Other mice will recover spontaneously and can be used for future experiments (they are considered sensitized).
13. Monitoring anaphylaxis:
    a. A clinical anaphylaxis score (CAS) was developed based on clinical features of mice experiencing anaphylaxis; mice are scored at baseline, then every 5 min up to 30 min following induction: score 0 = normal activity, no signs of anaphylaxis; score 1 = decreased movement, hunched over; score 2 = mice begin to lay prone, loss of self-righting reflex; score 3 = mice become moribund with cool, blue extremities.

b. Because anaphylactic shock is associated with a decrease in core body temperature, rectal temperature is measured at baseline, then once at 15 min, and again at 30 min. This is considered a more objective measurement to monitor anaphylaxis. Lubricate the temperature probe before rectal insertion.
c. Confirmation of anaphylaxis is by the presence of an abnormality in both CAS (score 1 or greater) and a decrease in core body temperature.

Acknowledgment

We thank Rusung Tan and Jacquline Trudeau for teaching us (E. L.) and providing reagents for tetramer analysis.

References

1 Atkinson, M. A. and Leiter, E. H. (1999) The NOD mouse model of type 1 diabetes: as good as it gets? *Nat. Med.* ***5,*** *601–604.*
2 Yu, L., Robles, D. T., Abiru, N., Kaur, P., Rewers, M., Kelemen, K., et al. (2000) Early expression of antiinsulin autoantibodies of humans and the NOD mouse: evidence for early determination of subsequent diabetes. *Proc. Natl. Acad. Sci. USA* **97,** 1701–1706.
3 Grewal, I. S. and Flavell, R. A. (1997) New insights into insulin dependent diabetes mellitus from studies with transgenic mouse models. *Lab. Invest.* **76,** 3–10.
4 Moriyama, H., Wen, L., Abiru, N., Liu, E., Yu, L., Miao, D., et al. (2002) Induction and acceleration of insulitis/diabetes in mice with a viral mimic (polyinosinic-polycytidylic acid) and an insulin self-peptide. *Proc. Natl. Acad. Sci. USA* **99,** 5539–5544.
5 Thebault-Baumont, K., Dubois-LaForgue, D., Krief, P., Briand, J. P., Halbout, P., Vallon-Geoffroy, K., et al. (2003) Acceleration of type 1 diabetes mellitus in proinsulin 2-deficient NOD mice. *J. Clin. Invest.* **111,** 851–857.
6 Baekkeskov, S., Kanaani, J., Jaume, J. C., Kash, S. (2000) Does GAD have a unique role in triggering IDDM? *J. Autoimmun.* **15,** 279–286.
7 Wong, F. S., Karttunen, J., Dumont, C., Wen, L., Visintin, I., Pilip, I. M., et al. (1999) Identification of an MHC class I-restricted autoantigen in type 1 diabetes by screening an organ-specific cDNA library. *Nat. Med.* **5,** 1026–1031.
8 Trudeau, J. D., Kelly-Smith, C., Verchere, C. B., Elliott, J. F., Dutz, J. P., Finegood, D. T., et al. (2003) Prediction of spontaneous autoimmune diabetes in NOD mice by quantification of autoreactive T cells in peripheral blood. *J. Clin. Invest.* **111,** 217–223.
9 Chatenoud, L., Thervet, E., Primo, J., and Bach, J. F. (1994) Anti-CD3 antibody induces long-term remission of overt autoimmunity in nonobese diabetic mice. *Proc. Natl. Acad. Sci. USA* **91,** 123–127.
10 Hayward, A. R., Shriber, M., Cooke, A., and Waldmann, H. (1993) Prevention of diabetes but not insulitis in NOD mice injected with antibody to CD4. *J. Autoimmun.* **6,** 301–310.

11 Herold, K. C., Hagopian, W., Auger, J. A., Poumian-Ruiz, E., Taylor, L., Donaldson, D., et al. (2002) Anti-CD3 monoclonal antibody in new-onset type 1 diabetes mellitus. *N. Engl. J. Med.* **346,** 1692–1698.

12 Pulito, V. L., Roberts, V. A., Adair, J. R., Rothermel, A. L., Collins, A. M., Varga, S. S., et al. (1996) Humanization and molecular modeling of the anti-CD4 monoclonal antibody, OKT4A. *J. Immunol.* **156,** 2840–2850.

13 Chatenoud, L. (2001) Restoration of self-tolerance is a feasible approach to control ongoing beta-cell specific autoreactivity: its relevance for treatment in established diabetes and islet transplantation. *Diabetologia* **44,** 521–536.

14 Daniel, D. and Wegmann, D. R. (1996) Protection of nonobese diabetic mice from diabetes by intranasal or subcutaneous administration of insulin peptide B-(9–23). *Proc. Natl. Acad. Sci. USA* **93,** 956–960.

15 Abiru, N., Maniatis, A. K., Yu, L., Miao, D., Moriyama, H., Wegmann, D., et al. (2001) Peptide and MHC specific breaking of humoral tolerance to native insulin with the B:9–23 peptide in diabetes prone and normal mice. *Diabetes* **50,** 1274–1281.

16 Uchigata, Y., Yamamoto, H., Nagai, H., and Okamoto, H. (1983) Effect of poly(ADP-ribose) synthetase inhibitor administration to rats before and after injection of alloxan and streptozotocin on islet proinsulin synthesis. *Diabetes* **32,** 316–318.

17 Tanaka, S. I., Nakajima, A. S., Inoue, S., Takamura, Y., Aoki, I., Okuda, K. (1990) Genetic control by I-A subregion in H-2 complex of incidence of streptozotocin-induced autoimmune diabetes in mice. *Diabetes* **39,** 1298–1304.

18 Ewel, C. H., Sobel, D. O., Zeligs, B. J., and Bellanti, J. A. (1992) Poly I:C accelerates development of diabetes mellitus in diabetes-prone BB rat. *Diabetes* **41,** 1016–1021.

19 Guberski, D. L., Thomas, V. A., Shek, W. R., Like, A. A., Handler, E. S., Rossini, A. A., et al. (1991) Induction of type 1 diabetes by Kilham's rat virus in diabetes-resistant BB/Wor rats. *Science* **254,** 1010–1013.

20 Alleva, D. G., Gaur, A., Jin, L., Wegmann, D., Gottlieb, P. A., Pahuja, A., et al. (2002) Immunological characterization and therapeutic activity of an altered-peptide ligand, NBI-6024, based on the immunodominant type 1 diabetes autoantigen insulin B-chain (9–23) peptide. *Diabetes* **51,** 2126–2134.

21 Cohen, I. R. (2002) Peptide therapy for type I diabetes: the immunological homunculus and the rationale for vaccination. *Diabetologia* **45,** 1468–1474.

22 Liu, E., Moriyama, H., Abiru, N., Miao, D., Yu, L., Taylor, R. M., et al. (2002) Anti-peptide autoantibodies and fatal anaphylaxis in NOD mice in response to insulin self-peptides B:9–23 and B:13–23. *J. Clin. Invest.* **110,** 1021–1027.

23 Pedotti, R., Sanna, M., Tsai, M., DeVoss, J. J., Steinman, L., McDevitt, H., et al. (2003) Severe anaphylactic reactions to glutamic acid decarboxylase (GAD) self peptides in NOD mice that spontaneously develop autoimmune type 1 diabetes mellitus. *BMC Immunol.* **4,** 2.

24 Pedotti, R., Mitchell, D., Wedemeyer, J., Karpuj, M., Chabas, D., Hattab, E. M., et al. (2001) An unexpected version of horror autotoxicus: anaphylactic shock to a self-peptide. *Nat. Immunol.* **2,** 216–222.

25 Kappos, L., Comi, G., Panitch, H., Oger, J., Antel, J., Conlon, P., et al. (2000) Induction of a non-encephalitogenic type 2 T helper-cell autoimmune response in multiple sclerosis after administration of an altered peptide ligand in a placebo-controlled, randomized phase II trial. The Altered Peptide Ligand in Relapsing MS Study Group. *Nat. Med.* **6,** 1176–1182.

26. Bielekova, B., Goodwin, B., Richert, N., Cortese, I., Kondo, T., Afshar, G., et al. (2000) Encephalitogenic potential of the myelin basic protein peptide (amino acids 83–99) in multiple sclerosis: results of a phase II clinical trial with an altered peptide ligand. *Nat. Med.* **6,** 1167–1175.

12

Generation, Maintenance, and Adoptive Transfer of Diabetogenic T-Cell Lines/Clones From the Nonobese Diabetic Mouse

Martha J. Milton, Michelle Poulin, Clayton Mathews, and Jon D. Piganelli

Summary

The ability to generate, maintain, and use cloned lines of T cells reactive for self-antigens has opened up a new avenue of investigation for researchers. These T-cell clones allow the rapid induction of tissue-specific autoimmunity with the intent of dissecting the contribution of the different cell types involved. T cells from the diabetes-prone nonobese diabetic mouse are proving to be a vital asset for understanding the T-cell-mediated pathogenesis that leads to overt β-cell destruction. T-cell clone adoptive transfer protocols have been developed for use in immunodeficient strains, thus reducing the complexity of mechanism of disease initiation. Furthermore, these T-cell clones have been used to derive T-cell receptor transgenic (TCR-Tg) animals carrying only self-reactive T cells. The use of these TCR-Tg animals to study pathogenesis has also evolved from the ability to generate, maintain, and use T-cell cloned lines. This chapter focuses on primary culture for the generation of T-cell lines and clones, their long-term maintenance, and their use in disease transfer for studying the pathogenesis of end-organ autoimmunity.

Key Words: Adoptive transfer; end-organ autoimmunity; islet; nonobese diabetic mouse; T cell; type I diabetes.

1. Introduction

Type I diabetes (TID) is a chronically progressive, T-cell-mediated autoimmune disease that affects humans and some inbred strains of rodents, such as the nonobese diabetic (NOD) mouse and the diabetes-prone biobreeding (BB)

From: *Methods in Molecular Medicine, Vol. 102: Autoimmunity: Methods and Protocols*
Edited by: A. Perl © Humana Press Inc., Totowa, NJ

rat ***(1)***. In humans, the progression of clinical symptoms associated with diabetes can take years, and in mice and rats, the disease manifests within months ***(2,3)***. TID is characterized by T-cell-mediated mononuclear cell infiltration of the pancreatic islets, leading to autoimmune destruction of insulin-producing pancreatic β-cells. Studies conducted in the NOD mouse have determined that the infiltrate within the islets (insulitis) is composed of $CD4^+$ and $CD8^+$ T lymphocytes, B lymphocytes, macrophages, and dendritic cells ***(4–9)***.

T-cell subsets play an obligatory role in disease initiation as T-cell deficient NOD mice carrying the *Prkdc*^{scid} (NOD.*scid*) mutation or with a targeted disruption of the Recombination activating gene 1 (*Rag1*) (NOD.*Rag*) develop neither diabetes nor insulitis. In the NOD mouse, it has been demonstrated that $CD8^+$ T cells are critical for the initiation of disease progression; the $CD4^+$ population is necessary for the mobilization of the mononuclear cell infiltrate. Although $CD8^+$ T cells are critical in the diabetes process, $CD8^+$ T cells isolated from either prediabetic or overtly diabetic NOD mice cannot independently initiate TID ***(4,10,11)***. $CD4^+$ T lymphocytes isolated from prediabetic NOD donors can home to the islets, but they cannot initiate TID in the absence of $CD8^+$ T cells. However, $CD4^+$ T cells isolated from the spleens of overtly diabetic NOD mice can transfer TID to NOD.*scid* recipients ***(4)***. Thus, it appears that the $CD8^+$ T-cell population that contributes to TID development in the prediabetic NOD mouse depends on helper functions provided by $CD4^+$ T cells ***(12)*** and that the $CD4^+$ cell activation may require $CD8^+$-induced β-cell necrosis to initiate the antigen-presenting cell (APC) presentation of β-cell antigens and to activate autoreactive $CD4^+$.

The $CD4^+$ and $CD8^+$ T-cell receptor (TCR) transgenic (TCR-Tg) mouse models that express a TCR from diabetogenic clones support this concept of critical expansion for initiation of disease. Interestingly, T cells from either $CD4^+$ ***(13)*** or $CD8^+$ ***(12)*** TCR-Tg strains, in which the T-cell repertoire is skewed to a single $CD4^+$ or $CD8^+$ TCR, can independently initiate diabetes. This suggests that, when overwhelming numbers of β-cell autoreactive T cells are present, these cells can initiate TID. Although the progression to frank diabetes in TCR-Tg mice is accelerated compared to that in humans or NOD mice, methods for increasing the progression of T-cell-mediated β-cell destruction allow the investigator to study the pathogenesis at a much faster rate.

This chapter focuses on the primary culture of T cells for the generation of T-cell lines and clones and their use in disease transfer, as well as the use of spleen cells from spontaneously diabetic NOD mice in an adoptive transfer model of accelerated diabetes in young NOD and NOD.*Rag* mice. These accelerated models aid in rapid dissection of the precise mechanisms of β-cell destruction.

2. Materials

2.2. Mice

1. Spleen donors: adult male NOD mice age 6–9 wk and spontaneously diabetic (approx 16-wk-old) NOD female mice.
2. Recipients: NOD or NOD.*Rag* mice age 3–14 d.

2.2. Medium/Solutions

1. Complete medium (CM) with 10% fetal calf serum (FCS) (*see* **Note 1** for primary culture): 500 mL high-glucose Dulbecco's modified Eagle's medium (DMEM), 55 mL FCS (low endotoxin), 1.5 m*M* L-glutamine, 10 mL MEM nonessential amino acids (100X stock; Invitrogen, Carlsbad, CA), 50 mg/mL gentamicin, 5 m*M* HEPES, 1 m*M* sodium pyruvate, 50 μ*M* 2-mercaptoethanol. Add all supplements to DMEM and sterile filter.
2. Sterile red blood cell (RBC) lysis buffer (ACK lysis buffer): 150 m*M* NH_4Cl, 10 m*M* $KHCO_3$, 0.1 m*M* ethylenediaminetetraacetic acid (EDTA) at pH 7.2.
3. Trypan blue.
4. Sterile Hanks balanced salt solution (HBSS).
5. 95% and 70% ethanol.
6. Normal mouse serum (NMS) (*see* **Note 2**).
7. Nonenzymatic cell dissociation buffer (Invitrogen).
8. Indomethacin (Sigma, St. Louis, MO, I7378).

2.3. Equipment

1. 15-mL conical tubes.
2. Sterile, autoclavable scissors and forceps (2 pairs of each).
3. Sterile, autoclavable glass homogenizer (7 mL for up to two spleens, 2 mL for one spleen or lymph nodes, LNs).
4. Hemocytometer and coverslip.
5. Microcentrifuge tubes for counting cells.
6. Cell strainer (70-μm cutoff).
7. Filters (0.22 μm) for medium/HBSS.
8. Sterile 1-mL syringes and 26-ga needles.
9. 162, 75, 25 cm^2 tissue culture flasks.

3. Methods

The methods detailed in the following section outline (a) the isolation and preparation of the diabetic donor spleen cells from female diabetic NOD mice, (b) the primary culture for isolation as well as maintenance and expansion of antigen-specific T-cell clones in vitro (5–7,14), (c) the adoptive transfer of the prepared diabetogenic spleen cells or T-cell clones/lines by intraperitoneal injection of young (6- to 10-d-old) NOD and NOD.Rag mice (7,14–18), and (d) urine and blood glucose monitoring of recipient mice for detection of glucosuria and hyperglycemia after adoptive transfer of diabetogenic T cells.

3.1. Sterile Removal of Lymph Nodes and Spleen (see Note 3)

1. Prior to sacrificing mice (by approved animal care protocol), have an ice bucket with 100 mL 95% ethanol in a beaker for maintaining sterility of surgical utensils, 10 mL of DMEM plus 0.3–0.5% supplemented with normal mouse serum (NMS) (DMEM-NMS) in a 15-mL conical tube on ice, sterile tools, and a sterile pad.
2. In a biosafety hood on a sterile blue pad, lay the mouse flat on its back and coat the exposed fur with 70% ethanol. Designate one pair of scissors and forceps as the outside pair and the other set as the inside pair prior to making an incision. Use the outside forceps to lift the skin away from the mouse at the urethral opening and make an incision beginning at the urethral opening to the chin of the mouse (**Fig. 1**).
3. Next, make an incision on either side of the first incision down to the knee, resulting in an incision that looks like an upside-down Y. This should expose the organs and leave the peritoneal wall intact.
4. Put the designated outside tools back in the beaker of 95% ethanol and use the inside forceps to lift the peritoneal layer and cut it to expose the organs. At this point, you are ready to remove the LNs (*see* **Fig. 2**). If the animal was immunized prior to LN harvest, only the draining LN from the site of injection need be removed. Use the forceps to hold the spleen gently while using the scissors to detach it from the pancreas and intestines. Immediately place the spleen in the DMEM-NMS.
5. Pour the spleen(s)/LN and medium into a glass homogenizer and pour off 5 mL of DMEM-NMS, leaving the spleen and 5 mL of DMEM-NMS in the homogenizer. Grind to a single-cell suspension and pour the cells into a 15-mL conical tube. Pour the remaining 5 mL of media into the base of the homogenizer and repeat the grinding.
6. Spin the cells at 330*g* for 5 min. Aspirate the supernatant (SN) and gently resuspend the pellet in 3 mL of RBC lysis buffer per spleen. Incubate for 5 min at room temperature. Immediately add an equal volume of DMEM-NMS, mix by gentle pipetting, and spin at 330*g* for 5 min. Repeat the wash (*see* **Note 4**). Resuspend the pellet from one spleen in 5 mL of DMEM-NMS and pour through a cell strainer into a sterile conical tube. Wash tube and strainer with an additional 5 mL per spleen for a total of 10 mL per spleen or LN. The single-cell suspension of spleen/LN is now ready for primary culture.

3.2. Primary Culture of T Cells

1. For primary cultures, cells are normally seeded at 1×10^7 cells in 1–2 mL of medium in 24-well tissue culture plates. The 1×10^7 LN/spleen cells are put into culture with the appropriate antigen at the desired concentration (*see* **Note 5**).
2. The cultures are then adjusted to the final volume with medium. No cytokine is added at this time to avoid generating interleukin (IL)-2-dependent T cells.

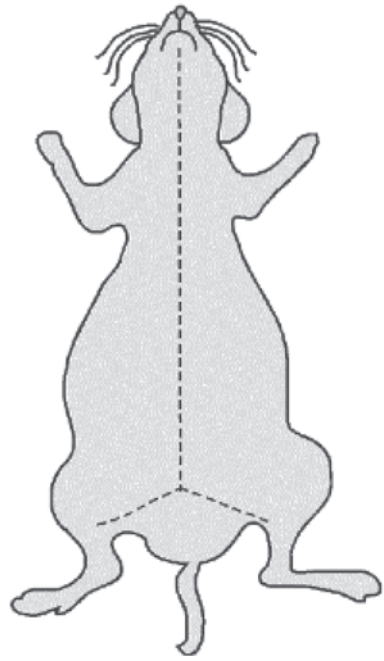

Fig. 1. Diagram of subcutaneous incision for isolation of LNs and spleen from diabetic and antigen-specific immunized mice. Animals are soaked in 70% ethanol to create an aseptic environment and matt the fur. The first incision is from the urethral opening to the chin, then from the urethral opening to either side of the knee. The incision is made to keep the peritoneal wall intact so the organs remain within the peritoneal cavity. (Obtained with permission from The Virtual Mouse Necropsy, www.geocities.com/virtualbiology/necropsy.html.)

3. The cells are cultured for 5 d at 37°C and 5% CO_2. After the 5-d incubation, the cells are ready to be restimulated according to the standard restimulation protocol (*see* **Subheading 3.3.**). This protocol is carried out every 2 wk (*see* **Note 6**). At this point, the primary culture contents can be switched into complete medium (CM).

3.3. Restimulation of Th1 T-Cell Clones

3.3.1. Responder T Cells

1. Responder T cells from a 2-wk restimulation flask are considered resting T cells and are used to continue the propagation of the antigen-specific T cells in a new 2-wk restimulation cycle. After resuspending the cells thoroughly, remove 100 µL to determine cell count and viability.
2. Add 20 mL trypan blue to identify dead cells, and count viable cells using a hemacytometer.

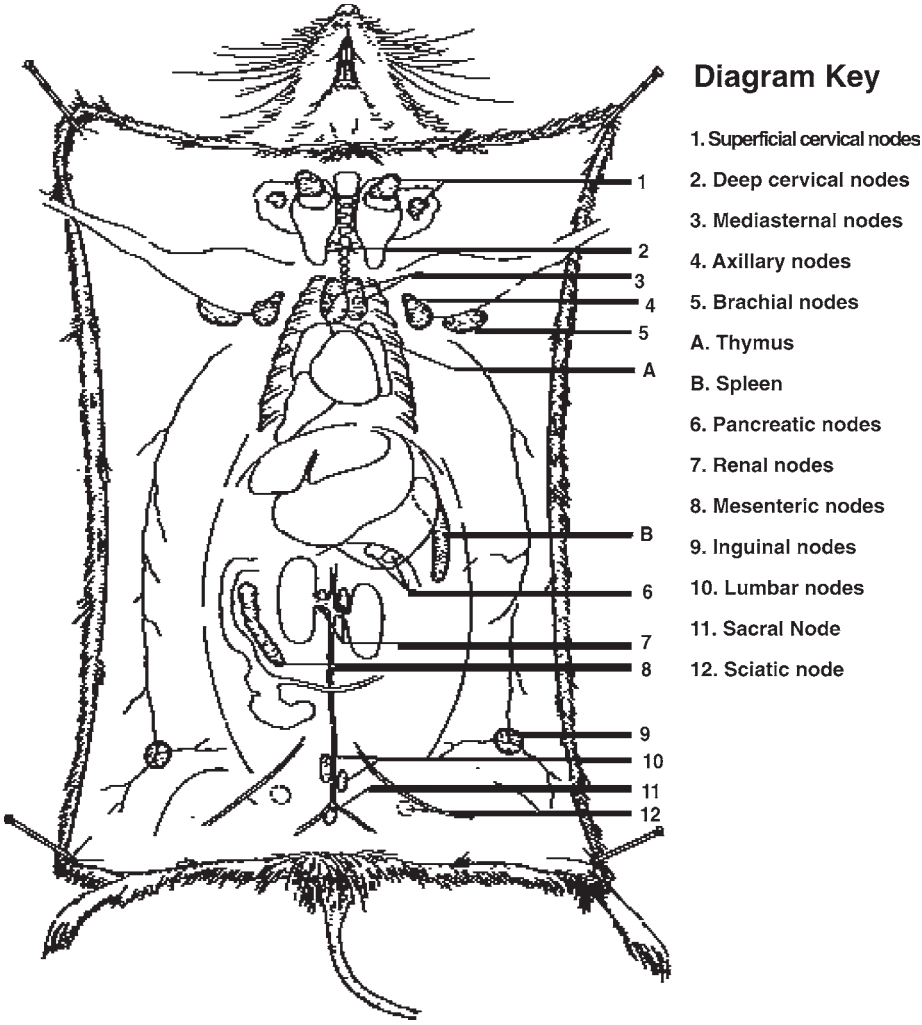

Fig. 2. Diagram of LNs located subcutaneously or in the connective tissues between muscles. If the animals have been immunized prior to harvesting the LNs, it will not be difficult to locate the nodes. If the animal has not been immunized, the nodes may be difficult to see. Look for bead-shape structures, which can range in color from a yellowish white to tan, depending on the strain of the mouse. Clearly, if the mouse is pigmented, the nodes will be darker than those of an albino mouse.

3.3.2. Preparation of APCs

1. Aseptically remove spleens from nondiabetic NOD mice not younger than age 6 wk and place in snap-cap tubes containing 2 mL CM.
2. In a homogenizer, break up organ to the point at which a single-cell suspension is achieved as described in **Subheading 3.2.**
3. Prepare a 1:50 dilution by adding 20 µL of spleen cells to 980 mL CM. Pipet 100 µL of cells into a 0.6-mL centrifuge tube containing 20 mL trypan blue. Count viable cells (not RBCs) using a hemacytometer (*see* **Note 7**).
4. APCs must be irradiated at 3500 rad or treated with mitomycin C (25 µg/mL) prior to addition to restimulation cultures. These treatments block lymphocyte proliferation, but allow processing and presentation of antigen by APCs. In addition, peritoneal macrophages may be used as a source of APCs without the need for irradiation (*see* **Note 8**).

3.3.3. Antigen for Whole Islet/Islet-Antigen Reactive T Cells

Irradiated (3500 rad) islet cells, islet fractions, or specific islet-associated antigen(s) may be used (*see* **Note 8**).

3.3.4. Components of Restimulation Culture

1. In a 25-cm^2 tissue culture flask, combine 1×10^6 responder T cells (5 mL at 2×10^5 cells/mL) and 2.5×10^7 irradiated or mitomycin C-treated APCs (25 µg/mL) (2.5 mL at 1×10^7 cells/mL).
2. If carrying T cells on islet cells use 5×10^4 islet cells (2.5×10^3 cells/mL) or other desired antigen and 7 U/mL recombinant IL-2 (rIL-2).
3. Bring to a volume of 20 mL with CM, loosen caps slightly to allow for gassing (if not vented), and tighten after 24 h.
4. Incubate flasks upright at 37°C and 5% CO_2 for 2 wk.

3.4. Assay of Antigen-Specific Response of T-Cell Clones

3.4.1. Responders (T Cells)

Resting T cells from 2-wk restimulation culture are counted as described in **Subheading 3.3.1.** and diluted to 2×10^5 cells/mL with fresh CM after centrifugation at 330*g* for 10 min.

3.4.2. APCs for Antigen-Specific T-Cell Response

The procedure is as described in **Subheading 3.3.2.** for APC isolation. Count viable cells (not RBCs) using a hemacytometer.

3.4.3. Antigen

Islet cells are prepared as for restimulation (5000 irradiated islet cells/well) (*see* **Note 8**). Use peptides or other antigens to test (various concentrations to be determined empirically).

3.4.4. In Vitro Antigen Recall Assay

To assess antigen specificity of T cells from primary culture, an in vitro antigen recall assay is performed. In a 96-well, flat-bottom tissue culture plate, add the following:

Responder T cells: 20,000 cells/well in 100 μL
APCs: 5×10^5 cells/well in 50 μL
Antigen: Appropriate concentration in 50 μL
Indomethacin: 50 μL of 100 m*M* solution, 20 m*M* final concentration.
Control wells: Responder T cells alone and responder T cells plus APC (no antigen), both in triplicate (*see* **Note 9**).
Bring control wells to a volume of 200 μL with CM. At 65 h, plates can be pulsed with 1 μCi/well tritiated thymidine and harvested on glass filter mats 6–8 h later using a cell harvester. Proliferation quantified by thymidine incorporation can then be determined by counts per minute on a scintillation counter. Alternatively, assessment of antigen specificity can be determined by harvesting SNs at 72 h for enzyme-linked immunosorbent assay analysis of interferon-γ.

3.4.5. Cloning of Antigen-Specific T Cells for Generation of T-Cell Clones

Once it has been established that the T cells from the restimulation flask are antigen specific in an in vitro antigen-specific recall assay, the T-cell lines can be cloned under limiting dilution conditions. The T-cell lines are cloned by limiting dilution in 96-well, round-bottom plates containing 5×10^5 irradiated APCs, 5×10^3 irradiated islet cells or specific islet cell protein as antigen and rIL-2 (7 U/mL).

3.5. Preparation of Cells for Adoptive Transfer

3.5.1. Expansion of T-Cell Clones or Lines

For the expansion of T-cell clones for use in adoptive transfer assays, it is necessary to prepare additional restimulation flasks as described in **Subheading 3.3.**. These additional flasks are used to seed the larger expansion cultures to generate the required number of T cells for transfer into recipient.

1. On day 4 after restimulation, prepare fresh CM. Add rIL-2 (14 U/mL) and CM to appropriately sized flasks (*see* **Table 1**).
2. Set on ice for 20 min to help facilitate removal of the cells from the bottom of the flask.
3. Remove 100 μL for counting.Transfer remaining volume to expansion flask.
4. For cells that stick to the bottom of the flask even after ice treatment, it is necessary to remove the medium, rinse the bottom of the flask with HBSS (calcium and magnesium free) or PBS, add 1 mL of nonenzymatic cell dissociation buffer, and incubate for 3 min at 37°C. Vigorously tap the flask to resuspend and remove cells. Rinse the flask with reserved medium and retain.

Table 1
Components Expansion Culture

Components	162-cm^2 flask[a]	75-cm^2 flask[a]	75-cm^2 flask[a]	25-cm^2 flask[a]
T-cell clones	20 mL	10 mL	5 mL	2 mL
CM	95.2 mL	47.6 mL	23.8 mL	7.6 mL
Total volume	120 mL	60 mL	30 mL	10 mL

[a]Recombinant IL-2 (rIL-2) (14 U/mL) is added to the flask to facilitate T-cell expansion.

5. Centrifuge the cells at 330*g* for 5 min. Resuspend the cell pellet in 20 mL of fresh CM and add to a 162-cm^2 flask with CM and rIL-2 according to **Table 1**.
6. Culture the cells for 4 d at 37°C and 5% CO_2 with the flasks lying flat.
7. On day 4 of subculture (day 8 since restimulation), remove and save the supernatant (SN) in 50-mL tubes. Rinse the flask with 5 mL HBSS and save with SN. Add 7 mL dissociation buffer to each 162-cm^2 flask (4 mL dissociation buffer for 75-cm^2 flasks) and incubate for 3 min at 37°C. Strike the flask hard with the heel of a gloved hand to bring cells off the flask bottom (cells tend to come off in a sheet).
8. Resuspend the cells with a pipet. Pour the reserved SN back into the flask, mix, and remove an aliquot for counting. Note the volume for calculation of cell yield.

3.5.2. Preparation of Expanded T-Cell Lines/Clones for Injection

1. Centrifuge cells in 50-mL tubes at 330*g* for 10 min.
2. Remove SN and resuspend cells with HBSS. Pool cells into a 50-mL tube and bring to a volume of 30–50 mL with HBSS.
3. Wash cells by centrifugation at 330*g* for 10 min. Repeat the washing and resuspend cells in HBSS at the appropriate concentration for injection (2×10^8 cells/mL for intraperitoneal injection of 10^7 cells in 50 μL).
4. Keep the cells on ice. Inject the cells as soon as possible. Mix well (do not vortex) before filling syringe. When loading syringe, remove needle and pull up cells (pulling cells through the needle will shear the cells).

3.5.3. Preparation of Diabetic Spleen Cells for Adoptive Transfer

1. Single-cell suspensions of spleen cells from diabetic NOD mice are prepared in HBSS using a glass tissue homogenizer and adjusted to 2×10^8 cells/mL.
2. For adoptive transfer experiments, mononuclear cells are counted, and cell viability is determined using trypan blue, a hemocytometer, and phase contrast microscopy or via a Coulter counter (*see* **Note 10**).
3. For phenotypic analyses, RBCs are lysed in spleen cell preparations by incubation in ACK lysis buffer (150 mM NH_4Cl, 10 mM $KHCO_3$, 0.1 mM EDTA at pH 7.2) for 5 min at room temperature before determining mononuclear cell counts and viability.

3.5.6. Monitoring of Recipient Mice for Glucosuria and Hyperglycemia

Beginning 5–7 d after adoptive transfer, recipient NOD or NOD.*Rag* mice should be monitored daily for elevated urine glucose. When mice exhibit glucosuria, blood or plasma glucose levels should be determined. There are many reliable methods for testing circulating glucose levels. Some are more laborious than others. Most laboratories use handheld glucometers such as those used by diabetic patients. We currently use the Precision QID glucometer (MediSense, Waltham, MA). Mice with blood glucose levels above 16.5 m*M* (300 mg/dL) are considered overtly diabetic.

4. Notes

1. Avoid use of medium containing FCS in primary cultures because it will increase the chances of generating T cells specific to antigens in the FCS. These cells can be common in the NOD mouse. After two passes of T cells in primary culture, assessment of antigen specificity will determine at which point the cultures can be switched to DMEM plus 10% FCS (CM).
2. Normal mouse serum refers to serum obtained from a nonautoimmune mouse strain (i.e., C57BL/6, BALB/c). Serum from NOD mice or related strains should not be used. Use at 0.3–0.5% when fresh. If NMS is not fresh, it is necessary to use 1–2% as a supplement for media. Medium must be filtered after serum has been added.
3. It is very important to keep the splenocytes and any material or solution that comes in contact with the splenocytes sterile because recipient young NOD mice and NOD.*Rags* are especially susceptible to infection. Also, minimize the time between sacrificing the animal and removing the spleen. Submersion of the mouse in 70% ethanol, skinning the mouse, and turning the hair and outside skin under and away from the sterile (blue pad) surface reduce the chances of bacterial contamination.
4. If the RBC lysis buffer is left on the cells for too long, it will lead to lymphocyte cell death.
5. The donor mice for primary cultures (T-cell line/clone derivation) should be female to avoid problems with reactivity to H-Y antigen later in immunocompetent female recipients of adoptively transferred cells. Depending on the nature of the desired cells, a 1:1 ratio of LN cells to spleen cells tends to work the best for primary cultures. We do not add cytokine to primary cultures because addition of IL-2 can lead to IL-2-dependent cells growing out in the culture rather than antigen-specific cells; addition of IL-4 leads to an outgrowth of B cells. If cell number allows, it is a good idea to try several concentrations of antigen in the primary cultures.
6. If growth in the primary cultures is poor, cells can be restimulated in the wells with addition of APCs (irradiated spleen cells; *see* APC preparation, **Subheading 3.3.2.**), antigen, and rIL-2 and grown for an additional 2 wk in the 24-well plate before they are expanded to 20-mL restimulation cultures. When expanding

cells from the 24-well plate to 20-mL restimulation flasks, add all cells from 1 well to 1 flask even if the cell count is above 1×10^6.

7. Notes on APCs: For calculation, divide the hemacytometer cell count by 4 (the number of quadrants counted) and multiply by the dilution factor 10^4/mL. Also, multiply by the dilution factor in the counting sample (50) as well as that of adding trypan blue (1.2). Finally, multiply by the volume of cells (× milliliters) to find the total number of cells. Dilute spleen cells to 1×10^7 cells/mL with CM. Spleen cells should be kept on ice whenever possible until used. Irradiation (3500 R) can be done on a single-cell suspension or intact spleens using a cesium or cobalt source. Another option is to treat the APC preparation with mitomycin C (25 μg/mL). An alternative to having to irradiate the APC population for in vitro recall assays is to use peritoneal macrophages as APCs. These cells are isolated using a peritoneal wash protocol: Use 10 mL of CM to wash the peritoneum of NOD mice aseptically to obtain peritoneal cells (PCs) (mainly macrophages) following the protocol for exposing the intact peritoneal wall described regarding **Fig. 1**. Then, make a small incision near the top of the exposed area. Hold open the incision with forceps or a hemastat. Wash the peritoneum with 1 mL at a time of CM until the total 10-mL volume has been used. Wash once at 330*g* for 10 min. Resuspend in 2 mL CM. Count viable cells, excluding RBCs, using a hemacytometer. Dilute the PCs to 5×10^5 cells/mL with CM. Do not irradiate the PCs. Because these cells produce large amounts of prostaglandins, which can inhibit T-cell proliferation and cytokine production ***(19)***, it is necessary to culture them with the nonsteroidal anti-inflammatory agent indomethacin (Sigma I7378). A working stock of 1 m*M* in CM is heated in a tube in boiling water to get the indomethacin into solution and then dilute). Aliquots of stock and working solution should be stored at –20°C. Indomethacin (100 μ*M*) should be added at 50 μL to wells containing PC in in vitro antigen recall assays. The final concentration of indomethacin is 20 μ*M*.
8. The islet isolation protocol for the use of whole islets as a source of antigen should follow the protocol of Ablamunits et al. ***(20)***. It should be noted that islet cells are not whole islets. To generate islet cells from a whole-islet isolation, islets must be incubated in cell dissociation buffer for an additional time to generate single islet cells. These single islet cells are then counted to give the correct number of cells to use in the in vitro recall assay. Whenever possible, the use of a known antigen is always an easier method for generating the T-cell lines/clones.
9. The background values of responder T cells alone and responder T cells plus APC should be 10% or less of the values from the antigen-pulsed wells.
10. Because each recipient mouse should receive 10^7 diabetic splenocytes and one diabetic NOD spleen yields about 7×10^7 splenocytes after lysing, estimate how many mice need to be sacrificed, allotting for extra cells and error. For cell counting, a "Coulter counter" may be used in lieu of a hemocytometer. Our laboratory currently uses a Beckman Coulter® Z1 Cell and Particle Counter. For counting, the cells should be diluted. We recommend using a greater dilution because at high concentrations the probability of two or more cells passing through the aper-

ture simultaneously and being counted as one cell is high. Put 0.02 mL of the suspension of cells into a Coulter Accuvette 200 containing 20 mL of diluent (such as Coulter Isoton II). Mix the sample thoroughly before counting as the cells may settle to the bottom. This type of instrument has been available for a few decades, and depending on the model and manufacturer, the basic operation will differ. For the older machines, all calculations will need to be performed manually; the output of newer equipment can be set to display cell concentration in the cell suspension directly. The length of the count should be approx 13 s, from when the first number appears in the register to when the counts are displayed. If the counting time is longer than 13 s, the aperture may be clogged with debris and should be cleaned gently with the brush provided. Any count that is obtained when the aperture is obstructed or clogged has an unpredictable coincidence and should be repeated. For older devices, the count displayed is the number of cells in 0.5 mL. If 0.02 mL of cell suspension was diluted into 20 mL, multiply the number displayed by 2 to obtain the total counts per milliliter and then by 1000 (dilution factor) to determine the number of cells per milliliter in the original culture/cell suspension. Then, multiply by the total volume (in milliliters) of cell suspension to determine the total number of cells in the suspension.

Acknowledgment

We wish to thank Dr. Hubert Tse for his critical reading and suggestions for this chapter.

References

1 Greiner, D. L., Rossini, A. A., and Mordes, J. P. (2001) Translating data from animal models into methods for preventing human autoimmune diabetes mellitus: *caveat emptor* and *primum non nocere*. *Clin. Immunol.* **100,** 134–143.
2 Eisenbarth, G. S. (1993) Molecular aspects of the etiology of type I diabetes mellitus. *J Diabetes Complications* **7,** 142–50.
3 Bach, J. F. (1994) Insulin-dependent diabetes mellitus as an autoimmune disease. *Endocrinology Rev.* **4,** 516–542.
4 Christianson, S. W., Shultz, L. D., and Leiter, E. H. (1993) Adoptive transfer of diabetes into immunodeficient NOD-scid/scid mice. Relative contributions of $CD4^+$ and $CD8^+$ T-cells from diabetic vs prediabetic NOD.NON-Thy-1a donors. *Diabetes* **42,** 44–55.
5 Haskins, K., Portas, M., Bradley, B., Wegmann, D., and Lafferty, K. (1988) T-lymphocyte clone specific for pancreatic islet antigen. *Diabetes* **37,** 1444–1448.
6 Haskins, K., Portas, M., Bergman, B., Lafferty, K., and Bradley, B. (1989) Pancreatic islet-specific T-cell clones from nonobese diabetic mice. *Proc. Natl. Acad. Sci. USA* **86,** 8000–8004.
7 Haskins, K. and McDuffie, M. (1990) Acceleration of diabetes in young NOD mice with a $CD4^+$ islet-specific T cell clone. *Science* **249,** 1433–1436.

8 Miller, B. J., Appel, M. C., O'Neil, J. J., and Wicker, L. S. (1988) Both the Lyt-2+ and L3T4+ T cell subsets are required for the transfer of diabetes in nonobese diabetic mice. *J. Immunol.* **140,** 52–58.
9. O'Reilly, L. A., Hutchings, P. R., Crocker, P. R., Simpson, E., Lund, T., Kioussis, D., et al. (1991) Characterization of pancreatic islet cell infiltrates in NOD mice: effect of cell transfer and transgene expression. *Eur. J. Immunol.* **21,** 1171–1180.
10 DiLorenzo, T. P., Graser, R. T., Ono, T., Christianson, G. J., Chapman, H. D., Roopenian, D. C., et al. (1998) Major histocompatibility complex class I-restricted T cells are required for all but the end stages of diabetes development in nonobese diabetic mice and use a prevalent T cell receptor alpha chain gene rearrangement. *Proc. Natl. Acad. Sci. USA* **95,** 12,538–12,543.
11 Serreze, D. V., Chapman, H. D., Varnum, D. S., Gerling, I., Leiter, E. H., and Shultz, L. D. (1997) Initiation of autoimmune diabetes in NOD/Lt mice is MHC class I- dependent. *J. Immunol.* **158,** 3978–3986.
12 Graser, R. T., DiLorenzo, T. P., Wang, F., Christianson, G. J., Chapman, H. D., Roopenian, D. C., et al. (2000) Identification of a CD8 T cell that can independently mediate autoimmune diabetes development in the complete absence of CD4 T cell helper functions. *J. Immunol.* **164,** 3913–3918.
13 Katz, J. D., Wang, B., Haskins, K., Benoist, C., and Mathis, D. (1993) Following a diabetogenic T cell from genesis through pathogenesis. *Cell* **74,** 1089–1100.
14 Poulin, M. and Haskins, K. (2000) Induction of diabetes in nonobese diabetic mice by Th2 T cell clones from a TCR transgenic mouse. *J. Immunol.* **164,** 3072–3078.
15 Peterson, J. D., Pike, B., McDuffie, M., and Haskins, K. (1994) Islet-specific T cell clones transfer diabetes to nonobese diabetic (NOD) F1 mice. *J. Immunol.* **153,** 2800–2806.
16 Peterson, J. D., Berg, R., Piganelli, J. D., Poulin, M., and Haskins, K. (1998) Analysis of leukocytes recruited to the pancreas by diabetogenic T cell clones. *Cell Immunol.* **189,** 92–98.
17 Dobbs, C. M. and Haskins, K. (2001) Comparison of a T cell clone and of T cells from a TCR transgenic mouse: TCR transgenic T cells specific for self-antigen are atypical. *J. Immunol.* **166,** 2495–2504.
18 Piganelli, J. D., Flores, S. C., Cruz, C., Koepp, J., Batinic-Haberle, I., Crapo, J., et al. (2002) A metalloporphyrin-based superoxide dismutase mimic inhibits adoptive transfer of autoimmune diabetes by a diabetogenic T-cell clone. *Diabetes* **51,** 347–355.
19 Metzger, Z., Hoffeld, J. T., and Oppenheim, J. J. (1980) Macrophage-mediated suppression. I. Evidence for participation of both hydrogen peroxide and prostaglandins in suppression of murine lymphocyte proliferation. *J. Immunol.* **124,** 983–988.
20. Ablamunits, V., Elias, D., and Cohen, I. R. (1999). The pathogenicity of islet-infiltrating lymphocytes in the non-obese diabetic (NOD) mouse. *Clin. Exp. Immunol.* **115,** 260–267.

13

Experimental Use of Murine Lupus Models

Stanford L. Peng

Summary

Murine models of systemic lupus erythematosus provide fertile research systems for the pathogenesis and therapy of systemic autoimmune disease. Their phenotypes span the broad range of clinical manifestations of human lupus and consist of both spontaneous and experimentally induced disease in both inbred and targeted mutant animals. This chapter contrasts the clinical characteristics of these various models, providing an outline for the use and analysis of these in vivo autoimmune systems.

Keywords: Arthritis; autoantibodies; autoimmune diseases; glomerulonephritis; hemolytic anemia; lupus; inbred mice; knockout mice; mutant mice; transgenic mice.

1. Introduction

Systemic lupus erythematosus (SLE) remains a prototypical systemic autoimmune disease capable of affecting virtually any organ; it is hallmarked by the presence of autoantibodies against a wide spectrum of ubiquitous autoantigens, including DNA and ribonucleoproteins ***(1,2)***. Because of such myriad manifestations, studies of disease pathogenesis and clinical therapeutics have often turned toward animal models, primarily mice, which have disease that often highly resembles the serological and histopathological findings of human SLE ***(3,4)***. Dogs ***(5)*** and perhaps cats ***(6)*** may also develop lupus, but the murine system has remained the foremost focus of scientific investigations, in large part because of the availability of genetically homogeneous yet susceptible strains as well as immunological and genetic reagents.

This chapter provides an overview of these various murine models, focusing on their experimental utility and the assessment of their most commonly studied disease manifestations, autoantibodies and renal disease (**Tables 1–3**). A

From: *Methods in Molecular Medicine, Vol. 102: Autoimmunity: Methods and Protocols*
Edited by: A. Perl © Humana Press Inc., Totowa, NJ

Table 1
Genetics of Lupus-Prone Mice

Strain	H-2	Vα	Vβ	IgH-C	IgH-V	IgK
BXSB/Mp	b	b	b		b	c
50% C57BL/6	b	b	a	b	b	c
50% SB/Le	b					
C3H/HeJ-*gld*/*gld*	k	a	b	j		
CBA/K1Jms-*lpr*^{cg}	k	a	b	j		
MRL/Mp-+/+	k	a	b	j	j	a
12.6% AKR	k	a	b	d	d	a
12.1% C3H/Di	k	a	b	j	k	c
0.3% C57BL/6	b	b	b	b	b	c
75% LG/J	d/f	a			j	j
MRL/Mp-*lpr*/*lpr*	k	a	b	j	j	a
NZB.H-2^{bm12}	bm12	c	b	n	d	b
(NZB × NZW)F1	d/z					
NZB	d	c	b	n	d	b
NZW	z	d	[a]	n	d	c
(NZB × SWR)F1	d/q	c	a/b	n/p		
(NZW × BXSB)F1				[b]		
(SWR × SJL)F1	q/s		a			
SWR	q	c	a	p		
SJL	s	c	a	b		

(Assembled and adapted from **refs. *260–270***.)
[a]Deletion of Cβ1-Dβ2-Jβ2.
[b]d at IgH-4,5,6 (γ,δ,μ); e at IgH-1,2,3,7 (γ2a, α,γ2b,ε)

complete discussion of lupus pathogenesis as gleaned from these animal models is beyond the scope of this chapter and can be found in several other reviews ***(7–16)***.

1.1. New Zealand Strains

1.1.1. Origins

The most well-described New Zealand (NZ) lupus strains include the NZ black (NZB) × NZ white (NZW) F1 and NZ mixed (NZM). Their initial origins are somewhat obscure, but NZB appears to have originated in the late 1940s during inbreeding of outbred stocks at the University of Otago School of Medical Sciences, New Zealand, during efforts to develop mouse strains for cancer research ***(17–19)***, and NZW was derived separately in 1952 during selective

Table 2
Histopathology of Lupus-Prone Mice

Strain	Life span	Glomerulonephritis	Arthritis	Miscellaneous
BXSB/Mp	161 (m) 574 (f)	Exudative, proliferative	None Neutrophilic infiltrate	
MRL/Mp-+/+	546 (m) 476 (f)	F > D > M > MP	75% pannus and infiltrate	Sialoadenitis 95% Conjunctivitis 50% Band keratopathy 90% Vasculitis 7.6%
MRL/Mp-*lpr*/*lpr*	154 (m) 143 (f)	D > F > MP > M Monocytic infiltrate	75% Pannus and infiltrate	Sialoadenitis 100% Conjunctivitis 85% Band keratopathy 90% Vasculitis 55.8% Oophritis 72% Choroiditis 100%
NZB	469 (m) 430 (f)	Chronic without Ig	None	Peptic ulcer 50%
NZB/W F1	406 (m) 245 (f)	Crescentic	None	Sialoadenitis? Conjunctivitis? Oophritis 35% Choroiditis 60–90%
SWR/SJL F1		IgG/C3 deposits	None	

Assembled and adapted from **refs.** ***7,17,22,26,101,103,104,185,*** **and** *190***.**
D, diffuse; F, focal; M, membranous; MP, membranoproliferative.

Table 3
Autoantibody Production in Lupus-Prone Mice

Strain	dsDNA	snRNP	RF	RBC	gp70	Cryo	Miscellaneous
BXSB/Mp	100 (4–5 mo)	0	0	20–40	+	+	Albumin Transferrin
MRL/Mp-+/+	100 (4–5 mo)	83 (9 mo)	+	10	+	+	Albumin Transferrin La, Ro Ribosome P, S10 RNA poly I
MRL/Mp-*lpr*/*lpr*	100 (4–5 mo)	37 (5 mo)	+	10	+	+	Albumin Transferrin La, Ro, Su Ribosome P, S10 RNA poly I Laminin Cardiolipin Collagen Ubiquitin mitochondria
NZB/W F1	100 (4–5 mo)	0	–	20–40	+	+	RNA poly I RNA IL-2, ubiquitin
SWR/SJL F1	21 (40 wk)	70 (40 wk)	?	?	?	?	

Assembled and adapted from **refs. *7*,*17*,*22*,*26*,*101*,*103*,*104*,*185*,** and ***190***.

Numbers indicate frequency of specific autoantibody (at tested age, if known). Cryo, cryoglobulins; dsDNA, double-stranded DNA; RF, rheumatoid factor; RBC, erythrocyte; RNA poly I, RNA polymerase I; snRNP, small nuclear ribonucleoprotein.

inbreeding for white coat color ***(20,21)***. Subsequent intercrosses revealed that the NZB/W F1 progeny developed lethal glomerulonephritis, reminiscent of human SLE ***(22)***. In the late 1980s, efforts to understand the contribution of major histocompatibility complex (MHC) genes to disease pathogenesis led to the development of the NZB.H-2^{bm12} congenic strain through backcrosses of the spontaneously mutant I-A gene ***(23)***. Similarly, to facilitate genetic studies, inbreeding of NZB/W F1 offspring led to the development of several NZM strains, including the most well characterized, NZM/Aeg2410 ***(24,25)***.

1.1.2. Clinical Features

NZB/W F1 animals are primarily studied for the development of autoimmune glomerulonephritis, as well as autoimmune hemolytic anemia ***(7,17,22,26)***. The former develops in close relationship to anti-double-stranded DNA (dsDNA) antibodies, which develop in virtually all animals. In contrast, antierythrocyte antibodies form in only approx 20–40% ***(22,27–31)***; several other autoantibody specificities have been described, but are less well characterized, including ribonucleoprotein ***(32–34)***, anticardiolipin ***(35,36)***, anti-Fcγ receptor (FcγR) ***(37)***, and anti-transfer RNA (tRNA) ***(38)***.

1.1.3. Use in the Study of Lupus Pathogenesis

The NZ system has received growing attention as a result of its use in dissecting genetic susceptibility to autoimmunity. Mapping of the *Sle* loci of the NZM strains, particularly NZM2410, has identified at least two susceptibility genes, *Cr2* (CR1/CR2; ***39***), and *Ifi202* ***(40)***, in addition to MHC ***(41–47)*** and perhaps tumor necrosis factor (TNF)-α ***(48,49)***. Several other loci remain to be identified fully ***(25,50–54)***.

NZB/W F1 animals have generally served as particularly useful models for the pathogenesis of anti-dsDNA and related immune complex glomerulonephritis, serving as the basis for many T-cell-focused models. Studies were performed demonstrating the importance of helper T cell–MHC class II interactions ***(55,56)*** in the selection of clonally selected, cationic charge binding specificity in anti-DNA antibodies ***(57–59)***; the identification of T-cell peptide epitopes derived from chromatin or nucleosomes ***(60–62)***; and the importance of pathogenic targets like complement ***(63)***, FcγR ***(64,65)***, CTLA4Ig, and CD154 ***(66–70)***. In addition, many studies have explored the relevance to disease of autoantigen epitope spreading ***(71–73)*** and idiotype networking ***(74–78)***. Other investigations have demonstrated the importance of the Th1 cytokine interferon (IFN)-γ ***(79–81)***, but have found conflicting roles for TNF-α ***(48,82)***, interleukin (IL)-2 ***(83)***, IL-4 or IL-12 ***(84,85)***, IL-6 ***(86)***, and IL-10 ***(87)***.

At the same time, NZ animals are characterized by intrinsically abnormal B cells, which can be solely responsible for disease induction ***(88–96)***. They possess unusual B1 cells ***(93,97)*** and/or $CD1^{hi}$ B-cell populations ***(98)***, which play a uniquely prominent role.

1.2. Murphy's Recombinant Large/MpJ

1.2.1. Origins

Murphy's recombinant large (MRL)/Mp mice developed from efforts in the 1960s to develop inbred mouse strains for the study of obesity ***(20,99)***, but they were found to develop autoantibodies and end-organ disease highly reminiscent of human SLE. They currently are estimated to consist of 75% LG/J, 12.6% AKR, 12.1% C3H/Di, and 0.3% C57BL/6 lineages. During the 12th brother-by-sister intercross, the spontaneous lymphoproliferation (*lpr*) mutation developed, associated with massive lymphadenopathy and precocious autoimmunity (***100–102***; *see* **Subheading 1.6.1.**).

1.2.2. Clinical Features

Of the available lupus-prone strains, MRL/Mp and their congenic MRL/Mp-*lpr*/*lpr* strains develop the most systemic and severe form of autoimmunity, involving multiple autoantibody specificities, such as anti-dsDNA, ribonucleoprotein (including small nuclear ribonucleoproteins [snRNPs], Ro, La, Su), ribosomal, and erythrocyte, as well as rheumatoid factor and cryoglobulins. End-organ disease includes not only varying and severe forms of glomerulonephritis, but also sialoadenitis in about 90–95% and inflammatory arthritis in about 75%, as well as less-often described but often seen inflammatory lesions of the liver, eyes, blood vessels, reproductive organs, and nervous system ***(7,101,103,104)***.

1.2.3. Use in the Study of Lupus Pathogenesis

MRL animals have sometimes been preferred in the study of autoimmunity because of their many clinical manifestations. Like NZ mice, MRL mice have been amenable to studies of anti-DNA responses, for which autoantibody responses support a T-cell-dependent, autoantigen-driven maturation ***(57,105)***; but perhaps because the autoimmune response of these animals is not as restricted as in NZ or BXSB animals, MRL pathogenesis has proven somewhat more complex, associated with diffuse, nonspecific, intrinsic hyperactivation of T and B cells ***(90,106,107)***. Here, many investigations have delineated the clonal evolution of polyspecific autoantibodies ***(108–120)***, including the diversification of autoantibody responses ***(121,122)***, as well as the possible contribution of receptor editing and revision ***(123–125)***. Transgenic

approaches have furthered such investigations by facilitating the identification and tracking of autoreactive B cells ***(126–129)***. Genetically altered animals have been particularly helpful in delineating roles for specific cell populations ***(130–134)***, cytokines and chemokines ***(135–138)***, complement ***(139,140)***, costimulatory molecules ***(141–144)***, and other receptors (e.g., ***145–147***).

In contrast to NZ models, genetic analysis of MRL autoimmune susceptibility has remained somewhat elementary ***(148–152)***. However, the successful development and use of MRL embryonal stem cells suggests that future genetic manipulations may be facilitated ***(153,154)***.

Interestingly, and in many cases fortunately, the *lpr* mutation primarily accelerates and amplifies underlying disease processes ***(155–157)*** rather than imposes an autoimmune diathesis. As such, many researchers prefer MRL/Mp-*lpr/lpr* mice to accelerate their in vivo assay of autoimmunity. On the other hand, however, because of defects in CD95 (apoptosis)-related pathways, *lpr* animals develop severe lymphadenopathy because of the massive accumulation of $CD3^+CD4^-CD8^-$ T cells, which often eventually infiltrate end organs, potentially confusing some histological assessments (*see* **Subheading 1.6.1.**).

1.3. BXSB Animals

1.3.1. Origins

BXSB mice originated at the Jackson Laboratory in Bar Harbor, Maine, through inbred selection of the satin, nonbeige phenotype after a C57BL/6 × SB intercross ***(20)***. Y-chromosome-linked autoimmunity was observed by the late 1970s ***(100–102,158)***.

1.3.2. Clinical Features

Like NZ animals, disease in BXSB consists predominantly of anti-DNA antibodies and glomerulonephritis; antierythrocyte antibodies have been described, but are not well characterized. Unlike other lupus models, however, BXSB develops a male-predominant disease because of the Y-linked autoimmune accelerator (Yaa; *see* **refs. *158*** and ***159***), inherited from the SB/Le parental strain ***(160)***, which is solely responsible for conferring disease to susceptible strains ***(161,162)***.

1.3.3. Use in the Study of Lupus Pathogenesis

Although less well studied than NZ or MRL mice, BXSB animals have also been used in studies of lupus genetics ***(163–166)***, and for studies of the T-cell-dependent development of pathogenic anti-DNA antibodies ***(105,167,168)***. The roles of some cell lineages, cytokines, and costimulatory molecules have been investigated ***(169–172)***, and some transgenic studies have implicated the impor-

tance of abnormalities of antigen presentation ***(45,173)***. Like other lupus models, BXSB animals are characterized by intrinsically abnormal B cells, but they may possess more T-cell dependence than NZ or MRL cells ***(90,100,106,174–176)***. Like MRL/Mp-*lpr*/*lpr*, embryonal stem cells have been derived, opening the possibility for direct genetic manipulation ***(153)***.

1.4. Other Spontaneous Models

Similar to the traditional New Zealand models, the (NZB × SWR) F1 (SNF1) model has been often used to characterize the anti-DNA response, including the recognition of nucleosomal peptides by autoreactive T cells ***(60,62,177)***, as well as the importance of specific residues and motifs in anti-DNA antibodies ***(57)***, often in "receptor presentation" ***(178)***. Some genetic studies have begun ***(179,180)***, and as in NZ strains, some studies have confirmed potential roles for peptide tolerization ***(61)*** and costimulatory blockade ***(181)***.

The (NZW × BXSB) F1 model resembles the traditional BXSB model in several respects, including the dominant importance of *Yaa* ***(182)***. Interestingly, however, these animals develop glomerulonephritis in both sexes (resembling BXSB in males, NZB × NZW F1's in females), as well as immune-mediated thrombocytopenic purpura, degenerative vascular lesions, and coronary artery disease, which may be related to anticardiolipin antibodies ***(183–187)***. Still, few studies to date have directly investigated pathogenic processes in this model, with only a few preliminary genetic studies involving MHC and other loci ***(188,189)***.

Other, even less-well-characterized models include the NZW (female) × SB/Le (male) F1, which develops disease virtually identical to BXSB ***(160)***, and the experimental autoimmune encephalomyelitis-susceptible SWR × SJL F1, which develops several autoantibodies and glomerulonephritis similar to human SLE ***(190,191)***. The spontaneous crescentic glomerulonephritis-forming mouse/Kinjoh (SCG/Kj) was derived from a BXSB/Mp × MRL/Mp-*lpr*/*lpr* F1 hybrid ***(192)*** and interestingly develops antineutrophil cytoplasmic antibodies that crossreact with anti-DNA ***(193)***.

1.5. Experimentally Induced Models

Few widely used, experimentally induced models exist for lupus. Graft-vs-host disease models have been sometimes studied because of the concomitant development of lupuslike autoimmunity; however, given the importance of allogeneity, its physiology probably represents a mode of pathogenesis distinct from the other lupus models described here ***(194)*** (*see also* Chapter 14). Alternatively, when exposed to bacillus Calmette-Guerin, nonobese diabetic mice have been demonstrated to develop hemolytic anemia, autoantibodies, worsened sialadenitis, and immune complex-mediated glomerulonephritis ***(195)***, but

follow-up studies have not been reported. Otherwise, two major models have been utilized predominantly by two research groups: pristane and 16/6 idiotype (Israel).

1.5.1. Pristane

The aliphatic hydrocarbon pristane (2,6,10,14-tetramethyl-pentadecane) has long been known to induce plasmacytomas ***(196–199)*** and arthritis ***(200–204)*** in susceptible BALB/c mice. Relatively recently, it was found to induce, in several strains, many different serological autoimmune phenomena, including anti-DNA and antiribonucleoprotein antibodies and glomerulonephritis ***(205–208)***, through mechanisms dependent on IFN-γ ***(209)***, IL-6 ***(210)***, and CD95–CD95L interactions ***(211)***. In some strains, antiribosomal P antibodies are seen as well ***(212)***. Because plasmacytoma induction by pristane exhibits both strain and housing dependence, it remains unclear whether this model will be widely useful in the study of murine lupus ***(213,214)***.

1.5.2. 16/6 Idiotype (Israel)

When immunized with the common human anti-DNA idiotype 16/6, C3H mice develop a syndrome highly reminiscent of lupus after a booster, including anti-DNA and antiribonucleoprotein autoantibodies, leukopenia, proteinuria, and renal immune deposits and sclerosis ***(215)***, as well as anticardiolipin antibodies and antiphospholipid antibody syndrome ***(216–218)***. This model is particularly susceptible to modulation by idiotype-derived complementary determining regions ***(219,220)*** and interestingly requires MHC class I ***(221)*** and TNF-α ***(222)***, in contrast to studies in human lupus. One English study failed to reproduce this model ***(223)***, also suggesting housing dependence to the penetrance of the disease, possibly limiting this model's generalized usefulness.

1.6. Lupus-Prone Mice With Defined Mutations

1.6.1. lpr/gld and Other CD95 Pathway Mutations

This group of recessive mutations share in common defective signaling via the CD95 (Fas)–CD95 ligand apoptosis pathway. The CD95 mutant *lpr* arose spontaneously during inbreeding of the MRL/Mp strain ***(100–102)*** because of a disabling insertion of an endogenous retrotransposon ***(224–227)***. The *gld* mutant arose spontaneously in C3H/HeJ mice ***(228)*** as a point mutation in CD95 ligand ***(229,230)***. Lpr^{cg} arose spontaneously in a Japanese CBA/KlJms colony ***(231–236)***. CD95-deficient animals were generated purposefully by gene targeting ***(237,238)***.

In general, mice with defects in the CD95 pathway resemble the human autoimmune lymphoproliferative syndromes, which include mutations in CD95

(Canale-Smith syndrome; ***239–241***), CD95 ligand ***(242)***, and caspase-10 ***(243)***. These syndromes share in common the development of severe lymphadenopathy because of $CD3^+CD4^-CD8^-$ T cells and the high incidence of often lupuslike autoimmune disease. CD95 defects alone generally do not convey autoimmunity *per se*, but rather accelerate and amplify any underlying autoimmune diathesis: For example, C57BL/6-*lpr* animals develop mild inflammatory disease consisting of lymphadenopathy, anti-single-stranded DNA (anti-ssDNA) antibodies, and mild, if any, glomerular disease; MRL/Mp-*lpr* animals develop widespread inflammation, including lymphadenopathy, autoantibodies of multiple specificities including anti-dsDNA, antiribonucleoprotein, anticardiolipin, and antiribosomal P, immune complex glomerulonephritis, as well as sialadenitis and hepatitis (*see* **Subheading 1.2.**; ***155–157***). Thus, these mutations have often been used in murine lupus to accelerate the in vivo assay.

Otherwise, these animals have typically been combined with their wild-type congenic counterparts to analyze the role of the CD95 system in immune regulation, such as the regulation of autoreactive B cells by T cells ***(126,244–246)***. They are also sometimes used as part of a model for graft-vs-host disease, in which donor *lpr* bone marrow cells induce a wasting disease in non-*lpr* recipients ***(247)***.

1.6.2. Other Defined Mutations

Several other mutant animal models have been found incidentally to develop systemic autoimmune manifestations, such as antinuclear antibodies and renal immune deposits, with or without overt glomerulonephritis (**Table 4**). Because detailed autoimmune analysis of these animals has not been performed, their use as a lupus model and relevance to human lupus remain on the whole undetermined.

1.7. Conclusions: The Selection of Murine Lupus Models

The diverse array of inbred and genetically altered mice provides many models for systemic lupus erythematosus, each with particular clinical manifestations and unique pathogenesis (**Tables 1–4**). Investigators should therefore choose models based on areas or phenomena of interest within the lupus autoimmune spectrum: For instance, studies focusing on anti-dsDNA antibody responses, T-cell autoreactivity, or hemolytic anemia may find the best supporting literature and precedence in the NZ systems. In contrast, studies of diversification and diversity of autoantibody repertoires and multisystem autoimmune disease may prefer MRL models. Congenic autoimmune-prone CD95-mutant animals, like MRL/Mp-*lpr*/*lpr*, may provide particularly rapid assay systems, but investigators should beware of possible confounding from the concomitant, severe lymphadenopathic process. Finally, studies with interests

Table 4
Targeted Genes With Lupus-Like Phenotypes

Locus	Mutation	Reference
Apoptosis and cell cycle-related molecules		
CD95	Dominant-interfering transgenic	***271***
CDK	Knockout[a]	***272,273***
bcl-2	Transgenic	***274***
bim	Knockout	***275,276***
E2F2	Knockout	***277***
GADD45	Knockout	***278***
Pten	Heterozygote	***279***
	T-cell-specific knockout	***280***
Receptors		
B7RP-1	Transgenic	***281***
CD21/CD35	Knockout	***282***
CD22	Knockout	***283***
CD45	Phosphatase deficiency	***284***
CD152	Knockout	***285,286***
FcγRII	Knockout	***287***
G2A	Knockout	***288***
IL-2Rβ	Knockout	***289***
PD-1	Knockout	***290***
TCR-α	Knockout	***291***
Miscellaneous		
Aiolos	Knockout	***292***
C1q	Knockout	***293,294***
BLys/BAFF/TALL-1	Transgenic	***295–297***
Cbl-b/Vav-1	Knockout	***298***
C4	Knockout	***282***
IEX-1	Transgenic	***299***
Lyn	Knockout	***300–302***
MER	Knockout	***303***
Mgat5	Knockout	***304***
Stra13	Knockout	***305***
TGF-β	Knockout	***306,307***

[a]May be strain dependent.

in some specific genes might benefit from the lupuslike phenotypes that occur in animals genetically altered in those respective genes. Here, we describe a typical necroscopic assessment of the lupus-prone mouse, with particular focus on serological and renal assessment, which together remain the hallmark manifestations of murine lupus.

2. Materials

2.1. The Lupus-Oriented Necropsy

1. Blood collecting tubes, heparin coated, Natelson or Caraway (e.g., Fisher, Hampton, NH, cat. no. 02-668-10 or 02-668-25).
2. Dissecting tools: scissors, forceps.
3. Dissection board (e.g., a styrofoam box lid).
4. Dry ice.
5. 10% buffered formalin.
6. 70% and absolute ethanol.
7. Medium for tissue culture (depending on follow-up applications).
8. 22- to 27-ga needles.
9. Optimal cutting temperature (OCT) Tissue-Tek medium (Andwin Scientific, Warner Center, CA, cat. no. 4583).
10. Pasteur pipets.
11. Phosphate-buffered saline (PBS).
12. 1- to 3-mL and 10-mL syringes.
13. Microcentrifuge tubes.

2.2. Analysis of Serum

2.2.1. Immunoglobulin Isotype Titers by Enzyme-Linked Immunosorbent Assay (ELISA)

1. Alkaline phosphatase (AP) substrate (e.g., Sigma, St. Louis, MO, 104-105 tablets).
2. Antibodies
   a. For capture (e.g., from Southern Biotechnology Associates, Birmingham, AL):
      - goat F(ab')2 antimouse immunoglobulin (Ig) (SBA 1012-01) for IgM, IgA, and IgG
      - rat antimouse IgE (23G3, SBA 1130-01)
   b. For detection:
      - goat antimouse IgM-AP (SBA 1020-04)
      - goat antimouse IgA-AP (SBA 1040-04)
      - goat antimouse IgG1-AP (SBA 1070-04)
      - goat antimouse IgG2a-AP (SBA 1080-04)
      - goat antimouse IgG2b-AP (SBA 1090-04)
      - goat antimouse IgG3-AP (SBA 1100-04)
      - rat antimouse IgE-AP (SBA 1130-04)

c. For standards:
   - purified mouse IgM, IgA, IgG1, IgG2a, IgG2b, IgG3, IgE (e.g., myeloma proteins)

3. 2% bovine serum albumin (BSA) in PBS.
4. Carbonate buffer: 325 mL 0.1 *M* $NaHCO_3$, 50 mL 0.1 *M* Na_2CO_3.
5. DEA buffer: mix 49 mg $MgCl_2 \cdot 6H_2O$ and 96 mL diethanolamine in 800 mL H_2O, titrate to pH 9.8 by HCl, raise to 1 L, and store at 4°C in foil protected from light).
6. PBS.
7. PBS-Tween: PBS with 0.05% Tween-20.
8. High-absorbancy 96-well microtiter plates (e.g., Nunc Maxisorp 430341, Nunc, Rochester, NY).
9. Microplate reader capable of $OD_{405.}$

Optional:

10. 20- to 200-μL multichannel pipets.
11. Microplate washer.

2.2.2. Fluorescent Antinuclear Antibody Test

1. Cover slips for microscope slides.
2. HEp-2 cell substrate, mounted on microscope slide (e.g., INOVA Diagnostics, Zeus Scientific, etc.).
3. Fluorescein isothiocyanate (FITC)-antimouse IgG (e.g., cat. no. 31541, Pierce, Rockford, IL).
4. Fluorescence-ready microscope.
5. Mounting medium.
6. PBS.

2.2.3. Anti-dsDNA: Crithidia

1. Coverslips for microscope slides.
2. *Crithidia* cell substrate, mounted on microscope slide (e.g., Antibodies Incorporated, Inc., Davis, CA).
3. FITC-antimouse IgG (e.g., Pierce 31541).
4. Fluorescence-ready microscope.
5. Mounting medium.
6. PBS.

2.2.4. Total Rheumatoid Factor ELISA

1. AP substrate (e.g., Sigma 104-105 tablets).
2. Antibodies
   a. purified murine IgG1, λ; IgG2a, λ; IgG2b, λ; and IgG3, λ (e.g., myeloma proteins).
   b. antimouse Igκ-AP (e.g., SBA 1050-04).
3. 2% BSA in PBS.
4. Carbonate buffer: 325 mL 0.1 *M* $NaHCO_3$, 50 mL 0.1 *M* Na_2CO_3.

5. DEA buffer: mix 49 mg $MgCl_2 \cdot 6H_2O$ and 96 mL diethanolamine in 800 mL H_2O, titrate to pH 9.8 by HCl, raise to 1 L, and store at 4°C in foil protected from light.
6. PBS.
7. PBS-Tween: PBS with 0.05% Tween-20.
8. High-absorbancy 96-well microtiter plates (e.g., Nunc Maxisorp 430341).
9. Microplate reader capable of OD_{405}.

Optional:

10. 20- to 200-µL multichannel pipets.
11. Microplate washer.

2.3. Renal Disease Assessment

2.3.1. Light Microscopy

1. Acid/alcohol differentiator: 10% acetic acid in 95% ethanol.
2. Coverslips for microscope slides.
3. Eosin Y Alcoholic (e.g., EM Science, Gibbstown, NJ, 588X-75).
4. 100, 95, 90, and 70% ethanol.
5. Mercury-free Harris Hematoxylin (e.g., EM Science 638A-71).
6. Poly-L-lysine-coated microscope slides.
7. Mounting media.
8. Paraffin.
9. Distilled or deionized and tap water.
10. Xylene.

2.3.2. Immunofluorescence for Immune Deposits

1. Acetone (at –20°C).
2. Coverslips for microscope slides.
3. Cryostat.
4. FITC-antimouse IgG (e.g., Pierce 31541).
5. Fluorescence-ready microscope.
6. Poly-L-lysine-coated microscope slides.
7. Mounting media.
8. PBS.

3. Methods

3.1. The Lupus-Oriented Mouse Necropsy

3.1.1. Tissue Harvest

1. Collect urine for analysis (e.g., ***248***), if desired (*see* **Note 1**).
   a. Cover the bottom of an empty mouse cage with plastic wrap (i.e., no bedding).
   b. Place mouse on plastic wrap.
   c. After 10–15 s, remove the mouse.
   d. Collect urine with a micropipet or Pasteur pipet.

2. Collect blood by retroorbital (RO) approach (e.g., http://www.upenn.edu/regulatoryaffairs/animal/annex9.html; *see* **Note 2**).
   a. Anesthetize the mouse.
   b. Apply pressure to the external jugular vein caudal to the mandible with thumb and gently elevate the upper eyelid with the index finger of the same hand.
   c. Insert a hematocrit tube into the medial canthus of the eye.
   d. Gently direct the hematocrit tube in a ventrolateral direction until blood is obtained.
   e. Once the desired amount of blood is obtained, discontinue the external jugular pressure and remove the hematocrit tube.
   f. Gentle pressure on the globe may be used to provide hemostasis.
   g. Empty the collected blood into a 1.5-mL Eppendorf tube or equivalent.
3. Euthanize mouse by CO_2 inhalation.
4. Collect peritoneal cells, if desired (*see* **Note 3**).
   a. Nick the abdominal skin below the sternum, taking care not to nick the peritoneum.
   b. Grab the two sides of the cut and gently pull apart the abdominal skin with a firm but gentle movement, exposing the sternum and the pelvis.
   c. Fit a 10-mL syringe with a 26- to 27-ga half-inch needle; fill with 5–7 mL of medium and 2–3 mL of air. Air is necessary to allow for intraperitoneal movement of fluid.
   d. Holding the sternum, fill the abdominal cavity with the medium and air. Remove the needle; the peritoneum self-seals.
   e. Vigorously shake the mouse in a supine position, caudad-cephalad, about 10–15 times.
   f. Prepare a Pasteur pipet with a rubber pipetter.
   g. Holding the sternum and peritoneum with forceps, insert the air-filled Pasteur pipet into the peritoneal cavity with a swirling movement.
   h. Express the air from the pipet into the peritoneum as much as possible.
   i. Collect as much fluid as possible into the pipet.
   j. Longitudinally cut the peritoneum from sternum to pelvis and collect the remaining fluid.
5. Fix the mouse on a flat surface (e.g., styrofoam box cover or dissecting tray) with 22- and/or 24-ga needles.
6. Spray fur with 70% ethanol. The ethanol prevents fur from loosening and interfering with the dissection.
7. Cut the skin (not the peritoneum) from leg to leg, arm to arm, and perineum to chin.
8. Pull apart the fur, exposing the neck, thorax, and abdomen. Pin the anterior skin flaps to the dissecting board with needles, exposing the mammary glands.
9. If the lung is to be harvested for histopathology, use a 1- to 3-mL syringe and 25- to 27-ga needle to cannulate the trachea and infuse approx 1 mL of fixative. This step expands the alveolar spaces prior to final fixation.

10. Superficial lymph nodes are easily recognizable in the mouse as small, grayish nodules resembling peas or beans.
    a. Harvest the inguinal lymph nodes at the crossing of the mammary arteries and superficial epigastric vein by grasping with forceps the fat pad in which it is contained.
    b. Harvest the submandibular lymph nodes located just distal to the darker submandibular glands, which lie inferior to the mandible. Use forceps to grasp the nodes and scissors to dissect them away from the glands (*see* **Note 4**).
    c. Harvest axillary lymph nodes in the axillary fossae.
    d. Harvest brachial lymph nodes just posterolateral to the axillae and near the scapular angle.
11. Harvest the submandibular glands, if desired.
12. Open the peritoneum (if not already done) and harvest the spleen just inferior to the stomach.
13. Cut away a piece of liver approximately the size of a spleen.
14. Remove kidneys.
15. Open the thorax by cutting the ribs on either side and cutting along the diaphragm in between. Gently lift the sternum to reveal the intrathoracic contents.
16. Harvest the thymus by holding it and dissecting the mediastinal tissue with scissors.
17. Remove the heart and lungs, if desired.
18. Harvest bones for bone marrow, if desired.
    a. Long bone dissection
        i. Insert the tips of a closed sharp pair of scissors in the thigh muscles just inferior to the femoral artery, meeting the femoral shaft.
        ii. Slide the closed scissors anterior to the femur and open them, detaching the anterior muscles from the femur.
        iii. Repeat steps 18.a.i. and 18.a.ii. on the posterior side of the femur.
        iv. Gently dislocate the femoral head from the acetabulum.
        v. Gently dislocate the distal femoral diaphysis from the knee.
        vi. Tibiae and humeri can be isolated in fashions similar to steps 18.a.i.–18.a.v.
    b. Vertebrae dissection.
        i. Remove all the visceral organs and most of the retroperitoneal tissue.
        ii. Deeply incise the left and right psoas muscles as close to the spinous processes as possible.
        iii. Cut the spine at the base of the thoracic vertebrae (at the level of the ribs).
        iv. Cut the spine at the base of the lumbar vertebrae (at the level of the pelvis).
        v. Remove the lumbar spine en bloc.

3.1.2. Tissue Processing

1. Serum isolation from whole blood (*see* **Note 5**).
   a. Allow the blood to clot at 4°C for 2 h to overnight.
   b. Microcentrifuge the sample at maximum speed (e.g., 20,800*g*) for 5 min.
   c. Collect the serum (the beige-colored, clear supernatant) with a micropipet.
2. For routine histopathology, use buffered formalin (*see* **Note 6**):
   a. Fix tissues of interest in 30 volume equivalents of 10% buffered formalin for 8–10 h at room temperature or 24 h at 4°C.
   b. Wash once with PBS (2–24 h) and transfer to 70% ethanol. Store at room temperature or 4°C until ready for processing.
3. For frozen tissue specimens (*see* **Note 7**):
   a. Prepare a dry ice-ethanol bath.
   b. Cut tissue into pea-size specimens still containing the anatomy of interest (e.g., for kidney, this usually equals about one-half of a hemisphere).
   c. Cut off the cap from a microcentrifuge tube for use as a mounting board. Place tissue on the cap (or other mounting apparatus as desired). Embed with OCT medium using just enough to cover the tissue.
   d. Immediately place the cap–tissue complex into the superchilled ethanol. Store at –70°C or below until sectioning.
   e. Section and stain per protocol for specific antigens (e.g., mouse IgG for kidneys).
4. Specimens to be analyzed in tissue culture or by flow cytometry can be rinsed in PBS and/or placed directly in complete cell culture medium.

3.2. Analysis of Serum (see Note 8)

3.2.1. Immunoglobulin Isotype Titers by ELISA

1. Coat 96-well plates with 50 µL/well of 2 µg/mL capture antibody in carbonate buffer at 4°C overnight (*see* **Note 9**).
2. Remove coating solution by tapping.
3. Block with 200 µL/well 2% BSA in PBS at 37°C for 2 h (*see* **Note 10**).
4. Remove blocking solution by tapping.
5. Make serial dilutions of each serum sample, such as 1:100, 1:200, 1:400, and so on, up to 1:102,400 in PBS and add 50 µL per well in duplicate (*see* **Note 11**).
6. Make serial dilutions of isotype standard control (e.g., 4000, 2000, 1000, 500, 250, 125 ng/mL) and add 50 µL per well in duplicate. Use a separate standard curve for each plate (*see* **Note 12**).
7. Incubate at room temperature for 1–2 h.
8. Wash each well four to six times with 200 µL PBS-Tween.
9. Dilute detection antibody 1:1000 to 1:2000 in PBS (according to manufacturer's instructions) and add 50 µL per well. Incubate at room temperature for 45–60 min.
10. Wash each well four to six times with 200 µL PBS-Tween.

11. Dissolve phosphatase substrate in DEA buffer to 1 mg/mL (e.g., one 5-mg tablet in 5 mL) and add 50 μL per well. Watch yellow color development in standard curve.
12. Read OD_{405} in a spectrophotometer. Interpolate and extrapolate Ig concentration in each sample using the standard curve and dilutions, averaging the duplicate samples. Serial OD readings may be necessary to obtain interpretable results for every sample. Discard sample readings outside the range of the standard curve. Note that optical density (OD) and concentration have a semilog relationship (*see* **Note 13**).

*3.2.2. Fluorescent Antinuclear Antibody Test (*see ***Note 14****)*

1. For screening, dilute test serum 1:40 or 1:50 in PBS and add 50 μL to a slide well of fixed, permeabilized HEp-2 cells. Incubate for 30–45 min at room temperature.
2. Wash slide four to six times with PBS in a Coplin jar, 5 min each time. Blot the excess fluid away after the last wash.
3. Dilute FITC-antimouse IgG 1:500 in PBS or as directed by manufacturer and add 50 μL to each well. Incubate for 30–45 min at room temperature protected from light.
4. Wash slide four to six times with PBS in a Coplin jar, 5 min each time. Blot the excess fluid away after the last wash.
5. Add three to five drops of mounting medium and coverslip to the slide. Observe slide immediately by fluorescence microscopy.
6. Titers less than 1:40 are generally considered negative. Positive samples, identified by the presence of any type of apple-green nuclear staining, can be fully titered by making serial dilutions (1:40, 1:80, 1:160, etc.) and repeating **steps 1–5** until an end point is reached.

3.2.3. Anti-dsDNA Assessment: Crithidia luciliae *Immunofluorescence (*see ***Note 15****)*

1. Dilute test serum 1:10 in PBS, add 25 μL to a slide well of fixed, permeabilized *Crithidia*. Incubate for 30–45 min at room temperature.
2. Wash slide four to six times with PBS in a Coplin jar, 5 min each time. Blot the excess fluid away after the last wash.
3. Dilute FITC-antimouse IgG 1:500 in PBS or as directed by manufacturer and add 25 μL to each well. Incubate for 30–45 min at room temperature protected from light.
4. Wash slide four to six times with PBS in a Coplin jar, 5 min each time. Blot the excess fluid away after the last wash.
5. Add three to five drops of mounting media and coverslip to the slide. Observe slide immediately by fluorescence microscopy.
6. Titers of less than 1:10 are generally considered negative. Positive samples are identified by the presence of apple-green fluorescence of both the nucleus (indicating positive antinuclear antibodies) and kinetoplast, the dsDNA-containing organelle near the base of the flagellum.

3.2.4. Total Rheumatoid Factor Assessment (ELISA) (see **Note 16**)

1. Coat 96-well plates with 50 μL/well of 0.5 μg/mL each of IgG1, λ; IgG2a, λ IgG2b, λ; and IgG3, λ in carbonate buffer at 4°C overnight.
2. Remove coating solution by tapping.
3. Block with 200 μL/well 2% BSA in PBS at 37°C for 2 h.
4. Remove blocking solution by tapping.
5. Make serial dilutions of each serum sample, such as 1:100, 1:200, 1:400, and so on up to 1:102,400 in PBS and add 50 μL per well in duplicate.
6. Make serial dilutions of a positive control, if available, and add 50 μL per well in duplicate. Use a separate standard curve for each plate.
7. Incubate at room temperature for 1–2 h.
8. Wash each well four to six times with 200 μL PBS-Tween.
9. Dilute AP-conjugated antimouse IgK antibody 1:1000 to 1:2000 in PBS (according to manufacturer's instructions) and add 50 μL per well. Incubate at room temperature for 45–60 min.
10. Wash each well four to six times with 200 μL PBS-Tween.
11. Dissolve phosphatase substrate in DEA buffer to 1 mg/mL (e.g., one 5-mg tablet in 5 mL) and add 50 μL per well. Watch yellow color development in standard curve.
12. Read OD_{405} in a spectrophotometer. Total rheumatoid factor (RF) activity is usually expressed as the absolute OD reading, but can be titrated against a positive control (e.g., a diseased MRL/Mp-*lpr*/*lpr* mouse).

3.3. Renal Disease Assessment

3.3.1. Light Microscopic

1. Embedding of tissue.
   a. Dehydrate tissue in 70% ethanol at room temperature for 1 h.
   b. Dehydrate tissue in 90% ethanol at room temperature for 1 h.
   c. Dehydrate tissue in 100% ethanol at room temperature for 1 h.
   d. Clear the tissue with three changes of xylene at room temperature for 1 h.
   e. Infiltrate the tissue with two changes of paraffin wax at 65°C.
   f. Reinfiltrate the tissue with paraffin wax at 65°C under vacuum.
   g. Embed the tissue and allow to set.
2. Cut 5- to 7-μm sections of kidney, placing them on a poly-L-lysine-coated slide.
3. Dewax slides at room temperature.
   a. Change twice in xylene, 3 min each.
   b. Change twice in absolute ethanol, 2 min each.
   c. Change twice in 95% ethanol, 1 min each.
   d. Change twice in 70% ethanol, 2 min each.
   e. Place in distilled water for 5 min.
4. Stain with hematoxylin and eosin.
   a. Stain with hematoxylin for 6–8 min.

b. Rinse in tap water for 45 s.
c. Rinse in acid/alcohol differentiator for 30–45 s.
d. Rinse with distilled water for 1 min.
e. Rinse with tap water for 1 min.
f. Stain in eosin Y alcoholic for 20–40 s.
g. Place in 95% ethanol for 30 s.
h. Change twice in absolute ethanol for 1 min each.
i. Change three times in xylene for 1 min each.

5. Add three to five drops of mounting media and coverslip to the slide. Allow to set overnight in fume hood before observing under light microscopy.
6. Disease can be assessed in three locations (*see* **Note 17**).
   a. Glomerular, for the presence of glomerulonephritis, typically diffusely proliferative and necrotizing, often with crescents. Focal, segmental, membranous, and/or sclerotic lesions are common as well.
   b. Tubular, for the presence of tubulointerstitial inflammation, typically composed of dense infiltrates of granulocytes and mononuclear cells, most common in the MRL strains.
   c. Perivascular, for the presence of perivascular inflammation, typically composed of dense infiltrates of granulocytes, lymphocytes, monocytes, and plasmacytoid cells, most common in MRL/Mp-*lpr*/*lpr* and related strains.

3.3.2. Immunofluorescence for Immune Deposits

1. Place the frozen kidney in OCT in the cryostat chamber for 10–20 min to allow the block to equilibrate in temperature. This is critical for quality of sections.
2. Place the tissue block on the cryostat specimen disk. Face the block until desired tissue is exposed.
3. Cut 5- to 7-μm sections of frozen kidney in OCT, placing them on a poly-L-lysine-coated slide (*see* **Note 18**).
4. Fix sections in cold acetone at –20°C for 2 min.
5. Wash slide three times in PBS at room temperature.
6. Add FITC-antimouse IgG, diluted 1:500 in PBS, just enough to cover the tissue (typically 25–50 μL). Incubate in a humidified chamber at room temperature and protected from light (*see* **Note 19**).
7. Wash slide three times in PBS at room temperature.
8. Add three to five drops of mounting media and coverslip to the slide. Observe slide immediately by fluorescence microscopy.
9. Positive samples are identified by apple-green fluorescence at the glomeruli (*see* **Note 20**).

3.3.3. Surrogate Assays for Renal Function

1. Serum analysis can be performed using commercially available kits for creatinine and/or urea nitrogen (e.g., Sigma), if desired.
2. Urine protein excretion can be quantified by various protein assays (e.g., Pierce), if desired.

3.4. Diagnosis of Murine Lupus

At present, there is no consensus as to the diagnosis of lupus in murine models, but in general, most studies judge experimental interventions based on the presence of antinuclear antibodies, including anti-dsDNA, and immune-deposit-related glomerulonephritis. Thus, minimal analysis includes assessment of the fluorescent antinuclear antibody test and anti-dsDNA antibodies and histopathological analysis of kidneys, often including immunofluorescence for IgG. The assessment of other organs, such as salivary glands or joints, has not been broadly studied or codified. In some investigations, serial analysis has been performed for antinuclear antibodies and/or specific autoantibodies (**Subheading 3.2.**), serum creatinine and urea nitrogen, urine proteinuria (**Subheading 3.3.**), and even kidney biopsies ***(249)***; unfortunately, such use remains nonstandardized, and the predictive value of any of these tests is incompletely known ***(250)***. Consequently, most experiments are performed as cross-sectional, necropsy studies in animals at a specified age, typically between 12 and 18 wk (since birth or immunization), based principally on serology and histopathology.

4. Notes

1. Mice usually urinate without provocation within 5–10 s or so by this method. Alternatively, multiple animals can be sampled simultaneously using a multicompartment tray. Wire mesh-bottom cages, such as used in metabolic assays, can be used, but are somewhat cumbersome for the present purposes.
2. Blood collection by cardiac puncture is not preferred because spilled blood may contaminate organs to be collected. The RO approach provides a rapid means to obtain blood; many investigators have found that anesthesia and postprocedure global pressure are unnecessary. However, proper training is required because ocular trauma may result. In addition, it is not amenable to multiple serial samples in a short period of time, although switching eyes allows for at least two relatively closely timed samples. The following techniques are adapted from http://www.upenn.edu/regulatoryaffairs/animal/annex9.html.
    a. Alternative 1: Lateral saphenous vein technique. This approach is often suggested because of its amenability to multiple serial sampling and low potential for animal harm and distress. However, like RO collection, it requires proper training; unlike RO, it generally requires specialized restraints or additional personnel and often requires 1 to 2 min for collection because of reduced blood flow (***251***; currently at http://www.uib.no/vivariet/mou_blood/Blood_coll_mice_.html).
        i. Restrain the mouse; this may require two people or a restraining device ***(252)***.
        ii. Shave the hair covering the lateral saphenous vein with a scalpel blade (the vein is located caudal and lateral to the fibula and tibia).

iii. Clean the shaved area.
iv. Apply pressure around the leg above the stifle (knee); this will help improve venous filling.
v. Puncture the saphenous vein with a 25-ga needle.
vi. Collect the blood accumulating over the incision using a hematocrit tube.
vii. Apply direct pressure to the incision for 1–3 min to facilitate hemostasis.
viii. Repeated blood samples may be obtained by removing the scab.

b. Alternative 2: Tail sectioning. This approach is a rapid, simple procedure that does not require significant training. Serial blood samples can be performed, but must be limited because of the length of the tail and the increased risk of inducing pain and distress. In general, a restraining device is required, but anesthesia is not ***(253)***.

i. Restrain the mouse ***(252)***.
ii. Clean the tail with an appropriate antiseptic solution.
iii. With a sterile scalpel blade, make a transverse section through the long axis of the tail 2 mm from the tip.
iv. Use a hematocrit tube or blood-collecting tube to collect blood dripping from the sectioned tail.
v. Massage the tail by passing the thumb and index finger from the base to the tip of the tail if blood flow is inadequate.
vi. Apply direct pressure to the incision for 1–3 min to facilitate hemostasis.
vii. Repeated blood sampling may be obtained by removing the clot or following **steps 1–6** with a new cut 1 mm from tip.

c. Alternative 3: Tail vein aspiration. This technique can potentially allow multiple serial samples with little harm to the animal, but requires significant proficiency to avoid permanent damage to the vein, which would disallow future aspirations. Restraint is required, and blood collection is often slow.

i. Anesthetize the mouse.
ii. Clean the area over the tail vein 3 cm from the base of the tail; use an acceptable antiseptic scrub.
iii. Make a small transverse incision partially through the lateral tail vein with a sterile scalpel blade.
iv. Use a hematocrit tube or blood collection tube to collect the blood dripping from the incision.
v. Apply direct pressure to the incision for 1–3 min to facilitate hemostasis.
vi. Subsequent blood samplings may be obtained in awake animals by removing the scab; if a new incision is required, the animal must be anesthetized.

3. Peritoneal cell collection is particularly used for B1 cell studies in NZ mice. During harvesting, too much force will cause laceration of the large vessels and intraperitoneal bleeding. Care should be taken to keep the needle hole as small

as possible. Best results are generally obtained if a firm hold on the sternum is maintained until the end of the peritoneal fluid harvest.

4. Here, investigators often also take several nodes from the nearby cervical chain, located just superior to the submandibular glands.
5. The stated protocol is a routine serum collection method that allows the blood to clot fully before serum collection. Alternatively, the serum can be collected immediately after blood collection (skipping **step 2**), as long as care is taken to avoid aspirating unclotted blood. Regardless, this type of serum collection will miss cold-precipitable cryoglobulins, which often comprise a significant part of the autoantibody repertoire of lupus-prone animals ***(102,254,255)***.
   a. Alternative: cryoglobulin serum collection.
      i. Collect blood at 37°C with prewarmed instruments and without anticoagulants (e.g., non-heparin-coated hematocrit tubes).
      ii. Allow the blood to clot at 37°C for 1–2 h.
      iii. Collect the serum by centrifugation at 37°C (e.g., by microcentrifuge at maximum speed for 5 min).
      iv. Incubate the serum at 0–4°C for 24–120 h and observe the development of a precipitate; the packed (centrifuged) volume of the precipitate is expressed as a percentage of the original serum volume, the cryocrit.
      v. Often, further confidence in the cryocrit is obtained by washing the precipitate three to six times in normal saline solution to reduce the possibility of precipitated salts or other proteins. In addition, the precipitate often is redissolved in saline at 37°C to confirm the warm solubility of the CGs; at this time, CG concentration can be determined by spectrophotometry, and further characterization can be accomplished by immunoelectrophoresis, ELISA, or other specific immunological assay ***(256)***.
6. Prolonged fixation does not affect morphology, but will affect immunodetection. Larger specimens will obviously need longer fixation times, but care should be taken because the outer regions of a large specimen will be fixed longer than the center, resulting in differential antigen availability during immunohistochemistry. For bone or bone marrow specimens, decalcification (e.g., via Decal; Decal Chemical Corp.) should be performed according to manufacturer protocol prior to ethanol dehydration.
7. Here, larger specimens are sometimes technically difficult to section. Also, a mount is helpful to allow the histopathologist to section through as much of the specimen as possible. Excess OCT will prolong the sectioning time. During sectioning, care should be taken that the cap does not fall away from the tissue with manipulation. However, once frozen, this usually is not a problem. Alternatively, many investigators simply place their tissue in a tissue cassette, add OCT or other embedding medium compatible with frozen specimens, and douse the

sample directly into the dry ice/ethanol bath. The tissue quality is no different from the protocol described in **Subheading 3.1.2.**, but the tissue will need to be processed without a mount.

8. For other specificities than those mentioned, many commercial sources produce ELISA systems with recombinant human autoantigens, which may be used for the assessment of murine autoantibodies, such as specificities against snRNPs (including Sm and RNP), Ro, La, and antiphospholipid. Some investigators have successfully purified their own autoantigens, such as chromatin or snRNPs, for their own autoantibody ELISA systems; unfortunately, the sensitivity and specificity of such protocols can be variably dependent on the quality of the antigen preparation. Immunoblot and immunoprecipitation techniques are also available, but also generally require the purification of autoantigen(s) and/or lengthy assays and so have generally not been widely used ***(257)***.
9. Several alternative capture–detection antibody combinations are available (e.g., BD Pharmingen). Note that most IgG2a reagents, including those listed in **Subheading 2.2.1**, capture and detect only $IgG2a^a$, not $IgG2a^b$, which is found in strains like C57BL/6 or SJL; such strains require the use of allotype-specific reagents (e.g., BD Pharmingen). In addition, coating can be performed for shorter periods, like 4 h at 37°C or 8 h at room temperature, but the efficiency of bonding seems diminished.
10. Longer periods, like overnight at 4°C, tend to overblock, leading to diminished OD signals.
11. High-titer dilutions are necessary to allow the detection of the extreme hypergammaglobulinemia seen in many lupus strains.
12. Higher concentrations than stated tend to exceed the binding capacity of most assay plates, leading to nonlinear signals.
13. The OD of a sample should lie within the linear range of the standard curve (on semilog paper) for proper interpretation.
14. Although HEp-2 cells are of human epithelial origin, they remain the most popular substrate because of their widespread commercial availability as part of human diagnostic kits and the ability of murine autoantibodies to crossreact with human antigens. Some investigators have elected to grow and/or prepare their own murine targets, such as murine spleen or liver, but the convenient, commercial HEp-2 substrates have largely supplanted such classical assays.
15. For most investigators, anti-dsDNA assessment by the *Crithidia* immunofluorescence technique affords the best compromise among reliability, reproducibility, and convenience ***(257)***. In contrast, the Farr radioimmunoassay is often considered the gold standard assay, but requires radioactivity and is somewhat unwieldy. Many ELISA systems are available, including many commercial systems, but they significantly vary in terms of their specificity and convenience, most commonly because dsDNA often denatures to ssDNA during the coating process. In addition, DNA binds poorly to many microtiter plate materials, prompting some investigators to use various conjugation methods to enhance substrate binding (e.g., precoating the microtiter plate with avidin and then adding biotinylated

dsDNA), but such a protocol also risks the development of ssDNA during the conjugation process. As such, many anti-dsDNA ELISAs are reported simply as anti-DNA to indicate the likely assessment of total anti-DNA, rather than specific anti-dsDNA, activity.

16. This rheumatoid factor ELISA generally provides the best compromise among reliability, reproducibility, and convenience. Limitations include the use of denatured, rather than native, autoantigen (IgG) and the detection of only κ-chain containing immunoglobulins. In addition, this technique does not discriminate among rheumatoid factor isotypes, so activity is generally reported in this assay as "total RF activity." IgM, IgA, and IgE rheumatoid factors could be assayed using appropriate secondary antibodies, but IgG RFs could not because the secondary antibodies would crossreact with the coated substrates. On the other hand, RF activity by this assay correlates strongly with disease activity in many murine models (e.g., ***258***). Investigators should remember that the IgG2a component of the target will need to be changed to IgG2c/IgG2a^b during the assessment of IgH^b allotype strains (e.g., C57BL/6). Otherwise, classical rheumatoid factor assays include solid-phase assays like radioimmunoassays, which are somewhat tedious, but nonetheless can discriminate specific RF isotypes.
17. Many studies evaluate only the glomerular lesions, which is the only area of consistent involvement across lupus-prone strains. These lesions have not been codified into pathological groups, so descriptions remain largely investigator dependent.
18. Some investigators use uncoated slides, but the sections have a tendency to detach from the slide in **steps 5** and **7**.
19. Blocking (e.g., with BSA or serum) is not necessary in this protocol. Other isotype-specific antibodies, such as for IgG subtypes or IgA, can be used here as well ***(259)***.
20. Often, nuclear staining is of the tubular epithelial cells is present, which probably reflects serum antinuclear antibodies not renal-specific immune deposits. Sometimes, staining of the tubular epithelium or glomerular capsule is present, but is of unclear significance.

References

1 Boumpas, D. T., Austin, H. A., 3rd, Fessler, B. J., Balow, J. E., Klippel, J. H., and Lockshin, M. D. (1995) Systemic lupus erythematosus: emerging concepts. Part 1: Renal, neuropsychiatric, cardiovascular, pulmonary, and hematologic disease. *Ann. Intern. Med.* **122,** 940–950.

2 Boumpas, D. T., Fessler, B. J., Austin, H. A., 3rd, Balow, J. E., Klippel, J. H., and Lockshin, M. D. (1995) Systemic lupus erythematosus: emerging concepts. Part 2: Dermatologic and joint disease, the antiphospholipid antibody syndrome, pregnancy and hormonal therapy, morbidity and mortality, and pathogenesis. *Ann. Intern. Med.* **123,** 42–53.

3 Burkhardt, H. and Kalden, J. R. (1997) Animal models of autoimmune diseases. *Rheumatol. Int.* **17,** 91–99.

4 Stoll, M. L. and Gavalchin, J. (2000) Systemic lupus erythematosus-messages from experimental models. *Rheumatology* **39,** 18–27.
5 Jones, D. R. (1993) Canine systemic lupus erythematosus: new insights and their implications. *J. Comp. Pathol.* **108,** 215–228.
6 Lusson, D., Billiemaz, B., and Chabanne, J. L. (1999) Circulating lupus anticoagulant and probable systemic lupus erythematosus in a cat. *J. Feline Med. Surg.* **1,** 193–196.
7 Theofilopoulos, A. N. and Dixon, F. J. (1985) Murine models of systemic lupus erythematosus. *Adv. Immunol.* **37,** 269–390.
8 Cohen, P. L. and Eisenberg, R. A. (1991) *Lpr* and *gld*: single gene models of systemic autoimmunity and lymphoproliferative disease. *Annu. Rev. Immunol.* **9,** 243–269.
9 Brey, R. L., Sakic, B., Szechtman, H., and Denburg, J. A. (1997) Animal models for nervous system disease in systemic lupus erythematosus. *Ann. N. Y. Acad. Sci.* **823,** 97–106.
10 Furukawa, F. (1997) Animal models of cutaneous lupus erythematosus and lupus erythematosus photosensitivity. *Lupus* **6,** 193–202.
11 Peng, S. L. and Craft, J. (1997) The regulation of murine lupus. *Ann. N. Y. Acad. Sci.* **815,** 128–138.
12. Scofield, R. H. and James, J. A. (1999) Immunization as a model for systemic lupus erythematosus. *Sem. Arthritis Rheum.* **29,** 140–147.
13 Izui, S., Ibnou-Zekri, N., Fossati-Jimack, L., and Iwamoto, M. (2000) Lessons from BXSB and related mouse models. *Int. Rev. Immunol.* **19,** 447–472.
14 Kono, D. H. and Theofilopoulos, A. N. (2000) Genetics of systemic autoimmunity in mouse models of lupus. *Int. Rev. Immunol.* **19,** 367–387.
15 Nose, M., Nishihara, M., and Fujii, H. (2000) Genetic basis of the complex pathological manifestations of collagen disease: lessons from MRL/*lpr* and related mouse models. *Int. Rev. Immunol.* **19,** 473–498.
16 Shlomchik, M. J., Craft, J. E., and Mamula, M. J. (2001) From T to B and back again: positive feedback in systemic autoimmune disease. *Nat. Rev. Immunol.* **1,** 147–153.
17 Bielschowsky, M., Helyer, B. J., and Howie, J. B. (1959) Spontaneous haemolytic anemia in mice of the NZB/BL strain. *Proc. Univ. Otago Med. Sch.* **37,** 9.
18. Bielschowsky, M. and Goodall, C. M. (1970) Origin of inbred NZ mouse strains. *Cancer Res.* **30,** 834–836.
19. Hall, W. H. and Simpson, L. O. (1975) The origins of some hitherto undescribed inbred mouse strains. *Lab. Animals* **9,** 139–142.
20 Beck, J. A., Lloyd, S., Hafezparast, M., Lennon-Pierce, M., Eppig, J. T., Festing, M. F., et al. (2000) Genealogies of mouse inbred strains. *Nat. Genet.* **24,** 23–25.
21. Jackson Laboratory website, http://jaxmice.jax.org/jaxmice-cgi/jaxmicedb.cgi?objtype=pricedetail&stock=001058&dest=N.
22. Burnet, F. M. and Holmes, M. C. (1965) The natural history of the NZB/NZW F1 hybrid mouse: a laboratory model of systemic lupus erythematosus. *Aust. Ann. Med.* **14,** 185–191.

23 Chiang, B. L., Bearer, E., Ansari, A., Dorshkind, K., and Gershwin, M. E. (1990) The *BM12* mutation and autoantibodies to dsDNA in NZB.H-2^{bm12} mice. *J. Immunol.* **145,** 94–101.

24 Rudofsky, U. H., Evans, B. D., Balaban, S. L., Mottironi, V. D., and Gabrielsen, A. E. (1993) Differences in expression of lupus nephritis in New Zealand mixed H-2z homozygous inbred strains of mice derived from New Zealand black and New Zealand white mice. Origins and initial characterization. *Lab. Invest.* **68,** 419–426.

25 Morel, L., Rudofsky, U. H., Longmate, J. A., Schiffenbauer, J., and Wakeland, E. K. (1994) Polygenic control of susceptibility to murine systemic lupus erythematosus. *Immunity* **1,** 219–229.

26 Helyer, B. J. and Howie, J. B. (1963) Renal disease associated with positive lupus erythematosus test in a cross-bred strain of mice. *Nature* **197,** 197.

27 Hicks, J. D. and Burnet, F. M. (1966) Renal lesions in the "auto-immune" mouse strains NZB and F1 NZBxNZW. *J. Pathol. Bacteriol.* **91,** 467–476.

28 Hicks, J. D. (1966) Vascular changes in the kidneys of NZB mice and F1 NZBxNZW hybrids. *J. Pathol. Bacteriol.* **91,** 479–486.

29 Russell, P. J., Hicks, J. D., and Burnet, F. M. (1966) Cyclophosphamide treatment of kidney disease in (NZB × NZW) F1 mice. *Lancet* **1,** 1280–1284.

30. Miyasato, F., Manaligod, J. R., and Pollak, V. E. (1967) Auto-immune disease in NZB and NZB-NZW F1 mice. Natural history and pathology. *Arch. Pathol. Lab. Med.* **83,** 20–30.

31 Russell, P. J. and Hicks, J. D. (1968) Cyclophosphamide treatment of renal disease in (NZB × NZW) F1 hybrid mice. *Lancet* **1,** 440–441.

32 Deshmukh, U. S., Lewis, J. E., Gaskin, F., Dhakephalkar, P. K., Kannapell, C. C., Waters, S. T., et al. (2000) Ro60 peptides induce antibodies to similar epitopes shared among lupus-related autoantigens. *J. Immunol.* **164,** 6655–6661.

33 Monneaux, F., Dumortier, H., Steiner, G., Briand, J. P., and Muller, S. (2001) Murine models of systemic lupus erythematosus: B and T cell responses to spliceosomal ribonucleoproteins in MRL/Fas(*lpr*) and (NZB × NZW) F_1 lupus mice. *Int. Immunol.* **13,** 1155–1163.

34 Suen, J. L., Wu, C. H., Chen, Y. Y., Wu, W. M., and Chiang, B. L. (2001) Characterization of self-T-cell response and antigenic determinants of U1A protein with bone marrow-derived dendritic cells in NZB × NZW F1 mice. *Immunology* **103,** 301–309.

35 Matsuura, E., Igarashi, Y., Yasuda, T., Triplett, D. A., and Koike, T. (1994) Anticardiolipin antibodies recognize β_2-glycoprotein I structure altered by interacting with an oxygen modified solid phase surface. *J. Exp. Med.* **179,** 457–462.

36 Haruta, K., Kobayashi, S., Hirose, S., Horiai, A., Ohyanagi, M., Tanaka, M., et al. (1998) Monoclonal anti-cardiolipin antibodies from New Zealand black × New Zealand white F1 mice react to thrombomodulin. *J. Immunol.* **160,** 253–258.

37 Boros, P., Chen, J. M., Bona, C., and Unkeless, J. C. (1990) Autoimmune mice make anti-Fcγ receptor antibodies. *J. Exp. Med.* **171,** 1581–1595.

38 Eilat, D., Schechter, A. N., and Steinberg, A. D. (1976) Antibodies to native tRNA in NZB/NZW mice. *Nature* **259,** 141–143.
39 Boackle, S. A., Holers, V. M., Chen, X., Szakonyi, G., Karp, D. R., Wakeland, E. K., et al. (2001) Cr2, a candidate gene in the murine Sle1c lupus susceptibility locus, encodes a dysfunctional protein. *Immunity* **15,** 775–785.
40 Rozzo, S. J., Allard, J. D., Choubey, D., Vyse, T. J., Izui, S., Peltz, G., et al. (2001) Evidence for an interferon-inducible gene, Ifi202, in the susceptibility to systemic lupus. *Immunity* **15,** 435–443.
41 Hirose, S., Nagasawa, R., Sekikawa, I., Hamaoki, M., Ishida, Y., Sato, H., et al. (1983) Enhancing effect of H-2-linked NZW gene(s) on the autoimmune traits of (NZB × NZW) F1 mice. *J. Exp. Med.* **158,** 228–233.
42 Kotzin, B. L. and Palmer, E. (1987) The contribution of NZW genes to lupus-like disease in (NZB × NZW) F1 mice. *J. Exp. Med.* **165,** 1237–1251.
43 Schiffenbauer, J., McCarthy, D. M., Nygard, N. R., Woulfe, S. L., Didier, D. K., and Schwartz, B. D. (1989) A unique sequence of the NZW I-Eβ chain and its possible contribution to autoimmunity in the (NZB × NZW) F1 mouse. *J. Exp. Med.* **170,** 971–984.
44 Babcock, S. K., Appel, V. B., Schiff, M., Palmer, E., and Kotzin, B. L. (1989) Genetic analysis of the imperfect association of H-2 haplotype with lupus-like autoimmune disease. *Proc. Natl. Acad. Sci. USA* **86,** 7552–7555.
45 Ibnou-Zekri, N., Iwamoto, M., Fossati, L., McConahey, P. J., and Izui, S. (1997) Role of the major histocompatibility complex class II Ea gene in lupus susceptibility in mice. *Proc. Natl. Acad. Sci. U S A* **94,** 14,654–14,659.
46 Vyse, T. J., Rozzo, S. J., Drake, C. G., Appel, V. B., Lemeur, M., Izui, S., et al. (1998) Contributions of Ea(z) and Eb(z) MHC genes to lupus susceptibility in New Zealand mice. *J. Immunol.* **160,** 2757–2766.
47 Vyse, T. J., Halterman, R. K., Rozzo, S. J., Izui, S., and Kotzin, B. L. (1999) Control of separate pathogenic autoantibody responses marks MHC gene contributions to murine lupus. *Proc. Natl. Acad. Sci. USA* **96,** 8098–8103.
48 Jacob, C. O. and McDevitt, H. O. (1988) Tumour necrosis factor-α in murine autoimmune "lupus" nephritis. *Nature* **331,** 356–358.
49 Jongeneel, C. V., Acha-Orbea, H., and Blankenstein, T. (1990) A polymorphic microsatellite in the tumor necrosis factor α promoter identifies an allele unique to the NZW mouse strain. *J. Exp. Med.* **171,** 2141–2146.
50 Knight, J. G. and Adams, D. D. (1978) Three genes for lupus nephritis in NZB × NZW mice. *J. Exp. Med.* **147,** 1653–1660.
51 Ozaki, S., Honda, H., Maruyama, N., Hirose, S., Hamaoki, M., Sato, H., et al. (1983) Genetic regulation of erythrocyte autoantibody production in New Zealand black mice. *Immunogenetics* **18,** 241–254.
52 Drake, C. G., Babcock, S. K., Palmer, E., and Kotzin, B. L. (1994) Genetic analysis of the NZB contribution to lupus-like autoimmune disease in (NZB × NZW) F1 mice. *Proc. Natl. Acad. Sci. USA* **91,** 4062–4066.
53. Kono, D. H., Burlingame, R. W., Owens, D. G., Kuramochi, A., Balderas, R. S., Balomenos, D., et al. (1994) Lupus susceptibility loci in New Zealand mice. *Proc. Natl. Acad. Sci. USA* **91,** 10,168–10,172.

54 Rahman, Z. S., Tin, S. K., Buenaventura, P. N., Ho, C. H., Yap, E. P., Yong, R. Y., et al. (2002) A novel susceptibility locus on chromosome 2 in the (New Zealand black × New Zealand white) F1 hybrid mouse model of systemic lupus erythematosus. *J. Immunol.* **168,** 3042–3049.
55 Adelman, N. E., Watling, D. L., and McDevitt, H. O. (1983) Treatment of (NZB × NZW) F1 disease with anti-I-A monoclonal antibodies. *J. Exp. Med.* **158,** 1350–1355.
56 Wofsy, D. and Seaman, W. E. (1985) Successful treatment of autoimmunity in NZB/NZW F1 mice with monoclonal antibody to L3T4. *J. Exp. Med.* **161,** 378–391.
57 Datta, S. K., Patel, H., and Berry, D. (1987) Induction of a cationic shift in IgG anti-DNA autoantibodies. Role of T helper cells with classical and novel phenotypes in three murine models of lupus nephritis. *J. Exp. Med.* **165,** 1252–1268.
58 Tillman, D. M., Jou, N. T., Hill, R. J., and Marion, T. N. (1992) Both IgM and IgG anti-DNA antibodies are the products of clonally selective B cell stimulation in (NZB × NZW) F1 mice. *J. Exp. Med.* **176,** 761–779.
59 Friedmann, D., Yachimovich, N., Mostoslavsky, G., Pewzner-Jung, Y., Ben-Yehuda, A., Rajewsky, K., et al. (1999) Production of high affinity autoantibodies in autoimmune New Zealand black/New Zealand white F1 mice targeted with an anti-DNA heavy chain. *J. Immunol.* **162,** 4406–4416.
60 Kaliyaperumal, A., Mohan, C., Wu, W., and Datta, S. K. (1996) Nucleosomal peptide epitopes for nephritis-inducing T helper cells of murine lupus. *J. Exp. Med.* **183,** 2459–2469.
61 Kaliyaperumal, A., Michaels, M. A., and Datta, S. K. (1999) Antigen-specific therapy of murine lupus nephritis using nucleosomal peptides: tolerance spreading impairs pathogenic function of autoimmune T and B cells. *J. Immunol.* **162,** 5775–5783.
62 Kaliyaperumal, A., Michaels, M. A., and Datta, S. K. (2002) Naturally processed chromatin peptides reveal a major autoepitope that primes pathogenic T and B cells of lupus. *J. Immunol.* **168,** 2530–2537.
63 Wang, Y., Hu, Q., Madri, J. A., Rollins, S. A., Chodera, A., and Matis, L. A. (1996) Amelioration of lupus-like autoimmune disease in NZB/WF1 mice after treatment with a blocking monoclonal antibody specific for complement component C5. *Proc. Natl. Acad. Sci. USA* **93,** 8563–8568.
64 Clynes, R., Dumitru, C., and Ravetch, J. V. (1998) Uncoupling of immune complex formation and kidney damage in autoimmune glomerulonephritis. *Science* **279,** 1052–1054.
65 Pritchard, N. R., Cutler, A. J., Uribe, S., Chadban, S. J., Morley, B. J., and Smith, K. G. (2000) Autoimmune-prone mice share a promoter haplotype associated with reduced expression and function of the Fc receptor FcγRII. *Curr. Biol.* **10,** 227–230.
66 Finck, B. K., Linsley, P. S., and Wofsy, D. (1994) Treatment of murine lupus with CTLA4Ig. *Science* **265,** 1225–1227.
67 Early, G. S., Zhao, W., and Burns, C. M. (1996) Anti-CD40 ligand antibody treatment prevents the development of lupus-like nephritis in a subset of New Zealand black × New Zealand white mice. Response correlates with the absence of an anti-antibody response. *J. Immunol.* **157,** 3159–3164.

68 Mihara, M., Tan, I., Chuzhin, Y., Reddy, B., Budhai, L., Holzer, A., et al. (2000) CTLA4Ig inhibits T cell-dependent B-cell maturation in murine systemic lupus erythematosus. *J. Clin. Invest.* **106,** 91–101.
69 Daikh, D. I. and Wofsy, D. (2001) Cutting edge: reversal of murine lupus nephritis with CTLA4Ig and cyclophosphamide. *J. Immunol.* **166,** 2913–2916.
70 Wang, X., Huang, W., Mihara, M., Sinha, J., and Davidson, A. (2002) Mechanism of action of combined short-term CTLA4Ig and anti-CD40 ligand in murine systemic lupus erythematosus. *J. Immunol.* **168,** 2046–2053.
71 Gilkeson, G. S., Pippen, A. M., and Pisetsky, D. S. (1995) Induction of cross-reactive anti-dsDNA antibodies in preautoimmune NZB/NZW mice by immunization with bacterial DNA. *J. Clin. Invest.* **95,** 1398–1402.
72 Gilkeson, G. S., Ruiz, P., Pippen, A. M., Alexander, A. L., Lefkowith, J. B., and Pisetsky, D. S. (1996) Modulation of renal disease in autoimmune NZB/NZW mice by immunization with bacterial DNA. *J. Exp. Med.* **183,** 1389–1397.
73 Riemekasten, G., Kawald, A., Weiss, C., Meine, A., Marell, J., Klein, R., et al. (2001) Strong acceleration of murine lupus by injection of the SmD1(83–119) peptide. *Arthritis Rheum.* **44,** 2435–2445.
74 Hahn, B. H. and Ebling, F. M. (1983) Suppression of NZB/NZW murine nephritis by administration of a syngeneic monoclonal antibody to DNA. Possible role of anti-idiotypic antibodies. *J. Clin. Invest.* **71,** 1728–1736.
75 Singh, R. R., Kumar, V., Ebling, F. M., Southwood, S., Sette, A., Sercarz, E. E., et al. (1995) T cell determinants from autoantibodies to DNA can upregulate autoimmunity in murine systemic lupus erythematosus. *J. Exp. Med.* **181,** 2017–2027.
76 Singh, R. R., Ebling, F. M., Sercarz, E. E., and Hahn, B. H. (1995) Immune tolerance to autoantibody-derived peptides delays development of autoimmunity in murine lupus. *J. Clin. Invest.* **96,** 2990–2996.
77 Hahn, B. H., Singh, R. R., Wong, W. K., Tsao, B. P., Bulpitt, K., and Ebling, F. M. (2001) Treatment with a consensus peptide based on amino acid sequences in autoantibodies prevents T cell activation by autoantigens and delays disease onset in murine lupus. *Arthritis Rheum.* **44,** 432–441.
78 Beger, E., Deocharan, B., Edelman, M., Erblich, B., Gu, Y., and Putterman, C. (2002) A peptide DNA surrogate accelerates autoimmune manifestations and nephritis in lupus-prone mice. *J. Immunol.* **168,** 3617–3626.
79 Jacob, C. O., van der Meide, P. H., and McDevitt, H. O. (1987) In vivo treatment of (NZB × NZW) F1 lupus-like nephritis with monoclonal antibody to γ interferon. *J. Exp. Med.* **166,** 798–803.
80 Ozmen, L., Roman, D., Fountoulakis, M., Schmid, G., Ryffel, B., and Garotta, G. (1995) Experimental therapy of systemic lupus erythematosus: the treatment of NZB/W mice with mouse soluble interferon-γ receptor inhibits the onset of glomerulonephritis. *Eur. J. Immunol.* **25,** 6–12.
81 Haas, C., Ryffel, B., and Le Hir, M. (1998) IFN-γ receptor deletion prevents autoantibody production and glomerulonephritis in lupus-prone (NZB × NZW) F1 mice. *J. Immunol.* **160,** 3713–3718.

82 Kontoyiannis, D. and Kollias, G. (2000) Accelerated autoimmunity and lupus nephritis in NZB mice with an engineered heterozygous deficiency in tumor necrosis factor. *Eur. J. Immunol.* **30,** 2038–2047.
83 Altman, A., Theofilopoulos, A. N., Weiner, R., Katz, D. H., and Dixon, F. J. (1981) Analysis of T cell function in autoimmune murine strains. Defects in production and responsiveness to interleukin 2. *J. Exp. Med.* **154,** 791–808.
84 Nakajima, A., Hirose, S., Yagita, H., and Okumura, K. (1997) Roles of IL-4 and IL-12 in the development of lupus in NZB/W F1 mice. *J. Immunol.* **158,** 1466–1472.
85 Santiago, M. L., Fossati, L., Jacquet, C., Muller, W., Izui, S., and Reininger, L. (1997) Interleukin-4 protects against a genetically linked lupus-like autoimmune syndrome. *J. Exp. Med.* **185,** 65–70.
86 Finck, B. K., Chan, B., and Wofsy, D. (1994) Interleukin 6 promotes murine lupus in NZB/NZW F1 mice. *J. Clin. Invest.* **94,** 585–591.
87 Ishida, H., Muchamuel, T., Sakaguchi, S., Andrade, S., Menon, S., and Howard, M. (1994) Continuous administration of anti-interleukin 10 antibodies delays onset of autoimmunity in NZB/W F1 mice. *J. Exp. Med.* **179,** 305–310.
88 Goldings, E. A., Cohen, P. L., McFadden, S. F., Ziff, M., and Vitetta, E. S. (1980) Defective B cell tolerance in adult (NZB × NZW) F1 mice. *J. Exp. Med.* **152,** 730–735.
89 Brooks, M. S. and Aldo-Benson, M. (1986) Defects in antigen-specific immune tolerance in continuous B cell lines from autoimmune mice. *J. Clin. Invest.* **78,** 784–789.
90 Klinman, D. M. and Steinberg, A. D. (1987) Systemic autoimmune disease arises from polyclonal B cell activation. *J. Exp. Med.* **165,,** 1755–1760.
91 Klinman, D. M. (1990) Polyclonal B cell activation in lupus-prone mice precedes and predicts the development of autoimmune disease. *J. Clin. Invest.* **86,** 1249–1254.
92 Reininger, L., Radaszkiewicz, T., Kosco, M., Melchers, F., and Rolink, A. G. (1992) Development of autoimmune disease in SCID mice populated with long-term "in vitro" proliferating (NZB × NZW) F1 pre-B cells. *J. Exp. Med.* **176,** 1343–1353.
93 Murakami, M., Yoshioka, H., Shirai, T., Tsubata, T., and Honjo, T. (1995) Prevention of autoimmune symptoms in autoimmune-prone mice by elimination of B-1 cells. *Int. Immunol.* **7,** 877–882.
94 Reininger, L., Winkler, T. H., Kalberer, C. P., Jourdan, M., Melchers, F., and Rolink, A. G. (1996) Intrinsic B cell defects in NZB and NZW mice contribute to systemic lupus erythematosus in (NZB × NZW) F1 mice. *J. Exp. Med.* **184,** 853–861.
95 Cassese, G., Lindenau, S., de Boer, B., Arce, S., Hauser, A., Riemekasten, G., et al. (2001) Inflamed kidneys of NZB/W mice are a major site for the homeostasis of plasma cells. *Eur. J. Immunol.* **31,** 2726–2732.
96 Wellmann, U., Letz, M., Schneider, A., Amann, K., and Winkler, T. H. (2001) An Ig mu-heavy chain transgene inhibits systemic lupus erythematosus immunopathology in autoimmune (NZB × NZW) F1 mice. *Int. Immunol.* **13,** 1461–1469.
97 Ishikawa, S., Sato, T., Abe, M., Nagai, S., Onai, N., Yoneyama, H., et al. (2001) Aberrant high expression of B lymphocyte chemokine (BLC/CXCL13) by

C11b$^+$CD11c$^+$ dendritic cells in murine lupus and preferential chemotaxis of B1 cells towards BLC. *J. Exp. Med.* **193,** 1393–1402.

98 Zeng, D., Lee, M. K., Tung, J., Brendolan, A., and Strober, S. (2000) Cutting edge: a role for CD1 in the pathogenesis of lupus in NZB/NZW mice. *J. Immunol.* **164,** 5000–5004.

99. Murphy, E. D. (1981) Lymphoproliferation (*lpr*) and other single-locus models for murine lupus, in *Immunologic Defects in Laboratory Animals* (Gershwin, M. E., and Merchant, B., eds.), Plenum Press, New York, Vol. 1, pp. 143–173.

100 Izui, S., McConahey, P. J., and Dixon, F. J. (1978) Increased spontaneous polyclonal activation of B lymphocytes in mice with spontaneous autoimmune disease. *J. Immunol.* **121,** 2213–2219.

101 Andrews, B. S., Eisenberg, R. A., Theofilopoulos, A. N., Izui, S., Wilson, C. B., McConahey, P. J., et al. (1978) Spontaneous murine lupus-like syndromes. Clinical and immunopathological manifestations in several strains. *J. Exp. Med.* **148,** 1198–1215.

102 Dixon, F. J., Andrews, B. S., Eisenberg, R. A., McConahey, P. J., Theofilopoulos, A. N., and Wilson, C. B. (1978) Etiology and pathogenesis of a spontaneous lupus-like syndrome in mice. *Arthritis Rheum.* **21,** S64–S67.

103. Murphy, E. D. and Roths, J. B. (1976) A single gene model for massive lyphoproliferation with immune complex disease in new mouse strain MRL. *Proc. 16th Int. Cong. Hematol.*, 69.

104. Murphy, E. D. and Roths, J. B. (1978) New inbred strains. *Mouse News Lett.* **58,** 51.

105 Burlingame, R. W., Rubin, R. L., Balderas, R. S., and Theofilopoulos, A. N. (1993) Genesis and evolution of antichromatin autoantibodies in murine lupus implicates T-dependent immunization with self antigen. *J. Clin. Invest.* **91,** 1687–1696.

106 Hang, L., Slack, J. H., Amundson, C., Izui, S., Theofilopoulos, A. N., and Dixon, F. J. (1983) Induction of murine autoimmune disease by chronic polyclonal B cell activation. *J. Exp. Med.* **157,** 874–883.

107 Vratsanos, G. S., Jung, S., Park, Y. M., and Craft, J. (2001) CD4(+) T cells from lupus-prone mice are hyperresponsive to T cell receptor engagement with low and high affinity peptide antigens: a model to explain spontaneous T cell activation in lupus. *J. Exp. Med.* **193,** 329–337.

108 Eisenberg, R. A., Craven, S. Y., Warren, R. W., and Cohen, P. L. (1987) Stochastic control of anti-Sm autoantibodies in MRL/Mp-*lpr/lpr* mice. *J. Clin. Invest.* **80,** 691–697.

109 Shlomchik, M. J., Marshak-Rothstein, A., Wolfowicz, C. B., Rothstein, T. L., and Weigert, M. G. (1987) The role of clonal selection and somatic mutation in autoimmunity. *Nature* **328,** 805–811.

110 Shlomchik, M. J., Aucoin, A. H., Pisetsky, D. S., and Weigert, M. G. (1987) Structure and function of anti-DNA autoantibodies derived from a single autoimmune mouse. *Proc. Natl. Acad. Sci. USA* **84,** 9150–9154.

111 Shlomchik, M., Mascelli, M., Shan, H., Radic, M. Z., Pisetsky, D., Marshak-Rothstein, A., et al. (1990) Anti-DNA antibodies from autoimmune mice arise by clonal expansion and somatic mutation. *J. Exp. Med.* **171,** 265–292.

112 Bloom, D. D., Davignon, J. L., Retter, M. W., Shlomchik, M. J., Pisetsky, D. S., Cohen, P. L., et al. (1993) V region gene analysis of anti-Sm hybridomas from MRL/Mp-*lpr*/*lpr* mice. *J. Immunol.* **150,** 1591–1610.
113 Bloom, D. D., Davignon, J. L., Cohen, P. L., Eisenberg, R. A., and Clarke, S. H. (1993) Overlap of the anti-Sm and anti-DNA responses of MRL/Mp-*lpr*/*lpr* mice. *J. Immunol.* **150,** 1579–1590.
114 Ishigatsubo, Y., Igarashi, T., Ohno, S., Ueda, A., Okubo, T., and Klinman, D. M. (1993) Cross-reactivity of IgM- and IgG-secreting B cells in autoimmune mice. *Arthritis Rheum.* **36,** 1003–1006.
115 Klinman, D. M., Dellacqua, D. K., Conover, J., and Huppi, K. (1993) VH family utilization by IgG anti-DNA-secreting lymphocytes derived from autoimmune MRL-*lpr*/*lpr* mice. *Arthritis Rheum.* **36,** 561–568.
116 Fatenejad, S., Brooks, W., Schwartz, A., and Craft, J. (1994) Pattern of anti-small nuclear ribonucleoprotein antibodies in MRL/Mp-*lpr*/*lpr* mice suggests that the intact U1 snRNP particle is their autoimmunogenic target. *J. Immunol.* **152,** 5523–5531.
117 Kita, Y., Sumida, T., Iwamoto, I., Yoshida, S., and Koike, T. (1994) V gene analysis of anti-cardiolipin antibodies from (NZW × BXSB) F1 mice. *Immunology* **82,** 494–501.
118 Shan, H., Shlomchik, M. J., Marshak-Rothstein, A., Pisetsky, D. S., Litwin, S., and Weigert, M. G. (1994) The mechanism of autoantibody production in an autoimmune MRL/*lpr* mouse. *J. Immunol.* **153,** 5104–5120.
119 Retter, M. W., Cohen, P. L., Eisenberg, R. A., and Clarke, S. H. (1996) Both Sm and DNA are selecting antigens in the anti-Sm B cell response in autoimmune MRL/*lpr* mice. *J. Immunol.* **156,** 1296–1306.
120 Brard, F., Shannon, M., Prak, E. L., Litwin, S., and Weigert, M. (1999) Somatic mutation and light chain rearrangement generate autoimmunity in anti-single-stranded DNA transgenic MRL/*lpr* mice. *J. Exp. Med.* **190,** 691–704.
121. Fatenejad, S., Mamula, M. J., and Craft, J. (1993) Role of intermolecular/intrastructural B- and T-cell determinants in the diversification of autoantibodies to ribonucleoprotein particles. *Proc. Natl. Acad. Sci. USA* **90,** 12,010–12,014.
122 Scofield, R. H., Farris, A. D., Horsfall, A. C., and Harley, J. B. (1999) Fine specificity of the autoimmune response to the Ro/SSA and La/SSB ribonucleoproteins. *Arthritis Rheum.* **42,** 199–209.
123 Gay, D., Saunders, T., Camper, S., and Weigert, M. (1993) Receptor editing: an approach by autoreactive B cells to escape tolerance. *J. Exp. Med.* **177,** 999–1008.
124 Klonowski, K. D., Primiano, L. L., and Monestier, M. (1999) Atypical VH-D-JH rearrangements in newborn autoimmune MRL mice. *J. Immunol.* **162,** 1566–1572.
125 Klonowski, K. D. and Monestier, M. (2000) Heavy chain revision in MRL mice: a potential mechanism for the development of autoreactive B cell precursors. *J. Immunol.* **165,** 4487–4493.
126 Roark, J. H., Kuntz, C. L., Nguyen, K. A., Mandik, L., Cattermole, M., and Erikson, J. (1995) B cell selection and allelic exclusion of an anti-DNA Ig transgene in MRL-*lpr*/*lpr* mice. *J. Immunol.* **154,** 4444–4455.

127 Chen, C., Nagy, Z., Radic, M. Z., Hardy, R. R., Huszar, D., Camper, S. A., et al. (1995) The site and stage of anti-DNA B-cell deletion. *Nature* **373,** 252–255.
128 Santulli-Marotto, S., Retter, M. W., Gee, R., Mamula, M. J., and Clarke, S. H. (1998) Autoreactive B cell regulation: peripheral induction of developmental arrest by lupus-associated autoantigens. *Immunity* **8,** 209–219.
129 Santulli-Marotto, S., Qian, Y., Ferguson, S., and Clarke, S. H. (2001) Anti-Sm B cell differentiation in Ig transgenic MRL/Mp-*lpr*/*lpr* mice: altered differentiation and an accelerated response. *J. Immunol.* **166,** 5292–5299.
130 Ma, J., Xu, J., Madaio, M. P., Peng, Q., Zhang, J., Grewal, I. S., et al. (1996) Autoimmune *lpr*/*lpr* mice deficient in CD40 ligand: spontaneous Ig class switching with dichotomy of autoantibody responses. *J. Immunol.* **157,** 417–426.
131 Peng, S. L., Madaio, M. P., Hughes, D. P., Crispe, I. N., Owen, M. J., Wen, L., et al. (1996) Murine lupus in the absence of αβ T cells. *J. Immunol.* **156,**, 4041–4049.
132 Peng, S. L., Madaio, M. P., Hayday, A. C., and Craft, J. (1996) Propagation and regulation of systemic autoimmunity by γδ T cells. *J. Immunol.* **157,** 5689–5698.
133 Peng, S. L., Fatenejad, S., and Craft, J. (1996) Induction of nonpathologic, humoral autoimmunity in lupus-prone mice by a class II-restricted, transgenic alpha beta T cell. Separation of autoantigen-specific and -nonspecific help. *J. Immunol.* **157,** 5225–5230.
134 Chan, O. T., Madaio, M. P., and Shlomchik, M. J. (1999) The central and multiple roles of B cells in lupus pathogenesis. *Immunol. Rev.* **169,** 107–121.
135 Peng, S. L., Moslehi, J., and Craft, J. (1997) Roles of interferon-γ and interleukin-4 in murine lupus. *J. Clin. Invest.* **99,** 1936–1946.
136 Balomenos, D., Rumold, R., and Theofilopoulos, A. N. (1998) Interferon-γ is required for lupus-like disease and lymphoaccumulation in MRL-*lpr* mice. *J. Clin. Invest.* **101,** 364–371.
137 Schwarting, A., Wada, T., Kinoshita, K., Tesch, G., and Kelley, V. R. (1998) IFN-γ receptor signaling is essential for the initiation, acceleration, and destruction of autoimmune kidney disease in MRL-Fas(*lpr*) mice. *J. Immunol.* **161,** 494–503.
138 Tesch, G. H., Maifert, S., Schwarting, A., Rollins, B. J., and Kelley, V. R. (1999) Monocyte chemoattractant protein 1-dependent leukocytic infiltrates are responsible for autoimmune disease in MRL-Fas(*lpr*) mice. *J. Exp. Med.* **190,** 1813–1824.
139 Sekine, H., Reilly, C. M., Molano, I. D., Garnier, G., Circolo, A., Ruiz, P., et al. (2001) Complement component C3 is not required for full expression of immune complex glomerulonephritis in MRL/*lpr* mice. *J. Immunol.* **166,** 6444–6451.
140 Bao, L., Haas, M., Boackle, S. A., Kraus, D. M., Cunningham, P. N., Park, P., et al. (2002) Transgenic expression of a soluble complement inhibitor protects against renal disease and promotes survival in MRL/*lpr* mice. *J. Immunol.* **168,** 3601–3607.
141 Lloyd, C. M., Gonzalo, J. A., Salant, D. J., Just, J., and Gutierrez-Ramos, J. C. (1997) Intercellular adhesion molecule-1 deficiency prolongs survival and protects against the development of pulmonary inflammation during murine lupus. *J. Clin. Invest.* **100,** 963–971.

142 Tada, Y., Nagasawa, K., Ho, A., Morito, F., Koarada, S., Ushiyama, O., et al. (1999) Role of the costimulatory molecule CD28 in the development of lupus in MRL/*lpr* mice. *J. Immunol.* **163,** 3153–3159.

143 Kinoshita, K., Tesch, G., Schwarting, A., Maron, R., Sharpe, A. H., and Kelley, V. R. (2000) Costimulation by B7-1 and B7-2 is required for autoimmune disease in MRL-Faslpr mice. *J. Immunol.* **164,** 6046–6056.

144 Liang, B., Kashgarian, M. J., Sharpe, A. H., and Mamula, M. J. (2000) Autoantibody responses and pathology regulated by B7-1 and B7-2 costimulation in MRL/*lpr* lupus. *J. Immunol.* **165,** 3436–3443.

145 Jevnikar, A. M., Grusby, M. J., and Glimcher, L. H. (1994) Prevention of nephritis in major histocompatibility complex class II-deficient MRL-*lpr* mice. *J. Exp. Med.* **179,** 1137–1143.

146 Christianson, G. J., Blankenburg, R. L., Duffy, T. M., Panka, D., Roths, J. B., Marshak-Rothstein, A., et al. (1996) β2-Microglobulin dependence of the lupus-like autoimmune syndrome of MRL-*lpr* mice. *J. Immunol.* **156,** 4932–4939.

147 Chan, O. T., Paliwal, V., McNiff, J. M., Park, S. H., Bendelac, A., and Shlomchik, M. J. (2001) Deficiency in β2-microglobulin, but not CD1, accelerates spontaneous lupus skin disease while inhibiting nephritis in MRL-Fas(*lpr*) nice: an example of disease regulation at the organ level. *J. Immunol.* **167,** 2985–2990.

148 Watson, M. L., Rao, J. K., Gilkeson, G. S., Ruiz, P., Eicher, E. M., Pisetsky, D. S., et al. (1992) Genetic analysis of MRL-*lpr* mice: relationship of the Fas apoptosis gene to disease manifestations and renal disease-modifying loci. *J. Exp. Med.* **176,** 1645–1656.

149 Gu, L., Weinreb, A., Wang, X. P., Zack, D. J., Qiao, J. H., Weisbart, R., et al. (1998) Genetic determinants of autoimmune disease and coronary vasculitis in the MRL-*lpr*/*lpr* mouse model of systemic lupus erythematosus. *J. Immunol.* **161,** 6999–7006.

150 Vidal, S., Kono, D. H., and Theofilopoulos, A. N. (1998) Loci predisposing to autoimmunity in MRL-Fas *lpr* and C57BL/6-Faslpr mice. *J. Clin. Invest.* **101,** 696–702.

151 Nishihara, M., Terada, M., Kamogawa, J., Ohashi, Y., Mori, S., Nakatsuru, S., et al. (1999) Genetic basis of autoimmune sialadenitis in MRL/*lpr* lupus-prone mice: additive and hierarchical properties of polygenic inheritance. *Arthritis Rheum.* **42,** 2616–2623.

152 Kamogawa, J., Terada, M., Mizuki, S., Nishihara, M., Yamamoto, H., Mori, S., et al. (2002) Arthritis in MRL/*lpr* mice is under the control of multiple gene loci with an allelic combination derived from the original inbred strains. *Arthritis Rheum.* **46,** 1067–1074.

153 Kawase, E., Suemori, H., Takahashi, N., Okazaki, K., Hashimoto, K., and Nakatsuji, N. (1994) Strain difference in establishment of mouse embryonic stem (ES) cell lines. *Int. J. Dev. Biol.* **38,** 385–390.

154 Goulet, J. L., Wang, C. Y., and Koller, B. H. (1997) Embryonic stem cell lines from MRL mice allow genetic modification in a murine model of autoimmune disease. *J. Immunol.* **159,** 4376–4381.

155 Kelley, V. E. and Roths, J. B. (1985) Interaction of mutant *lpr* gene with background strain influences renal disease. *Clin. Immunol. Immunopathol.* **37,** 220–229.
156 Eisenberg, R. A., Craven, S. Y., Fisher, C. L., Morris, S. C., Rapoport, R., Pisetsky, D. S., et al. (1989) The genetics of autoantibody production in MRL/*lpr* lupus mice. *Clin. Exp. Rheumatol.* **7,** S35–S40.
157. Peng, S. L. and Craft, J. (1999) Lessons from knockout and transgenic lupus-prone mice, in *Lupus: Molecular and Cellular Pathogenesis* (Kammer, G. M. and Tsokos, G. C., eds.), Humana Press, Totowa, NJ, pp. 152–166.
158 Murphy, E. D. and Roths, J. B. (1979) A Y chromosome associated factor in strain BXSB producing accelerated autoimmunity and lymphoproliferation. *Arthritis Rheum.* **22,** 1188–1194.
159 Morel, L., Croker, B. P., Blenman, K. R., Mohan, C., Huang, G., Gilkeson, G., et al. (2000) Genetic reconstitution of systemic lupus erythematosus immunopathology with polycongenic murine strains. *Proc. Natl. Acad. Sci. USA* **97,** 6670–6675.
160 Izui, S., Masuda, K., and Yoshida, H. (1984) Acute SLE in F1 hybrids between SB/Le and NZW mice; prominently enhanced formation of gp70 immune complexes by a Y chromosome-associated factor from SB/Le mice. *J. Immunol.* **132,** 701–704.
161 Hudgins, C. C., Steinberg, R. T., Klinman, D. M., Reeves, M. J., and Steinberg, A. D. (1985) Studies of consomic mice bearing the Y chromosome of the BXSB mouse. *J. Immunol.* **134,** 3849–3854.
162 Izui, S., Higaki, M., Morrow, D., and Merino, R. (1988) The Y chromosome from autoimmune BXSB/MpJ mice induces a lupus-like syndrome in (NZW × C57BL/6) F1 male mice, but not in C57BL/6 male mice. *Eur. J. Immunol.* **18,** 911–915.
163 Hogarth, M. B., Slingsby, J. H., Allen, P. J., Thompson, E. M., Chandler, P., Davies, K. A., et al. (1998) Multiple lupus susceptibility loci map to chromosome 1 in BXSB mice. *J. Immunol.* **161,** 2753–2761.
164 Haywood, M. E., Hogarth, M. B., Slingsby, J. H., Rose, S. J., Allen, P. J., Thompson, E. M., et al. (2000) Identification of intervals on chromosomes 1, 3, and 13 linked to the development of lupus in BXSB mice. *Arthritis Rheum.* **43,** 349–355.
165 Maibaum, M. A., Haywood, M. E., Walport, M. J., and Morley, B. J. (2000) Lupus susceptibility loci map within regions of BXSB derived from the SB/Le parental strain. *Immunogenetics* **51,** 370–372.
166 Haywood, M. E., Vyse, T. J., McDermott, A., Thompson, E. M., Ida, A., Walport, M. J., et al. (2001) Autoantigen glycoprotein 70 expression is regulated by a single locus, which acts as a checkpoint for pathogenic anti-glycoprotein 70 autoantibody production and hence for the corresponding development of severe nephritis, in lupus-prone BXSB mice. *J. Immunol.* **167,** 1728–1733.
167 Hahn, B. H. and Ebling, F. M. (1984) A public idiotypic determinant is present on spontaneous cationic IgG antibodies to DNA from mice of unrelated lupus-prone strains. *J. Immunol.* **133,** 3015–3019.
168 Lawson, B. R., Koundouris, S. I., Barnhouse, M., Dummer, W., Baccala, R., Kono, D. H., et al. (2001) The role of αβ+ T cells and homeostatic T cell proliferation in Y-chromosome-associated murine lupus. *J. Immunol.* **167,** 2354–2360.

169 Wofsy, D. (1986) Administration of monoclonal anti-T cell antibodies retards murine lupus in BXSB mice. *J. Immunol.* **136,** 4554–4560.

170 Chu, E. B., Hobbs, M. V., Wilson, C. B., Romball, C. G., Linsley, P. S., and Weigle, W. O. (1996) Intervention of $CD4^+$ cell subset shifts and autoimmunity in the BXSB mouse by murine CTLA4Ig. *J. Immunol.* **156,** 1262–1268.

171 Adachi, Y., Inaba, M., Sugihara, A., Koshiji, M., Sugiura, K., Amoh, Y., et al. (1998) Effects of administration of monoclonal antibodies (anti-CD4 or anti-CD8) on the development of autoimmune diseases in (NZW × BXSB) F1 mice. *Immunobiology* **198,** 451–464.

172 Kono, D. H., Balomenos, D., Park, M. S., and Theofilopoulos, A. N. (2000) Development of lupus in BXSB mice is independent of IL-4. *J. Immunol.* **164,** 38–42.

173 Merino, R., Iwamoto, M., Fossati, L., Muniesa, P., Araki, K., Takahashi, S., et al. (1993) Prevention of systemic lupus erythematosus in autoimmune BXSB mice by a transgene encoding I-Eα chain. *J. Exp. Med.* **178,** 1189–1197.

174. Prud'homme, G. J., Balderas, R. S., Dixon, F. J., and Theofilopoulos, A. N. (1983) B cell dependence on and response to accessory signals in murine lupus strains. *J. Exp. Med.* **157,** 1815–1827.

175 Umland, S. P., Go, N. F., Cupp, J. E., and Howard, M. (1989) Responses of B cells from autoimmune mice to IL-5. *J. Immunol.* **142,** 1528–1535.

176 Merino, R., Fossati, L., Lacour, M., and Izui, S. (1991) Selective autoantibody production by Yaa+ B cells in autoimmune Yaa(+)-Yaa- bone marrow chimeric mice. *J. Exp. Med.* **174,** 1023–1029.

177 Decker, P., Le Moal, A., Briand, J. P., and Muller, S. (2000) Identification of a minimal T cell epitope recognized by antinucleosome Th cells in the C-terminal region of histone H4. *J. Immunol.* **165,** 654–662.

178 Zhang, X., Smith, D. S., Guth, A., and Wysocki, L. J. (2001) A receptor presentation hypothesis for T cell help that recruits autoreactive B cells. *J. Immunol.* **166,** 1562–1571.

179 Ghatak, S., Sainis, K., Owen, F. L., and Datta, S. K. (1987) T-cell-receptor β- and I-Aβ-chain genes of normal SWR mice are linked with the development of lupus nephritis in NZB × SWR crosses. *Proc. Natl. Acad. Sci. USA* **84,** 6850–6853.

180 Xie, S., Chang, S., Yang, P., Jacob, C., Kaliyaperumal, A., Datta, S. K., et al. (2001) Genetic contributions of nonautoimmune SWR mice toward lupus nephritis. *J. Immunol.* **167,** 7141–7149.

181 Kalled, S. L., Cutler, A. H., Datta, S. K., and Thomas, D. W. (1998) Anti-CD40 ligand antibody treatment of SNF1 mice with established nephritis: preservation of kidney function. *J. Immunol.* **160,** 2158–2165.

182 Merino, R., Iwamoto, M., Gershwin, M. E., and Izui, S. (1994) The Yaa gene abrogates the major histocompatibility complex association of murine lupus in (NZB × BXSB) F1 hybrid mice. *J. Clin. Invest.* **94,** 521–525.

183 Hang, L. M., Izui, S., and Dixon, F. J. (1981) (NZW × BXSB) F1 hybrid. A model of acute lupus and coronary vascular disease with myocardial infarction. *J. Exp. Med.* **154,** 216–221.

184 Berden, J. H., Hang, L., McConahey, P. J., and Dixon, F. J. (1983) Analysis of vascular lesions in murine SLE. I. Association with serologic abnormalities. *J. Immunol.* **130,** 1699–1705.

185 Oyaizu, N., Yasumizu, R., Miyama-Inaba, M., Nomura, S., Yoshida, H., Miyawaki, S., et al. (1988) (NZW × BXSB) F1 mouse. A new animal model of idiopathic thrombocytopenic purpura. *J. Exp. Med.* **167,** 2017–2022.

186 Hashimoto, Y., Kawamura, M., Ichikawa, K., Suzuki, T., Sumida, T., Yoshida, S., et al. (1992) Anticardiolipin antibodies in NZW × BXSB F1 mice. A model of antiphospholipid syndrome. *J. Immunol.* **149,** 1063–1068.

187 Mizutani, H., Kurata, Y., Kosugi, S., Shiraga, M., Kashiwagi, H., Tomiyama, Y., et al. (1995) Monoclonal anticardiolipin autoantibodies established from the (New Zealand white × BXSB) F1 mouse model of antiphospholipid syndrome cross-react with oxidized low-density lipoprotein. *Arthritis Rheum.* **38,** 1382–1388.

188 Ida, A., Hirose, S., Hamano, Y., Kodera, S., Jiang, Y., Abe, M., et al. (1998) Multigenic control of lupus-associated antiphospholipid syndrome in a model of (NZW × BXSB) F1 mice. *Eur. J. Immunol.* **28,** 2694–2703.

189 Ibnou-Zekri, N., Iwamoto, M., Gershwin, M. E., and Izui, S. (2000) Protection of murine lupus by the Ead transgene is MHC haplotype-dependent. *J. Immunol.* **164,** 505–511.

190 Vidal, S., Gelpi, C., and Rodriguez-Sanchez, J. L. (1994) (SWR × SJL) F1 mice: a new model of lupus-like disease. *J. Exp. Med.* **179,** 1429–1435.

191 Yu, M., Johnson, J. M., and Tuohy, V. K. (1996) A predictable sequential determinant spreading cascade invariably accompanies progression of experimental autoimmune encephalomyelitis: a basis for peptide-specific therapy after onset of clinical disease. *J. Exp. Med.* **183,** 1777–1788.

192 Kinjoh, K., Kyogoku, M., and Good, R. A. (1993) Genetic selection for crescent formation yields mouse strain with rapidly progressive glomerulonephritis and small vessel vasculitis. *Proc. Natl. Acad. Sci. USA* **90,** 3413–3417.

193 Jethwa, H. S., Nachman, P. H., Falk, R. J., and Jennette, J. C. (2000) False-positive myeloperoxidase binding activity due to DNA/anti-DNA antibody complexes: a source for analytical error in serologic evaluation of anti-neutrophil cytoplasmic autoantibodies. *Clin. Exp. Immunol.* **121,** 544–550.

194. Portanova, J. P. and Kotzin, B. L. (1988) Lupus-like autoimmunity in murine graft-vs-host disease. *Concepts Immunopathol.* **6,** 119–140.

195 Silveira, P. A. and Baxter, A. G. (2001) The NOD mouse as a model of SLE. *Autoimmunity* **34,** 53–64.

196 Anderson, P. N. and Potter, M. (1969) Induction of plasma cell tumours in BALB-c mice with 2,6,10,14-tetramethylpentadecane (pristane). *Nature* **222,** 994–995.

197 Mock, B. A., Krall, M. M., and Dosik, J. K. (1993) Genetic mapping of tumor susceptibility genes involved in mouse plasmacytomagenesis. *Proc. Natl. Acad. Sci. USA* **90,** 9499–9503.

198 Zhang, S., Ramsay, E. S., and Mock, B. A. (1998) Cdkn2a, the cyclin-dependent kinase inhibitor encoding p16INK4a and p19ARF, is a candidate for the plasmacytoma susceptibility locus, Pctr1. *Proc. Natl. Acad. Sci. USA* **95,** 2429–2434.

199 Kovalchuk, A. L., Kim, J. S., Park, S. S., Coleman, A. E., Ward, J. M., Morse, H. C., 3rd, et al. (2002) IL-6 transgenic mouse model for extraosseous plasmacytoma. *Proc. Natl. Acad. Sci. USA* **99,** 1509–1514.

200 Potter, M. and Wax, J. S. (1981) Genetics of susceptibility to pristane-induced plasmacytomas in BALB/cAn: reduced susceptibility in BALB/cJ with a brief description of pristane-induced arthritis. *J. Immunol.* **127,** 1591–1595.

201 Wooley, P. H., Seibold, J. R., Whalen, J. D., and Chapdelaine, J. M. (1989) Pristane-induced arthritis. The immunologic and genetic features of an experimental murine model of autoimmune disease. *Arthritis Rheum.* **32,** 1022–1030.

202 Beech, J. T., Siew, L. K., Ghoraishian, M., Stasiuk, L. M., Elson, C. J., and Thompson, S. J. (1997) $CD4^+$ Th2 cells specific for mycobacterial 65-kilodalton heat shock protein protect against pristane-induced arthritis. *J. Immunol.* **159,** 3692–3697.

203 Thompson, S. J., Francis, J. N., Siew, L. K., Webb, G. R., Jenner, P. J., Colston, M. J., et al. (1998) An immunodominant epitope from mycobacterial 65-kDa heat shock protein protects against pristane-induced arthritis. *J. Immunol.* **160,** 4628–4634.

204 Corrigall, V. M., Bodman-Smith, M. D., Fife, M. S., Canas, B., Myers, L. K., Wooley, P., et al. (2001) The human endoplasmic reticulum molecular chaperone BiP is an autoantigen for rheumatoid arthritis and prevents the induction of experimental arthritis. *J. Immunol.* **166,** 1492–1498.

205 Satoh, M. and Reeves, W. H. (1994) Induction of lupus-associated autoantibodies in BALB/c mice by intraperitoneal injection of pristane. *J. Exp. Med.* **180,** 2341–2346.

206 Satoh, M., Kumar, A., Kanwar, Y. S., and Reeves, W. H. (1995) Anti-nuclear antibody production and immune-complex glomerulonephritis in BALB/c mice treated with pristane. *Proc. Natl. Acad. Sci. USA* **92,** 10,934–10,938.

207 Satoh, M., Langdon, J. J., Hamilton, K. J., Richards, H. B., Panka, D., Eisenberg, R. A., et al. (1996) Distinctive immune response patterns of human and murine autoimmune sera to U1 small nuclear ribonucleoprotein C protein. *J. Clin. Invest.* **97,** 2619–2626.

208. Satoh, M., Richards, H. B., Shaheen, V. M., Yoshida, H., Shaw, M., Naim, J. O., et al. (2000) Widespread susceptibility among inbred mouse strains to the induction of lupus autoantibodies by pristane. *Clin. Exp. Immunol.* **121,** 399–405.

209 Richards, H. B., Satoh, M., Jennette, J. C., Croker, B. P., Yoshida, H., and Reeves, W. H. (2001) Interferon-γ is required for lupus nephritis in mice treated with the hydrocarbon oil pristane. *Kidney Int.* **60,** 2173–2180.

210 Richards, H. B., Satoh, M., Shaw, M., Libert, C., Poli, V., and Reeves, W. H. (1998) Interleukin 6 dependence of anti-DNA antibody production: evidence for two pathways of autoantibody formation in pristane-induced lupus. *J. Exp. Med.* **188,** 985–990.

211 Satoh, M., Weintraub, J. P., Yoshida, H., Shaheen, V. M., Richards, H. B., Shaw, M., et al. (2000) Fas and Fas ligand mutations inhibit autoantibody production in pristane-induced lupus. *J. Immunol.* **165,** 1036–1043.
212 Satoh, M., Hamilton, K. J., Ajmani, A. K., Dong, X., Wang, J., Kanwar, Y. S., et al. (1996) Autoantibodies to ribosomal P antigens with immune complex glomerulonephritis in SJL mice treated with pristane. *J. Immunol.* **157,** 3200–3206.
213 Morse, H. C., 3rd, Riblet, R., Asofsky, R., and Weigert, M. (1978) Plasmacytomas of the NZB mouse. *J. Immunol.* **121,** 1969–1972.
214 Byrd, L. G., McDonald, A. H., Gold, L. G., and Potter, M. (1991) Specific pathogen-free BALB/cAn mice are refractory to plasmacytoma induction by pristane. *J. Immunol.* **147,** 3632–3637.
215 Mendlovic, S., Brocke, S., Shoenfeld, Y., Ben-Bassat, M., Meshorer, A., Bakimer, R., et al. (1988) Induction of a systemic lupus erythematosus-like disease in mice by a common human anti-DNA idiotype. *Proc. Natl. Acad. Sci. USA* **85,** 2260–2264.
216 Blank, M., Cohen, J., Toder, V., and Shoenfeld, Y. (1991) Induction of anti-phospholipid syndrome in naive mice with mouse lupus monoclonal and human polyclonal anti-cardiolipin antibodies. *Proc. Natl. Acad. Sci. U S A* **88,** 3069–3073.
217 Blank, M., Krause, I., Ben-Bassat, M., and Shoenfeld, Y. (1992) Induction of experimental anti-phospholipid syndrome associated with SLE following immunization with human monoclonal pathogenic anti-DNA idiotype. *J. Autoimmun.* **5,** 495–509.
218 Shoenfeld, Y. and Ziporen, L. (1998) Lessons from experimental APS models. *Lupus* **7,** S158–S161.
219 Waisman, A., Ruiz, P. J., Israeli, E., Eilat, E., Konen-Waisman, S., Zinger, H., et al. (1997) Modulation of murine systemic lupus erythematosus with peptides based on complementarity determining regions of a pathogenic anti-DNA monoclonal antibody. *Proc. Natl. Acad. Sci. USA* **94,** 4620–4625.
220 Eilat, E., Dayan, M., Zinger, H., and Mozes, E. (2001) The mechanism by which a peptide based on complementarity-determining region-1 of a pathogenic anti-DNA auto-Ab ameliorates experimental systemic lupus erythematosus. *Proc. Natl. Acad. Sci. USA* **98,** 1148–1153.
221 Mozes, E., Kohn, L. D., Hakim, F., and Singer, D. S. (1993) Resistance of MHC class I-deficient mice to experimental systemic lupus erythematosus. *Science* **261,** 91–93.
222 Segal, R., Dayan, M., Zinger, H., and Mozes, E. (2001) Suppression of experimental systemic lupus erythematosus (SLE) in mice via TNF inhibition by an anti-TNFα monoclonal antibody and by pentoxiphylline. *Lupus* **10,** 23–31.
223 Isenberg, D. A., Katz, D., Le Page, S., Knight, B., Tucker, L., Maddison, P., et al. (1991) Independent analysis of the 16/6 idiotype lupus model. A role for an environmental factor? *J. Immunol.* **147,** 4172–4177.
224 Watanabe-Fukunaga, R., Brannan, C. I., Copeland, N. G., Jenkins, N. A., and Nagata, S. (1992) Lymphoproliferation disorder in mice explained by defects in Fas antigen that mediates apoptosis. *Nature* **356,** 314–317.

225 Adachi, M., Watanabe-Fukunaga, R., and Nagata, S. (1993) Aberrant transcription caused by the insertion of an early transposable element in an intron of the Fas antigen gene of *lpr* mice. *Proc. Natl. Acad. Sci. USA* **90,** 1756–1760.

226 Chu, J. L., Drappa, J., Parnassa, A., and Elkon, K. B. (1993) The defect in Fas mRNA expression in MRL/*lpr* mice is associated with insertion of the retrotransposon, ETn. *J. Exp. Med.* **178,** 723–730.

227 Wu, J., Zhou, T., He, J., and Mountz, J. D. (1993) Autoimmune disease in mice due to integration of an endogenous retrovirus in an apoptosis gene. *J. Exp. Med.* **178,** 461–468.

228 Roths, J. B., Murphy, E. D., and Eicher, E. M. (1984) A new mutation, gld, that produces lymphoproliferation and autoimmunity in C3H/HeJ mice. *J. Exp. Med.* **159,** 1–20.

229 Lynch, D. H., Watson, M. L., Alderson, M. R., Baum, P. R., Miller, R. E., Tough, T., et al. (1994) The mouse Fas-ligand gene is mutated in gld mice and is part of a TNF family gene cluster. *Immunity* **1,** 131–136.

230 Takahashi, T., Tanaka, M., Brannan, C. I., Jenkins, N. A., Copeland, N. G., Suda, T., et al. (1994) Generalized lymphoproliferative disease in mice, caused by a point mutation in the Fas ligand. *Cell* **76,** 969–976.

231 Matsuzawa, A., Moriyama, T., Kaneko, T., Tanaka, M., Kimura, M., Ikeda, H., et al. (1990) A new allele of the *lpr* locus, lprcg, that complements the gld gene in induction of lymphadenopathy in the mouse. *J. Exp. Med.* **171,** 519–531.

232 Kimura, M., Mohri, H., Shimada, K., Wakabayashi, T., Kanai, Y., and Matsuzawa, A. (1990) Serological and histological characterization of the new mutant strain of *lpr* mice, CBA/KlJms-lprcg/lprcg. *Clin. Exp. Immunol.* **79,** 123–129.

233 Kimura, M., Katagiri, T., Kikuchi, Y., Shimada, K., Nariuchi, H., Wakabayashi, T., et al. (1991) Role of bone marrow cells in autoantibody production and lymphoproliferation in the novel mutant strain of mice, CBA/KlJms-lprcg/lprcg. *Eur. J. Immunol.* **21,** 63–69.

234 Kimura, M., Ikeda, H., Katagiri, T., and Matsuzawa, A. (1991) Characterization of lymphoproliferation induced by interactions between lprcg and gld genes. *Cell. Immunol.* **134,** 359–369.

235 Matsuzawa, A., Kimura, M., Muraiso, T., Kominami, R., and Katagiri, T. (1991) Genotype-restricted lymphoproliferation in autoimmune *lpr* mice. *Eur. J. Immunol.* **21,** 1535–1542.

236 Kimura, M., Ogata, Y., Shimada, K., Moriyama, T., and Matsuzawa, A. (1991) New mutant mice of autoimmunity, CBA/KiJms-lprcg/lprcg, that could link the *lpr* and *gld* genes. *Autoimmunity* **9,** 359–361.

237 Adachi, M., Suematsu, S., Suda, T., Watanabe, D., Fukuyama, H., Ogasawara, J., et al. (1996) Enhanced and accelerated lymphoproliferation in Fas-null mice. *Proc. Natl. Acad. Sci. USA* **93,** 2131–2136.

238 Senju, S., Negishi, I., Motoyama, N., Wang, F., Nakayama, K. I., Nakayama, K., et al. (1996) Functional significance of the Fas molecule in naive lymphocytes. *Int. Immunol.* **8,**423–431.

239 Fisher, G. H., Rosenberg, F. J., Straus, S. E., Dale, J. K., Middleton, L. A., Lin, A. Y., et al. (1995) Dominant interfering Fas gene mutations impair apoptosis in a human autoimmune lymphoproliferative syndrome. *Cell* **81,** 935–946.

240 Rieux-Laucat, F., Le Deist, F., Hivroz, C., Roberts, I. A., Debatin, K. M., Fischer, A., et al. (1995) Mutations in Fas associated with human lymphoproliferative syndrome and autoimmunity. *Science* **268,** 1347–1349.

241 Drappa, J., Vaishnaw, A. K., Sullivan, K. E., Chu, J. L., and Elkon, K. B. (1996) Fas gene mutations in the Canale-Smith syndrome, an inherited lymphoproliferative disorder associated with autoimmunity. *N. Engl. J. Med.* **335,** 1643–1649.

242 Wu, J., Wilson, J., He, J., Xiang, L., Schur, P. H., and Mountz, J. D. (1996) Fas ligand mutation in a patient with systemic lupus erythematosus and lymphoproliferative disease. *J. Clin. Invest.* **98,** 1107–1113.

243 Wang, J., Zheng, L., Lobito, A., Chan, F. K., Dale, J., Sneller, M., et al. (1999) Inherited human Caspase 10 mutations underlie defective lymphocyte and dendritic cell apoptosis in autoimmune lymphoproliferative syndrome type II. *Cell* **98,** 47–58.

244 Roark, J. H., Kuntz, C. L., Nguyen, K. A., Caton, A. J., and Erikson, J. (1995) Breakdown of B cell tolerance in a mouse model of systemic lupus erythematosus. *J. Exp. Med.* **181,** 1157–1167.

245 Mandik-Nayak, L., Seo, S. J., Sokol, C., Potts, K. M., Bui, A., and Erikson, J. (1999) MRL-*lpr*/*lpr* mice exhibit a defect in maintaining developmental arrest and follicular exclusion of anti-double-stranded DNA B cells. *J. Exp. Med.* **189,** 1799–1814.

246 Seo, S. J., Fields, M. L., Buckler, J. L., Reed, A. J., Mandik-Nayak, L., Nish, S. A., et al. (2002) The impact of T helper and T regulatory cells on the regulation of anti-double-stranded DNA B cells. *Immunity* **16,** 535–546.

247 Theofilopoulos, A. N., Balderas, R. S., Gozes, Y., Aguado, M. T., Hang, L. M., Morrow, P. R., et al. (1985) Association of *lpr* gene with graft-vs-host disease-like syndrome. *J. Exp. Med.* **162,** 1–18.

248 Kurien, B. T. and Scofield, R. H. (1999) Mouse urine collection using clear plastic wrap. *Lab. Anim.* **33,** 83–86.

249 Kimura, M., Nagase, M., Hishida, A., and Honda, N. (1987) Intramesangial passage of mononuclear phagocytes in murine lupus glomerulonephritis. *Am. J. Pathol.* **127,** 149–156.

250 Hoffsten, P. E., Hill, C. L., and Klahr, S. (1975) Studies of abluminuria and proteinuria in normal mice and mice with immune complex glomerulonephritis. *J. Lab. Clin. Med.* **86,** 920–930.

251 Hem, A., Smith, A. J., and Solberg, P. (1998) Saphenous vein puncture for blood sampling of the mouse, rat, hamster, gerbil, guinea pig, ferret and mink. *Lab. Anim.* **32,** 364–368.

252 Furner, R. L. and Mellett, L. B. (1975) Mouse restraining chamber for tail-vein injection. *Lab. Anim. Sci.* **25,** 648.

253 Durschlag, M., Wurbel, H., Stauffacher, M., and Von Holst, D. (1996) Repeated blood collection in the laboratory mouse by tail incision—modification of an old technique. *Phys. Behav.* **60,** 1565–1568.

254 Hijmans, W., Radema, H., van Es, L., Feltkamp, T. E., van Loghem, J. J., and Schaap, O. L. (1969) Cryoglobulins in New Zealand black mice. *Clin. Exp. Immunol.* **4,** 227–239.

255. Reininger, L., Berney, T., Shibata, T., Spertini, F., Merino, R., and Izui, S. (1990) Cryoglobulinemia induced by a murine IgG3 rheumatoid factor: skin vasculitis and glomerulonephritis arise from distinct pathogenic mechanisms. *Proc. Natl. Acad. Sci. USA* **87,** 10,038–10,042.

256 Dammacco, F., Sansonno, D., Piccoli, C., Tucci, F. A., and Racanelli, V. (2001) The cryoglobulins: an overview. *Eur. J. Clin. Invest.* **31,** 628–638.

257. Peng, S. L. and Craft, J. (2001) Antinuclear antibodies, in *Kelly's Textbook of Rheumatology* (Ruddy, S., Harris, E. D., and Sledge, C. B., eds.), Saunders, Philadelphia, PA, pp. 161–174.

258 Shlomchik, M. J., Madaio, M. P., Ni, D., Trounstein, M., and Huszar, D. (1994) The role of B cells in *lpr/lpr*-induced autoimmunity. *J. Exp. Med.* **180,** 1295–1306.

259 Peng, S. L., Cappadona, J., McNiff, J. M., Madaio, M. P., Owen, M. J., Hayday, A. C., et al. (1998) Pathogenesis of autoimmunity in αβ T cell-deficient lupus-prone mice. *Clin. Exp. Immunol.* **111,** 107–116.

260 Kofler, R., Perlmutter, R. M., Noonan, D. J., Dixon, F. J., and Theofilopoulos, A. N. (1985) Ig heavy chain variable region gene complex of lupus mice exhibits normal restriction fragment length polymorphism. *J. Exp. Med.* **162,** 346–351.

261 Kotzin, B. L., Barr, V. L., and Palmer, E. (1985) A large deletion within the T-cell receptor β-chain gene complex in New Zealand white mice. *Science* **229,** 167–171.

262 Noonan, D. J., Kofler, R., Singer, P. A., Cardenas, G., Dixon, F. J., and Theofilopoulos, A. N. (1986) Delineation of a defect in T cell receptor β genes of NZW mice predisposed to autoimmunity. *J. Exp. Med.* **163,** 644–653.

263 Yanagi, Y., Hirose, S., Nagasawa, R., Shirai, T., Mak, T. W., and Tada, T. (1986) Does the deletion within T cell receptor β-chain gene of NZW mice contribute to autoimmunity in (NZB × NZW) F1 mice? *Eur. J. Immunol.* **16,** 1179–1182.

264 Singer, P. A., McEvilly, R. J., Balderas, R. S., Dixon, F. J., and Theofilopoulos, A. N. (1988) T-cell receptor α-chain variable-region haplotypes of normal and autoimmune laboratory mouse strains. *Proc. Natl. Acad. Sci. USA* **85,** 7729–7733.

265 Wilson, R. K., Lai, E., Concannon, P., Barth, R. K., and Hood, L. E. (1988) Structure, organization and polymorphism of murine and human T-cell receptor α and β chain gene families. *Immunol. Rev.* **101,** 149–172.

266 Jouvin-Marche, E., Morgado, M. G., Trede, N., Marche, P. N., Couez, D., Hue, I., et al. (1989) Complexity, polymorphism, and recombination of mouse T-cell receptor α gene families. *Immunogenetics* **30,** 99–104.

267 Klotz, J. L., Barth, R. K., Kiser, G. L., Hood, L. E., and Kronenberg, M. (1989) Restriction fragment length polymorphisms of the mouse T-cell receptor gene families. *Immunogenetics* **29,** 191–201.

268 Theofilopoulos, A. N., Kofler, R., Singer, P. A., and Dixon, F. J. (1989) Molecular genetics of murine lupus models. *Adv. Immunol.* **46,** 61–109.

269 Noonan, D. J., McConahey, P. J., and Cardenas, G. J. (1990) Correlations of autoimmunity with H-2 and T cell receptor β chain genotypes in (NZB × NZW) F2 mice. *Eur. J. Immunol.* **20,** 1105–1110.

270. Hansen, T. H., Carreno, B. M., and Sachs, D. H. (1993) The major histocompatibility complex, in *Fundamental Immunology* (Paul, W. E., ed.), Raven Press, New York, pp. 577–628.

271 Choi, Y., Ramnath, V. R., Eaton, A. S., Chen, A., Simon-Stoos, K. L., Kleiner, D. E., et al. (1999) Expression in transgenic mice of dominant interfering Fas mutations: a model for human autoimmune lymphoproliferative syndrome. *Clin. Immunol.* **93,** 34–45.

272 Balomenos, D., Martin-Caballero, J., Garcia, M. I., Prieto, I., Flores, J. M., Serrano, M., et al. (2000) The cell cycle inhibitor p21 controls T-cell proliferation and sex-linked lupus development. *Nat. Med.* **6,** 171–176.

273 Lawson, B. R., Kono, D. H., and Theofilopoulos, A. N. (2002) Deletion of p21 (WAF-1/Cip1) does not induce systemic autoimmunity in female BXSB mice. *J. Immunol.* **168,** 5928–5932.

274 Strasser, A., Whittingham, S., Vaux, D. L., Bath, M. L., Adams, J. M., Cory, S., et al. (1991) Enforced BCL2 expression in B-lymphoid cells prolongs antibody responses and elicits autoimmune disease. *Proc. Natl. Acad. Sci. USA* **88,** 8661–8665.

275 Bouillet, P., Metcalf, D., Huang, D. C., Tarlinton, D. M., Kay, T. W., Kontgen, F., et al. (1999) Proapoptotic Bcl-2 relative Bim required for certain apoptotic responses, leukocyte homeostasis, and to preclude autoimmunity. *Science* **286,** 1735–1738.

276 Bouillet, P., Purton, J. F., Godfrey, D. I., Zhang, L. C., Coultas, L., Puthalakath, H., et al. (2002) BH3-only Bcl-2 family member Bim is required for apoptosis of autoreactive thymocytes. *Nature* **415,** 922–926.

277 Murga, M., Fernandez-Capetillo, O., Field, S. J., Moreno, B., Borlado, L. R., Fujiwara, Y., et al. (2001) Mutation of E2F2 in mice causes enhanced T lymphocyte proliferation, leading to the development of autoimmunity. *Immunity* **15,** 959–970.

278 Salvador, J. M., Hollander, M. C., Nguyen, A. T., Kopp, J. B., Barisoni, L., Moore, J. K., et al. (2002) Mice lacking the p53-effector gene Gadd45a develop a lupus-like syndrome. *Immunity* **16,** 499–508.

279 Di Cristofano, A., Kotsi, P., Peng, Y. F., Cordon-Cardo, C., Elkon, K. B., and Pandolfi, P. P. (1999) Impaired Fas response and autoimmunity in Pten ± mice. *Science* **285,** 2122–2125.

280 Suzuki, A., Yamaguchi, M. T., Ohteki, T., Sasaki, T., Kaisho, T., Kimura, Y., et al. (2001) T cell-specific loss of Pten leads to defects in central and peripheral tolerance. *Immunity* **14,** 523–534.

281 Yoshinaga, S. K., Zhang, M., Pistillo, J., Horan, T., Khare, S. D., Miner, K., et al. (2000) Characterization of a new human B7-related protein: B7RP-1 is the ligand to the co-stimulatory protein ICOS. *Int. Immunol.* **12,** 1439–1447.

282 Prodeus, A. P., Goerg, S., Shen, L. M., Pozdnyakova, O. O., Chu, L., Alicot, E. M., et al. (1998) A critical role for complement in maintenance of self-tolerance. *Immunity* **9,** 721–731.

283. O'Keefe, T. L., Williams, G. T., Davies, S. L., and Neuberger, M. S. (1996) Hyperresponsive B cells in CD22-deficient mice. *Science* **274,** 798–801.

284 Majeti, R., Xu, Z., Parslow, T. G., Olson, J. L., Daikh, D. I., Killeen, N., et al. (2000) An inactivating point mutation in the inhibitory wedge of CD45 causes lymphoproliferation and autoimmunity. *Cell* **103,** 1059–1070.

285 Tivol, E. A., Borriello, F., Schweitzer, A. N., Lynch, W. P., Bluestone, J. A., and Sharpe, A. H. (1995) Loss of CTLA-4 leads to massive lymphoproliferation and fatal multiorgan tissue destruction, revealing a critical negative regulatory role of CTLA-4. *Immunity* **3,** 541–547.

286 Waterhouse, P., Penninger, J. M., Timms, E., Wakeham, A., Shahinian, A., Lee, K. P., et al. (1995) Lymphoproliferative disorders with early lethality in mice deficient in Ctla-4. *Science* **270,** 985–988.

287 Bolland, S. and Ravetch, J. V. (2000) Spontaneous autoimmune disease in FcγRIIB-deficient mice results from strain-specific epistasis. *Immunity* **13,** 277–285.

288 Le, L. Q., Kabarowski, J. H., Weng, Z., Satterthwaite, A. B., Harvill, E. T., Jensen, E. R., et al. (2001) Mice lacking the orphan G protein-coupled receptor G2A develop a late-onset autoimmune syndrome. *Immunity* **14,** 561–571.

289 Suzuki, H., Kundig, T. M., Furlonger, C., Wakeham, A., Timms, E., Matsuyama, T., et al. (1995) Deregulated T cell activation and autoimmunity in mice lacking interleukin-2 receptor β. *Science* **268,** 1472–1476.

290 Nishimura, H., Nose, M., Hiai, H., Minato, N., and Honjo, T. (1999) Development of lupus-like autoimmune diseases by disruption of the PD-1 gene encoding an ITIM motif-carrying immunoreceptor. *Immunity* **11,** 141–151.

291 Wen, L., Roberts, S. J., Viney, J. L., Wong, F. S., Mallick, C., Findly, R. C., et al. (1994) Immunoglobulin synthesis and generalized autoimmunity in mice congenitally deficient in αβ(+) T cells. *Nature* **369,** 654–658.

292 Wang, J. H., Avitahl, N., Cariappa, A., Friedrich, C., Ikeda, T., Renold, A., et al. (1998) Aiolos regulates B cell activation and maturation to effector state. *Immunity* **9,** 543–553.

293 Nash, J. T., Taylor, P. R., Botto, M., Norsworthy, P. J., Davies, K. A., and Walport, M. J. (2001) Immune complex processing in C1q-deficient mice. *Clin. Exp. Immunol.* **123,** 196–202.

294 Botto, M., Dell'Agnola, C., Bygrave, A. E., Thompson, E. M., Cook, H. T., Petry, F., et al. (1998) Homozygous C1q deficiency causes glomerulonephritis associated with multiple apoptotic bodies. *Nat. Genet.* **19,** 56–59.

295 Mackay, F., Woodcock, S. A., Lawton, P., Ambrose, C., Baetscher, M., Schneider, P., et al. (1999) Mice transgenic for BAFF develop lymphocytic disorders along with autoimmune manifestations. *J. Exp. Med.* **190,** 1697–1710.

296 Gross, J. A., Johnston, J., Mudri, S., Enselman, R., Dillon, S. R., Madden, K., et al. (2000) TACI and BCMA are receptors for a TNF homologue implicated in B-cell autoimmune disease. *Nature* **404,** 995–999.

297 Khare, S. D., Sarosi, I., Xia, X. Z., McCabe, S., Miner, K., Solovyev, I., et al. (2000) Severe B cell hyperplasia and autoimmune disease in TALL-1 transgenic mice. *Proc. Natl. Acad. Sci. USA* **97,** 3370–3375.

298 Krawczyk, C., Bachmaier, K., Sasaki, T., Jones, G. R., Snapper, B. S., Bouchard, D., et al. (2000) Cbl-b is a negative regulator of receptor clustering and raft aggregation in T cells. *Immunity* **13,** 463–473.

299 Zhang, Y., Schlossman, S. F., Edwards, R. A., Ou, C. N., Gu, J., and Wu, M. X. (2002) Impaired apoptosis, extended duration of immune responses, and a lupus-like autoimmune disease in IEX-1-transgenic mice. *Proc. Natl. Acad. Sci. USA* **99,** 878–883.

300 Hibbs, M. L., Tarlinton, D. M., Armes, J., Grail, D., Hodgson, G., Maglitto, R., et al. (1995) Multiple defects in the immune system of Lyn-deficient mice, culminating in autoimmune disease. *Cell* **83,** 301–311.

301 Nishizumi, H., Taniuchi, I., Yamanashi, Y., Kitamura, D., Ilic, D., Mori, S., et al. (1995) Impaired proliferation of peripheral B cells and indication of autoimmune disease in *lyn*-deficient mice. *Immunity* **3,** 549–560.

302 Cornall, R. J., Cyster, J. G., Hibbs, M. L., Dunn, A. R., Otipoby, K. L., Clark, E. A., et al. (1998) Polygenic autoimmune traits: Lyn, CD22, and SHP-1 are limiting elements of a biochemical pathway regulating BCR signaling and selection. *Immunity* **8,** 497–508.

303 Scott, R. S., McMahon, E. J., Pop, S. M., Reap, E. A., Caricchio, R., Cohen, P. L., et al. (2001) Phagocytosis and clearance of apoptotic cells is mediated by MER. *Nature* **411,** 207–211.

304 Demetriou, M., Granovsky, M., Quaggin, S., and Dennis, J. W. (2001) Negative regulation of T-cell activation and autoimmunity by Mgat5 *N*-glycosylation. *Nature* **409,** 733–739.

305 Sun, H., Lu, B., Li, R. Q., Flavell, R. A., and Taneja, R. (2001) Defective T cell activation and autoimmune disorder in Stra13-deficient mice. *Nat. Immunol.* **2,** 1040–1047.

306 Yaswen, L., Kulkarni, A. B., Fredrickson, T., Mittleman, B., Schiffman, R., Payne, S., et al. (1996) Autoimmune manifestations in the transforming growth factor-β1 knockout mouse. *Blood* **87,** 1439–1445.

307. Gorelik, L. and Flavell, R. A. (2000) Abrogation of TGFβ signaling in T cells leads to spontaneous T cell differentiation and autoimmune disease. *Immunity* **12,** 171–181.

14

The Anti-DNA Knock-In Model of Systemic Autoimmunity Induced by the Chronic Graft-vs-Host Reaction

Robert Eisenberg and Arpita Choudhury

Summary

The injection of spleen cells from bm12 mice into C57BL/6 recipients induces a chronic graft-vs-host reaction characterized by systemic autoimmunity, including anti-double-stranded DNA (anti-dsDNA) autoantibodies and immune complex-type proliferative glomerulonephritis. If the B6 recipient mice express an anti-DNA Vh site-directed transgene, the repertoire is skewed even more toward the anti-DNA response. Over a period of several weeks, high titers of serum anti-DNA antibodies appear and the mice develop renal damage. This permits the examination of the role of somatic immunoglobulin genetics and B-cell tolerance in a model of systemic lupus erythematosus.

Key Words: Anti-DNA; autoimmunity; B cells; GVH; SLE; tolerance.

1. Introduction

The described method combines two important approaches to modeling systemic autoimmunity in mice: the chronic graft-vs-host (cGVH) reaction, driven by major histocompatibility complex (MHC) class II recognition ***(1–3)***, and the use of site-directed transgenics (Tgs) of immunoglobulin genes from anti-DNA (anti-DNA) autoantibodies ***(4,5)***. This provides several distinct advantages. First, the cGVH allows the precise time of induction of the autoimmune syndrome to be fixed. Second, it permits comparison to the preautoimmune state, which is entirely normal. Thus, B cells that recognize important autoantigens can be studied in the tolerant state before the induction of the cGVH and in the autoimmune state after the syndrome is initiated. Third, the use of normal C57BL/6 (B6) mice as recipients permits the facile adaptation of

From: *Methods in Molecular Medicine, Vol. 102: Autoimmunity: Methods and Protocols*
Edited by: A. Perl © Humana Press Inc., Totowa, NJ

the system to the large number of Tg strains on the B6 background to test the role of various genes ***(6)***. In fact, the model described here utilizes just such a modification, in this case with the anti-DNA knockin Tgs ***(7,8)***. Fourth, the anti-DNA Tgs provide the additional advantage of a repertoire skewed toward production of a known autoantibody specific for systemic lupus erythematosus (SLE), as well as potential markers to permit analyses to focus on the autoreactive B cells themselves. Finally, the site-directed or knockin Tgs offer substantial benefit over traditional Tgs. Because the rearranged immunoglobulin genes are inserted in a nearly physiological manner into the appropriate genetic locus, they are subject to the normal mechanisms of class switching, secondary rearrangements, and somatic mutations.

Another significant feature of the cGVH model we utilize is that the recipient strain (B6) differs from the donor B6.CH2bm12/Kheg (bm12) only by a change of three amino acids in the β-chain of MHC class II molecule I-A (although the site-directed heavy chain gene might be considered an additional difference) ***(9)***. This allows the transfer of parental bm12 cells into parental B6 recipients. That is, we do not need to use F1 recipients to prevent a host-vs-graft reaction because the donor T cells do not express MHC class II. The donor B cells, of course, do express I-A, but they do not appear to be stimulated by the host T cells, and they disappear fairly quickly after transfer ***(10)***. The reciprocal transfer of B6 donors into bm12 recipients creates a similar model, but is generally less useful because of the very limited number of Tg and congenic strains available on the bm12 background ***(11)***.

Although the allogeneic T-cell stimulus that drives autoantibody production in the cGVH is unlikely to be directly applicable to spontaneous SLE, either in mice or in humans, the pattern of loss of B-cell tolerance, as evidenced in the spectrum of autoantibodies produced and in fact those that are not produced ***(12–15)***, is so strikingly parallel to the natural disease that the elucidation of the cellular and biochemical mechanisms of the cGVH is highly likely to provide important insights into the processes of loss of B-cell tolerance in general.

2. Materials

2.1. Mice

The C576BL/6J (B6) and B6.CH2bm12/Kheg (bm12) mice are originally obtained from the Jackson Laboratory (Bar Harbor, ME). We maintain our own breeding colony as a matter of convenience and cost. The site-directed Tgs are available from Dr. Martin Weigert (University of Chicago, Chicago, IL) or from us. These include mice with the 3H9 and 56R anti-DNA rearranged site-directed Tg heavy chain ***(16)***. Additional anti-DNA site-directed Tgs are under development by Dr. Weigert.

2.2. Mouse Typing

The following polymerase chain reaction (PCR) primers are used ***(17)***:

1. 5'CTGTCAQGGAACTGCAGGTAAGG3((Invitrogen, Carlsbad, CA).
2. 5'CATAACATAGGAATATTTACTCCTCGC3((Invitrogen).

The PCR mixture contains 18.6 μL distilled water, 0.75 μL 50 m*M* $MgCl_2$, 2.5 μL 10X PCR buffer, 2.0 μL 10 m*M* deoxyribonucleotide triphosphates (dNTPs), 0.25 μL of each of the primers from 100 m*M* solutions, 0.15 μL Taq, and 0.4 μL sample DNA. The $MgCl_2$, 10X PCR buffer, and Taq all come from Invitrogen. The dNTPs come from Applied Biosystems (Foster City, CA). DNA is extracted with tail lysis buffer, which contains 50 m*M* Tris-HCl, 50 m*M* KCl, 2.5 m*M* ethylene-diaminetetraacetic acid (EDTA), 0.45% Tween-20, and 0.45% NP-40 at pH 8.0. Proteinase K is obtained from Roche (Indianapolis, IN) as a 14-mg/mL solution.

2.3. Cell Preparation

Cell preparation is done in Hanks balanced salt solution (HBSS), obtained from Mediatech (Herndon, VA).

2.4. Induction of cGVH

No special reagents are required for induction of cGVH.

2.5. Follow-Up

Uristix to measure urinary protein come from Miles Laboratories (Elkhart, IN).

2.6. Sacrifice

Fixation for routine histology is done in 4% formalin (Fisher Scientific, Fairlawn, NJ). Kidneys are frozen in Tissue-Tek OCT (Sakura Finetechnical, Tokyo, Japan).

2.7. Serologies

The basic enzyme-linked immunosorbent assay (ELISA) buffer is borate-buffered saline (BBS), which consists of 0.2 *M* borate plus 0.075 *M* NaCl at pH 8.4. For coating plates to block nonspecific binding and for diluting samples and other binding reagents, the BBS is supplemented with 0.5% bovine serum albumin (Sigma-Aldrich, St. Louis, MO), 0.4% Tween-80 (Fisher Scientific), and 0.1% NaN_3 (BBT).

Antigens include the following:

1. Double-stranded DNA (dsDNA) is prepared by extracting calf thymus DNA (Sigma-Aldrich) with chloroform:isoamyl alcohol (24:1) five times, treating with

S1 nuclease (4 μL of a 25,000 U/mL stock from Pharmacia [Piscataway, NJ] for 500 mg DNA in 10 mL 0.1 *M* acetate at pH 5.0 plus 1 m*M* $ZnCl_2$) for 45 min at 37°C to remove single-stranded portions and precipitating with 95% ethanol.

2. Chromatin is prepared by hypotonic lysis of chicken erythrocyte nuclei ***(18)*** as follows: Chicken blood is collected in 20-mL anticoagulant buffer (0.15 *M* NaCl, 0.01 *M* HEPES, 0.01 *M* EDTA at pH 7.4), washed and resuspended in 15 mL of buffer A (0.08 *M* NaCl, 0.02 *M* EDTA at pH 7.5), lysed with 1.5% Triton X-100, layered over 2 mL 2.25 *M* sucrose and 18 mL 1.7 *M* sucrose in buffer A, and centrifuged for 90 min at 112,700*g* in a Beckman SW27 rotor at 4°C. The nuclear pellet is lysed by homogenization in 0.1 m*M* EDTA at pH 8.0 using a Dounce homogenizer and then aliquotted and stored in 0.1 m*M* EDTA. $IgG1^b$ and $IgG2b^b$ are prepared from the supernatants of MOPC245 and BPC4, respectively, by protein G.
3. The developing antibodies include biotinylated goat antimouse IgG, pFc'-specific and alkaline phosphatase antirabbit immunoglobulin G (IgG; Jackson ImmunoResearch Laboratories, West Grove, PA); rabbit antimouse $IgG2a^a$ and antimouse $IgG2a^b$ (Nordic Immunological Laboratories, Tilburg, Netherlands); and avidin-alkaline phosphatase (Zymed Laboratories, South San Francisco, CA).
4. 96-well flexible polyvinyl plastic microtiter plates (Dynatech Laboratories, Alexandria, VA).
5. Paranitrophenyl phosphate alkaline phosphatase substrate (Sigma-Aldrich).
6. Poly-L-lysine (Sigma Aldrich).

2.8. Cellular Analysis

The following antibodies from BD Pharmingen (San Diego, CA) are used:

1. Fluorescein isothiocyanate (FITC)/PE/biotin anti-B220 (RA3-6B2).
2. FITC anti-CD21 (7G6).
3. FITC anti-Igλ1/2/3 (R26-46).
4. FITC anti-IgG1 (A85-1).
5. PE anti-CD86 (GL1).
6. PE anti-CD23 (B3B4).
7. PE anti-CD24 (M1/69).
8. PE anti-IgD^b (217-170).
9. PE anti-IgM^a (DS-1).
10. Biotin anti-Fas (Jo2).
11. Biotin anti-IgD^a (AMS9.1).
12. Biotin anti-IgM (II/1).
13. Streptavidin cytochrome.

HEPES comes from Gibco (Grand Island, NY) as a 1 *M* stock.

2.9. Hybridoma Production

SP2/0 line was used as a fusion partner.

3. Methods

3.1. Mouse Maintenance

Mice used for the cGVH are bred in our specific-pathogen-free facility. The bm12 mice are paired as brothers with two sisters, with attention to keep contemporaneous mice in a single generation as much as possible. Subsequent generations are derived from a single breeder cage (stem) so that individual sublines do not develop. C57BL/6-anti-DNA Tg (B6-Tg) mice are bred by crossing them B6 mice bred by brother–sister mating in our colony, as for bm12. The transgene-positive B6 can be either the female or the male mate. Mice are used between ages 6 and 12 wk. The anti-DNA transgene thus is always maintained in the heterozygous state, and the offspring of each generation include about 50% transgene-positive and 50% transgene-negative individuals, which can be used as controls.

3.2. Mouse Typing

Mice are "tailed" (1- to 2-mm piece of distal tail is cut off with a scalpel at age 2 wk), and DNA is extracted from the tail by 100 μL of tail lysis buffer plus 0.7 μL proteinase K at 56°C overnight. The mixture is vortexed, quick spun, and then can be stored at –20°C. The presence of the transgene is determined by PCR as follows: Denature at 94°C for 5 min, then cycled 35 times at 94°C for 30 s, 59°C for 30 s, and 72°C for 30 s. Finally, the sample is annealed at 72°C for 7 min and held at 4°C.

3.3. Cell Preparation

Spleen cells are prepared from bm12 donor mice for transfer into B6-Tg recipients. As each recipient is given 10^8 mononuclear cells, two donors are sacrificed per recipient to ensure that sufficient cells will be available at the end of the day. Donors are sacrificed by cervical dislocation. After wiping down the fur with 70% ethanol, the abdominal skin is grasped with a forceps, and an incision is made with a pair of scissors. Care must be taken to cut through all layers to expose fully the contents of the peritoneum without injuring any of the internal organs, particularly the gut or the spleen itself.

The spleen is readily identified in the left upper quadrant. Its pedicle can be grasped with a pair of bent forceps. With gentle, persistent retraction of the spleen at this point, the organ should be delivered intact and free of any other structures.

A single-cell suspension is prepared from the spleen by pressing through a wire mesh screen in HBSS. The cells are washed in HBSS, and red blood cells are lysed with 5 mL 0.15 *M* ammonium chloride plus 0.01 *M* potassium carbonate plus 0.1 m*M* EDTA at pH 7.2–7.4 for 5 min at room temperature. Cells

are pelleted at 400*g* for 5 min, washed twice with HBSS, and resuspended at 3.3×10^8 live cells/mL in the same medium. They are kept on ice for injection into recipients the same day. Control recipients receive comparable cells prepared from B6 donors.

3.4. Induction of cGVH

Bm12 spleen cells are injected intraperitoneally with a 30-ga needle, 0.3 mL per recipient. Care must be taken to ensure that the needle enters the peritoneal cavity and not the gut itself. In all cases, the sex of the donors and recipients must match so that the male-specific antigen is not recognized as foreign. In any experiment in which the reactivity of the donor is tested, an appropriate positive control must be included that receives aliquots of the same bm12 spleen cell preparation. Positive control recipients could be B6 or B6-Tg mice.

3.5. Follow-Up

The development of disease is followed by periodic bleeds, measurement of proteinuria, and general observation for signs of systemic illness. Bleeds are taken either from the tail or from the retroorbital sinus into a glass Pasteur pipet and transferred to microcentrifuge tubes for clotting. The clots are "rimmed" with an applicator stick to detach them from the walls of the tube, and the serum is separated by centrifugation in a microfuge at 9300*g* for 30 s. Serum is removed with a Pasteur pipet and stored as a single aliquot in a labeled microfuge tube with 1 µL of 10% NaN_3 added as a preservative. Bleeds are normally done just before the induction of cGVH and then at 1, 2, and 4 wk and monthly thereafter.

Proteinuria is assessed whenever a bleed is taken by wetting a urinary protein dipstick (Uristix) with a drop of mouse urine and comparing the resultant color with the scale on the bottle. The mouse may be induced to urinate by grasping it with one hand by the scruff of the neck and the tail (the thumb and index finger hold the neck skin, and the tail is wrapped around the pinkie) and credéing the bladder with a single finger of the other hand.

For clinical disease, the mice are observed twice a week for ruffling of the fur, hunched posture, weight loss, and difficult movements. Mice that appear to be seriously ill are euthanized.

3.6. Sacrifice

Mice are sacrificed either when they are clinically seriously ill or at a predetermined end point, such as 12 wk. They are euthanized by cervical dislocation. Autopsy permits harvesting of the kidneys, spleen, lymph nodes, and bone marrow. The kidneys are removed with bent forceps by grasping the kidneys at the pedicle, as for the spleen. One kidney is fixed in formalin for light micros-

copy, and the other is frozen in OCT compound for immunofluorescence analysis. A blinded observer reads the renal histology on a 4-point scale to judge the degree of glomerular, interstitial, and vascular involvements separately ***(19)***.

Lymph nodes may be found in the inguinal and submandibular regions. The bone marrow is flushed from the tibia and femur by inserting a 22-ga needle parallel to the long axis of the bone through the epiphysis into the marrow cavity and expressing about 3 mL HBSS into a sterile Petri dish. Spleen and lymph node suspensions are prepared by pressing the organs through a wire mesh.

3.7. Serologies

The development of serological abnormalities indicative of the cGVH is assessed in saved serum samples ***(6,20)***. For comparisons over time, all samples must be tested in a single assay for a given specificity. Assays for total serum IgG, IgG antichromatin, IgG anti-dsDNA, and IgM anti-IgG1 or IgM anti-IgG2b^b are generally performed. The total serum IgG assay is described in detail, whereas the other assays are described only insofar as they differ from it.

3.7.1. ELISA for Total Serum IgG

By means of a 12-multichannel pipettor, microtiter plates are loaded with 100 μL of polyclonal goat antimouse IgG (H-chain specific) diluted to 3 μg/mL in phosphate-buffered saline. Plates are incubated at room temperature for 4 h or overnight at 4°C. Between all additions, the plates must not be allowed to dry. All incubations are done with hard plastic covers over the plates to limit evaporation and to prevent contamination. The incubating plates are held in a flat Tupperware container with a moist atmosphere provided by a thin layer of wet towels to minimize evaporation of samples.

The plates are aspirated with a multichannel aspirator with short lengths of plastic tubing attached to the tips to protect the plate and then filled with 200 μL per well of BBT with a multichannel pipet. After further incubation at room temperature for 1 h, samples are loaded into appropriate wells.

Samples are prepared during the previous incubation periods by diluting serum to 10^{-5} in two steps. The first dilution can then be used for the other serological tests. All serum dilutions are made in BBT. Samples are loaded in duplicate with a 100-μL multichannel pipettor. When all samples have been added, the plates are incubated overnight at 4°C in a cold room.

The next day, the plates are aspirated with an automatic plate washer and washed with BBS plus 0.05 % Tween-20 five times. One plate at a time, the final wash solution is flicked out manually, the plates are quickly patted dry with paper towels, and the detecting antibody, goat antimouse IgG conjugated to biotin, is added at a 1/2000 dilution in BBT. This is incubated at room tem-

perature for 3 h, the plates are washed again five times, and streptavidin-conjugated alkaline phosphatase is added diluted 1/8000 in BBT for an additional 3 h incubation. After further washing, 1 mg/mL paranitrophenyl phosphate substrate in 0.01 *M* diethanolamine at pH 9.8 is added. A standard curve is made with serial twofold dilutions of a purified monoclonal IgG, such as HB63.

3.7.2. ELISA for Antichromatin

The ELISA for antichromatin assay is performed essentially the same as the one for total serum IgG except that the initial coating is with chicken chromatin at 3 μg/mL, the serum is added at a dilution of 1/500, and the standard curve is with an MRL/*lpr-Igh*^{b} serum in serial twofold dilutions. The optical density for each sample is referred to the standard curve, and the corresponding dilution of the MRL/*lpr-Igh*^{b} serum is multiplied by 10^6 and times the dilution factor (500) to give an equivalent dilution factor ***(21)***.

3.7.3. ELISA for Anti-DNA

The ELISA for anti-DNA is performed the same as the antichromatin assay except that the plates are precoated with 0.01% poly-L-lysine in distilled water for 3 h at room temperature, washed with distilled water, and then dried before further coating with DNA diluted to 3 μg/mL.

3.7.4. ELISA for Rheumatoid Factor

The ELISA for rheumatoid factor is performed the same as the antichromatin assay except that the initial coating is with purified IgG1^b at 5 μg/mL or IgG2b^b at 3 μg/mL, and the bound antibody is detected with biotinylated monoclonal antibody against mouse IgM.

3.8. Cellular Analysis

The phenotype of lymphoid cells in the spleen, bone marrow, and lymph nodes is detected with appropriate monoclonal antibody in 96-well, round-bottom microtiter plates ***(3,22)***. Single-cell suspensions in HBSS are washed with FACS buffer (HBSS, 0.15 *M* HEPES, 3% bovine serum albumin, 0.1% NaN_3) and blocked with 50 μL (hybridoma supernatant) 2.4G2 anti-FcγRc at a concentration of 1.5×10^6 cells for 20 min on ice. They are then incubated for 30 min with labeled antibodies, washed twice, and incubated an additional 20 min with streptavidin-cytochrome or secondary antibody. After washing twice with FACS buffer, they are washed once with HBSS plus 0.1% NaN_3, and then they are fixed in phosphate-buffered saline with 1% paraformaldehyde. They are analyzed on a FACscan (BD Biosciences, Mountainview, CA).

3.9. Hybridoma Production

The repertoire of autoantibody-producing cells can be sampled by producing hybridomas from the spleens of mice undergoing cGVH ***(23)***. Single-cell spleen suspensions are fused with SP2/0 partners without further stimulation. They are plated at limiting dilution in 96-well microtiter plates in the presence of 10% Origen and hypoxanthine azaserine (Sigma). Wells bearing single colonies are expanded, and those secreting Ig are selected for further study. The molecular biological approaches to analyzing the use of Ig genes in these hybridomas are beyond the scope of this review.

4. Notes

1. We have maintained the anti-DNA knock-in Tgs in the heterozygous state in general. This permits additional rearrangements to occur on the endogenous chromosome, which has a different heavy chain allotype (Igh^b; the Tg chromosome is Igh^a) ***(7,8)***. These site-directed Tgs can be bred to homozygosity, but this will change the immunoglobulin genetics of the model. On the other hand, it will provide twice as many Tg offspring for experimentation, and plain B6 mice can be used as controls.
2. The described PCR works for the 3H9 and 56R transgenes. It does not give an explicit identification of non-Tg chromosomes, so it cannot be used to distinguish heterozygotes from homozygotes.
3. The CD4 donor cells are the key constituent of the spleen. If necessary, this subset can be purified and transferred in smaller numbers. We do not have direct experience, but others have used 10^7 CD4 T cells per recipient ***(24)***.
4. In the past, we have used intravenous injection of the same number of cells (10^8). We found no difference in the disease produced with intravenous vs intraperitoneal injection. Intravenous injection is technically more difficult, but one can be sure at the time of injection that the cells were appropriately delivered to the host. In all experiments, there is substantial variability in the response of individual cGVH recipients; not uncommonly, some mice will fail to make any autoantibodies. It is clear that the cell dose is critical. If fewer than 10^8 cells are transferred (e.g., 5×10^7), much less of a cGVH reaction is seen.
5. In the Tg system, anti-DNA antibodies appear by 1 wk after injection. Other changes in B-cell phenotype may occur even earlier in the first week. The levels of antibodies increase over several weeks and then start to decrease after 4–8 wk. The kidney disease is apparent at 3 wk; we have not looked earlier.
6. The level of spontaneous mortality from cGVH in this model is variable for unknown reasons.
7. Other serologies have been reported in the cGVH, including anticollagen IV and antidipeptidyl peptidase IV ***(25,26)***. With the site-directed Tg recipients, the response is very much skewed toward anti-dsDNA, such that the levels of antibodies seen with this specificity are much higher than in non-Tg cGVH B6 mice; most of the

antibody-producing hybridomas recovered are directed against dsDNA. We have not looked extensively for additional specificities in this model.

8. The curious aspect of the cellular analysis of recipient B cells is that the entire B-cell population appears to be affected. For example, the peak of $CD19^+$ B cells is shifted upward in its expression of CD86. This uniform response is not a result of the restricted repertoire of the Tg recipient because non-Tg B6 recipients show the same phenotypic changes. Rather, there appears to be a polyclonal effect of the allohelp of the cGVH on the recipient B cells that is separate from the antigen-specific induction of autoantibody production.
9. We have so far analyzed fusions taken 10 wk after the induction of cGVH. Preliminary data indicate that a 3-wk fusion in the 56R recipients gives similar results.

References

1 Morris, S. C., Cheek, R. L., Cohen, P. L., and Eisenberg, R. A. (1990) Autoantibodies in chronic graft vs host result from cognate T-B interactions. *J. Exp. Med.* **171,** 503–517.

2 Eisenberg, R. A. and Cohen, P. L. (1983) Class II major histocompatibility antigens and the etiology of systemic lupus erythematosus. *Clin. Immunol. Immunopathol.* **29,** 1–6.

3 Feuerstein, N., Chen, F., Madaio, M., Maldonado, M., and Eisenberg, R. A. (1999) Induction of autoimmunity in a transgenic model of B cell receptor peripheral tolerance: changes in coreceptors and B cell receptor-induced tyrosine-phosphoproteins. *J. Immunol.* **163,** 5287–5297.

4 Chen, C., Prak, E. L., and Weigert, M. (1997) Editing disease-associated autoantibodies. *Immunity* **6,** 97–105.

5 Prak, E. L., Trounstine, M., Huszar, D., and Weigert, M. (1994) Light chain editing in kappa-deficient animals: a potential mechanism of B cell tolerance. *J. Exp. Med.* **180,** 1805–1815.

6 Chen, F., Maldonado, M. A., Madaio, M., and Eisenberg, R. A. (1998) The role of host (endogenous) T cells in chronic graft-vs-host autoimmune disease. *J. Immunol.* **161,** 5880–5885.

7 Sekiguchi, D. R., Jainandunsing, S. M., Fields, M. L., Maldonado, M. A., Madaio, M. P., Erickson, J., et al. (2002) Chronic graft-vs-host in Ig knockin transgenic mice abrogates B cell tolerance in anti-double-stranded DNA B cells. *J. Immunol.* **168,** 4142–4153.

8 Sekiguchi, D. R., Eisenberg, R. A., and Weigert, M. (2003) Secondary heavy chain rearrangement: a mechanism for generating anti-double-stranded DNA B cells. *J. Exp. Med.* **197,** 27–39.

9 Tse, H. Y., Kanamori, S., Walsh, W. D., and Hansen, T. H. (1985) The murine bm12 gene conversion provides evidence that T cells recognize predominantly Ia conformation. *Proc. Natl. Acad. Sci. USA* **82,** 7058–7062.

10 Morris, S. C., Cheek, R. L., Cohen, P. L., and Eisenberg, R. A. (1990) Allotype-specific immunoregulation of autoantibody production by host B cells in chronic graft-vs-host disease. *J. Immunol.* **144,** 916–922.

11 Morris, S. C., Cohen, P. L., and Eisenberg, R. A. (1990) Experimental induction of systemic lupus erythematosus by recognition of foreign Ia. *Clin. Immunol. Immunopathol.* **57,** 263–273.
12 van der Veen, F. M., Rolink, A. G., and Gleichmann, E. (1982) Autoimmune disease strongly resembling systemic lupus erythematosus (SLE) in F1 mice undergoing graft-vs-host reaction (GVHR). *Adv. Exp. Med. Biol.* **149,** 669–677.
13 Gleichmann, E., Van Elven, E. H., and Van der Veen, J. P. (1982) A systemic lupus erythematosus (SLE)-like disease in mice induced by abnormal T-B cell cooperation. Preferential formation of autoantibodies characteristic of SLE. *Eur. J. Immunol.* 12, **152–159.**
14 van Rappard-Van der Veen, F. M., Kiesel, U., Poels, L., Schuler, W., Melief, C. J., Landegent, J., et al. (1984) Further evidence against random polyclonal antibody formation in mice with lupus-like graft-vs-host disease. *J. Immunol.* **132,** 1814–1820.
15 van Rappard-van der Veen, F. M., Kong, Y. M., Rose, N. R., Kimura, M., and Gleichmann, E. (1984) Injection of mouse thyroglobulin and/or adult thymectomy do not break tolerance to thyroglobulin during the lupus like graft vs host disease in mice. *Clin. Exp. Immunol.* **55,** 525–534.
16 Chen, C., Nagy, Z., Prak, E. L., and Weigert, M. (1995) Immunoglobulin heavy chain gene replacement: a mechanism of receptor editing. *Immunity* **3,** 747–755.
17 Erikson, J., Radic, M. Z., Camper, S. A., Hardy, R. R., Carmack, C., and Weigert, M. (1991) Expression of anti-DNA immunoglobulin transgenes in non-autoimmune mice. *Nature* **349,** 331–334.
18 Fowler, E. and Cheng, N. (1983) Comparison of radioimmunoassay and ELISA methods for detection of antibodies to chromatin components. *J. Immunol. Methods* **62,** 297–303.
19 Shlomchik, M. J., Madaio, M. P., Ni, D., Trounstein, M., and Huszar, D. (1994) The role of B cells in lpr/lpr-induced autoimmunity. *J. Exp. Med.* **180,** 1295–1306.
20 Bradley, D. S., Jennette, J. C., Cohen, P. L., and Eisenberg, R. A. (1994) Chronic graft vs host disease-associated autoimmune manifestations are independently regulated by different MHC class II loci. *J. Immunol.* **152,** 1960–1969.
21 Fisher, C. L., Eisenberg, R. A., and Cohen, P. L. (1988) Quantitation and IgG subclass distribution of antichromatin autoantibodies in SLE mice. *Clin. Immunol. Immunopathol.* **46,** 205–213.
22 Reap, E. A., Piecyk, M. L., Oliver, A., Sobel, E. S., Waldschmidt, T., Cohen, P. L., et al. (1996) Phenotypic abnormalities of splenic and bone marrow B cells in lpr and gld mice. *Clin. Immunol. Immunopathol.* **78,** 21–29.
23 Chen, C., Radic, M. Z., Erikson, J., Camper, S. A., Litwin, S., Hardy, R. R., et al. (1994) Deletion and editing of B cells that express antibodies to DNA. *J. Immunol.* **152,** 1970–1982.
24 Bensinger, S. J., Bandeira, A., Jordan, M. S., Caton, A. J., and Laufer, T. M. (2001) Major histocompatibility complex class II-positive cortical epithelium mediates the selection of CD4(+)25(+) immunoregulatory T cells. *J. Exp. Med.* **194,** 427–438.

25 Bruijn, J. A., van Leer, E. H., Baelde, H. J., Corver, W. E., Hogendoorn, P. C., and Fleuren, G. J. (1990) Characterization and in vivo transfer of nephritogenic autoantibodies directed against dipeptidyl peptidase IV and laminin in experimental lupus nephritis. *Lab. Invest.* **63,** 350–359.

26. Bruijn, J. A., Hogendoorn, P. C., Corver, W. E., van den Broek, L. J., Hoedemaeker, P. J., and Fleuren, G. J. (1990) Pathogenesis of experimental lupus nephritis: a role for anti-basement membrane and anti-tubular brush border antibodies in murine chronic graft-vs-host disease. *Clin. Exp. Immunol.* **79,** 115–122.

15

Murine Models of Lupus Induced by Hypomethylated T Cells

Bruce Richardson, Donna Ray, and Raymond Yung

Summary

CD4+ T-cell DNA hypomethylation may contribute to the development of drug-induced and idiopathic human lupus. Inhibiting DNA methylation in mature CD4+ T cells causes autoreactivity specific to the major histocompatibility complex in vitro. The lupus-inducing drugs hydralazine and procainamide also inhibit T-cell DNA methylation and induce autoreactivity, and T cells from patients with active lupus have hypomethylated DNA and a similarly autoreactive T-cell subset. Further, T cells treated with DNA methylation inhibitors demethylate the same sequences that demethylate in T cells from patients with active lupus. The pathological significance of the autoreactivity induced by inhibiting T-cell DNA methylation has been tested by treating murine T cells in vitro with drugs that modify DNA methylation, then injecting the cells into syngeneic female mice. Mice receiving CD4+ T cells demethylated by a variety of agents, including procainamide and hydralazine, develop a lupuslike disease. This chapter describes the protocols for inducing autoreactivity in murine T cells in vitro and using the cells to induce autoimmunity in vivo.

Key Words: Animal models; autoimmunity; drug-induced lupus; DNA methylation; lupus.

1. Introduction

1.1. Background

DNA methylation is an essential determinant of chromatin structure and gene expression. DNA methylation refers to the postsynthetic methylation of deoxycytosine bases at the 5 position to form deoxymethylcytosine (d^mC). Nearly all d^mC is found in CpG dinucleotides, although only 70–80% of the CpG pairs are methylated. In general, the methylation of CG pairs in regulatory sequences results in transcriptional suppression; demethylation permits active transcription. Methylation patterns are established during differentia-

From: *Methods in Molecular Medicine, Vol. 102: Autoimmunity: Methods and Protocols*
Edited by: A. Perl © Humana Press Inc., Totowa, NJ

tion and serve to suppress expression of genes not necessary for the function of fully differentiated cells. The enzymes responsible for establishing methylation patterns include Dnmt3a and Dnmt3b, referred to as *de novo* methyltransferases. The methylation patterns are then maintained during mitosis by maintenance methyltransferases, including Dnmt1 ***(1)***.

The importance of DNA methylation is evidenced by its role in differentiation, genomic imprinting, and X chromosome inactivation ***(1)***. Disrupting both *DNMT1* alleles in embryonal stem cells results in embryonic death, indicating that DNA methylation is important in ontogeny ***(2)***. Dnmt3a and Dnmt3b are also essential for mammalian development: Homozygous Dnmt3a deficiency causes runting and death at age 4 wk; Dnmt3b deficiency is embryonic lethal ***(3)***.

Inhibiting DNA methylation in differentiated cells can have profound effects on cells. For example, treating the mouse fibroblast cell line 10T1/2 with the irreversible DNA methyltransferase inhibitor 5-azacytidine (5-azaC) causes the cells to differentiate into myocytes, adipocytes, and chondrocytes ***(4)***.

1.2. DNA Methylation and T-Cell Function

DNA methylation is also important in regulating T-lymphocyte gene expression. Methylation patterns change during thymic maturation ***(5)***, similar to the changes that occur during differentiation of other cell types. DNA methylation is implicated in the differentiation of Th0 cells into Th1 and Th2 phenotypes as well: The interferon (IFN)-γ gene is methylated in nonexpressing Th2 cells, but demethylated in Th1 cells; the interleukin (IL)-4 gene is methylated in Th1, but not in Th2, cells ***(6,7)***. Also, 5-azaC can modify T-cell gene expression. Examples include effects on IFN-γ and perforin expression in $CD4^+$ T cells ***(8,9)***.

Demethylating T-cell DNA with 5-azaC can change T-cell reactivity and function. Treating $CD4^+$ T-cell clones, as well as polyclonal $CD4^+$ T cells, with DNA methylation inhibitors causes autoreactivity. The treated cells lose restriction for nominal antigen and respond to self-class II major histocompatibility complex (MHC) molecules without added antigen ***(10,11)***. The autoreactivity is because of overexpression of the adhesion molecule LFA-1 (CD11a/CD18), and causing LFA-1 overexpression by transfection induces a similar MHC-restricted autoreactivity ***(12–14)***. The autoreactivity may reflect overstabilization of the normally low-affinity interaction between the TCR and MHC class II molecules presenting inappropriate antigen ***(15)***. 5-azaC increases steady-state levels of CD11a but not CD18 mRNA, and the increase in CD11a messenger RNA (mRNA) appears to be because of demethylation of repetitive elements 5' to the CD11a promoter ***(13,16)***. In contrast, $CD8^+$ T cells do not become autoreactive following 5-azaC treatment ***(11)***, and the reason is unexplored.

1.3. T-Cell DNA Hypomethylation and Autoimmunity

The pathological significance of 5-azaC-induced autoreactivity has been tested in animal models. The approach is to treat stimulated $CD4^+$ T cells with 5-azaC in vitro, culture for at least one to two cell cycles, then inject the treated cells into syngeneic recipients. The 5-azaC and other DNA methylation inhibitors prevent the methylation of newly synthesized DNA during S phase, referred to as passive demethylation. Thus, these agents are only effective when added to dividing cells. Further, one to two rounds of cell division are often required before changes in gene expression are observed ***(17)***. Adoptive transfer of murine $CD4^+$ T cells, made autoreactive either by treatment with 5-azaC or by transfection with CD18, causes a lupuslike disease in syngeneic recipients ***(14)***. The disease induced closely resembles chronic graft-vs-host disease in mice, in which features of lupuslike autoimmunity are also induced by $CD4^+$ T cells responding to host MHC class II molecules ***(18)***.

The DNA hypomethylation model has been used successfully with polyclonal $CD4^+$ T cells in DBA/2 mice ***(19)***, cloned Th2 cells in AKR mice ***(20)***, and cloned Th1 cells in B10.A mice ***(21)***. We have also used a panel of DNA methylation inhibitors, including 5-azaC, procainamide, hydralazine, and the ERK pathway inhibitor U0126 to induce autoimmunity ***(22,23)***. 5-azaC and procainamide are DNA methyltransferase inhibitors ***(17,24)***; hydralazine and the ERK pathway inhibitors prevent the upregulation of Dnmt1 and Dnmt3a during T-cell stimulation ***(23)***. All the DNA hypomethylation models develop anti-DNA antibodies, but vary to some degree with respect to the histologic changes induced, caused by either the different repertoire of effector functions displayed by the treated cells or host-specific genetic influences. The mechanism common to all models is promiscuous killing of host macrophages (Mθ). This may contribute to the development of anti-DNA antibodies by increasing the total amount of potentially antigenic apoptotic material ***(25)*** and/or by removing the cells responsible for removing apoptotic debris, analogous to knockout mice with defective clearance of apoptotic material that develop anti-DNA antibodies ***(26)***.

1.4. Relevance to Human Lupus

At least five lines of evidence support the contention that the DNA hypomethylation model has relevance to human lupus. First, the two drugs that most clearly cause a lupuslike disease in people, procainamide and hydralazine, are T-cell DNA methylation inhibitors ***(27)***. Cloned murine Th2 cells treated with these drugs induce a lupuslike disease identical to that caused by 5-azaC ***(22)***, suggesting a mechanism by which they might cause lupus in

humans. Second, T cells from patients with active lupus have decreased levels of total genomic d^mC, similar to 5-azaC-treated cells ***(28)***. Third, T cells from patients with active lupus overexpress LFA-1 on an autoreactive T-cell subset ***(13)***, and the overexpression is associated with hypomethylation of the same sequences flanking the CD11a promoter that demethylates following 5-azaC treatment ***(16)***. Fourth, T cells from patients with active lupus have a selective defect in ERK pathway signaling, the pathway inhibited by hydralazine ***(29)***, and inhibiting this pathway with hydralazine or U0126 causes a lupuslike disease in the adoptive transfer model ***(23)***. Finally, LFA-1-overexpressing T cells isolated from patients with active lupus spontaneously kill autologous monocytes with a specificity identical to experimentally hypomethylated T cells ***(13)*** and by the same mechanisms (FasL, TRAIL, and TWEAK) as experimentally hypomethylated T cells ***(30,31)***. Together, these studies strongly suggest that similar mechanisms contribute to the development of autoimmunity in the DNA hypomethylation model and in drug-induced and idiopathic human lupus.

2. Materials

1. Mice: Young (6- to 8-wk-old) female AKR and B10.A mice are obtained from Jackson Laboratories (Bar Harbor, ME), and DBA/2 mice are obtained from Charles River (Wilmington, MA).
2. Cell Lines: D10.G4.1 (D10) cells are obtained from the American Type Culture Collection (Manassas, VA) (ATCC). AE7 cells were obtained from Dr. Ronald Schwartz.
3. 5-Azacytidine: The 5-azaC (Aldrich, St. Louis, MO) is dissolved in tissue culture media, typically at 0.25–8.0 mM, and is made fresh just before use (*see* **Subheading 4.1.1.**). The solution is filter sterilized before adding to culture. 5-Aza-2'-deoxycytidine may also be used and is more potent (*see* **Subheading 4.1.1.**). The 5-azaC is potentially mutagenic and should be handled with appropriate precautions.
4. Interleukin 2: The IL-2-secreting T-cell line MLA-144, obtained from the ATCC, is cultured in RPMI-1640 supplemented with 3% fetal calf serum (FCS). Three times a week, the cells are sedimented by centrifugation; the conditioned media is filtered to remove any remaining cells and then stored frozen at –20°C.
5. For growth of polyclonal T cells, use RPMI-1640 supplemented with 10% heat-inactivated FCS, 40% IL-2-containing conditioned media, 2 m*M* glutamine, 100 IU/mL penicillin, 100 μg/mL streptomycin, and 5×10^{-5} M 2-mercaptoethanol.
6. For growth of D10 cells, use Click's medium supplemented with 10% FCS, 40% IL-2-containing conditioned media, 2 m*M* glutamine, 100 IU/mL penicillin, 100 μg/mL streptomycin, and 5×10^{-5} *M* 2-mercaptoethanol.
7. For growth of AE7 cells, use 50% Click's medium/50% RPMI-1640 supplemented with 10% FCS, 40% IL-2-containing conditioned media, 2 m*M* glutamine, 100 IU/mL penicillin, 100 μg/mL streptomycin, and 5×10^{-5} M 2-mercaptoethanol.

3. Methods

3.1. Cells and 5-Azacytidine Treatment

3.1.1. Polyclonal $CD4^+$ T-Cell Lines

Spleens are removed from young (6- to 8-wk-old) female DBA/2 ($H\text{-}2^d$) mice and dissociated with forceps, followed by forcing through a sterile disposable plastic screen with a syringe piston. Splenocytes are then isolated by density gradient centrifugation through Lympholyte-M (Cedarlane). $CD8^+$ cells are depleted with magnetic beads (Miltenyi, Auburn, CA) according to the manufacturer's instructions, then 10^6 $CD4^+$ cells are cultured in 2 mL of IL-2-containing media (*see* **Subheading 2.5.**) and stimulated with either 10^6 irradiated (3000 R) allogeneic splenocytes (e.g., C57BL/6, $H\text{-}2^b$) or 5 μg/mL concanavalin A (Pharmacia) using flat-bottom. 24-well plates. The cultures are maintained at 37°C in 5% CO_2 and humidified atmosphere and rocked on a rocker platform (Bellco) at 5–6 cycles/min (*see* **Subheading 4.1.2.**).

The lines are maintained by the addition of fresh IL-2-containing media every 2–3 d and restimulating every 7–10 d using approx 10^6 cells/well and equal numbers of irradiated allogeneic splenocytes or $0.5–1.0 \times 10^6$ irradiated syngeneic splenocytes plus 1 μg/mL concanavalin A, as appropriate. One day after restimulation, the cells are treated with 5-azaC; 6 d later, the cells are tested for autoreactivity and/or used for adoptive transfer. The cells should also be tested for CD4 and CD8 expression by flow cytometry at this point to exclude overgrowth by $CD8^+$ cells.

3.1.2. D10 Cells

D10.G4.1 (D10) cells (ATCC) are maintained in IL-2-containing media (*see* **Subheading 2.5.2.**) using flat-bottom, 24-well plates and a rocker platform as for polyclonal cells. The line is maintained by challenging $0.1–1.0 \times 10^6$ D10 cells with 5×10^5 irradiated (3000 R) AKR splenocytes and 100 μg/mL conalbumin (Sigma) every 7–10 d. The D10 line contains an autoreactive subset (*see* **Subheading 4.1.3.**) and must be subcloned by limiting dilution and a nonautoreactive subclone selected prior to use. Cells are treated with 5-azaC and used for functional characterization or given in adoptive transfer at least 6 d after treatment.

3.1.3. AE7 Cells

AE7 cells are maintained in IL-2-containing media (*see* **Subheading 2.5.3.**) and stimulated weekly with irradiated syngeneic (B10.A) splenocytes and antigen (100 μg/mL pigeon cytochrome C) on a rocker platform as described for polyclonal $CD4^+$ cells and D10 cells. To induce autoreactivity, the cells are treated with 5-aza-2'-deoxycytidine (*see* **Subheading 4.1.4.**) and used 6 d later.

3.1.4. Variations

See **Subheading 4.1.5.**

3.2. Autoreactivity Assays

3.2.1. Proliferation Assays

For D10 cells, 2×10^4 treated or untreated cells are cultured with graded numbers ($2–10 \times 10^4$) of irradiated syngeneic (AKR) splenocytes in 200 μL of the same media without IL-2, with or without 100 μg/mL conalbumin, using round-bottom, 96-well plates. Proliferation is tested 4–5 d later by adding 1 μCi tritiated thymidine/well and 6 h later determining ^3H incorporation into DNA. Polyclonal $CD4^+$ T cells are similarly tested using 5×10^4 T cells and approx 10^5 irradiated syngeneic splenocytes/well (range 5×10^4 to 5×10^5), using allogeneic splenocytes or concanavalin A as appropriate for the positive control. In all cases, determinations are performed in triplicate or quadruplicate.

3.2.2. Cytotoxicity Assays

For D10 cells, thioglycollate-elicited syngeneic (AKR) macrophages (Mø) are labeled with 100 μCi ^{51}Cr in 1 mL RPMI/10% FCS for 1 h at 37°C in a round-bottom culture tube. The cells are washed, then 5000 labeled Mø are cultured with 125,000 D10 cells with or without 100 μg/mL conalbumin in a total volume of 200 μL of sterile media lacking IL-2, using round-bottom microtiter plates. Chromium release is measured 18 h later using a scintillation spectrometer ***(30)***. AE7 killing assays are performed similarly, except that an effector:target ratio of 10:1 is used, and the antigen (positive control) is 100 μg/mL pigeon cytochrome C. Splenocyte killing assays are similarly performed, using an effector:target ratio of 25:1. Percentage cytotoxicity is calculated as follows ***(19)***:

$$[(\text{Experimental} - \text{Background release})/(\text{Total incorporation} - \text{Background release})] \times 100$$

3.3. Adoptive Transfer of Autoreactive Cells

All models are performed similarly. The treated cells are washed, dead cells are removed by centrifugation through Lympholyte M, then 5×10^6 viable cells are suspended in 0.2 mL sterile phosphate-buffered saline (PBS) and injected into the tail vein of young (<12 wk) syngeneic female mice using a 26-ga needle. A total of six injections are performed, spaced 2 wk apart. The rationale for repeated adoptive transfers derives from the observation that 5-azaC-induced autoreactivity is self-limited ***(11)***. Four weeks after the last injection, the mice are euthanized and studied for the development of serological and histological evidence of autoimmunity. The development of proteinuria and

hematuria may be monitored by holding Chemstrips (Boehringer Mannheim) under the mouse while picking it up (*see* **Subheading 4.3.**).

3.4. Immunoglobulin G, Immunoglobulin M, and Anti-DNA Antibody Assays

Total serum immunoglobulin G (IgG) and IgM concentrations are measured using Immulon 4 plates (Dynatech Laboratories, Chantilly, VA) coated with 2.5 μg antimouse IgG or IgM (Sigma) in 100 μL 0.01 *M* PBS at pH 7.4 for 18 h at 4°C. The plates are washed three times with PBS containing 0.05% Tween-20, then 200 μL of PBS supplemented with 3% bovine serum albumin; 0.1% gelatin and 0.05% Tween-20 are added, and the mix is incubated 2 h at 23°C. Serum samples or purified standards (murine IgG or IgM; Sigma) are diluted to the desired concentrations in PBS containing 3% bovine serum albumin and 0.1% gelatin, added to the wells, and incubated 18 h at 4°C, then washed three times. Next, 100 μL horseradish peroxidase-conjugated goat antimouse IgG (heavy and light chains) or IgM (μ-chain specific) are added at a final dilution of 1:2500 in PBS containing 0.05% Tween-20, and the mix is incubated for 2 h at room temperature. The plates are developed using Sigma Fast tablets (Sigma, St. Louis, MO) according to the manufacturer's instructions.

Anti-single-stranded DNA (anti-ssDNA) and anti-double-stranded DNA (anti-dsDNA) titers are determined by coating Immulon 4 plates with 2.5 Mg purified ssDNA (Sigma) or dsDNA (cesium chloride-purified KS^+-SV2CAT plasmid) in 100 μL 0.01 *M* PBS at pH 7.4 for 18 h at 4°C. The protocols used are the same as for the immunoglobulin ELISAs described above except for coating the wells. Horseradish peroxidase-conjugated goat antimouse polyvalent (IgG, IgM, IgA) antibody (Sigma) is again used as the secondary antibody before developing with Sigma Fast tablets. Positive controls should include pooled serum from 6-mo or older female New Zealand black/white mice or 5-mo or older MRL/*lpr* mice.

4. Notes

1. The 5-azaC and 5-aza-2'-deoxycytidine are unstable in aqueous media ***(17)***, and must be prepared just before use. The purchased chemicals have some variability in potency, and each lot should be tested. Typical concentrations for 5-azaC are 0.25–8.0 m*M*, with 1 m*M* most often effective. 5-Aza-2-deoxycyti-dine is more specific for DNA methylation inhibition and is also more potent ***(17)***, so lower concentrations may be used. Both compounds inhibit both DNA methylation and DNA synthesis, and concentrations inhibiting DNA methylation are only slightly lower than concentrations inhibiting DNA synthesis ***(17)***. Further, treated cells must undergo one to two cycles of cell division for the changes in gene expression to occur ***(17)***, highlighting the importance of establishing optimal concentrations. Significant cell death also occurs during treatment. Changes in T-cell

gene expression are typically seen 3–6 d after treatment, and kinetic analysis should be performed to determine the optimal time.
2. Cell–cell contact is maximized in flat-bottom culture plates using a rocker platform, and the cultures should be rocked for at least 24 h following stimulation.
3. With prolonged culture, D10 cells tend to lose the restriction for antigen and proliferate to syngeneic antigen-presenting cells (APCs) without added antigen. The mechanism is unknown, but adoptive transfer of these cells does not induce autoimmunity ***(20)***. The cells also tend to lose the requirement for IL-2 for sustained growth over time, causing high backgrounds in proliferation assays. Consequently, it is necessary to subclone this line repeatedly and to select antigen-specific cells. Alternatively, multiple aliquots of quality-tested subcloned cells may be stored in liquid nitrogen and thawed as needed.
4. AE7 cells are more refractory to the induction of autoreactivity than normal T cells or D10 cells. Treatment with 5-aza-2'-deoxycytidine is required, and concentrations up to 8 μ*M* are sometimes needed ***(21)***. Also, in our hands, proliferation assays are less reliable than cytotoxicity assays for both antigen reactivity and autoreactivity.
5. Activated T cells can be modified with other DNA methylation inhibitors or by transfection as needed. Our group has found D10 cells are the best suited for these studies, and we have successfully compared procainamide with *N*-acetylprocainamide and hydralazine with phthalazine in this model ***(22)***. Similarly, we have used the ERK pathway inhibitor U0126 ***(23)*** and used D10 cells transfected with CD18 ***(14)***. Other modifications of the cells may be similarly tested.
6. If desired, MHC specificity of the autoreactivity assays may be tested using monoclonal antibodies to the relevant MHC class II molecules or congenic mouse strains.
7. Following injection of 5-azaC-treated polyclonal $CD4^+$ T cells from DBA/2 mice, hematuria is first seen between weeks 1 and 3 and usually lasts 7–14 d, then resolves. Proteinuria, defined as a level above 30 mg/dL, was more persistent. Immunofluorescent evidence of renal Ig deposition correlates with active hematuria and resolves at later times.
8. Sometimes, the control sera give a relatively high background in the anti-DNA ELISAs. The specificity of the ELISAs may be tested by adding 5 μg/mL of soluble ssDNA or dsDNA as appropriate to replicate wells. Lack of inhibition is indicative of nonspecificity; inhibition is indicative of autoantibodies.

References

1 Attwood, J. T., Yung, R. L., and Richardson, B. C. (2002) DNA methylation and the regulation of gene transcription. *Cell Mol. Life Sci.* **59,** 241–257.
2 Li, E., Bestor, T. H., and Jaenisch, R. (1992) Targeted mutation of the DNA methyltransferase gene results in embryonic lethality. *Cell* **69,** 915–926.
3 Okano, M., Bell, D. W., Haber, D. A., Li, E. (1999) DNA methyltransferases Dnmt3a and Dnmt3b are essential for *de novo* methylation and mammalian development. *Cell* **99,** 247–257.

4 Taylor, S. M. and Jones, P. A. (1979) Multiple new phenotypes induced in 10T1/2 and 3T3 cells treated with 5-azacytidine. *Cell* **17,** 771–779.
5 Golbus, J., Palella, T. D., and Richardson, B. C. (1990) Quantitative changes in T cell DNA methylation occur during differentiation and ageing. *Eur. J. Immunol* **20,** 1869–1872.
6 Young, H. A. (1996) Regulation of interferon-gamma gene expression. *J. Interferon Cytokine Res.* **16,** 563–568.
7 Santangelo, S., Cousins, D. J., Winkelmann, N. E., Staynov, D. Z. (2002) DNA methylation changes at human Th2 cytokine genes coincide with DNase I hypersensitive site formation during CD4(+) T cell differentiation. *J. Immunol.* **169,** 1893–1903.
8 Young, H. A., Ghosh, P., Ye, J., Lederer, J., Lichtman, A., Gerard, J. R., et al. (1994) Differentiation of the T helper phenotypes by analysis of the methylation state of the IFN-gamma gene. *J. Immunol.* **153,** 3603–3610.
9 Lu, Q., Wu, A., Ray, D., Deng, C., Attwood, J., Hanash, S., Pipkin, M., et al. (2003) DNA methylation and chromatin structure regulate T cell perforin gene expression. *J. Immunol.* **170,** 5124–5132.
10 Richardson, B. C., Liebling, M. R., and Hudson, J. L. (1990) $CD4^+$ cells treated with DNA methylation inhibitors induce autologous B cell differentiation. *Clin. Immunol. Immunopathol.* **55,** 368–381.
11 Richardson, B. (1986) Effect of an inhibitor of DNA methylation on T cells. II. 5-Azacytidine induces self-reactivity in antigen-specific T4+ cells. *Hum. Immunol.* **17,** 456–470.
12 Richardson, B., Powers, D., Hooper, F., Yung, R. L., O'Roarke, K. (1994) Lymphocyte function-associated antigen 1 overex-pression and T cell autoreactivity. *Arthritis Rheum.* **37,** 1363–1372.
13 Richardson, B. C., Strahler, J. R., Pivirotto, T. S., Quddus, J., Bayliss, G. E., Gross, L. A., et al. (1992) Phenotypic and functional similarities between 5-azacytidine-treated T cells and a T cell subset in patients with active systemic lupus erythematosus. *Arthritis Rheum*. **35,** 647–662.
14 Yung, R., Powers, D., Johnson, K., Amento, E., Carr, D., Laing, T., et al. (1996) Mechanisms of drug-induced lupus. II. T cells overexpressing lymphocyte function-associated antigen 1 become autoreactive and cause a lupuslike disease in syngeneic mice. *J. Clin. Invest.* **97,** 2866–2871.
15 Kaplan, M.J., Beretta, L., Yung, R. L., Richardson, B. (2000) LFA-1 overexpression and T cell autoreactivity: mechanisms. *Immunol. Invest.* **29,** 427–442.
16 Lu, Q., Kaplan, M., Ray, D., Ray, D., Zacharek, S., Gutsch, D., et al. (2002) Demethylation of ITGAL (CD11a) regulatory sequences in systemic lupus erythematosus. *Arthritis Rheum.* **46,** 1282–1291.
17. Jones, P. A. (1984) Gene activation by 5-azacytidine, in *DNA Methylation. Biochemistry and Biological Significance* (Razin, C. H. and Riggs, A., eds.), Springer-Verlag, New York, pp. 165–187.
18 van der Veen, F. M., Rolink, A. G., and Gleichmann, E. (1982) Autoimmune disease strongly resembling systemic lupus erythematosus (SLE) in F1 mice undergoing graft-vs-host reaction (GVHR). *Adv. Exp. Med. Biol.* **149,** 669–677.

19 Quddus, J., Johnson, K. J., Gapalchin, J., Amento, E. P., Chrisp, C. E., Yung, R. FL., et al. (1993) Treating activated $CD4^+$ T cells with either of two distinct DNA methyltransferase inhibitors, 5-azacytidine or procainamide, is sufficient to cause a lupus-like disease in syngeneic mice. *J. Clin. Invest.* **92,** 38–53.

20 Yung, R. L., Quddus, J., Chrisp, C. E., Johnson, K. J., Richardson, B. C. (1995) Mechanism of drug-induced lupus. I. Cloned Th2 cells modified with DNA methylation inhibitors in vitro cause autoimmunity in vivo. *J. Immunol.* **154,** 3025–33035.

21 Yung, R., Kaplan, M., Ray, D., Schneider, K., Mo, R. R., Johnson, K., et al. (2001) Autoreactive murine Th1 and Th2 cells kill syngeneic macrophages and induce autoantibodies. *Lupus* **10,** 539–546.

22 Yung, R., Chang, S., Hemati, N., Johnson, K., Richardson, B. (1997) Mechanisms of drug-induced lupus. IV. Comparison of procainamide and hydralazine with analogs in vitro and in vivo. *Arthritis Rheum.* **40,** 1436–1443.

23 Deng, C., Lu, Q., Zhang, Z., Rao, T., Attwood, J., Yung, R., et al. (2003) Hydralazine may induce autoimmunity by inhibiting extracellular signal-regulated kinase pathway signaling. *Arthritis Rheum.* **48,** 746–756.

24 Scheinbart, L. S., Johnson, M. A., Gross, L. A., Edelstein, S. R., Richardson, B., et al. (1991) Procainamide inhibits DNA methyltransferase in a human T cell line. *J. Rheumatol.* **18,** 530–534.

25 Mevorach, D., Mevorach, D., Zhou, J. L., Song, X., Elloon, K. B . (1998) Systemic exposure to irradiated apoptotic cells induces autoantibody production. *J. Exp. Med.* **188,** 387–392.

26 Walport, M. J. (2000) Lupus, DNase and defective disposal of cellular debris. *Nat. Genet.* **25,** 135–136.

27 Cornacchia, E., Golbus, J., Maybaum, J., Strahler, J., Hanark, S., Richardson, B. (1988) Hydralazine and procainamide inhibit T cell DNA methylation and induce autoreactivity. *J. Immunol.* **140,** 2197–2200.

28 Richardson, B., Scheinbart, L., Strahler, J., Gross, L., Hanark, S., Johnson, M. (1990) Evidence for impaired T cell DNA methylation in systemic lupus erythematosus and rheumatoid arthritis. *Arthritis Rheum.* **33,** 1665–1673.

29 Deng, C., Kaplan, M., Yang, J., Zhang, Z., McCune, W. J., Hanark, S., et al. (2001) Decreased Ras-mitogen-activated protein kinase signaling may cause DNA hypomethylation in T lymphocytes from lupus patients. *Arthritis Rheum.* **44,** 397–407.

30 Kaplan, M. J., Lewis, E. E., Sheldon, E. A., Somers, E., Paulic, R., McCune, W. J., et al. (2002) The apoptotic ligands TRAIL, TWEAK, and Fas ligand mediate monocyte death induced by autologous lupus T cells. *J. Immunol.* **169,** 6020–6029.

31. Kaplan, M. J., Ray, D., Mo, R. R., Yung, R. L., Richardson, B. (2000) TRAIL (Apo2 ligand) and TWEAK (Apo3 ligand) mediate $CD4^+$ T cell killing of antigen-presenting macrophages. *J. Immunol.* **164,** 2897–2904.

16

The Mouse Model of Collagen-Induced Arthritis

David D. Brand, Andrew H. Kang, and Edward F. Rosloniec

Summary

Collagen-induced arthritis (CIA) is an experimental autoimmune disease that can be elicited in susceptible strains of rodents (rat and mouse) and nonhuman primates by immunization with type II collagen (CII), the major constituent protein of articular cartilage. Following immunization, these animals develop an autoimmune polyarthritis that shares several clinical and histological features with rheumatoid arthritis. Susceptibility to CIA in rodents is linked to the class II molecules of the major histocompatibility complex (MHC), and the immune response to CII is characterized by both the stimulation of collagen-specific T cells and the production of high titers of antibody specific for both the immunogen (heterologous CII) and the autoantigen (mouse CII). Histologically, murine CIA is characterized by an intense synovitis that corresponds precisely with the clinical onset of arthritis. Because of the pathological similarities between CIA and rheumatoid arthritis, the CIA model has been the subject of extensive investigation. Here, we describe the specifics for establishing the murine model of CIA, including specific requirements for the handling and preparation of the CII antigen, procedures for immunization, selection of susceptible mouse strains for study, and procedures for the evaluation and quantitation of the autoimmune arthritis.

Key Words: Arthritis; autoimmunity; Freund's complete adjuvant; inflammation; mouse; mycobacteria; type II collagen.

1. Introduction

Collagen-induced arthritis (CIA) is an animal model of autoimmune arthritis induced by immunization with type II collagen (CII). This model of autoimmunity shares several clinical and pathological features with rheumatoid arthritis (RA) and has become the most widely studied model of RA. CIA in the mouse model was first described by Courtney et al. in 1980 ***(1)***, and the major histocompatibility complex (MHC) genetics controlling the susceptibility were analyzed in detail by Wooley et al. ***(2)***.

From: *Methods in Molecular Medicine, Vol. 102: Autoimmunity: Methods and Protocols*
Edited by: A. Perl © Humana Press Inc., Totowa, NJ

Like RA, susceptibility to CIA is regulated by the class II molecules of the MHC. It is induced by a simple immunization with CII emulsified in Freund's complete adjuvant (FCA); however, the solubilization and handling of the CII requires special attention. The major characteristics of the murine CIA model are (a) disease susceptibility is strongly linked to the class II molecules of the MHC, specifically to the I-A^q and I-A^r alleles ***(2)***; (b) CIA can be induced in susceptible mouse strains by immunization with a variety of CIIs from different species, but the susceptibility to these collagens differs among different strains of mice; (c) although stimulation of CII-specific T cells is required to induce arthritis, high levels of circulating antibody to CII are strongly associated with the development of autoimmune arthritis (*see* **Note 1**).

In support of a dominant role of antibody in this model is that CIA can be passively transferred to both naive syngeneic and allogeneic mice with purified polyclonal antibodies or a mixture of monoclonal antibodies specific for CII ***(3,4)*** (*see* **Note 2**). These antibodies can be detected bound to the cartilage of arthritic joints along with deposition of the complement component C3, and the fixation of complement appears to be a major mechanism by which antibody to CII initiates the inflammatory response ***(5)***. Thus, this model offers a wide range of opportunities for the study of autoimmune arthritis and its associated inflammatory response.

In the following sections, we describe how to handle and prepare the CII properly for immunization, discuss the selection of mouse strains available for studying CIA and the immunization techniques most successful in establishing disease, and describe the various means of evaluating and quantitating the incidence and severity of the autoimmune inflammatory response. Like most animal models, there are specific details that must be adhered to for successful initiation of the autoimmune disease, but these procedures can be mastered quickly by anyone familiar with the use of mouse models.

2. Materials

1. CII (Chondrex, Redmond, WA).
2. Freund's incomplete adjuvant (FIA; BD Biosciences, San Jose, CA).
3. FCA (BD Biosciences).
4. Heat-killed, freeze-dried *Mycobacterium tuberculosis* (BD Biosciences) (optional).
5. Mortar and pestle.
6. 1 cc glass or polystyrene syringes (must have Luer lock).
7. 26-ga needles.
8. 50 m*M* acetic acid.
9. VirTis high-speed homogenizer or other mechanical means of emulsification (VirTis Inc., Gardiner, NY) (optional).
10. Constant tension caliper (optional).

3. Methods

3.1. Antigen Selection and Preparation

3.1.1. Structure of CII

Structurally, CII is different from all other autoantigens studied in autoimmune models. It is a homotrimer of α1(II)-polypeptide chains and has a molecular weight of 285 kDa ***(6)*** . Typical of most collagens, as a mature protein the structure of CII is an extended α-helix composed of repeating Gly-X-Y sequences in which X or Y is frequently a proline. In addition, the structure is also unusual in that many of the prolines and lysines in the Y positions are posttranslationally hydroxylated, and some of the hydroxylated lysines are glycosylated. The tissue distribution of CII is restricted to hyaline cartilage and the vitreous body of the eye and is normally absent in all other tissues.

Like other interstitial collagens, native CII is highly resistant to most proteolytic enzymes, with the exception of collagenase. However, CII is very susceptible to denaturation, especially by temperatures near or above 38°C. Denaturation not only adversely affects the arthritogenic capacity of CII, but also renders the individual α-chains of CII highly susceptible to rapid degradation by a number of proteases. This is the primary reason that native CII must be kept cold at all times, including during emulsification (described in **Subheading 3.3.1.**).

3.1.2. Sources of CII

Although CII can be obtained from several commercial vendors, it is our experience that not all forms of commercially available collagens are suitable for use in the induction of arthritis. As detailed in **Subheading 3.1.3.**, to maintain arthritogenicity, great care must be taken during the purification and subsequent handling of CII. With these concepts in mind, high-quality arthritogenic CII is available from a few sources. Bovine, chick, porcine, and human CII are available from Chondrex Inc. (www.chondrex.com) and from MD Biosciences (www.mdbiosciences.com); highly purified bovine CII is also available from the authors at www.utmem.edu/ctr. In addition, protocols for preparation of CII as well as isolation of α1(II)-chains and other arthritogenic fractions are also available ***(7)***. Although it is time consuming to purify, large quantities (grams) of CII can be prepared in a single purification; properly stored, the CII can last a long time.

3.1.3. Handling and Storage

The proper handling and storage conditions for CII are an important concern. If CII is stored for great lengths of time in any form, crosslinks between the α1(II)-chains will slowly begin to occur, rendering it difficult to solubilize

even in acetic acid. Although CII is easily lyophilized and can be stored dry at room temperature, we find that the best method for CII storage that results in the least amount of crosslinking is to store it in aliquots at –80°C (ultralow freezer) at 4 mg/mL in 50 m*M* acetic acid. We find that 50 m*M* acetic acid is an optimal concentration of acid to maintain solubility of the CII, and the 4-mg/mL concentration is preferred because it makes it much easier to achieve higher concentrations of emulsified CII, thus requiring less injection volume in the tails of the experimental mice (*see* **Subheading 3.3.2.**).

Small aliquots (5 mL) are suggested because it is recommended that repeated freeze–thaw cycles be avoided. It is important that the vials be thawed at 4°C instead of warming them to room temperature or subjecting them to a warm water bath. Placing the vial of frozen CII at 4°C for 20 min and then transferring it to a prechilled beaker of water (also at 4°C) can be done to speed up the thawing process without compromising the native structure of the CII. Once a vial is thawed, it can be safely stored for several months at 4°C. The acetic acid in which the CII is dissolved helps considerably in this regard as the acid conditions tend to retard the growth of most microbes.

3.1.4. Solubilization

If obtained in lyophilized form, CII should be dissolved in 50 m*M* acetic acid at 4 mg/mL in prechilled glassware (*see* **Notes 3** and **4**). Time is a big consideration in this process; depending on the condition of the lyophilized CII (age, degree of purity, maintenance of low moisture content), usually 24 h of stirring is required to dissolve it completely. Very small quantities (<1 mL) can be effectively dissolved in Eppendorf tubes using a microstir bar (approx 2–3 mm).

If the age of the lyophilized CII is in question, close inspection of the dissolved product is recommended. When CII is dissolved at 4 mg/mL in acetic acid at 4°C, it should be a clear, colorless solution with a significant viscosity that is readily apparent. If there is more than a subtle haze to the solution, centrifugation of the CII solution at 10,000*g* for 30 min with a prechilled rotor in a refrigerated centrifuge is recommended. Of course, if there is a recognizable pellet, then the collagen can no longer be considered dissolved at 4 mg/mL. Should this occur, the soluble portion of the CII can be relyophilized and redissolved in 50 m*M* acetic acid to the desired concentration.

3.2. Mouse Strain Selection

The murine model of CIA is particularly advantageous for study given the vast number of inbred strains available and their corresponding immunologic reagents. However, there are several criteria that must be considered in selecting a mouse strain for CIA studies. First, in the case of genetics, susceptibility to CIA is highly regulated by the MHC. Only mice expressing the mouse class

Table 1
Susceptibility of Various Mouse Strains to CIA

Strain	Class II haplotype	CIA susceptibility
DBA/1LacJ	q	+++
DBA/1J	q	+++[a]
B10.RIII	r	+++
B10.Q	q	+++
B10._QBr	q	+++
BUB	q	+++
SWR	q	–[b]
NFR/N	q	++
B10.CAS2	w17	+
B10.M-DR1	DRA1*0101/DRB1*0101, I-A^f	+++
B10.M-DR4	DRA1*0101/DRB1*0401, I-A^f	+++[c]
B10.M	I-A^f	–[d]
HLA-DQ8	DQA1*0301/DQB1*0302	+++

[a] Although both the DBA/1J and the DBA/1LacJ mice are both highly susceptible to CIA, there may be a slightly higher incidence of arthritis in the DBA1/LacJ mice.

[b]This strain is resistant apparently because of a genetic deficiency in the production of the complement component C5 ***(16,17)***.

[c]Although there are no differences in severity of arthritis between the DR4 and DR1 mouse, the DR4 strain has a slightly lower incidence of arthritis. This is likely because of gene dosage differences of the transgenes ***(8)***.

[d]Although this strain is considered resistant to arthritis induction, a small incidence (<5%) has been observed ***(8,9)***.

II genes I-A^q and I-A^r are susceptible. The DBA/1 and B10.Q (both H-2^q) and B10.RIII (H-2^r) are the most commonly used and are widely available commercially (**Table 1**). In addition to these strains, several transgenic strains expressing HLA-DR or DQ genes have also been shown to be susceptible to CIA ***(8–11)***.

The second consideration is that the strain selected must be paired with the appropriate species of CII. For example, susceptibility of H-2^r mice differs significantly from that of H-2^q in terms of the species of CII used for immunization. H-2^r mice are susceptible to CIA when immunized with bovine or porcine CII, but not with chick or human CII. Conversely, H-2^q mice are susceptible to CIA when immunized with bovine, chick, and human, but not porcine, CII. The HLA-DR and HLA-DQ transgenic mice have been less well studied in this regard, but all are susceptible when immunized with bovine CII, and at least the DR transgenics are susceptible to immunization with human

CII. Arthritis can also be induced in some strains by immunization with either purified α1(II)-chains or large cyanogen bromide fragments of CII, such as CB11, CII(124–402) for H-2^q ***(12,13)*** and CB8, CII(403–551) for H-2^r ***(14)***. However, there is lower incidence and decreased severity of arthritis in comparison to that for immunization with native CII, and the time of onset can be delayed. Other less-common H-2^q strains shown in **Table 1** have also been shown to be susceptible to CIA, with the exception of the SWR strain, which has a complement deficiency ***(15–17)***.

Finally, male mice are frequently preferred for CIA studies because the incidence of arthritis appears to be marginally higher in comparison to that in female mice. The age of mice can also be an important factor in eliciting disease. Mice as young as age 6 wk tend to be resistant, and mice of minimally age 8 wk are generally preferred for CIA experiments. DBA/1 mice remain highly susceptible to arthritis at least through age 6 mo.

3.3. Induction of Arthritis

3.3.1. Emulsification of Antigen

Typically, immunizations for the induction of CIA consist of 100 μg of *M. tuberculosis* and 100 μg of CII in a total volume of 50–100 μL; however, arthritis can be induced with as little as 10 μg of native CII. FCA is the adjuvant of choice for the induction of CIA, and the proper emulsification of CII in FCA is critical for achieving a reproducible, high incidence of arthritis in the mouse model of CIA.

There are two options for selecting the FCA: commercially prepared FCA or FIA supplemented with freshly ground *M. tuberculosis* H37Ra. In our experience, freshly ground *M. tuberculosis* mixed with FIA at 4 mg/mL results in the highest incidence of arthritis. The best approach is to grind 40 mg of *M. tuberculosis* to a fine powder with a mortar and pestle and add it to a 10-mL vial of FIA. This FCA can be stored for several months without any loss of activity; however, it is critical that the FCA be vortexed vigorously to resuspend the *M. tuberculosis* completely prior to using it to prepare an emulsion.

Commercially prepared FCA has also been used successfully by a number of investigators, with only some drawbacks. Arthritis induction may be delayed or may develop at a lower incidence, depending on the source of FCA, but some of these problems can be overcome by using a booster immunization of CII in FIA at 2–3 wk after the primary immunization. The following is the procedure:

1. Dissolve the CII in 50 m*M* acetic acid by stirring overnight at 4°C in preparation for emulsification in adjuvant. For 50-μL injection volumes containing 100 μg of CII, dissolve CII at 4 mg/mL; for 100-μL injection volumes, dissolve CII at 2 mg/mL. It is important that native CII be kept cold while being dissolved to prevent

denaturation. Once denatured, its efficacy in eliciting arthritis will drop by approximately one-half or more in comparison to native CII.

2. Prepare FCA by adding heat-killed *M. tuberculosis* that has been finely ground in a mortar and pestle to FIA at 4 mg/mL final concentration (*see* **Note 8**). Commercially prepared FCA may also be used, but may result in a lower incidence and decreased severity of arthritis.
3. Emulsify CII in an equal volume of FCA just prior to immunization. If using a homogenizer to emulsify, add the required amount of FCA to a 10-cc syringe that has been cut down to the 5-cc level. Seal the needle end of the syringe and clamp it into place in an ice bucket mounted on the stage of the homogenizer. Add the FCA to the syringe (*see* **Note 9**) and lower the impeller of the homogenizer so that it is as close as possible to the bottom of the syringe without touching the walls. Start the impeller spinning at 10,000 rpm and slowly, dropwise, add the CII solution. After it has all been added, increase the speed to 40,000 rpm for 1–2 min or until a stable emulsion is achieved (*see* **Note 10**). Remember to keep it cold throughout the procedure.

If the collagen is dissolved at 4 mg/mL, then 50-μL immunizations will be possible (and are easier to perform than 100-μL immunizations.) Because of loss of material during processing and handling, an additional 0.5 mL (at least) of emulsion should be prepared. Using the procedure described above, the resulting emulsion should be the consistency of shaving cream (*see* **Note 11**). The emulsion can then be transferred to a 1-cc syringe for injection using either tubing or a stopcock with Luer locks to connect the two syringes (*see* **Note 12**). Because of the consistency of the emulsion, it is imperative that the syringe for the injections be equipped with a Luer lock. The press-fit needles will come off of the syringe during injection, resulting in a complete loss of the emulsion. Glass syringes with locking hubs are preferable for injecting FCA emulsions.

3.3.2. Immunization

CIA in mice is induced by immunization with the CII: FCA emulsion intradermally at the base of the tail using a 26-ga needle. The needle should be inserted under the tail skin at about 1.5 cm from the base of the tail (**Fig. 1**) and carefully threaded up the tail under the epidermis about 0.5 cm. This both creates a space to deposit the emulsion and helps prevent the emulsion from leaking out the tail during the injection. Avoid depositing the emulsion onto the dorsum of the mouse; the emulsion should be confined to the tail itself.

When injected properly, the emulsion will be clearly visible through the epidermis of the mouse tail and will impart a temporary "stiffness" to the tail. If the tip of the needle accidentally exits the skin and makes a second hole in the tail, another immunization site on the tail will have to be used or the adjuvant will leak out of the tissue. Simply move further up the tail (proximal) or roll the tail to either side to generate a new immunization site. Finally, if desired, a

Fig. 1. Immunization of mice for the induction of CIA.

booster immunization of 50–100 μg of CII emulsified in FIA can be given 2–3 wk after the primary immunization. This is generally not necessary if the CII was properly handled and a stable emulsion was achieved with the 4 mg/mL FCA; however, it may be helpful if commercial FCA was used to make the emulsion or when either α1(II)-chains or purified cyanogen bromide fragments of CII were used to induce arthritis.

Injection of the mouse with an emulsion containing FCA can result in the formation of an injection site reaction. Ulceration at the site of the injection is not uncommon, and frequent monitoring is suggested to make sure these ulcers do not become infected. In addition, a small percentage of male mice may develop orchitis as a result of the immunization. Because of the severity of the inflammatory response associated with the development of arthritis, it is recommended that soft bedding be used as a cage bottom instead of wire mesh, and that at the peak of disease severity, the animals be monitored closely to be certain that they are able to reach food and water without difficulty (*see* **Note 5**). Because it is the inflammatory response that serves as the point of study for this disease model, analgesics that can interfere with the inflammatory response are not recommended.

3.4. Evaluation of Arthritis

3.4.1. Visual Scoring for Incidence and Severity

Although the presence or absence of arthritis in the mouse model is relatively easy to ascertain, assessing or quantitating the degree of severity of the disease is somewhat more difficult. As shown in **Fig. 2**, arthritic limbs are easily recognized by their swelling and erythema in the early stages of disease. Any or all of the four paws may be affected. At its peak, the inflammation extends from above the tarsal joint (ankle) or the carpus joint (wrist) of the paw all the way through the digits.

Generally, there are three stages of arthritis gross pathology: early swelling, which may be minimal, followed by progression to a severely inflamed paw that may limit the animal's mobility, and finally ankylosis of the joint, although not all arthritic limbs progress to this end point. After approx 20 d postimmunization with CII or at first signs of arthritis development, each paw should be examined two to three times a week (*see* **Note 6**). It is not uncommon for a limb to appear normal one day, yet be severely swollen and inflamed the next. Although the arthritis in CIA is monophasic, new arthritic limbs can appear up to 8 wk after immunization. The inflammation in the affected limbs either resolves to a point at which the paw appears normal or progresses to a deformed, ankylosed joint in which the inflammation has diminished.

The incidence of CIA in most mouse strains following immunization with native CII should be 80% or greater. As shown in **Fig. 3**, for most of the models, arthritis begins to appear around day 20 and continues to develop through day 50. Accelerated models of CIA have been developed using a T-cell receptor transgene specific for CII (DBA/1-Vb8.3; **Fig. 3**) ***(18)***. In these mice, arthritis appears as early as day 10 and is complete by day 40. In the DBA/1 and B10.RIII model, an incidence of 25–50% is expected either when using cyanogen bromide fragments of CII such as CB11 (DBA/1) or CB8 (B10.RIII) or when using α1(II)-chains to induce arthritis. The failure to induce arthritis or the induction of only mild disease at a low incidence in a given experiment can usually be attributed to inadvertent denaturation of the collagen, a poor-quality adjuvant or emulsion, or poor injection technique. Booster immunizations do little to correct these problems.

The biggest difficulty in characterizing the arthritis is evaluating the severity of the inflammation. The most common means of quantitating the severity of the inflammation is based on a subjective assignment of a severity score ranging from 0 (no inflammation) to 4, where 4 represents extensive swelling and erythema of the entire paw (**Fig. 2**). This scoring system is described in detail in **Table 2**, and examples of varying degrees of inflammation in the mouse model are shown in **Fig. 2**.

Fig. 2. Examples of varying degrees of inflammation in the CIA mouse model. **(A)** normal front paws; **(B)** front paw with grade 2 inflammation; **(C)** front paw with grade 4 inflammation; **(D)** normal hind paw; **(E)** hind paw with grade 3 inflammation; **(F)** hind paw with grade 4 inflammation.

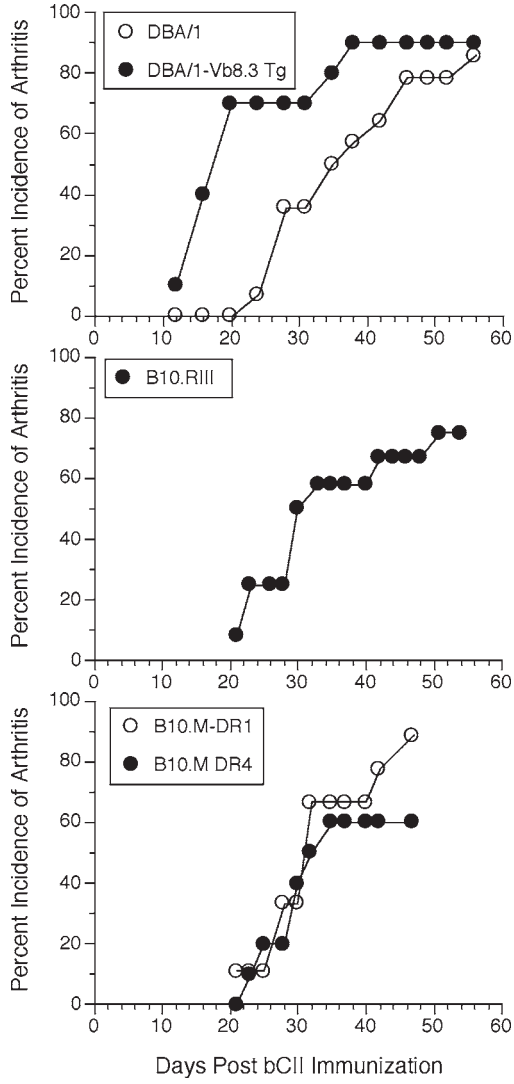

Fig. 3. Kinetics of arthritis development among CIA-susceptible strains. Mice were immunized with bovine CII emulsified in FCA and were observed for the development of arthritis. The "DR4-boosted" mice received a second injection of CII in FIA at day 21. The DBA/1-Vb8.3 mice express a transgene of a TCR Vb8.3 chain derived from a CII-specific, I-A^q-restricted T cell.

Table 2
Visual Scoring System for Evaluating Arthritis Severity in CIA Mouse Models

Severity score	Gross pathology
0	No evidence of erythema and swelling
1	Erythema or mild swelling confined to the midfoot (tarsals) or ankle joint
2	Erythema and mild swelling extending from the ankle to the midfoot
3	Erythema and moderate swelling extending from the ankle to the metatarsal joints
4	Erythema and severe swelling encompassing the ankle, foot, and digits

If there is any question as to whether a limb is arthritic, it is either in the very early stages or not arthritic. Repeat observations documenting the progression of severity will confirm the presence of disease. It is rare that a limb will become minimally swollen (score of 1) and quickly resolve to normal appearance over a day or two. Although the swelling of a single digit is occasionally observed, this observation alone does not necessarily indicate that arthritis has developed. Because we occasionally observe swollen digits in naïve mice, we do not consider these to be a an indication of autoimmune arthritis unless the inflammation progresses to the rest of the paw. The unskilled observer may find it difficult to distinguish between severity scores of 3 and 4, especially in the front paws, and may wish to modify the scoring system to a 1 through 3, reserving a grade of 4 for the ankylosed joint.

The greatest drawback of subjective swelling is accounting for the resolution of synovitis. Occasionally, reduced joint involvement is evident to the eye, but erythema and swelling still persist in the same anatomic distribution, necessitating no change in the score. To help reduce the subjectivity and prevent bias, two separate examiners should be used, with at least one unaware of the identity of the treatment groups.

In attempts to reduce the subjectivity of the severity scores, two other methods have also been used occasionally to evaluate arthritis severity, mercury displacement and caliper measurement of foot pad thickness *(7)*. However, both of these approaches also have drawbacks. The mercury displacement approach requires quantities of mercury that may constitute a significant chemical hazard, and the measurements are subject to variations in how much limb is immersed. In the case of the caliper-based measurements of footpad thickness, there are concerns that the footpad alone is a subset of the total

inflammation, and caliper application to soft tissue swelling can vary based on the amount of force applied and in the long term can alter the inflammatory response.

3.4.2. Immunological Assessment

Disease induction in CIA is more complex than that found in many of the other autoimmune disease models, such as experimental autoimmune encephalomyelitis, in that CIA requires both the activation of T cells and B-cell production of antibodies specific for the immunogen and the autoantigen, murine CII. Therefore, in addition to visual inspection of the mice, the effectiveness of the immunization with CII can be evaluated by measuring both cellular and humoral immune responses. Like most antigen systems, T-cell responses peak around days 10–12 postimmunization, but still can be detected after several weeks (*see* **Note 7**). Serum antibody levels peak as the incidence and severity of arthritis peaks, and within a given strain, the levels of antibody correlate well with the presence or absence of arthritis. Among different susceptible and nonsusceptible strains, antibody levels can vary widely. Some nonsusceptible strains produce significant amounts of CII-specific antibody, yet fail to develop arthritis ***(2)***.

CII-specific antibody can be easily measured using a standard indirect enzyme-linked immunosorbent assay (ELISA) in which the CII is adsorbed to the plate ***(7)***. Serum collected 35–42 d (peak arthritis) in the mouse model should yield positive results by ELISA at minimally a 1:1000 dilution. High-responder mouse strains (DBA/1 and B10.RIII) frequently yield positive ELISA results at serum dilutions ranging from 1:10,000 to 1:100,000. T-cell responses to CII using draining lymph node cells can be evaluated both by microtiter proliferation assays and by the production of interferon (IFN)-γ using a solid-phase ELISA.

T cells can be stimulated using CII, α1(II)-chains, fragments of CII, or synthetic peptides of CII that have been identified as antigenic determinants ***(8,9,12,14)***. In the DBA/1 model (H-2^q), the proliferative response is dominated by recognition of the CII(260–267) determinant ***(12)***, and IFN-γ production can be detected to both CII(260–267) and CII(181–210) ***(19–21)***. The dominant response in CIA-susceptible H-2^r (B10.RIII) mice is directed to CII(610–618), although a second T-cell determinant is present in CB8, CII(442–456) ***(14,22)***.

3.4.3. Histological Evaluation

Histological sectioning of arthritic joints can also provide evidence of the severity of the inflammation associated with CIA, but is largely an impractical approach to quantitating the degree of inflammation in every mouse of every group. Nonetheless, "representative" sections should be obtained from each

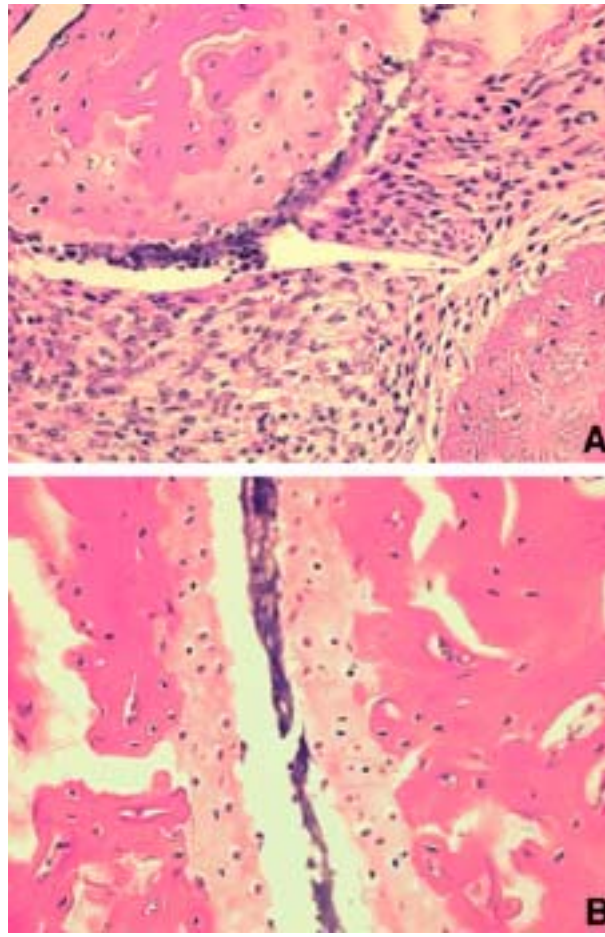

Fig. 4. Histological analysis of normal and arthritic limbs from mice developing CIA. Mouse limbs were amputated, the skin was removed, and the limb was placed in 10% phosphate-buffered formalin at pH 6.9–7.1 for 2–3 d. The limbs were then transferred to decalcification solution (0.1 *M* Tris-base, 10% ethylenediaminetetraacetic acid at pH 7.4) for 2 wk, changing solutions every week. Tissues were then embedded in paraffin, sectioned, and stained with eosin and hematoxylin. **(A)** hind leg joint from mouse with CIA; **(B)** hind leg joint from an untreated mouse.

experiment to verify that the inflammatory response observed in treatment groups is consistent with the known pathogenesis of CIA. **Figure 4** is an example of a CIA arthritic joint compared to a normal joint. Large numbers of inflammatory cells are clearly evident, as are synovial hyperplasia and erosions of the cartilage lining the joint. At the peak of arthritis, the majority of the cells infiltrating the joint are polymorphonuclear cells with some mononuclear cells evident.

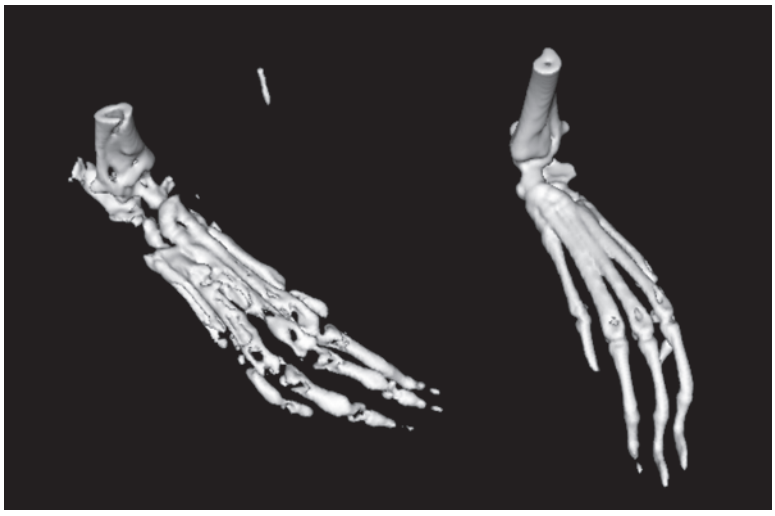

Fig. 5. CT scan of an arthritic limb (L) and a normal hind paw (R) from a mouse that developed CIA. Arthritic and normal limbs were imaged with a GE eXplore MS micro CT using a setting of 90 kVp at 0.18 mA and reconstructed using the Feldkamp conebeam algorithm.

3.4.4. Micro Computer-Aided Tomography

Micro computer-aided tomography analysis of rodents is fast becoming a new approach for studying the pathology of disease models, especially those involving the bone. As shown in **Fig. 5**, this approach enables new views of the arthritis in CIA that were not previously possible. Although this approach is still not suitable for repeated use in quantitating severity of each mouse in an experimental group, it can be used to study individual mice at multiple times throughout the development and resolution of arthritis. Although these instruments are still quite expensive, their use has enormous potential for gaining new insights into the understanding of the pathogenesis of autoimmune arthritis and the efficacy of new and old therapies.

4. Notes

1. Most of these techniques can be applied to the rat model of CIA directly, with the exception that FIA is used. Many rat strains develop arthritis to FCA alone, but not FIA.
2. Adoptive transfer of monoclonal antibodies specific for CII can be used to induce a fast-developing, transient arthritis that is useful for those interested in studying inflammation. Susceptibility to this adoptive transferred arthritis is not strain specific, providing all the required inflammatory mediator genes are present.

3. The acetic acid solution used to dissolve the collagen must be prechilled to 4°C. When it is necessary to work with collagen in a neutral buffer, dissolve the collagen first in acetic acid and then dialyze the solution into the desired buffer in the cold.
4. High concentrations of native CII, up to 6 mg/mL, are achievable but come at the expense of a highly viscous solution. Acetic acid concentrations greater than 100 m*M* should be avoided as they only cause pain on injection and irritation at the injection site.
5. Once arthritis has developed, it is helpful to add food to the bottom of the cages as severely arthritic mice may have difficulty feeding from the cage top.
6. Too frequent handling of the mice after immunization can adversely affect the development of arthritis. Examination two to three times per week is sufficient. Experiments involving daily treatment of mice following immunization with CII need to be carefully controlled.
7. Generally, draining lymph node cells are the better source of T cells for proliferation assays. If spleen cells are used as the source of CII-stimulated T cells, red blood cells must first be lysed with Gey's solution. Nonpurified mouse lymph node cells already contain sufficient numbers of antigen-presenting cells.
8. Grinding the *M. tuberculosis* can be a tedious process, and care must be taken not to create aerosols. This process can be made safer and easier by adding a drop or two of the adjuvant oil to the mortar while grinding the mycobacteria with the pestle.
9. Because of the highly viscous nature of paraffin oil, the FIA is very difficult to measure accurately with a standard laboratory pipet. It is more accurate and convenient to use a positive-displacement instrument (such as a syringe) to measure the FIA accurately. Alternatively, adding the ground mycobacteria directly to a fresh vial of FIA circumvents some of this problem.
10. If using a VirTis homogenizer (or substitute) to create the emulsion directly in the syringe, care must be taken to ensure that the impeller does not come into contact with the syringe, thus creating plastic shavings certain to clog the needle during the immunization.
11. The quality of the emulsion preparation should be assessed by placing a small drop of the emulsion on the surface of a small volume of water. If the emulsion is prepared properly, the drop will maintain its integrity. If the CII and adjuvant are not completely emulsified or the emulsion has been allowed to sit for too long before use, the drop will separate and form an oily slick on the surface of the water.
12. If the emulsion was prepared in a syringe, it can easily be transferred to the injection syringe with minimal loss by connecting the two syringes with a small piece of appropriate size Tygon tubing or a syringe stopcock. The biggest difficulty in successfully transferring the emulsion is eliminating the air pocket formed when the plunger of the 10-cc syringe is placed into the barrel containing the emulsion. This problem can be avoided by calculating the expected total volume of emulsion and using a 16-ga needle to make a hole in the side of the barrel of the 10-cc

syringe at the level of the expected emulsion volume. As the plunger of the 10-cc syringe is placed in the barrel, the trapped air can exit through the hole punched in the side of the syringe, but the hole will become occluded after the plunger passes and reaches the level of the emulsion.

13. Delivering a small volume of emulsion just after the needle is inserted in the tail of the mouse causes a small bleb to form in front of the bevel of the needle and allows the needle to be advanced into the intradermal space without reemerging from the surface of the tail.

Acknowledgments

This work was supported by US Public Health Service grants AR-39166 and AR-47379 (A. H. Kang); grants from the Office of Research and Development, Medical Research Service, Department of Veterans Affairs (E. R. Rosloniec and A. H. Kang); and an Arthritis Foundation Biomedical Grant (D. D. Brand).

References

1 Courtenay, J. S., Dallman, M. J., Dayan, A. D., Martin, A., and Mosedale, B. (1980) Immunisation against heterologous type II collagen induces arthritis in mice. *Nature* **283,** 666–668.

2 Wooley, P. H., Luthra, H. S., Stuart, J. M., and David, C. S. (1981) Type II collagen induced arthritis in mice. I. Major histocompatibility complex (I region) linkage and antibody correlates. *J. Exp. Med.* **154,** 688–700.

3 Terato, K., Hasty, K. A., Reife, R. A., Cremer, M. A., Kang, A. H., and Stuart, J. M. (1992) Induction of arthritis with monoclonal antibodies to collagen. *J. Immunol.* **148,** 2103–2108.

4 Stuart, J. M. and Dixon, F. J. (1983) Serum transfer of collagen induced arthritis in mice. *J. Exp. Med.* **158,** 378–392.

5 Hietala, M. A., Jonsson, I. M., Tarkowski, A., Kleinau, S., and Pekna, M. (2002) Complement deficiency ameliorates collagen-induced arthritis in mice. *J. Immunol.* **169,** 454–459.

6 Miller, E. J. (1971) Isolation and characterization of the cyanogen bromide peptides from the α1(II) chain of chick cartilage collagen. *Biochemistry* **10**, 3030–3035.

7 Rosloniec, E. F., Kang, A. H., Myers, L. K., and Cremer, M. A. (1997). Collagen-induced arthritis, in *Current Protocols in Immunology*, (Coico, R., and Shevach, E., eds.) Wiley, New York, Unit 15.5, pp. 15.15.11–15.15.24.

8 Rosloniec, E. F., Brand, D. D., Myers, L. K., Esaki, Y., Whittington, K. B., Zaller, D. M., et al. (1998) Induction of autoimmune arthritis in HLA-DR4 (DRB1*0401) transgenic mice by immunization with human and bovine type II collagen. *J. Immunol.* **160,** 2573–2578.

9. Rosloniec, E. F., Brand, D. D., Myers, L. K., Whittington, K. B., Gumanovskaya, M., Zaller, D. M., et al. (1997) An HLA-DR1 transgene confers susceptibility to collagen-induced arthritis elicited with human type II collagen. *J. Exp. Med.* **185,** 1113–1122.

10 Andersson, E. C., Hansen, B. E., Jacobsen, H., Madsen, L. S., Andersen, C. B., Engberg, J., et al. (1998) Definition of MHC and T cell receptor contacts in the HLA-DR4restricted immunodominant epitope in type II collagen and characterization of collagen-induced arthritis in HLA-DR4 and human CD4 transgenic mice. *Proc. Natl. Acad. Sci. U S A* **95,** 7574–7579.

11 Nabozny, G. H., Baisch, J. M., Cheng, S., Cosgrove, D., Griffiths, M. M., Luthra, H. S., et al. (1996) HLA-DQ8 transgenic mice are highly susceptible to collagen-induced arthritis: a novel model for human polyarthritis. *J. Exp. Med.* **183**, 27–37.

12 Brand, D. D., Myers, L. K., Whittington, K. B., Stuart, J. M., Kang, A. H., and Rosloniec, E. F. (1994) Characterization of the T cell determinants in the induction of autoimmune arthritis by bovine α1(II)-CB11 in H-2^q mice. *J. Immunol.* **152**, 3088–3097.

13 Terato, K., Hasty, K. A., Cremer, M. A., Stuart, J. M., Townes, A. S., and Kang, A. H. (1985) Collagen induced arthritis in mice: localization of an arthritigenic determinant to a fragment of the type II collagen molecule. *J. Exp. Med.* **162**, 637–646.

14 Myers, L. K., Miyahara, H., Terato, K., Seyer, J. M., Stuart, J. M., and Kang, A. H. (1995) Collagen-induced arthritis in B10.RIII mice (H-2^r): identification of an arthritogenic T-cell determinant. *Immunology* **84**, 509–513.

15 Watson, W. C. and Townes, A. S. (1985) Genetic susceptibility to murine collagen II autoimmune arthritis. Proposed relationship to the IgG2 autoantibody subclass response, complement C5, major histocompatibility complex (MHC) and non MHC loci. *J. Exp. Med.* **162,** 1878–1891.

16 Wetsel, R. A., Fleischer, D. T., and Haviland, D. L. (1990) Deficiency of the murine fifth complement component (C5). A 2-base pair gene deletion in a 5'-exon. *J. Biol. Chem.* **265,** 2435–2440.

17 Ooi, Y. M. and Colten, H. R. (1979) Genetic defect in secretion of complement C5 in mice. *Nature* **282,** 207–208.

18 Brand, D. D., Myers, L. K., Whittington, K. B., Latham, K. A., Stuart, J. M., Kang, A. H., et al. (2002) Detection of early changes in autoimmune T cell phenotype and function following intravenous administration of type II collagen in a TCR transgenic model. *J. Immunol.* **168,** 490–498.

19 Myers, L. K., Stuart, J. M., Seyer, J. M., David, C. S., and Kang, A. H. (1993) T cell epitopes of type II collagen which regulate murine collagen-induced arthritis. *J. Immunol.* **151,** 500–505.

20 Myers, L. K., Terato, K., Seyer, J. M., Stuart, J. M., and Kang, A. H. (1992) Characterization of a tolerogenic T cell epitope of type II collagen and its relevance to collagen-induced arthritis. *J. Immunol.* **149,** 1439–1443.

21 Myers, L. K., Stuart, J. M., Seyer, J. M., and Kang, A. H. (1989) Identification of an immunosuppressive epitope of type II collagen that confers protection against collagen-induced arthritis. *J. Exp. Med.* **170,** 1999–2010.

22. Miyahara, H., Myers, L. K., Rosloniec, E. F., Brand, D. D., Seyer, J. M., Stuart, J. M., et al. (1995) Identification and characterization of a major tolerogenic T cell epitope of type II collagen which suppresses arthritis in B10.RIII mice. *Immunology* **86,** 110–115.

17

Proteoglycan Aggrecan-Induced Arthritis

A Murine Autoimmune Model of Rheumatoid Arthritis

Tibor T. Glant and Katalin Mikecz

Summary

This chapter describes the major principals, methods, and immunization protocols for the induction of a systemic autoimmune arthritis in genetically susceptible murine strains. The model is called proteoglycan-induced arthritis (PGIA) because the antigenic/arthritogenic material is isolated from cartilage. This autoimmune systemic disease is induced by intraperitoneal immunization of either BALB/c or certain C3H colonies with cartilage proteoglycan, an abundant component in articular cartilage. The chapter presents (a) methodological details on how to purify cartilage proteoglycan aggrecan by cesium chloride gradient centrifugation; (b) substitution of this highly purified antigenic/arthritogenic material with a crude cartilage extract obtained from knee joint cartilages removed during joint replacement surgery; and (c) substitution of human cartilage proteoglycan with pig, dog, sheep, or bovine cartilage proteoglycans for arthritis induction. The cartilage proteoglycan aggrecan requires partial deglycosylation, and necessary materials, methods, and protocols are described. In addition, basic methods for measuring antigen-specific T-cell-dependent immune responses, antibody production, serum cytokine levels, and alternative solutions for adoptive transfers are also described.

Key Words: Adjuvants; adoptive transfer; autoantibodies; cartilage; cytokine; arthritis; inflammation; mouse models; PGIA; proteoglycan; proteoglycan-induced arthritis; T-cell responses.

1. Introduction

Rheumatoid arthritis is probably the least-understood systemic autoimmune disease that affects approx 1% of the human population. Several lines of evidence indicate that the effector mechanism, which initially attacks small joints, is T-cell driven. As a result, an aggressive synovial pannus develops

From: *Methods in Molecular Medicine, Vol. 102: Autoimmunity: Methods and Protocols*
Edited by: A. Perl © Humana Press Inc., Totowa, NJ

that destroys articular cartilage and bone, leading to massive ankylosis and deformities of peripheral joints. The disease has a progressive character, with the involvement of more and more joints. Although the primary target organ is the synovial joint, there is no clear evidence that any macromolecule of cartilaginous tissues, bone, or synovium would be a preferential autoantigen.

Although immunity to the cartilage proteoglycan (PG) aggrecan has been less extensively studied than immunity to type II collagen, cartilage PGs are also considered a causal factor in some rheumatoid joint diseases ***(1–4)***. Both humoral and cellular immunities to human cartilage PGs have occasionally been detected in patients with rheumatoid arthritis and juvenile rheumatoid arthritis ***(1,2,5–7)***. It is of special interest that cellular immunity to adult cartilage PGs has been detected quite frequently in patients with ankylosing spondylitis ***(1,6)***, and PG-specific T-cell lines and clones have been isolated from such patients ***(7,8)***.

There are numerous animal models in rodents that simulate some or many of the clinical, immunological, or histopathological features of the disease. The most relevant animal models of rheumatoid arthritis appear to be those induced by cartilage matrix components such as type II collagen and PG. Systemic immunization of genetically susceptible DBA/1 mice with cartilage-specific type II collagen ***(9)*** or BALB/c or C3H mice with human cartilage PG ***(10,11)*** depleted of both chondroitin sulfate (CS) and KS (keratan sulfate) side chains ***(12–14)*** leads to the development of progressive polyarthritis. Both models have similarities and differences, advantages and disadvantages, and mimic certain clinical or laboratory characteristics of rheumatoid arthritis when compared to the other ***(15)***.

Prior to the use of any of the two autoimmune arthritis models, investigators should carefully consider these differences (**Table 1**) and then select the appropriate model system for the specific research purpose. It is important to note that PG-induced arthritis (PGIA)-susceptible strains of mice, which respond to immunization with type II collagen, are completely resistant to collagen-induced arthritis (CIA), and vice versa, CIA-susceptible mice respond to PG immunization, but are fully resistant to PGIA ***(11,14)***.

This chapter summarizes the current knowledge of, and technical approaches to, PGIA in mice; Chapter 16 considers the same aspects of CIA. It is noteworthy that, although the major histocompatibility complex (MHC) is a critical predisposing factor of each autoimmune disease and its corresponding animal model, the non-MHC genetic components are at least as important factors as the MHC. Many of the differences between the two murine models of arthritis dictated by these MHC- and non-MHC-related genetic components together determine arthritis susceptibility and severity.

Table 1
Comparison of Major Differences Between Collagen-Induced Arthritis (CIA) and Proteoglycan (Aggrecan)-Induced Arthritis (PGIA) in Mice

Characteristics	CIA[a]	PGIA
Antigen	Type II collagen	Cartilage PG
MHC haplotype	H-2q or H-2r	H-2d or H-2k
Non-MHC genetic background	DBA/1 or C57BL	BALB/c or C3H
Required injections	1–2 (intracutaneous)	2–4 (intraperitoneal)
Peak of onset (days)	30–40	50–70
Range of incidence	60–90%	80–100%
Preferred age and sex	5- to 8-wk-old males	Retired breeders (females)
Inheritance	Dominant	Recessive in matched haplotype, and dominant if MHC is unmatched
IFN-γ deficiency	Increases susceptibility	Resistant to PGIA
Spondylitis	Unknown	Characteristic (1–2 mo after the onset of arthritis in synovial joints)
Disease progression	Variable, acute inflammation is usually followed by chronic inflammation	Progressive, acute followed by chronic inflammation (recovery never occurs); joint deformities and ankylosis are characteristics

[a]CIA can be induced in genetically susceptible rats ***(50)*** and mice ***(9)***, but only mouse strains (BALB/c and C3H) are known to be susceptible to PGIA ***(4,20,21,29)***.

2. Materials

2.1. Source of Cartilage Antigen

Cartilage PG is a large and complex macromolecule (approx $2–3 \times 10^6$ Da), especially in composition ***(13)***. The PG molecule contains a central protein core to which 100–120 glycosaminoglycan (GAG; e.g., CS and KS) side chains are attached together with O-linked and N-linked oligosaccharides (**Fig. 1**). Many of the T-cell epitopes of the core protein are masked by these GAG side chains. PGIA originally was described in BALB/c mice after immunization with fetal human cartilage PG depleted of CS. PG in fetal human cartilage

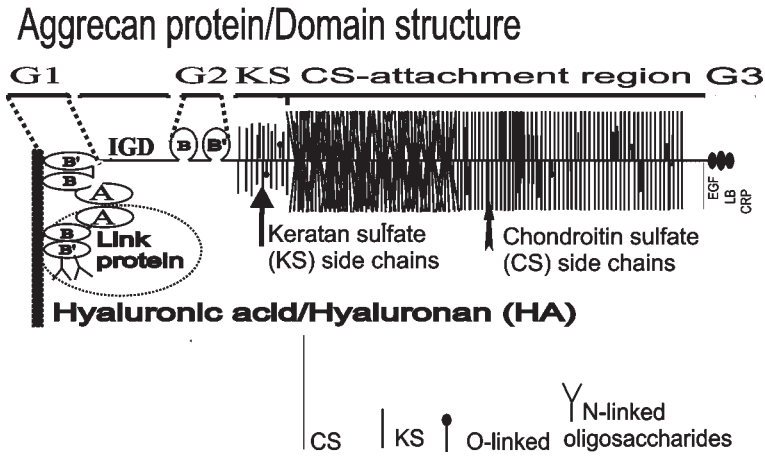

Fig. 1. Schematic presentation of the structure of cartilage proteoglycan (PG) aggrecan. This cartilage PG (M_r approx 2–3 × 10^6 Da) consists of a central protein core (M_r approx 2.2 × 10^5 Da) to which glycosaminoglycan (GAG), chondroitin sulfate (CS; M_r approx 2–3 × 10^4 Da), and keratan sulfate (KS; M_r approx 1–2 × 10^4 Da) side chains are attached together with O-linked and N-linked oligosaccharides. (Hundreds of PG aggrecan molecules bind to a single hyaluronan chain, stabilized by link protein, forming large, multimillion Dalton size aggregates.) The various domains/subdomains of the central protein core are the G1 domain with A, B, and B' loops; IGD (interglobular domain between G1 and G2 domains); G2 domain with B and B' loops; KS (a KS-rich region between the G2 domain and the CS attachment region); CS attachment regions; and a G3 domain containing EGF (epidermal growth factorlike), LB (lectin-binding), and CRP (complement regulatory protein-like) subdomains. Approximately 100–120 CS side chains are attached to a long, but restricted, region of the core protein (CS attachment region). Although most of the KS chains are localized in a narrow region (KS), KS side chains are also present along the entire core protein and frequently mask T-cell epitopes. CS and KS side chains mask the T-cell epitopes of the core protein, and many of the T-cell epitopes can be processed by the MHC only if the GAG side chains are removed.

essentially has no KS chain ***(16,17)***. In contrast, PG in adult human cartilage is substantially glycosylated with KS side chains, a GAG that is nondegradable in the mammalian system, but masks a number of T-cell epitopes ***(5,13,18)***.

It was found that PGs from several other species are as effective for arthritis induction as the PG from fetal human cartilage if both CS and KS side chains are removed. Human, canine, and porcine cartilage PGs are the most effective ***(19)***, but sheep and bovine (in this order) can also induce PGIA with lesser incidence and severity. Mouse, rat, guinea pig, rabbit, and chicken PGs, although

they provoke immune responses when injected with adjuvants, are unable to induce arthritis in the susceptible BALB/c strain. Technically, an unlimited source of PG antigen is human osteoarthritic knee cartilage removed during the process of joint replacement surgery ***(14)***. The yield of cartilage from other osteoarthritic joints (shoulder, hip) is low, and macromolecules in cartilage (especially the core protein of PG) are extensively degraded. Similarly, knee cartilage from patients with rheumatoid arthritis, because of the extensive degradation, is not recommended for PG isolation ***(14)***.

2.2. Chemicals, Laboratory Disposal, and Equipment for Antigen Preparation

1. Regular (standard) laboratory chemicals (analytical grade) and cesium chloride, dimethyl methylene blue (DMMB), CS, conconavalin A.
2. Sodium acetate buffer: 0.1 *M*, pH 5.8; and Tris-HCl/sodium acetate buffer: both 0.1 *M*, pH 7.6.
3. Enzyme inhibitors: phenymethyl-sulfonyl-fluoride (PMSF), iodoacetamide, pepstatin A, ethylenediaminetetraacetic acid (EDTA) (*see* **Note 2**).
4. 4 *M* guanidinium chloride in 0.1 *M* sodium acetate buffer (pH 5.8) (*see* **Note 1**).
5. Glycosidases: endo-β-galactosidase (0.1 U/vial) (Seikagaku/Assoc. of Cape Cod, Falmouth, MA or Sigma Aldrich, St. Louis, MO), chondroitinase ABC (Seikagaku or Sigma Aldrich) or testicular hyaluronidase (usually 400–600 USP/Nfu nits/mg; Worthington Biochemicals, Freehold, NJ).
6. Antibodies (peroxidase-labeled antimouse immunoglobulin G1 [IgG1], IgG2a, IgG3), antibodies to cell surface markers, and mouse isotype standards are available from Zymed (San Francisco, CA), BD Pharmingen (San Francisco, CA), or Accurate Chemical and Scientific Corporation (Westbury, NY).
7. Kits for protein assay (Pierce, Rockford, IL; or Bio-Rad, Hercules, CA), cytokine enzyme-linked immunosorbent assay (ELISA) kits (R&D Systems, Minneapolis, MN; BD Pharmingen; or BioSource, Camarillo, CA).
8. Dialysis tubes (molecular weight cutoff 12,000–14,000 Da), polyallomer Quick-Seal ultracentrifuge tubes, polycarbonate high-speed centrifuge tubes.
9. Equipment: ultracentrifuge, high-speed centrifuge (Beckman, Newton, CT, or Sorvall, Fullerton, CA), freezing mill (Spex CertiPrep Inc., Metuchen, NJ) or cryostat, water baths or incubators, shaker, vortex, freeze-dryer, spectrophotometer or microplate reader, microwave, micropipets, cell harvester, scintillation counter, and tissue culture facility (equipment, plastic ware, media, sera).
10. Adjuvants: Freund's complete adjuvant (FCA) and Freund's incomplete adjuvant (Difco Laboratories, Detroit, MI), dimethyl-dioctadecyl ammonium bromide (DDA; Sigma-Aldrich or Fluka).
11. Laboratory glass and plastic wares, 96-well plates for ELISA.
12. [^{3}H]-Thymidine (low specific activity 6.7 Ci/m*M*), CTLL-2 cell line (American Type Culture Collection, Manassas, VA).

2.3. Susceptible Strains of Mice

The strain of mice and adjuvant used for immunization are as critical as the source of antigen. A wide range of different colonies of BALB/c strain (H-2d haplotype) is susceptible to PGIA, although some differences in both susceptibility (50–100%) and severity are known. Other strains with H-2d haplotype (e.g., NZB or DBA/2) are resistant to PGIA. Depending on the antigen and adjuvant, BALB/c colonies of Charles River Laboratories (Kingston, NY, Portage, MI, or Raleigh, NC) and BALB/AnNCr (National Cancer Institute [NCI], Frederick, MD) are 98–100% susceptible to PGIA. If no genetic contamination occurred in a BALB/c colony, the least-susceptible colony (e.g., BALB/cBy from Jackson Laboratory) using Freund's adjuvants must have at least 50% incidence.

Because of parvovirus or hepatitis infections, companies frequently establish new colonies, which may show some variability in onset, severity, or incidence of PGIA when compared to the previous colony used by the same investigator. Susceptibility may be higher in spring or summer than in other seasons (unpublished observation, Dr. T. Glant). The inheritance of PGIA in hybrid or congenic mice of BALB/c origin is recessive; that is, F1 hybrids of BALB/c and any resistant strain combination are completely resistant to arthritis.

If Freund's adjuvants are used for immunization, it is highly recommended to use females because of both the aggressive behavior and the high mortality of BALB/c males after repeated intraperitoneal injections with FCA. When using DDA as the adjuvant, the differences among BALB/c colonies in susceptibility is minor, and mortality is lower, but the disease is more acute and dramatic than when Freund's adjuvants are used. Older females (older than 16–20 wk or retired breeders) develop more severe arthritis with an earlier onset than young (6- to 8-wk-old) female BALB/c mice, but the use of younger mice for in vitro T-cell tests or T-cell separation may be considered.

The other PGIA-susceptible strain is the C3H (H-2k haplotype), but there is an extremely wide variety among C3H colonies ***(11)***. Other murine strains with H-2k alleles (e.g., AKR and CBA) are resistant to PGIA. The most susceptible C3H colonies are those maintained by the NCI (C3H/HeJCr) and Charles River Laboratories (C3H/ChR), whereas C3H/HeJ (Jackson Laboratory) or C3H/BiDACr (NCI) colonies are almost completely resistant to PGIA (less than 10% susceptibility) ***(11,20)***. There are no real differences in onset, severity, or susceptibility between susceptible C3H females and males, and the age difference is less evident than in the BALB/c strain. The inheritance of PGIA in F1 hybrids of susceptible C3H and a resistant strain is dominant; that is, over 50% of the F1 hybrids develop arthritis in response to PG immunization ***(21)*** (**Table 1**).

3. Methods

3.1. Antigen Preparation

3.1.1. Preparation of Crude Extract of Cartilage

Harvested cartilage samples can be stored at 4°C for a few hours, but should be cut into small pieces and placed on ice as soon as possible, ready for extraction, and stored at –80°C until use (*see* **Note 3**). Samples from an operating room (osteoarthritic knee joint cartilage and osteophytes from the marginal zone of the articular surface) should be removed from the underlying subchondral bone by scalpel, cut to small pieces, and stored at –80°C. For the most effective yield of PG extraction, cartilage pieces should be cut as small (thin) pieces as possible (thinner than 1 mm). For the best extraction, 0.5–1.0 g pieces of cartilage can be frozen in block (in a plastic cylinder 0.5–1.0 cm high) and, after removing the cylinder, sectioned by cryostat (20–50 μm thickness).Frozen cartilage pieces can be pulverized under liquid nitrogen in a freezing mill. Low-speed homogenization is insufficient to generate small pieces of cartilage, whereas the high-speed homogenization (>20,000*g*) is not recommended because of a high splitting force, which may mechanically damage macromolecules.

Pig, sheep, or bovine articular cartilages from a slaughterhouse should be harvested as soon as possible and shipped on ice. If bovine or pig nasal cartilage is harvested, the perichondrium and blood vessels should be carefully removed and blood washed away with cold water prior to freezing for either sectioning or pulverization. Mouse cartilage can be collected from newborn (4–6 d old) skeletal tissue after removing the soft tissue (newborn cartilage) or from adult mice by removing the cartilage "cap" from the femoral heads with toothed forceps (*see* **Note 7**).

Second, cartilage powder or sections should be extracted with 4 *M* guanidinium chloride in 50 m*M* sodium acetate at pH 5.8 and containing protease inhibitors at 4°C for 24 h ***(22,23)***. A standard cocktail of protease inhibitors contains 10 m*M* EDTA, 2 m*M* PMSF, 2 m*M* iodoacetamide, and 5 μg/mL pepstatin A. PMSF and pepstatin A should be prepared freshly in alcohol. The final ratio of cartilage weight to the 4 *M* guanidinium chloride is 1:10 (w/v).

If the cartilage pieces are larger than 20–30 μm (i.e., chopped by blades or scalpels [0.5–1.0 mm in thickness] or pulverized under liquid nitrogen), a 48-h extraction is required at 4°C. In this case, the cartilage extract should be harvested by centrifugation after 24 h, and fresh 4 *M* guanidinium chloride containing fresh protease inhibitors should be added at a ratio of 1:5 to the cartilage pellet. Guanidinium chloride extract is collected by high-speed centrifugation (2000*g*, 15–20 min at 4°C) after 24–48 h, and supernatant containing all salt-soluble proteins of cartilage can be further processed immediately or stored at –20°C for months.

This guanidine extract without additional purification is called *crude extract*. The crude extract then can be used for purification on cesium chloride gradient centrifugation to obtain high-quality PG (*see* **Subheading 3.1.2.**) or exposed to deglycosylation (*see* **Subheading 3.1.3.**), which is also sufficient for immunization and arthritis induction. Even so, using deglycosylated PGs in a crude extract for arthritis induction (*see* **Subheading 3.2.**), the investigator may need highly purified PG for antibody or T-cell assays.

3.1.2. Preparation of Highly Purified Cartilage PG

There are several methods to purify high-density cartilage PG (aggrecan). The method described here is called dissociative gradient centrifugation because the 4 *M* guanidine chloride concentration is maintained during the entire purification procedure (*see* **Note 1**). The original protocol ***(24)*** divided the gradient into six equal portions and numbered them from bottom (D1 fraction) to top (D6 fraction). High-density cartilage PG (aggrecan) was recovered in the bottom two fractions (D1 and D2; density > 1.56 g/mL). This high-density PG (aggrecan) typically contained 6.5–7.5% protein in fetal samples and 11.5–12.5% in adult samples and mostly preserved their in vitro aggregating capacities to hyaluronic acid (hyaluronan, HA) ***(23)***. However, the retained aggregating capacity of PG to HA or the gross biochemical characteristics of the molecule does not exclude some degradation of the C-terminal end of the core protein, which is especially characteristic of a cartilage sample obtained from knee joints of patients with osteoarthritis ***(23,25,26)***. As described in **Points 3** and **4** in this subheading, if the cartilage extract is highly contaminated with blood, muscle, or other soft tissue (newborn skeletal tissue of mice, chondrosarcoma or nasal cartilage), the dissociative cesium chloride gradient centrifugation should be repeated at least twice to obtain a highly purified cartilage PG sample.

1. Guanidine (crude) extracts of cartilages can be purified by cesium chloride gradient centrifugation ***(22,24,27)***. The density of the 4 *M* guanidinium extract is approx 1.12 g/mL. The required starting density is 1.5 g/mL; thus, approx 68–70 g solid cesium chloride should be added to 100 mL 4 *M* guanidinium extract to achieve this starting density. A relatively large volume of nuclear and membrane components in the extract makes the solution "dirty," which is especially evident after adding the cesium chloride to the extract. A 10- to 15-min high-speed centrifugation (200–2500*g*, 4°C; balance tubes carefully because of the high-density solution) is recommended to preclean the cartilage extract prior to adjusting the starting density for a linear gradient centrifugation.
   The lipid-rich layer from the top can be removed by a teaspoon or spatula and, if necessary, prefiltered on a multilayer gauze. The density of this still-opalescent cartilage extract then can be measured by a microbalance using a calibrated

micropipet. Use dry (new) tips for each measurement and measure the density of the sample at least three times. For a more accurate calibration of the viscous extract, the 1- to 2-mm end of the 1-mL blue tip can be cut off. Solid cesium chloride can be added to increase, or 4 *M* guanidinium chloride stock solution to reduce, the density of the extract to 1.50–1.51 g/mL. Cartilage extract with the desired starting density then should be transferred into polyallomer heat-sealing (Quick-Seal) ultracentrifuge tubes, which had been stored on ice, by syringe with a 15- to 18-ga needle. Transfer the extract slowly into the tube without introducing air bubbles, which may be difficult to remove prior to heat sealing of the tube.

2. Heat-sealed centrifuge tubes are transferred into a precooled rotor (4–10°C), which is then returned to the ultracentrifuge. The gravidity at the middle of the tube should be 100,000*g*. Program the ultracentrifuge to hold at 10°C and run the sample for at least 48 h. A stable gradient is formed, and a longer run (e.g., 60–72 h) will not modify the established density. Stop centrifugation in the morning hours to have sufficient time for further processing of the sample. Do not use the deceleration program (brake) of the centrifuge when stopping it. Depending on the size of the tubes (i.e., the volume of the extract) or the rotor available, different speeds are required to reach the required centrifugation force. Typically, use 33,000 rpm for a Beckman or Sorvall Ti50 rotor (38-mL tubes) or 38,000 rpm for a Ti70 rotor (12-mL tubes).
3. Remove the tubes gently from the rotor by an appropriate forceps into an ice bucket and cut (remove) the very top segment (sealed neck) of the tube with a blade. If gradient slicer equipment is available (e.g., Beckman), cut the gradient at the one-third bottom level. This bottom fraction contains the PG minimally contaminated with other proteins. If the gradient slicer equipment is not available, remove the upper two-thirds volume by a transfer pipet and then the bottom one-third fraction with a clean 5- to 10-mL glass or plastic pipet using a pipet-aid. Alternatively, after removing the lipid/cell membrane layer from the top, the bottom fraction can be removed by a 12- to 15-cm long lumbar puncture needle connected to a syringe or a peristaltic pump. If clean and washed articular cartilage, which does not contain blood, blood vessels, or perichondrium, was used for extraction, no additional ultracentrifugation is necessary. In this case, transfer the one-third bottom fraction directly to a dialyzing tube. If the original sample was heavily contaminated with soft tissue, proteins with small molecular weights are uniformly distributed in the tube (from bottom to top); thus, repeated ultracentrifugation is required to obtain a highly purified PG sample. The overall density of the bottom one-third fraction must be 1.56–1.57 g/mL (4°C), which is the best indicator of the quality of the gradient density centrifugation.
4. Contaminated samples must be recentrifuged. If the same sample was distributed in several tubes prior to the density gradient centrifugation, bottom fractions can be pooled before readjusting the density. Adjust the density of the harvested bottom one-third fractions (typically 1.56–1.57 g/mL) to the 1.50–1.51 g/mL starting density by adding 4 *M* guanidinium chloride with protease inhibitors. Density is measured by a microbalance using a calibrated micropipet. The volume of the

density-readjusted sample (e.g., 100 mL) should be diluted with an excess volume of approx 40–50% (additional 40–50 mL), with a stock solution (4 *M* guanidine chloride with cesium chloride of 1.50 g/mL density) prepared in advance. Typically, the second (or third) centrifugation in the rotor requires approximately half of the space (tubes) used for the first gradient centrifugation. All procedures and gradient and volume adjustments should be performed at 4°C on ice. Second, or third, ultracentrifugation should be performed in the same conditions as used for the first gradient centrifugation (minimum 48 h at 10°C), and the sample collection is also the same as described in **Point 3**.

5. Total/crude cartilage extracts (if used directly for enzymatic treatment), or the one-third bottom density gradient fraction (as described above), must be dialyzed first against 0.1 *M* sodium acetate (1:20 v/v, 2 × 12 h) to dissociate the guanidine from the PG and then dialyzed exhaustively (3–4 d at 4°C) against distilled water prior to freeze-drying. Freeze-dried sample, although hygroscopic, can be stored in a hermetically closed vial for years at 4°C or –20°C. Stock solution can be prepared for composition (biochemical) analysis or deglycosylation, which is crucial to retrieve the arthritogenicity of the PG molecule.

3.1.3. Deglycosylation of Highly Purified Cartilage PG or Crude Extract for Immunization

Technically, for induction of PGIA, either a crude cartilage extract containing essentially all soluble components of cartilage or highly purified cartilage PG is sufficient. However, there are four major criteria of arthritis induction using PG for immunization: (a) source of cartilage (human, dog, pig; less effective are the sheep and bovine cartilage); (b) PG must be deglycosylated (depleted) of both CS and KS; (c) the strain of mice (BALB/c and some C3H colonies); and (d) the immunization protocol (including the type of adjuvant).

The CS side chains can be removed with either chondroitinase ABC (**Subheading 3.1.3.1.**) or testicular hyaluronidase (**Subheading 3.1.3.2.**). Similarly, the KS can be removed with either endo-β-galactosidase (**Subheading 3.1.3.3.**) or keratanases. Either combination of enzymes is sufficient, but both CS and KS must be removed. In all cases, the presence of an appropriate concentration of protease inhibitors is crucial because all enzymes are contaminated with proteases, which can degrade the core protein of cartilage PG, and the arthritogenicity of the sample can be lost.

Deglycosylated crude extract of cartilage can be used (**Subheading 3.1.1.**) because neither the BALB/c nor susceptible C3H colonies develop arthritis with immunization of type II collagen or other matrix components ***(14)***, except BALB/c mice for "link protein" immunization ***(28)***. (Link protein is a 38-kDa glycoprotein that stabilizes the interaction between HA and PG in cartilage; **Fig. 1**.) In contrast, none of the other murine strains develop arthritis in response to PG immunization ***(4,14,20,21,29)***. The crude extract of car-

tilage, if deglycosylated in an appropriate manner, is as effective as the highly purified cartilage PG, and there is no antigen competition, which would modify the clinical or laboratory feature of arthritis. However, highly purified PG is necessary for testing PG-specific T- or B-cell responses.

3.1.3.1. Removal of the CS Side Chains by Chondroitinase ABC

Typically, 100 mg lyophilized (purified) cartilage PG or 250–300 mg crude extract can be depleted of CS with 5 U (1 vial) of chondroitinase ABC at 37°C within 18–24 h. Dissolve sample (e.g., 100 mg PG or 250 mg crude extract) in 10 mL 0.1 *M* Tris-HCl-sodium acetate buffer (pH 7.4–7.6) containing protease inhibitors and mix with 5 U chondroitinase ABC dissolved in 0.5 mL of the same buffer. Repeated shaking in the first 2–3 h can accelerate the digestion, which is proportional to the loss of viscosity of the sample.

3.1.3.2. Removal of CS Side Chains With Testicular Hyaluronidase

Testicular hyaluronidase is less expensive than chondroitinase ABC but contains significantly more proteases. Therefore, the presence of fresh enzyme inhibitors is critical. A double concentration of protease inhibitors (10 m*M* EDTA, 5 m*M* PMSF, 5 m*M* iodoacetamide, and 5–10 μg/mL pepstatin A) is recommended. Typically, 100 mg purified PG or 200 mg crude extract are dissolved in 10 mL 0.1 *M* sodium acetate buffer (pH 5.0) containing protease inhibitors (listed above), 50 m*M* $MgCl_2$, and 50 m*M* NaCl. After complete dissolution, 50 U of testicular hyaluronidase in 100 μL, dissolved in the same buffer (sodium acetate/$MgCl_2$/NaCl, pH 5.0) as the sample, are added to 100 mg purified PG or 250 mg crude extract. Digestion is completed within 24 h at 37°C, and the loss of viscosity indicates the degradation of the CS side chains.

3.1.3.3. Removal of KS With Digestion of Endo-β-galactosidase

The pH samples treated with either chondroitinase ABC (pH 7.4–7.6) or testicular hyaluronidase (pH 5.0) should be adjusted to 5.8 with 0.5 *M* acetic acid or 0.1 *M* sodium hydroxide. Fresh protease inhibitors should be added to the sample prior to mixing with endo-β-galactosidase. Add 0.05 U (half a vial) to each 100 mg purified PG or 250 mg of crude extract dissolved in a volume of 10–11 mL. Digestion is performed at 37°C for 24 h. Double-digested samples are transferred into dialysis tubes and dialyzed exhaustively against deionized water at 4°C. This requires at least 2–3 d, changing the precooled dialyzing water at least twice a day. Finally, samples are lyophilized, and the chemical composition is determined. Alternatively, KS can be removed with keratanase I and keratanase II (both enzymes are also endo-β-galactosidases) as described in detail in **ref. *22***.

3.1.3.4. Special Treatment of Crude Extract of Cartilage

Whenever a crude extract is used for deglycosylation, the rehydrated sample first should be centrifuged at a high speed (5000–6000*g* for 30 min at 4°C) to remove insoluble components extracted with 4 *M* guanidinium chloride. A significant portion of this insoluble material is salt-soluble collagen. As the deglycosylation is a critical step and the crude extract is rehydrated in buffer, some proteins that otherwise are insoluble in deionized water during dialysis are redissolved in the sample (enzyme) buffer. After digestion (e.g., with testicular hyaluronidase and endo-β-galactosidase), just prior to the dialysis, samples should be recentrifuged at 5000–6000*g* for 30 min at 4°C and then supernatant dialyzed against water.

3.1.3.5. Purification of PG Core Protein

GAG side chains are fragmented into di- and tetrasaccharides by enzymes (**Subheadings 3.1.3.1.–3.1.3.4.**) and removed during dialysis ***(13)***. Enzymes used for deglycosylation do not interfere with the anti-PG immune response or arthritis induction in vivo; therefore, it is unnecessary to remove them. Low titers of antibodies against these enzymes, and antibodies to contaminating cartilage proteins if crude extracts were used for immunization, can be detected, which may be additive to the overall (anti-PG) immune response measured by ELISA. However, T-cell responses against contaminating enzymes cannot be detected. Therefore, whenever a crude extract is used for immunization and the anti-PG immune responses are measured, a highly purified PG sample is necessary for in vitro tests. This is the same whenever the autoimmune response to mouse (self) cartilage PG is measured.

Thus, preparation of a stock of highly purified cartilage PGs (**Subheading 3.1.2.**), especially after deglycosylation, is a critical issue. This highly purified cartilage PG, after cesium chloride gradient centrifugation and deglycosylation, can be obtained by column chromatography using, for instance, Sepharose CL-4B (at least 80-cm-long gel) or an equivalent high-performance liquid chromatographic column ***(17,22)*** equilibrated in 0.1 *M* sodium acetate buffer (pH 5.8). Deglycosylated core protein (approx 220,000 Da) is eluted in the voided volume, and then should be dialyzed against deionized water and lyophilized.

3.1.4. Characterization of Cartilage PG, Crude Extract, and Deglycosylated Samples

A 10-mg lyophilized sample/milliliter is an optimal concentration for measuring either protein or GAG content. Purified PG is highly soluble in deionized water, whereas deglycosylated crude extract is less soluble. Therefore, it is recommended to rehydrate samples in phosphate-buffered saline (PBS; pH 7.4), especially the crude extract, which can also be used for induc-

tion of PGIA. Protein content can be measured by bicinchoninic acid assay (Pierce) or Bio-Rad Protein Assay (Bio-Rad) following the manufacturer's instruction. Protein content may vary depending on the source (species and age) of the sample (*see* **Note 3**). Purified PG (prior to deglycosylation) from fetal/newborn human cartilage contains significantly lesser amounts, whereas PG from adult cartilage contains higher amounts of protein (**Table 2**). A more precise measurement can be performed using monoclonal antibodies against composite-specific epitopes (core protein, CS, KS). A brief summary with the corresponding basic literature for these assays is given in **Note 9**.

3.1.4.1. DMMB Assay: Preparation of DMMB Reagent

To prolong the activity of the DMMB, it is desirable first to solubilize the reagent in organic solvents before diluting it into a mostly aqueous environment. This is why it is suggested in **ref. *30*** that the DMMB reagent first be dissolved in an ethanol-formate solution.

1. Dissolve 16 mg DMMB (Polysciences Inc., cat. no. 03610) in 5.0 mL absolute ethanol. Solubilize for 15 min at room temperature.
2. Add 2.0 mL formic acid and 2.0 g sodium formate (mol wt 68.01) to approx 20 mL double-distilled water (ddH_2O). Dissolve and add to the ethanol-DMMB solution.
3. Allow to shake for 20 min.
4. Add ddH_2O to less than 1 L.
5. Adjust the pH to 6.8.
6. Add ddH_2O to a final volume of 1 L. (Note that by adjusting the pH before making the final volume 1 L the dye solution should be more reproducible.)
7. Final dye solution: 16 mg/mL DMMB, 0.03 *M* sodium formate, 0.2% formic acid at pH 6.8.

Do not filter or refrigerate the DMMB reagent. DMMB activity is transient, so shelf life is only 1 mo.

3.2. Immunization Protocols and Assessment of Arthritis

Technically, 250–300 μg of lyophilized human cartilage PG depleted of both CS and KS represents100 μg core protein of PG (a single dose for injection of an arthritis-susceptible mouse). This amount of 100 μg PG core protein is present in approx 1.0–1.4 mg deglycosylated (testicular hyaluronidase and endo-β-galactosidase-treated) crude extract of human adult or osteoarthritic cartilage (*see* **Note 4**). A more "accurate" calculation for the required dose (approx 100 μg PG core protein) of immunization can be achieved by measuring the GAG stubs by DMMB assay or by monoclonal antibodies to CS and KS. Empirically, 250–300 μg of CS (measured by DMMB assay) is equivalent to (represents) approx 100 μg PG core protein in deglycosylated and lyophilized crude extract.

Table 2
Biochemical Comparison of Intact (Nondeglycosylated) Cartilage Proteoglycans[a]

	Protein (%)	Chondroitin sulfate (%)	Keratan sulfate[b] (relative %)
Human PGs[c]			
Fetal (24–27 wk)	5.9	39.9	28
Newborn	6.1	25.2	36
Adult (52–56 yr)	10.2	15.9	100
PGs from animal cartilages[d]			
Mouse (newborn)	6.1	36.5	<2.0
Mouse (adult, 5–10 mo)	7.4	32.0	<2.0
Fetal calf (21 wk)	6.7	34.7	56
Bovine (18 mo)	15.2	29.3	94
Fetal pig (6–12 wk)	4.2	29.8	86
Porcine (12–16 mo)	12.8	24.3	49
Newborn lamb (<2 wk)	8.0	36.7	n.d.
Sheep (24–30 mo)	11.2	18.4	82
Newborn canine (<2 wk)	9.4	29.8	75
Canine (2–8 yr)	13.0	18.3	86
Newborn rabbit (2 wk)	9.3	19.2	68
Chicken sternal (3 mo)	7.2	18.5	91
Guinea pig rib (6 mo)	11.2	23.8	44

n.d., not determined.

[a]High-density cartilage PGs (aggrecan) were purified on cesium chloride gradient centrifugation.

[b]KS content was measured by monoclonal antibody EFG-11 ***(49)*** in ELISA as described in **ref. *51*** and expressed as a relative amount compared to human adult cartilage PG (100%).

[c]Age of cartilage sample is indicated.

[d]Articular cartilages were used except for the guinea pig rib and chicken sternal cartilages.

Two different methods are available for immunization using either Freund's adjuvants or DDA. The major difference between the two adjuvants (Freund's or DDA) is that the development of PGIA using Freund's adjuvant requires a longer time, and the inflammation of joints is less dramatic. Therefore, the overall clinical picture and progression of the disease is more chronic than the arthritis induced by PG in DDA. Spine involvement in PG/Freund's adjuvant-induced arthritis may occur months after the first clinical symptoms in synovial joints, whereas spondylitis can be detected almost simultaneously in mice immunized with PG in DDA. In summary, it appears that PGIA using Freund's adjuvant is more chronic, thus more resembling rheumatoid arthritis, whereas

PGIA using PG in DDA is extremely acute. To the end, articular cartilage is completely destroyed in all affected joints, and peripheral joints become deformed and ankylotized using either Freund's or DDA adjuvant. Special advantages of using DDA are (a) avoidance of the coeffects of the exogenous heat shock proteins present in mycobacteria in FCA, (b) significantly shorter onset time, and (c) lower mortality (no abdominal adhesions develop, which are typical in FCA-injected animals).

3.2.1. Immunization of Susceptible Mice With PG in Freund's Adjuvant

Young retired breeder female BALB/c mice from Charles River (Kingston, NY, Portage, MI, or Raleigh, NC colonies) or NCI (Kingston colony) are the most susceptible to PGIA (98–100% incidence). The optimal dose of highly purified and CS-depleted aggrecan of human fetal cartilage for arthritis induction was determined to be approx 100 μg per intraperitoneal injection ***(10,12,13,31)***. Therefore, the material prepared for injection (either purified density gradient fractions or crude cartilage extracts) should contain approximately this amount (100 μg) of PG core protein. Use an emulsion of 100 μg PG protein in 100 μL PBS and 100 μL Freund's adjuvant per mouse and injected intraperitoneally (*see* **Note 5**). Higher doses of PG do not increase the susceptibility or severity of PGIA.

The first intraperitoneal injection should be given in FCA; all other injections can be given in incomplete Freund's adjuvant on days 21, 42, and, if necessary, on days 63–70 to achieve a 100% incidence. Usually, an animal is boosted three or four times only if it remains asymptomatic for 3–4 wk after the previous injection. It is typical that, if an animal once develops any small symptom of inflammation (e.g., in the interphalangeal joint of one paw; arthritis score <1.0) (**Fig. 2B**), this mouse will develop severe arthritis sooner or later without additional injections (**Fig. 2**). Usually, the small joints (interphalangeal, carpo-metacarpo-phalangeal, or tarso-metatarso-phalangeal joints) are first involved. Disease may flare up in one or in a few joints, symmetrically or asymmetrically, when the inflammation in other joints is regressed. Along the progression of the disease, more and more joints are involved until severe deformities and ankylosis develops. Once an animal develops arthritis, it will never regress spontaneously.

3.2.2. Immunization of Susceptible Mice With PG in DDA Adjuvant

DDA is a novel adjuvant used more recently for immunization of mice ***(20)***. (DDA is a lipophilic quaternary ammonium salt, an adjuvant successfully used for vaccination of pregnant women and children without side effect ***[(32)]***.) Although the clinical and immunological features of the "classic" form of PGIA ***(10–14,31)*** are preserved, the onset of the disease is faster, and the

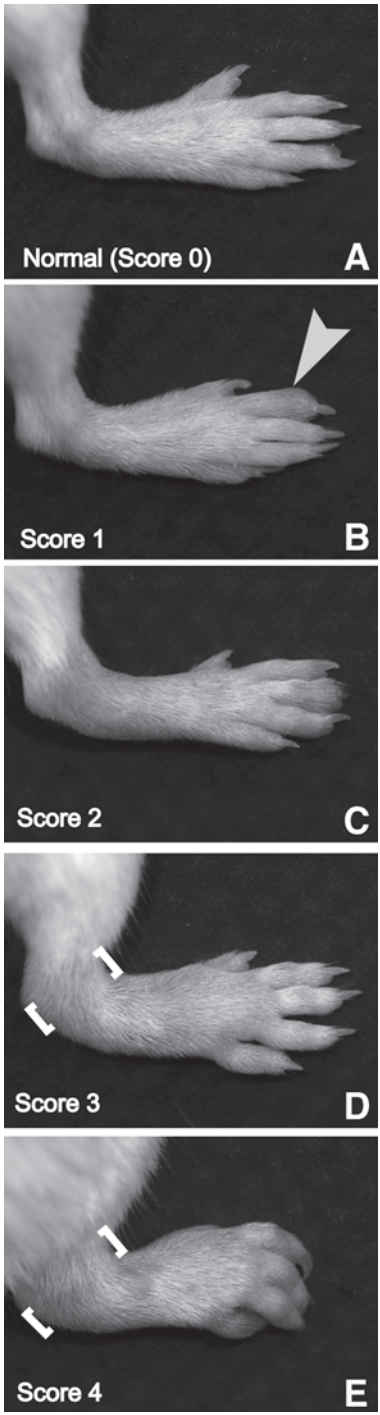

Fig. 2. Representative macroscopic images of a right hind paw before the onset of arthritis (**A**, normal) and subsequently as the disease progressed. Corresponding and representative clinical (arthritis) scores from 1 to 4 are shown in **B–D**. Arrowhead in **B** shows the inflamed second digit, whereas swollen digits 2–5 of the paw can be seen a few days later (**C**). White brackets in **D** and **E** indicate massive swelling of the ankle joints as well, and swollen and ankylotized fingers can be seen in **E**.

severity is even greater when arthritogenic PGs are given in DDA intraperitoneally. Deglycosylation of PG is still the most critical issue in revealing the arthritogenic character of a PG molecule, and no additional inbred strains, other than BALB/c or C3H, are susceptible using PG in DDA ***(20)***.

Using DDA as adjuvant, however, numerous PGs that are otherwise weakly arthritogenic when administered in FCA (e.g., bovine and sheep) almost uniformly induces severe arthritis in mice of all BALB/c and susceptible C3H colonies. On the other hand, even though immunization of susceptible BALB/c or C3H mice with mouse, rat, or chicken cartilage PGs in either FCA or DDA can provoke anti-PG immune responses, none of these cartilage PGs can induce arthritis.

Prepare a 10 mg/mL solution of DDA in PBS, heat to 50–60°C (e.g., microwave or water bath) and chill on ice. Mix the equal volume of antigen in PBS with DDA in PBS. The dose per mouse is 100 μg/PG protein in 100 μL (1 mg) DDA in PBS.

3.2.3. Assessment of Arthritis

The limbs of mice should be examined at least three times a week after the second injection of DDA, or after the third injection of Freund's adjuvants, to record abnormalities because of arthritic changes of the joints ***(10,11,20,31,33)***. The appearance of joint swelling should be recorded at the onset of arthritis. An acute clinical (arthritis) score, which is a cumulative arthritis score of the four limbs of each animal, should be determined by the same person over the entire experimental period in a blind manner.

Each paw is given a grade ranging from 0 to 4 (**Fig. 2**). Slight swelling of the paw or small joints (e.g., interphalangeal joints) is recorded as 1, whereas the maximum redness and swelling of a paw, or ankylotized joint(s), is graded as 4 (**Fig. 2**). Therefore, each mouse at each time is scored from 0 to 16 ***(11,31,33–35)***. For standard histopathological assessments of arthritis, paws can be fixed in formalin, decalcified, embedded in paraffin, sectioned, and stained as described elsewhere ***(10,11,14,15,29)***.

3.3. Measuring Immune Responses and Cytokines in PGIA

3.3.1. T-Cell Responses

Mouse spleen and joint-draining lymph node cells ($2–3 \times 10^5$/200 μL/well) can be seeded in 96-well tissue culture plates in either Dulbecco's modified Eagle's medium or RPMI-1640 supplemented with 0.5 μ*M* 2-mercaptoethanol, 1% nonessential amino acids, 1% sodium pyruvate, 100 μg/mL gentamicin, and 1% pooled normal mouse and 5–10% heat-inactivated fetal calf serum (all tissue culture grade). Cells can be cultured alone (nonstimulated cultures) or in

the presence of concanavalin A (2.5–5.0 μg/mL; positive control) or chondroitinase ABC-digested human or mouse PGs (20–50 μg protein/mL); the depletion of the CS side chains supports a more effective antigen presentation.

Antigen (PG)-specific T-cell responses are measured by interleukin (IL)-2, interferon (IFN)-γ, and IL-4 production and T-cell proliferation. T-cell proliferation is measured by a 16-h incorporation of 0.5 μCi of [^{3}H]-thymidine into the DNA using quadruplicate samples. Cells are harvested on day 5, and incorporated [^{3}H]-thymidine is determined by scintillation counter. Values are expressed either as delta count per minute (Δcpm), which is the difference of counts per minute measured in antigen-stimulated and nonstimulated cultures, or as a stimulation index (SI), which is the ratio of counts per minute measured in antigen-stimulated cell cultures relative to the counts per minute measured in nonstimulated cell cultures.

A CTLL (American Type Culture Collection, Manassas, VA) bioassay is used for measuring IL-2 production in supernatants of antigen-stimulated vs nonstimulated cultures. The same system described for T-cell proliferation is used, except that 100 μL of a 36- to 48-h culture medium is transferred to a new 96-well plate containing 1×10^5 IL-2-sensitive CTLL-2 cells/well. The use of a multichannel pipet makes the transfer process fast and accurate. Next, 24 h later, 0.5 μCi of [^{3}H]-thymidine in 10 μL medium is added to each well for 12 h, and then cells are harvested. Incorporated [^{3}H]-thymidine is counted as described above for T-cell proliferation.

IFN-γ and IL-4 production can be measured in culture supernatants using capture ELISA methods. If possible, cultures established in 48- or 24-well plates are used for cytokine assays. In a 48-well tissue culture plate, 1.5×10^6 spleen or 1×10^6 lymph node cells in 600 μL medium (with or without PG antigen) produce sufficient amounts of these cytokines, which can be measured in day 3 or 4 supernatants by ELISA ***(11,21,33)***.

To detect transforming growth factor (TGF)-β production, spleen cells should be cultured in serum-free HL-1 medium (Biowhittaker, Walkersville, MD), and then TGF-β can be measured after acid treatment of samples using a TGF-β ELISA kit (Promega, Madison, WI) ***(36)***.

In an extreme or critical case, when the antigen or cell number is limited, cytokine production and T-cell proliferation can be measured in the same culture system. In this case, 100 μL of culture supernatants are transferred on CTLL-2 cells on day 2, and the removed medium is replaced with fresh (original) medium. However, it is unnecessary to add fresh PG if the medium is partially replaced on day 2 or later. [^{3}H]-Thymidine in 10 μL medium is added to each well for 12 h on day 5. Prior to the cell harvesting, supernatants are transferred into antibody-coated ELISA plates for cytokine assays, and then cells are harvested, washed, and counted for [^{3}H]-thymidine incorporation.

Evidently, special attention should be given to using isotope-containing supernatants for ELISA.

3.3.2. Antibody Production and Antibody Isotypes

Blood samples can be collected from the retrobulbar venous plexus during immunization, or serum can be prepared at the end of the experiment. Maxisorp immunoplates (Nalgene Nunc International, Rochester, NY) do not require additional steps and bind well the negatively charged cartilage PG (*see* **Note 6**). Wells are coated with human or mouse cartilage PGs (0.1 μg protein/100 μL/well) for ELISA ***(11,35,37)***. Sera should be applied at increasing dilutions from 1:500 to 1:62,500, and the titer of isotypes of PG-specific antibodies can be determined using peroxidase-conjugated rat antimouse IgG1 or IgG2a or IgG2b secondary antibodies ***(21,37–39)***. Alternatively, total anti-PG antibodies can be measured using peroxidase-labeled antimouse IgGAM. The optimal dilution of isotype-specific second antibodies should be determined in preliminary experiments.

Serum antibody levels can be normalized to mouse IgG1 and IgG2a, or IgG3, isotype standards. The control immunoglobulin isotypes can be purchased from companies or purified from irrelevant (non-PG-specific) monoclonal antibody-containing ascites fluids by protein A/G. Serial dilutions of these standards are immobilized on the microplate's surface at linear concentrations ranging from 0.2 to 200 ng/well. Peroxidase substrate (H_2O_2) and any appropriate color reagents (*o*-phenylene diamine or 3,3',5,5'-tetramethyl benzidine) can be used for quantification of the peroxidase reaction by an ELISA plate reader.

3.3.3. Cytokines

Various cytokines (IL-1, IL-5, IL-6, IL-10, IL-12, IFN-γ, tumor necrosis factor-α, etc.) can be measured by capture ELISAs. These ELISAs are commercially available and have appropriate manufacturer's instructions and protocols. Although most of these cytokines cannot be detected in normal mouse serum, eventually all are measurable in sera of arthritic animals.

ELISA kits are very expensive. If many animals and assays are designed, the purchase of the capture and detection antibodies in a set is the most economical approach. Both capture and detection antibodies are available from either R&D Systems (Duo-Set), BD Pharmingen (BD OptEIA ELISA set), or BioSource (CytoSet Antibody Pair), but the investigator has to adopt the protocol, purchase ELISA plates, and prepare buffer solutions.

3.4. Adoptive Transfer of PGIA

T-cell homeostasis is a physiological function of the immune system that maintains a balance in the numbers and ratios of T cells at the periphery. A self-MHC/self-peptide ligand can induce weak (covert) signals via the T-cell

receptor (TCR), thus providing an extended life span for naïve T cells. A low number of T cells can repopulate the lymphoid organs, but only in syngeneic condition, which allows for recognition of a wide range of self-MHC-associated/(self)peptide ligands by matched TCRs ***(40–42)***.

Technically, the adoptive transfer of PGIA from BALB/c donors into genetically matched (both MHC and non-MHC genes) BALB/c or SCID mice can be achieved. If syngeneic BALB/c mice are used, a whole body irradiation (500 rad) is necessary, which is followed by bone marrow transplantation ***(29)***. The use of SCID mice, especially in BALB/c background, is a more ideal system for studying T-cell restoration in a T-cell-mediated autoimmune disease, such as PGIA.

Uniformly, 2×10^7 unseparated spleen cells or 1×10^7 B- or T-cell-depleted lymphocytes or in vitro-stimulated lymphocytes can be injected intraperitoneally on days 0 and 7 in transfer experiments ***(38)***. For a successful transfer, cells must be injected together with 100 μg PG on day 0, or cells should be stimulated in vitro with cartilage PG for 4 d prior to the transfer. In vitro mitogen-stimulated cells from arthritic mice do not transfer PGIA. Anti-PG antibodies or B cells alone or together do not transfer arthritis. Successful arthritis transfer requires both T and B cells.

Although the source of donor T cells (from arthritic mice) is critical, PG-specific B cells from nonarthritic animals, or from animals immunized with nonarthritogenic PG (e.g., rat chondrosarcoma), can help or support the transfer. These antigen (PG)-specific B cells are the most superior PG antigen-presenting cells (APCs) for T cells ***(14)***. These PG-specific B cells are probably the first joint homing lymphocytes, which may be activated by PG fragments released during the normal metabolic turnover of cartilage and then recruit PG-specific (arthritogenic) T cells to the joint ***(29,38,43)***.

4. Notes

1. The quality of solid guanidine hydrochloride and cesium chloride is critical. For example, if a crystal-clear 6–8 *M* guanidinium chloride solution cannot be prepared from the solid guanidine hydrochloride, do not use this solid guanidine for preparation of 4 *M* guanidine chloride.
2. The use of enzyme inhibitors is absolutely critical, and the sample should never be warmed above 10°C. The use of two to three times more protease inhibitor does not damage the molecular structure or influence the deglycosylation, but a smaller amount or stored protease inhibitors may not prevent the proteolytic degradation. PMSF and pepstatin A should be dissolved freshly in organic solvent and added dropwise to the heavily mixed sample. These protease inhibitors have a very short half-life even at 4°C, and they become inactive after a few hours.
3. Avoid freezing and thawing of cartilage samples, which lead to damage of chondrocytes. Many proteolytic enzymes are released from dead chondrocytes,

which degrade macromolecules of cartilage matrix. One of the most sensitive macromolecules is the core protein of PG, and proteolytic degradation may lead to the loss of T-cell epitopes.

4. As described in **Subheading 3.2.** for routine experiments, the use of deglycosylated crude extract of human cartilage is sufficient, convenient, and relatively inexpensive. Endo-β-galactosidase (Seikagaku) and testicular hyaluronidase (Worthington) are the least-expensive combination for deglycosylation. In this case, use endo-β-galactosidase treatment first; after 24 h digestion, adjust pH 5.8 to pH 5.0 with acetic acid, add $MgCl_2$ and NaCl, and apply the testicular hyaluronidase digestion as a last step. Typically, 1.0–1.2 mg deglycosylated, dialyzed, and lyophilized crude extract contains approx 100 μg PG core protein (a dose/injection/mouse). Some proteins in the crude extract are insoluble in PBS after deglycosylation, but this is mostly the KS-free G1 domain, which contains arthritogenic epitopes ***(5,44,45)***. Therefore, do not remove insoluble material from this final stock solution. Most of the contaminations as insoluble proteins were removed before the last dialysis.
5. Smear exhaustively the emulsion after intraperitoneal injection; otherwise, it remains in a drop and induces massive adhesion.
6. Whenever a crude extract is used for immunization, highly purified PG is also needed for testing T- and B-cell responses in vitro. The purification and chemical characterization of a relatively large quantity of cartilage PG (**Subheading 3.1.2.**) may be sufficient for years.
7. There are no real differences in the chemical compositions of neonatal and adult mouse cartilage PGs. However, the yield is different: approx 10 mg PG can be purified from the cartilage of 600–800 femoral heads (300–400 adult mice) and approx 100 mg PG from skeletal tissue of 80–120 neonatal (3- to 6-d-old) mice. However, these skeletal tissue extracts have to be purified at least three times with cesium chloride gradient centrifugation.
8. There is a common step, the 4 *M* guanidinium chloride extraction, in preparation of cartilage PG (or crude extract of cartilage) and type II collagen. Using PG for purification or immunization, the 4 *M* guanidinium chloride extract is needed; the insoluble cartilage extract, mostly containing type II collagen, is discarded. This insoluble cartilage residue can be used for type II collagen isolation after washing, pepsin digestion, and repeated sodium chloride precipitation (*see* Chapter 16). Therefore, with human cartilage (from either necropsy or from joint replacement surgery), both PG and type II collagen can be isolated, and both antigenic materials may be simultaneously available for both collagen-induced and PG-induced arthritis.
9. The protein content of the crude extract is variable. Precise measurement of the core protein content of PG aggrecan is a difficult task as this large molecule (M_r about $2–3 \times 10^6$) is extensively degraded during aging processes or especially in osteoarthritic cartilage; the type and level of degradation vary from cartilage to cartilage ***(23)***. In addition, chondrocytes of diseased cartilage synthesize aggrecan characteristic of fetal cartilage, and the size and composition of this molecule is

significantly different from that synthesized by normal adult articular chondrocytes ***(23,46)***. None of the currently available chemical (DMMB or uronic acid assay, toluidine blue or safranin-O staining) or immunological (protein or glycosaminoglycan epitope) methods is able to determine precisely the core protein content of aggrecan in diseased cartilage. With awareness of this problem, a panel of monoclonal antibodies must be used to quantify, and then correlate, aggrecan content in extracts of osteoarthritic cartilages. Methods have been fully described elsewhere ***(17,22,23,47,48)***, and monoclonal antibodies are available either from Chemicon International Limited (Temecula, CA), ICN Biochemicals (Costa Mesa, CA), or the Developmental Studies Hybridoma Bank at Johns Hopkins University School of Medicine (Baltimore, MD). In summary, and at the conclusion of a large number of assays performed and described in **Subheading 3.2.**, approx 250–300 μg of lyophilized human cartilage PG depleted of both CS and KS represent 100 μg PG core protein (100 μg PG core protein is present in approx 1.0–1.4 mg deglycosylated [testicular hyaluronidase and endo-β-galactosidase-treated] crude extract of human adult or osteoarthritic cartilage). The quality of undigested cartilage samples or purified PG can be tested in agarose-polyacrylamide composite gel electrophoresis ***(23)***. Gels can be stained directly with toluidine blue, or PGs should be transferred onto positively charged nylon membrane (Amersham, Arlington Heights, IL) and then stained with PG-specific monoclonal antibodies ***(17,22,23,47,49)***.

References

1 Glant, T., Csongor, J., and Szücs, T. (1980) Immunopathologic role of proteoglycan antigens in rheumatoid joint diseases. *Scand. J. Immunol.* **11,** 247–252.

2. Poole, A. R., Glant, T. T., and Mikecz, K. (1988) Autoimmunity to cartilage collagen and proteoglycan and the development of chronic inflammatory arthritis, in *The Control of Tissue Damage* (Glaurer, A. M., ed.), Elsevier (Biomedical Division), Amsterdam, The Netherlands, pp. 55–65.

3 Glant, T. T., Fülöp, C., Mikecz, K., Buzás, E., Molnár, G., and Erhardt, P. (1990) Proteoglycan-specific autoreactive antibodies and T-lymphocytes in experimental arthritis and human rheumatoid joint diseases. *Biochem. Soc. Trans.* **18,** 796–799.

4. Glant, T. T., Mikecz, K., Thonar, E. J. M. A., and Kuettner, K. E. (1992) Immune responses to cartilage proteoglycans in inflammatory animal models and human diseases, in *Cartilage Degradation: Basic and Clinical Aspects* (Woessner, J. F. and Howell, D. S., eds.), Dekker, New York, pp. 435–473.

5 Guerassimov, A., Zhang, Y. P., Banerjee, S., Cartman, A., Leroux, J. Y., Rosenberg, L. C., et al. (1998) Cellular immunity to the G1 domain of cartilage proteoglycan aggrecan is enhanced in patients with rheumatoid arthritis but only after removal of keratan sulfate. *Arthritis Rheum.* **41,** 1019–1025.

6 Golds, E. E., Stephen, I. B. M., Esdaile, J. M., Strawczynski, H., and Poole, A. R. (1983) Lymphocyte transformation to connective tissue antigens in adult and juvenile rheumatoid arthritis, osteoarthritis, ankylosing spondylitis, systemic

lupus erythematosus and a non-arthritic control population. *Cell. Immunol.* **82,** 196–209.

7 Li, N. L., Zhang, D. Q., Zhou, K. Y., Cartman, A., Leroux, J. Y., Poole, A. R., et al. (2000) Isolation and characteristics of autoreactive T cells specific to aggrecan G1 domain from rheumatoid arthritis patients. *Cell Res.* **10,** 39–49.

8 Mikecz, K., Glant, T. T., Baron, M., and Poole, A. R. (1988) Isolation of proteoglycan specific T-cells from patients with ankylosing spondylitis. *Cell. Immunol.* **112,** 55–63.

9. Courtenay, J. S., Dallman, M. J., Dayan, A. D., Martin, A., and Mosedale, B. (1980) Immunization against heterologous type II collagen induces arthritis in mice. *Nature* **282,** 666–668.

10 Glant, T. T., Mikecz, K., Arzoumanian, A., and Poole, A. R. (1987) Proteoglycan-induced arthritis in BALB/c mice. Clinical features and histopathology. *Arthritis Rheum.* **30,** 201–212.

11 Glant, T. T., Bárdos, T., Vermes, C., Chandrasekaran, R., Valdéz, J. C., Otto, J. M., et al. (2001) Variations in susceptibility to proteoglycan-induced arthritis and spondylitis among C3H substrains of mice. Evidence of genetically acquired resistance to autoimmune disease. *Arthritis Rheum.* **44,** 682–692.

12 Mikecz, K., Glant, T. T., and Poole, A. R. (1987) Immunity to cartilage proteoglycans in BALB/c mice with progressive polyarthritis and ankylosing spondylitis induced by injection of human cartilage proteoglycan. *Arthritis Rheum.* **30,** 306–318.

13 Glant, T. T., Buzás, E. I., Finnegan, A., Negroiu, G., Cs-Szabó, G., and Mikecz, K. (1998) Critical role of glycosaminoglycan side chains of cartilage proteoglycan (aggrecan) in antigen recognition and presentation. *J. Immunol.* **160,** 3812–3819.

14 Glant, T. T., Cs-Szabó, G., Nagase, H., Jacobs, J. J., and Mikecz, K. (1998) Progressive polyarthritis induced in BALB/c mice by aggrecan from human osteoarthritic cartilage. *Arthritis Rheum.* **41,** 1007–1018.

15. Glant, T. T., Finnegan, A., and Mikecz, K. (2003) Proteoglycan-induced arthritis: immune regulation, cellular mechanisms and genetics. *Crit. Rev. Immunol.* **23,** 199–250.

16 Roughley, P. J. and White, R. J. (1980) Age-related changes in the structure of the proteoglycan subunits from human articular cartilage. *J. Biol. Chem.* **255,** 217–224.

17 Glant, T. T., Mikecz, K., Roughley, P. J., Buzás, E., and Poole, A. R. (1986) Age-related changes in protein-related epitopes of human articular-cartilage proteoglycans. *Biochem. J.* **236,** 71–75.

18 Brennan, F. R., Negroiu, G., Buzás, E. I., Fülöp, C., Mikecz, K., and Glant, T. T. (1995) Presentation of cartilage proteoglycan to a T cell hybridoma derived from a mouse with proteoglycan-induced arthritis. *Clin. Exp. Immunol.* **100,** 104–110.

19. Glant, T. T., Fülöp, C., Cs-Szabó, G., Buzás, E. I., Ragasa, D. R., and Mikecz, K. (1995) Mapping of arthritogenic/autoimmune epitopes of cartilage aggrecans in proteoglycan-induced arthritis. *Scand. J. Rheumatol.* **24,** 43–49.

20. Hanyecz, A., Berlo, S. E., Szánto, S., Broeren, C. P. M., Mikecz, K., and Glant, T. T. (2003) Achievement of a synergistic adjuvant effect on arthritis induction by activation of innate immunity and forcing the immune response toward the Th1 phenotype. *Arthritis Rheum.* **50,** in press.
21 Otto, J. M., Chandrasekaran, R., Vermes, C., Mikecz, K., Finnegan, A., Rickert, S. E., et al. (2000) A genome scan using a novel genetic cross identifies new susceptibility loci and traits in a mouse model of rheumatoid arthritis. *J. Immunol.* **165,** 5278–5286.
22 Glant, T. T., Mikecz, K., and Poole, A. R. (1986) Monoclonal antibodies to different protein-related epitopes of human articular cartilage proteoglycans. *Biochem. J.* **234,** 31–41.
23. Cs-Szabó, G., Roughley, P. J., Plaas, A., and Glant, T. T. (1995) Large and small proteoglycans of osteoarthritic and rheumatoid articular cartilage. *Arthritis Rheum.* **38,** 660–668.
24 Hascall, V. C. and Sajdera, S. W. (1969) Protein polysaccharide complex from bovine nasal cartilage. The function of glycoprotein in the formation of aggregates. *J. Biol. Chem.* **244,** 2384–2396.
25 Witter, J., Roughley, P. J., Webber, C., Roberts, N., Keystone, E., and Poole, A. R. (1987) The immunologic detection and characterization of cartilage proteoglycan degradation products in synovial fluids of patients with arthritis. *Arthritis Rheum.* **30,** 519–529.
26 Lohmander, L. S., Neame, P. J., and Sandy, J. D. (1993) The structure of aggrecan fragments in human synovial fluid. Evidence that aggrecanase mediates cartilage degradation in inflammatory joint disease, joint injury, and osteoarthritis. *Arthritis Rheum.* **36,** 1214–1222.
27 Sajdera, S. W. and Hascall, V. C. (1969) Protein polysaccharide complex from bovine nasal cartilage. A comparison of low and high shear extraction procedures. *J. Biol. Chem.* **244,** 77–87.
28 Zhang, Y., Guerassimov, A., Leroux, J.-Y., Cartman, A., Webber, C., Lalic, R., et al. (1998) Induction of arthritis in BALB/c mice by cartilage link protein. Involvement of distinct regions recognized by T- and B lymphocytes. *Am. J. Pathol.* **153,** 1283–1291.
29 Mikecz, K., Glant, T. T., Buzás, E., and Poole, A. R. (1990) Proteoglycan-induced polyarthritis and spondylitis adoptively transferred to naive (nonimmunized) BALB/c mice. *Arthritis Rheum.* **33,** 866–876.
30 Muller, G. and Hanschke, M. (1996) Quantitative and qualitative analyses of proteoglycans in cartilage extracts by precipitation with 1,9-dimethylmethylene blue. *Connect. Tissue Res.* **33,** 243–248.
31 Mikecz, K., Brennan, F. R., Kim, J. H., and Glant, T. T. (1995) Anti-CD44 treatment abrogates tissue edema and leukocyte infiltration in murine arthritis. *Nat. Med.* **1,** 558–563.
32 Stanfield, J. P., Gall, D., and Bracken, P. M. (1973) Single-dose antenatal tetanus immunisation. *Lancet* **1,** 215–219.

33 Adarichev, V. A., Valdez, J. C., Bárdos, T., Finnegan, A., Mikecz, K., and Glant, T. T. (2003) Combined autoimmune models of arthritis reveal shared and independent qualitative (binary) and quantitative trait loci. *J. Immunol.* **170,** 2283–2292.
34. Buzás, E. I., Brennan, F. R., Mikecz, K., Garzó, M., Negroiu, G., Holló, K., et al. (1995) A proteoglycan (aggrecan)-specific T cell hybridoma induces arthritis in BALB/c mice. *J. Immunol.* **155,** 2679–2687.
35 Otto, J. M., Cs-Szabó, G., Gallagher, J., Velins, S., Mikecz, K., Buzás, E. I., et al. (1999) Identification of multiple loci linked to inflammation and autoantibody production by a genome scan of a murine model of rheumatoid arthritis. *Arthritis Rheum.* **42,** 2524–2531.
36 Bourdeau, A., Faughnan, M. E., McDonald, M. L., Paterson, A. D., Wanless, I. R., and Letarte, M. (2001) Potential role of modifier genes influencing transforming growth factor- beta1 levels in the development of vascular defects in endoglin heterozygous mice with hereditary hemorrhagic telangiectasia. *Am. J. Pathol.* **158,** 2011–2020.
37. Holló, K., Glant, T. T., Garzó, M., Finnegan, A., Mikecz, K., and Buzás, E. I. (2000) Complex pattern of Th1 and Th2 activation with a preferential increase of autoreactive Th1 cells in BALB/c mice with proteoglycan (aggrecan)-induced arthritis. *Clin. Exp. Immunol.* **120,** 167–173.
38. Bárdos, T., Mikecz, K., Finnegan, A., Zhang, J., and Glant, T. T. (2002) T and B cell recovery in arthritis adoptively transferred to SCID mice: antigen-specific activation is required for restoration of autopathogenic $CD4^+$ Th1 cells in a syngeneic system. *J. Immunol.* **168,** 6013–6021.
39 Adarichev, V. A., Bárdos, T., Christodoulou, S., Phillips, M. T., Mikecz, K., and Glant, T. T. (2002) Major histocompatibility complex controls susceptibility and dominant inheritance, but not the severity of the disease in mouse models of rheumatoid arthritis. *Immunogenetics* **54,** 184–192.
40 Mackall, C. L., Hakim, F. T., and Gress, R. E. (1997) Restoration of T-cell homeostasis after T-cell depletion. *Semin. Immunol.* **9,** 339–346.
41 Ernst, B., Lee, D. S., Chang, J. M., Sprent, J., and Surh, C. D. (1999) The peptide ligands mediating positive selection in the thymus control T cell survival and homeostatic proliferation in the periphery. *Immunity* **11,** 173–181.
42 Viret, C., Wong, F. S., and Janeway, C. A., Jr. (1999) Designing and maintaining the mature TCR repertoire: the continuum of self-peptide:self-MHC complex recognition. *Immunity* **10,** 559–568.
43. Buzás, E., Mikecz, K., Brennan, F. R., and Glant, T. T. (1994) Mediators of autopathogenic effector cells in proteoglycan-induced arthritic and clinically asymptomatic BALB/c mice. *Cell. Immunol.* **158,** 292–304.
44. Buzás, E. I., Mikecz, K., Finnegan, A., Hudecz, F., and Glant, T. T. (1999) T-cell recognition of differentially tolerated epitopes of cartilage proteoglycan (aggrecan) in arthritis. *Arthritis Rheum.* **42,** S259.
45. Zhang, Y., Guerassimov, A., Leroux, J.-Y., Cartman, A., Webber, C., Lalic, R., et al. (1997) Arthritis induced by proteoglycan aggrecan G1 domain in BALB/c

mice: the immunosuppressive influence of keratan sulfate on recognition of T- and B-cell epitopes. *Arthritis Rheum.* **40,** S56.

46 Rizkalla, G., Reiner, A., Bogoch, E., and Poole, A. R. (1992) Studies of the articular cartilage proteoglycan aggrecan in health and osteoarthritis. Evidence for molecular heterogeneity and extensive molecular changes in disease. *J. Clin. Invest.* **90,** 2268–2277.

47. Cs-Szabó, G., Melching, L. I., Roughley, P. J., and Glant, T. T. (1997) Changes in messenger RNA and protein levels of proteoglycans and link protein in human osteoarthritic cartilage samples. *Arthritis Rheum.* **40,** 1037–1045.

48. Negroiu, G., Roughley, P. J., Cs-Szabó, G., Otto, J. M., and Glant, T. T. (1996) Localization of autoimmune/arthritogenic B cell epitopes of cartilage proteoglycans (PGs) by autoreactive antibodies to mouse aggrecan. *Arthritis Rheum.* **39,** S285.

49 Poole, C. A., Glant, T. T., and Schofield, J. R. (1991) Chondrons from articular cartilage. (IV) Immunolocalization of proteoglycan epitopes in isolated canine tibial chondrons. *J. Histochem. Cytochem.* **39,** 1175–1187.

50 Trentham, D. E., Townes, A. S., and Kang, A. H. (1977) Autoimmunity to type II collagen: an experimental model of arthritis. *J. Exp. Med.* **146,** 857–868.

51. Thonar, E. J. M. A., Lenz, M. E., Maldonado, B., Otten, L., Glant, T., and Kuettner, K. E. (1990) Measurement of antigenic keratan sulfate by an enzyme-linked immunosorbent assay, in *Methods in Cartilage Research* (Maroudas, A. and Kuettner, K. E., eds.), Academic Press, London, pp. 170–172.

18

Mouse Models of Multiple Sclerosis

Experimental Autoimmune Encephalomyelitis and Theiler's Virus-Induced Demyelinating Disease

Kevin G. Fuller, Julie K. Olson, Laurence M. Howard, J. Ludovic Croxford, and Stephen D. Miller

Summary

Experimental autoimmune encephalomyelitis (EAE) and Theiler's murine encephalitis virus-induced demyelinating disease (TMEV-IDD) are two clinically relevant murine models of multiple sclerosis (MS). Like MS, both are characterized by mononuclear cell infiltrate into the central nervous system and demyelination. EAE is induced by either the administration of protein or peptide in adjuvant or by the adoptive transfer of encephalitogenic T-cell blasts into naïve recipients. The relative merits of each of these protocols are compared. Depending on the type of question asked, different mouse strains and peptides are used. Different disease courses are observed with different strains and different peptides in active EAE. These variations are addressed, and grading of mice in EAE is discussed. In addition to EAE induction, useful references for other disease indicators, such as delayed-type hypersensitivity, in vitro proliferation, and immunohistochemistry, are provided. TMEV-IDD is a useful model for understanding the potential viral etiology of MS. This chapter provides detailed information on the preparation of viral stocks and subsequent intracerebral infection of mice. In addition, virus plaque assay and disease assessment are discussed. Recombinant TMEV strains have been created for the study of molecular mimicry; these strains incorporate 30 various amino acid myelin epitopes within the leader region of TMEV.

Key Words: Active induction; adoptive transfer; EAE; emulsion; encephalitogenic; epitope spreading; experimental autoimmune encephalomyelitis; MBP; MOG; multiple sclerosis; myelin; neurodegeneration; PLP; relapsing-and-remitting; T cell blasts; Theiler's murine encephalomyelitis virus-induced demyelinating disease; TMEV-IDD; VP2; VP3.

From: *Methods in Molecular Medicine, Vol. 102: Autoimmunity: Methods and Protocols*
Edited by: A. Perl © Humana Press Inc., Totowa, NJ

1. Introduction

The mouse models of demyelinating disease have been useful in both the demonstration of T-cell-mediated demyelination and in the characterization of immune-mediated demyelinating disease. This chapter describes the methods for inducing and characterizing two models of demyelinating disease: experimental autoimmune encephalomyelitis (EAE) and Theiler's murine encephalomyelitis virus-induced demyelinating disease (TMEV-IDD).

In EAE, peripheral immunization with myelin antigen(s) results in a $CD4^+$ T-cell-mediated demyelinating disease characterized by the presence of activated T cells and macrophages in the brain and spinal cord. The pathological mechanisms observed in central nervous system (CNS) lesions of this model bear very strong similarity to that found in brain lesions of patients with MS ***(1–13)***. Oligoclonal immunoglobulin G (IgG) can be found in the CSF of both EAE mice and patients with multiple sclerosis (MS) ***(2,7,14)***, along with infiltration of T cells, macrophages, and B cells within the white matter of the CNS ***(11,15–18)***.

Discrete foci of demyelination can be observed in both EAE and MS ***(15,17,19)***, and these are associated with infiltrating immune cells ***(15,18,19)***. These infiltrating immune cells express proinflammatory cytokines, chemokines, and reactive oxygen species thought to mediate the physical destruction of myelin-sheathed nerves ***(7,15,18,19)***.

In addition, foam cell-like macrophages, containing phagocytosed hydrophobic myelin debris, have been demonstrated within active lesions ***(20–22)***. Ascending hind-limb paralysis (described in **Subheading 3.1.3.**) is associated with inflammation and demyelination of axonal tracks. Transfer of activated myelin-specific Th1 cells to naïve recipient mice alone can induce demyelinating disease, demonstrating that T cells can initiate the disease process ***(23–25)***. However, to do this, T cells must first be obtained from the lymph nodes of mice previously immunized using the active induction protocol described above ***(23,26)***.

Adoptive transfer protocols have numerous advantages over that of the active induction protocols: (a) the day of adoptive transfer serves as a definitive point of introducing encephalitogenic T cells to the recipient mice; (b) there is no antigen depot to maintain *de novo* activation of naïve T cells; (c) it is considered a more direct way of characterizing T-cell effector function in the CNS in a highly defined system; (d) it can be used to track encephalitogenic T cells in vivo and to study infiltration and to isolate antigen-specific T cells from the CNS ***(27,28)***. In the SJL mouse, both active induction and adoptive transfer of disease typically take a relapsing-and-remitting (R/R) form.

TMEV-IDD has been defined as a mouse model for human multiple sclerosis ***(29,30)***. TMEV is a natural mouse pathogen that belongs to the cardiovirus group of the Picornaviridae ***(31,32)***, and it is composed of a single, positive-strand RNA genome surrounded by a capsid containing viral protein (VP)1, VP2, and VP3. TMEV is divided into two subgroups based on the pathogenesis of the viruses. The first subgroup, which includes GDVII, is highly virulent and induces fatal encephalitis in infected mice. The second group, which is defined as the Theiler's original subgroup, includes Daniels (DA) and BeAn 8386 strains, which have low virulence and do not induce severe encephalitis, but do establish persistent infections of the CNS associated with immune-mediated demyelination ***(33)***.

TMEV-IDD is an immune-mediated demyelinating disease dependent on persistent virus infection of the macrophage/microglia cell population of the CNS ***(34,35)***. TMEV-IDD is associated with a mononuclear cell infiltrate consisting predominantly of $CD4^+$ T cells, macrophages, and B cells. The chronic phase of TMEV-IDD is mediated by a $PLP_{139–151}$-specific, $CD4^+$ Th1-type T-cell response that can be detected at approx 55 d postinfection ***(36)***. As the disease progresses, epitope spreading leads to autoimmune responses to additional myelin antigens ***(37)***. The inflammation and demyelination observed in TMEV-IDD is similar to the pathological descriptions in patients with MS ***(38,39)***. Importantly, epidemiological studies suggested a viral etiology for MS, providing additional importance for TMEV-IDD as a model for MS ***(40,41)***. Infection of SJL mice with the BeAn strain has been directly associated with the development of a chronic progressive demyelinating disease arising approx 30–35 d postinfection and characterized by spastic hind-limb paralysis and primary demyelination ***(42)***.

This chapter addresses the basic methods in inducing both active and adoptive transfer of EAE and the induction of TMEV-IDD. Although different mouse strains have various susceptibilities to both models of disease, we focus primarily on the induction in the most commonly used strain of mouse, the SJL. In addition, the induction of TMEV-IDD is described using the BeAn strain of TMEV. Mouse strain susceptibilities and variation in disease are discussed in **Subheading 4.2.**

2. Materials

2.1. Induction of Active EAE

1. SJL mice (Harlan Laboratories, Indianapolis, IN).
2. Encephalitogenic protein or peptide or spinal cord homogenate.
3. Phosphate-buffered saline (PBS).
4. *Mycobacterium tuberculosis*, H37 RA (Difco, Detroit, MI).

5. Freund's incomplete adjuvant (Bacto, Detroit, MI).
6. Three-way nylon stopcock (Luer connector) (Kontes Glass Co., Vineland, NJ) or Sorvall Omni-Mixer (Dupont Instruments, Newton, CT).
7. 5-mL snap-cap tubes (Falcon).
8. Small-animal clippers (Golden A5, Oster/Sunbeam, Boca Raton, FL).
9. 18- and 25-ga needles (Becton Dickinson, Franklin Lakes, NJ).
10. *Pertussis* toxin (List Biological Labs, Campbell, CA).
11. Carbol fuchsin dye.
12. Ear tags (Gey Band and Tag, Norristown, PA).

2.2. Adoptive Transfer of EAE

1. SJL mice (Harlan Laboratories).
2. Balanced salt solution (BSS).
3. Dulbecco's modified Eagle's medium (DMEM; Sigma, St. Louis, MO).
4. Heat-inactivated fetal calf serum (FCS, Sigma).
5. 200 m*M* L-glutamine (Sigma).
6. 5.5 m*M* β2-mercaptoethanol (Sigma).
7. 1000 U/mL penicillin, 1000 μg/mL streptomycin.
8. Light microscope and hemocytometer.
9. 75-cm^2 sterile tissue culture flasks.
10. Myelin antigen or myelin peptide.
11. 10-mL sterile pipet.
12. 100-ga sterile wire mesh and 90-mm sterile Petri dishes.
13. 3- and 10-mL syringes.
14. 25-ga needle.

2.3. Induction of TMEV-IDD

1. DMEM (Sigma).
2. FCS (Sigma).
3. Tryptose phosphate broth (Sigma).
4. Antibiotic-antimycotic (Gibco BRL, Gaithersburg, MD).
5. BHK-21 cells (American Type Culture Collection, Manassas, VA).
6. 25-, 75-, 162-cm^2 tissue culture flasks (Corning, Corning, NY).
7. Versene 1:5000 (Gibco BRL).
8. 15- and 50-mL centrifuge tubes.
9. Polyethylene glycol.
10. Tris base.
11. Sodium chloride.
12. Sodium dodecyl sulfate (SDS).
13. Sucrose.
14. 21-, 23-, and 27-ga needles.
15. Cesium sulfate (Cs_2SO_4; Sigma).
16. PBS.
17. 60-mm tissue culture dishes (Nunc, Rochester, NY).

18. Noble agar (Sigma).
19. Penicillin/streptomycin (Invitrogen, Carlsbad, CA).
20. Crystal violet (Sigma).
21. ClaI restriction enzyme (Promega, Madison, WI).
22. DH5α max efficient *Escherichia coli* (Invitrogen).
23. Sp6/T7 in vitro transcription kit (Roche, Indianapolis, IN).
24. Lipofectin reagent (Gibco BRL).
25. SJL mice (Harlan Laboratories).
26. Gentamicin (Gibco BRL).
27. [4]Isoflurane (Abbott Laboratories, Abbott Park, IL)

3. Methods

3.1. Induction of Active and Adoptive Transfer of R/REAE

3.1.1. Induction of Active R/REAE Disease

EAE can be induced in susceptible strains of mice using proteolipid protein (PLP), myelin basic protein (MBP), myelin oligodendrocyte glycoprotein (MOG), or peptides corresponding to the encephalitogenic portions of these proteins. Peptides (>98% purity based on mass spectrophotometry) or spinal cord homogenate to be used in priming are first dissolved in PBS and irradiated at 6000 rad for sterilization purposes. For peptides insoluble in PBS (pH 7.0), the pH can be increased until the peptide dissolves. The pH can then be decreased to physiological levels.

However, pH has little influence on disease induction with peptide in Freund's complete adjuvant (FCA). Peptide should be diluted in PBS to a final concentration of 2 mg/mL. An equal volume of peptide/PBS is added to FCA (4 mg/mL; desiccated *M. tuberculosis*, H37 RA in incomplete Freund's adjuvant). This is then thoroughly mixed to form a thick peptide/FCA emulsion. For small volumes, the emulsion can be prepared directly between two 1-mL tuberculin syringes using a three-way stopcock with a Luer connector. For larger volumes, the emulsion can be prepared using a mechanical mixer with the emulsion on ice. Emulsion should be removed from the mixer with a standard laboratory spatula and placed in a 5-mL snap-cap tube. The emulsion is then gently centrifuged. The emulsion should be loaded into 1-mL tuberculin syringes using an 18-ga needle, taking care not to introduce air bubbles into the syringe. The 18-ga needle is replaced with a 27-ga needle for immunization. **Table 1** provides a comprehensive list of different peptides of PLP, MBP, and MOG proteins that can be used to initiate disease in different inbred mouse strains.

The backs of animals to be primed are shaved using small animal clippers. Ideally, animals receive approx 100 μL of emulsion subcutaneously, divided equally across three sites on the dorsal flank (on each hip and one along the

Table 1
Mouse Strain and Encephalitogenic Peptides in Active EAE

Mouse strain	H-2 type	Peptide[a]	Sequence[a]	Reference
SJL	H-2^s	$MBP_{89–101}$	VHFFKNIVTPRTP	***53***
		$MBP_{84–104}$	VHFFKNIVTPRTPPPSQGKGR	***4***
		$PLP_{139–151}$[b]	HSLGKWLGHPDKF	***51,54***
		$PLP_{104–117}$	KTTICGKGLSATVT	***54***
		$PLP_{178–191}$	NTWTTCQSIAFPSK	***55***
		$PLP_{57–70}$	YEYLINVIHAFQYV	***56***
		$MOG_{92–106}$	DEGGYTCFFRDHSYQ	***57***
PL/J, B10.PL	H-2^u	$MBP_{Ac1–11}$	Ac-ASQKRPQRHG	***58***
		$PLP_{178–191}$	NTWTTCQSIAFPSK	Unpubl. (B10.PL)
		$MBP_{35–47}$	TGILDSIGRFFSG	***58***
		$PLP_{43–64}$	EKLIETYFSKNYQDYEYLINVI	***59***
(PL/J × SJL) F1	H-$2^{s/u}$	$MBP_{Ac1–11}$	Ac-ASQKRPQRHG	***58***
		$PLP_{43–64}$	EKLIETYFSKNYQDYEYLINVI	***59***
		$PLP_{139–151}$	HSLGKWLGHPDKF	***51***
C57BL/6	H-2^b	$MOG_{35–55}$	MEVGWYRSPFSRVVHLYRNGK	***60***
		$PLP_{178–191}$	NTWTTCQSIAFPSK	***61***
C3H	H-2^k	$PLP_{103–116}$	YKTTICGKGLSATV	***62***
SWR	H-2^q	$PLP_{215–232}$	PGKVCGSNLLSICKTAEF	***63***
(SJL × B10.PL) F1	H-$2^{s/q}$	$PLP_{139–151}$	HSLGKWLGHPDKF	Unpubl.
		$PLP_{178–191}$	NTWTTCQSIAFPSK	Unpubl.
		$MBP_{Ac1–11}$	Ac-ASQKRPQRHG	Unpubl.
(SJL × C3H/HeJ) F1[c]	H-$2^{s/k}$	$PLP_{190–209}$	SKTSASIGSLCADARMYGVL	***64***
		$PLP_{215–232}$	PGKVCGSNLLSICKTAEFQ	***56***
BALB/cPt[c]	H-2^d	$PLP_{178–191}$	NTWTTCQSIAFPSK	***55***
NOD	H-2^{g7}	$PLP_{48–70}$	TYFSKNYQDYEYLINIHAFQYV	***65***
		$MOG_{35–55}$	MEVGWYRSPFSRVVHLYRNGK	***66***

[a]Sequences for MBP peptides are based on different species variants of MBP that have different numbering systems; sequences for PLP peptides are based on the mouse sequence. Consult the indicated references for more detailed information.

[b]The $PLP_{139–151}$ sequence has a serine-for-cysteine substitution at position 140 to enhance solubility.

[c]The EAE observed in these mice is nonclassical. In (SJL × C3H/HeJ) F1 mice, the disease causes imbalance and axial rotatory movement (rotatory EAE). The BALB/cPt mice show lack of balance and forelimb paralysis in the absence of hind-limb paralysis.

midline of the back between the shoulders) using a 25-ga needle. As necessary, animals should be marked for grading purposes. White and light-brown mice can be marked with a red dye (carbol fuchsin). We routinely mark with large spots on the head, midback, base of tail, and left and right sides. For black mice, the tails can be marked with permanent markers (e.g., Sharpies), reapplied as necessary (one, two, three stripes, etc.), or use numbered ear tags.

3.1.2. Adoptive Transfer of R/REAE

The 8- to 12-wk-old mice are immunized as described for active induction of EAE ***(23,26)***. In some cases, such as the adoptive transfer of myelin-specific transgenic T cells and encephalitogenic T-cell lines maintained by in vitro passage, this step is not necessary. Once immunized, the mice are left for 7–14 d, as described for different models in notes. The ratio of donor mice to recipient mice varies according to how many activated cells are required from adoptive transfer. Typically, for induction of $PLP_{139–151}$-induced disease in the SJL mouse, one donor mouse for two recipient mice is usually sufficient. In the C57BL/6 model, typically the ratio is one to one. When large numbers of cells are to be transferred, higher ratios are required.

In models in which donor mice are immunized, inguinal, axillary, and brachial lymph nodes are pooled from primed mice and placed in BSS solution. Cell suspensions should be kept on ice at all times. The pooled lymph nodes are then placed onto a sterile 100-ga wire mesh in a 90-mm Petri dish. Using the plunger of a sterile 10-mL syringe, the lymph nodes are crushed to produce a single-cell suspension. The cell suspension is centrifuged at 300*g* for 5 min at 4°C in a sterile 50-mL sterile conical centrifuge tube. The pellet is resuspended in fresh BSS by vigorous manual agitation or repeated pipetting using a sterile 10-mL pipet. The cells are washed once more with BSS and again pelleted as previously described. After centrifugation, the cells are resuspended in complete culture medium (DMEM containing 10% FCS, 2 m*M* L-glutamine, 100 U/mL penicillin, 100 μg/mL streptomycin, and 50 μ*M* β2-mercaptoethanol). For each donor mouse used to obtain lymph node cells, 3 mL of culture medium are added.

Primed lymph node cells are resuspended at a final concentration of 8×10^6 cells/mL in complete DMEM medium, and 30 mL (2.4×10^8 total cells) are placed into a sterile 75-cm^2 tissue culture flask. Myelin protein or peptide antigen is added to the lymph node suspension at the concentrations indicated in **Table 2**. Cells are cultured for 3–4 d (37°C, 100% humidity, 5% CO_2) for the times indicated in **Table 2** for the various models. In transfer systems in which T-cell lines or naïve transgenic T cells (e.g., B10.PL–MBP_{Ac1-11}-specific transgenic T cells) are to be reactivated or activated, respectively, different protocols are followed and can be obtained from the relevant sources ***(43,44)***. In these systems, addition of recombinant interleukin (IL)-12 to the culture

Table 2
Summary of General Parameters for Various EAE Adoptive Transfer Models[a]

Mouse strain	Antigen specificity	Donor immunization period (days)	In vitro antigen concentration (μg/mL)	In vitro IL-12 (ng/mL)	In vitro culture time (h)	Number of blast transfers ($\times 10^6$)	Disease type	Disease severity
SJL	PLP	7–14	50–100	—	72–96	5–10	R/R	Severe
	$PLP_{139–151}$	7–14	20	—	72–96	1–5	R/R	Severe
	MBP	7–14	50–100	—	72–96	40–60	R/R	Moderate
	$MBP_{84–104}$	7–14	50	—	72–96	10–20	R/R	Moderate
C57BL/6	MBP	10–14	50–100	—	72–96	50	Monophasic/ chronic	Mild
	$MBP_{84–104}$	10–14	50	—	72–96	50	Monophasic/ chronic	Mild
	MOG	10–14	50	25	72–96	20	R/R	Moderate
	$MOG_{35–55}$	10–14	10	25	72–96	20	R/R	Moderate
B10.PL[b]	$MBP_{Ac1–11}$	—	50	10	72	1	Monophasic	Moderate
B10.S	MBP	10–11	25	20	96	35	Monophasic	Moderate
	$MBP_{87–106}$	10–11	50	20	96	35	Monophasic	Moderate

[a]These parameters have been optimized in different laboratories as previously described: SJL protocol parameters from **refs. *26, 27, and 67–73***; C57BL/6 protocol parameters from **refs. *60* and *74–77***; B10.PL protocol parameters from **ref. *43***; and B10.S protocol parameters from ***44***.

[b]Note that the B10.PL system employs T-cell receptor transgenic donors, which do not require in vivo priming, only in vitro culture with MBPAc1–11 peptide and recombinant IL-12.

medium is sometimes required for efficient induction of clinical disease in naïve recipient mice. In some cases, neutralizing antibody to IL-4 has also been used ***(43)***.

After 3 to 4 d of in vitro culture, the cells are resuspended by repeated pipetting and are pelleted in a 50-mL conical tube. Cells are washed twice with BSS and resuspended in approx 10 mL of BSS for each 30 mL tissue culture volume. This blast preparation consists mainly of $CD4^+$ T cells. If required, $CD8^+$ T cells and any remaining B cells and macrophages can be depleted using magnetic bead separation techniques or other standard depletion methods.

The number of viable T-cell blasts are determined using a hemocytometer. Both the total numbers of cells and the total numbers of T-cell blasts are determined. Unstimulated T cells appear small, quite regular in shape, and with a cytoplasm relatively clear, compared to the large, often irregular, and granular appearance of T-cell blasts. Typically, in the SJL transfer system, blasts account for 30–40% of total cells. In other systems, the percentage may be lower; in transgenic systems, it may be higher. Cells are resuspended at a concentration of 2×10^6 to 1.2×10^8 T-cell blasts/mL in BSS, depending on the adoptive transfer system and the number of blasts transferred.

The T-cell blasts, derived above, can be injected into naïve syngeneic recipients either intraperitoneally or intravenously to induce effective clinical disease. However, intravenous injection is typically more effective, with clinical disease developing faster than delivery via intraperitoneal injection. Usually, the required numbers of cells are injected in a volume of 0.25–0.5 mL using a disposable 1-mL tuberculin syringe and a 25-ga or 27-ga needle.

3.1.3. Clinical Grading of Active and Adoptively Transferred EAE

Following priming, mice should be monitored every other day for the development of disease. The appearance of EAE disease induced by active immunization varies considerably based on mouse strain and peptide used. For most strains and peptides, disease appears between the second and fourth weeks following priming. The disease is characterized by an ascending hind-limb paralysis that begins in the tail and spreads to involve the hind limbs and forelimbs. The disease is graded on a 0-to-5 scale. Depending on strain and peptide, mice do not always reach the higher disease grades before disease resolution or disease plateau.

Grade 0: There is no observable difference from naïve animals.
Grade 1: This grade is assigned to mice that have lost tail tonicity or show hind-limb weakness (but not both). Loss of tail tonicity is judged in mice that, when held aloft by the base of the tail, show sagging of the tail, and the tail cannot be lifted. In addition, the tip of the tail fails to curl. Hind-limb weakness is defined by the objective criterion that, when placed on the wire screen of the cage, the

animal's legs fall through the screen as it tries to walk. A waddling gait can also be observed as the animal walks on a flat surface. The rear limbs are splayed, and the rear posture is lowered.

Grade 2: This grade is assigned to mice that present both a limp tail and show hind-limb weakness as defined in grade 1.

Grade 3: This assignment is given to mice that show partial hind-limb paralysis, defined as the ability of a mouse to move one or both hind limbs to some extent, but not maintain posture or walk.

Grade 4: This grade is assigned to mice that cannot move their hind limbs. The animal moves only by dragging itself with its front limbs. A spastic paralysis and atrophy of the hind limbs and lower body are often observed at this point. Mice at this stage are given food (that can be moistened) on the cage floor, bottles with long sipper tubes, and daily injections of subcutaneous saline to prevent death by dehydration.

Grade 5: This grade is assigned to the most severe end-stage assessment of EAE. These mice show a complete inability to move because of paralysis in all limbs. In addition, any animals that consistently show high grades and die ("death by EAE") should be given a grade of 5. Mice that reach this stage and are moribund with EAE should be sacrificed for humane reasons.

Histopathologically, the disease is characterized by a $CD4^+$ T-cell and F4/80^+ (macrophage) inflammatory cell infiltrate that tends to be found in both diffuse and focal patterns. In most EAE models, the pattern of infiltrate tends to concentrate in the thoracic section of the spinal cord, with less involvement in other regions of the cord or the brain.

3.1.4. Clinical Disease Course

The first clinical episode is referred to as acute-phase disease, which is preceded by pronounced weight loss. Mice will experience this acute episode for variable times, depending on whether the disease is R/R, monophasic, or chronic/progressive in nature. The point at which disease reaches its highest score is referred to as the peak of acute disease. After the initial episode or a subsequent relapse, some strains of mice experience a recovery (remission). If the recovery lasts for at least 2 d and drops by at least one grade level, the recovery is deemed an authentic remission. These recoveries are observed in mice that show R/R (SJL) and monophasic disease (B10.PL) profiles. Mice that remit from the initial disease episode and recover fully or stabilize at a reduced disease score are referred to as monophasic (e.g., B10.PL primed with $MBP_{Ac1\text{-}11}$). Mice that have an acute disease that never shows a full grade reduction in disease are said to experience a chronic disease. This chronic disease is characterized by sustained antigen-specific T-cell responses to the priming antigen (e.g., C57BL/6 following $MOG_{35–55}$ priming).

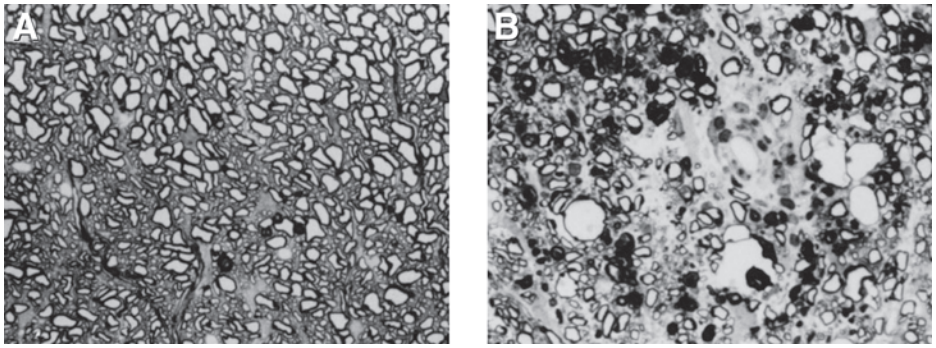

Fig. 1. Histopathological evaluation of 1-μm thick, Epon-embedded spinal cord sections. **(A)** Spinal cord section from a normal mouse. Note the presence of profuse and evenly distributed ringed structures that reflect myelinated axons with no infiltrating immune cells. **(B)** Spinal cord section from an SJL mouse with severe EAE. Note the few and unevenly distributed myelinated axonal ringed structures with large bare areas, along with large numbers of infiltrating immune cells throughout the section, which appear as dense and dark spots. Magnification ×220.

In adoptive transfer, clinical disease is evaluated using the same scale as for actively induced EAE. The type of disease, day of onset, and peak severity of disease depend on the system used. Onset to peak disease is rapid, necessitating daily evaluation of mouse clinical signs. Results are typically presented as mean clinical score of mouse groups plus or minus the standard error of the mean. Other critical measures include mean day of onset, mean peak score, mean day of remission, and relapse (the last two are relevant to R/R disease). Typically, mice reach peak disease within 1–2 d after disease onset and remain at peak disease longer than in the active EAE induction (average 5 vs 3 d). Disease incidence is normally greater than 90%. Clinical disease may also be evaluated using a terminal evaluation of histopathology in which fixed, Epon-embedded sections of spinal cord are stained with toluidine blue as described in **ref. *13*** (**Fig. 1**).

3.2. Induction of TMEV-IDD

3.2.1. TMEV Infecting Stock

Virus is produced in BHK-21 cells. BHK-21 cells are grown in DMEM supplemented with 10% FCS, 0.295% tryptose phosphate broth, 1.0% gentamicin, and 1% antimycotic-antibiotic. Cells are maintained in culture at 37°C

and 5% CO_2 and grown to confluency. BHK-21 cells are removed from the flask by rinsing with versene (1:5000), resuspended in complete medium, and seeded (1:10 split) in a new flask. These BHK-21 cells are grown to confluency (2–3 d), and washed with DMEM without serum or supplements.

Medium is removed from the cells, and TMEV, BeAn 8386 strain, is added at a multiplicity of infection of 5 in a minimal volume of serum-free medium, ensuring that the cell monolayer is covered with medium. The infected cells are incubated at room temperature for 1 h with intermittent rocking of the culture flask. After the 1-h incubation, DMEM with 2% FCS is added to the flask at the appropriate volume. The flasks are incubated at 33°C and 5% CO_2 until the cells are lysed (detached from plate surface), usually within 24 h.

The medium is removed from the flask, and the cell debris is pelleted by centrifugation. The cell lysate is removed and stored on ice, leaving a small volume on top of the pelleted cells. The pelleted cells are then sonicated using brief pulses to lyse the cells completely, and the resulting cell debris is again pelleted by centrifugation. The lysate is added to the stored lysate collected from the first spin, and this is aliquoted into small volumes and stored at –70°C. The titer of the infecting virus stock is determined by plaque assay (as described in **Subheading 3.3.3.**).

3.2.2. Purification of TMEV

Virus is produced in large stocks as described in **Subheading 3.2.2.** until the point of removing the supernatant from the infected cells. The supernatant is removed from the infected cells, and the pH is adjusted with HCl to a pH below 7.0. The supernatant is frozen in bottles at –20°C. The bottles are thawed in a 37°C shaking water bath without allowing the supernatant to become too warm.

To each 500 mL of lysate, 14.5 g NaCl and 30 g polyethylene glycol are added, and the lysate is stirred overnight at 4°C. The precipitated lysate is centrifuged at 5000*g* in a Sorvall HB-4 swinging bucket rotor for 45 min at 4°C. The supernatant is discarded, and the pellet is immediately resuspended in 18 mL hypertonic TNE buffer (0.02 *M* Tris base, 0.5 *M* NaCl, 0.002 *M* EDTA).

The resuspended pellets are sonicated to separate the virus from cellular debris and DNA. The sonicates are pooled, warmed, and incubated with 1 mL 10% SDS for each 9 mL of resuspended pellets for 30 min at 37°C. The lysate is then centrifuged to remove any membranous debris. The supernatant is transferred to clear ultracentrifuge tubes and overlaid onto 22 mL of a 35% sucrose solution. The virus is pelleted through the sucrose by centrifuging in a SW28 rotor at 72,128*g* (SW28 rotor at 20,000 rpm) for 20 h at room temperature.

Following the centrifugation, the pellet is resuspended in 2 mL hypertonic TNE buffer and sonicated to remove clumps. The virus solution is then incubated with 0.1 mL 10% SDS for each 1 mL solution for at least 10 min at 37°C to remove the remaining membranous fractions. The virus solution is then clarified by centrifugation and 2–3 mL of the resulting supernatant overlaid on 20–70% sucrose gradients in clear centrifuge tubes. The gradients are centrifuged at 35,000 rpm for 3 h at room temperature. Following the centrifugation, a blue band containing the virus is visible by ultraviolet or halogen light about 2–3 cm from the bottom of the tube. The virus-containing band is collected by puncturing the side of the tube using a syringe fitted with a 21-ga needle. The bands are pooled in new tubes up to a maximum volume of 1.5 mL per tube, and 2.2 mL of 1 g/mL Cs_2SO_4 solution is then added to each tube. The tubes are filled with hypotonic TNE buffer, mixed thoroughly, and centrifuged at 144,000*g* for 22 h at 4°C in a 50Ti rotor.

The following day, the virus, contained in a white band about 1 cm from the bottom of the tube, is collected using a syringe fitted with a 23-ga needle. The virus-containing bands are pooled in a new centrifuge tube (2–3 mL per tube), and the tubes are then filled with hypotonic TNE buffer, mixed, and centrifuged at 110,000*g* for 3 h at 5°C. After the centrifugation, the virus pellet is resuspended in 0.2 mL PBS and incubated for 24 h at 4°C. To increase virus yields, sonication of the suspension will help separate virus particles and remove virus adhering to the tube wall. Quantitate the virus by measuring the average absorbance at wavelength 280 cps A_{280} and determine amount of virus using the following equation:

$$\text{Average } A_{280} \times (10/35) = \text{mg virus}$$

Purity is assessed by SDS polyacrylamide gel electrophoresis.

3.2.3. TMEV Plaque Assay

BHK-21 cells are cultured in 35-mm culture dishes to confluency as described in **Subheading 3.2.1.** The BHK-21 cells are washed twice with serum-free DMEM. Dilutions of the virus stock or tissue homogenate are made in serum-free DMEM, and 0.5 mL of each dilution is added to the BHK-21 cells in duplicate. The cells are incubated at room temperature for 1 h with occasional rocking of the dishes. Meanwhile, a 2% solution of noble agar is autoclaved and maintained at 55°C. A 1:1 solution of the 2% noble agar and 2X DMEM supplemented with 2% FCS and 2% penicillin/streptomycin is then prepared.

After the 1-h incubation, 6 mL of the 1:1 agar:DMEM solution is added to each culture dish. The cells are then incubated at 33°C and 5% CO_2 for 5–6 d. The agar is removed from the dish with a lab spatula, and the cells are fixed

with methanol and stained with a crystal violet solution (0.8 g crystal violet, 100 mL ethanol, 400 mL H_2O) for 5 min. The plate is then rinsed in a dish with water to remove the excess stain. Plaques are counted, and the number of plaque-forming units (PFUs) is calculated based on the dilution and volume added to each culture dish.

3.2.4. Construction of TMEV Containing Molecular Mimics of Myelin Peptides

The complementary DNA (cDNA) for the BeAn genome has been inserted into pGEM plasmid for molecular manipulations. A ClaI restriction enzyme site was inserted into the leader sequence of the BeAn genome along with a deletion of 23 amino acids. Molecular mimic sequences for myelin epitopes as described in **ref. *45*** are inserted into the ClaI restriction site. Polymerase chain reaction mutagenesis was conducted to insert ClaI sites flanking the sequence into the virus genome. The mimic sequences are 30 amino acids long to restore the deletion in the leader protein. The mimic sequence is ligated into the ClaI site in the BeAn cDNA, and DH5α *E. coli* are transformed with the ligated product to produce a BeAn cDNA containing the mimic sequence in the correct orientation.

Next, in vitro transcription of the BeAn cDNA containing the mimic sequence is driven by an upstream T7 promoter using an Sp6/T7 in vitro transcription kit. This produces a single positive-stranded RNA. The resulting RNA is transfected into BHK-21 cells in a 60-mm culture dish with DMEM supplemented with 2% FBS using lipofectin reagent as described by the manufacturer's protocol. The transfected cells are incubated overnight at 33°C. Following the incubation, the medium is removed from the cells, replaced with DMEM containing 2% serum, and incubated for an additional 2–3 d at 33°C until the cells begin to lyse, indicating virus production.

Virus is isolated from the cells following the procedure described in **Subheading 3.2.1.**. The virus is amplified beginning with very small volumes until the virus titer reaches 10^4 PFU/mL. Larger volumes can be used to produce recombinant virus for infecting stocks. The viral titer of the recombinant viruses is determined by plaque assay as described in **Subheading 3.2.3.**

3.2.5. Induction of TMEV-IDD

Female SJL mice 6–7 wk old are anesthetized with aerosolized isoflurane and inoculated with either 3×10^7 PFU of wild-type TMEV (BeAn 8386 strain) infecting stock (produced as described in **Subheading 3.2.1.**) or recombinant mimic-expressing viruses (produced as described in **Subheading 3.2.4.**) in 30 μL in the right cerebral hemisphere by free-hand injection with a 27-ga needle. Mice are marked to allow for individual evaluation of clinical and histological disease.

3.2.6. Clinical Assessment of TMEV-IDD

The clinical disease presentation seen in susceptible mouse strains, such as SJL, depends on the strain of TMEV used for infection. Following inoculation with the brain-derived DA strain of virus, mice first develop a flaccid paralysis. Mice recover in approx 2 wk, indicating that this phase of disease is self-limiting. However, 2–3 wk after infection, mice then develop a spastic paresis of the hind limbs, which in SJL mice has a chronic disease course, resulting in severe spastic paralysis ***(42)***.

In contrast, infection of SJL mice with the tissue culture-adapted BeAn 8386 strain does not produce clinical evidence of a first-phase disease. Infected mice begin to show signs of clinical disease between 30 and 40 d post-TMEV infection and develop a chronic, progressive paralysis with no recovery or remitting episodes, similar to primary progressive MS. Unlike EAE, clinical signs develop slowly, with no drastic changes in gait from day to day. Mice are monitored for disease progression two to three times per week, continuing until 100 d post-infection. Each mouse is assigned a numerical score between 0 and 5 based on the severity of their impairment: 0, asymptomatic; 1, mild gait abnormalities; 2, severe gait abnormalities; 3, loss of ability to right self associated with mild spastic paralysis; 4, spastic paralysis in both hind limbs combined with urinary incontinence and dehydration; 5, moribund.

Infection with recombinant TMEV containing different molecular mimic sequences leads to different disease profiles, depending on the epitope expressed. Mice infected with the leader deletion recombinant virus ΔClaI-BeAn do not develop signs of demyelinating autoimmune disease ***(45)***. In contrast, mice infected with the recombinant PLP139-BeAn virus exhibit earlier onset and more severe clinical disease, with onset between days 7 and 10 post-infection ***(45)***.

3.2.7. Immunological Aspects of TMEV-IDD

Numerous immunological assays can be performed to determine the specificity, class, and timing of immune system involvement in disease pathology following TMEV infection. Support for a $CD4^+$ T-cell-mediated pathogenesis of TMEV-IDD derives from studies showing that susceptibility strongly correlates with the development of chronic high levels of TMEV- and myelin-specific delayed-type hypersensitivity (DTH) reactions. DTH to TMEV capsid epitopes in BeAn-infected, susceptible SJL mice develop within 5–10 d postinfection, preceding the appearance of clinical signs. These levels remain high for at least 100 d postinfection ***(46)***. VP2 contains the immunodominant Th1 determinant in TMEV-infected SJL mice as 80–90% of the DTH response is directed against this virion protein ***(47)***.

The immunodominant myelin epitope in SJL mice is $PLP_{139–151}$, and responses to this self-antigen are first observed around 45–50 d postinfection (i.e., 2–3 wk after clinical disease onset) ***(37)***. As disease progresses, epitope spreading occurs in a hierarchical order, with intramolecular spreading to $PLP_{178–191}$ and $PLP_{56–70}$ and intermolecular epitope spreading to $MOG_{92–106}$ and $MBP_{84–104}$ occurring during the chronic late phase of TMEV-IDD by day 100 postinfection ***(36,37)***. These responses can be detected by both DTH and splenic T-cell proliferative responses.

$PLP_{139–151}$ responses can be detected between days 10 and 14 following infection with PLP139-BeAn ***(45)***. This is in contrast to wild-type TMEV-infected mice, for which myelin responses arise by day 50 postinfection. In addition, there is evidence for epitope spreading of myelin epitopes $PLP_{178–191}$ in PLP139-BeAn-infected mice ***(45,48)***.

In addition, cytokines play an important role in TMEV-IDD. The release of the proinflammatory cytokines interferon-γ and lymphotoxin (LT)/tumor necrosis factor-β by both viral and myelin-specific Th1 cells in the CNS leads to the recruitment and activation of monocytes and macrophages, which cause myelin destruction by a terminal nonspecific *bystander* mechanism ***(39)***. These cytokines can be quantitated using enzyme-linked immunosorbent assay, enzyme-linked immunospot, and other cytokine measures.

In conclusion, following TMEV infection of the CNS, bystander damage to myelin is initiated by virus-specific $CD4^+$ Th1 cells, which leads to the release, processing, and presentation of myelin autoantigens by CNS antigen-presenting cells (APCs). This presentation to autoreactive T cells leads, via epitope spreading, to an autoimmune response directed against CNS myelin, which perpetuates chronic clinical pathology.

4. Notes

1. General Considerations on the Induction of EAE and TMEV-ID: These protocols have been developed by numerous laboratories, with some variation between each protocol. Variation in optimal culture conditions and immunization conditions are apparent. As such, it is important for each laboratory to optimize the culture system for their environment and reagents. Thus, listed concentrations may need to be adjusted.
2. Mouse Strains Used in Active and Adoptive Transfer of EAE (Tables 1 and 2): **Susceptible strains:** Varieties of mouse strains are used to study EAE. The most common are SJL, B10.PL, C57BL/6, C3H, SWR, and the F1 progeny of several of these parental strains. The importance of pertussis toxin and the type of disease course (chronic vs R/R) for each of these strains is discussed in **Note 3**. **Table 1** describes the haplotype and reported encephalitogenic peptides for each of these susceptible strains.

Resistant strains: Although many mouse strains are useful in the study of EAE, not all mouse strains are susceptible to EAE induction. For instance, A/J, C3H/HeJ, AKR, NZW, and DBA/2 appear to be resistant to EAE after priming with known myelin antigens *(49)*.

3. For efficient disease induction in some strains, administration of pertussis toxin is required on days surrounding peptide priming. For this, 200 ng (200 μL of a 1 μg/mL stock in PBS) is administered intraperitoneally on the day of priming and again the following day. Pertussis should be dissolved at least 24 h prior to use to prevent death associated with administration of fresh pertussis. Pertussis toxin is required to initiate EAE in C57BL/6 and B10.PL mice and their F1 progeny, as well as (SJL × BALB/c) F1 mouse strains. Efficient disease induction in SJL mice requires the use of pertussis toxin only with certain neuroantigens (e.g., intact MBP and $MPB_{84–104}$).
4. In addition to induction of disease and clinical disease, several other techniques have been used to assay the presence and persistence of T-cell responses (and, importantly, antigen-specific responses) following the development of EAE. These include DTH ***(50)***, proliferation assay ***(51)***, immunohistochemistry ***(52)***, and histopathology (**Fig. 1**). Complete descriptions of these techniques can be found in the respective citations.
5. The disease course and immune reactivity described in these methods relate to the BeAn strain of TMEV. The DA strain also induces a demyelinating disease with some differences in clinical disease and different immune reactivities. In addition, the GDVII strain of TMEV induces a lethal encephalitis and thus does not result in a late-onset demyelinating disease.
   The mouse strain described in these methods is the SJL mouse, which is susceptible to BeAn strain TMEV-IDD. C57/BL6 are resistant to BeAn strain TMEV-IDD. BALB/c have varying susceptibility to TMEV-IDD, depending on the substrain, with BALB/cAnNCr mildly susceptible and BALB/cByJ resistant to TMEV-IDD.

References

1 Brown, A., MFCArlin, D. E., and Raine, C. S. (1982) Chronologic neuropathology of relapsing experimental allergic encephalomyelitis in the mouse. *Lab. Invest.* **46,** 171–185.
2 Karcher, D., Lassmann, H., Lowenthal, A., Kitz, K., and Wisniewski, H. M. (1982) Antibodies-restricted heterogeneity in serum and cerebrospinal fluid of chronic relapsing experimental allergic encephalomyelitis. *J. Neuroimmunol.* **2,** 93–106.
3 Lassmann, H. (1983) Chronic relapsing experimental allergic encephalomyelitis: its value as an experimental model for multiple sclerosis. *J. Neurol.* **229,** 207–220.
4 Tan, L. J., Kennedy, M. K., and Miller, S. D. (1992) Regulation of the effector stages of experimental autoimmune encephalomyelitis via neuroantigen-specific tolerance induction. II. Fine specificity of effector T cell inhibition. *J. Immunol.* **148,** 2748–2755.

5 Eng, L. F., Ghirnikar, R. S., and Lee, Y. L. (1996) Inflammation in EAE: role of chemokine/cytokine expression by resident and infiltrating cells. *Neurochem. Res.* **21,** 511–525.
6 Miller, S. D. and Karpus, W. J. (1994) The immunopathogenesis and regulation of T-cell mediated demyelinating diseases. *Immunol. Today* **15,** 356–361.
7. Williams, K. C., Ulvestad, E., and Hickey, W. F. (1994) Immunology of multiple sclerosis. *Clin. Neurosci.* **2,** 229–245.
8 Lublin, F. D. (1985) Relapsing experimental allergic encephalomyelitis. An autoimmune model of multiple sclerosis. *Springer Semin. Immunopathol.* **8,** 197–208.
9 Arnason, B. G. (1983) Relevance of experimental allergic encephalomyelitis to multiple sclerosis. *Neurol. Clin.* **1,** 765–782.
10 Lassmann, H. and Wisniewski, H. M. (1979) Chronic relapsing experimental allergic encephalomyelitis: clinicopathological comparison with multiple sclerosis. *Arch. Neurol.* **36,** 490–497.
11 Traugott, U., Stone, S. H., and Raine, C. S. (1979) Chronic relapsing experimental allergic encephalomyelitis. Correlation of circulating lymphocyte fluctuations with disease activity in suppressed and unsuppressed animals. *J. Neurol. Sci.* **41,** 17–29.
12 Raine, C. S., Barnett, L. B., Brown, A., Behar, T., and MFCArlin, D. E. (1980) Neuropathology of experimental allergic encephalomyelitis in inbred strains of mice. *Lab. Invest.* **43,** 150–157.
13 Dal Canto, M. C., Melvold, R. W., Kim, B. S., and Miller, S. D. (1995) Two models of multiple sclerosis: experimental allergic encephalomyelitis (EAE) and Theiler's murine encephalomyelitis virus (TMEV) infection—a pathological and immunological comparison. *Microsc. Res. Tech.* **32,** 215–229.
14. Colover, J. (1988) Immunological and cytological studies of autoimmune demyelination and multiple sclerosis. *Brain, Behav. and Immun.* **2,** 341–345.
15 Traugott, U., MFCArlin, D. E., and Raine, C. S. (1986) Immunopathology of the lesion in chronic relapsing experimental autoimmune encephalomyelitis in the mouse. *Cell. Immunol.* **99,** 395–410.
16 Boyle, E. A. and McGeer, P. L. (1990) Cellular immune response in multiple sclerosis plaques. *Am. J. Pathol.* **137,** 575–584.
17 McCallum, K., Esiri, M. M., Tourtellotte, W. W., and Booss, J. (1987) T cell subsets in multiple sclerosis. Gradients at plaque borders and differences in nonplaque regions. *Brain* **110,** 1297–1308.
18 Renno, T., Krakowski, M., Piccirillo, C., Lin, J. Y., and Owens, T. (1995) TNF-alpha expression by resident microglia and infiltrating leukocytes in the central nervous system of mice with experimental allergic encephalomyelitis. Regulation by Th1 cytokines. *J. Immunol.* **154,** 944–953.
19 Swanborg, R. H. (1995) Experimental autoimmune encephalomyelitis in rodents as a model for human demyelinating disease. *Clin. Immunol. Immunopathol.* **77,** 4–13.
20 Epstein, L. G., Prineas, J. W., and Raine, C. S. (1983) Attachment of myelin to coated pits on macrophages in experimental allergic encephalomyelitis. *J. Neurol. Sci.* **61,** 341–348.

21 Smith, M. E. (1993) Phagocytosis of myelin by microglia in vitro. *J. Neurosci. Res.* **35,** 480–487.
22 Sommer, M. A., Forno, L. S., and Smith, M. E. (1992) EAE cerebrospinal fluid augments in vitro phagocytosis and metabolism of CNS myelin by macrophages. *J. Neurosci. Res.* **32,** 384–394.
23 Cross, A. H. and Raine, C. S. (1990) Serial adoptive transfer of murine experimental allergic encephalomyelitis: successful transfer is dependent on active disease in the donor. *J. Neuroimmunol.* **28,** 27–37.
24 Raine, C. S., Mokhtarian, F., and MFCArlin, D. E. (1984) Adoptively transferred chronic relapsing experimental autoimmune encephalomyelitis in the mouse. Neuropathologic analysis. *Lab. Invest.* **51,** 534–546.
25 Zamvil, S., Nelson, P., Trotter, J., Mitchell, D., Knobler, R., Fritz, R., et al. (1985) T-cell clones specific for myelin basic protein induce chronic relapsing paralysis and demyelination. *Nature* **317,** 355–358.
26 McRae, B. L., Kennedy, M. K., Tan, L. J., Dal Canto, M. C., and Miller, S. D. (1992) Induction of active and adoptive chronic-relapsing experimental autoimmune encephalomyelitis (EAE) using an encephalitogenic epitope of proteolipid protein. *J. Neuroimmunol.* **38,** 229–240.
27 Kim, C. and Tse, H. Y. (1993) Adoptive transfer of murine experimental autoimmune encephalomyelitis in SJL.Thy-1 congenic mouse strains. *J. Neuroimmunol.* **46,** 129–136.
28 Howard, L. M. and Miller, S. D. (2001) Autoimmune intervention by CD154 blockade prevents T cell retention and effector function in the target organ. *J. Immunol.* **166,** 1547–1553.
29. Lipton, H. L., Miller, S. D., Melvold, R., and Fujinami, R. S. (1986). Theiler's murine encephalomyelitis virus (TMEV) infection in mice as a model for MS, in *Concepts in Viral Pathogenesis II* (Notkins, A. L. and Oldstone, M. B. A., eds.), Springer-Verlag, New York, pp. 248–254.
30. Miller, S. D. (1995) Pathogenesis of Theiler's murine encephalomyelitis virus-induced demyelinating disease—a model of multiple sclerosis. *ACLAD Newslett.* **16,** 4–6.
31 Pevear, D. C., Borkowski, J., Luo, M., and Lipton, H. (1988) Sequence comparison of a highly virulent and a less virulent strain of Theiler's virus. Amino acid differences on a three- dimensional model identify the location of possible immunogenic sites. *Ann. NY Acad. Sci.* **540,** 652–653.
32 Pevear, D. C., Calenoff, M., Rozhon, E., and Lipton, H. L. (1987) Analysis of the complete nucleotide sequence of the picornavirus Theiler's murine encephalomyelitis virus indicates that it is closely related to cardioviruses. *J. Virol.* **61,** 1507–1516.
33 Lipton, H. L. (1980) Persistent Theiler's murine encephalomyelitis virus infection in mice depends on plaque size. *J. Gen. Virol.* **46,** 169–177.
34 Clatch, R. J., Miller, S. D., Metzner, R., Dal Canto, M. C., and Lipton, H. L. (1990) Monocytes/macrophages isolated from the mouse central nervous system contain infectious Theiler's murine encephalomyelitis virus (TMEV). *Virology* **176,** 244–254.

35 Peterson, J. D., Karpus, W. J., Clatch, R. J., and Miller, S. D. (1993) Split tolerance of Th1 and Th2 cells in tolerance to Theiler's murine encephalomyelitis virus. *Eur. J. Immunol.* **23,** 46–55.

36 Katz-Levy, Y., Neville, K. L., Padilla, J., Rahbe, S. M., Begolka, W. S., Girvin, A. M., et al. (2000) Temporal development of autoreactive Th1 responses and endogenous antigen presentation of self myelin epitopes by CNS-resident APCs in Theiler's virus-infected mice. *J. Immunol.* **165,** 5304–5314.

37 Miller, S. D., Vanderlugt, C. L., Begolka, W. S., Pao, W., Yauch, R. L., Neville, K. L., et al. (1997) Persistent infection with Theiler's virus leads to CNS autoimmunity via epitope spreading. *Nat. Med.* **3,** 1133–1136.

38 Prineas, J. (1975) Pathology of the early lesion in multiple sclerosis. *Hum. Pathol.* **6,** 531–554.

39 Dal Canto, M. C. and Lipton, H. L. (1975) Primary demyelination in Theiler's virus infection. An ultrastructural study. *Lab. Invest.* **33,** 626–637.

40 Nathanson, N. and Miller, A. (1978) Epidemiology of multiple sclerosis: critique of evidence for a viral etiology. *Am. J. Epidemiol.* **107,** 451–461.

41. Kurtzke, J. F. (1997). The epidemiology of multiple sclerosis, in *Multiple Sclerosis: Clinical and Pathogenetic Basis* (Raine C. S. and MFCArlin, H. F. T. W. W., eds.), Chapman and Hall, London, pp. 91–139.

42 Lipton, H. L. (1975) Theiler's virus infection in mice: an unusual biphasic disease process leading to demyelination. *Infect. Immun.* **11,** 1147–1155.

43 Walker, M. R. and Mannie, M. D. (2002) Acquisition of functional MHC class II/peptide complexes by T cells during thymic development and CNS-directed pathogenesis. *Cell Immunol.* **218,** 13–25.

44 Segal, B. M. and Shevach, E. M. (1996) IL-12 unmasks latent autoimmune disease in resistant mice. *J. Exp. Med.* **184,** 771–775.

45 Olson, J. K., Croxford, J. L., Calenoff, M., Dal Canto, M. C., and Miller, S. D. (2001) A virus-induced molecular mimicry model of multiple sclerosis. *J. Clin. Invest.* **108,** 311–318.

46 Clatch, R. J., Lipton, H. L., and Miller, S. D. (1986) Characterization of Theiler's murine encephalomyelitis virus (TMEV)-specific delayed-type hypersensitivity responses in TMEV-induced demyelinating disease: correlation with clinical signs. *J. Immunol.* **136,** 920–927.

47 Gerety, S. J., Clatch, R. J., Lipton, H. L., Goswami, R. G., Rundell, M. K., and Miller, S. D. (1991) Class II-restricted T cell responses in Theiler's murine encephalomyelitis virus-induced demyelinating disease. IV. Identification of an immunodominant T cell determinant on the N- terminal end of the VP2 capsid protein in susceptible SJL/J mice. *J. Immunol.* **146,** 2401–2408.

48 Miller, S. D., Olson, J. K., and Croxford, J. L. (2001) Multiple pathways to induction of virus-induced autoimmune demyelination: lessons from Theiler's virus infection. *J. Autoimmun.* **16,** 219–227.

49 Duong, T. T., Finkelman, F. D., Singh, B., and Strejan, G. H. (1994) Effect of anti-interferon-gamma monoclonal antibody treatment on the development of experi-

mental allergic encephalomyelitis in resistant mouse strains. *J. Neuroimmunol.* **53,** 101–107.

50 Zamvil, S. S. and Steinman, L. (1990) The T lymphocyte in experimental allergic encephalomyelitis. *Annu. Rev. Immunol.* **8,** 579–621.

51 McRae, B. L., Vanderlugt, C. L., Dal Canto, M. C., and Miller, S. D. (1995) Functional evidence for epitope spreading in the relapsing pathology of experimental autoimmune encephalomyelitis. *J. Exp. Med.* **182,** 75–85.

52 Begolka, W. S., Vanderlugt, C. L., Rahbe, S. M., and Miller, S. D. (1998) Differential expression of inflammatory cytokines parallels progression of central nervous system pathology in two clinically distinct models of multiple sclerosis. *J. Immunol.* **161,** 4437–4446.

53 Sakai, K., Zamvil, S. S., Mitchell, D. J., Lim, M., Rothbard, J. B., and Steinman, L. (1988) Characterization of a major encephalitogenic T cell epitope in SJL/J mice with synthetic oligopeptides of myelin basic protein. *J. Neuroimmunol.* **19,** 21–32.

54. Tuohy, V. K. and Thomas, D. M. (1993) A third encephalitogenic determinant of myelin proteolipid protein (PLP) for SJL/J mice. *J. Immunol.* **150,** 194A.

55 Greer, J. M., Kuchroo, V. K., Sobel, R. A., and Lees, M. J. (1992) Identification and characterization of a second encephalitogenic determinant of myelin proteolipid protein (residues 178–191) for SJL mice. *J. Immunol.* **149,** 783–788.

56 Greer, J. M., Sobel, R. A., Sette, A., Southwood, S., Lees, M. B., and Kuchroo, V. K. (1996) Immunogenic and encephalitogenic epitope clusters of myelin proteolipid protein. *J. Immunol.* **156,** 371–379.

57 Amor, S., Groome, N., Linington, C., Morris, M. M., Dornmair, K., Gardinier, M. V., et al. (1994) Identification of epitopes of myelin oligodendrocyte glycoprotein for the induction of experimental allergic encephalomyelitis in SJL and Biozzi AB/H mice. *J. Immunol.* **153,** 4349–4356.

58 Zamvil, S. S., Mitchell, D. J., Moore, A. C., Kitamura, K., Steinman, L., and Rothbard, J. B. (1986) T-cell epitope of the autoantigen myelin basic protein that induces encephalomyelitis. *Nature* **324,** 258–260.

59 Whitham, R. H., Jones, R. E., Hashim, G. A., Hoy, C. M., Wang, R. Y., Vandenbark, A. A., et al. (1991) Location of a new encephalitogenic epitope (residues 43 to 64) in proteolipid protein that induces relapsing experimental autoimmune encephalomyelitis in PL/J and (SJL × PL)F1 mice. *J. Immunol.* **147,** 3803–3808.

60 Mendel, I., Kerlero, D. R., and Ben-Nun, A. (1995) A myelin oligodendrocyte glycoprotein peptide induces typical chronic experimental autoimmune encephalomyelitis in H-2b mice: fine specificity and T cell receptor V beta expression of encephalitogenic T cells. *Eur. J. Immunol.* **25,** 1951–1959.

61 Tompkins, S. M., Padilla, J., Dal Canto, M. C., Ting, J. P., Van Kaer, L., and Miller, S. D. (2002) *De novo* central nervous system processing of myelin antigen is required for the initiation of experimental autoimmune encephalomyelitis. *J. Immunol.* **168,** 4173–4183.

62 Tuohy, V. K., Lu, Z. J., Sobel, R. A., Laursen, R. A., and Lees, M. B. (1988) A synthetic peptide from myelin proteolipid protein induces experimental allergic encephalomyelitis. *J. Immunol.* **141,** 1126–1130.
63. Endoh, M., Kunishita, T., Nihei, J., Nishizawa, M., and Tabira, T. (1990) Susceptibility to proteolipid apoprotein and its encephalitogenic determinants in mice. *Int. Arch. Allergy Appl. Immunol.* **92,** 433–438.
64 Muller, D. M., Pender, M. P., and Greer, J. M. (2000) A neuropathological analysis of experimental autoimmune encephalomyelitis with predominant brain stem and cerebellar involvement and differences between active and passive induction. *Acta Neuropathol. (Berl.)* **100,** 174–182.
65 Maron, R., Hancock, W. W., Slavin, A., Hattori, M., Kuchroo, V., and Weiner, H. L. (1999) Genetic susceptibility or resistance to autoimmune encephalomyelitis in MHC congenic mice is associated with differential production of pro- and anti-inflammatory cytokines. *Int. Immunol.* **11,** 1573–1580.
66 Slavin, A., Ewing, C., Liu, J., Ichikawa, M., Slavin, J., and Bernard, C. C. (1998) Induction of a multiple sclerosis-like disease in mice with an immunodominant epitope of myelin oligodendrocyte glycoprotein. *Autoimmunity* **28,** 109–120.
67 Miller, S. D., Tan, L. J., Kennedy, M. K., and Dal Canto, M. C. (1991) Specific immunoregulation of the induction and effector stages of relapsing EAE via neuroantigen-specific tolerance induction. *Ann. NY Acad. Sci.* **636,** 79–94.
68 Tuohy, V. K. and Thomas, D. M. (1995) Sequence 104-117 of myelin proteolipid protein is a cryptic encephalitogenic T cell determinant for SJL/J mice. *J. Neuroimmunol.* **56,** 161–170.
69 Skundric, D. S., Kim, C., Tse, H. Y., and Raine, C. S. (1993) Homing of T cells to the central nervous system throughout the course of relapsing experimental autoimmune encephalomyelitis in Thy-1 congenic mice. *J. Neuroimmunol.* **46,** 113–121.
70 Fritz, R. B. and Zhao, M. L. (1994) Encephalitogenicity of myelin basic protein exon-2 peptide in mice. *J. Neuroimmunol.* **51,** 1–6.
71 Segal, B. M., Raine, C. S., MFCArlin, D. E., Voskuhl, R. R., and MFCArland, H. F. (1994) Experimental allergic encephalomyelitis induced by the peptide encoded by exon 2 of the MBP gene, a peptide implicated in remyelination. *J. Neuroimmunol.* **51,** 7–19.
72 Pettinelli, C. B. and MFCArlin, D. E. (1981) Adoptive transfer of experimental allergic encephalomyelitis in SJL/J mice after in vitro activation of lymph node cells by myelin basic protein: requirement for Lyt 1^+ $2^($ T lymphocytes. *J. Immunol.* **127,** 1420–1423.
73. Pettinelli, C. B., Fritz, R. B., Chou, C. H. J., and MFCArlin, D. E. (1982) Encephalitogenic activity of guinea pig myelin basic protein in the SJL mouse. *J. Immunol.* **129,** 1209–1211.
74 Shaw, M. K., Kim, C., Hao, H. W., Chen, F., and Tse, H. Y. (1996) Induction of myelin basic protein-specific experimental autoimmune encephalomyelitis in C57BL/6 mice: mapping of T cell epitopes and T cell receptor V beta gene segment usage. *J. Neurosci. Res.* **45,** 690–699.

75 Clark, R. B., Grunnet, M., and Lingenheld, E. G. (1997) Adoptively transferred EAE in mice bearing the *lpr* mutation. *Clin. Immunol. Immunopathol.* **85,** 315–319.
76 Mendel, I. and Shevach, E. M. (2002) Differentiated Th1 autoreactive effector cells can induce experimental autoimmune encephalomyelitis in the absence of IL-12 and CD40/CD40L interactions. *J. Neuroimmunol.* **122,** 65–73.
77. Segal, B. M., Dwyer, B. K., and Shevach, E. M. (1998) An interleukin (IL)-10/IL-12 immunoregulatory circuit controls susceptibility to autoimmune disease. *J. Exp. Med.* **187,** 537–546.

19

Experimental Autoimmune Encephalomyelitis

Praveen Rao and Benjamin M. Segal

Summary

Experimental autoimmune encephalomyelitis (EAE) is an inflammatory demyleinating disease of the central nervous system that is induced in laboratory animals by the generation of an immune response against myelin epitopes. It has been used as a prototype of Th1-driven, organ-specific autoimmunity and as a model for the human disease multiple sclerosis. This chapter describes two classic protocols for EAE induction (active immunization and adoptive transfer). **Subheading 3.3.** describes methods for rating clinical disease in symptomatic animals. **Subheading 3.4.** includes instructions for the isolation of mononuclear cells from the inflamed spinal cords from mice with EAE.

Key Words: Active immunization; adoptive transfer; experimental autoimmune encephalomyelitis; myelin basic protein; myelin oligodendrocyte glycoprotein; proteolipid protein.

1. Introduction

Experimental autoimmune encephalomyelitis (EAE) is an inflammatory disease of the central nervous system (CNS) that is induced in laboratory animals via the generation of an autoimmune response against the myelin sheath, an insulating covering around nerve fibers. The typical clinical course is an ascending paralysis that correlates with inflammation and tissue damage in the thoracolumbar regions of the spinal cord, although the optic nerves and brain (particularly the subpial white matter and brain stem) are also frequently affected ***(1)***. The classic pathological features of EAE are (a) perivascular inflammatory infiltrates (composed of lymphocytes, macrophages, and activated microglia) and (b) adjacent areas of demyelination, characterized by destruction of myelin with relative preservation of axons. However, there is growing evidence for early axonal transection as well, which might actually correlate more strongly with long-term disability ***(2,3)***.

From: *Methods in Molecular Medicine, Vol. 102: Autoimmunity: Methods and Protocols*
Edited by: A. Perl © Humana Press Inc., Totowa, NJ

EAE is widely used as an animal model of multiple sclerosis (MS) because of the striking clinical and histopathological similarities shared by the animal and human diseases. Indeed, many recent advances in MS therapeutics, including the introduction of glatiramer acetate and antibodies against very later antigen (VLA)-4, arose from EAE studies ***(4–7)***. However, beyond its usefulness as a model of MS, EAE is arguably the best-defined experimental model of Th1-driven, organ-specific autoimmunity. Many principles initially observed in EAE have been extended to other models of autoimmune disease, with tissue targets as diverse as the joints (collagen-induced arthritis), uvea, thyroid, and bowel. For example, the roles of $CD4^+$ effector T cells and interleukin (IL)-12p40 monokines during the induction phase, now recognized as critical in all of the above models, were initially worked out in EAE ***(8–17)***.

In early versions of the EAE model, disease was induced using subpial white matter homogenate, myelin extracts, or whole myelin proteins (such as myelin basic protein [MBP], proteolipid protein [PLP], and myelin oligodendrocyte glycoprotein [MOG]) as the immunogen. A wide spectrum of mammals were found to be susceptible, including mice, rats, pigs, and nonhuman primates ***(18)***. However, as the model has evolved, it has become common practice to induce the disease in well-defined inbred mouse strains by targeting single major histocompatibility complex (MHC) class II-restricted myelin epitopes. A list of the most popular EAE-susceptible murine strains and corresponding encephalitogenic peptides is provided in **Table 1.**

From a practical standpoint, murine EAE holds many advantages. With most of the current protocols, the disease is induced with a high degree of incidence (80–100%) and reproducibility. Unlike other models of autoimmune disease, which take months to become manifest, clinical signs begin within 5–16 d of induction. Furthermore, different clinical courses simulating various subcategories of multiple sclerosis can be triggered based on the particular strain and autoantigen employed. For example, SJL mice immunized with a peptide of proteolipid protein ($PLP_{139–151}$) or injected with $PLP_{139–151}$-specific T cells exhibit a relapsing–remitting course reminiscent of the most common form of MS. By contrast, C57BL/6 mice actively immunized against a peptide of MOG ($MOG_{35–55}$) develop a progressive form of EAE characteristic of later stages of MS.

EAE in the mouse can be triggered either by active immunization or by the adoptive transfer of myelin-specific $CD4^+$ T-cell lines. Both protocols are described in detail in the following sections. This is followed by a description of a clinical scale used to rate mice with EAE based on the severity of their neurological deficits. From an immunological standpoint, the encephalitogenic T-cell response has traditionally been measured by subjecting draining lymph node cells and/or splenocytes to standard T-cell assays, such as thymi-

Table 1
Peptides Used to Induce EAE in Susceptible Mouse Strains

Mouse strain	Protein	Peptide	Reference
SJL	PLP	139–151	***20***
	MBP	89–101	***21***
	MBP	84–104	***22***
C57 BL6	MOG	92–106	***23***
B10.PL	MBP	35–47	***24***
	PLP	43–64	***25***
	MBP	Ac 1–11	***26***
SWR	PLP	215–232	***27***
C3H	PLP	103–116	***28***

dine incorporation and interferon-γ/IL-2 enzyme-linked immunosorbent assays or enzyme-linked immunospots. In **Subheading 3.4.**, we concentrate on methods more specific to the EAE model, namely, the isolation and analysis of CNS-infiltrating leukocytes.

2. Materials

2.1. Active Immunization

1. Freund's complete adjuvant (FCA) with killed *Mycobacterium tuberculosis* H37Ra at 4 mg/mL. Supplement standard FCA (Difco, Detroit, MI; containing 1 mg/mL *M. tuberculosis*) or Freund's incomplete adjuvant (FIA; containing no bacterial products) with desiccated *M. tuberculosis* H37Ra (also available from Difco) to reach the desired concentration.
2. Synthetic myelin peptides (*see* **Tables 1** and **2**), at 90% or greater high-performance liquid chromatographic purity are obtained in lyophilized form, dissolved in phosphate-buffered saline (PBS) at high concentration, sterile filtered, and stored at –80°C.
3. PBS.
4. 1-, 5-, or 10-cc glass syringes.
5. Plastic stopcock.
6. 1-mL plastic syringes.
7. 25- and 27-ga needles.
8. Avertin, for which stock solution (50X) is prepared by dissolving 2,2,2-tribromoethanol (Sigma, St. Louis, MO) in tertiary amyl alcohol (5g/6.5 mL). Store at –20°C in 0.5- to 1-mL aliquots.
9. Pertussis toxin (salt free; List Biological Laboratories, San Jose, CA); sold as a lyophilized powder. Reconstitute with PBS to a final concentration of 2 μg/mL and store at 4°C.

Table 2
Sequences of Encephalitogenic Peptides Used to Induce EAE in Mouse

Peptide[a]	Sequence
PLP 43–64	EKLIETYFSKNYQDYEYLINVI
PLP 103–116	YKTTICGKGLSATV
PLP 139–151[b]	HSLGKWLGHPDKF
PLP 215–232	PGKVCGSNLLSICKTAEF
MBP Ac 1–11	Ac-ASQKRPSQRHG
MBP 89–101	VHFFKNIVTPRTP
MBP 84–104	VHFFKNIVTPRTPPPSQGKGR
MBP 35–47	TGILDSIGRFFSG
MOG 92–106	DEGGYTCFFRDHSYQ

[a]References are provided in **Table 1**.
[b]To increase solubility, the synthetic peptide differs from the native sequence by the substitution of serine for cysteine at position 140.

10. 8- to 12-wk-old female mice (the most commonly used strains are SJL, C57BL/6, and B10.PL). Mice should be housed under specific pathogen-free conditions with routine testing of sentinels for infections, including mouse hepatitis virus.
11. 2-mm ear punch (Roboz, Gaithersburg, MD).

Peptides should be sterile filtered following resuspension. PBS, syringes, stopcock, and needles must be sterile.

2.2. Lymph Node Cell Culture for Passive Transfer

1. Tissue culture media (TCM) consisting of the following ingredients (all ingredients should be stored at 4°C except for penicillin/streptomycin and fetal bovine serum, both of which should be stored at –20°C):
   - 500 mL RPMI-1640 with L-glutamine (Gibco BRL, Carlsbad, CA).
   - Fetal bovine serum (Gibco BRL), heat denatured at 58°C for 45 min and filter sterilized prior to use. Add 100 mL.
   - 2-Mercaptoethanol (Sigma); prepare stock at 5×10^{-5} *M*. Add 1 mL.
   - 100 m*M* sodium pyruvate (Gibco BRL). Add 10 mL.
   - 10 m*M* nonessential amino acid solution (Gibco BRL). Add 10 mL.
   - Penicillin/streptomycin solution (10,000 U penicillin and 10 mg streptomycin/mL; Gibco BRL). Add 10 mL.
   - 1 *M* HEPES (Gibco BRL). Add 12.5 mL.
2. Sterile Hank's balanced salt solution (HBSS).
3. Sterile disposable nylon 70-μm cell strainers (BD Falcon, Millville, NJ).
4. 50-mL conical polypropylene centrifuge tubes.

5. Trypan blue.
6. Hematocytometer.
7. 24-well plates treated for tissue culture.
8. Synthetic myelin peptide (Macromolecular Resources, Fort Collins, CO; *see* **Tables 1** and **2**).

2.3. Spinal Cord Harvest and Isolation of CNS Mononuclear Cells

1. Peristaltic pump (cat. no. 54856-075, VWR Scientific, West Chester, PA).
2. Collagenase (Worthington Biochemical Corp., Lakewood, NJ); prepare stock solution of 8 mg/mL in HBSS or RPMI-1640. Store 5-mL aliquots at –80°C.
3. DNAse I (Sigma); prepare stock solution of 20 mg/mL in PBS. Store 1-mL aliquots at –20°C.
4. Percoll (Amersham, Piscataway, NJ). Store at 4°C.
5. Sterile 15- and 50-mL polypropylene tubes.

3. Methods

There are two basic approaches for induction of EAE: active immunization and passive transfer. In active immunization, the entire disease process, from autoreactive T-cell priming to CNS infiltration and demyelination, takes place in the same animal. Depending on the mouse strain and myelin epitope, it is sometimes necessary to inject the recipient with pertussis toxin to attain a high rate of incidence and to synchronize the course between experimental subjects. (The mechanism of action of pertussis toxin is unknown, but it is widely believed that it acts by increasing the permeability of the blood–brain barrier, thereby expediting migration of effector cells into the brain and spinal cord ***(19)***.

Adoptive transfer allows the separation of the induction and effector phase, which might be advantageous depending on the experimental question posed. Myelin peptide-primed lymph node cells are reactivated with antigen in vitro for 96 h prior to disease transfer. The in vitro stimulation step is critical for successful disease transfer. Presumably, it allows the selective expansion of myelin-reactive T cells and/or their terminal differentiation into encephalitogenic effector cells.

3.1. Induction of EAE by Active Immunization

1. Estimate the amount of peptide and FCA needed: Irrespective of the specific model, we find that immunization of mice with 100 μg of myelin peptide in 100 μL of an emulsion with FCA is sufficient for the reproducible induction of EAE at high incidence. Therefore, the total amount of peptide needed in micrograms equals $100 \times n$, where n is the number of mice to be immunized. Dilute the appropriate amount of peptide (from stock solution) with sterile PBS to a final concentration of 2 μg/μL. To prepare the emulsion, FCA is mixed with aqueous peptide solution in equal parts (v/v). The final volume (in microliters) needed of FCA as well as peptide solution is $50n$.

2. Prepare the emulsion: Mix FCA and peptide solution by repetitive passage between two glass syringes connected by a stopcock. The syringes should be partly submerged in ice. At periodic intervals, test the emulsion by placing a drop in a Petri dish containing PBS. If the droplet breaks up and comes apart, continue mixing. If, on the other hand, the droplet remains intact, the emulsion is ready for injection. Generally, 10–15 min of mixing is sufficient.
3. Load plastic syringes with emulsion: Pump all of the emulsion into one of the glass syringes. Remove the empty glass syringe from the stopcock and replace it with a plastic 1-cc syringe. Slowly transfer emulsion to the plastic syringe. Repeat until all of the emulsion is dispensed into plastic syringes.
4. Anesthetize mice: Dilute stock solution of Avertin in sterile PBS (200 μL into 10 mL, respectively), vortex, and heat to 56°C prior to use. Inject intraperitoneally at a dose of 250 mg/kg mouse body weight (or approx 0.33 mL for a mouse weighing 20 g) using a 27-ga needle. Periodically assess the mouse's level of consciousness by toe pinch. The animal is properly anesthetized when it fails to withdraw the limb. Mice should be anesthetized within several minutes of the injection.
5. Immunize mice: Subcutaneously inject a total of 0.1 cc of emulsion per mouse in its back. Distribute the immunogen equally among four sites over the flanks.
6. Administer pertussis toxin systemically: Inject pertussis toxin intraperitoneally or intravenously (300 ng in 0.1 mL PBS per mouse) on days 0 and 2 postimmunization.
7. Identify mice by ear punch.
8. Score mice: Monitor mice on a daily basis starting on day 7 for development of neurological deficits (*see* **Subheading 3.3.** for details).

3.2. Induction of EAE by Passive Transfer (Fig. 1)

1. Immunize donor mice as described in **Subheading 3.1.**, but do not inject pertussis toxin.
2. Sacrifice mice between days 10 and 16 postimmunization.
3. Harvest draining lymph nodes (four axillary and two inguinal) under aseptic conditions and place in HBSS.
4. Prepare a single-cell suspension by pressing the lymph node cells through a cell strainer or mesh screen with a plunger from a sterile 3- or 5-mL syringe. We use disposable nylon 70-μm cell strainers, which fit over a 50-mL conical tube. (Alternatively, use a 100-mesh screen from Fisher. Clean and flame sterilize the screen prior to each use.) During the preparation of the suspension, periodically douse the strainer with 1- to 2-mL aliquots of sterile HBSS to wash adherent cells through to the 50-mL conical tube. Remove debris and connective tissue with sterile forceps as they accumulate on the screen.
5. Once the single-cell suspension is finished, centrifuge the 50-mL tube at 300*g* at 4°C for 7 min.
6. Resuspend the pellet in 20 mL fresh HBSS and spin cells again. Repeat for two washes.

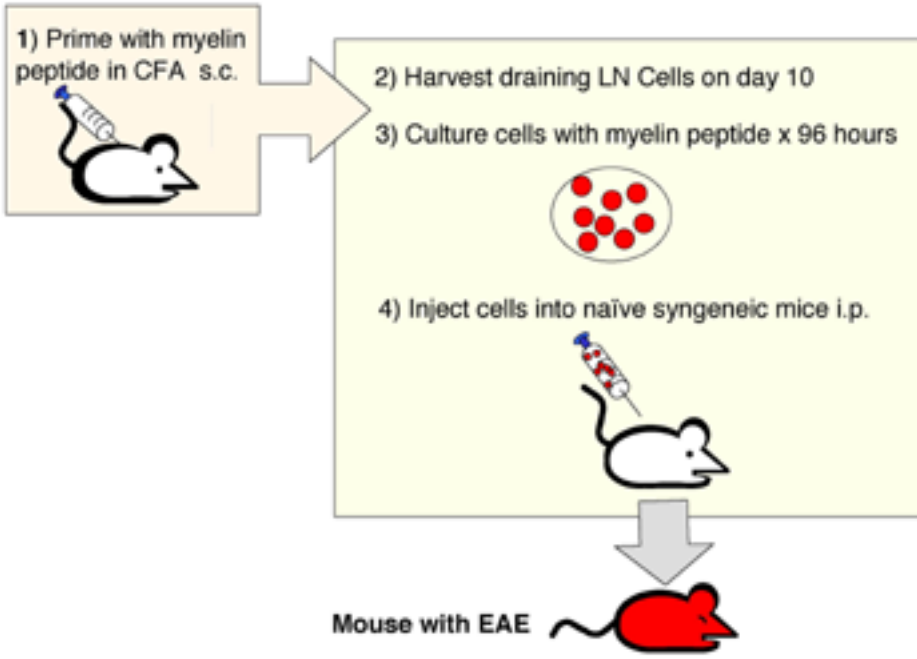

Fig. 1. Diagrammatic illustration of the adoptive transfer protocol (described in **Subheading 3.2.**).

7. Count viable cells with a hematocytometer using trypan blue exclusion. Expected yield is 50–70 × 10^6 cells/mouse.
8. Resuspend cells in TCM and dilute to a final concentration of 4 × 10^6 cells/mL. Add myelin peptide at a concentration of 50 μg/mL.
9. Transfer cell suspension to 24-well plates in 2-mL aliquots per well. Incubate at 37°C in a 7.5% CO_2 tissue culture incubator.
10. After 96 h of culture, collect the cells in 50-mL tubes with a sterile transfer pipet. Centrifuge at 300*g* for 12 min. Discard supernatants and resuspend each pellet in a relatively small volume of HBSS. Pool cell suspensions together. Centrifuge again and wash with HBSS twice.
11. Count viable cells by trypan blue exclusion. Cell yield will be 60–80% of the cells at the start of the culture.
12. Spin cells and resuspend the pellet with PBS to a final concentration of 25 × 10^6 cells/0.1 cc.
13. Inject 0.2 cc of cell suspension per mouse intraperitoneally or intravenously using a 1-cc plastic syringe attached to a 25-ga needle.
14. Examine mice on a daily basis starting on day 5 and score for degree of neurological impairment (*see* **Subheading 3.3.**). Animals generally develop clinical signs between days 5 and 8 after cell transfer.

3.3. Clinical Assessment of Mice With EAE

1. Observe the mouse as it ambulates on a smooth surface.
2. If there is no obvious limb paresis, hold the mouse by the scruff of the neck and note whether it spontaneously raises its tail. If the tail does not move or is only lifted transiently, assess its tone by flicking gently with your index finger.
3. Next, while holding the tail between thumb and index finger, flip the animal on its back and time how long it takes to assume an upright position. A healthy mouse will turn itself over immediately. A delay suggests hind-limb weakness.
4. Place the mouse on a wire cage top or metal grid and observe as it crosses from one side to the other. Pay particular attention to whether the hind limbs slip between the bars.
5. Score according to the following 5-point scale:
   0: Healthy mouse. No signs of neurological dysfunction.
   1: Limp tail only. The tail remains flaccid when the mouse is picked up.
   2: Hind-limb paresis, but without frank leg dragging. The mouse fails the backflip test and has a waddling gait. When placed on a wire cage top, the mouse frequently slips, with one or more limbs falling in between the bars.
   3: Partial hind-limb weakness with one or both hind limbs dragging, but some movement preserved.
   4: Complete hind-limb paralysis (depicted in **Fig. 2**).
   5: Moribund. The mouse is paralyzed in both hind limbs and possibly one forelimb. Inevitably, there is weight loss. Breathing appears labored.

3.4. Isolation of Mononuclear Cells From Inflamed Spinal Cords

1. Anesthetize mice with Avertin as described in **Subheading 3.1.**, but at double the dose (500 mg/kg).
2. Perfuse mice with PBS by the intracardiac route using a peristaltic pump set to low flow and low speed.
3. Remove the entire spinal column by gross dissection.
4. Fill a 10-cc syringe with PBS and attach an 18-ga needle to the tip.
5. Hold the spinal column with forceps and insert the 18-ga needle at the caudal end.
6. Eject the spinal cord into a Petri dish filled with HBSS by applying steady pressure on the plunger.
7. Prepare an "enzyme cocktail" composed of 5 mL collagenase stock solution, 1 mL DNAse I, and 14 mL HBSS.
8. Transfer the spinal cords to a Petri dish filled with the enzyme cocktail and mince into small sections with a scalpel.
9. Incubate the dish at 37°C for 45–60 min.
10. Draw the digested material up and down through a large-bore needle several times to dissociate the CNS cells further into a cell suspension.
11. Prepare a 30/70% Percoll gradient in 15 mL polystyrene tubes (with 4 mL of each phase per tube). Carefully overlay the cell suspension (4–5 mL suspension per tube).

Fig. 2. Photograph of a mouse with EAE. The arrow points to a female SJL mouse 15 d after injection with 50×10^6 $PLP_{139–151}$ reactive T cells (according to the protocol described in **Subheading 3.2.**) At this point, the mouse had reached a clinical score of 4 (*see* **Subheading 3.3.**). Neurological signs initially presented as a flaccid tail on day 10 after cell transfer and then evolved into hind-limb paralysis. A naïve, healthy littermate is shown for the sake of comparison.

12. Centrifuge at 1085*g* for 20 min at room temperature with the brake disengaged.
13. Collect cells from the 30/70% interface and transfer to a 50-mL tube containing HBSS with 5% fetal bovine serum.
14. Centrifuge at 575*g* at 4°C for 10 min.
15. Resuspend the pellet in 10 mL HBSS and transfer to a 15-mL tube.
16. Centrifuge at 322*g* at 4°C for 7 min.
17. Decant the supernatant and resuspend cells in 1–2 mL TCM.
18. Count viable cells by trypan blue exclusion. The cell yield depends on the particular EAE model and the stage of disease at which mice are sacrificed. However, a reasonable estimate is 5×10^5 cells/cord (range 3–7 $\times 10^5$ cells/cord).
19. Isolated cells can now be used for various studies, including flow cytometric analysis, RNA extraction for reverse transcriptase polymerase chain reaction and enzyme-linked immunospot assays.

4. Notes

4.1. Immunization

1. Peptides should be sterile filtered following resuspension in PBS prior to storage. PBS, syringes, stopcock, and needles must be sterile as well.
2. Prepare 10–25% more emulsion than actually required as some volume is lost to dead space in the syringe tips and needles. In addition, material is inevitably lost during the course of mixing and transferring.
3. Vortex FCA rigorously before adding it to the glass syringe. Mycobacterial particles settle to the bottom of the tube during storage.
4. Attempt to remove air bubbles before mixing the emulsion by tapping on the side of the glass syringe after the FCA and peptide solution has been added to the barrel. Air bubbles can hamper the emulsification process.
5. In the case of SJL mice immunized against $PLP_{139–151}$, injection of pertussis toxin is not absolutely necessary for disease induction. Mice will still succumb to EAE, although at a slightly lower incidence (70–80% as opposed to 90–100%) and in a less-synchronized manner.

4.2. Adoptive Transfer

6. Mix cells gently immediately before they are transferred to the syringe for in vivo injection. This will help ensure that a uniform number of cells are injected per mouse.
7. Cells should be injected slowly to prevent lysis. Prior to withdrawal, leave the needle in for several seconds after the cells are dispensed. This will help minimize leakage.
8. When designing experiments, be aware of the fact that 20–40% of the cells from the start will be lost by the end of the 96-h culture. This is because of the death of T cells that are not specific for the myelin antigen as well as the turnover of other (non-T-) cell types.
9. If you want to avoid introducing mycobacterial products in the donor mice, it is possible to generate encephalitogenic T cells from mice that are immunized with myelin antigen in FIAincomplete Freund's adjuvant by adding recombinant IL-12 to the culture (10 pg/mL).

4.3. Clinical Scoring

10. The clinical scale described in **Subheading 3.3.** is appropriate for mice that experience the most common course of EAE, namely, ascending paralysis. This course correlates with predominant spinal cord pathology. Occasionally, a mouse will develop a cerebellar lesion, manifested by a tilt in its posture and/or gait. We rate an animal with such a deficit as a 3 (because there is an obvious neurological sign, immediately apparent, but not severe enough to interfere with essential activities). As the disease progresses, the mouse may continually lie on its side, unable to assume an upright stance, or might even exhibit repetitive rolling. Such a mouse is rated a 4 or 5 regarding whether breathing and/or body weight are affected.

11. Our practice is to sacrifice mice before they progress to a score of 5.
12. In addition to rating neurological deficits, some investigators weigh mice on a daily basis and use weight loss as a "surrogate marker" of EAE.

4.4. Isolation of Mononuclear Cells From Inflamed Spinal Cords

13. The enzyme cocktail can be made slightly in advance and kept on ice. It should be warmed at 37°C immediately prior to use.
14. Percoll solutions should be kept at room temperature.
15. HBSS without calcium and magnesium is preferred for washing as this is believed to result in higher cell yields.

References

1 Raine, C. S., Barnett, L. B., Brown, A., Behar, T., and MFCArlin, D. E. (1980) Neuropathology of experimental allergic encephalomyelitis in inbred strains of mice. *Lab. Invest.* **43,** 150–157.

2 Trapp, B. D., Peterson, J., Ransohoff, R. M., Rudick, R., Mork, S., and Bo, L. (1998) Axonal transection in the lesions of multiple sclerosis. *N. Engl. J. Med.* **338,** 278–285.

3 Wujek, J. R., Bjartmar, C., Richer, E., Ransohoff, R. M., Yu, M., Tuohy, V. K., et al. (2002) Axon loss in the spinal cord determines permanent neurological disability in an animal model of multiple sclerosis. *J. Neuropathol. Exp. Neurol.* **61,** 23–32.

4 Baron, J. L., Madri, J. A., Ruddle, N. H., Hashim, G., and Janeway, C. A., Jr. (1993) Surface expression of alpha 4 integrin by CD4 T cells is required for their entry into brain parenchyma. *J. Exp. Med.* **177,** 57–68.

5 Keith, A. B., Arnon, R., Teitelbaum, D., Caspary, E. A., and Wisniewski, H. M. (1979) The effect of Cop 1, a synthetic polypeptide, on chronic relapsing experimental allergic encephalomyelitis in guinea pigs. *J. Neurol. Sci.* **42,** 267–274.

6 Teitelbaum, D., Arnon, R., Sela, M., and Abramsky, O. (1989) Clinical trial of copolymer 1 in multiple sclerosis. *Harefuah* **116,** 453–456.

7 Tubridy, N., Behan, P. O., Capildeo, R., Chaudhuri, A., Forbes, R., Hawkins, C. P., et al. (1999) The effect of anti-alpha4 integrin antibody on brain lesion activity in MS. The UK Antegren Study Group. *Neurology* **53,** 466–472.

8 Segal, B. M., Dwyer, B. K., and Shevach, E. M. (1998) An interleukin (IL)-10/IL-12 immunoregulatory circuit controls susceptibility to autoimmune disease. *J. Exp. Med.* **187,** 537–546.

9 Segal, B. M. and Shevach, E. M. (1996) IL-12 unmasks latent autoimmune disease in resistant mice. *J. Exp. Med.* **184,** 771–775.

10 Segal, B. M., Chang, J. T., and Shevach, E. M. (2000) CpG oligonucleotides are potent adjuvants for the activation of autoreactive encephalitogenic T cells in vivo. *J. Immunol.* **164,** 5683–5688.

11 Tarrant, T. K., Silver, P. B., Chan, C. C., Wiggert, B., and Caspi, R. R. (1998) Endogenous IL-12 is required for induction and expression of experimental autoimmune uveitis. *J. Immunol.* **161,** 122–127.

12 Trembleau, S., Penna, G., Bosi, E., Mortara, A., Gately, M. K., and Adorini, L. (1995a) Interleukin 12 administration induces T helper type 1 cells and accelerates autoimmune diabetes in NOD mice. *J. Exp. Med.* **181,** 817–821.

13 Trembleau, S., Germann, T., Gately, M. K., and Adorini, L. (1995b) The role of IL-12 in the induction of organ-specific autoimmune diseases. *Immunol. Today* **16,** 383–386.

14 Neurath, M. F., Fuss, I., Kelsall, B. L., Stuber, E., and Strober, W. (1995) Antibodies to interleukin 12 abrogate established experimental colitis in mice. *J. Exp. Med.* **182,** 1281–1290.

15 Moiola, L., Galbiati, F., Martino, G., Amadio, S., Brambilla, E., Comi, G., et al. (1998) IL-12 is involved in the induction of experimental autoimmune myasthenia gravis, an antibody-mediated disease. *Eur. J. Immunol.* **28,** 2487–2497.

16 Matthys, P., Vermeire, K., Mitera, T., Heremans, H., Huang, S., and Billiau, A. (1998) Anti-IL-12 antibody prevents the development and progression of collagen-induced arthritis in IFN-gamma receptor-deficient mice. *Eur. J. Immunol.* **28,** 2143–2151.

17 Malfait, A. M., Butler, D. M., Presky, D. H., Maini, R. N., Brennan, F. M., and Feldmann, M. (1998) Blockade of IL-12 during the induction of collagen-induced arthritis (CIA) markedly attenuates the severity of the arthritis. *Clin. Exp. Immunol.* **111,** 377–383.

18 Martin, R., MFCArland, H. F., and MFCArlin, D. E. (1992) Immunological aspects of demyelinating diseases. *Annu. Rev. Immunol.* **10,** 153–187.

19 Linthicum, D. S. (1982) Development of acute autoimmune encephalomyelitis in mice: factors regulating the effector phase of the disease. *Immunobiology* **162,** 211–220.

20 McRae, B. L. and Miller, S. D. (1994) Fine specificity of $CD4^+$ T cell responses to the dominant encephalitogenic PLP 139-151 peptide in SJL/J mice. *Neurochem. Res.* **19,** 997–1004.

21 Sakai, K., Zamvil, S. S., Mitchell, D. J., Lim, M., Rothbard, J. B., and Steinman, L. (1988) Characterization of a major encephalitogenic T cell epitope in SJL/J mice with synthetic oligopeptides of myelin basic protein. *J. Neuroimmunol.* **19,** 21–32.

22 Tan, L. J., Kennedy, M. K., and Miller, S. D. (1992) Regulation of the effector stages of experimental autoimmune encephalomyelitis via neuroantigen-specific tolerance induction. II. Fine specificity of effector T cell inhibition. *J. Immunol.* **148,** 2748–2755.

23 Amor, S., Groome, N., Linington, C., Morris, M. M., Dornmair, K., Gardinier, M. V., et al. (1994) Identification of epitopes of myelin oligodendrocyte glycoprotein for the induction of experimental allergic encephalomyelitis in SJL and Biozzi AB/H mice. *J. Immunol.* **153,** 4349–4356.

24 Zamvil, S. S., Mitchell, D. J., Powell, M. B., Sakai, K., Rothbard, J. B., and Steinman, L. (1988) Multiple discrete encephalitogenic epitopes of the autoantigen myelin basic protein include a determinant for I-E class II-restricted T cells. *J. Exp. Med.* **168,** 1181–1186.

25 Whitham, R. H., Bourdette, D. N., Hashim, G. A., Herndon, R. M., Ilg, R. C., Vandenbark, A. A., et al. (1991) Lymphocytes from SJL/J mice immunized with spinal cord respond selectively to a peptide of proteolipid protein and transfer relapsing demyelinating experimental autoimmune encephalomyelitis. *J. Immunol.* **146,** 101–107.

26 Zamvil, S. S., Mitchell, D. J., Moore, A. C., Kitamura, K., Steinman, L., and Rothbard, J. B. (1986) T-cell epitope of the autoantigen myelin basic protein that induces encephalomyelitis. *Nature* **324,** 258–260.

27 Endoh, M., Rapoport, S. I., and Tabira, T. (1990) Studies of experimental allergic encephalomyelitis in old mice. *J. Neuroimmunol.* **29,** 21–31.

28. Tuohy, V. K., Sobel, R. A., and Lees, M. B. (1988) Myelin proteolipid protein-induced experimental allergic encephalomyelitis. Variations of disease expression in different strains of mice. *J. Immunol.* **140, 1868–1873.**

20

Animal Models of Scleroderma

Gabriella Lakos, Shinsuke Takagawa, and John Varga

Summary

Although no single animal model of systemic sclerosis (SSc) faithfully reproduces all features of the human disease, certain animal models that display some of the features of SSc are potentially useful as they may be helpful in gaining a better understanding of the pathogenesis of SSc as well as developing novel therapeutic interventions. This chapter gives the detailed description of the two most useful animal models of SSc: bleomycin-induced skin fibrosis and the sclerodermatous graft-vs-host disease in mice. It provides the methodology of the induction as well as the repertoire of the different approaches that can be used to investigate the skin fibrosis in these models, including histopathology, immunohistochemistry, dermal thickness, hydroxyproline content of the skin, and analysis of dermal cells by flow cytometry.

Key Words: Bleomycin; collagen; flow cytometry; immunohistochemistry; scleroderma; sclerodermatous graft-vs-host disease; skin fibrosis; skin thickness; transforming growth factor-β.

1. Introduction

1.1. Scleroderma

Scleroderma or systemic sclerosis (SSc) is a chronic acquired connective tissue disease of unknown etiology and poorly understood pathogenesis. There are currently no effective treatments, and 5-yr mortality approaches 30% ***(1)***. Like other connective tissue diseases, SSc occurs more frequently in women, with highest incidence in the third through fifth decades. The striking constellation of autoimmune, vascular, and fibrotic alterations, which develop in virtually all patients, makes SSc unique among connective tissue diseases.

The most frequent initial manifestation is Raynaud phenomenon, representing reversible vascular injury that may precede other manifestations by years. With progression of the disease, vascular injury becomes irreversible, with

From: *Methods in Molecular Medicine, Vol. 102: Autoimmunity: Methods and Protocols*
Edited by: A. Perl © Humana Press Inc., Totowa, NJ

digital ischemia and infarctions, telangiectasia in the skin and stomach, and evidence of widespread microvascular damage most prominent in the pulmonary circulation. Mononuclear cell inflammation occurs early in skin and other affected organs and is associated with the local production of growth factors such as transforming growth factor (TGF)-β, and chemokines such as monocyte chemotactic protein 1. Most patients show a highly restricted autoimmune response, with circulating autoantibodies directed against topoisomerase-1 or kinetochore (centromere). A type 2 (Th2) immune response predominates, with elevated levels of interleukin (IL)-4, IL-6, and IL-13 and low or absent interferon (IFN)-γ ***(2)***.

With time, progressive fibrosis affects the skin, lungs, heart, and gastrodigestive tract as well as joints, tendons, and ligaments and medium-size blood vessels in most visceral organs. In late SSc, lesional tissues show a paucity of inflammatory cells; in contrast, a subpopulation of resident fibroblasts is activated, with elevated production of collagen and other extracellular matrix components, increased levels of surface integrins, and transdifferentiation into myofibroblasts. The normal equilibrium between matrix synthesis and matrix turnover is disrupted, with excessive accumulation of connective tissue, resulting in progressive displacement of normal tissue architecture and failure of affected organs. In **Table 1**, the major clinical and pathological features of SSc are contrasted with those seen in the animal models discussed next.

1.2. Animal Models of Scleroderma

Perhaps because of its unique triad of autoimmune/vascular/fibrotic features, as well as the marked heterogeneity of clinical manifestations from one individual to the next, understanding the pathogenesis of SSc presents an enormous challenge. It is not surprising that no single animal model of SSc faithfully reproduces the human disease. However, there are animal models that display some of the features of SSc. These models are of enormous potential utility because they may be helpful in gaining a better understanding of the pathogenesis of SSc as well as in developing of novel therapeutic interventions. Reviews provided excellent overview of animal models of SSc ***(3,4)***. Here, we focus on the advantages and limitations of selected animal models, then present methodological considerations.

Most animal models of SSc have been developed in the mouse, a natural choice in light of the large body of genetic information available. The models can be divided into those in which disease is induced (by an exogenous substance such as bleomycin or through manipulation of the immune system) and those for which disease develops spontaneously through an inherited mutation or through genetic manipulation. In the first group, the antibiotic and antitumor agent bleomycin ***(5)*** is widely used to study fibrosis in a variety of organs of rodents. Administered intratracheally, bleomycin induces pulmonary

Table 1
Comparison of SSc and Selected Animal Models

Systemic sclerosis	Mouse models of scleroderma		
	Bleomycin-induced; C3H mouse strain	Graft-vs-host disease; BALB/c (recipient) and B10.D2 (donor) mouse strains	Tsk-1, B10.D2 mouse strain
Acquired	Acquired	Acquired	Inherited (autosomal dominant)
Female predominance	No gender predominance	No gender predominance	No gender predominance
Generally insidious progression	Skin fibrosis evolving by 21 d	Skin fibrosis evolving by 21 d	Skin fibrosis detectable by day 7
Early inflammation in lesional tissue	Early inflammation in lesional tissue	Early inflammation in lesional tissue	No inflammation in lesional tissue
Skin fibrosis	Skin fibrosis	Skin fibrosis	Skin fibrosis
Lung fibrosis	Lung fibrosis	Lung fibrosis	Emphysema
Gastrointestinal tract fibrosis	?	No gastrointestinal involvement	?
Systemic vascular injury	Systemic vascular injury	No vascular injury	No vascular injury
Autoantibodies	No autoantibodies	No autoantibodies	± Autoantibodies

inflammation, fibroblast accumulation, and fibrosis ***(6)***. The histological changes resemble those seen in the lungs of patients with SSc ***(7)***. Susceptibility to lung fibrosis is strongly influenced by the genetic background of the mouse ***(8–10)***.

Injection of bleomycin by the subcutaneous route is associated with early inflammation, with striking numbers of monocytes accumulating in the lesional dermis ***(11–13)***. The inflammatory infiltrate also contains mast cells and occasional eosinophils ***(14)***. After 1–2 wk of daily injections, progressive dermal fibrosis develops (**Fig. 1**). At this stage, the lesional dermis is thickened and relatively acellular, with excessive accumulation of collagen. The indurated lesion remains highly localized and persists for at least 6 wk after the last administration of bleomycin. Fibroblasts in the lesional dermis may show elevated expression of Hsp47, a marker for ongoing collagen synthesis ***(15)***, and sustained activation of the intracellular TGF-β/Smad signal transduction pathway ***(13)***. Many fibroblasts stain positive for α-smooth muscle actin, indicating their transdifferentiation into smooth muscle-like myofibroblasts ***(16)***. Administration of neutralizing antibody to TGF-β prevents the development of fibrosis ***(17)***.

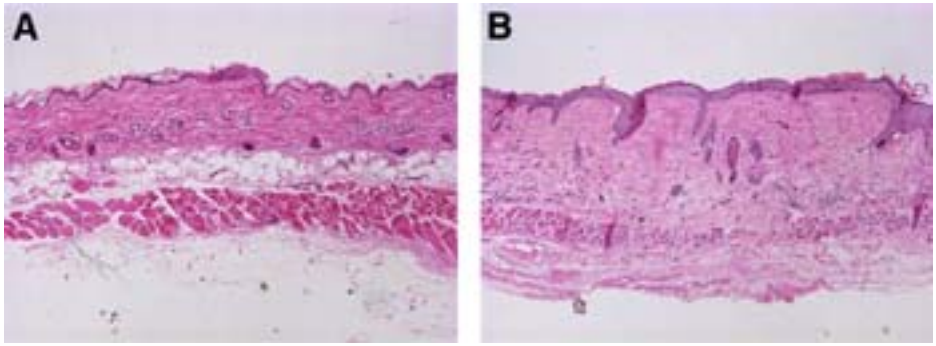

Fig. 1. Dermal sclerosis in the bleomycin-induced mouse scleroderma model. C3H mice were injected daily with **(A)** PBS or **(B)** 100 μg/mL bleomycin for 3 wk. Note extensive dermal thickening; fat layer is replaced by connective tissue.

Another animal model that shows intriguing similarities with SSc is a form of graft-vs-host disease (GVHD), which can be induced in lethally irradiated BALB/c mice by transplanting bone marrow or spleen cells from B10.D2 mice compatible at major, but not minor, histocompatibility loci ***(18)***. The recipients show skin and lung fibrosis by day 21 after bone marrow transplantation, preceded by infiltration with monocytes and T cells of donor origin and elevated tissue levels of messenger RNA (mRNA) for TGF-β1 and monocyte chemotactic protein 1. The donor cells infiltrating the dermis show evidence of activation and display H-2 and class A scavenger receptor molecules. Increased numbers of mast cells and evidence of mast cell activation/degranulation have also been described ***(19)***. In contrast to SSc, there is no evidence of vascular injury or of autoantibodies.

Tight skin (Tsk1) mice develop fibrosis spontaneously as a result of a stably inherited genetic alteration. A mutation on chromosome 2 results in an in-frame duplication of exons 17 through 40 of the fibrillin-1 gene ***(20)***. The duplicated region is inserted between exons 40 and 41, yielding a mutant 450-kDa fibrillin-1 protein that has two extra TGF-β-binding domains. Homozygous Tsk1 mice die *in utero* at 8–10 d of gestation, whereas heterozygous mice develop skin thickening by day 7. Cutaneous fibrosis is associated with marked collagen accumulation and increased transcription of the α2-chain of type I collagen gene in dermal fibroblasts ***(21)***. In addition to scleroderma, Tsk1/+ mice also develop cardiac fibrosis, but no lung fibrosis; rather, they have greatly distended lungs with emphysemalike alveolar dilatation. The pathogenesis of skin and cardiac fibrosis in the Tsk1/+ mouse, and the role of TGF-β, remain obscure.

Another animal model of SSc is provided by MRL/*lpr* mice lacking the IFN-γ receptors (MRL/*lpr*γR–/–). The MRL/*lpr* mice, widely used as a model for systemic lupus erythematosus, have a mutation of the gene encoding Fas and develop glomerulonephritis, vasculitis, and lymphadenopathy associated with autoantibody production. Because IFN-γ is an important antifibrotic signal, the loss of IFN-γ responsiveness in the MRL/*lpr*γR–/– mouse results in dermal fibrosis and collagen accumulation accompanied by evidence of vascular injury (J. Oates, S. Takagawa, and J. Varga, unpublished, 2003).

In summary, induced and naturally occurring forms of fibrosis in the mouse reproduce important clinical or pathological features of SSc, especially dermal fibrosis. Because the severity, time course, and extent of dermal fibrosis in these models can be accurately monitored, it provides a useful experimental "readout."

2. Materials

2.1. Induction of Scleroderma in Mice by Subcutaneous Injection of Bleomycin

1. 15 U Bleomycin for injection, USP (Gensia Sicor Pharmaceuticals Inc., Irvine, CA).
2. Phosphate-buffered saline (PBS) at pH 7.4.
3. 1-mL U-100 insulin syringe with 28-ga needle (309309 Becton Dickinson, Franklin Lakes, NJ).
4. Millex-GP 0.22-μm syringe-driven filter unit (SLGP033RS Millipore Corp., Bedford, MA).

2.2. Induction of Sclerodermatous GVHD in Mice (Bone Marrow Transplantation)

1. 100 μL heparin (10,000 U/mL; Sigma, St. Louis, MO) for injection of each donor mouse.
2. Iodine solution and 75% ethanol to disinfect skin before collecting bone marrow and spleen cells.
3. Surgical instruments (strong scissors, fine scissors, forceps).
4. Sterile Petri dishes with medium containing heparin (RPMI-1640, BioWhittaker, Frederick, MD, with 20 U/mL heparin, Fisher Scientific, Pittsburgh, PA).
5. Sterile 50-mL falcon tubes to collect cells.
6. Autoclaved stainless steel mesh.
7. Gammacel ^{137}Cs source.
8. 27-ga needles.
9. 5-mL syringes preloaded with medium/heparin (**item 4**).
10. Microisolator cages (Lab Products, Seaford, DE).
11. Autoclaved acidified water (pH 2.5 with acetic acid) and autoclaved chow.

2.3. Processing Skin for Histological and Immunohistochemical Analysis

1. Histoprep tissue capsule (15-182-218, Fisher Scientific).
2. 10% formalin (buffered formalde-fresh SF93-4, Fisher Scientific).
3. Ethanol (70, 80, 90, 95, and 100%).
4. Xylene (HC700 HistoPrep xylenes, Fisher Scientific).
5. Paraffin (Paraplast X-tra tissue embedding medium 23-021401, Fisher Scientific).
6. Vacuum incubator.
7. Histoprep mold release (SH70-250D, Fisher Scientific).
8. Histoprep stainless steel base mold (15-182-505, Fisher Scientific).
9. Embedding cassettes (15-182-500, Fisher Scientific).
10. Tissue embedder (Histoembedder 038621439 B, Leica Instruments GmbH, Nussloch, Germany).
11. Microtome (Biocut 2030, Leica Instruments).
12. Disposable Microtome blades (818, Leica Instruments).
13. Superfrost/Plus microscope slide (12-550-15, Fisher Scientific).
14. Histobond adhesive (23-245692, Fisher Scientific).
15. Water bath.
16. Slide warmer (26020, Lab-Line Instruments Inc., Melrose Park, IL).

2.4. Hematoxylin and Eosin Staining, Determination of Dermal Thickness

1. Hematoxylin solution (HHS-16 Accustain Harris hematoxylin solution, modified, Sigma-Aldrich Co., St. Louis, MO).
2. Eosin Y solution (HT-110-1-16 Accustain eosin Y solution, alcoholic, Sigma-Aldrich).
3. Xylene (HC700 HistoPrep xylenes, Fisher Scientific).
4. Ethanol (100, 95, and 80%).
5. 0.5% acid alcohol solution (1 mL concentrated HCl plus 199 mL 70% ethanol).
6. Ammonia water (1 mL 28% NH_4OH plus 199 mL distilled water).
7. Mounting medium (SP15-100 Permount, Fisher Scientific).
8. Staining jars.
9. Coverslips (FISHERfinest premium cover glass 12-544-14, Fisher Scientific).
10. Microscope equipped with digital camera and suitable software to transfer the photos to the computer (for example, charge coupled device camera and SPOT Insight, Diagnostic Instruments, Sterling Heights, MI).
11. SPOT Advanced software (Diagnostic Instruments) for image analysis.

2.5. Immunohistochemistry

1. DAKO pen (S2002, DAKO Corp., Carpinteria, CA).
2. Steamer, such as Favor Scenter steamer deluxe (HS2776, Black and Decker, Towson, MD).
3. DAKO Target Retrieval solution (S1699, DAKO Corp.).

4. 3% H_2O_2.
5. TBS-T: 50 m*M* Tris-HCl, 300 m*M* NaCl at pH7.8, and 0.1% Tween-20.
6. DAKO Protein Block, serum free (X0909, Dako Corp.).
7. Hematoxylin solution (HHS-16 Accustain Harris hematoxylin solution, modified, Sigma-Aldrich).
8. Xylene (HC700 HistoPrep xylenes, Fisher Scientific).
9. Ethanol (100, 95, and 80%).
10. 0.5% acid alcohol solution (1 mL concentrated HCl plus 199 mL 70% ethanol).
11. Ammonia water (1 mL 28% NH_4OH plus 199 mL distilled water).
12. Mounting medium (SP15-100 Permount, Fisher Scientific).
13. Staining jars.
14. Coverslips (FISHERfinest premium cover glass 12-544-14, Fisher Scientific).

2.6. Digestion of Tissue for Single-Cell Suspension for Flow Cytometric Analysis

1. PBS at pH 7.4.
2. Dulbecco's modified Eagle's medium (15-017-CM, Mediatech (800) Cellgro, Herndon, VA).
3. HEPES (H-7523, Sigma-Aldrich).
4. Dispase (354235, BD Biosciences, San Diego, CA). Working solution: 50 U/mL. Store stock solution aliquoted at –70°C. Avoid repeated freezing and thawing.
5. Hyaluronidase (H-3506, Sigma-Aldrich). Working solution: 1000 U/mL. Store stock solution aliquoted at –70°C. Avoid repeated freezing and thawing.
6. Deoxyribonuclease (D-5025, Sigma-Aldrich). Working solution: 0.01%. Store stock solution aliquoted at –70°C. Avoid repeated freezing and thawing.
7. Collagenase I (C-9891, Sigma-Aldrich). Working solution: 0.27%. Store stock solution aliquoted at –70°C. Avoid repeated freezing and thawing.
8. Scalpel, forceps, scissors.
9. 40-μm pore size cell strainer (352340, Becton Dickinson).
10. 50-mL polypropylene conical tubes (352070, Becton Dickinson).
11. Trypan blue dye, hemacytometer.
12. Flow cytometry wash buffer: PBS with 1% bovine serum albumin and 0.05% sodium azide.

2.7. Determination of Hydroxyproline Content of the Skin

1. 6*N* HCl (H 0636, Sigma-Aldrich).
2. Chloramine T (C 9887, Sigma-Aldrich).
3. Sodium acetate trihydrate (S 9513, Sigma-Aldrich).
4. NaOH (S 8045, Sigma Aldrich).
5. Isopropanol (2-propanol I 9516, Sigma-Aldrich).
6. 4-(Dimethylamino)benzaldehyde (D 2004, Sigma-Aldrich).
7. Perchloric acid 69.0–72.0% (24,425-2, Sigma-Aldrich).
8. Citric acid monohydrate (C 1909, Sigma-Aldrich).

9. Glacial acetic acid (A 6283, Sigma-Aldrich).
10. Stock solution: 5 g citric acid, 1.2 mL glacial acetic acid, 12 g sodium acetate trihydrate, 3.4 g NaOH in 100 mL of deionized water (stable at +4°C for 2 wk).
11. Chloramine-T reagent: Dissolve 1.4 g chloramine-T in 20 mL deionized water, add 30 mL propanol and 50 mL stock solution (stable at +4°C for 2 wk).
12. Hydroxyproline standards (Trans-4-hydroxy-L-proline H 5534, Sigma-Aldrich).
13. Dimethylaminobenzaldehyde reagent: Dissolve 15 g dimethylaminobenzaldehyde in 60 mL isopropanol and slowly add 30 mL of 70% perchloric acid. Must be freshly prepared under hood.
14. 6-mm dermal biopsy punch (33-36, Miltex Instrument Co. Inc., Bethpage, NY).
15. Glass tubes.
16. Vacuum incubator.
17. 96-well polystyrene plate.
18. Enzyme-linked immunosorbent assay photometer.

3. Methods

3.1. Induction of Scleroderma by Subcutaneous Injection of Bleomycin

Repeated daily subcutaneous injections of bleomycin (0.1–1 mg/mL) induce dermal sclerosis in various strains of mice. There appears to be some degree of strain variability in susceptibility to fibrosis; for example, fibrosis develops after 4 wk in BALB/c mice, but after 3 wk in C3H mice (*see* **Note 1**). Fibrosis remains confined to the injected area (approx 0.5 cm^2).

1. Sterilize PBS by filtration through 0.22-μm syringe-driven filter unit. Dissolve bleomycin in PBS (100 μg/mL) and sterilize by filtration (*see* **Note 2**). Sterilized solutions should be aliquoted and stored at –20°C.
2. Shave the backs of 6-wk-old C3H mice (*see* **Note 3**).
3. Using the 28-ga needle, inject 100 μL bleomycin or PBS (as control) subcutaneously into the shaved back. Two different spots on the back of the mice can be shaved and injected to have more lesional tissue for study.
4. Injections at the same site should be carried out daily for up to 3 wk (*see* **Note 4**).

3.2. Induction of Sclerodermatous GVHD

1. Mouse strains: The donor/recipient mouse strain pair used to generate sclerodermatous GVHD is B10.D2 (nSNJ H-2^d, Mls-2^a, Mls3^a) transplanted to BALB/cJ (H-2^d, Mls2^a, Mls3^a) (both from Jackson Laboratory, Bar Harbor, ME). Male or female mice can be utilized as donors and recipients at approx 6–8 wk of age. When male mice from different littermates are placed together, the fighting that ensues can lead to unwanted injuries with scarring of the skin; therefore, female mice are generally used as recipients. It is helpful to transplant bone marrow and spleen from male mice into female mice to track donor cells by polymerase chain reaction analysis of Y-chromosome sequences. Transplantation with syngeneic BALB/c bone marrow/spleen cells is always performed (control group).

2. Donor and recipient mice are allowed to adapt for approx 1 wk after shipping and are maintained from time of arrival in Microisolator cages (three to five mice per cage).
3. Recipient mice are irradiated early on the day of transplantation in groups of 5–8 with 700 cGy using a Gammacel ^{137}Cs source. Increased mortality unrelated to GvHD occurs at higher doses in BALB/c mice, which are sensitive to ionizing radiation.
4. A standard protocol for preparation of the transplantation inoculum is used and is briefly described here ***(22)***:
   a. Preparation of bone marrow cells (source of hematopoietic precursors for engraftment). Donor mice are sedated with ketamine and injected intraperitoneally with 100 μL of heparin before sacrifice by cervical dislocation. The skin is disinfected by dipping in iodine solution, then in 75% ethanol. Using ethanol-cleaned surgical instruments, the lower extremity skin is stripped away starting at the Achilles tendon with an incision. The leg is released by disarticulation of the femur from the pelvic socket with heavy scissors. Fine scissors are then used to strip the soft tissue from femur and tibia, and the fibula is discarded. The ends of each bone are clipped using heavy scissors and discarded. Three cleaned bones from each leg (femur, knee joint, and tibia) are then placed in a sterile Petri dish with media/heparin. Using 27-ga needles and 5-mL syringes preloaded with media/heparin, bone marrow is flushed from the bone marrow canal into a 50-mL falcon tube. Bone marrow cells are resuspended in a final volume of 50 mL media/heparin, washed two times in media/heparin, and counted for total number and viability using trypan blue dye exclusion. The bone marrow preparation is kept at room temperature until use. Bone marrow from four to five mice yields approx 50–150 × 10^6 bone marrow cells for transplantation. 5-Fluorouracil, 150 μg/mouse, injected intraperitoneally 2 d before collection of bone marrow will increase yield. The bone marrow cells must be handled carefully after 5-fluorouracil mobilization because they appear to be more fragile.
   b. Preparation of spleen cells (source of mature T cells to generate GVHD). Spleen is removed at the same time that leg bones are collected. After mincing the spleen with a sharp scalpel in a sterile Petri dish with media/heparin, cells are disaggregated by pressing pieces through an autoclaved stainless steel wire mesh screen over a 50-mL falcon tube. The mesh is washed in media/heparin, and spleen cells are collected into 50 mL media/heparin. Cells are then washed two times in media/heparin and counted for total number and viability. They are also kept at room temperature.
   c. Transplantation. Bone marrow and spleen cells are combined to deliver a ratio of 2:1 bone marrow (2 × 10^6) and spleen (1 × 10^6) cells in a volume of 0.2 mL per mouse (standard dose for generating GVHD). The bone marrow/spleen preparation is kept at room temperature. The preparation is drawn up repeatedly in a 5-cc syringe with an 18-ga needle to disaggregate clots before use. To have viable transplanted cells, transplantation must occur within 6 h of

fresh bone marrow/spleen collection. Variability in skin thickening at given times after transplantation may occur in animals receiving less than the full transplantation inoculum because they may develop GVHD at a slower rate. Deaths during the transplantation procedure itself are usually because of emboli (clotted bone marrow/spleen preparations or air emboli) during tail vein injections. Deaths at early times (1–2 wk after transplantation) are because of failure of engraftment. To confirm that the irradiation dose was lethal, irradiated but not transplanted mice are included in each experiment. These mice typically die between 7 and 10 d postirradiation. Engraftment can be evaluated by examination of spleen in sacrificed animals. Within 4–5 d after transplantation, numerous colonies should be present in spleens of engrafted animals.

d. Transplanted animals are maintained in Microisolator cages and given autoclaved acidified water (pH 2.5 with acetic acid) and autoclaved chow. Antibiotics are not used in drinking water.

3.3. Processing Skin for Histological and Immunohistochemical Analysis

1. Euthanize mice. Shave the injected areas. Harvest the injected spot (about 1 cm^2) of the skin. If necessary, label the injection site before harvesting. Place and extend the tissue on a piece of cardboard paper. This prevents skin curling during the procedure. Place skin samples into tissue basket.
2. Fix samples in 10% formalin for 6–24 h. For proper fixation, the ratio of formalin to tissue should be 10:1. Agitation of the specimen with a shaker also enhances fixation.
3. Wash samples with tap water for 10 min, dehydrate by ascending strain of alcohol (70, 80, 90, 95, and 100% twice), and proceed to alcohol-xylene mixture (50:50%), xylene twice, xylene-paraffin mixture (50:50%), and finally paraffin twice. Each step requires 2 h (*see* **Note 5**).
4. Wet embedding mold with Histoprep mold release agent and pour in melted paraffin. Stand fixed skin exactly vertical in the mold (preferably in diagonal position, with the epidermis upside; *see* **Note 6**). Once paraffin starts to solidify, put the embedding cassette on the top of the mold, pour in more paraffin until the mold is full, and cool. After solidifying and cooling, take the paraffin block out of the mold. Paraffin blocks can be stored at room temperature.
5. Cool paraffin blocks on ice for 10–15 min before cutting.
6. Make 5-μm sections (**Fig. 2**) and float on 35–38°C water bath containing 1% Histobound adhesive (this facilitates the sections to adhere better to the slides) to stretch paraffin ribbon (*see* **Note 7**).
7. Pick up sections on slides. Make consecutive sections and label the slides by order. This helps identify structures during immunohistochemical processes. Dry the sections overnight on a slide warmer or in a 37°C incubator. The slides can be stored at room temperature.

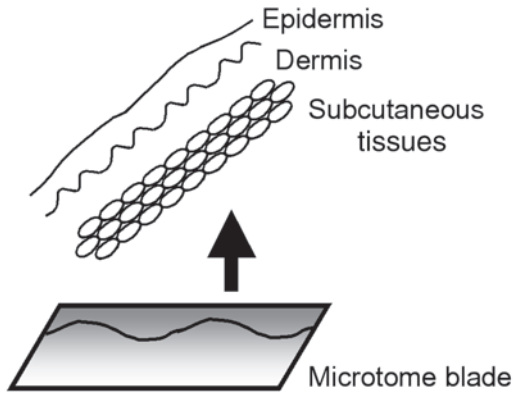

Fig. 2. Position of the skin sample and blade for sectioning. The microtome blade (moving from the bottom of the paraffin block to the top) should move from the softer to the harder layer. Cutting angle should be vertical.

3.4. Hematoxylin and Eosin Staining, Determination of Dermal Thickness

In bleomycin-treated mice, skin fibrosis appears as thickening of the dermal layer, with swollen and homogeneous collagen bundles (**Fig. 1**). The dermis contains only a few cells (fibroblasts), and the fat layer of the reticular dermis is replaced with extracellular matrix. In sclerodermatous GVHD, skin is thickened, and increased numbers of inflammatory cells are present at the dermis–fat interface.

The extent of dermal sclerosis can be measured by several methods. Quantifying the hydroxyproline content of the affected area provides information on the degree of collagen accumulation. Only semiquantitative information can be obtained by the collagen-specific Masson's trichrome or sirius red tissue staining ***(23)*** or by immunohistochemical detection of collagen in the dermis. The degree of dermal sclerosis can be best estimated by measuring dermal thickness because it provides information on the production of all types of extracellular matrices (collagen, fibronectin, proteoglycans). Dermal thickness should be measured from the epidermal–dermal junction to the dermal–fat junction (**Fig. 3**).

1. Deparaffinize sections in xylene for 5 min twice. Blot excess xylene before going into ethanol.
2. Rehydrate sections in descending ethanol dilutions: 100% twice for 3 min, 95% twice for 3 min, 80% for 3 min, distilled water for 5 min.

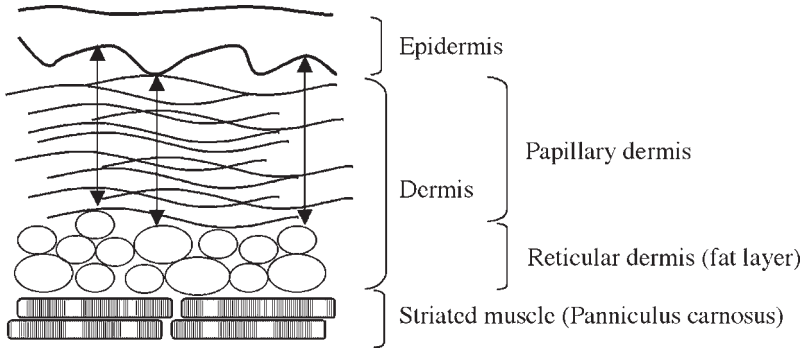

Fig. 3. Schematic of mouse skin. Dermal thickness should be measured from the epidermal–dermal junction to the dermal fat junction.

3. Stain them in hematoxylin solution for 5 min.
4. Wash the sections in distilled water. Change water at least twice.
5. Dip the slides into 0.5% acid alcohol solution one or two times (*see* **Note 8**).
6. Wash the sections in distilled water. Change water at least twice.
7. Dip the slides into ammonia water for approx 30 s (*see* **Note 9**).
8. Wash the sections in distilled water. Change water at least twice.
9. Stain in eosin Y solution for 2 min.
10. Differentiate and dehydrate the sections in ascending ethanol dilutions: 95% for 2 min twice, 100% for 2 min twice.
11. Clear the sections in xylene for 2 min twice.
12. Mount the sections with Permount and let them dry for 24 h.
13. Take a picture at ×100 magnification on the selected area (*see* **Note 10**). Store image as a Joint Photographic Experts Group (Jpeg) file.
14. Subject file to image analysis using SPOT software. Calibrate the software by a hemacytometer (to determine number of pixels corresponding to a given distance). Determine dermal thickness at five randomly selected sites in several microscopic fields.

3.5. Immunohistochemistry

Immunohistochemical analysis, performed on either frozen or formalin-fixed, paraffin-embedded tissue sections, is suitable for identifying cell types by their specific antigen expression and investigating the expression of surface and intracellular molecules such as receptors, transcription factors, and differentiation markers. A large variety of antibodies is commercially available. We prefer paraffin-embedded sections because the morphological characteristics are better preserved. Here, we describe a procedure for a paraffin-embedded section. The type of the secondary antibody and the method of detection are

determined by the primary antibody. There are many commercially available, ready-to-use kits that include all of the reagents needed after the incubation with the primary antibody. These kits make procedures easier and more reproducible.

1. Deparaffinize and rehydrate sections as for hematoxylin and eosin staining.
2. Place slides in a plastic jar filled with antigen retrieval solution.
3. Put jar in boiling steamer and leave 10 min (or as recommended for the particular primary antibody).
4. Remove jar from steamer and let the slides cool at room temperature for 20 min.
5. Wash slides in distilled water for 2 min twice. Do not let the slides dry during the whole procedure because this may cause nonspecific reactions.
6. Draw a circle around the sample with DAKO pen. This circle will keep the drops of antibody and all of the other reagents on the section.
7. Incubate slides with 3% H_2O_2 for 10 min to block endogenous peroxidase activity of the tissue when using peroxidase-labeled secondary antibody.
8. Wash slides in TBS-T 2 min twice.
9. Apply blocking reagent and incubate 20 min at room temperature. Blocking reagent may be diluted serum from the same species as the secondary antibody or serum-free blocking solution, such as DAKO protein block.
10. Apply primary antibody or negative control. Negative control reagent should be the same immunoglobulin class and animal species and diluted to the same protein concentration as the diluted primary antibody. If using monoclonal antibody, the negative control should be the same immunoglobulin subclass as the primary antibody.
11. Follow the manufacturer's instructions up to developing. Use TBS-T for washing between steps.
12. After color development, proceed with counterstaining with hematoxylin (*see* **Note 11**).
13. Dehydrate sections in ascending ethanol dilutions: (80, 90, and 100% twice for 2 min each) and clear them in xylene for 5 min twice.
14. Mount the sections with Paramount and dry for 24 h.

3.6. Digestion of Skin for Single-Cell Suspension for Flow Cytometric Analysis

Flow cytometric analysis is a powerful tool for investigation of the number, composition, and activation state of the cells infiltrating the dermis, as well as of resident cells. Flow cytometric analysis offers objective information about thousands (usually 10,000) of cells simultaneously, providing a useful alternative or additional method for immunohistochemistry. Flow cytometry is suitable for detecting cell-specific antigens, activation markers, and receptors by surface staining and for measuring intracytoplasmic molecules by cytoplasmic labeling ***(18)***. The initial and critical step is to obtain a suspension of a suffi-

cient number of viable single cells from the dermis. As inflammatory infiltration is an early event in the bleomycin-induced scleroderma model, infiltrating cells can be best studied by flow cytometric analysis during the first week.

1. Euthanize mice. Shave the injected area. Harvest lesional tissue (about 0.5–1 cm^2 of skin). If necessary, label the injection site before harvesting; a larger piece exceeding the injected area may contain normal tissue, thus "diluting" the results.
2. Place the harvested skin into PBS (1 mL) containing 50 U/mL dispase in a microtube. Vortex thoroughly. Incubate at 4°C overnight.
3. Remove the epidermis (*see* **Note 12**).
4. Place tissue in a Petri dish, cut it into pieces as small as possible with a scalpel, and place in 1mL Dulbecco's modified Eagle's medium containing 10 m*M* HEPES, 0.27% collagenase, 0.01% deoxyribonuclease, and 1000 U/mL hyaluronidase. Vortex thoroughly. Incubate at 37°C for 1 h in a shaker water bath or vortex microtube every 10 min (*see* **Note 13**).
5. Place a 40-μm pore size cell strainer on a 50-mL tube and filter the digested skin by centrifuging at 500*g* for 3 min.
6. Wash cells twice in 3 mL of flow cytometry wash buffer and place on ice.
7. Check cell viability by trypan blue staining and count the cells. Usually, 2–4 × 10^6 cells can be obtained from 1 cm^2 dermis.
8. Process the cells for flow cytometry. Red blood cells present in the suspension should be lysed by PharM Lyse ammonium chloride lysing reagent (555899, BD Biosciences) during the staining procedure.

3.7. Determination of Hydroxyproline Content of the Skin

Type I collagen is the major component of the dermal extracellular matrix. The collagen content of the dermis is a reliable measure of the extent/severity of skin fibrosis. However, staining of collagen by Masson's trichrome or sirius red or immunohistochemical detection of collagen fibers can provide only qualitative information. As collagens are the only proteins that contain 3- and 4-hydroxyproline molecules (up to 10–15% of their amino acids), the hydroxyproline content of a tissue sample is an accurate measure of collagen content. The amount of hydroxyproline may be normalized by the dry weight of the sample.

1. Obtain lesional skin tissue by 6-mm diameter punch biopsy. Freeze samples in liquid nitrogen and store at –80°C until processing.
2. Hydrolyze samples in 2 mL of 6*N* HCl at 110°C for 18 h in glass tubes.
3. Dry samples under vacuum overnight at 110°C.
4. Dissolve pellets in 1 mL distilled water at room temperature.
5. Make hydroxyproline standards containing 0, 25, 50, 100, and 200 μg/mL hydroxyproline.
6. Prepare 1.5-mL microtubes containing 500 μL of chloramine-T reagent.

7. Add 200 μL of sample or standard, mix thoroughly, and incubate for 20 min at room temperature.
8. Add 500 μL of dimethylaminobenzaldehyde reagent and incubate at 60°C for 15 min.
9. Transfer 100 μL of final reaction solution into 96-well plate (triplicate measurements for each sample) and read optical density at 557 (550) nm.
10. Create a calibration curve plotting the optical densities of the standards against their hydroxyproline content and calculate the hydroxyproline content of the samples.

4. Notes

1. Different strains of mice have different susceptibilities for fibrosis. Several publications found C3H/HeJ and Balb/c mice were resistant, and C57BL/6 mice were prone to develop chemical or irradiation induced lung or skin fibrosis ***(10,24–26)***.
2. The amount of bleomycin can be given as milligrams or units. The conversion factor is 1.5–2.0 U/mg.
3. Injections in the same spot. To specify injection site, shave only a small area (about 1 cm × 1 cm).
4. Some reported similar results by injections on every second day ***(12)***.
5. Paraffin should be kept in an incubator (56–58°C) under vacuum. This will prevent bubble trapping in tissues, which may appear as holes in sections.
6. Skin consists of three different layers: epidermis (hard), dermis, and subcutaneous tissues (soft), so sectioning the skin is more difficult than for other tissues. The microtome blade (moving from the bottom of the paraffin block to the top) should go from softer layer to harder layer. The vertical and diagonal position of the tissue ensures the appropriate cutting angle. The cutting angle should be vertical; however, the measurement of the dermal thickness is not accurate.
7. In case of problems such as shrinking or shattering the paraffin ribbon during sectioning, the block should be cooled on ice, or the blade should be changed. These options solve most of the problems in tissue sectioning. The time that the paraffin ribbon stays on the bath water and the temperature of the bath are both critical. If time is too long or the water is too warm, the paraffin ribbon will spread, and significant artifacts will occur. This results in holes and spaces in the dermis that preclude accurate measurement of dermal thickness.
8. Usually, one dip is enough. Check sections after one dip and rinsing with distilled water. Too much time in the acid alcohol may result in faint colors of the nuclei.
9. Ammonia water turns the purple color of the nuclei to blue. Check sections after 30 s. Repeat the step if necessary.
10. In bleomycin-induced murine scleroderma, the affected area is small, so care should be taken to identify the exact location.
11. Follow the procedure described in **Subheading 3.4.** but omit eosin. Increase the time in the acid alcohol solution to have lighter blue nuclei than in regular hematoxylin staining. This helps differentiate the specific staining.

12. The epidermis can be easily removed by gentle scraping with a scalpel.
13. The incubation time can be varied according to the type and age of animal and the degree of dermal fibrosis. Digestion is complete when 90% of the small pieces are disintegrated. Longer incubation times may affect cell viability.

References

1 Bryan, C., Knight, C., Black, C. M., and Silman, A. J. (1999) Prediction of 5-year survival following presentation with scleroderma: development of a simple model using three disease factors at first visit. *Arthritis Rheum.* **42,** 2660–2665.

2 Hasegawa, M., Fujimoto, M., Kikuchi, K., and Takehara, K. (1997) Elevated serum levels of interleukin 4 (IL-4), IL-10, and IL-13 in patients with systemic sclerosis. *J. Rheumatol.* **24,** 328–332.

3 Zhang, Y. and Gilliam, A. C. (2002) Animal models for scleroderma: an update. *Curr. Rheumatol. Rep.* **4,** 150–162.

4 Jimenez, S. A. and Christner, P. J. (2002) Murine animal models of systemic sclerosis. *Curr. Opin. Rheumatol.* **14,** 671–680.

5 Adamson, I. V. R. (1984) Drug-induced pulmonary fibrosis. *Environ. Health Perspect.* **55,** 25–36.

6 Lazo, J. S., Hoyt, D. G., Sebti, S. M., and Pitt, B. R. (1990) Bleomycin: a pharmacologic tool in the study of the pathogenesis of interstitial pulmonary fibrosis. *Pharmacol. Ther.* **47,** 347–358.

7 Adamson, I. Y. and Bowden, D. H. (1974) The pathogenesis of bleomycin-induced pulmonary fibrosis in mice. *Am. J. Pathol.* **77,** 185–197.

8 Haston, C. K., Amos, C. I., King, T. M., and Travis, E. L. (1996) Inheritance of susceptibility to bleomycin-induced pulmonary fibrosis in the mouse. *Cancer Res.* **56,** 2596–2601.

9 Warshamana, G. S., Pociask, D. A., Sime, P., Schwartz, D. A., and Brody, A. R. (2002) Susceptibility to asbestos-induced and transforming growth factor-beta1-induced fibroproliferative lung disease in two strains of mice. *Am. J. Respir. Cell Mol. Biol.* **27,** 705–713.

10 Kolb, M., Bonniaud, P., Galt, T., Sime, P. J., Kelly, M. M., Margetts, P. J., et al. (2002) Differences in the fibrogenic response after transfer of active transforming growth factor-beta1 gene to lungs of "fibrosis-prone" and "fibrosis-resistant" mouse strains. *Am. J. Respir. Cell Mol. Biol.* **27,** 141–150.

11 Mountz, J. D., Downs Minor, M. B., Turner, R., Thomas, M. B., Richards, F., and Pisko, E. (1983) Bleomycin-induced cutaneous toxicity in the rat: analysis of histopathology and ultrastructure compared with progressive systemic sclerosis (scleroderma). *Br. J. Dermatol.* **108,** 679–686.

12 Yamamoto, T., Takagawa, S., Katayama, I., Yamazaki, K., Hamazaki, Y., Shinkai, H., et al. (1999) Animal model of sclerotic skin. I: Local injections of bleomycin induce sclerotic skin mimicking scleroderma. *J. Invest. Dermatol.* **112,** 456–462.

13 Takagawa, S., Lakos, G., Mori, Y., Yamamoto, T., Nishioka, K., and Varga, J. (2003) Sustained activation of fibroblast TGF-β/Smad signaling in murine scleroderma. *J. Invest. Dermatol.* **121,** 41–50.

14 Yamamoto, T., Takahashi, Y., Takagawa, S., Katayama, I., and Nishioka, K. (1999) Animal model of sclerotic skin. II. Bleomycin induced scleroderma in genetically mast cell deficient WBB6F1-W/W(V) mice. *J. Rheumatol.* **26,** 2628–2634.
15 Sasaki, H., Sato, T., Yamauchi, N., Okamoto, T., Kobayashi, D., Iyama, S., et al. (2002) Induction of heat shock protein 47 synthesis by TGF-beta and IL-1 beta via enhancement of the heat shock element binding activity of heat shock transcription factor 1. *J. Immunol.* **168,** 5178–5183.
16 Yamamoto, T. and Nishioka, K. (2002) Animal model of sclerotic skin. V: Increased expression of alpha-smooth muscle actin in fibroblastic cells in bleomycin-induced scleroderma. *Clin. Immunol.* **102,** 77–83.
17 Yamamoto, T., Takagawa, S., Katayama, I., and Nishioka, K. (1999) Anti-sclerotic effect of transforming growth factor-beta antibody in a mouse model of bleomycin-induced scleroderma. *Clin. Immunol.* **92,** 6–13.
18 Zhang, Y., McCormick, L. L., Desai, S. R., Wu, C., and Gilliam, A. C. (2002) Murine sclerodermatous graft-vs-host disease, a model for human scleroderma: cutaneous cytokines, chemokines, and immune cell activation. *J. Immunol.* **168,** 3088–3098.
19 Hawkins, R. A., Claman, H. N., Clark, R. A., and Steigerwald, J. C. (1985) Increased dermal mast cell populations in progressive systemic sclerosis: a link in chronic fibrosis? *Ann. Intern. Med.* **102,** 182–186.
20 Siracusa, L. D., McGrath, R., Ma, Q., Moskow, J. J., Manne, J., Christner, P. J., et al. (1996) A tandem duplication within the fibrillin 1 gene is associated with the mouse tight skin mutation. *Genome Res.* **6,** 300–313.
21 Denton, C. P., Zheng, B., Shiwen, X., Zhang, Z., Bou-Gharios, G., Eberspaecher, H., et al. (2001) Activation of a fibroblast-specific enhancer of the proalpha2(I) collagen gene in tight-skin mice. *Arthritis Rheum.* **44,** 712–722.
22 Korngold, R. and Sprent, J. (1991) Graft-vs-host disease in experimental allogeneic bone marrow transplantation. *Proc. Soc. Exp. Biol. Med.* **197,** 12–18.
23. Sheehan, D. and Hrapchak, B. (1980) *Theory and Practice of Histotechnology*, 2nd ed., Battelle Press, Columbus, OH, pp. 189–191.
24 Kolb, M., Bonniaud, P., Galt, T., Sime, P. J., Kelly, M. M., Margetts, P. J., et al. (2002) Differences in the fibrogenic response after transfer of active transforming growth factor-beta1 gene to lungs of "fibrosis-prone" and "fibrosis-resistant" mouse strains. *Am. J. Respir. Cell Mol. Biol.* **27,** 141–150.
25 Johnston, C. J., Wright, T. W., Rubin, P., and Finkelstein, J. N. (1998) Alterations in the expression of chemokine mRNA levels in fibrosis-resistant and -sensitive mice after thoracic irradiation. *Exp. Lung Res.* **24,** 321–337.
26. Yamamoto, T., Kuroda, M., and Nishioka, K. (2000) Animal model of sclerotic skin. III: Histopathological comparison of bleomycin-induced scleroderma in various mice strains. *Arch. Dermatol. Res.* **292,** 535–541.

21

Rodent Models of Experimental Autoimmune Uveitis

Rajeev K. Agarwal and Rachel R. Caspi

Summary

The model of experimental autoimmune uveitis (EAU) in mice and in rats is described. EAU targets immunologically privileged retinal antigens and serves as a model of autoimmune uveitis in humans as well as a model for autoimmunity in a more general sense. EAU is a well-characterized, robust, and reproducible model that is easily followed and quantitated. It is inducible with synthetic peptides derived from retinal autoantigens in commonly available strains of rats and mice. The ability to induce EAU in various gene-manipulated, including HLA-transgenic, mouse strains makes the EAU model suitable for the study of basic mechanisms as well as in clinically relevant interventions.

Key Words: Autoimmunity; EAU; IRBP; S-Ag; T cells; Th1; Th2; tolerance; uveitis; uveoretinitis.

1. Introduction

Experimental autoimmune uveitis (EAU) is an organ-specific, T-cell-mediated autoimmune disease that targets the neural retina and related tissues; it is induced by immunization with retinal antigens ***(1–3)***. The pathology of EAU closely resembles human uveitic diseases of a putative autoimmune nature in which patients display immunological responses to retinal antigens. Examples of such diseases, which have similar pathology to EAU and in which patients frequently have circulating lymphocytes that respond to retinal proteins, are sympathetic ophthalmia, birdshot retinochoroidopathy, Behcet's disease, and others ***(4,5)***. In the United States alone, there are approx 70,000 cases of uveitis per year, and autoimmune uveitis is estimated to account for approx 10% of severe vision loss.

Although none of the animal models mimics all the features of human disease, each has distinguishing characteristics reminiscent of different aspects of clinical uveitis. Even if the retinal antigens that might be involved in human

From: *Methods in Molecular Medicine, Vol. 102: Autoimmunity: Methods and Protocols*
Edited by: A. Perl © Humana Press Inc., Totowa, NJ

uveitis have not been definitively identified, many uveitis patients respond to the retinal soluble antigen (S-Ag, arrestin) and to a lesser extent to other retinal antigens.

The EAU model has served as an invaluable tool to evaluate novel immunotherapeutic and conventional therapeutic strategies. The EAU model is also useful for study of basic mechanisms of tolerance and autoimmunity to organ-specific antigens in immunologically privileged sites ***(5)***. Thus, EAU is useful as a tool for clinical and for basic studies of ocular and organ-specific autoimmunity.

EAU can be induced in susceptible animals by peripheral immunization with a number of evolutionarily well-conserved uveitogens (purified protein antigens extracted from the retina or their peptides) in adjuvant or by adoptive transfer of lymphocytes specific to these antigens ***(2,5,6)***. In many cases, the sequence of these proteins is known, and the pathogenic fragments have been identified. The majority of the studies have been performed using heterologous bovine antigens because autologous rat or mouse retinal proteins cannot be obtained in sufficient quantities. Uveitogenic retinal proteins are molecules with homologues that can be found as far down the phylogenetic scale as the invertebrates ***(7–9)***. The uveitogenic retinal proteins identified so far are as follows:

1. S-Ag, arrestin. This 48-kDa intracellular photoreceptor protein is involved in the phototransduction cascade. It binds to photoactivated-phosphorylated rhodopsin, thereby apparently preventing the transducin-mediated activation of phosphodiesterase ***(10)***.
2. Interphotoreceptor retinoid-binding protein (IRBP). This 148-kDa protein is found in the interphotoreceptor matrix, which helps in transporting vitamin A derivatives between the photoreceptor and the retinal pigment epithelium. IRBP is composed of four evolutionary conserved homologous domains, which are thought to have arisen by gene duplication ***(8)***.
3. Rhodopsin and its illuminated form, opsin. This 40-kDa membrane protein is the rod visual pigment ***(7)***. Pathogenicity of this protein appears to be conformation dependent as rhodopsin is more pathogenic than opsin ***(11)***.
4. Recoverin, which is a 23-kDa calcium-binding protein.
5. Phosducin, which is 33-kDa soluble cytosolic photoreceptor protein.

Susceptibility to EAU is genetically controlled. It has been observed that different species, and strains within species, vary in their susceptibility. Thus, rats develop EAU after immunization with either S-Ag or IRBP. Guinea pigs are susceptible to S-Ag, but not to IRBP, and mice develop severe disease with IRBP, but not with S-Ag.

Within each species, there are susceptible and resistant strains. In mice and in rats, both major histocompatibility complex (MHC) and non-MHC gene

control have been implicated ***(12,13)***. MHC control is likely connected to the ability to bind and present uveitogenic epitopes. Non-MHC control is more complex and controlled by multiple genetic pathways that are not all defined.

One important factor is the type of effector response that a given strain is genetically programmed to mount. Strains that are dominant Th1 responders tend to be susceptible, whereas strains that are genetically low Th1 responders (e.g., AKR mouse, F344 rat) or overt Th2 responders (e.g., BALB/c mouse) tend to be resistant ***(14,15)***. Furthermore, skewing of the response toward a Th2-like phenotype, such as by treatment with the regulatory cytokines interleukin (IL)-4 and IL-10, can ameliorate EAU ***(16)***. Another factor is different levels of expression of retinal antigens in the thymus, provoking efficient central tolerance to antigens expressed in "adequate" amounts ***(17)***. Other factors, including the hypothalamus–pituitary–adrenal axis control and the number of mast cells in the eye, have also been implicated ***(18,19)***. Genetic control of clinical and experimental uveitis has been reviewed ***(20)***.

Although in many clinical diseases and in some autoimmunity models there is a gender bias of susceptibility, in EAU there does not seem to be an obvious difference in susceptibility between males and females. However, reduced susceptibility is seen in pregnant females ***(21)*** and in animals harboring an active infection (R. Caspi et al., unpublished). Both phenomena may be connected to the cytokine milieu elicited by the physiological state of the individual. Pregnant mice were found to have elevated transforming growth factor (TGF)-β levels ***(21)***, and infection elicits production of interferon (IFN)-γ, which has a protective role in tissue-specific autoimmunity, including EAU ***(22)***. There are no controlled studies of age dependency of susceptibility. We used animals between ages 6 wk and 8 mo without any noticeable differences in disease development (R. Caspi et al., unpublished observations).

EAU in many poorly susceptible strains can be enhanced by treatment with *Bordetella pertussis* in the form of heat-killed bacteria or, better yet, as purified pertussis toxin (PT), concurrent with immunization. This is similar to other autoimmune disease models, such as experimental autoimmune encephalomyelitis. Administration of PT concurrent with uveitogenic immunization permits expression of disease in resistant strains and enhances it in susceptible strains ***(14,23,24)***. The mechanism has for a long time been thought to involve the opening of the blood–organ barrier by PT ***(25,26)***; however, recently we showed that a dominant effect of PT in EAU is to enhance the Th1 response ***(14,23)***. This effect is at least in part because of maturation of dendritic cells by PT ***(15)*** and is mediated by the B subunit of PT ***(27)***. It is important to point out that PT can have strong inhibitory effects on disease as well if it is present at the time of cell migration to the target organ because of its inhibitory effects on chemokine receptor signaling through G protein inhibition ***(28)***. Therefore, not only the

timing of PT administration, but also the amount administered are important because excess PT administered at the time of immunization will persist into the effector stage of the disease and inhibit its expression ***(29)***.

In mice and in rats, EAU induced with the different uveitogenic proteins or their peptides appears to share essentially the same immunological mechanisms and histological features; however, there are species-specific and strain-specific differences in the course of disease ***(1,3,5,30,31)***. The type, number, and size of lesions serve as a basis for a semiquantitative grading system used to score disease severity. A degree of familiarity with ocular histology is needed to grade the disease in a specific fashion. In practice, disease scores assigned by different observers will not always be identical; however, when performed by the same person, grading should be consistent.

Although originally developed in the guinea pig, the two major EAU models in use today are the mouse and the rat. Each has its unique advantages. The mouse is immunologically well characterized, and many congenic and gene-manipulated strains are available that permit sophisticated studies of basic immunological mechanisms. The rat's larger size permits therapeutic and surgical manipulations that are more difficult to do in the mouse; traditionally, the rat is the preferred model for endocrine and physiological studies. More specific attributes of EAU in the rat and mouse models are described in **Subheading 3.** EAU models in the guinea pig, the rabbit, and the monkey have been reviewed elsewhere ***(1,5,32)***. The choice of model will therefore depend on the specific needs of the study.

The methods and descriptions in this chapter deal with the rat and the mouse models of EAU induced by defined synthetic peptides of retinal antigens. Synthetic peptides were chosen because they can be synthesized in every laboratory and do not require access to native retinal antigens from natural or recombinant sources. Last, **Subheading 4.** contains general information and troubleshooting information.

2. Materials

1. Mice (B10.RIII and C57BL/6) (Jackson Laboratories, Bar Harbor, ME).
2. Lewis rats (Charles River Laboratories, Wilmington, MA).
3. Pertussis toxin (cat. no. P-7208, Sigma, St. Louis, MO).
4. IRBP and S-Ag peptides.
5. Dulbecco's modified Eagle's medium (DMEM) and RPMI-1640 (Hyclone Laboratories, Logan, UT).
6. L-Glutamine, sodium pyruvate, nonessential amino acids, gentamicin (Invitrogen, Carlsbad, CA) as medium additives.
7. Fetal bovine serum (FBS; Gemini Bio-Products, Woodland, CA).
8. Freund's complete adjuvant (FCA) and *Mycobacterium tuberculosis* (Difco, Detroit, MI).

Table 1
Susceptibility to EAU of Some Inbred Rat Strains[a]

Strain	MHC	Susceptibility	Antigen	Reference
Lewis	$RT1^{l}$	High	S-Ag, IRBP	***(3,18)***
F344	$RT1^{lv1}$	Low	S-Ag, IRBP peptide R16	***(3,18,29)***
CAR	$RT1^{l}$	High	S-Ag	***(3,18)***
BN	$RT1^{n}$	Low[c]	S-Ag	***(5)***
PVG	$RT1^{c}$	High	S-Ag	***(37)***

[a]Please see other references for more detailed list ***(39,40)***.
[b]Resistance of this strain may vary in different colonies ***(18)***.
[c]Resistance is not overcome by PT treatment.

9. 10% glutaraldehyde (Fisher Scientific, Fair Lawn, NJ) solution was prepared in phosphate-buffered saline (PBS).
10. 10% phosphate-buffered formaldehyde (Fisher Scientific, Fair Lawn, NJ).
11. Ophthalmic dilating solutions: 1% tropicamide (Alcon Laboratories Inc., Fort Worth, TX) and phenylephrine (Akron Inc., Buffalo Grove, IL) for fundus examination procedure.
12. Sterile eye-irrigating physiological solution (Ciba Vision Ophthalmics, Atlanta, GA).

3. Methods

3.1. EAU in Rats

The model of EAU, originally established in the guinea pig using homologous uveal tissue ***(33–35)***, was adapted to the rat in 1973 by Wacker and Kalsow ***(36)*** using whole retinal extracts and was subsequently refined by de Kozak et al. using the retinal S-Ag ***(37)***. IRBP was shown to be uveitogenic in rats ***(38)***.

Susceptibility of EAU varies among different rat strains. The strain most commonly used for EAU studies is the Lewis rat. In the Lewis rat, the disease is monophasic, which develops characteristically severe uveitis and has served as a "standard" against which responses of other strains are compared. It appears that both MHC and non-MHC genes play a role ***(12)***; however, because of the limited availability of congenic and MHC-recombinant rat strains, their relative effects have not been well separated. **Table 1** summarizes the susceptibility of some common inbred rat strains to EAU induced with the native S-Ag or IRBP. A more detailed list has been published elsewhere ***(39,40)***.

The retinal uveitogenic proteins have historically been defined as such in the Lewis rat model, the most highly susceptible rat strain known. The normal

dose is 30–50 μg of S-Ag or IRBP or 50–100 μg of rhodopsin emulsified in FCA. Lewis rats do not require PT as part of the immunization protocol to develop disease, but if used, PT will cause earlier onset and enhanced disease scores. The immunizing protocol of 30 μg of peptide R16 of bovine IRBP (**Table 2**) in FCA normally results in disease onset on day 9 or 10. In contrast, immunization with 30 μg of S-Ag in FCA usually results in onset between days 12 and 14. Other strains may require PT as an additional adjuvant. Subcutaneous immunization in the thighs and base of the tail with an emulsion of S-Ag or IRBP in FCA was as good or better than the footpad route for induction of disease ***(41)***.

Table 2 shows the commonly used epitopes found consistently pathogenic in the Lewis strain. The peptides that are pathogenic at low doses are considered to contain a major pathogenic epitope.

3.1.1. Induction of EAU in the Lewis Rat by Active Immunization

The Lewis rat strain is highly susceptible to EAU. (In strains that are less susceptible, such as the F344, PT must be used as an additional adjuvant, and a higher dose of antigen is recommended.) Two peptides are recommended as strongly and consistently uveitogenic in the Lewis rat: peptide R16 of bovine IRBP (residues 1177–1191, sequence ADGSSWEGVGVVPDV) and peptide S35 of human S-Ag (residues 341–360, sequence GFLGELTSSEVATEVP FRLM). S35 tends to cause stronger disease, but onset is a day or two later than with R16.

1. Use 6- to 8-wk-old female Lewis rats (preferably housed in specific pathogen-free environment) with food and water *ad libitum*. If rats are procured from an outside vendor, it is best to acclimate them for a few days before immunization.
2. Prepare an emulsion of the chosen peptide: 30 μg of R16 or S35 in FCA (1:1 v/v) (**Support Protocol 3.3.3.**) by sonication to provide 30 μg of peptide in 200 μL per rat. Spin at 900*g* to remove any air bubbles embedded in the emulsion. A well-prepared emulsion should have the consistency of thick cream.
3. A 16-ga blunt-end needle is used to draw the emulsion into a 1-mL glass syringe, preferably with a Luer lock tip (rubber plungers in plastic syringes tend to soften and stick because of the oil in FCA). Carefully remove any residual air bubbles trapped in the syringe. Change to a 23-ga needle and subcutaneously inject 100 μL at the base of the tail and 50 μL in each thigh.
4. At 7–9 d after immunization, start inspecting the eyes with a flashlight for loss of red reflex (**Fig. 1**). Grade the disease on a scale of 0 (no disease) to 4 (severe disease) based on the scoring method in **Table 3**.
5. Approximately 16 d after immunization (or at least 7 d after onset of the disease), euthanize the rats. Remove the eyes and process them for histopathology (**Support Protocol 3.3.2.**).
6. Examine the hematoxylin- and eosin-stained sections under a microscope and grade the disease histopathologically following the guidelines listed in **Table 4**.

Table 2
Retinal Protein-Derived Peptides Pathogenic for Lewis Rats[a]

Source	Nickname (if any)	Position[b]	Amino acid sequence[c]	Minimal dose[d]	Reference
Bovine S-Ag	Peptide N	281–302 (287–297)	VPLLANNRERRGIALDGKIKHE	50 μg	***50***,***51***
	Peptide M	303–320 (303–317)	DTNLASSTIIKEGIDKTV	50 μg	***52***
Bovine IRBP	R23	1091–1115	PNNSVSELWTLSQLEGERYGSKKSM	100 n*M* (280 μg)	***53***
	R4	1158–1180	HVDDTDLYLTIPTARSVGAADGS	67 μg	***54***
	R14	1169–1191(1182–1190)	PTARSVGAADGSSWEGVGVVPDV	0.1 n*M* (0.2 μg)	***6***,***55***
	R16	1177–1191 (1182–1190)	ADGSSWEGVGVVPDV	0.1 n*M* (0.2 μg)	***6***
Human S-Ag	Peptide 19	181–200	VQHAPLEMGPQPRAEATWQF	25 μg	***56***
	Peptide 35	341–360 (343–356)	GFLGELTSSEVATEVPFRLM	5 μg	***56***,***57***
	Peptide 36	351–370 (356–366)	VATEVPFRLMHPQPEDPAKE	50 μg	***56***,***58***
Human IRBP	H-IRBP 715	521–540 (527–534)	YLLTSHRTATAAEEFAFLMQ[e]	0.1 μg	***59***

[a]More detailed list of other peptides pathogenic to Lewis rats can be found elsewhere ***(39***,***40)***.
[b]Parenthetical numbers indicate position of minimal sequence (if known).
[c]The minimal pathogenic sequence (if known) is underlined.
[d]Pathogenicity was tested in most cases using PT as an additional adjuvant ($1–2 \times 10^{10}$ heat-killed organisms per rat).
[e]An additional epitope may be encoded by the N-terminus (sequence YLLTSHRTATAA).

Table 3
Clinical Grading of EAU in the Rat

Grade[a]	Criteria
0	No disease; eye is translucent and reflects light (red reflex)
0.5 (trace)	Dilated blood vessels in the iris
1	Engorged blood vessels in iris; abnormal pupil contraction
2	Hazy anterior chamber; decreased red reflex
3	Moderately opaque anterior chamber, but pupil still visible; dull red reflex
4	Opaque anterior chamber and obscured pupil; red reflex absent; proptosis

[a]Each higher grade includes the criteria of the preceding one.

Table 4
Scoring EAU Histopathologically in the Rat

Grade	Area of retinal section affected	Criteria
0	None	No disease; normal retinal architecture
0.5 (trace)	<1/4	Mild inflammatory cell infiltration of the retina with or without photoreceptor damage
1	≥1/4	Mild inflammation and/or photoreceptor outer segment damage
2	≥1/4	Mild-to-moderate inflammation and/or lesion extending to the outer nuclear layer
3	≥1/4	Moderate-to-marked inflammation and/or lesion extending to the inner nuclear layer
4	≥1/4	Severe inflammation and/or full-thickness retinal damage

3.1.2. Induction of EAU in the Lewis Rat by Adoptive Transfer

EAU is a $CD4^+$ T-cell-mediated disease. The full histopathological picture can be obtained by adoptive transfer of immune lymph node or spleen cells or long-term $CD4^+$, MHC class II-restricted T-cell lines in the absence of detectable titers of serum antibodies ***(2,42)***. The cells must be activated with antigen or mitogen just prior to transfer to mediate disease efficiently, suggesting that

activation-dependent functions (lymphokine production, expression of adhesion molecules, etc.) are important. The minimal number of cells required to transfer the disease depends on their source and specificity ***(2,42,43)***. The following protocol describes induction of disease using primary cultures of lymph node cells and peptide antigen.

1. Rats to be used as cell donors are immunized as mentioned in **Subheading 3.1.1.** The donor rats are sacrificed 10–12 d postimmunization, and draining lymph nodes (inguinal and iliac) are harvested and cultured with the immunizing peptide as follows.
2. Keep isolated lymph nodes in RPMI-1640 media containing 1% FBS or rat serum. Prepare single-cell suspension by crushing the nodes using a plunger from a disposable plastic syringe on a sterile mesh in a Petri dish, with some sterile media to release the cells.
3. Transfer the cells to a 50-mL centrifuge tube and wash the Petri dish with additional media. Spin the cells at 300*g* and discard the supernatant. Resuspend the pellet in fresh media and repeat the washing procedure one or two times. Resuspend the final cell pellet in a small volume of RPMI-1640 media containing 1% FBS.
4. Count viable cells using an exclusion dye such as trypan blue.
5. Adjust the cell suspension to 5×10^6 cells/mL by adding complete RPMI media (**Support Protocol 3.3.4.**). Add the peptide used for immunization of the cell donors (R16 or S35) to a final concentration of 5 μg/mL.
6. Distribute 2-mL aliquots into 12-well tissue culture plates and incubate the culture at 37°C for 3 d in 5% CO_2 tissue incubator.
7. After 72 h, collect, wash, and count the cells (as described in **Subheading 3.1.2.**, **steps 3** and **4**). All procedures are preferably done using RPMI-1640 media with 1% serum for maximal cell viability.
8. Inject to $30–50 \times 10^6$ cells (in 0.3 to 0.5 mL) intraperitoneally into recipient Lewis rats.
9. Starting on day 3 after adoptive transfer, inspect the recipients for disease by examining the eyes with a flashlight for loss of red reflex (**Fig. 1**) and grade the disease as described in **Table 3**.
10. Between 11 and 14 d after adoptive transfer (around 7 d after disease onset), euthanize the rats, collect the eyes (**Support Protocol 3.3.2.**) and process them for histopathological grading of EAU according to **Table 4**.

3.1.3. Expected Course of Disease

The course of disease in the Lewis rat is typically acute and short. The time of onset will vary depending on severity of the developing disease, the antigen, and the antigen dose. S-Ag and its peptides tend to give more severe disease but a later onset than IRBP and its peptides. For instance, 30 μg of S35 peptide in FCA without PT results in onset around days 12–14, and a similar dose of R16 in FCA without PT results in onset around days 10–12. If pertussis is used

as additional adjuvant, the time of onset will be shortened by 2 d and will usually be more uniform than without pertussis. The amount of antigen used to elicit disease can be reduced severalfold if PT is used.

Onset of EAU induced by adoptive transfer is usually on days 4–7 (i.e., about a week earlier than for active immunization). The active EAU in the Lewis rats lasts 1–2 wk, and the disease does not relapse. The rapid onset and acute course of EAU in the Lewis rat makes it difficult to evaluate therapeutic intervention during active disease. Alternatively, to look at efferent stage disease, begin intervention 7 d after immunization, when immune lymphocytes are already present, or use an adoptive transfer system.

3.1.4. Quantitation

3.1.4.1. Clinical

Onset of disease in the albino Lewis rat can be recognized by inspecting the eyes with the aid of a good flashlight (**Fig. 1**). The normal eye appears translucent and reflects the light (red reflex). The first sign of uveitis is engorgement of blood vessels in the iris and an irregular pupil that cannot contract in response to light (caused by the iris adhering to the lens). Leukocyte infiltration and deposition of fibrin is first seen as dulling of the red reflex, progressing to complete opacification of the anterior chamber. The eye swells and can protrude from its socket (proptosis). In very severe cases, hemorrhages in the anterior chamber and even perforation of the cornea can occur. In the last case, the animal should be euthanized. We grade clinical EAU on a scale of 0 (no disease) to 4 (severe disease) using the criteria listed in **Table 3**.

3.1.4.2. Histopathology

EAU is defined primarily as a posterior segment disease because the target antigens reside in the retina. Lewis rats can develop very severe anterior chamber inflammation, which can lead to corneal perforation. Therefore, although clinical follow-up by anterior chamber inflammation is important and yields valuable information, the final readout should be recorded by histopathology. We grade EAU by histopathology based on number and extent of lesions and use an arbitrary scale of 0 (none) to 4 (maximum severity), in half-point increments, as shown in **Table 4** ***(40)***. Typical EAU vs normal histology is shown in **Fig. 3**. Although Fig. 3 shows EAU histopathology in the mouse, it is representative of that seen in the rat.

3.2. EAU in Mice

Mice are highly resistant to EAU induction with S-Ag, but some strains can develop severe EAU after immunization with IRBP ***(31)***. As in rats, age and

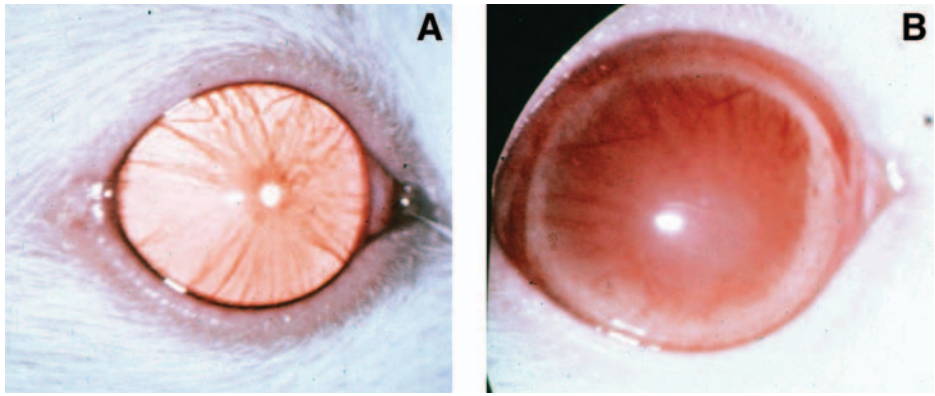

Fig. 1. Clinical appearance of EAU in the Lewis rat by anterior chamber examination. **(A)** Normal eye; translucent appearance; pupil and iris blood vessels are clearly visible, and the vessels are not congested. **(B)** Uveitic eye; the eye appears larger because of swelling and proptosis; red reflex is absent, and pupil is obscured.

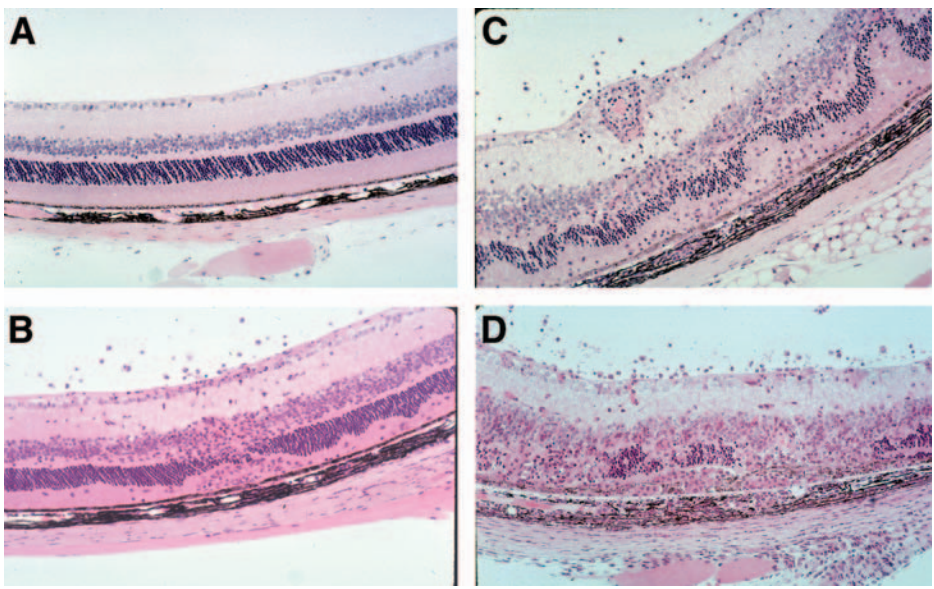

Fig. 3. Histopathology of EAU in the B10.RIII mouse. **(A)** No disease (score 0); note well-preserved photoreceptor cell layer. **(B)** Mild disease (score 1–2). **(C)** Moderate disease (score 2–3). **(D)** Severe disease (score 3–4). EAU in the rat shows essentially the same type of histopathology.

Table 5
Susceptibility of Different Mouse Strains to IRBP EAU[a]

Strain	H-2	Susceptibility[b]	Epitope, position, and reference
B10.RIII	r	Very high	SGIPYIISYLHPGNTILHVD (161–180) ***(46)***
B10.A	a (I-A^k)	High	ADKDVVVLTSSRTGGV (201–216) ***(45)***
B10.BR	k	High	Same as B10.A
A/J	a (I-A^k)	Medium	Same as B10.A
C57BL/6	b	Medium	GPTHLFQPSLVLDMAKVLLD (1–20) ***(44)***
C57BL/10	b	Medium	Same as C57BL/6

[a]More detailed list of other mouse strains can be found elsewhere ***(39)***.
[b]Mice were immunized by the split-dose method with 100 μg IRBP in FCA in the footpads and were given 1 μg of PT intraperitoneally. Eyes were harvested at 5 weeks. Adapted from Caspi et al. ***(13,22)***.

sex do not appear to have a major influence on susceptibility to disease. **Table 5** lists some common EAU-susceptible mouse strains and IRBP epitopes that have been found to induce disease in each.

The epitopes of the IRBP molecule pathogenic for the H-2^b, H-2^r, and H-2^k haplotypes have been identified ***(44–46)***. In the B10.A mouse (K^k, A^k, E^k, D^d), MHC control of susceptibility has been tentatively mapped to the I-A region, with modifying influences from the I-E region ***(13)***. In addition to a susceptible H-2 haplotype, which can bind and present the uveitogenic epitopes, the strain must also have a "permissive" background to express disease. Studies with MHC-congenic mice showed that a nonpermissive background can completely prevent expression of disease in mice with a "susceptible" H-2. Known susceptible H-2 haplotypes include $H2^r$, H-2^k, H-2^a (shares class II subregion with H-2^k), H-2^b, H-2^q, and H-2^d. The last two, initially thought to be resistant, can in fact be shown to be EAU susceptible when IFN-γ is neutralized or knocked out (***22*** and R. Grajewski and R. Caspi, unpublished, 2003).

The most susceptible mouse strain currently known is B10.RIII (H-2^r). Unlike other mouse strains, this strain does not require PT to develop disease by active immunization either with IRBP or with its major pathogenic epitope, residues 161–180 of human IRBP. B10.RIII does, however, require PT if the murine sequence of peptide 161–180 is used. This is likely because of thymic elimination of high-affinity T cells reacting with the endogenous version of peptide 161–180 (***46a***). In less-susceptible mouse strains, such as B10.A or C57BL/6, a higher dose of IRBP (50–150 μg) or of the peptide appropriate for the haplotype in FCA is injected subcutaneously concurrent with PT (0.5 μg) given intraperitoneally.

One of the strengths of the mouse model of EAU is the ready availability of many gene-manipulated mouse strains. Knockouts and transgenics for various immunologically relevant genes have been, and continue to be, instrumental in unraveling the basic mechanisms in uveitis. EAU can be induced with human IRBP residues 1–20 in mice of the H-2^b haplotype, which is expressed by the C57BL/6 and 129 strains, that typically serves for production of transgenics and knockouts ***(44)***.

It is also important to mention here one newly established model, the "humanized" EAU model in HLA class II transgenic mice. Uveitic diseases in humans show strong associations with specific HLA class I or class II alleles, which vary depending on the disease and the population studied. The genetic associations in uveitis have recently been reviewed ***(20)***. MHC association strongly supports a role for antigen presentation by HLA molecules in the etiology of uveitis. HLA class I and II transgenic mice afford a model to study these effects. Both HLA class I (A29) and class II transgenic (DR3, DR4, DR2, DQ6, DQ8) mice have been used to study uveitis. HLA A29 transgenics develop a spontaneous uveitis ***(47)***, whereas the various class II transgenic mice develop EAU after immunization with IRBP ***(48)***. Importantly, HLA-DR3 transgenic mice develop severe uveitis after immunization with S-Ag, which is thought to be involved in human uveitis but is not uveitogenic in wild-type mice. These humanized models support an etiological role for retinal antigens, which are uveitogenic in animals, in human uveitis and validate use of the EAU model for the study of human disease.

3.2.1. Induction of EAU in the B10.RIII Mouse by Immunization

The following protocol is given for B10.RIII mice, the most susceptible mouse strain currently known. Human IRBP peptide 161–180 is used. This peptide does not require PT as part of the immunization protocol, although PT will promote more severe disease and an earlier onset ***(23)***. A variation of the protocol is given for use in C57BL/6 mice.

1. Use 6- to 8-wk-old female B10.RIII mice ($H2^r$), preferably housed under specific pathogen-free conditions with food and water available *ad libitum*. If purchased from an outside vendor, let acclimate to animal facility for a few days before immunization.
2. Emulsify IRBP peptide 161–180 (*see* sequence in **Table 5**) in FCA (1:1 v/v) by sonication to provide 10–25 μg peptide in 0.2 mL emulsion per mouse. Severity of disease obtained will depend on the amount of peptide used ***(23)***. Spin at 900*g* to remove air bubbles trapped in the emulsion. A well-prepared emulsion has the consistency of thick cream.
3. Use a 16-ga blunt-end needle to draw the emulsion in a 1-mL glass syringe with a Luer lock tip (rubber plungers in plastic syringes tend to soften and stick

Table 6
Clinical Scoring of EAU in the Mouse

Grade	Criteria
0	No change
0.5 (trace)	Few (1–2) very small, peripheral focal lesions; minimal vasculitis/ vitritis
1	Mild vasculitis; <5 small focal lesions; ≤1 linear lesion
2	Multiple (>5) chorioretinal lesions and/or infiltrations; severe vasculitis (large size, thick wall, infiltrations); few linear lesions (<5)
3	Pattern of linear lesions; large confluent lesions; subretinal neovascularization; retinal hemorrhages; papilledema
4	Large retinal detachment; retinal atrophy

because of the oil in FCA). Carefully remove any air bubbles trapped in the syringe. Change to a 23-ga needle and inject each mouse subcutaneously with 0.2 mL emulsion, dividing the dose among the two thighs (50 μL each) and base of the tail (100 μL).

4. At 12 d postimmunization, monitor the eyes of these mice for disease induction by inspecting the fundus under a binocular microscope (**Support Protocol 3.3.1.**). Grade the animals on a scale of 0 (no disease) to 4 (severe disease) using the criteria described in **Table 6**.
5. Approximately 21 d after immunization (or 7 d after the disease onset), euthanize the mice and remove eyes for histopathology (**Support Protocol 3.3.2.**).
6. Examine the hematoxylin- and eosin-stained sections under a microscope and grade the disease histopathologically following the guidelines in **Table 7**.

3.2.2. Alternative Protocol: Induction of EAU in the C57BL/6 Mouse by Immunization

1. Use 6- to 8-wk-old female C57BL/6 mice ($H2^b$), preferably housed under specific pathogen-free conditions with food and water available *ad libitum*. If purchased from an outside vendor, let acclimate to animal facility for a few days before immunization.
2. Emulsify human IRBP peptide 1–20 (*see* sequence in **Table 5**) in FCA (1:1 v/v) by sonication to provide 200–300 μg peptide in 0.2 mL emulsion per mouse. Severity of disease obtained will depend on the amount of peptide used ***(44)***. Spin at 900*g* to remove air bubbles trapped in the emulsion. A well-prepared emulsion has the consistency of thick cream.
3. Prepare PT as adjuvant. Pertussis bacteria are not as potent as the purified toxin. If reconstituting a lyophilized preparation, bring up in PBS to 1 mg/mL or another convenient concentration with 1% mouse serum. The serum serves to prevent

Table 7
Grading EAU Histopathologically in the Mouse

Grade	Criteria
0	No change
0.5 (trace)	Mild inflammatory cell infiltration; no tissue damage
1	Infiltration; retinal folds and focal retinal detachments; few small granulomas in choroid and retina, perivasculitis
2	Moderate infiltration; retinal folds, detachments, and focal photo receptor cell damage; small-to-medium-size granulomas, perivas culitis, and vasculitis
3	Medium-to-heavy infiltration; extensive retinal folding with detachments, moderate photoreceptor cell damage; medium-size granulomatous lesions; subretinal neovascularization
4	Heavy infiltration; diffuse retinal detachment with serous exudate and subretinal bleeding; extensive photoreceptor cell damage; large granulomatous lesions; subretinal neovascularization

adsorption of the PT to plastic and glass tubes, pipets, and syringes. The stock solution can be kept at 4°C for up to 1 mo. For injection, prepare solution of 5 μg/mL just before use by diluting 1:20 in PBS with 1% syngeneic serum (0.1 mL will result in a dose of 0.5 μg).

4. Proceed as described in **Subheading 3.2.1.** for the B10.RIII mouse, starting from **step 3**.

3.2.3. Induction of EAU in B10.RIII or C57BL/6 Mice by Adoptive Transfer

Adoptive transfer of primed uveitogenic effector cells, just like in rats, can induce EAU in mice. Primary cultures from immunized donors, as described in the protocol in this section, can be used as a source of effector cells. Alternatively, long-term antigen-specific T-cell lines, which are typically $CD4^+$ cells of the Th1 phenotype, can be derived from draining lymph node cells of IRBP- or peptide-immunized mice ***(46)***.

1. Immunize donor mice as described in **Subheading 3.2.1.** and **3.2.2.** using peptide 161–180 of human IRBP for B10.RIII mice and peptide 1–20 of human IRBP for C57BL/6 mice, respectively.
2. After 10–14 d, harvest draining lymph nodes (inguinal and iliac) as well as spleens from donor mice.
3. Place isolated lymph nodes and spleens in DMEM media containing 1% FBS or mouse serum. Prepare a single-cell suspension (lymph nodes and spleen) by disrupting the spleens and the lymph nodes using a sterile rubber plunger from a

disposable plastic syringe on a sterile mesh in a Petri dish with some sterile media to release the cells.
4. Pool the suspensions of lymph node cells and of splenocytes and transfer to 50-mL centrifuge tubes. Wash the cells by centrifuging at 300*g*. Discard the supernatant and resuspend the pellet in fresh media. Repeat the washing one or two times. Resuspend the final cell pellet in a small volume of DMEM media containing 1% serum to maintain maximal viability of the cells.
5. Take a small aliquot and count the viable cells using a vital dye such as trypan blue.
6. Adjust the cell concentration to 10×10^6 live cells/mL in complete DMEM media (**Support Protocol 3.3.4.**) containing 20–25 μg/mL of the immunizing peptide. Optionally, including 5 ng/mL of IL-12 in the culture will result in a more highly Th1-polarized population that will transfer disease with fewer cells ***(44)***.
7. Distribute 150-mL aliquots into 175-cm^2 tissue culture flasks and incubate for 3 d in a humidified 37°C tissue incubator with 10% CO_2.
8. Important: After 24 h and again after 48 h of culture, bring the nonadherent cells into suspension by gently rocking the flasks and transfer the entire suspension to a new flask of the same size. This gets rid of excess (adherent) macrophages that produce inhibitory factors.
9. After 72 h of culture, collect, wash, and count the viable cells. There usually are many dead cells in the culture at this point. Purifying the cells by centrifugation over Ficoll (Lympholyte M, Accurate Biochemicals, Westbury, NY) can help obtain a more pure population of live cells and facilitate counting. Suspend the counted cells in DMEM media with 1% normal serum.
10. Inject cells intraperitoneally into syngeneic recipients in a volume of 0.5 mL or less. For B10.RIII mice, inject $30–50 \times 10^6$ cells. For recipient C57BL/6 mice, inject $50–100 \times 10^6$ cells. If IL-12 was used during culture, this number may be reduced.
11. Starting 4 d after adoptive transfer, inspect the recipients for disease induction by fundus examination (*see* **Support Protocol 3.3.1.**).
12. Between 12 and 14 d after adoptive transfer (at least 7 d after disease onset), euthanize the mice, collect the eyes, and process the eyes for histopathology. Score the eyes according to the criteria listed in **Table 7**.

3.2.4. Expected Course of Disease

The severity and clinical course of EAU induced with peptide 161–180 in B10.RIII mice is typically monophasic, resembling that for the Lewis rat, and lasts for 2–3 wk. High-intensity immunization results in an acute form of disease, with onset as early as day 8 or 9, and widespread photoreceptor damage, whereas a lower intensity immunization will result in milder disease with progressively later onset ***(23)***. In other strains (e.g., B10.A) it is possible to observe relapsing disease after a low-to-intermediate intensity protocol ***(49)***. As in the Lewis rat, the rapid onset and acute course of EAU induced with

peptide 161–180 in B10.RIII mice makes it difficult to evaluate therapeutic intervention during active disease. Alternatively, to look at efferent stage disease, begin intervention 7 d after immunization, when immune lymphocytes are already present, or use an adoptive transfer system.

3.2.5. Quantitation

3.2.5.1. Clinical

Unlike rats, in susceptible strains of mice (B10 background), black pigmentation of the eyes and an often mild involvement of the anterior chamber preclude detection of disease by anterior chamber examination. However, in pigmented strains, it is possible to observe changes in the fundus of the eye under a binocular microscope after dilating the pupil (**Support Protocol 3.3.1.**) (**Fig. 2**). Visualization of the fundus is possible if the anterior chamber does not become infiltrated with cells or after the infiltrate clears (usually within a few days after onset). The nature, number, and severity of the lesions are used as criteria for clinical scoring on a scale of 0 (no change) to 4 (severe disease) (**Table 6**).

3.2.5.2. Histopathology

Histological grading is the final readout of the disease and is performed on methacrylate-embedded tissue sections (**Support Protocol 3.3.2.**). Disease is scored on a scale of 0 (no disease) to 4 (maximum disease) in half-point increments according to a semiquantitative system described in **ref. *31***. Examples of various grades of pathology are shown in **Fig. 3**.

3.3. Support Protocols

3.3.1. Funduscopic Examination

Funduscopic examination can be used to detect and evaluate EAU in pigmented animals, provided that the anterior segment of the eye remains clear. In this procedure, the retina of the eye is examined through the dilated pupil under a microscope. Funduscopy is a good tool for determining the onset and clinical grading of disease in pigmented animals, but not in albinos. The following materials are used:

1. Ophthalmic dilating solutions: 1% tropicamide and phenylephrine.
2. Sterile physiological solution (either normal saline, PBS, or artificial tears).
3. Binocular microscope with coaxial illumination.
4. Microscope coverslip.

Anesthetize the animals and dilate the pupil with one to two drops of dilating solution. It takes several minutes for the medication to take effect. Place a

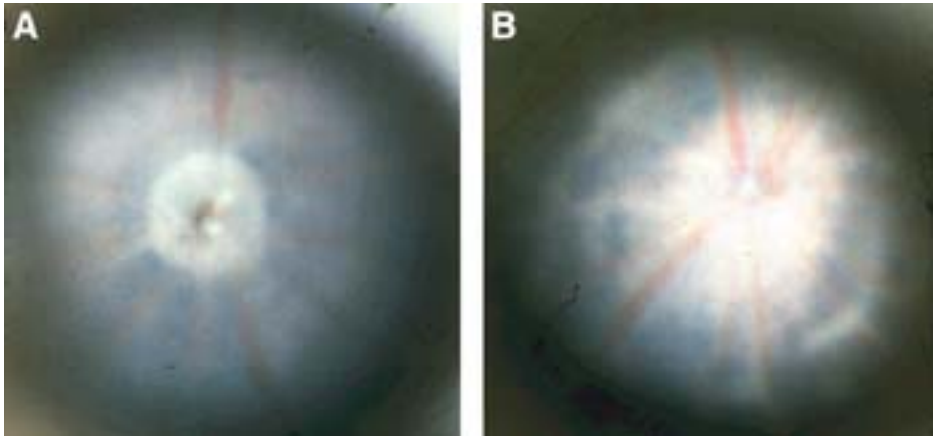

Fig. 2. Clinical appearance of EAU in the B10.A mouse by funduscopic exam. **(A)** Normal eye; note blood vessels radiating from the optic nerve head. **(B)** Uveitic eye; note retinal detachment obscuring the optic nerve head and numerous white linear lesions.

drop of sterile physiological solution and a microscope coverslip on the cornea to equalize refraction. Manipulate the head of the mouse under the microscope to inspect as far up the sides of the retina as possible. Look for engorged blood vessels, constricted blood vessels ("cuffing"), white linear lesions, subretinal hemorrhages, and retinal detachment. Typical appearance of a uveitic fundus is shown in **Fig. 2**. If you have difficulty in grading the disease, please *see* **Subheadings 4.1.** and **4.2.** for some possible reasons and solutions.

3.3.2. Handling of Eyes for Histopathology

Eyes should be collected within 15 min of euthanasia; otherwise, autolysis may preclude correct evaluation of the results. Enucleation in rats should be performed by carefully dissecting the globe from the periocular tissues and the optic nerve without applying pressure on the globe to avoid maceration of delicate ocular tissues, which become even more fragile when inflamed. In mice for enucleation, the eye should be made to protrude by applying pressure on the skull and plucked free of the tissue with a curved forceps.

Freshly enucleated eyes are fixed in 4% phosphate-buffered glutaraldehyde for 1 h and then transferred into 10% phosphate-buffered formaldehyde at least overnight or until processing. The brief fixation in 4% glutaraldehyde prevents artifactual detachment of the retina from the choroid. However, leaving the eyes in glutaraldehyde for too long will cause excessive hardening of the lens,

which will make sectioning difficult. The grading is conveniently done on methacrylate- or paraffin-embedded tissue sections cut up to 8 µ thick and stained with hematoxylin and eosin. To arrive at the final grading, several sections cut through the pupillary–optic nerve axis should be examined for each eye.

It should be remembered that, in this type of visual scoring, there is always an element of subjectivity. Therefore, it is important that the results be read in a masked fashion, preferably always by the same person. Whenever possible, both eyes should be evaluated for the disease as disease may be unilateral. If it becomes experimentally necessary to take only one eye, always collect the same eye to average out this random variation. Please *see* **Subheading 4.3.** for some potential problems and solutions.

3.3.3. Freund's Complete Adjuvant (FCA)

Using a porcelain mortar and pestle, 100 mg heat-killed *M. tuberculosis* (strain H37Ra) is crushed into a fine powder. Mix with 70 mL of FCA (1.0 mg/mL of *M. tuberculosis*). Store at 4°C until used. The suspension must be thoroughly mixed before each use as the mycobacterial particles settle quickly to the bottom.

3.3.4. Complete Medium for Cell Culture (RPMI-1640 or DMEM)

1. 500-mL bottle of RPMI-1640 or DMEM.
2. 50 mL FBS (10% final).
3. 5 mL 200 m*M* L-glutamine (2 m*M* final).
4. 5 mL 100 m*M* sodium pyruvate (1 m*M* final).
5. 5 mL 10 m*M* nonessential amino acids (0.1 m*M* final).
6. 0.5 mL 50 mg/mL gentamicin (50 µg/mL final).
7. 0.05 mL 0.5 *M* 2-mercaptoethanol (5 µ*M* final).

Filter though 0.2-µm filter and store up to 4 wk at 4°C.

4. Notes

1. Although the EAU model is very robust, problems can arise with the technique at a number of levels. If no disease is obtained, the following questions should be considered (some may seem trivial or obvious, but we have encountered all of them):
   a. Has the antigen been uveitogenic in previous experiment? If this is a new synthesis, a synthesis error might have changed the pathogenic epitope.
   b. Has a sufficient dose of antigen been used?
   c. Has the adjuvant been prepared correctly: use of enough mycobacteria, mixed before sampling (mycobacteria may have settled), use of a well-prepared (thick) emulsion?

d. Has the correct strain and substrain of mouse or rat been used? Substrains of the same strain, and even the same strain from a different vendor, may vary in their susceptibility.
e. Are the animals in poor health, stressed, or harboring an infection? Mice that are unhealthy, chronically stressed (have elevated corticosteroid levels), or actively infected (high levels of circulating interferon) will frequently fail to develop disease.
f. Have the mice developed abscesses at the site of immunization (reaction to the mycobacteria in FCA) and been promptly treated by the facility veterinarian with a nonsteroidal anti-inflammatory agent such as ibuprofen? These agents may inhibit induction of disease.

Susceptibility varies with strain. For some commonly used mouse strains immunized with IRBP, hierarchy of susceptibility is B10.RIII > B10.A = B10.BR > C57BL/10 > C57BL/6 ≥ 129.

Chronic exposure to strong light can damage photoreceptor cells and cause retinal degeneration. Albino animals are especially sensitive to this because of lack of pigment in their eyes. For this reason, it is important to protect animals that will be used in EAU experiments from strong light because the resulting retinal damage may confound correct EAU assessment. This includes frequent and prolonged funduscopies.

Some common laboratory mouse strains carry the rd (retinal degeneration) mutation and congenitally lack photoreceptor cells. These strains of course are not appropriate for EAU studies as they do not possess the target tissue. Strains carrying the rd gene include FVB/N, CBA, SLJ/J, PL/J, and most C3H substrains. However, F1 hybrids of these strains with a sighted strain such as B10.RIII or C57BL/6 will be sighted. As determined by crosses between sighted strains, a hybrid's susceptibility is usually intermediate between the two parental strains.

If a strain other than B10.RIII or a B10.RIII hybrid with a less-susceptible strain is used, PT may be needed. It is important to bring up lyophilized PT in a solution containing serum as carrier and to keep the reconstituted stock of PT for no longer than 1 mo. PT solution that has deteriorated will fail to support disease induction. Because different commercial lots of PT may vary in potency, each lot should be titrated for optimal disease-promoting activity. Depending on the lot and the manufacturer, this will usually be between 0.4 and 1 mg for mice and approximately double that for rats.

When anesthetizing animals for any reason, including funduscopy, it is important to keep in mind that anesthetized animals sleep with their eyes open and do not blink. Therefore, if animals are going to be asleep for more than just a few minutes, it is necessary to place an ointment on the eyes to prevent drying of the cornea. Drying of the eyes will inevitably result in exposure keratitis, which will cause corneal opacification and will make follow-up of clinical disease difficult or impossible.

2. Funduscopy is best done under general anesthesia. With some practice, funduscopy can be performed on nonanesthetized animals, but if disease is borderline or

severity scores are to be assigned, it advisable to anesthetize the mouse lightly prior to funduscopy to facilitate a more thorough inspection. Note that the dilating drops cause temporary opacification of the lens within 5–10 min after application, so it is important to complete the funduscopy within that time frame.

3. When cutting the embedded eye tissue, it is important to make sure that the cut is made through the pupillary–optic nerve plane. If the inflammation is mild, pathology is often most apparent around the optic nerve head. Therefore, if sections are cut more laterally, it can be missed. Especially in mild cases, specimens positive on funduscopy may appear to be negative on histology because of the fact that pathology is focal, and the sectioning may have missed it. Therefore, it is important to prepare and examine several nonconsecutive sections.

References

1 Caspi, R. R. (1989). Basic mechanisms in immune-mediated uveitic disease, in *Immunology of Eye Disease* (Lightman, S. L., ed.), Kluwer, Lancaster, UK, Vol. Ch. 5, pp. 61–86.

2. Caspi, R. R., Roberge, F. G., McAllister, C. G., el Saied, M., Kuwabara, T., Gery, I., et al. (1986) T cell lines mediating experimental autoimmune uveoretinitis (EAU) in the rat. *J. Immunol.* **136,** 928–933.

3 Gery, I., Robinson, W. G., Jr., Shichi, H., El-Saied, M., Mochizuki, M., Nussenblatt, R. B., et al. (1985) Differences in susceptibility to experimental autoimmune uveitis among rats of various strains, in *Advances in Immunology and Immunopathology of the Eye (Proceedings of the Third International Symposium on Immunology and Immunopathology of the Eye)* (Chandler, J. W. and O'Conner, G. R., eds.), Masson, New York, Vol. Ch. 59, pp. 242–245.

4. Nussenblatt, R. B., Whitcup, S. M., and Palestine, A. G. (1996) *Uveitis: Fundamentals and Clinical Practice*, 2nd ed., Mosby/Year Book, St. Louis, MO.

5. Gery, I., Mochizuki, M., and Nussenblatt, R. B. (1986) Retinal specific antigens and immunopathogenic processes they provoke. *Prog. Retinal Res.* **5,** 75–109.

6 Sanui, H., Redmond, T. M., Kotake, S., Wiggert, B., Hu, L. H., Margalit, H., et al. (1989) Identification of an immunodominant and highly immunopathogenic determinant in the retinal interphotoreceptor retinoid-binding protein (IRBP). *J. Exp. Med.* **169,** 1947–1960.

7 Applebury, M. L. and Hargrave, P. A. (1986) Molecular biology of the visual pigments. *Vision Res.* **26,** 1881–1895.

8 Borst, D. E., Redmond, T. M., Elser, J. E., Gonda, M. A., Wiggert, B., Chader, G. J., et al. (1989) Interphotoreceptor retinoid-binding protein. Gene characterization, protein repeat structure, and its evolution. *J. Biol. Chem.* **264,** 1115–1123.

9 Mirshahi, M., Boucheix, C., Collenot, G., Thillaye, B., and Faure, J. P. (1985) Retinal S-antigen epitopes in vertebrate and invertebrate photoreceptors. *Invest. Ophthalmol. Vis. Sci.* **26,** 1016–1021.

10 Pfister, C., Chabre, M., Plouet, J., Van Tuyen, V., De Kozak, Y., Faure, J. P., et al. (1985) Retinal S antigen identified as the 48K protein regulating light-dependent phosphodiesterase in rods. *Science* **228,** 891–893.

11 Schalken, J. J., Winkens, H. J., van Vugt, A. H., Bovëe-Geurts, P. H., de Grip, W. J., and Broekhuyse, R. M. (1988) Rhodopsin-induced experimental autoimmune uveoretinitis: dose-dependent clinicopathological features. *Exp. Eye Res.* **47,** 135–145.
12 Hirose, S., Ogasawara, K., Natori, T., Sasamoto, Y., Ohno, S., Matsuda, H., et al. (1991) Regulation of experimental autoimmune uveitis in rats—separation of MHC and non-MHC gene effects. *Clin. Exp. Immunol.* **86,** 419–425.
13 Caspi, R. R., Grubbs, B. G., Chan, C. C., Chader, G. J., and Wiggert, B. (1992) Genetic control of susceptibility to experimental autoimmune uveoretinitis in the mouse model: concomitant regulation by MHC and non-MHC genes. *J. Immunol.* **148,** 2384–2389.
14 Caspi, R. R., Silver, P. B., Chan, C. C., Sun, B., Agarwal, R. K., Wells, J., et al. (1996) Genetic susceptibility to experimental autoimmune uveoretinitis in the rat is associated with an elevated Th1 response. *J. Immunol.* **157,** 2668–2675.
15 Sun, B., Rizzo, L. V., Sun, S. H., Chan, C. C., Wiggert, B., Wilder, R. L., et al. (1997) Genetic susceptibility to experimental autoimmune uveitis involves more than a predisposition to generate a T helper-1-like or a T helper-2-like response. *J. Immunol.* **159,** 1004–1011.
16 Rizzo, L. V., Xu, H., Chan, C. C., Wiggert, B., and Caspi, R. R. (1998) IL-10 has a protective role in experimental autoimmune uveoretinitis. *Int. Immunol.* **10,** 807–814.
17 Egwuagu, C. E., Charukamnoetkanok, P., and Gery, I. (1997) Thymic expression of autoantigens correlates with resistance to autoimmune disease. *J. Immunol.* **159,** 3109–3112.
18 Caspi, R. R., Chan, C.-C., Fujino, Y., Oddo, S., Najafian, F., Bahmanyar, S., et al. (1992) Genetic factors in susceptibility and resistance to experimental autoimmune uveoretinitis. *Curr. Eye Res.* **11**(Suppl.), 81–86.
19 Mochizuki, M., Kuwabara, T., Chan, C. C., Nussenblatt, R. B., Metcalfe, D. D., and Gery, I. (1984) An association between susceptibility to experimental autoimmune uveitis and choroidal mast cell numbers. *J. Immunol.* **133,** 1699–1701.
20 Pennesi, G. and Caspi, R. R. (2002) Genetic control of susceptibility in clinical and experimental uveitis. *Int. Rev. Immunol.* **21,** 67–88.
21 Agarwal, R. K., Chan, C. C., Wiggert, B., and Caspi, R. R. (1999) Pregnancy ameliorates induction and expression of experimental autoimmune uveitis. *J. Immunol.* **162,** 2648–2654.
22 Caspi, R. R., Chan, C. C., Grubbs, B. G., Silver, P. B., Wiggert, B., Parsa, C. F., et al. (1994) Endogenous systemic IFN-gamma has a protective role against ocular autoimmunity in mice. *J. Immunol.* **152,** 890–899.
23 Silver, P. B., Chan, C. C., Wiggert, B., and Caspi, R. R. (1999) The requirement for pertussis to induce EAU is strain-dependent: B10.RIII, but not B10.A mice, develop EAU and Th1 responses to IRBP without pertussis treatment. *Invest. Ophthalmol. Vis. Sci.* **40,** 2898–2905.
24 Arimoto, H., Tanuma, N., Jee, Y., Miyazawa, T., Shima, K., and Matsumoto, Y. (2000) Analysis of experimental autoimmune encephalomyelitis induced in F344 rats by pertussis toxin administration. *J. Neuroimmunol.* **104,** 15–21.

25 Ma, R. Z., Gao, J., Meeker, N. D., Fillmore, P. D., Tung, K. S., Watanabe, T., et al. (2002) Identification of Bphs, an autoimmune disease locus, as histamine receptor H1. *Science* **297,** 620–623.
26 Sudweeks, J. D., Todd, J. A., Blankenhorn, E. P., Wardell, B. B., Woodward, S. R., Meeker, N. D., et al. (1993) Locus controlling *Bordetella pertussis*-induced histamine sensitization (Bphs), an autoimmune disease-susceptibility gene, maps distal to T-cell receptor beta-chain gene on mouse chromosome 6. *Proc. Natl. Acad. Sci. U S A* **90,** 3700–3704.
27 Su, S. B., Silver, P. B., Wang, P., Chan, C. C., and Caspi, R. R. (2003) Dissociating the enhancing and inhibitory effects of pertussis toxin on autoimmune disease. *J. Immunol.* **171,** 2314–2319.
28 Su, S. B., Silver, P. B., Zhang, M., Chan, C. C., and Caspi, R. R. (2001) Pertussis toxin inhibits induction of tissue-specific autoimmune disease by disrupting G protein-coupled signals. *J. Immunol.* **167,** 250–256.
29 Agarwal, R. K., Sun, S. H., Su, S. B., Chan, C. C., and Caspi, R. R. (2002) Pertussis toxin alters the innate and the adaptive immune responses in a pertussis-dependent model of autoimmunity. *J. Neuroimmunol.* **129,** 133–140.
30 Caspi, R. R. (1993) Immunogenetic aspects of clinical and experimental uveitis. *Reg. Immunol.* **4,** 321–330.
31. Caspi, R. R., Roberge, F. G., Chan, C. C., Wiggert, B., Chader, G. J., Rozenszajn, L. A., et al. (1988) A new model of autoimmune disease. Experimental autoimmune uveoretinitis induced in mice with two different retinal antigens. *J. Immunol.* **140,** 1490–1495.
32. Faure, J. P. (1980) Autoimmunity and the retina. *Curr. Topics Eye Res.* **2,** 215–301.
33. Aronson, S. B., Hogan, M. J., and Zweigart, P. (1963) Homoimmune uveitis in the guinea-pig. I. General concepts of auto- and homoimmunity, methods and manifestations. *Arch. Ophthalmol.* **69,** 105–109.
34. Aronson, S. B., Hogan, M. J., and Zweigart, P. (1963) Homoimmune uveitis in the guinea-pig. III. Histopathologic manifestations of the disease. *Arch. Ophthalmol.* **69,** 208–219.
35. Aronson, S. B., Hogan, M. J., and Zweigart, P. M. (1963) Homoimmune uveitis in the guinea-pig. II. Clinical manifestations. *Arch. Ophthalmol.* **69,** 203–207.
36. Wacker, W. B. and Kalsow, C. M. (1973) Autoimmune uveo-retinitis in the rat sensitized with retina photoreceptor cell antigen. *Int. Arch. Allergy Appl. Immunol.* **45,** 582–592.
37 de Kozak, Y., Sakai, J., Thillaye, B., and Faure, J. P. (1981) S antigen-induced experimental autoimmune uveo-retinitis in rats. *Curr. Eye Res.* **1,** 327–337.
38 Gery, I., Wiggert, B., Redmond, T. M., Kuwabara, T., Crawford, M. A., Vistica, B. P., et al. (1986) Uveoretinitis and pinealitis induced by immunization with interphotoreceptor retinoid-binding protein. *Invest. Ophthalmol. Vis. Sci.* **27,** 1296–1300.
39. Caspi, R. (1996) Experimental autoimmune uveoretinitis (EAU)—mouse and rat, in *Current Protocols in Immunology* (Kruisbeek, A., Margulies, D., Shevach, E., and Strober, W., eds.), Wiley, New York, January, Unit 15.16.11–15.16.18.

40. Caspi, R. R. (1994) Experimental autoimmune uveoretinitis—rat and mouse, in *Animal Models for Autoimmune Diseases: A Guidebook* (Cohen, I. R. and Miller, A., eds.), Academic Press, New York, Vol. Ch. 5, pp. 57–81.
41. Mozayeni, R. M., Chan, C. C., Grubbs, B. E., Stober, D. I., Wiggert, B., Chader, G. J., et al. (1995) Alternative methods of immunization for the induction of experimental autoimmune uveoretinitis (EAU) in rodent models: a comparison. *Ocul. Immunol. Inflamm.* **3,** 81–87.
42 Mochizuki, M., Kuwabara, T., McAllister, C., Nussenblatt, R. B., and Gery, I. (1985) Adoptive transfer of experimental autoimmune uveoretinitis in rats. Immunopathogenic mechanisms and histologic features. *Invest. Ophthalmol. Vis. Sci.* **26,** 1–9.
43 Beraud, E., Kotake, S., Caspi, R. R., Oddo, S. M., Chan, C. C., Gery, I., et al. (1992) Control of experimental autoimmune uveoretinitis by low dose T cell vaccination. *Cell. Immunol.* **140,** 112–122.
44 Avichezer, D., Silver, P. B., Chan, C. C., Wigge rt, B., and Caspi, R. R. (2000) Identification of a new epitope of human IRBP that induces autoimmune uveoretinitis in mice of the H-2b haplotype. *Invest. Ophthalmol. Vis. Sci.* **41,** 127–131.
45 Namba, K., Ogasawara, K., Kitaichi, N., Matsuki, N., Takahashi, A., Sasamoto, Y., et al. (1998) Identification of a peptide inducing experimental autoimmune uveoretinitis (EAU) in H-2Ak-carrying mice. *Clin. Exp. Immunol.* **111,** 442–449.
46 Silver, P. B., Rizzo, L. V., Chan, C. C., Donoso, L. A., Wiggert, B., and Caspi, R. R. (1995) Identification of a major pathogenic epitope in the human IRBP molecule recognized by mice of the H-2r haplotype. *Invest. Ophthalmol. Vis. Sci.* **36,** 946–954.
46a. Avichezer, D., Grajewski, R.S., Chan, C. C., Mattapallil, M. J., Silver, P. B., Raber, J. A., et al. (2003) An immunologically privileged retinal antigen elicits tolerance: major role for central selection mechanisms. *J. Exp. Med.* **198,** 1665–1676.
47 Szpak, Y., Vieville, J. C., Tabary, T., Naud, M. C., Chopin, M., Edelson, C., et al. (2001) Spontaneous retinopathy in HLA-A29 transgenic mice. *Proc. Natl. Acad. Sci. U S A* **98,** 2572–2576.
48 Pennesi, G., Mattapallil, M. J., Sun, S. H., Avichezer, D., Silver, P. B., Karabekian, Z., et al. (2003) A humanized model of experimental autoimmune uveitis in HLA class II transgenic mice. *J. Clin. Invest.* **111,** 1171–1180.
49 Chan, C. C., Caspi, R. R., Ni, M., Leake, W. C., Wiggert, B., Chader, G. J., et al. (1990) Pathology of experimental autoimmune uveoretinitis in mice. *J. Autoimmun.* **3,** 247–255.
50 Donoso, L. A., Yamaki, K., Merryman, C. F., Shinohara, T., Yue, S., and Sery, T. W. (1988) Human S-antigen: characterization of uveitopathogenic sites. *Curr. Eye Res.* **7,** 1077–1085.
51 Singh, V. K., Nussenblatt, R. B., Donoso, L. A., Yamaki, K., Chan, C. C., and Shinohara, T. (1988) Identification of a uveitopathogenic and lymphocyte proliferation site in bovine S-antigen. *Cell. Immunol.* **115,** 413–419.

52 Donoso, L. A., Merryman, C. F., Sery, T. W., Shinohara, T., Dietzschold, B., Smith, A., et al. (1987) S-antigen: characterization of a pathogenic epitope which mediates experimental autoimmune uveitis and pinealitis in Lewis rats. *Curr. Eye Res.* **6,** 1151–1159.

53 Kotake, S., Redmond, T. M., Wiggert, B., Vistica, B., Sanui, H., Chader, G. J., et al. (1991) Unusual immunologic properties of the uveitogenic interphotoreceptor retinoid-binding protein-derived peptide R23. *Invest. Ophthalmol. Vis. Sci.* **32,** 2058–2064.

54 Sanui, H., Redmond, T. M., Hu, L. H., Kuwabara, T., Margalit, H., Cornette, J. L., et al. (1988) Synthetic peptides derived from IRBP induce EAU and EAP in Lewis rats. *Curr. Eye Res.* **7,** 727–735.

55 Kotake, S., de Smet, M. D., Wiggert, B., Redmond, T. M., Chader, G. J., and Gery, I. (1991) Analysis of the pivotal residues of the immunodominant and highly uveitogenic determinant of interphotoreceptor retinoid-binding protein. *J. Immunol.* **146,** 2995–3001.

56 de Smet, M. D., Bitar, G., Roberge, F. G., Gery, I., and Nussenblatt, R. B. (1993) Human S-antigen: Presence of multiple immunogenic and immunopathogenic sites in the Lewis rat. *J. Autoimmun.* **6,** 587–599.

57 Merryman, C. F., Donoso, L. A., Zhang, X. M., Heber-Katz, E., and Gregerson, D. S. (1991) Characterization of a new, potent, immunopathogenic epitope in S-antigen that elicits T cells expressing V beta 8 and V alpha 2-like genes. *J. Immunol.* **146,** 75–80.

58 Gregerson, D. S., Merryman, C. F., Obritsch, W. F., and Donoso, L. A. (1990) Identification of a potent new pathogenic site in human retinal S-antigen which induces experimental autoimmune uveoretinitis in LEW rats. *Cell. Immunol.* **128,** 209–219.

59. Donoso, L. A., Merryman, C. F., Sery, T., Sanders, R., Vrabec, T., and Fong, S. L. (1989) Human interstitial retinoid binding protein. A potent uveitopathogenic agent for the induction of experimental autoimmune uveitis. *J. Immunol.* **143,** 79–83.

22

Autoimmune Depigmentation Following Sensitization to Melanoma Antigens

Arthur A. Hurwitz and Qingyong Ji

Summary

Generating an antitumor immune response can be thought of as eliciting an immune response to cells derived from self-tissue. As such, tumor immunity may result in autoimmunity. Melanoma patients undergoing immunotherapy often develop a form of autoimmune depigmentation referred to as vitiligo, in which T cells with antigenic specificity for pigmentation antigens destroy normal melanocytes. The models described in this chapter can be used to study immunity to melanoma antigens. These models employ a well-characterized pigmentation antigen relevant to melanoma and a common transplantable murine melanoma cell line. As more sophisticated approaches to cancer therapy are developed, models such as these may be key in understanding how immunity to self-antigens can be manipulated to elicit tumor immunity.

Key Words: Autoimmunity; depigmentation; melanoma; murine model; T cells; tumor immunity; tyrosinase-related protein 2 (TRP-2); vitiligo.

1. Introduction

Immunotherapy of patients with melanoma has often been associated with an autoimmune depigmentation referred to as vitiligo. This autoimmune syndrome is presumed to be the result of T-cell reactivity directed against pigmentation antigens coexpressed by melanoma cells and melanocytes ***(1–4)***. In some mouse models of melanoma, notably the C57BL/6-derived B16 model, a similar depigmentation occurs following vaccination with cell-based vaccines, therapy based on DNA, or peptide-based therapy ***(5–12)***. These models all suggest that a highly potent antitumor response may be associated with autoimmune depigmentation, although some vaccines may not be sufficiently potent to elicit autoimmunity ***(13)***.

From: *Methods in Molecular Medicine, Vol. 102: Autoimmunity: Methods and Protocols*
Edited by: A. Perl © Humana Press Inc., Totowa, NJ

This chapter describes two approaches to elicit autoimmune depigmentation in mice. The first model employs B16 tumor cells genetically modified to express the proinflammatory cytokine granulocyte-macrophage colony-stimulating factor (GM-CSF). Sensitization of syngeneic mice with this vaccine, in combination with anti-CTLA-4, results in vitiligo-like depigmentation in approx 70% of mice. The second model takes advantage of a defined epitope contained within the melanogenic enzyme, tyrosinase-related protein 2 (TRP-2). TRP-$2_{180–188}$ is an H-2 K^b-restricted, immunodominant epitope. Mice sensitized to the synthetic peptide emulsified in complete Freund's adjuvant (CFA), in combination with anti-CTLA-4, develop small areas of depigmentation. In both models, depigmentation is dependent on $CD8^+$ T cells, but not $CD4^+$ T cells. These two models provide the opportunity to study autoimmunity to antigens relevant to cancer.

2. Materials

1. B16 tumor cells (American Type Culture Collection) cultured in Dulbecco's modified Eagle's medium with 10% fetal calf serum.
2. Purified anti-CTLA-4 antibody (BD Pharmingen or American Type Culture Collection).
3. C57BL/6 mice (Jackson Laboratories or NCI).
4. TRP-$2_{180–188}$ peptide (New England Peptide).
5. CFA (Fisher Scientific).
6. Heat-killed *Mycobacterium tuberculosis* H37Ra (Difco/Fisher Scientific).
7. 1-cc syringes.
8. 23-, 25-, 18-, and 21-ga 1-in. needles.
9. Emulsifying needle (18-ga) and glass syringes or homogenizer.
10. Oster clippers with no. 40 blades.
11. Irradiator (cesium source or X-ray).
12. Ruler or caliper.

3. Methods

The methods in this subheading describe the use of the vaccine based on GM-CSF-expressing B16 cells (**Subheading 3.1.**) and TRP-2 peptide (**Subheading 3.2.**) to induce depigmentation in C57BL/6 mice. Also described is a grading system for monitoring depigmentation (**Subheading 3.3.**).

3.1. Sensitization to the B16 Cell-Based Vaccine

The B16 melanoma is a C57BL/6-derived pigmenting melanoma with several variant sublines. The F_0 subline is considered parental. The F_{10} subline is often used for experimental metastasis models following intravenous challenge. The BL6 variant is the most aggressive and also forms pulmonary metastases after intravenous challenge. The GM-CSF-expressing variant (GM-B16) needs

to be prepared by gene transfer or can be obtained from other investigators. The production of GM-CSF can be confirmed and estimated by commercially available enzyme-linked immunosorbent assay kits and should be in the range of 5–20 ng/mL for 1×10^6 cells/24 h. The efficacy of lower or higher values has not been determined. Prior to injection, cells should be handled using aseptic techniques.

1. On day 0, lift GM-B16 cells from cell culture dishes using trypsin and wash three times in serum-free medium or saline to remove excess fetal calf serum and trypsin.
2. Resuspend the cells at a density of 1×10^7 cells/mL and place tube on ice.
3. Irradiate cells using a dosage of 12,000 rad, maintaining cells on ice.
4. Load cells into 1-cc syringe capped with a 23-ga needle.
5. Inject 0.1 mL of cell solution into the shaved dorsal surface of mice. Between injections, invert syringe to maintain constant cell density.
6. On day 1, inject mice intraperitoneally with 100 μg of anti-CTLA-4 antibody.
7. Repeat **steps 1–6** twice every 3 d (starting days 3 and 6). Subsequent subcutaneous injection of cells can be performed in adjacent areas. The cell vaccine persists for 3–6 d at the site of injection.
8. Two weeks after antibody injection, begin monitoring for depigmentation of hairs (**Protocol 3.3.**).

3.2. Sensitization to TRP-2$_{180–188}$ Peptide

1. Prepare aqueous peptide solution at a 1.5 mg/mL. Peptide should first be solubilized in dimethyl sulfoxide at an approximate concentration of 10 mg/mL. This solution can then be diluted with phosphate-buffered saline to a final concentration of 1.5 mg/mL.
2. Separately, prepare the CFA solution using CFA supplemented with *M. tuberculosis* H37RA to a final concentration of 8 mg/mL. This solution is very viscous and should be distributed with a wide-bore pipet tip.
3. Mix an equal volume of CFA and antigen in a 50-mL conical tube and transfer the solution to two appropriate size glass syringes using 18-ga needles. Remove the needles and attach the emulsifying needle to one of the syringes. Fill the emulsifying needle with the antigen/adjuvant solution and then cap the opposite end of the emulsifying needle with the other glass syringe. Taking care to avoid air in the needle at this point eliminates the problem of having air in the emulsion when sensitizing mice later.
4. Emulsify the mixture by transferring the solution between the two syringes. This process can take from 5 to 15 min. The solution should change from an ivory-colored solution to a white color. The efficiency of emulsification can be tested by expelling a small amount of the emulsion onto the surface of a water-filled beaker. If emulsification is complete, there will be minimal spreading of the solution, and it will have a consistency like marshmallow Fluff®.

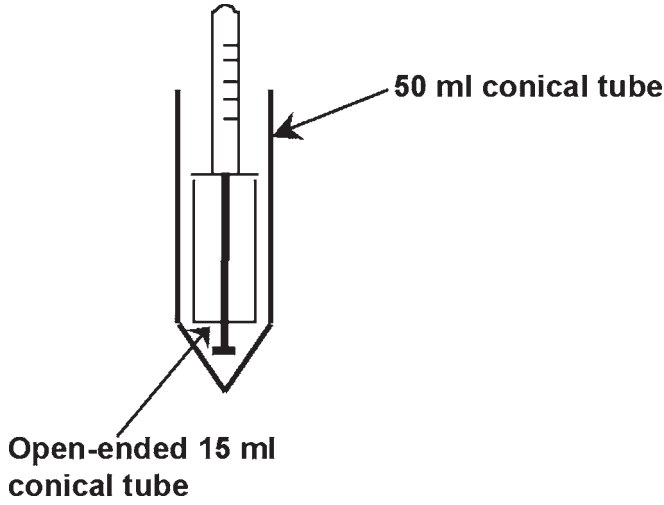

Fig. 1. Preparation of syringe with emulsified adjuvant: A 1-cc tuberculin syringe is inverted and placed into a cut 15-mL conical tube. This combination is placed in a 50-mL conical tube, and the complex is spun at 1000 rpm for 6 min.

5. When the solution is completely emulsified, it can be transferred into 1-cc syringes. Either glass or plastic can be used for injection. If plastic syringes are used, care should be taken when attaching the syringe to the emulsifying needle because most 1-cc syringes are not Luer lock compatible. In addition, care should be taken to avoid getting the emulsion on the tip of the syringe as the oily residue can cause the needle to slip off the syringe during injections. A 21-ga needle should be used for adjuvant injection.
6. An alternative way to make the emulsion is to use a tissue homogenizer. This approach is usually faster, and there is less loss of the emulsion. The syringes need to be loaded carefully to avoid getting air bubbles in the emulsion. To avoid the presence of air bubbles, the loaded syringe can be spun inverted using a low-speed centrifuge. The inverted syringe is placed in an open-ended 15-mL conical tube placed in a 50-mL conical tube (*see* **Fig. 1**). After spinning (<500 rpm), the air can be expelled from the syringe. A 21-ga needle should be used for adjuvant injection.
7. Each mouse should be injected with 200 μL of antigen emulsion at two sites, preferably on contralateral sides, on the shaved, dorsolateral surface. Extreme care should be taken while injecting mice. If there is little animal handling experience, it is suggested to anesthetize the mice using either an inhaled or injectable anesthetic.
8. Two days after sensitization to the TRP-2 peptide, mice should be treated with anti-CTLA-4. As described in **Subheading 3.1.**, this requires three 100-μg injec-

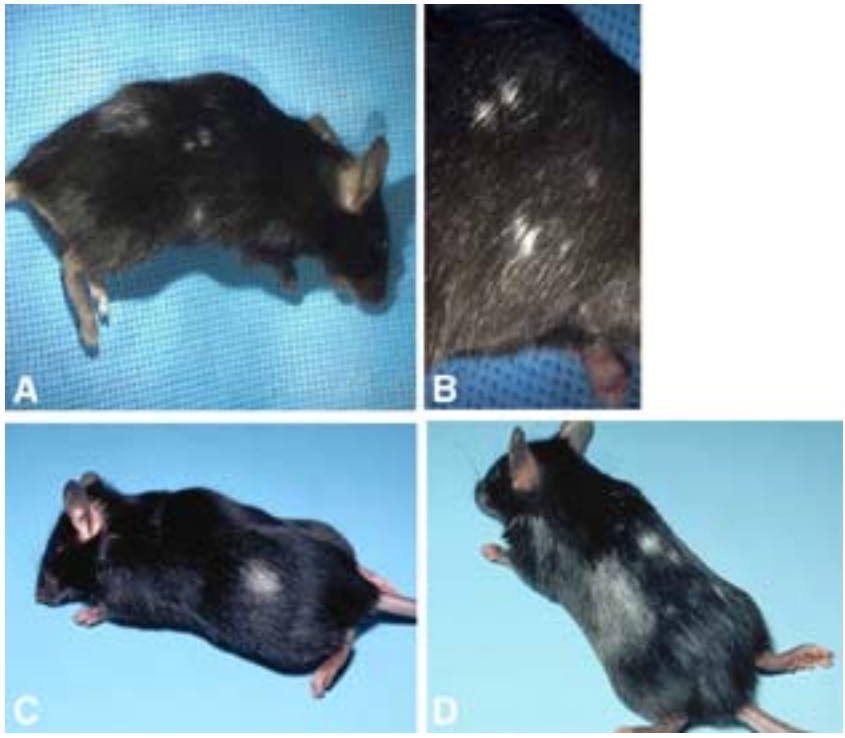

Fig. 2. Vitiligolike depigmentation in mice. Mice were sensitized to (**A,B**) TRP-2 180–188, (**C,D**) GM-CSF-expressing B16 tumor cells in combination with anti-CTLA-4. Depigmentation usually begins at the site of vaccination and sometimes extends to distal areas of the surface in mice vaccinated with the B16 vaccine.

tions given at 3-d intervals. This injection can be administered either intraperitoneally or intravenously.

9. In this model, depigmentation begins to appear within 4 wk of injection. As such, depigmentation should be monitored beginning 3 wk after sensitization.

As a safety note, extreme care should be taken when handling FAC solutions and emulsion. Although the *M. tuberculosis* is not pathogenic, it can cause an individual to seroconvert.

3.3. Scoring Depigmentation of Hairs in Mice

In general, depigmentation appears within 4 wk of sensitization to either the B16 vaccine or the TRP-2 peptide. Thus, it is advisable to begin monitoring the mice within 2–3 wk after sensitization. The depigmentation usually appears adjacent to the site of sensitization (**Fig. 2A,B**). The area of depigmentation is always larger in mice sensitized to the B16 vaccine (**Fig. 2C,D**) and can be

measured using a ruler or caliper. An example of depigmentation has been published ***(11)***. The following grading system is used:

0 = no depigmentation
1 = small, random areas of depigmentation
2 = area of depigmentation less than 5 mm
3 = area of depigmentation between 5 and 20 mm
4 = area of depigmentation greater than 20 mm

Mice can be monitored for up to 8 wk. In the B16 vaccine model, depigmentation is progressive for the entire period. In the TRP-2 sensitization model, the area of depigmentation (without manipulation) usually does not exceed 20 mm.

References:

1 Phan, G. Q., Attia, P., Steinberg, S. M., White, D. E., and Rosenberg, S. A. (2001) Factors associated with response to high-dose interleukin-2 in patients with metastatic melanoma. *J. Clin. Oncol.* **19,** 3477–3482.

2 Rosenberg, S. A. and White, D. E. (1996) Vitiligo in patients with melanoma: normal tissue antigens can be targets for cancer immunotherapy. *J. Immunother. Emphasis Tumor Immunol.* **19,** 81–84.

3 Phan, G. Q., Yang, J. C., Sherry, R. M., Hwu, P., Topalian, S. L., Schwartzentruber, D. J., et al. (2003) Cancer regression and autoimmunity induced by cytotoxic T lymphocyte-associated antigen 4 blockade in patients with metastatic melanoma. *Proc. Natl. Acad. Sci. U S A* **100,** 8372–8377.

4 Dudley, M. E., Wunderlich, J. R., Robbins, P. F., Yang, J. C., Hwu, P., Schwartzentruber, D. J., et al. (2002) Cancer regression and autoimmunity in patients after clonal repopulation with antitumor lymphocytes. *Science* **298,** 850–854.

5 Overwijk, W. W., Lee, D. S., Surman, D. R., Irvibe, K. R., Touloukian, C. E., Chan, C.-C., et al. (1999) Vaccination with a recombinant vaccinia virus encoding "self" antigen induces autoimmune vitiligo and tumor cell destruction in mice: requirement for $CD4^+$ T lymphocytes. *Proc. Natl. Acad. Sci.* **96,** 2982–2987.

6 van Elsas, A., Sutmuller, R. P., Hurwitz, A. A., Ziskin, J., Villasenor, J., Medema, J. P., et al. (2001) Elucidating the autoimmune and antitumor effector mechanisms of a treatment based on cytotoxic T lymphocyte antigen-4 blockade in combination with a B16 melanoma vaccine: comparison of prophylaxis and therapy. *J. Exp. Med.* **194,** 481–489.

7 Bowne, W. B., Srinivasan, R., Wolchok, J. D., Hawkins, W. G., Blachere, N. E., Dyall, R., et al. (1999) Coupling and uncoupling of tumor immunity and autoimmunity. *J. Exp. Med.* **190,** 1717–1722.

8 Naftzger, C., Takechi, Y., Kohda, H., Hara, I., Vijayasaradhi, S., and Houghton, A. N. (1996) Immune response to a differentiation antigen induced by altered antigen: a study of tumor rejection and autoimmunity. *Proc. Natl. Acad. Sci.* **93,** 14,809–14,814.

9 Schreurs, M. W., Eggert, A. A., de Boer, A. J., Vissers, J. L., van Hall, T., Offringa, R., et al. (2000) Dendritic cells break tolerance and induce protective immunity against a melanocyte differentiation antigen in an autologous melanoma model. *Cancer Res.* **60,** 6995–7001.

10 Shimizu, K., Thomas, E. K., Giedlin, M., and Mule, J. J. (2001) Enhancement of tumor lysate- and peptide-pulsed dendritic cell-based vaccines by the addition of foreign helper protein. *Cancer Res.* **61,** 2618–2624.

11 van Elsas, A., Hurwitz, A. A., and Allison, J. P. (1999) Combination immunotherapy of B16 melanoma using anti-cytotoxic T lymphocyte-associated antigen 4 (CTLA-4) and granulocyte/macrophage colony-stimulating factor (GM-CSF)-producing vaccines induces rejection of subcutaneous and metastatic tumors accompanied by autoimmune depigmentation. *J. Exp. Med.* **190,** 355–366.

12 Weber, L. W., Bowne, W. B., Wolchok, J. D., Srinivasan, R., Qin, J., Moroi, Y., et al. (1998) Tumor immunity and autoimmunity induced by immunization with homologous DNA. *J. Clin. Invest.* **102,** 1258–1264.

13. Bronte, V., Apolloni, E., Ronca, R., Zamboni, P., Overwijk, W. W., Surman, D. R., et al. (2000) Genetic vaccination with "self" tyrosinase-related protein 2 causes melanoma eradication but not vitiligo. *Cancer Res.* **60,** 253–258.

Index